Mechanistische Charakterisierung und Anwendung von Light-oxygen-voltage Rezeptoren

DISSERTATION

zur Erlangung des akademischen Grades einer Doktorin
der Naturwissenschaften (Dr. rer. nat.)
an der Fakultät für Biologie, Chemie und Geowissenschaften
der Universität Bayreuth

vorgelegt von

Julia Dietler, geb. Hennemann

aus *Lichtenfels*Bayreuth, 2021

Die vorliegende Arbeit wurde in der Zeit von Februar/2017 bis Januar/2021 in Bayreuth

am Lehrstuhl Biochemie unter Betreuung von Herrn Professor Dr. Andreas Möglich

angefertigt.

Vollständiger Abdruck der von der Fakultät für Biologie, Chemie und Geowissenschaf-

ten der Universität Bayreuth genehmigten Dissertation zur Erlangung des akademi-

schen Grades einer Doktorin der Naturwissenschaften (Dr. rer. nat.).

Dissertation eingereicht am: 29.01.2021

Zulassung durch Promotionskommission: 24.02.2021

Wissenschaftliches Kolloquium: 05.07.2021

Amtierender Dekan: Prof. Dr. Matthias Breuning

Prüfungsausschuss:

Prof. Dr. Andreas Möglich (Gutachter)

Prof. Dr. Birgitta Wöhrl (Gutachterin)

Prof. Dr. Roland Marschall (Vorsitz)

Prof. Dr. Andreas Greiner

Inhalt

Abkürzungen	5
Abstract	7
Zusammenfassung	9
1 Einleitung	11
1.1 Light-oxygen-voltage (LOV) Photorezeptoren	13
1.1.1 Architektur und topologische Vielfalt	14
1.1.2 Struktureller Aufbau von LOV Domänen	18
1.1.3 Photozyklus und initiale Signalweiterleitung in LOV Re	ezeptoren19
1.1.4 Allosterische Signalweiterleitung in LOV Rezeptoren	23
1.2 Erstellung künstlicher Photorezeptoren	25
1.2.1 Designstrategien von LOV-basierten optogenetischen W	Verkzeugen26
1.2.2 Bakterielle LOV-basierte Genexpressionssysteme	30
1.3 Ziele der Arbeit	33
2 Synopsis	34
2.1 Gepulste Beleuchtung in der Optogenetik und Photobiolog	gie34
2.1.1 Erstellung programmierbarer Beleuchtungsapparaturen	36
2.1.2 Präzise und sequenzielle Kontrolle bakterieller Genexpi	ression37
2.2 Signaltransduktion in LOV Rezeptoren	39
2.3 Charakterisierung, Anwendung und Optimierung einer lic	-
LOV Domäne	
2.4 Blaulichtgesteuerte Assemblierung von Goldnanopartikeln	151
2.5 Fazit	53
3 Literaturverzeichnis	54
4 Eigenanteil	
4.1 Manuskript I	67
4.2 Manuskript II	67
4.3 Manuskript III	68
4.4 Manuskript IV	68
4.5 Manuskript V	69
5 Manuskripte	70
5.1 Manuskript I	70
5.2 Manuskript II	81
5.3 Manuskript III	103

5.4	Manuskript IV	155
5.5	Manuskript V	187
6	Publikationsliste	204
7	Danksagung	205
8	(Eidesstattliche) Versicherungen und Erklärungen	206

Abkürzungen

AsLOV2 Phototropin 1 LOV2 Domäne aus Avena sativa

ATP Adenosintriphosphat

AuNP Goldnanopartikel

BLUF blue light sensors using flavin adenine nucleotide

CA catalytic and ATP binding

c-di-GMP cyclic dimeric guanosine monophosphate, bis-(3'-5')-zyklisches di-Guanosin-

monophosphat

D dunkeladaptierter Zustand

DHp dimerization and histidine phosphotransfer

DsRed Optimierte Version des rot fluoreszierenden Proteins aus Discosoma species

FAD Flavin-Adenin-Dinukleotid

FKF1 Flavin binding-Kelch-Fbox-1

FMN Flavinmononukleotid

GEF Guanosintriphosphataustauschfaktor

GFP grün fluoreszierendes Protein

GTP Guanosintriphosphat

GTPase Guanosintriphosphatase

His₆ Hexahistidin

HisKA Histidin-Kinase-Phosphoakzeptor

HK Histidinkinase

HSQC Heteronuclear Single Quantum Coherence

HTH helix-turn-helix

I Intensität

ISC Intersystem Crossing

k Ratenkonstante

 $K_{\rm D}$ Dissoziationskonstante

L lichtadaptierter Zustand

LED *light-emitting diodes*

LOV *Light-oxygen-voltage*

mFGFR-1 murine fibroblast growth factor receptor 1

NMR Kernspinresonanz

NTA Nitrilotriessigsäure

PAS Per-Arnt-Sim

pGpG 5'-Phosphoguanylyl-(3'→5')-Guanosin

Pkinase Proteinkinase

Ptaur-LOV Isolierte Aureochrom 1a LOV Domäne aus Phaeodactylum tricornutum

PYP photoactive yellow protein

ROS reactive oxygen species, reactive Sauerstoffspezies

RR response regulator, Antwortregulator

RsLOV LOV Domäne aus Rhodobacter sphaeroides

RTK Rezeptortyrosinkinase

S₀ Singulettzustand

S₁ angeregter Singulettzustand

sLOV short LOV

SPR surface plasmon resonance, Oberflächenplasmonenresonanz

STAS sulfate transporter and anti-sigma factor antagonist

T₁ Triplettzustand

TCS two-component system, Zweikomponentensystem

TEM Transmissionselektronenmikroskopie

TetR Tet Repressor

TrpR Trp Repressor

Vfaur-LOV Isolierte Aureochrom 1a LOV Domäne aus Vaucheria frigida

WC-1 white collar-1

Abstract

Light-oxygen-voltage (LOV) photoreceptors enable a variety of organisms to sense and respond to (sun)light. The receptors feature modular architecture and comprise sensor and effector modules. The LOV sensor incorporates a flavin-nucleotide chromophore to detect blue light. Light absorption induces conformational changes within the sensor that are further propagated to the effector which in turn mediates a specific biological response. Due to the compact architecture of the LOV sensor and diverse allosteric strategies by which light signals are translated into changes of biological activity, LOV domains often operate in optogenetic systems. In optogenetics, sensory photoreceptors enable the minimally invasive control of diverse processes in cells and organisms with high spatiotemporal resolution. Recombination of sensor and effector modules from different proteins yields photoreceptor chimeras to put cellular signaling pathways under light control. Both, knowledge of precise regulation, sensitivity and signaling principles of underlying receptors are essential for their application as an optogenetic tool. The present work provides further insights into characteristics and signal transduction of LOV receptors and covers the engineering of new synthetic LOV-based (optogenetic) actuators.

Using the engineered photoreceptor YF1 and its derived gene expression systems pDusk and pDawn, it was initially shown that pulsed illumination allows precise and graduated control of downstream responses, whereas continuously applied light of the same color failed to do so. Further the employment of pulsed illumination schemes affords the reduction of the overall light dose and hence mitigates phototoxicity, photobleaching and sample heating. This thesis also demonstrates that photoreceptor proteins can be addressed separately with a single light color when differing in their dark recovery kinetics. In turn this allows the sequential control of several optogenetic systems.

In addition to light reception, subsequent signal transduction is decisive for the functionality of LOV receptors. Prior studies indicated that downstream signaling involves the rotation of a conserved glutamine residue and subsequent alteration of hydrogen bonding interactions adjacent to the flavin. Contrary to the prevalent view in the field, here it was shown that signals can be forwarded to expediently regulate downstream responses in YF1 even when devoid of the conserved glutamine. Signal transduction most likely occurs via an alternative mechanism and presumably does not hinge on the conventional hydrogen bonding pathway. Further characterization of a newly identified LOV-GGDEF receptor revealed that glutamine devoid LOV receptors exist in nature and equally facilitate blue light-dependent signal transduction.

LOV receptors do not only integrate light signals but can also sense other environmental stimuli. Within this thesis the light and temperature sensitivity of the LOV domain of *Rhodobacter*

sphaeroides (RsLOV), which dissociates upon blue light illumination, was further analyzed and characterized. For this purpose a new optogenetic tool that is based on the *E. coli* Tet repressor (TetR) and the RsLOV domain was developed. It provides blue light-controlled gene expression in *E. coli*, whereas an increase in temperature results in a loss of light regulation. This effect could be ascribed to the RsLOV domain. By using distinct approaches, two RsLOV variants were identified that restore light-dependent gene expression at 37°C. Biochemical analysis demonstrated that, one variant improves the weak homodimer affinity of the wildtype protein by two-fold, whereas the other reveals an enhanced thermodynamic stability. Owing to the revised homodimer affinity of the identified RsLOV variant, blue light-dependent control of a receptor tyrosine kinase was likewise established, while any attempts on light regulation using the wildtype RsLOV domain failed.

Finally this thesis demonstrates that the use of LOV domains is not limited to cellular contexts. By establishing the blue light-induced assembly of gold nanoparticles (AuNPs) it could be shown that LOV domains can successfully be utilized in extracellular applications. The assembly is based on the immobilization of the LOV domain VIVID from *Neurospora crassa* on the surface of functionalized AuNPs. In darkness, VIVID is monomeric, whereas blue light exposure triggers the dimerization which in turn resulted in the assembly and formation of huge AuNP clusters. The demonstrated combination of genetically encoded, light-switchable proteins with inorganic AuNPs augurs new applications in biology and material science.

Zusammenfassung

Light oxygen voltage (LOV) Photorezeptoren ermöglichen einer Vielzahl von Organismen die Wahrnehmung und Reaktion auf (Sonnen)-Licht. Die Rezeptoren sind modular aufgebaut und bestehen aus einem Sensor- und einem Effektormodul. Mit Hilfe eines Flavinderivats detektiert der Sensor Licht im blauen Bereich und leitet das Signal über konformationelle Änderungen an seinen Effektor weiter. Dieser übt sodann eine spezifische biologische Antwort aus. Auf Grund der kompakten Architektur des Sensors und der vielfältigen allosterischen Prinzipien zur Signalweiterleitung, fungieren diese oftmals als Werkzeug in optogenetischen Systemen. Optogenetik beschreibt die räumlich-zeitlich exakte und minimalinvasive Kontrolle zellulärer Prozesse mit Hilfe von sensorischen Photorezeptoren. Die Rekombination von Sensor- und Effektormodulen unterschiedlicher Ausgangsproteine erzeugt neue Chimäre, welche die Lichtsteuerung ausgewählter Signalwege erlaubt. Wesentlich für den Einsatz als optogenetisches Werkzeug ist sowohl das Verständnis über eine präzise Regulation, die Sensitivität, als auch das Wissen über die molekulare Wirkweise. Die vorliegende Arbeit gewährt weitere Einblicke in die Eigenschaften und Signaltransduktion von LOV Rezeptoren sowie beschäftigt sich mit der Erstellung neuer synthetischer LOV-basierter (optogenetischer) Schalter.

Anhand des künstlichen Photorezeptors YF1 und der abgeleiteten Genexpressionssysteme pDusk und pDawn wurde zunächst gezeigt, dass gepulste Beleuchtung im Gegensatz zu kontinuierlich verabreichtem Licht gleicher Farbe eine sehr präzise und gestaffelte Kontrolle der Signalantwort erlaubt. Darüber hinaus ermöglicht der Einsatz gepulster Beleuchtungsschemata die Reduzierung der Gesamlichtdosis, sodass mögliche Schäden im Gewebe, die durch hohe Lichtdosen entstehen, verhindert werden können. Ebenso wurde gezeigt, dass Photorezeptoren mit einer einzigen Lichtfarbe getrennt voneinander adressiert werden können, solange diese sich hinsichtlich ihrer Rückkehrkinetik unterscheiden. Dies ermöglicht die sequenzielle Kontrolle mehrerer optogenetischer Systeme.

Neben der Wahrnehmung des Lichts ist eine nachfolgende Signalweiterleitung maßgebend für die Funktionalität von LOV Rezeptoren. Vorhergehende Studien hierzu zeigten, dass eine blaulichtausgelöste Umlagerung eines chromophornahen, konservierten Glutamins sowie folgende Veränderungen am Wasserstoffbrückennetzwerk für die Signalweiterleitung entscheidend sind. Mittels Mutagenesestudien an YF1 konnte innerhalb dieser Arbeit hingegen gezeigt werden, dass Signale in fast vollem Umfang auch ohne das konservierte Glutamin an den Effektor übermittelt werden können. Die Signaltransduktion erfolgt dabei höchstwahrscheinlich über einen alternativen Mechanismus und verläuft nicht über den herkömmlichen Weg. Hinzukommend

konnte anhand eines neu identifizierten LOV-GGDEF Rezeptors gezeigt werden, dass glutaminfreie LOV Rezeptoren in der Natur existieren und eine blaulichtgesteuerte Signalübermittlung erlauben.

LOV Rezeptoren sind nicht nur empfindlich gegenüber Blaulicht, sondern können auch weitere umgebungsbedingte Reize wahrnehmen. Innerhalb dieser Arbeit wurden weitere Einblicke in die Licht- und Temperatursensitivität der auf Blaulicht hin dissoziierenden LOV Domäne aus *Rhodobacter sphaeroides* (*Rs*LOV) gewonnen. Hierfür wurde mit Hilfe des *E. coli* Tet Repressors (TetR) und der *Rs*LOV Domäne ein neues optogenetischen Werkzeugs entwickelt. Dieses ermöglicht blaulichtabhängige Genexpression in *E. coli*, wobei eine Erhöhung der Temperatur zum Verlust dieser führt und vermutlich auf die *Rs*LOV Domäne zurückzuführen ist. Unter Verwendung unterschiedlicher Herangehensweisen konnten zwei *Rs*LOV Varianten identifiziert werden, welche auch bei 37°C eine Lichtregulation gestatten. Die eine Variante erhöht die schwache Homodimerisierungsaffinität der wildtypischen Domäne um das zweifache, wohingegen die andere *Rs*LOV Variante eine ausgeprägtere thermodynamische Stabilität aufweist. Die verbesserten Dimerisierungseigenschaften der hier identifizierten *Rs*LOV Variante erbrachten zudem die blaulichtabhängige Steuerung einer Rezeptortyrosinkinase, welche bei Verwendung des wildtypischen Rezeptors nicht erreicht werden kann.

Zuletzt wird gezeigt, dass sich der Einsatz von LOV Domänen sich nicht nur auf zelluläre Kontexte beschränkt. Die in dieser Arbeit realisierte blaulichtinduzierte Assemblierung von Goldnanopartikeln (AuNP) demonstriert, dass LOV Domänen auch in extrazellulären Anwendungen gewinnbringend eingesetzt werden können. Grundlage dessen ist die Immobilisierung der Hexahistidin-markierten LOV Domäne VIVID aus *Neurospora crassa* auf der Oberfläche von funktionalisierten AuNP. In Dunkelheit bildet VIVID Monomere, wohingegen Blaulichtbestrahlung die Dimerisierung auslöst und so zur Assemblierung und Ausbildung großer AuNP-Netzwerke führt. Die hier gezeigte Kombination von genetisch kodierten, lichtschaltbaren Proteinen mit anorganischen Goldnanopartikeln verspricht neue Anwendungen in biologischen und materialwissenschaftlichen Bereichen.

1 Einleitung

Die Evolution des Lebens auf der Erde ist seit jeher geprägt durch die Gegenwart von Sonnenlicht. Zahlreiche Organismen haben daher die Fähigkeit entwickelt, Lichtreize wahrzunehmen und darauf zu reagieren. Seither dient Licht als essenzielle Energie- und Informationsquelle, welche das Wachstum und Überleben sichert. Lichtquanten werden von Pflanzen, Algen und bestimmten Bakterien benötigt, um im Rahmen der Photosynthese chemische Energie zu gewinnen, welche zum Aufbau energiereicher, organischer Verbindungen genutzt wird (Arnon 1959, Blankenship 2010). Daneben ermöglicht die Absorption von Licht die Anpassung des Organismus an seine Umgebung. Die Detektion des Lichts resultiert in diversen biologischen Antworten wie dem Phototropismus in Pflanzen, der Phototaxis in bestimmten Flagellaten und der visuellen Wahrnehmung in Tieren (Christie et al. 1998, Nagel 2002, Gehring 2005). Auf molekularer Ebene wird dies durch sensorische Photorezeptoren vermittelt. Diese sind wie viele andere Signaltransduktionsproteine modular aufgebaut und können vereinfacht durch zwei funktionelle Module, dem sogenannten Sensor- und dem Effektormodul, beschrieben werden (Abbildung 1) (Möglich et al. 2010b). Beide Module werden meist durch separate, globuläre Proteindomänen realisiert und können mittels verschiedener, oft helikaler Linker verbunden sein (Möglich und Moffat 2007).

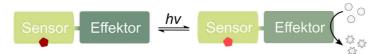


Abbildung 1: Vereinfachte Darstellung des Aufbaus eines sensorischen Photorezeptors, welcher sich aus einem N-terminalen Sensormodul (hellgrün) und einem C-terminalen Effektormodul (dunkelgrün) zusammensetzt. Die funktionellen Module sind oftmals durch einen helikalen Linkers miteinander verbunden. Der Sensor beinhaltet einen organischen Chromophor (Fünfeck), welcher Licht einer bestimmten Wellenlänge absorbiert. Resultierende strukturelle und dynamische Veränderungen innerhalb des Sensors werden an den Effektor weitergegeben und führen zu dessen Aktivierung.

Der vorwiegend N-terminal lokalisierte Sensor beinhaltet einen organischen Chromophor, welcher auf Grund seines konjugierten π-Elektronen-Systems die Detektion des Lichts ermöglicht. Chromophore gehen meist aus kleinen Metaboliten hervor oder können aus proteineigenen, aromatischen Seitenketten gebildet werden (Christie et al. 2012a, Wu et al. 2012). Im dunkeladaptierten Zustand absorbiert dieser Licht spezifischer Wellenlänge und durchläuft anschließend einen Photozyklus, welcher die Bildung eines (meta)stabilen (Signal-)Zustands zur Folge hat (Mathes 2016). Daraufhin erfährt das Sensormodul strukturelle und dynamische Veränderungen, die an das C-terminal gekoppelte Effektormodul übertragen werden. In einigen Photorezeptoren weicht jedoch die Abfolge der Module vom konventionellen Aufbau ab und die Architektur ist invers (Takahashi et al. 2007). Der Effektor besitzt häufig katalytische Aktivität und ist für die physiologische Antwort ausschlaggebend, wobei die biologische Vermittlung

entweder lichtinduziert oder lichtreprimiert erfolgen kann (Karniol und Vierstra 2003, Ziegler und Möglich 2015, Heintz und Schlichting 2016). Der lichtadaptierte Zustand kehrt entweder durch thermische Reversion über die Zeit oder durch Bestrahlung mit Licht einer anderen Wellenlänge in seinen Ausgangszustand zurück und der Photozyklus ist abgeschlossen (Losi und Gärtner 2012, Kreslavski et al. 2018).

Um präzise auf unterschiedliche Lichteinflüsse reagieren und diese möglichst effizient nutzen zu können, haben insbesondere Pflanzen viele verschiedene sensorische Photorezeptoren entwickelt (Kong und Okajima 2016). Diese unterscheiden sich hauptsächlich in ihrer Sensitivität zum einfallenden Licht, welche durch die Verwendung von unterschiedlichen Chromophoren realisiert wird. Anhand dieser und der damit einhergehenden Photochemie erfolgt eine Untergliederung in verschiedene Klassen (Abbildung 2) (Ziegler und Möglich 2015).

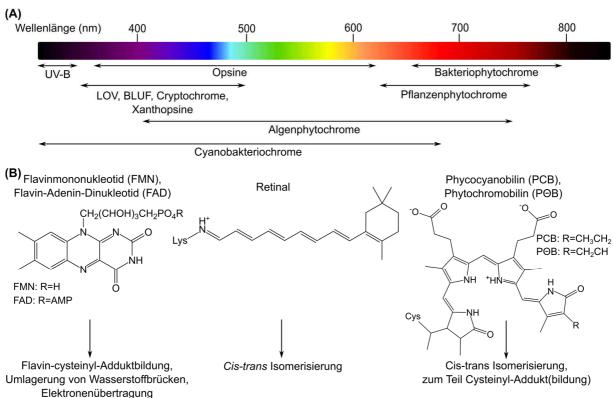


Abbildung 2: Beispielhafte Übersicht über natürlich vorkommende Photorezeptoren (A) Einordnung von sensorischen Photorezeptoren erfolgt anhand des verwendeten Chromophors, der Photochemie und der taxonomischen Herkunft. (B) Strukturen und primäre Photochemie möglicher Kofaktoren (Shcherbakova et al. 2015, Ziegler und Möglich 2015, Porter 2016).

Phytochrome stellen wohl auf Grund ihrer großen spektralen Bandbreite die vielfältigste Klasse an Photorezeptoren dar. Anfänglich wurden diese ausschließlich als Rot- und Fernrotlicht-Rezeptoren (600-780 nm) in Pflanzen beschrieben, mittlerweile konnten diese aber auch in Bakterien, Pilzen, Algen und Cyanobakterien identifiziert werden (van der Horst und Hellingwerf 2004). Dort vermitteln sie sie diverse biologische Funktionen wie Schattenvermeidung und Samenkeimung in Pflanzen oder Phototaxis in Mikroorganismen (Wilde et al. 2002, Franklin und

Whitelam 2005). Phytochrome binden lineare Tetrapyrrole, sogenannte Biline (Abbildung 2B), und können abhängig vom Protonierungszustand, Wasserstoffbrückennetzwerk und Torsionswinkel der zugrundeliegenden Pyrrolringe verschiedenste Wellenlängen absorbieren (Rockwell und Lagarias 2010, Kottke et al. 2018).

Opsine decken hingegen vorrangig mit Hilfe von 11-cis-Retinal (Abbildung 2B) oder in einigen wenigen Fällen unter Benutzung von all-*trans*-Retinal den Bereich des für den Menschen sichtbaren Lichts (380-780 nm) ab. In Vertebraten sind sie für das Sehen verantwortlich (Hao und Fong 1999, Ernst et al. 2014, Nagata et al. 2018).

Light-oxygen-voltage (LOV), blue light sensors using flavin adenine nucleotide (BLUF) Rezeptoren und Cryptochrome nutzen hingegen Flavinderivate als Chromophor, um vorranging energiereiches nah-UV bis blaues Licht wahrzunehmen (Abbildung 2B). Während LOV Rezeptoren in Pflanzen, Bakterien, Pilzen und Cyanobakterien vorkommen, wurden BLUF Rezeptoren bislang hautsächlich in Bakterien und Algen gefunden (Gomelsky und Klug 2002, Christie et al. 2012b, Losi und Gärtner 2012). Cryptochrome sind in allen Lebensformen zu finden und regulieren hierbei beispielsweise das Wachstum in Pflanzen oder sind an der Aufrechterhaltung der zirkadianen Rhythmik beteiligt (Chaves et al. 2011, Shcherbakova et al. 2015). Die Klasse der Xanthopsine ist ebenso Bestandteil der Blaulichtrezeptoren und bedient sich 4-Hydroxyzimtsäure als Chromophor (Losi et al. 2018). Zu ihnen zählt das photoactive yellow protein (PYP), welches in halotoleranten Bakterien in der Vermittlung negativer Phototaxis eine Rolle spielt (Sprenger et al. 1993). Auf Grund seiner sehr guten Löslichkeit, seiner Stabilität und der schnellen Ausbildung von Kristallen wurde es als Modellsystem für die Untersuchung photochemischer und Proteinfaltungs-Prozesse verwendet (Hellingwerf et al. 2003). UV-B-Rezeptoren verwenden hingegen keinen zusätzlichen Chromophor sondern absorbieren Licht im nahen UV-Bereich (280-315 nm) mit Hilfe proteineigener Tryptophane. In Arabidopsis thaliana vermittelt beispielsweise UVR8 den Schutz vor energiereicher UV-B-Strahlung, um so DNA- und Zellschäden entgegenzuwirken (Brown et al. 2005, Christie et al. 2012a). Im Folgenden wird näher auf die Klasse der dieser Arbeit zu Grunde liegenden blaulichtsensitiven LOV Rezeptoren eingegangen.

1.1 Light-oxygen-voltage (LOV) Photorezeptoren

Seit der Entdeckung von LOV Rezeptoren in Phototropinen in *A. thaliana* als blaulichtabhängige Regulatoren von diversen physiologischen Prozessen, wie etwa dem Phototropismus, der Chloroplastenrelokalisation oder der Stomataöffnung, konnten auch in anderen Organismen

noch viele weitere identifiziert werden (Christie et al. 2002, Harada et al. 2003). LOV Rezeptoren spielen beispielsweise in Bakterien, Archaeen und Pilzen eine Rolle in der Vermittlung von Stressantworten und Virulenz, aber auch in der Regulation des Tagesrhythmus (Herrou und Crosson 2011). Die Sensormodule von LOV Rezeptoren bestehen aus kleinen Proteindomänen (110-120 Aminosäuren) und detektieren UV-A Strahlung oder Licht im blauen Bereich (320-500 nm). Im dunkeladaptierten Zustand liegt ein nicht kovalent gebundenes Flavinderivat, entweder Flavinmononukleotid (FMN) oder Flavin-Adenin-Dinukleotid (FAD), als Chromophor vor (siehe Abbildung 2B) (Möglich und Moffat 2007, Zoltowski et al. 2007). Die durch den Sensor vermittelte Blaulichtsensitivität beeinflusst dabei mehr als 100 verschiedene Effektoren (Glantz et al. 2016).

1.1.1 Architektur und topologische Vielfalt

Der modulare Aufbau von sensorischen Photorezeptoren bedingt, dass sowohl Rezeptoren mit einem einzigen Sensor umgeben von einem einzigen Effektor, aber auch Multidomänenrezeptoren, welche etwa zwei LOV Sensoren beinhalten, existieren. Sogenannte Tandem-LOV-Sensoren wurden bisher nur in Landpflanzen und Protisten beschrieben. Möglicherweise verstärken diese dort die Sensitivität des Systems gegenüber einfallendem Licht, um beispielsweise die Photosyntheserate nutzbringend anzupassen (Christie 2007, Okajima et al. 2014). Die Vielzahl von physiologischen Prozessen, welche LOV Rezeptoren vermitteln, ist auf die topologische Vielfalt möglicher Effektordomänen zurückzuführen.

Eine Studie zur Datenbankanalyse von LOV Sensor-Effektor Beziehungen erfasste über 6500 verschiedene LOV Rezeptoren und verdeutlicht die große Diversität möglicher Effektor in unterschiedlichen Organismen (Abbildung 3) (Glantz et al. 2016). Dabei konnte gezeigt werden, dass die Architektur von LOV Rezeptoren vorwiegend von der Art des Effektors abhängig ist; verschiedene Effektortypen präferieren dabei entweder eine N- oder C- terminale Lokalisation. LOV Sensordomänen sind häufig von Per-Arnt-Sim (PAS) Domänen, Histidin-Kinase-Phosphoakzeptor Domänen (HisKA), Serin-Threonin Kinasen (Pkinase) oder F-box Domänen umgeben, können in vielen Organismen aber auch ohne weitere Proteindomänen gefunden werden. PAS Domänen sind in allen Lebensformen vertreten, detektieren ein breites Spektrum an chemischen sowie physikalischen Signalen, vermitteln Proteindimerisierung und sind oftmals in der Signaltransduktion beteiligt (Möglich et al. 2009a, 2010a).

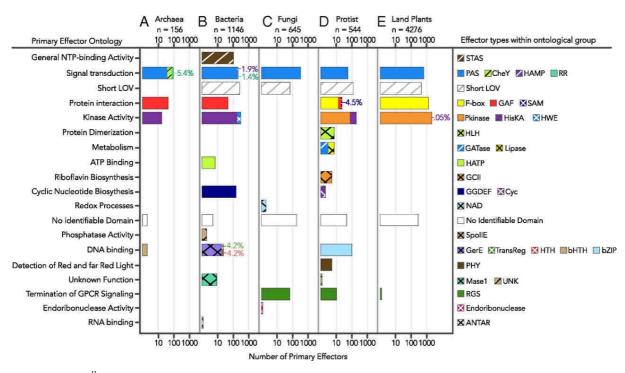


Abbildung 3: Übersicht über die Variabilität primärer Effektordomänen in LOV Rezeptoren und deren abgeleitete biologische Aktivität. Die Balken repräsentieren die Zahl an Effektoren eines funktionellen Clusters in logarithmischer Darstellung. Entnommen von (Glantz et al. 2016).

In LOV-HisKA Rezeptoren steht die Aktivität einer Histidin-Kinase (HK) unter der Kontrolle des LOV Sensors. HK bestehen aus einer Dimerisierungs- und Phosphoakzeptordomäne (dimerization and histidine phosphotransfer, DHp) sowie einer katalytischen und Adenosintriphosphat-bindenden Domäne (catalytic and ATP binding, CA). Sie kommen in der Regel als Dimere vor und operieren je nach Signalzustand entweder als Kinasen oder Phosphatasen (Gao und Stock 2017). Erst kürzlich konnte jedoch auch ein monomerischer LOV-HisKA-Rezeptor identifiziert und näher charakterisiert werden (Rivera-Cancel et al. 2014, Dikiy et al. 2019). Sensorische HK sind Teil von Zweikomponentensystemen (two-component system, TCS), welche in Archaeen, Bakterien und teilweise in Pflanzen eine wichtige Rolle in der Regulation von Chemo- und Phototaxis und der Virulenzvermittlung einnehmen (Swartz et al. 2007). Einfach aufgebaute TCS bestehen aus einer Sensorkomponente, der HK, und einer Effektorkomponente, dem sogenannten Antwortregulator (response regulater, RR) (Abbildung 4). Dieser umfasst meist eine Phosphoakzeptor- und eine Regulatordomäne (Trajtenberg und Buschiazzo 2020). Rund 70 % aller bekannten klassischen Antwortregulatoren beinhalten eine DNA-Bindedomäne und agieren somit als Transkriptionsfaktoren (Zschiedrich et al. 2016). Die signalabhängige Aktivierung der HK führt unter Verbrauch eines Adenosintriphosphats (ATP) zur Autophosphorylierung eines Histidinrests innerhalb der DHp-Domäne. In einem zweiten Schritt wird die Phosphorylgruppe auf ein Aspartat des Antwortregulators übertragen, welcher dadurch aktiviert wird (Purcell et al. 2007, Swartz et al. 2007). In der Regel katalysieren Histidinkinasen auch die Hydrolyse des Phospho-Aspartyl-Rests im phosphoryliertem RR. Entscheidend für die Nettoleistung der Histidinkinase und die resultierenden biologischen Antworten ist somit das dynamische Gleichgewicht zwischen den beiden Aktivitätszuständen (Möglich et al. 2009b, Möglich 2019).

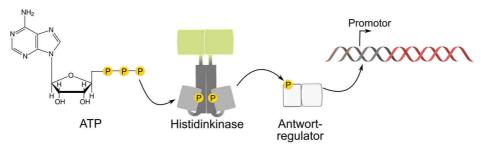


Abbildung 4: HisKA Domänen als Effektormodul in LOV-basierten Rezeptoren als Teil von Zweikomponentensystemen. Nach Adenosintriphosphat (ATP)-abhängiger Autophosphorylierung der Histidinkinase (HK) folgt der Transfer der Phosphatgruppe auf die Phosphoakzeptordomäne des Antwortregulators. Dieser fungiert oft als Transkriptionsfaktor und ermöglicht die Expression eines Zielgens (Möglich et al. 2009b).

Zu den in Bakterien stark verbreiteten Effektoren zählen des Weiteren *sulfate transporter and anti-sigma factor antagonist* (STAS) und GGDEF Domänen. STAS Domänen können meist Cterminal von bestimmten Sulfattransportern und in Antisigma-Faktor Antagonisten gefunden werden und agieren dort als Nukleotidbinde-Phosphoproteine oder Nukleotidasen (Aravind und Koonin 2000). Ebenso dienen sie als Interaktions- bzw. Transduktionsmodule in vielen Multidomänensensoren, die neben Licht auch Gasotransmitter oder zyklische Nukleotide wahrnehmen (Sharma et al. 2011). Beispielsweise aktiviert der LOV-STAS Rezeptor YtvA in *Bacillus subtilis* den für die Initiation der Transkription notwendigen Sigma-Faktor σ^B , und reguliert so in blaulichtabhängiger Art und Weise die generelle Stressantwort des Organismus (Avila-Perez et al. 2006, Gaidenko et al. 2006).

LOV Domänen, welche hingegen an GGDEF-EAL Domänen gekoppelt sind, regulieren die Synthese und Hydrolyse von bis-(3'-5')-zyklischem di-Guanosinmonophosphat (*cyclic dimeric guanosine monophosphate*, c-di-GMP) (Abbildung 5). Dieses dient als wichtiger sekundärer Botenstoff und reguliert eine Vielzahl von physiologischen Prozessen wie die Biofilmbildung, Motilität, den Zellzyklus oder die Vermittlung von Virulenz (Hengge 2009, Gomelsky 2011). Der Domänenname ist jeweils auf das konservierte GGDEF- bzw. EAL-Motiv (Gly-Gly-Asp-Glu-Phe und Glu-Ala-Leu) innerhalb des aktiven Zentrums zurückzuführen. Diguanylatzyklasen aus der GGDEF-Familie katalysieren dabei die Zyklisierung zweier Guanosintriphosphatmoleküle (GTP) in ein c-di-GMP Molekül (Navarro et al. 2009). Die Hydrolyse von c-di-GMP konnte hingegen in EAL-Domänen enthaltenen Proteinen nachgewiesen werden. Diese kann entweder direkt oder indirekt über 5'-Phosphoguanylyl-(3'→5')-Guanosin (pGpG) sowie mit

Hilfe eines anderen Proteins oder auch allein ablaufen (Schmidt et al. 2005). Bisher sind zwar nur sehr wenige LOV-GGDEF-EAL Rezeptoren funktionell untersucht worden, dennoch wird vermutet, dass diese eine ubiquitäre Rolle in der Anpassung des zytosolischen c-di-GMP-Spiegels spielen (Cao et al. 2010, Herrou und Crosson 2011).

Abbildung 5: GGDEF-EAL Domänen als Effektormodul in LOV-basierten Rezeptoren. Tandem-GGDEF-EAL Proteine katalysieren je nach Signalzustand mit Hilfe ihrer Diguanylatzyklaseaktivität die Synthese von bis-(3'-5')-zyklischem di-Guanosinmonophosphat (*cyclic dimeric guanosine monophosphate*, c-di-GMP) aus zwei Molekülen Guanosintriphosphat (GTP), oder dank ihrer Phosphodiesteraseaktivität die Hydrolyse von c-di-GMP zu 5'-Phosphoguanylyl-(3' \rightarrow 5')-Guanosin (pGpG). Als sekundärer Botenstoff beeinflusst c-di-GMP diverse biologische Prozesse.

Im Gegensatz zu den Multidomänenrezeptoren bestehen short LOV (sLOV) Rezeptoren lediglich aus einem photoaktiven Sensormodul und besitzen keine kovalent gebundene Effektordomäne. Stattdessen interagieren diese vermutlich mit anderen Proteinen, sogenannten Proteinpartnern, oder ihre flankierenden Enden besitzen selbst enzymatische, beziehungsweise DNA-Bindeaktivität (Chen et al. 2010, Hunt et al. 2010, Malzahn et al. 2010, Endres et al. 2015, Glantz et al. 2016). Funktionell und strukturell gut charakterisierte Beispiele für sLOV Rezeptoren umfassen PpSB1-LOV und PpSB2-LOV aus Pseudomonas putida, RsLOV aus Rhodobacter sphaeroides und VIVID aus Neurospora crassa (Crosson et al. 2003, Zoltowski et al. 2007, Herrou und Crosson 2011, Losi und Gärtner 2012, Pathak et al. 2012). Während der C-Terminus von RsLOV von einem helix-turn-helix (HTH) Motiv gebildet wird und bisher kein Proteinpartner identifiziert werden konnte, bindet VIVID im lichtadaptierten Zustand an white collar-1 (WC-1)-Dimere und schwächt hierdurch die Expression eines den tagesperiodischen Rhythmus regulierenden Gens (Hunt et al. 2010, Vaidya et al. 2011, Conrad et al. 2013). Neben der Vielfalt möglicher Effektorproteine weisen LOV Rezeptoren Cluster von konservierten Linkern, welche den Sensor und den Effektor verbinden, auf. Die Sequenz und Länge ist dabei vom Effektor abhängig, wobei oftmals eine Heptadenabhängigkeit in helikalen Verbindungsstücken festgestellt werden kann (Möglich et al. 2009b, 2009a, Ohlendorf et al. 2016).

1.1.2 Struktureller Aufbau von LOV Domänen

LOV Sensordomänen gehören strukturell der Klasse der PAS Familie an. Das konservierte PAS-Motiv besteht aus einem zentralen fünfsträngigen antiparallelen β -Faltblatt, welches von mehreren α -Helices umgeben ist (Abbildung 6). Der Isoalloxazinring des Chromophors ist zwischen dem β -Faltblatt und zwei benachbarten α -Helices eingebettet, wobei eine der beiden α -Helices zur Koordination des Flavinderivats ein konserviertes Konsensusmotiv (GXNCRFLQ) beherbergt (Abbildung 6) (Taylor und Zhulin 1999, Möglich und Moffat 2007, Möglich et al. 2009a, 2010b, Zoltowski und Gardner 2011). Während die Kernstruktur weitestgehend konserviert vorliegt, variieren die terminalen α -Helices, die sogenannten A' α - und J α -Helices, doch sehr stark. Es konnte gezeigt werden, dass diese einen großen Beitrag zur allosterischen Signalweiterleitung an das Effektormodul leisten (Anantharaman et al. 2006, Halavaty und Moffat 2007, Zoltowski et al. 2007, Nash et al. 2011, Conrad et al. 2013).

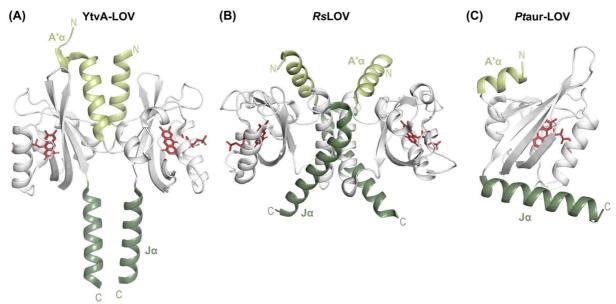


Abbildung 6: Kristallstrukturen dunkeladaptierter LOV Domänen mit den N- (hellgrün) und C-terminalen (dunkelgrün) flankierenden A'α- und Jα-Helices. Der Chromophor ist jeweils als Stäbchenmodell (rot) dargestellt. (A) Die YtvA-LOV Domäne (Reste 1-143, PDB: 4GCZ) aus *Bacillus subtilis* bildet ein Kopf-an-Kopf orientiertes Homodimer aus. Die Dimerisierungsfläche ist durch die superspiralisierten N- und C-terminalen Helices realisiert. (B) Die LOV Domäne aus *Rhodobacter sphaeroides* (*Rs*LOV, PDB: 4HIA) bildet ebenso ein Homodimer aus, wobei die Dimerisierungsfläche aus einem Bündel verlängerter flankierender Termini besteht. (C) Die isolierte Aureochrom 1a LOV Domäne aus *Phaeodactylum tricornutum* (*Pt*aur-LOV, PDB: 5DKK) liegt als Monomer vor.

Viele LOV Domänen neigen zur Ausbildung von Dimeren, welche ebenso lichtabhängig vonstattengehen kann. Die Dimerisierungsfläche wird entweder durch das β-Faltblatt-Gerüst der PAS Domäne gebildet oder durch die terminalen Helices jeder Untereinheit realisiert (Salomon et al. 2004, Möglich und Moffat 2007, Conrad et al. 2013, Banerjee et al. 2016). Beispielsweise liegt sowohl YtvA als auch seine isolierte LOV Domäne YtvA-LOV lichtunabhängig als konstitutives Homodimer vor (Abbildung 6A), während die *s*LOV Domäne aus *Rhodobacter*

sphaeroides RsLOV nur im dunkeladaptierten Zustand ein Homodimer bildet (Abbildung 6B) (Möglich und Moffat 2007, Jurk et al. 2010, Conrad et al. 2013). Blaulichtbestrahlung führt hier indessen zur Dissoziation (Conrad et al. 2013). Im Gegensatz dazu liegt die isolierte, dunkeladaptierte Aureochrom 1a LOV Domäne aus *Phaeodactylum tricornutum* (*Pt*aur-LOV) als Monomer vor (Abbildung 6C), wobei Blaulichtexposition deren Homoassoziation bewirkt (Banerjee et al. 2016).

1.1.3 Photozyklus und initiale Signalweiterleitung in LOV Rezeptoren

LOV Rezeptoren verbindet nicht nur das Vorkommen des konservierten PAS-Motivs, sondern auch das Durchlaufen eines blaulichtausgelösten Photozyklus (Abbildung 7A). Dieser unterscheidet LOV Rezeptoren von anderen flavin-basierten Photorezeptoren (Schleicher et al. 2004, Möglich et al. 2010b).

Im thermodynamisch stabilsten, dunkeladaptierten D₄₅₀ Zustand absorbiert der oxidierte, nicht kovalent gebundene Flavinchromophor mit einem charakteristischen Maximum im Bereich von 450 nm (D₄₅₀ Zustand) (Abbildung 7B). Absorption von Photonen des blauen Lichts führt zur Ausbildung eines angeregten Singulett-Zustands (S₁), welcher durch effizientes Intersystem Crossing (ISC) innerhalb weniger Nanosekunden in einen Triplettzustand übergeht (T₁, L₆₅₀ Zustand). Anschließend erfolgt binnen Mikrosekunden die Ausbildung eines kovalenten Thioaddukts zwischen dem C4a Atom des Flavins (FMN-C4a) und einem hochkonservierten, proximalen Cysteinrests (Swartz et al. 2001, Conrad et al. 2014). Die Adduktbildung läuft dabei höchstwahrscheinlich über Radikalintermediate ab. Es wird angenommen, dass der Triplettzustand konzertierte Elektronen- und Protonentransferreaktionen am C4a Atom und an der Schwefelgruppe des Cysteinrests auslöst, welche zur Reduktion des FMNs und der Ausbildung eines neutralen radikalischen Paars (FMNH•/Cys-S•) führt. Anschließend treffen die beiden Radikale aufeinander und es kommt zur Bildung des FMN-Cysteinyl-Thiol-Addukts (Bauer et al. 2011, Kutta et al. 2015, Chang et al. 2017). Der reduzierte Chromophor absorbiert mit einem ausgedehnten Maximum bei rund 390 nm (S_{Addukt}, S₃₉₀ Zustand) (Abbildung 7B).

Die formale Reduktion des Flavinchromophors durch Ausbildung des Photoadduktes erhöht dabei den p*Ka* des N5 Atoms und erleichtert dessen Protonierung. Zur Aufrechterhaltung des Wasserstoffbrückennetzwerks rotiert und verlagert sich infolgedessen die Seitenkette eines nahegelegenen, konservierten Glutaminrests (Abbildung 8B). Die ursprüngliche Wasserstoffbrückenbindung zum FMN-O4 wird aufgehoben und es kommt zur Ausbildung einer neuen FMN-N5H Wasserstoffbrücke. Die dadurch ausgelösten Veränderungen am gesamten Wasserstoffbrückenbindungsnetzwerk bedingen strukturelle und dynamische Änderungen innerhalb des β-

Faltblatts. Diese werden an die amphipathischen α -Helices der terminalen Enden propagiert und sind ausschlaggebend für die Signalweiterleitung an den jeweiligen Effektor (Avila-Perez et al. 2006, Möglich und Moffat 2007, Nash et al. 2008, Möglich et al. 2009b, 2009a, Ganguly et al. 2017, Henry et al. 2020, Polverini et al. 2020). Neuere Studien haben allerdings gezeigt, dass in Abwesenheit des konservierten Cysteinrests eine Reduktion des Flavins unter Bildung eines neutralen Semiquinons mit einhergehender N5 Protonierung stattfindet und ebenso Signalweiterleitung erfolgen kann (Yee et al. 2015).

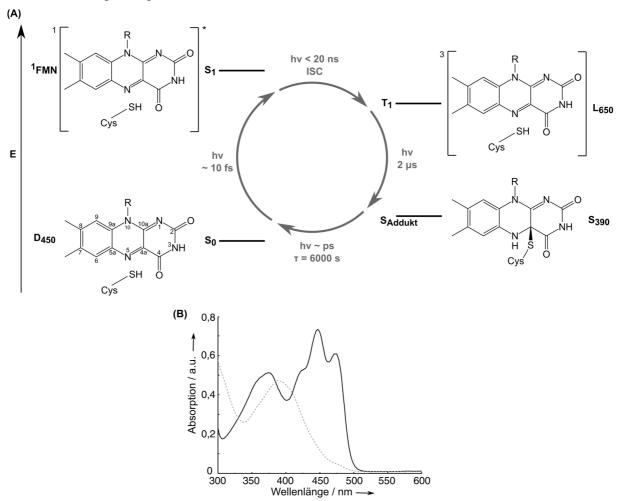


Abbildung 7: Photozyklus von LOV Rezeptoren. (A) Im dunkeladaptierten Zustand liegt der FMN Chromophor oxidiert und nicht kovalent an das Protein gebunden vor und zeigt eine ausgeprägte Absorption im Bereich von 450 nm (S_0 , D_{450} Zustand). Blaulichtbestrahlung führt zur Absorption von Photonen und Ausbildung eines angeregten Singulett-Zustands (S_1), welcher innerhalb von Nanosekunden mittels Intersystem Crossing (ISC) in einen Triplettzustand (T_1) übergeht. Mutmaßlich via eines bi-radikalischen Intermediats (nicht gezeigt) erfolgt sogleich die Ausbildung eines kovalenten Addukts zwischen dem C4a Atom des Isoalloxazinrings und einem konservierten Cysteinrest innerhalb der LOV Domäne (S_{Addukt}). Der lichtadaptierte Zustand zeigt eine ausgeprägte Absorption um 390 nm (S_{390} Zustand). Durch thermische Relaxation kehrt dieser anschließend in den dunkeladaptierten Zustand zurück. Verändert nach (Bauer et al. 2011, Chang et al. 2017). (B) Absorptionsspektrum eines typischen LOV Rezeptors in seinem dunkeladaptierten (schwarz) und lichtadaptierten (grau gestrichelt) Zustand.

Durch thermische Relaxation kehrt der lichtadaptierte Zustand vollständig via Deprotonierung des N5 Atoms und Auflösung des kovalenten Photoaddukts in seinen dunkeladaptierten Zustand zurück. Die Lebenszeit des Adduktzustands schwankt dabei abhängig von der jeweiligen LOV Domäne zwischen wenigen Sekunden bis zu mehreren Tagen und ist stark temperaturabhängig (Kottke et al. 2003, Alexandre et al. 2007, Zoltowski et al. 2009, Pudasaini et al. 2015). Ebenso wurde berichtet, dass die Bestrahlung mit nahem UV-Licht die Regeneration des dunkeladaptierten Zustands innerhalb weniger Pikosekunden herbeiführt (Kennis et al. 2004). Prinzipiell ist die Lebenszeit des lichtadaptierten Zustands einer LOV Domäne von folgenden Aspekten abhängig (Abbildung 8A): (i) Sterische Kontakte zum reaktiven Cysteinrest; (ii) Basenzugänglichkeit und Wasserstoffbrückenbindungen zum Chromophor; und (iii) konformationelle und elektronische Änderungen innerhalb des Isoalloxazinrings. Diese Faktoren werden größtenteils durch Aminosäurereste, welche die Lösungsmittelzugänglichkeit zur Chromophorregion beeinflussen oder durch stereoelektronische Effekte an der Unterseite des Flavins, der re-Seite, bestimmt (siehe Abbildung 8B). Mutation einer oder mehrerer dieser Aminosäuren kann infolgedessen großen Einfluss auf die Lebenszeit des lichtadaptierten Zustands haben.

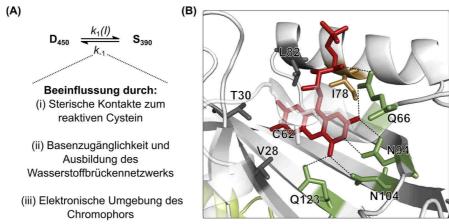


Abbildung 8: Beeinflussung der FMN-Cysteinyl-Thiol-Adduktbildung. (A) Unter konstanter Beleuchtung befindet sich der Photorezeptor in einem photostationären Gleichgewicht zwischen dem dunkeladaptierten D_{450} -Zustand und dem lichtadaptierten S_{390} -Zustand. Dieses ist bestimmt durch das Verhältnis der lichtinduzierten Vorwärtsreaktion $k_1(I)$ und der Rückreaktion k_1 . Mutationen innerhalb der Chromophorregion können die Ratenkonstante k_1 stark erniedrigen oder erhöhen. (B) Aminosäurereste in der Chromophorregion der YtvA-LOV Domäne (Reste 1-143, PDB: 4GCZ), welche bei Mutation Einfluss auf die Lebenszeit des lichtadaptierten Zustands haben. Die Reste Q66, N94, N104 und Q123 bilden Wasserstoffbrückenbindungen zum FMN (gestrichelte Linien), während V28, T30 und L82 hydrophobe Wechselwirkungen eingehen. I78 stabilisiert die Elektronendichte des Flavin-Nukleotid-Chromophors und stabilisiert den lichtadaptierten Zustand (Diensthuber et al. 2014, Polverini et al. 2020).

Studien an YtvA-LOV, Phototropin 1 LOV2 Domäne aus *Avena sativa* (*As*LOV2) und VIVID haben gezeigt, dass Aminosäuren, welche die Ausbildung und Aufrechterhaltung des FMN-Cysteinyl-Thiol-Addukts sterisch behindern, den lichtadaptierten Zustand destabilisieren (Christie 2007, Zoltowski et al. 2009, Kawano et al. 2013). Des Weiteren bewirken Aminosäu-

ren, die Wasserstoffbrückenausbildung in der Nähe des Isoalloxazinrings begünstigen und somit die Elektronendichte des Flavins stärken, eine Stabilisierung des lichtadaptierten Zustands. Im Gegenzug erleichtern Aminosäuren, die diese stören, die Rückkehr in den dunkeladaptierten Zustand. Beispielhaft führt der Austausch eines stark konservierten Asparaginrests (N94 in Ytva-LOV, siehe Abbildung 8B), welcher Wasserstoffbrücken zum Isoalloxazinrings ausbildet, durch Serin, Asparaginsäure oder Alanin eine fünf- bis 45-fache Beschleunigung der Rückkehr herbei (Raffelberg et al. 2011).

Faktoren, die zur Erhöhung der Lösungsmittelzugänglichkeit beitragen und folglich die Deprotonierung des FMN-N5H begünstigen, tragen ebenso zur Beschleunigung des Adduktzerfalls bei (Kottke et al. 2003, Purcell et al. 2010, Raffelberg et al. 2011, Zoltowski et al. 2011). Der Austausch eines Valinrests an Position 28 in YtvA-LOV (Abbildung 8B) gegen Threonin resultiert in einer erheblich kürzeren Halbwertszeit des lichtadaptierten Zustands. Der Austausch gegen das aliphatische Isoleucin hingegen führt zu dessen Erhöhung. Es wird vermutet, dass Mutationen an dieser Stelle zum einen die Zugänglichkeit zur Chromophorbindetasche und zum anderen die sterische Stabilität des Adduktzustands beeinflussen und so zu unterschiedlichen Lebenszeiten beitragen (Zoltowski et al. 2011, Kawano et al. 2013, Diensthuber et al. 2014). Ebenso kann die Adduktstabilität von bestimmten Aminosäureresten, welche an der re-Seite lokalisiert sind und veränderte sterische und elektronische Eigenschaften aufweisen, stark geschwächt werden. Es wurde berichtet, dass elektronenreiche Aminosäurereste einen schnelleren Zerfall des Addukts bewirken. Hingegen führt die Einführung von β-verzweigten aliphatischen Resten (vergleiche Abbildung 8B, Aminosäurerest I78) zur Stabilisierung der Elektronendichte des Flavins. Dies äußert sich sowohl in einem langlebigeren Adduktzustand als auch in der Stabilisierung von reduzierten Semiquinonspezies (Druhan und Swenson 1998, Yamamoto et al. 2008, Zoltowski et al. 2009, Vaidya et al. 2011).

Die Möglichkeit zur gezielten Veränderung der Lebenszeit des lichtadaptierten Zustands gestattet die Einstellung der effektiven Lichtsensitivität im photostationären Gleichgewicht unter konstanter Bestrahlung. Diese wird durch das Verhältnis der lichtinduzierten Vorwärtsreaktion $k_1(I)$ in Abhängigkeit der Lichtintensität I und der Rückreaktion k_{-1} bestimmt (Abbildung 8A). Um beispielsweise das photostationäre Gleichgewicht unter konstanter Bestrahlung im Falle einer beschleunigten Rückreaktion k_{-1} aufrecht zu erhalten, muss eine Erhöhung der Lichtintensität I erfolgen. Folglich ist die Empfindlichkeit des LOV Rezeptors gegenüber Licht herabgesetzt (Diensthuber et al. 2014, Ziegler und Möglich 2015). Im Falle einer deutlich verlangsamten Rückkehr in den dunkeladaptierten Zustand ist unter gleichen Annahmen die Empfindlichkeit des Rezeptors gegenüber Blaulicht erhöht.

1.1.4 Allosterische Signalweiterleitung in LOV Rezeptoren

Während die ersten Schritte der Signalweiterleitung in LOV Domänen infolge ihres konservierten Photozyklus ähnlich verlaufen, variiert die weitere Signalvermittlung zwischen unterschiedlichen Rezeptoren drastisch (Herrou und Crosson 2011). Eine entscheidende Rolle spielen dabei die N- und C-terminalen Helices, welche abhängig von der Architektur des LOV Rezeptors die Sensor- und Effektordomäne verbinden. Die Veränderung des Wasserstoffbrückenbindungsmusters und/oder der Elektronendichte innerhalb des β -Faltblatts nach Blaulichtexposition leitet konformationelle Änderungen ein, welche je nach LOV Rezeptor unterschiedlich stark ausfallen können (Zoltowski et al. 2009, 2011, Henry et al. 2020). Diese werden an die gesamte LOV Domäne weitergegeben und bedingen oftmals die Entfaltung und/oder Neuorientierung der terminalen α -Helices und modulieren so die Aktivität des Effektors. Abhängig davon ob LOV Rezeptoren infolge der Änderung der Lichtbedingung ihren oligomeren Zustand ändern, kann zwischen nicht-assoziierenden und assoziierenden Arten unterschieden werden (Abbildung 9) (Ziegler und Möglich 2015, Losi et al. 2018).

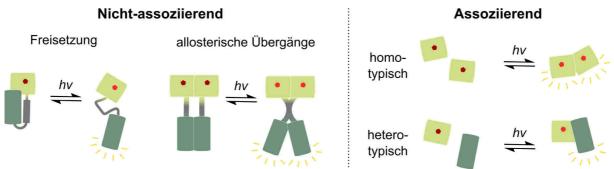


Abbildung 9: Allosterie von LOV Photorezeptoren. Die Signaltransduktionsmechanismen können anhand der Untergliederung in assoziierende und nicht-assoziierende Arten beschrieben werden. Die Signalweiterleitung von nicht-assoziierenden LOV Rezeptoren basiert auf lichtregulierten Ordnungs-Unordnungs-Übergängen, wie das lichtinduzierte Entfalten der Jα-Helix in AsLOV2 oder auf Änderungen in der Tertiär- oder Quartärstruktur. Im Falle von assoziierenden Photorezeptoren kommt es infolge des Lichtstimulus zur Änderung des oligomeren Status. Die Assoziation kann entweder blaulichtinduziert oder -reprimiert sowie zwischen identischen (homotypisch) oder unterschiedlichen Partnern (heterotypisch) erfolgen. Ferner können Dimere oder höhere Oligomere vorliegen. Das hellgrüne Rechteck veranschaulicht den Sensor und das dunkelgrüne Rechteck den Effektor, welche durch einen Linker/die terminale Helix verbunden sind. Dunkle und helle Farben des Fünfecks repräsentieren den oxidierten und reduzierten Zustand des Chromophors. Abbildung modifiziert nach (Ziegler und Möglich 2015, Losi et al. 2018).

Die allosterische Signalweiterleitung in *As*LOV2, der wohl meiststudierten LOV Domäne, ist ein prominentes Beispiel für einen nicht-assoziierenden Rezeptor. Hier induziert Blaulichtbestrahlung die konzertierte, reversible Entfaltung und Freisetzung der N-terminalen A'α-Helix und der C-terminalen Jα-Helix. Die Ablösung der Jα-Helix von der Kerndomäne moduliert sodann die Aktivität der C-terminal gelegenen Kinase (Harper et al. 2004, Schleicher et al. 2004, Halavaty und Moffat 2007, Nash et al. 2008, Alexandre et al. 2009, Zayner et al. 2012). Im

Falle der konstitutiv homodimeren YtvA-LOV Domäne schwächt Blaulichtbestrahlung die Interaktion des zentralen β -Faltblatts mit der N-terminalen A' α -Helix und führt so zu einer leichten Drehung und zum Auseinanderkippen der Monomer-Untereinheiten. Die Änderung der Quartärkernstruktur wird an die N-terminalen J α -Helices weitergegeben, welche sich daraufhin um ca. 3 Å auseinander bewegen und die mechanistische Grundlage für eine anschließende Signalweiterleitung an den Effektor bilden (Möglich und Moffat 2007, Berntsson et al. 2017a, 2017b, Engelhard et al. 2017, Möglich 2019).

Assoziierende LOV Rezeptor-Typen können am besten anhand von sLOV Rezeptoren beschrieben werden. Beispielsweise führt Blaulichtbestrahlung im Falle von N. crassa VIVID zu dessen Homodimerisierung (Zoltowski et al. 2007; Zoltowski and Crane 2008). Die Dimerisierung wird hierbei durch konformationelle Änderungen der besonders ausgeprägten N-terminalen Verlängerung, der sogenannten Ncap, vermittelt (Zoltowski et al. 2007, Zoltowski und Crane 2008). Zusätzlich können die Dimere mit WC-1-Dimeren interagieren und höhere Oligomere ausbilden (Hunt et al. 2010). Im Gegensatz dazu liegt RsLOV im dunkeladaptierten Zustand als Homodimer vor und dissoziiert bei Blaulichtbestrahlung. Die Dissoziation wird vermutlich ebenfalls durch strukturelle Änderungen der terminalen Enden, welche ein ungewöhnliches helikales Bündel in der Dimerisierungsfläche bilden, ausgelöst (Conrad et al. 2013). Weitere Beispiele umfassen die jeweils isolierten Aureochrom 1a LOV Domänen aus Vaucheria frigida (Vfaur-LOV) und Phaeodactylum tricornutum (Ptaur-LOV), welche ebenfalls eine blaulichtausgelöste Homodimerisierung erfahren (Takahashi et al. 2007, Banerjee et al. 2016). Anzumerken ist, dass der oligomere Zustand von isolierten LOV Sensoren und der des Volllängenproteins variieren kann. Während Ptaur-LOV eine blaulichtinduzierte Dimerisierung erfährt, liegt Ptaur wohl auf Grund des N-terminal lokalisierten bZIP Motivs als konstitutives Dimer vor. Dennoch wird angenommen, dass Blaulicht die Entfaltung von der terminalen A'α- und Jα-Helix auslöst und infolgedessen die LOV Domänen vom bZIP Motiv dissoziieren and anschließend dimerisieren. Dies erhöht die Flexibilität der bZIP Domäne und steigert deren Affinität für die Bindung der Ziel-DNA-Sequenz (Heintz und Schlichting 2016, Tian et al. 2020). Prinzipiell kann der oligomere Zustand eines Photosensors durch die Länge der terminalen Helices moduliert werden. Dies stellt ein wichtiges Schlüsselelement in der Erstellung künstlicher Photorezeptoren dar (Halavaty und Moffat 2013).

1.2 Erstellung künstlicher Photorezeptoren

Sensorische Photorezeptoren finden oftmals Anwendung in diversen sogenannten optogenetischen Systemen. Ursprünglich wurde die Optogenetik für die Neurobiologie entwickelt und nutzte die heterologe Expression von natürlichen Photorezeptoren, wie lichtempfindliche Channelrhodopsine, um zelluläre Prozesse durch gezielt angelegte optische Signale minimalinvasiv manipulieren zu können (Boyden et al. 2005, Deisseroth 2011). Sowohl das detaillierte Wissen über die Struktur und Funktionalität von natürlichen Photorezeptoren als auch ihr modularer Aufbau führte vor einigen Jahren zu der Idee der Erzeugung neuer künstlicher Photorezeptoren. Oftmals ermöglicht die Kombination einer gut charakterisierten Sensordomäne mit einer neuen, bis dato nicht lichtregulierten Effektordomäne deren Steuerung mittels Licht (Ziegler und Möglich 2015, Losi et al. 2018). Mit der Erstellung synthetischer Photorezeptoren vergrößerte sich sodann das Repertoire an Möglichkeiten biologische Funktionen und Signalwege mit exakter, räumlich-zeitlicher Auflösung zu erforschen (Möglich und Moffat 2010, Ziegler und Möglich 2015, Losi et al. 2018). Oftmals können auf Grund einer neu geschaffenen und gut zu detektierenden Signalausgabe von künstlichen Rezeptoren auch weitere Einblicke in den Mechanismus der Signaltransduktion gewonnen werden (Möglich et al. 2009b, Diensthuber et al. 2014, Yee et al. 2015).

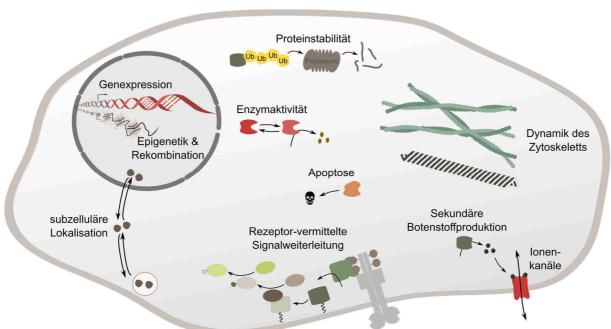


Abbildung 10: Übersicht über zelluläre Prozesse, welche durch synthetische LOV-basierte Photorezeptoren kontrolliert werden können. Verändert nach (Nack und Möglich 2017, Losi et al. 2018).

Auf Grund der ubiquitären Verfügbarkeit von Flavinen *in vivo*, des umfassenden molekularen Verständnisses und der Diversität der allosterischen Signalweiterleitung basieren bisher die meisten optogenetischen Schalter auf LOV Domänen (Kolar et al. 2018). So ist es z. B. möglich

blaulichtabhängig Sekretion, Rekrutierung und Abbau von unterschiedlichsten Proteinen, Aktivierung von Caspase/Apoptose und anderer Enzyme, Epigenetik oder Genexpression in vielen Pro- oder auch Eukaryoten zu steuern (Abbildung 10) (Lee et al. 2008, Möglich et al. 2009b, Lungu et al. 2012, Mills et al. 2012, Ohlendorf et al. 2012, Wang et al. 2012, Chen et al. 2013, Renicke et al. 2013, Bonger et al. 2014, Guntas et al. 2015, Kawano et al. 2015, Losi et al. 2018). Blaues Licht kann jedoch in hohen Dosen auf Grund von endogenen Photosensibilisatoren, welche reaktive Sauerstoffspezies (*reactive oxygen species*, ROS) generieren, einen phototoxischen Effekt hervorrufen und dringt zudem weniger tief in lebendes Gewebe als beispielsweise Rot- oder Fernrotlicht (Shcherbakova et al. 2015, Losi und Gärtner 2017).

Blaulichtsensitive künstliche Photorezeptoren dienen nicht nur als Werkzeug für die Kontrolle physiologischer Prozesse, vielmehr können diese auch für weitere Zwecke eingesetzt werden. Die relative hohe Fluoreszenzquantenausbeute von LOV Rezeptoren und die Möglichkeit diese durch bestimmte Mutationen zu steigern, ermöglicht den Einsatz als Fluoreszenzprotein (Drepper et al. 2007, Chapman et al. 2008, Guntas et al. 2015, Sanford und Palmer 2017). Zugleich dienen LOV Rezeptoren als Ausgangspunkt für genetisch kodierbare Photosensibilisatoren, welche blaulichtabhängig ROS generieren (Shu et al. 2011, Losi und Gärtner 2017).

Im Folgenden soll auf die Strategien zum Design neuer chimärer LOV-basierter Werkzeuge eingegangen werden.

1.2.1 Designstrategien von LOV-basierten optogenetischen Werkzeugen

Dem Design neuer LOV-basierter Photorezeptoren liegen allosterische Prinzipien zugrunde, die die Signalweiterleitung an mögliche Effektoren vermitteln. Eine Klassifizierung der möglichen Strategien erfolgt infolge der bereits getroffenen Einteilung in nicht assoziierende und assoziierende Photorezeptoren (siehe 1.1.4). Jede dieser Strategien basiert gleichwohl auf lichtausgelösten konformationellen Änderungen, welche entweder direkt die Aktivität des Effektors beeinflussen oder Hetero- sowie Homo-Oligomerisierung bewirken. Die folgenden Designstrategien beruhen vorwiegend der Fusion einer isolierten LOV Domäne mit einem bis dato lichtunempfindlichen Effektormodul.

Wegweisend für die Erstellung blaulichtabhängiger optogenetischer Aktoren war die Ausnutzung der lichtinduzierten Entfaltung und gleichzeitige Ablösung der terminalen A'α- und Jα-Helices der AsLOV2 Domäne. Beispielsweise erbrachte die Fusion der N-terminalen Helix des Escherichia coli Trp Repressorproteins (TrpR) mit der C-terminalen Jα-Helix der AsLOV2 Domäne die Erschaffung eines lichtregulierten DNA-Bindeproteins. Die Fusion verursacht dabei

eine sterische Interferenz der beiden Einheiten, sodass die gemeinsame Helix entweder die Faltung der AsLOV2 Domäne oder der TrpR Domäne erlaubt. Blaulichtexposition ermöglicht die korrekte Faltung von TrpR und infolgedessen die Bindung der Konsensussequenz (Strickland et al. 2008, 2010).

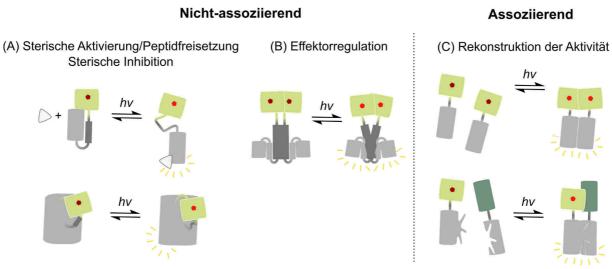


Abbildung 11: Designstrategien zur Erstellung blaulichtabhängiger Photorezeptoren. (A) Basierend auf natürlichen nicht-assoziierenden Rezeptoren kann mittels lichtinduzierter Ordnungs-Unordnungs-Übergänge eine sterische Aktivierung der Effektordomäne/Peptidfreisetzung oder sterische Inhibition der Aktivität des Effektors realisiert werden. (B) Lichtinduzierte Änderungen der Positionierung der Sensordomänen ermöglichen ebenso eine lichtabhängige Steuerung eines Effektors. (C) Assoziierende Photorezeptoren erlauben die Wiederherstellung vorher vorsätzlich geteilter Effektormodule in lichtabhängiger Art. Je nach oligomerem Zustand des zu regulierenden Effektors beruht das Design auf homo- oder heterotypischen Sensoren. Modifiziert nach (Ziegler und Möglich 2015, Losi et al. 2018).

Die lichtinduzierte Entfaltung der AsLOV2 Jα-Helix ist zudem Basis für viele weitere Designstrategien. Beispielsweise kann die Fusion der Jα-Helix von AsLOV2 an den N-Terminus ausgewählter Effektoren zu einer Blockierung deren aktiven Zentrums führen. Blaulichtinduzierte Entfaltung der Jα-Helix führt sodann zur Ablösung der Effektordomäne, wodurch sterische Einschränkungen aufgehoben werden und die biologische Aktivität begünstigt wird (Abbildung 11A) (Wu et al. 2009, Pham et al. 2011, Lungu et al. 2012, Mills et al. 2012).

Ein weiteres Prinzip setzt auf die Insertion von nicht-assoziierenden LOV Domänen in schleifenförmigen Oberflächenbereichen von Effektorproteinen (Abbildung 11A). Unter Ausnutzung der lichtinduzierten Entfaltung der terminalen AsLOV2 Helices und der einhergehenden konformationellen Änderung innerhalb des Fusionsproteins ist es etwa möglich verschiedene Signalproteine wie Kinasen, Guanosintriphosphatasen (GTPasen) und GTP-Austauschfaktoren (GEFs) in blaulichtabhängiger Weise zu steuern (Lee et al. 2008, Dagliyan et al. 2016).

Ebenso verbreitet ist der Ansatz natürliche Sensor- oder Effektormodule gegen homologe Domänen auszutauschen (Abbildung 11B) (Shcherbakova et al. 2015, Losi et al. 2018). Der Aus-

tausch der Häm-bindenden und Sauerstoff-detektierenden PAS-B Sensordomäne der *Bradyrhizobium japonicum* FixL Histidinkinase mit der strukturell homologen Sensordomäne YtvA-LOV ermöglichte die Erschaffung der lichtregulierten Histidinkinase YF1 (Abbildung 12A).

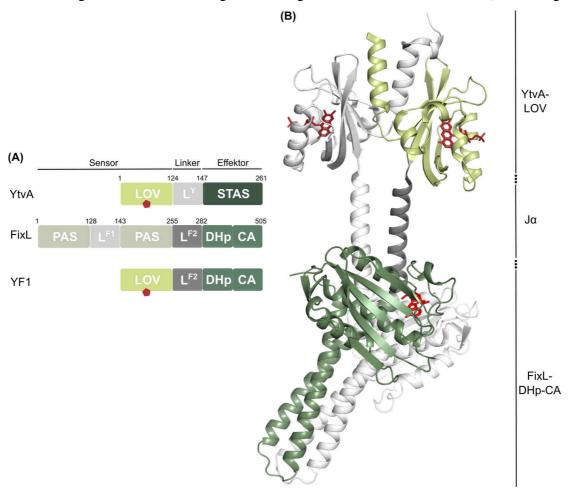


Abbildung 12: Architektur und Struktur der blaulichtreprimierten Histidinkinase YF1. (A) YF1 besteht aus der YtvA-LOV Sensordomäne aus *B. subtilis* und der FixL Histidinkinase (DHp und CA Domänen) aus *B. japonicum*. Der Linker der FixL Histidinkinase verbindet den Sensor und den Effektor. (B) Die Kristallstruktur von YF1 (PDB: 4GCZ) zeigt ein Homodimer mit superspiralisierten Jα-Helices, welche die Sensor- und Effektordomänen verbinden.

Im dunkeladaptierten Zustand agiert YF1 als HK, wohingegen Blaulichtexposition die Netto-Phosphorylierungsrate um ein 1000-faches reprimiert, da YF1 als Netto-Phosphatase fungiert. Biochemischen und spektroskopischen Daten zu Folge, weist YF1 jedoch nur Kinaseaktivität auf, wenn sich beide LOV Domänen im dunkeladaptierten Zustand befinden (Möglich et al. 2009b). Im funktionellen Homodimer verbinden die parallelen, superspiralisierten, helikalen Jα-Linker die N-terminal lokalisierte YtvA-LOV Sensordomäne mit der DHp- und der CA-Domäne der HK (Abbildung 12B). Blaulichtabsorption induziert das Auseinanderschwenken der Sensordomäne, welches eine linksgerichtete Spiralisierung der terminalen Jα-Helices auslöst und zur Neuorientierung der CA-Module führt. Im Zuge dessen kommt es zur Modulation der Kinaseaktivität (Berntsson et al. 2017a, 2017b, Engelhard et al. 2017, Möglich 2019). Die

Länge der α -helikalen Verbindung zwischen Sensor und Effektor ist dabei maßgebend für die katalytische Funktion und die Schaltbarkeit. Für lichtschaltbare Varianten sollte der Linker idealerweise auf Grund der superspiralisierten Helices, den sogenannten Coiled-Coils, eine Heptadenperiodizität aufweisen. Coiled-Coil-Strukturen zeichnen sich durch ihr periodisches Sequenzmuster aus, welches im Falle eines regelmäßigen, parallelen Coiled-Coils sieben Aminosäurereste und zwei α -Helixwindungen beinhaltet. Konstrukte mit einer Linkerlänge von 7n sowie 7n + 5 Aminosäuren zeigen lichtreprimierte Kinaseaktivität, wohingegen Linkerlängen von 7n + 1 Aminosäuren die Inversion der Lichtantwort bewirken (Ohlendorf et al. 2016). Die hier beobachtete Abhängigkeit verdeutlicht die Rolle des gewählten Linkers. Hier ist nicht nur die Länge, sondern auch die Struktur und Dynamik von besonderer Bedeutung.

Deutlich geringere Anforderungen an die Verbindungsstücke zwischen dem Sensor und dem Effektor beinhalten Designstrategien, welche auf assoziierenden LOV Rezeptoren basieren (Abbildung 11C). Hier ist es oftmals ausreichend überwiegend hydrophile, kurze und flexible Linkerelemente zu verwenden (Ziegler und Möglich 2015). Da viele biologische Prozesse in der Natur auf Oligomerisierungsreaktionen, insbesondere auf Dimerisierungen, zurückgreifen, beruhen einige blaulichtsensitive Schalter auf assoziierenden LOV Domänen. Beispielsweise erlaubt die Fusion eines zu assoziierenden Effektormoduls an eine dimerisierende LOV Domäne dessen Photoaktivierung. Auf diese Strategie greifen häufig lichtinduzierbare Genexpressionssysteme zurück. Die LOV Domäne VIVID bildet beispielsweise die Grundlage für das sogenannte "Light-ON"-System für die lichtinduzierte Expression von Genen in Eukaryoten. Die Fusion von VIVID an eine trunkierte Version des DNA-Bindeproteins Gal4 erlaubt dessen lichtinduzierte Dimerisierung und Bindung an seine Konsensussequenz (Wang et al. 2012). Weitere homodimerisierende LOV Domänen wurden unter anderem bereits an den intrazellulären C-terminalen Teil des murinen fibroblast growth factor receptor 1 (mFGFR-1) fusioniert. Blaulicht induziert sodann deren Dimerisierung und löst die MAPK/ERK-Signaltransduktionskaskade aus (Grusch et al. 2014). Ebenso gebräuchlich ist die photoinduzierte Rekonstruktion von vorsätzlich geteilten Effektormodulen (Abbildung 11C). Um deren Selektivität und Effizienz zu steigern, wird hier oftmals auf heterodimerisierende LOV Sensoren zurückgegriffen. Neben der Verwendung von natürlichen heterodimerisierenden Photorezeptoren wie Flavin binding-Kelch-Fbox-1 (FKF1) aus A. thaliana, welches lichtabhängig an das Protein GIGAN-TEA bindet, gelang basierend auf der LOV Domäne VIVID die Erstellung eines neuen heteroassoziierenden Schalters. Die Dimerisierungsfläche von VIVID wurde so verändert, dass durch elektrostatische Wechselwirkungen eine Homodimerisierung verhindert und eine Heterodimerisierung favorisiert wird (Kawano et al. 2015). Die sogenannten magnets weisen eine schnelle Dissoziationskinetik auf und finden Anwendung in diversen optogenetischen Systemen (Kawano et al. 2015, 2015, 2016, Nihongaki et al. 2015, Baumschlager et al. 2017, Furuya et al. 2017). Neuere Studien haben allerdings gezeigt, dass in einigen Fällen die Assoziationsstärke der *magnets* nicht ausreichend ist, um eine exakte räumlich-zeitliche Kontrolle bestimmter Signalwege zu gewährleisten (Benedetti et al. 2018).

Betrachtet man die Anzahl an diversen blaulichtgesteuerten optogenetischen Systemen, macht die Regulation der Genexpression einen der am häufigsten durch Licht manipulierten Bereiche aus. Daher soll auf diesen im Folgenden näher eingegangen werden.

1.2.2 Bakterielle LOV-basierte Genexpressionssysteme

Die Kontrolle der Genexpression stellt eines der ersten und wichtigsten Steuerelemente zur Untersuchung oder zur gezielten Modifikation eines zellulären Prozesses dar. Bereits seit einigen Jahren wurde versucht diese artifiziell durch Gabe externer chemischer Stimuli zu beeinflussen (Studier und Moffatt 1986, Gossen et al. 1995, Gottesfeld et al. 2001). Um die Limitierungen von chemischen Induktoren wie eine begrenzte Diffusionsrate (langsame Aktivierung) und schwierige Entfernung (langsame Deaktivierung) zu überwinden, stützen sich zahlreiche optogenetische Anwendungen auf die Kontrolle der Transkription. Die Tatsache, dass der molekulare Ablauf der Transkription gut untersucht ist und von modular aufgebauten Transkriptionsfaktoren initiiert werden kann, erleichtert das Design von künstlichen Photorezeptoren zur lichtregulierten Genexpressionskontrolle.

Oftmals wird beim Design lichtgesteuerter Transkriptionssysteme Gebrauch von der Modularität der Transkriptionsfaktoren gemacht und auf Grundlage dieser werden neue Fusionsproteine erstellt (Strickland et al. 2008, Li et al. 2020). Wie bereits im vorherigen Abschnitt erwähnt, stellt die Fusion des Trp Repressorproteins an die C-terminale Jα-Helix von *As*LOV2 eines der ersten lichtgesteuerten Transkriptionssysteme in Prokaryoten dar. Dieses findet aber auch nach Weiterentwicklung zum LOV-TAP angesichts seiner geringen DNA-Bindeaffinität nur geringen Einsatz (Abbildung 13) (Strickland et al. 2008, 2010, Ziegler und Möglich 2015).

Durchaus verbreiteter in der Anwendung ist der bakterielle, photosensitive Transkriptionsfaktor EL222 aus *Erythrobacter litoralis* (Abbildung 13). Dieser besteht aus einer photosensorischen LOV Domäne und einer HTH-DNA-Bindedomäne. In Abwesenheit von Blaulicht bindet die LOV Domäne die HTH-Bindedomäne und blockiert sterisch die 4α -Helix, welche für eine Dimerisierung und DNA-Bindung entscheidend ist. Blaulichtexposition hebt die inhibitorischen LOV-HTH-Interaktionen auf, worauf die Assoziation und Bindung an den Operator folgt (Nash et al. 2011, Rivera-Cancel et al. 2012, Zoltowski et al. 2013). Die kürzliche Entwicklung eines

bidirektionalen EL222-basierenden Promotorsystems erlaubt die Verwendung von EL222 als lichtinduzierten Aktivator oder Repressor in *E. coli* (Jayaraman et al. 2016).

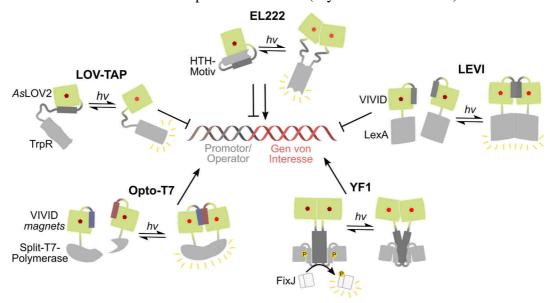


Abbildung 13: Bakterielle LOV-basierte Genexpressionssysteme, welche blaulichtabhängige Transkription eines gewünschten Gens ermöglichen. Modifiziert nach (Losi et al. 2018, Mathony und Niopek 2020).

Viele optogenetische Systeme nutzen den dimeren Charakter natürlich vorkommender, bisher nicht lichtregulierter Repressoren, welcher es ihnen erlaubt spezifische DNA-Sequenzen zu binden. Die Fusion einer trunkierten, monomeren Version des E. coli LexA Repressorproteins mit VIVID, benannt als LEVI, ermöglicht die blaulichtgesteuerte Dimerisierung und Wiederherstellung der Repressoraktivität (Abbildung 13) (Chen et al. 2016). Während diese Systeme aus einem einzelnen chimären Protein bestehen, setzen viele andere auf die Erstellung zweier unterschiedlicher Fusionsproteine. Jene basieren dann häufig auf heterodimerisierenden LOV Domänen, einer DNA-Binde- und einer Transkriptionsaktivierungsdomäne. Blaulichtexposition führt auf Grund der Interaktion des Photorezeptorpaars zur Rekrutierung der DNA-Bindeund der Aktivierungsdomäne und so zur Transkriptionsaktivierung (Lungu et al. 2012, Polstein und Gersbach 2012, Guntas et al. 2015). An diese Strategie anknüpfend wurde gezeigt, dass die Aktivität der in zwei Fragmente gespaltenen T7-Polymerase durch Fusion mit magnets in blaulichtabhängiger Weise wiederhergestellt werden kann (Abbildung 13) (Baumschlager et al. 2017, Han et al. 2017). Oftmals erlaubt der Anknüpfung viraler Transaktivierungsdomänen den Einsatz von genannten optogenetischen Schalter in Eukaryoten (Wang et al. 2012, Motta-Mena et al. 2014, Rullan et al. 2018).

Komplexere Systeme zur lichtinduzierten Genregulation stützen sich häufig auf Zweikomponentensysteme (siehe 1.1.1). Der am häufigsten angewandte, hierauf basierende, künstlich er-

stellte Photorezeptor ist YF1 (siehe 1.2.1). Die blaulichtreprimierte Histidinkinase dient als Basis für die Plasmide pDusk und pDawn, welche blaulichtgesteuerte Genexpression in *E. coli* erlauben (Abbildung 14).

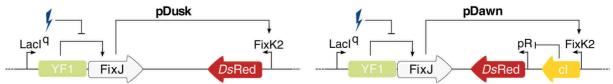


Abbildung 14: Die Plasmide pDusk und pDawn stützen sich auf das lichtsensitive YF1/FixJ Zweikompontentensystem und erlauben licht-reprimierte und licht-aktivierte Genexpression. Das Plasmid pDawn ist eine abgeleitete Version des pDusk-Systems und beherbergt eine Geninversionskasette basierend auf dem λ -Phagen Repressor cI. Modifiziert nach (Ohlendorf et al. 2012).

Das pDusk Plasmid beinhaltet YF1 und dessen zugehörigen Antwortregulator FixJ. Beide werden konstitutiv in einem bicistronischen Operon exprimiert. In Abwesenheit von Blaulicht phosphoryliert YF1 sein Partnerprotein FixJ. Dieses kann in seiner phosphorylierten Form an den FixK2 Promotor binden, welcher stromaufwärts von einer multiplen Klonierstelle beheimatet ist und so Genexpression ermöglicht. Umgekehrt vermindert Blaulichtbestrahlung die Netto-Kinaseaktivität von YF1, was zur Dephosphorylierung des Antwortregulators und zur Repression der Genexpression führt. Das pDawn Plasmid erlaubt hingegen blaulichtinduzierte Genexpression. Die Inversion basiert auf der Expression des λ -Phagen Repressors cI vom FixK2 Promotor. Da der Phagen-Repressor an den λ -Promotor pR bindet, inhibiert dieser sodann die Expression des gewünschten Zielgens (Ohlendorf et al. 2012). Die Tatsache, dass pDusk und pDawn jeweils auf einem einzigen Plasmid kodiert und somit leicht mit anderen Systemen kombiniert werden können, eröffnet ein großes Anwendungsspektrum (Farzadfard und Lu 2014, Magaraci et al. 2014, Jin und Riedel-Kruse 2018, Pu et al. 2018, Lalwani et al. 2019, 2020).

1.3 Ziele der Arbeit

LOV Rezeptoren besitzen als lichtsensitive Aktoren nicht nur große Wichtigkeit in diversen Organismen sondern finden immer größeren Einsatz in der Optogenetik und Photobiologie. In der vorliegenden, mehrgliedrigen Arbeit sollen zum einen die Charakteristika von LOV Rezeptoren weiter analysiert und zum anderen neue Anwendungsmöglichkeiten geschaffen werden. Zunächst soll untersucht werden, ob eine exakt staffelbare, sequenzielle Kontrolle mehrerer optogenetischer Systeme durch Variation der Intensität und Pulsfrequenz einer einzigen Lichtfarbe erzielt werden kann. Dafür sollen für die blaulichtsensitiven Genexpressionssysteme pDusk und pDawn, welche sich auf den künstlich erstellen Photorezeptor YF1 stützen, die Antworten auf gepulstes Blaulicht analysiert werden. Zudem wird der Einfluss der Modulation der Rückkehrzeiten von YF1 auf die Sensitivität des Systems näher betrachtet.

Daneben sollen in einem weiteren Projekt weitere Einblicke in die Signaltransduktion von LOV Rezeptoren geschaffen werden. Datenbankanalysen zeigen dabei, dass es LOV-artige Rezeptoren gibt, welche anstelle des konservierten, für die Signalweiterleitung wesentlichen Glutaminrests eine andere Aminosäure aufweisen. Ausgehend von Mutagenesestudien an YF1 soll geprüft werden, ob und inwieweit Signale auch ohne das chromophornahe Glutamin übermittelt werden können. Zudem wird die blaulichtvermittelte Signalantwort eines bisher noch nicht charakterisierten, natürlich vorkommenden, glutaminfreien LOV-GGDEF Rezeptors genauer analysiert.

Neben Licht können LOV-Rezeptoren vermutlich auch andere Reize wie Sauerstoff- oder Temperaturveränderungen wahrnehmen. Innerhalb dieser Arbeit soll die Licht- und Temperatursensitivität der LOV Domäne aus *Rhodobacter sphaeroides* (*Rs*LOV) näher charakterisiert werden. Hierfür wird unter zu Hilfenahme des *E. coli* Tet Repressors (TetR) und der auf Blaulicht hin dissoziierenden *Rs*LOV Domäne ein neues Genexpressionssystem erstellt. Dieses dient zum einen der Identifikation verbesserter *Rs*LOV Varianten und zum anderen, neben biochemischen Analysen, der Charakterisierung der Licht- und Temperaturantwort selbiger.

LOV Rezeptoren finden nicht nur breite Anwendung in der Optogenetik, sondern können auch im extrazellulären Kontext eingesetzt werden. Besonders im Bereich der Kolloidchemie ist etwa eine sorgfältige Reaktionskontrolle nützlich, welche durch LOV Rezeptoren mit hoher räumlich-zeitlicher Genauigkeit vermittelt werden könnte. Mit Hilfe der assoziierenden LOV Domäne VIVID wird innerhalb dieser Arbeit die prinzipielle Durchführbarkeit dieses Ansatzes untersucht. Insbesondere soll die photobiologisch gelenkte Assemblierung von Goldnanopartikeln etabliert werden.

2 Synopsis

Die vorliegende kumulative Dissertation umfasst insgesamt fünf wissenschaftliche Arbeiten:

- Kapitel 5.1: "Optogenetic Control by Pulsed Illumination"
- Kapitel 5.2: "Pulsatile Illumination for Photobiology and Optogenetics"
- Kapitel 5.3: "Signal Transduction in Light-Oxygen-Voltage Receptors Lacking the Active-Site Glutamine"
- Kapitel 5.4: "A Light-Oxygen-Voltage Sensor Integrates Light and Temperature"
- Kapitel 5.5: "Photobiologically Directed Assembly of Gold Nanoparticles"

Während von diesen Arbeiten vier bereits veröffentlicht (Kapitel 5.1, 5.2, 5.4 und 5.5) sind, wurde das fünfte Manuskript (Kapitel 5.3) im Fachjournal *Nature Chemical Biology* eingereicht.

Die einzelnen Manuskripte behandeln die Charakterisierung sowie die Anwendung von LOV Photorezeptoren. Die beiden ersten Arbeiten befassen sich mit der Möglichkeit zur Regulation optogenetischer Systeme mittels periodisch applizierten, unterschiedlich starken Lichts gleicher Wellenlänge. Zugleich beschreiben diese die Konstruktion programmierbarer Beleuchtungsapparate zur schnellen und parallelen Analyse biologischer Signale auf verschiedene Lichtverhältnisse hin. Das dritte Manuskript konzentriert sich auf den Mechanismus zur Übermittlung von Signalen in LOV Rezeptoren. Die beiden letzten Manuskripte befassen sich mit der Erstellung und Anwendung neuer LOV Rezeptoren. Insbesondere beschreibt die vierte Arbeit die Konstruktion und Optimierung eines blaulichtregulierten Genexpressionssystems und beschäftigt sich zudem mit der Temperatur- und Lichtsensitivität der eingesetzten LOV Domäne. Das fünfte Manuskript, zeigt das Anwendungspotential von LOV Rezeptoren außerhalb der Optogenetik. Es beschreibt die Möglichkeit der Kombination von biologischen und chemischen Bausteinen anhand der lichtgesteuerten Assemblierung von Goldnanopartikeln.

2.1 Gepulste Beleuchtung in der Optogenetik und Photobiologie

Die ersten beiden Veröffentlichungen (Kapitel 5.1 und 5.2) befassen sich mit der Reaktion optogenetischer Schaltkreise auf periodisch verabreichtes Licht unterschiedlicher Intensität und Pulsfrequenz. Im Fall eines monomeren Photorezeptors führt Lichtabsorption zum Übergang des dunkeladaptierten Zustands D in den lichtadaptierten Zustand L (Abbildung 15A). Dies erfolgt in Abhängigkeit der Lichtintensität mit einer Ratenkonstanten von k_1 ; die Rückreaktion findet hingegen mit einer Ratenkonstanten von k_1 statt. Numerische Simulationen zur Systemantwort zeigen, dass während einer Folge von Lichtpulsen eine monomerer Photorezeptor in Abhängigkeit der Ratenkonstanten k_1 und k_2 und der angelegten Pulsfrequenz wiederholt

zwischen den beiden Zuständen D und L hin und her wechselt (Abbildung 15B). Unterschiedliche Beleuchtungsschemata bei identischer Gesamtlichtdosis können so den Rezeptor in verschiedenem Umfang aktivieren. Zudem erlaubt der Einsatz von gepulster Beleuchtung zwei Photorezeptorsysteme, welche sich in ihrer Ratenkonstanten k-1 unterscheiden, diskriminieren zu können.

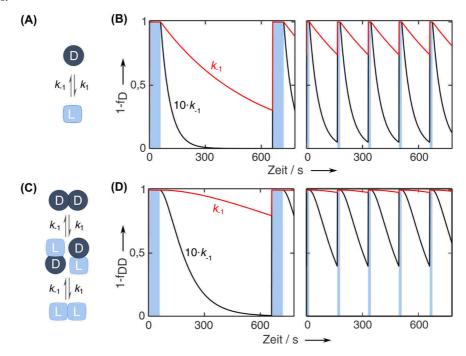


Abbildung 15: Simulationen zur Antwort lichtsensitiver Systeme auf gepulste Beleuchtung. (A) Licht bedingt die Konversion eines dunkeladaptierten monomeren Photorezeptors D in seinen lichtadaptierten Zustand L mit einer unimolekularen Ratenkonstanten von k_1 . Der Photorezeptor kehrt anschließend in den dunkeladaptierten Zustand mit einer Ratenkonstanten von k_1 zurück. (B) Das kinetische Modell aus (A) wurde in den angegebenen Zeiten unter periodischer Beleuchtung (blaue Balken) numerisch gelöst. Die Ordinate stellt die Fraktion des Rezeptors im lichtadaptieren Zustand dar. Gezeigt sind Simulationen für eine langsame (rot) und 10-fach schnellere (schwarz) Rückkehr in den D-Zustand. Die Pulsfrequenz wurde im rechten Diagramm vierfach erhöht und die Dauer der Lichtperiode um den gleichen Faktor reduziert, sodass die Gesamtlichtdosis konstant gehalten wird. (C) In dimeren Photorezeptoren erfolgt die Reaktion von DD nach LL und umgekehrt über eine zweischrittige Reaktion via DL/LD-Intermediate. Die Protomere gehen unabhängig voneinander mit Ratenkonstanten k_1 und k_2 in den D- bzw. L-Zustand über. (D) Analoge Simulationen zu (B), jedoch für dimere Photorezeptoren.

Im Falle eines dimeren Photorezeptors führt Lichtabsorption zum Übergang des dunkeladaptierten Zustands DD in den lichtadaptierten Zustand LL unter Durchlaufen der Intermediatszustände DL und LD (Abbildung 15C). Der Einfachheit halber wird hierbei angenommen, dass die beiden Untereinheiten unabhängig voneinander zwischen den Zuständen D und L mit einer Ratenkonstanten k_1 und k_{-1} übergehen. Wie bereits in mindesten einem dimeren Photorezeptor experimentell gezeigt wurde (Möglich et al. 2009b), kann weiterhin angenommen werden, dass die Zustände DL, LD und LL jeweils die gleiche Aktivität aufweisen. Anders als im monomeren Szenario kann die Rückkehr in den dunkeladaptierten Zustand nicht mit einer Einfachexponentialfunktion beschrieben werden, sondern ist durch einen sigmoidalen Reaktionsverlauf ge-

kennzeichnet. Infolgedessen zeigen analoge Simulationen zur Systemantwort dimerer Photorezeptoren, dass diese im Vergleich zu monomeren Rezeptoren in größerem Umfang aktiviert werden können, sofern der Photorezeptor mehrerer kürzerer Lichtpulse als einen seltenen, aber längeren Lichtpuls erfährt (Abbildung 15D). Ebenso bedingt der sigmoidale Reaktionsverlauf eine deutlich bessere Unterscheidung zweier Photorezeptorsysteme mit unterschiedlichen Rückkehrraten. Zusammengefasst legen die theoretischen Studien nahe, dass gepulste Beleuchtung neben der Möglichkeit die Dauer und Intensität von stetig appliziertem Licht zu variieren einen zusätzlichen Ansatzpunkt zur präzisen und sequenziellen Kontrolle mehrerer Photorezeptorsysteme erlauben können.

2.1.1 Erstellung programmierbarer Beleuchtungsapparaturen

Zur anschließenden systematischen Untersuchung der Antwort lichtsensitiver Systeme auf verschiedene Lichtintensitäten und Zeitschemata *in vivo* wurden auf Leuchtdioden- (*light-emitting diodes*, LED) Matrizen basierte Beleuchtungsvorrichtungen entworfen und optimiert (Abbildung 16). Diese erlauben eine parallele und programmierbare Beleuchtung von 64 Proben einer kommerziellen 96-Loch-Titerplatte von unten. Die zugrundeliegenden LED-Matrizen können individuell bestückt werden und basieren ausschließlich auf *open-source* Arduino-Bauteilen. Die Beleuchtungsvorrichtung kann mit geringem Aufwand und Kosten assembliert und mittels einer dazugehörigen graphischen Benutzeroberfläche leicht programmiert werden.

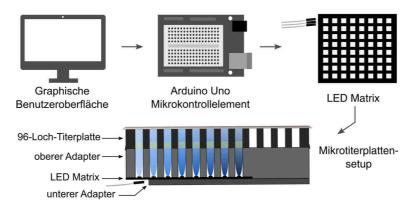


Abbildung 16: Schematische Darstellung der Anwendung des LED-Matrix basierten Beleuchtungsapparates. Eine graphische Benutzeroberfläche ermöglicht die Konfiguration der LED-Matrix. Die Konfigurationsdatei wird anschließend auf eine Arduino Uno Mikrokontrolleinheit, welche die Terminierung und Intensität der 64 LEDs regelt, hochgeladen. Die Matrix ist umhüllt von einem 3D-gedrucktem Gehäuse, welches die individuelle Beleuchtung der einzelnen Löcher einer Standard-96-Loch-Titerplatte von unten erlaubt.

Der hier beschriebene Beleuchtungsapparat ermöglicht das routinemäßige Testen von multiplen Beleuchtungsschemata nicht nur in optogenetischen Anwendungen, sondern auch in anderen lichtsensitiven (chemischen) Prozessen.

2.1.2 Präzise und sequenzielle Kontrolle bakterieller Genexpression

Unter Zuhilfenahme der programmierbaren Beleuchtungsvorrichtungen konnte anschließend die Reaktion des künstlich erstellen und gut verstandenen Photorezeptors YF1 auf periodisch verabreichtes Licht unterschiedlicher Intensität und Pulsfrequenz näher untersucht werden. Hierfür wurde auf die bereits etablierten, abgeleiteten Genexpressionssysteme pDusk- und pDawn zurückgegriffen (Ohlendorf et al. 2012). Entsprechende *E. coli* Kulturen wurden zunächst unter alternierenden Zyklen von Dunkelheit und Blaulichtbeleuchtung inkubiert. Die lichtabhängige Expression des *Ds*Red Express2 (*Ds*Red) Reportergens ermöglichte dabei die Erfassung der Systemantwort. Es zeigte sich, dass die Verwendung von gepulster Beleuchtung eine präzise und gestufte Kontrolle des Umfangs der *Ds*Red-Expression ermöglicht, welche durch konstante Beleuchtung nicht erreicht werden kann (Abbildung 17A).

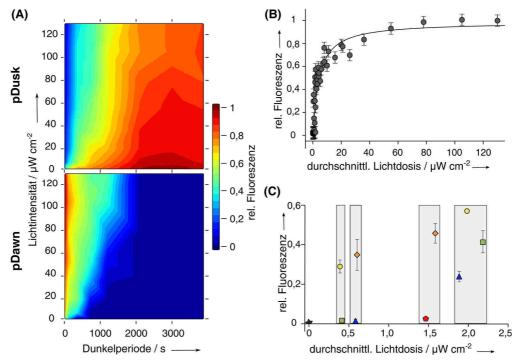


Abbildung 17: Kontrolle der Genexpression mittels Variation der Lichtintensität und Pulsfrequenz. (A) Die Konturdiagramme zeigen die normierte Expression von DsRed in Abhängigkeit der Länge der Dunkelperiode und der Intensität des applizierten Blaulichts im pDusk- und pDawn-DsRed Expressionskontext. (B) Die DsRed-Expression steigt mit zunehmender durchschnittlich verabreichter Lichtdosis hyperbolisch an. (C) Im Bereich von 0,5 und 2,5 μ W cm⁻² variiert die Antwort des Systems abhängig von der verwendeten Pulsfrequenz stark. Generell bewirkt die Verabreichung mehrerer Pulse mit geringerer Intensität eine höhere Aktivierung als die Verwendung eines einzelnen Pulses von hoher Intensität. Die Symbole verdeutlichen die verschiedene Lichtintensitäten (\bigstar : 0, \circlearrowleft : 2, \diamondsuit : 8, \blacksquare : 55, \blacktriangle : 78 und \spadesuit : 150 μ W cm⁻²).

Die Betrachtung der durchschnittlich eingesetzten Lichtdosis im pDawn-DsRed System zeigte einen hyperbolischen Anstieg der Reportergenfluoreszenz. Interessanterweise skaliert diese jedoch bei kleinen bis mittleren Lichtdosen, weit unterhalb des Sättigungsbereichs, nicht gleichbleibend mit der verabreichten Lichtdosis, sondern ist vor allem von der Pulsfrequenz der Be-

leuchtung abhängig. Dies impliziert, dass die Verabreichung gleicher Lichtdosen in diesem Bereich abhängig von der Häufigkeit des Lichtpulses zu unterschiedlichen Antworten führen kann und somit eine erweiterte Kontrolle des Systems erlaubt (Abbildung 17C). Der Einsatz von gepulstem Licht anstelle kontinuierlicher Beleuchtung kann überdies zu einer nahezu identischen Aktivierung des Systems führen, wobei gepulste Beleuchtung eine beträchtlich geringere Lichtdosisexposition mit sich bringt (Abbildung 17C). Auf diesen Erkenntnissen beruhend vermag die Entwicklung und Anwendung optimierter Beleuchtungsschemata dazu genutzt werden schädlichen phototoxischen Effekten im Gewebe, die bei langer Lichtexposition und hoher Lichtdosis entstehen können, entgegenzuwirken.

Basierend auf den Simulationen zur Systemantwort dimerer Photorezeptoren hinsichtlich gepulster Beleuchtung (siehe Abbildung 15) wurde erwartet, dass eine Veränderung der Rückkehrkinetik einen signifikanten Einfluss auf die Antwort des Systems unter periodisch verabreichtem Licht haben sollte. Um dies zu testen wurden zwei YF1 Varianten, V28T und V28I, welche eine zweifach beschleunigte bzw. 10-fach verlangsamte Rückkehr in den dunkeladaptierten Zustand aufweisen, erstellt und mittels des pDusk- bzw. pDawn-*Ds*Red Systems hinsichtlich der Sensitivität gegenüber periodisch verabreichtem Licht untersucht.

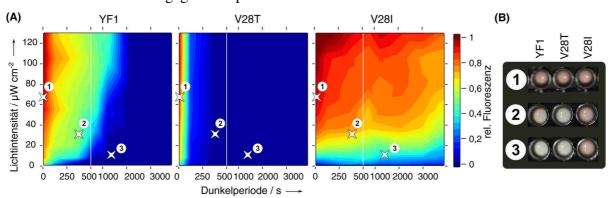


Abbildung 18: Modulation des Genexpressionsmusters durch Veränderung der Rückkehrraten von YF1 bei periodisch verabreichtem Licht. (A) Die normierte *Ds*Red Expression als Funktion der Pulsfrequenz und Lichtintensität zeigt eine erniedrigte bzw. erhöhte Lichtsensitivität der Varianten V28T bzw. V28I im Vergleich zu YF1. (B) Gepulste, gleichfarbige Beleuchtung ermöglicht die individuelle Kontrolle verschiedener lichtabhängiger Expressionssysteme. *E. coli* Kulturen, welche entweder YF1, die V28T oder V28I Variante im pDawn-*Ds*Red Kontext enthalten, wurden bei in A gekennzeichneten Beleuchtungsprotokollen inkubiert und spiegeln die resultierende Reportergenexpression wider.

Die Variante V28T zeigte dabei einhergehend mit der schnelleren Rückkehr eine erniedrigte Lichtsensitivität, wohingegen die Variante V28I, bedingt durch die verlangsamte Rückkehr in den dunkeladaptierten Zustand, eine deutlich erhöhte Sensitivität gegenüber Blaulicht aufweist (Abbildung 18A). Ein Vergleich der Expressionsmuster des pDawn-*Ds*Red Systems zeigt zudem, dass es Beleuchtungsregime gibt, in denen ein Teil der Varianten effektiv geschaltet werden kann und zugleich andere Varianten kaum Aktivierung aufweisen (Abbildung 18B). Dies

kann nur beobachtet werden sofern gepulste Beleuchtungsschemata eingesetzt wurden. Konstante Beleuchtung ist hingegen nicht ausreichend, um im gleichen Umfang eine individuelle und sequenzielle Aktivierung der Systeme herbeizuführen.

Zusammenfassend konnte hier gezeigt werden, dass periodisch verabreichtes, einfarbiges Licht genauere Kontrolle ermöglicht und diese für eine parallele Nutzung verschiedener Systeme und deren sequenzieller Steuerung eingesetzt werden kann. Auf Grundlage des Verständnisses der Möglichkeiten zur Modulation der Rückkehrkinetik durch bestimmte Aminosäuresubstitutionen, kann prinzipiell die Antwort eines Photorezeptors auf gepulste Beleuchtung hin adäquat für die jeweilige Anwendung eingestellt werden. Außerdem vermag die Möglichkeit verschiedene Photorezeptorsysteme mit Hilfe einer einzelnen Lichtfarbe unterschiedlich stark adressieren zu können, die Mehrfachnutzung verschiedener lichtregulierter Aktoren und Fluoreszenzreporter zu erleichtern.

2.2 Signaltransduktion in LOV Rezeptoren

Vorangegangene Studien zeigen, dass in LOV Domänen Blaulichtbestrahlung zur Ausbildung eines kovalenten Thioaddukts und zur Protonierung des N5 Atoms führt, was schließlich die Rotation bzw. Umlagerung eines konservierten Glutaminrests hervorruft. Es wird gemutmaßt, dass das Glutamin als entscheidender molekularer Hebel für die nachfolgende Signalweiterleitung fungiert und folglich unter anderem ausschlaggebend für die Aktivität des Effektors ist (Avila-Perez et al. 2006, Nash et al. 2008, Ganguly et al. 2017, Losi et al. 2018, Henry et al. 2020, Polverini et al. 2020). Eine Analyse der Sequenzdatenbanken zeigte jedoch, dass das chromophornahe Glutamin zwar stark konserviert vorliegt, aber auch einige LOV-artige Rezeptoren vorkommen, welche andere Aminosäuren an besagter Stelle aufweisen. Besonders häufig ist dabei das polare Glutamin gegen das unpolare Leucin substituiert.

Es stellt sich daher die Frage inwieweit auch ohne das konservierte Glutamin eine Signalweiterleitung stattfindet und eine Regulation des Effektors ausgelöst werden kann. Hierzu wurden zunächst YF1 Mutanten erstellt, welche anstelle des konservierten Glutamins eine beliebig andere Aminosäure aufweisen (Q123X). Diese wurden anschließend unter Zuhilfenahme des pDusk-*Ds*Red Genexpressionssystems auf blaulichtausgelöste Reportergenrepression untersucht (Abbildung 19A). Ein Vergleich mit YF1 zeigt, dass überraschenderweise bei nahezu allen Mutanten blaulichtinduzierte Signaltransduktion stattfindet. Einzig der Austausch gegen Prolin, Tryptophan, Tyrosin und Histidin bedingt eine konstitutive Reportergenexpression, wohingegen diese im Falle von YF1 Q123R weder im Licht noch im Dunkeln beobachtbar ist. Insbesondere löst Blaulichtbestrahlung im Falle von YF1 Q123L eine ebenso starke Repression der Reportergenexpression aus wie YF1.

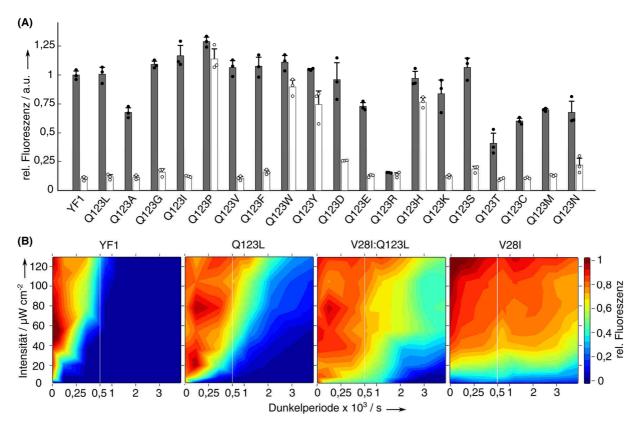


Abbildung 19: Aktivitätsmessungen von YF1 Varianten mit Hilfe des pDusk- und pDawn-*Ds*Red Genexpressionssysteme. (A) Blaulichtabhängige Reportergenexpression im pDusk-*Ds*Red Kontext. Im Falle von YF1 induziert Blaulicht (weiße Balken) eine zwölffache Repression der *Ds*Red Reportergenexpression im Vergleich zu in Dunkelheit inkubierten Kulturen (graue Balken). (B) Lichtsensitivität von YF1, YF1 Q123L, YF1 V28I:Q123L und YF1 V28I im Kontext des pDawn-*Ds*Red Genexpressionssystems. Die normierte *Ds*Red Expression als Funktion der Pulsfrequenz und Lichtintensität zeigt eine erhöhte Lichtsensitivität der Varianten Q123L, V28I:Q123L bzw. V28I im Vergleich zu YF1.

Da Leucin innerhalb der Datenbankanalyse eine der mit am häufigsten gefundenen Aminosäuresubstitutionen darstellt, wurde die Signalantwort von YF1 Q123L weiter mit Hilfe des pDawn-DsRed Genexpressionssystems untersucht. Im Falle von YF1 führt Blaulichtexposition zu einer ca. 65-fachen Erhöhung der Reportergenfluoreszenz, welche im gleichen Maß für YF1 Q123L beobachtet werden konnte. Durch Variation der Blaulichtintensität und Pulsfrequenz konnte zudem die Sensitivität des glutamindefizienten Rezeptors näher analysiert werden (Abbildung 19B). Dabei zeigte sich, dass YF1 Q123L deutlich sensibler auf Blaulicht reagiert, aber im Vergleich zu YF1 V28I, welches in vorangegangenen Studien ebenso als sensitive Variante identifiziert werde konnte (siehe Kapitel 2.1.2), weniger empfindlich ist. Eine Kombination der beiden Mutationen generierte eine Variante, welche eine erhöhte effektive Lichtsensitivität als YF1 Q123L aufweist, aber die von YF1 V28I nicht übertrifft.

Funktionale Studien an anderen LOV Rezeptoren, wie der blaulichtregulierten *As*LOV2-dCas9 Endonuklease oder dem blaulichtabhängig bindenden PAL Rezeptors, zeigen ebenso, dass auch in diesen Systemen in Gegenwart des unpolaren Leucins Signaltransduktion stattfindet.

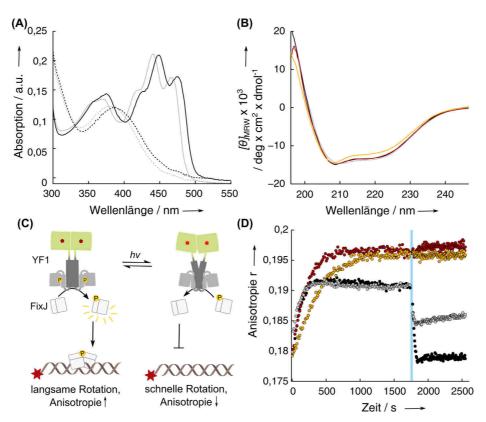


Abbildung 20: *In vitro* Analyse von YF1 Varianten. (A) UV/VIS-Absorptionsprofile von YF1 (schwarz) und YF1 Q123L (grau) im dunkeladaptierten (durchgezogene Linie) und lichtadaptierten (gestrichelt) Zustand. (B) Fern-UV CD spektroskopische Analyse von YF1 (schwarz), YF1 Q123L (grau), YF1 Q123P (orange) und YF1 Q123H (rot) im Dunkeln. (C) Schematische Darstellung der Interkation von FixJ mit dem fluoreszenzmarkiert FixK2-Epitop in Abhängigkeit der YF1-Aktivität. (D) Zeitaufgelöste Fluoreszenzanisotropie der Interaktion von FixJ und fluoreszenzmarkiertem DNA-Substrat in Gegenwart von YF1 (schwarz), YF1 Q123L (grau), YF1 Q123P (orange) und YF1 Q123H (rot) nach ATP-Zugabe. Der blaue Balken symbolisiert eine Bestrahlung mit Blaulicht.

Infolgedessen stellte sich die Frage welchen Einfluss der Austausch des konservierten Glutamins auf die biochemischen und biophysikalischen Eigenschaften ausübt. Während die Substitution gegen Arginin, wohl auf Grund seiner Größe, den Einbau des Chromophors gänzlich verhindert und zu einer partiellen Destabilisierung des Proteins führt, durchlaufen die YF1 Mutanten Q123L und Q123P den für LOV Domänen typischen Photozyklus (Abbildung 20A). Auf Grund des veränderten Wasserstoffbrückennetzwerks innerhalb der Chromophorregion im Vergleich zu YF1 kommt es hier jedoch zur Verschiebung der Feinstruktur der FMN-Absorption zu kleinerer Wellenlänge um bis zu 6 nm im Falle von YF1 Q123L (Nozaki et al. 2004, Jones et al. 2007, Kobayashi et al. 2020). Die Substitution gegen ein Histidin führt hingegen wohl auf Grund sterischer Hinderungen zum Verlust der photochemischen Schaltbarkeit und bedingt so das Ausbleiben einer Signaltransduktion. Die abgeänderten elektronischen Eigenschaften in der Nähe des Chromophors spiegeln sich ebenso in der Rückkehrkinetik wider. Für YF1 Q123L konnte beispielsweise im Vergleich zu YF1 eine zehnfach verlangsamte Rückkehr in den dunkeladaptierten Zustand beobachtet werden. Wie bereits die Reportergenmessungen zur gepulsten Beleuchtung gezeigt haben, wird hierdurch die Sensitivität gegenüber Blaulicht deutlich

erhöht (vgl. Abbildung 19B). Eine fern-UV CD spektroskopische Analyse der Sekundärstruktur zeigte, dass die Varianten Q123L, Q123P und Q123H ebenso wie YF1 einem gemischten α/β -Protein entsprechen und gefalten vorliegen (Abbildung 20B). Die Einführung der Mutationen führte daher zu keiner signifikanten Änderung der Sekundärstruktur.

Zur näheren Überprüfung der Signaltransduktion der YF1 Varianten wurde zudem Fluoreszenzanisotropie angewandt und die Drehbewegung eines fluoreszenzmarkierten DNA-Substrats in Lösung betrachtet (Abbildung 20C). Dieses weist die spezifische Bindestelle für FixJ auf. Im Dunkeln agiert YF1 als Nettohistidinkinase, sodass es nach Zugabe von ATP zur Phosphorylierung von FixJ durch YF1 kommt. Der phosphorylierte Antwortregulator FixJ interagiert anschließend mit der fluoreszenzmarkierten DNA. Die Größenänderung bedingt die Erhöhung des hydrodynamischen Radius und führt zur Einschränkung der Beweglichkeit wodurch die Anisotropie ansteigt. Blaulichtbestrahlung hingegen löst die Nettophosphataseaktivität von YF1 aus, was zur Dephosphorylierung von FixJ und letztendlich zur Aufhebung der FixJ-DNA-Interaktion führt. Infolgedessen kommt es zur Verringerung der Anisotropie. In Übereinstimmung mit den Erkenntnissen des pDusk-DsRed Genexpressionsassays konnte gezeigt werden, dass die Mutanten Q123L, Q123P und Q123H in Abwesenheit von Blaulicht als Histidinkinasen fungieren und Blaulichtbestrahlung nur im Falle der Q123L Mutante zur Erhöhung der Phosphataseaktivität führt (Abbildung 20D). Im Vergleich zu YF1 ist diese jedoch, anders als die in vivo Ergebnisse implizieren, schwächer ausgeprägt und ist womöglich auf eine weniger effiziente Signalweiterleitung zurückzuführen.

Interessanterweise durchläuft YF1 Q123P, anders als YF1 Q123H, zwar den typischen Photozyklus, dennoch bleibt vermutlich auf Grund des fehlenden Wasserstoffatoms der Peptidbindung eine blaulichtausgelöste Signalübertragung an den Effektor aus. Infolgedessen kommt es mutmaßlich zu einer Verschiebung des Gleichgewichts zwischen Kinase- und Phosphataseaktivität, wodurch deutlich höhere Anisotropiewerte erreicht werden. Diese Ergebnisse lassen vermuten, dass die blaulichtausgelöste, zur Signalweiterleitung essenzielle N5 Protonierung nicht allein von der Seitenkette des Glutamins, sondern auch durch Wechselwirkung mit dem Proteinrückgrat oder von Wassermolekülen innerhalb der Chromophorbindetasche wahrgenommen werden kann. Die veränderten Proteinrückgratwechselwirkungen würden konformationelle Änderungen innerhalb des Sensors einleiten und zur Modulation der Effektoraktivität führen.

Molekulardynamik-Simulationen zur Signalweiterleitung in AsLOV2 und YtvA-LOV legen nahe, dass für eine Signalweiterleitung wichtige zusätzliche Wasserstoffbrücken vermutlich

von zwei benachbarten Asparaginresten (entsprechend N94 und N104 in YF1) vermittelt werden (Abbildung 21A) (Iuliano et al. 2020, Polverini et al. 2020). Eine entsprechende Substitution in YF1 gegen Alanin zeigte, dass das Fehlen der Wasserstoffbrücken im Falle von N94 zum vollständigen Verlust der Signaltransduktion führt, wohingegen diese im Fall von N104 aufrechterhalten wird (Abbildung 21B). Interessanterweise bedingt jedoch die zusätzliche Einführung eines Leucins anstelle des konservierten Glutamins (YF1 N94A:Q123L) eine partielle Wiederherstellung der lichtabhängigen Signaltransduktion. Dies lässt vermuten, dass die Ausbildung der N94-vermittelten Wasserstoffbrücke für eine Signalweiterleitung in glutaminhaltigen Rezeptoren unerlässlich ist. In Abwesenheit des Glutamins vermag hingegen eine Signalweiterleitung unabhängig vom ausgebildeten Wasserstoffbrückennetzwerk stattfinden und durch konformationelle Änderungen des Peptidrückgrats oder von Wassermolekülen propagiert werden.

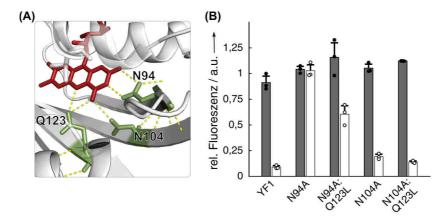


Abbildung 21: Signaltransduktion in Abhängigkeit von Wasserstoffbrücken innerhalb der Chromophorregion. (A) Ausbildung von Wasserstoffbrücken innerhalb der Chromophorregion in YF1 (PDB: 4GCZ). (B) Aktivitätsmessungen von YF1 Mutanten mit Hilfe des pDusk-DsRed Genexpressionssystems. Während Inkubation in Dunkelheit (grau) oder unter Blaulicht (weiß) im Falle von YF1 N94A eine konstitutive Histidinkinaseaktivität bedingt, kommt es in YF1 N94A:Q123L zu einer blaulichtausgelösten Signalweiterleitung.

Inwieweit eine Signalweiterleitung in YF1 in Abwesenheit des reaktiven Cysteinrests und dem gleichzeitigen Fehlen des hier untersuchten Glutminrests stattfinden kann, konnte innerhalb dieser Arbeit auf Grund der Sensibilität der verwendeten Methoden gegenüber entstehender ROS nicht ermittelt werden. Gleichzeitig durchgeführte Studien an AsLOV2 lassen dennoch vermuten, dass keiner der beiden Reste für eine Signaltransduktion nötig ist.

Neben den Studien zur Signalweiterleitung in Abwesenheit des konservierten Glutaminrests in gut untersuchten LOV Rezeptoren ist interessant, inwiefern die in der Datenbankanalyse identifizierten, von Natur aus glutaminfreien LOV Rezeptoren eine Signalweiterleitung erlauben. Zur Überprüfung wurde die Diguanylatzyklaseaktivität eines bislang nicht charakterisierten LOV-GGDEF Rezeptors aus *Mesorhizobium loti* mittels eines *lacZ*-basierten Reportertestsystems im Hinblick auf verschiedene Lichtverhältnisse genauer untersucht. Wie viele andere in

der Datenbank gefundene LOV-GGDEF Rezeptoren enthält dieser ein Methionin anstelle des Glutmaninrests. Da es infolge einer c-di-GMP Produktion zur Transkription von Genen aus dem csgBAC Operons kommt, gibt die Expression einer csgB::lacZ Fusion Auskunft über die Aktivität des GGDEF-haltigen Proteins (Abbildung 22A) (Römling et al. 1998, Sommerfeldt et al. 2009, Serra et al. 2013). Das E. coli lacZ Gen kodiert dabei das Enzym β -Galactosidase; dessen Aktivität kann infolge der Hydrolyse des synthetischen Substrates o-Nitrophenyl- β -D-galactopyranosid (ONPG) bestimmt werden (Miller 1972).

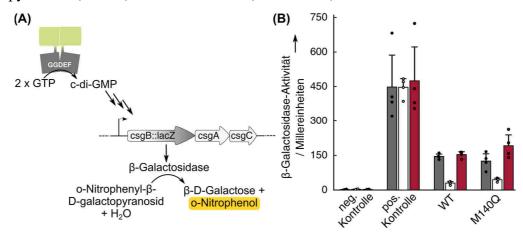


Abbildung 22: Diguanylatzyklaseaktivität von LOV-GGDEF Rezeptoren. (A) Schematische Darstellung des lacZ-basierten Reportertestsystems zur Bestimmung der Diguanylatzyklaseaktivität in $E.\ coli.$ (B) Spezifische β-Galactosidaseaktivität von $E.\ coli.$ Kulturen, welche eine genomische csgB::lacZ Fusion enthalten und LOV-GGDEF Varianten entweder in Dunkelheit (grau), in Anwesenheit von Blaulicht (weiß) oder von Rotlicht (rot) exprimieren. Die β-Galactosidaseaktivität wurde infolge der Hydrolyse des synthetischen Substrates o-Nitrophenyl- β -D-galactopyranosid nach (Miller 1972) bestimmt. Als Positivkontrolle diente ein Reporterstamm, welcher konstitutiv die Diguanlytatzyklase DgcE exprimiert und infolgedessen lichtunabhängig eine hohe β -Galactosidaseaktivität aufweist. Hingegen kommt es im diguanylatdefizienten $E.\ coli$ Reporterstamm zu keiner β -Galactosidaseexpression.

Zur Analyse der Signaltransduktion wurden zunächst LOV-GGDEF Varianten in einem diguanylatdefizienten *E. coli* Reporterstamm unter verschiedenen Lichtbedingungen exprimiert und die β-Galactosidaseaktivität bestimmt. Dabei zeigte sich, dass eine Inkubation in Dunkelheit oder unter Rotlicht die Diguanylatzyklasaeaktivität des wildtypischen LOV-GGDEF Rezeptors erlaubt, während Blaulichtbestrahlung diese signifikant reprimiert (Abbildung 22B). Der innerhalb dieser Arbeit erstmals untersuchte LOV-GGDEF Rezeptor agiert folglich als blaulichtreprimierte Diguanylatzyklase und demonstriert, dass natürlich vorkommende glutaminfreie LOV Rezeptoren eine Signaltransduktion erlauben. Die Anwesenheit des in anderen Rezeptoren stark konservierten Glutamins bewirkt dabei keine höhere Blaulichtschaltbarkeit und bringt folglich unter den getesteten Bedingungen keinen ersichtlichen Vorteil mit sich.

Die hier erbrachten Ergebnisse verdeutlichen, dass eine Signaltransduktion nicht zwingend bzw. nicht ausschließlich durch eine Neujustierung des konservierten Glutamins und damit verbundene Veränderungen am Wasserstoffbrückennetzwerk ausgelöst wird. Vielmehr konnte innerhalb dieser Arbeit gezeigt werden, dass es einen alternativen Mechanismus gibt, welcher es erlaubt Signale unabhängig vom konventionellen Wasserstoffbrückennetzwerk zu übermitteln, und dieser womöglich auch in natürlich vorkommenden glutamindefizienten LOV Rezeptoren ausgenutzt wird.

2.3 Charakterisierung, Anwendung und Optimierung einer licht- und temperatursensitiven LOV Domäne

Das vierte Manuskript (Kapitel 5.4) behandelt die Charakterisierung der Licht- und Temperatursensitivität einer LOV Domäne sowie die Erstellung und Optimierung eines neuen optogenetischen Werkzeugs. Anders als bei vielen anderen, in der Optogenetik bereits mehrfach eingesetzten, assoziierenden LOV Domänen, führt Blaulichtbestrahlung bei der LOV Domäne aus Rhodobacter sphaeroides (RsLOV) zur Dissoziation des Homodimers. Dies ermöglichte bereits die Konstruktion eines lichtschaltbaren Cas9-Proteins, welches jedoch auch auf Temperaturänderung reagiert (Richter et al. 2016, 2017). Obwohl die starke Temperaturabhängigkeit nur unzureichend verstanden ist, könnte sie in der RsLOV Domäne selbst verwurzelt sein und auf eine allgemeine Labilität des Proteins hinweisen. Innerhalb dieser Arbeit sollte daher die Reaktion der RsLOV Domäne auf blaues Licht und Temperatur genauer untersucht werden. Hierzu wurde zunächst mit Hilfe des konstitutiv dimeren E. coli Tet Repressors (TetR) ein neues blaulichtinduzierbares Genexpressionssystem entwickelt. Die Wirkweise des TetR ist sehr gut untersucht, sodass dieser als zuverlässiger Transkriptionsregulator in Bakterien, Pflanzen, Hefen und Säugerzellen breite Anwendung findet (Gatz und Quail 1988, Geissendörfer und Hillen 1990, Gossen et al. 1995, Lutz 1997, Belli 1998). In Abwesenheit von Tetrazyklinen bindet TetR an den tet-Operator und reprimiert die Transkription nachfolgender Gene. In Gegenwart seines Induktors kommt es zu konformationellen Änderungen und zur Aufhebung der TetR-DNA-Interaktion (Orth et al. 1998).

In einer vorangegangenen Arbeit führte die Kürzung des C-Terminus des TetR zur Unterbindung bzw. Schwächung der inhärenten Dimerisierung des TetR. Diese konnte anschließend durch die Fusion mit der RsLOV Domäne, welche im Dunkeln als Homodimer vorliegt, wiederhergestellt werden (Schuster & Möglich). Blaulichtexposition löst vermutlich die Dissoziation des Fusionsproteins aus und erlaubt die Aktivierung der Transkription (Abbildung 23A). Anhand des Vergleichs der Expressionsstärke des Reportergens DsRed von in Dunkelheit oder unter Blaulicht inkubierten E. coli Kulturen bei 29°C wurden verschiedene chimäre TetR-

RsLOV Varianten, welche sich in der Länge des TetR und des verbindenden Linkers unterscheiden, auf Lichtregulation geprüft. Die Fluoreszenz von E. coli Kulturen, welche ein entsprechendes Plasmid ohne das Reportergen tragen, wurde jeweils abgezogen.

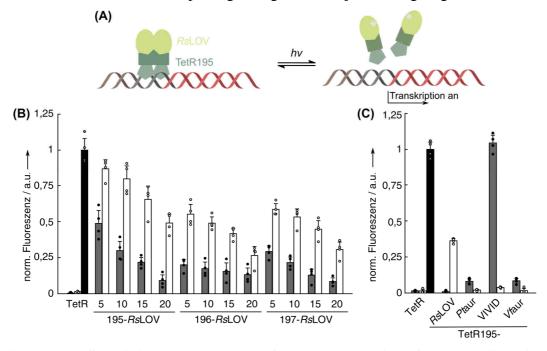


Abbildung 23: Das lichtschaltbare TetR-Genexpressionssystem. (A) Schematische Darstellung des TetR-RsLOV basierten Genexpressionssystems in E. coli (B) Die RsLOV Domäne wurde mittels unterschiedlich langer Linker (5, 10, 15, 20 Aminosäuren) an trunkierte Versionen des TetR Proteins (195, 196, oder 197 Aminosäuren) fusioniert. Die entsprechenden Proteine wurden in E. coli im Dunkeln (grau), unter Blaulicht (weiß) oder in Gegenwart von Anhydrotetrazyklin (schwarz) exprimiert und bei 29°C auf blaulichtausgelöste Reportergenexpression getestet. Die Hintergrundfluoreszenz von E. coli Kulturen, welche ein Plasmid ohne DsRed enthalten, wurde abgezogen. (C) Modifikation des Replikationsursprungs des zugrundeliegenden Vektors erhöhte die Schaltbarkeit des TetR195-20-RsLOV Konstrukts bei 29°C. Der Austausch gegen andere, auf Blaulicht hin dimerisierende LOV Domänen wie Ptaur-LOV aus Phaeodactylum tricornutum, VI-VID aus Neurospora crassa und Vfaur aus Vaucheria frigida führt zur Aktivierung im Dunkeln (grau) und Repression der Genexpression unter Blaulichtbedingungen (weiß).

Das Fusionsprotein TetR195-20-RsLOV zeigte dabei von allen getesteten Konstrukten die beste Repression im Dunkeln in Kombination mit einer moderaten Aktivierung der Reportergenexpression unter Blaulicht (Abbildung 23B). Die Chimäre beinhaltet die ersten 195 Aminosäuren des TetR, einen 20 Aminosäuren langen Linker sowie die RsLOV Domäne und wird im nachfolgendem als TetR195-RsLOV bezeichnet. Durch eine Erhöhung der Plasmidkopienzahl des zugrundeliegenden Vektors konnte innerhalb dieser Arbeit auf Grund einer größeren Repressorexpression dessen Schaltbarkeit von fünf- auf 40-fach gesteigert werden (Abbildung 23C) (Kim und Ryu 1991, French und Ward 1996). Das entwickelte Genexpressionssystem zeigt somit eine vergleichbare Schaltbarkeit wie das auf das Zweikomponentensystem YF1/FixJ basierte pDusk Genexpressionssystem und kann genauso wie dieses als potentes Werkzeug in der Optogenetik eingesetzt werden (Ohlendorf et al. 2012). Überdies konnte hier gezeigt werden, dass der Austausch der RsLOV Domäne gegen andere bereits beschriebene,

assoziierende LOV Domänen ebenso eine blaulichtgesteuerte Genexpression zulässt (Abbildung 23C). Da in diesen Fällen Blaulichtbestrahlung die Dimerisierung der Domänen bedingt (Zoltowski und Crane 2008, Nakatani und Hisatomi 2015, Banerjee et al. 2016), kommt es im Gegensatz zur Verwendung der *Rs*LOV Domäne zur blaulichtinduzierten Repression der Reportergenexpression. Anhand dieser Ergebnisse konnte gezeigt werden, dass die Aktivität der erstellen lichtsensitiven Repressorproteine auf die Dimerisierung der jeweiligen LOV Domänen zurückzuführen ist.

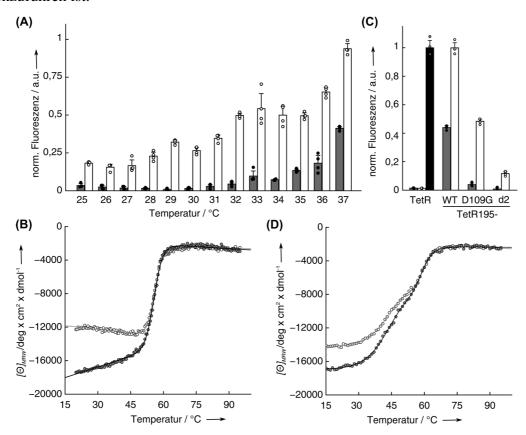


Abbildung 24: Temperatursensitivität der *Rs*LOV Domäne. (A) Eine Erhöhung der Inkubationstemperatur führt zum Verlust der Repressionsfähigkeit des TetR195-*Rs*LOV Konstrukts im Dunkeln (grau) und unter Blaulicht (weiß) in *E. coli*. Die Hintergrundfluoreszenz von *E. coli* Kulturen, welche ein Plasmid ohne *Ds*Red enthalten, wurde abgezogen. (B) CD spektroskopische Analyse zur Bestimmung der thermischen Stabilität der *Rs*LOV Domäne in Dunkelheit (grau) und nach Blaulichtbestrahlung (weiß). (C) Der Austausch von *Rs*LOV gegen optimierte Varianten im TetR195-*Rs*LOV-Kontext führt zu einer höheren Repression im Dunkeln (grau), aber ermöglicht ebenso blaulichtausgelöste (weiß) Reportergenexpression bei 37°C. Im Falle des ursprünglichen TetR kommt es in Gegenwart von Anhydrotetrazyklin (schwarz) zu einer ca. 70-fachen Steigerung der Genexpression. Die Hintergrundfluoreszenz von *E. coli* Kulturen, welche ein Plasmid ohne *Ds*Red enthalten, wurde abgezogen. (D) CD spektroskopische Analyse zur Bestimmung der thermischen Stabilität der *Rs*LOV d2 Mutante in Dunkelheit (grau) und nach Blaulichtbestrahlung (weiß).

Wie bereits frühere Studien an lichtschaltbaren *Rs*LOV basierten Cas9-Varianten zeigten (Richter et al. 2016), weist auch das hier erstellte Genexpressionssystem neben der Lichtsensitivität eine Temperaturabhängigkeit auf. Die Erhöhung der Inkubationstemperatur von 29°C auf 37°C führt dabei zum fast vollständigen Verlust der Repressionsfähigkeit des Fusionspro-

teins (Abbildung 24A), welche beim ursprünglichen TetR nicht festgestellt werden konnte. Folgende biochemische Studien zur thermischen Stabilität der RsLOV Domäne zeigen, dass bei Temperaturen unterhalb des Entfaltungsübergangs in Dunkelheit ein allmählicher Verlust der α -helikalen Struktur auftritt (Abbildung 24B). Im lichtadaptierten Zustand kann dies hingegen nicht beobachtet werden und deutet darauf hin, dass nicht nur Blaulicht sondern auch ein Temperaturanstieg zur teilweisen Entfaltung terminaler α -Helices und vermutlich zur Dissoziation des Dimers führen könnte.

Um die Temperaturempfindlichkeit des TetR195-*Rs*LOV-Systems zu umgehen, wurden zwei Strategien zur Optimierung der *Rs*LOV Domäne verfolgt. Nach Zufallsmutagenese des *Rs*LOV Proteins konnte mit Hilfe des TetR195-*Rs*LOV-Genexpressionssystems eine Variante identifiziert werden, welche bei 37°C eine deutlich bessere Repression im Dunkeln erlaubt (Abbildung 24C). Diese beherbergt in einer lösungsmittelexponierten Schleife fernab der Dimerisierungsfläche der *Rs*LOV Domäne ein Glycin anstelle eines Aspartatrests (Position 109). Zudem konnte mithilfe des *Protein Repair One-Stop Shop* (PROSS)-Algorithmus eine Proteinvariante (*Rs*LOV d2) identifiziert werden, die ebenso im TetR-basierten Genexpressionskontext bei 37°C eine erhöhte Repressionsfähigkeit im Dunkeln aufweist (Abbildung 24C). Die insgesamt sechs eingebrachten Mutationen befinden sich ebenfalls nicht in direkter Nähe der Dimerisierungsfläche, sondern sind an lösungsmittelexponierten Stellen lokalisiert.

Während die Repressionsstärke im Dunkeln bei beiden Varianten D109G und d2 nahezu gleich ausgeprägt ist, wird im Falle von RsLOV D109G eine deutlich höhere blaulichtinduzierte Genexpression erreicht (Abbildung 24C). Bei niedrigeren Inkubationstemperaturen erfolgt jedoch in keinem Fall eine Aktivierung der Genexpression. Die Repression und der Grad der Lichtregulierung der TetR195-RsLOV-Varianten konnte durch gezielte Destabilisierung des TetR moduliert werden. Ebenso brachte die Insertion einer C-terminalen Hexahistidinsequenz, welche vermutlich zur Beeinträchtigung der RsLOV Dimerisierung führt, auch bei niedrigen Temperaturen lichtschaltbare Konstrukte hervor. Durch einen Vergleich der Expressionsstärke der rekombinanten TetR195-RsLOV Proteine konnte ausgeschlossen werden, dass das verbesserte Repressionsvermögen auf das Vorliegen höherer Proteinkonzentrationen zurückzuführen ist. Um die Temperaturtoleranz der RsLOV Varianten D109G und d2 besser zu verstehen erfolgte eine biochemische Charakterisierung. Während die beiden Varianten die kanonische LOV-Photochemie aufwiesen und Gelfiltrationsstudien zu Folge in gleichem Ausmaß wie der wildtypische Rezeptor blaulichtabhängige Dissoziation erfahren, zeigten sich Unterschiede in ihren Reaktionen auf Licht und Temperaturerhöhung. CD spektroskopische Analysen zeigen, dass die Variante d2 einen weniger stark ausgeprägten blaulichtinduzierten Verlust an α-helikalen Strukturen erfährt als der Wildtyp und die Variante D109G (Abbildung 24D). Zudem verläuft die thermische Entfaltung der Variante d2 über ein stabiles Gleichgewichtsintermediat (Abbildung 24D), welches im Falle des wildtypischen Rezeptors und der D109G Variante nicht beobachtet werden kann. Die sich aus dem Gleichgewichtsintermediat ergebenen Übergänge zeigen je einen ca. 50%-igen Verlust an α -Helizität, was vermutlich auf die Entfaltung der terminalen Helices und auf die der Kerndomäne zurückzuführen ist. Bei Temperaturen unterhalb des ersten Übergangs kommt es im Gegensatz zum Wildtyp und der D109G Mutante kaum zum Verlust α -helikaler Strukturen. Der Verlust tritt hier erst bei höherer Temperatur auf und lässt auf eine gesteigerte Kooperativität der temperaturgesteuerten Entfaltung schließen. Die Unterschiede in der thermischen Stabilität der Variante d2 könnten somit die Ursache der erhöhten Temperaturtoleranz im TetR-Kontext sein.

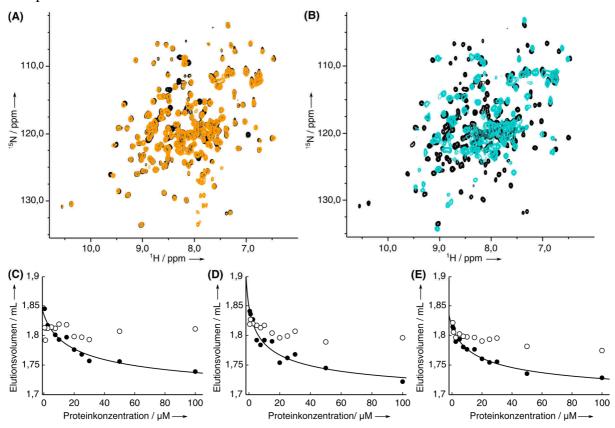


Abbildung 25: Biochemische Analyse von *Rs*LOV Varianten. (A) ¹H–¹⁵N HSQC-Spektren von dunkeladaptiertem *Rs*LOV (schwarz) und der Variante D109G (orange) bei 37°C. (B) ¹H–¹⁵N HSQC-Spektren von dunkeladaptiertem (schwarz) und lichtadaptiertem *Rs*LOV (türkis) bei 37°C. (C-E) Retentionsvolumina von Gelfiltrationsstudien in Abhängigkeit der Konzentration an wildtypischen *Rs*LOV (C), D109G (D) und d2 (E) im dunkeladaptierten (schwarz gefüllte Kreise) sowie lichtadaptierten Zustand (weiß gefüllte Kreise). Die Daten wurden an reversible Homodimerisierungsisothermen gefittet.

Um ferner Unterschiede zwischen der D109G Variante und dem wildtypischen LOV Rezeptor ausmachen zu können, wurde Kernspinresonanz (NMR)-Spektroskopie angewandt. ¹H-¹⁵N *Heteronuclear Single Quantum Coherence* (HSQC)-Experimente zeigten, dass beide Proteine bei 29°C im Dunkeln gefalten vorliegen und sich die Spektren in nur wenigen Resonanzwerten,

welche auf den mutierten Rest und die direkte Umgebung zurückzuführen sind, unterscheiden. Des Weiteren bedingt die Erhöhung der Temperatur auf 37°C keine signifikante Änderung Signale. Folglich kann angenommen werden, dass beide Proteine temperaturunabhängig eine ähnliche Struktur aufweisen (Abbildung 25A). Zur genaueren Beurteilung des oligomeren Zustands dunkeladaptierter Proteine wurden zudem NMR Relaxationsmessungen durchgeführt. Ausgehend von den Relaxationszeiten T_2 konnten für beide Proteine Rotationskorrelationszeiten τ_c von 17 ns bei 29°C und 16 ns bei 37°C berechnet werden. Diese deuten auf das Vorliegen von Homodimeren hin. $^1\text{H-}^{15}\text{N}$ HSQC-Spektren von lichtadaptierten wildtypischen RsLOV und RsLOV D109G bei 37°C unterscheiden sich drastisch von denen der dunkeladaptierten Proteine und weisen auf eine Entfaltung mehrerer Proteinsegmente hin (Abbildung 25B). Die hier beobachteten umfassenden, blaulichtausgelösten konformationellen Änderungen stehen somit in Einklang mit der CD spektroskopisch beobachteten α -helikalen Entfaltung. Unterschiede zwischen dem Wildtyp und der Mutante konnten wiederum nicht festgestellt werden, sodass davon ausgegangen werden kann, dass beide Proteine gleichartige, lichtinduzierte, strukturelle Veränderungen erfahren.

Angesichts des insgesamt ähnlichen biochemischen Verhaltens von *Rs*LOV und der D109G Mutante, könnte die verbesserte Temperaturtoleranz auf Unterschiede in der Homodimeraffinität zurückzuführen sein. Zur Überprüfung dessen wurden die jeweiligen Dissoziationskonstanten (*K*_D) im Dunkeln bei 4°C mittels Gelfiltrationsstudien bestimmt. Während die Retentionszeiten der lichtadaptierten *Rs*LOV Varianten über den Konzentrationsbereich von 0,5-100 μM kaum variierten, verringerten sich diese im Falle der dunkeladaptierten Probe mit steigenden Proteinkonzentrationen (Abbildung 25C, D, E). Diese Beobachtung ist konsistent mit einer zunehmenden Ausbildung von Dimeren. Unter Annahme einer reversiblen Homodimerisierung konnte für den wildtypischen Rezeptor und Variante d2 ein apparenter *K*_D-Wert von ca. 40 μM bestimmt werden. *Rs*LOV D109G weist hingegen eine rund zweifach höhere Homodimerisierungsaffinität auf, welche womöglich der Grund für das verbesserte Abschneiden im TetR-Kontext ist.

Zusammenfassend lässt sich sagen, dass innerhalb dieser Arbeit Einblicke in die Licht- und Temperatursensitivität der *Rs*LOV Domäne gewonnen und ein weiteres lichtsensitives Genexpressionssystem geschaffen wurde. Die Temperatursensitivität der *Rs*LOV Domäne konnte zwar nicht vollständig überwunden werden, dennoch gelang die Identifizierung zweier Varianten, welche auf Grund einer erhöhten thermodynamischen Stabilität bzw. Dimerisisierungsaffinität im TetR-Kontext lichtgesteuerte Genexpression bei 37°C zulassen. Ebenso zeigen Studien in Säugerzellen, dass der Einsatz einer der hier ermittelten *Rs*LOV Variante D109G zu

einer lichtsensitiven Rezeptortyrosionkinase führt, wohingegen die Verwendung des wildtypischen Rezeptors keine Lichtregulation zulässt.

2.4 Blaulichtgesteuerte Assemblierung von Goldnanopartikeln

Die fünfte wissenschaftliche Arbeit (Kapitel 5.5) konzentriert sich auf die Anwendung assoziierenden LOV Rezeptoren abseits optogenetischer Systeme. Die Vorteile der Kontrolle durch sensorische Photorezeptoren vermögen auch in dem Bereich der Reaktionskontrolle in der Kolloidchemie von Relevanz zu sein. Ziel dieser Arbeit war es daher mit Hilfe homodimerisierender LOV Domänen die Assemblierung von Goldnanopartikeln (AuNP) als Modelpartikel in blaulichtabhängiger Art und Weise zu kontrollieren und somit eine neue Möglichkeit zur Reaktionskontrolle zu etablieren.

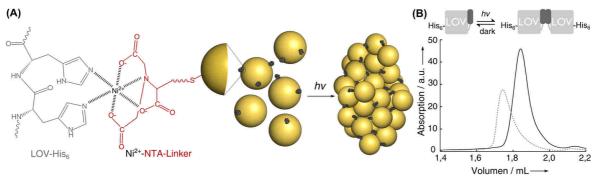


Abbildung 26: Strategie zur lichtinduzierten Assemblierung von Goldnanopartikeln. (A) Hexahistidin (His6)-markierte, assoziierende LOV Domänen werden auf der Oberfläche von Goldnanopartikeln mittels Nickel-koordinationschemie immobilisiert. Blaulicht löst die Dimerisierung der LOV Domäne aus, was folglich zur Assemblierung der Partikel führt. (B) Größenauschlusschromatographie von VIVID-His6 in Ab- (schwarz) und Anwesenheit von Blaulicht (grau gestrichelt).

Grundlage ist die Immobilisierung von assoziierenden LOV Domänen an der Oberfläche von Goldnanopartikeln mit Hilfe von Nickelkoordinationschemie. Hierfür wurden in einem Kooperationsprojekt AuNP synthetisiert und anschließend mit Nitrilotriessigsäure-(NTA) Liganden funktionalisiert. Diese ermöglichen zusammen mit Ni²⁺ als Chelator die Koordination Hexahistidin (His₆)-markierter LOV Domänen (Abbildung 26A). Innerhalb dieser Arbeit konnte gezeigt werden, dass ausschließlich eine C-terminale Markierung von VIVID (VIVID-His₆) zur Aufrechterhaltung der lichtgesteuerten Dimerisierung führt (Abbildung 26B).

Zunächst wurde die gewünschte Assoziation von VIVID-His6 an Ni²⁺-funktionalisierte AuNP mittels asymmetrischer Fluss-Feld-Fluss-Fraktionierung untersucht. Eine beobachtete Erhöhung des apparenten hydrodynamischen Radius von $(11,7 \pm 1,5)$ nm auf $(17,8 \pm 1,2)$ nm ließ auf eine Immobilisierung der LOV Proteine an der Oberfläche der funktionalisierten AuNP schließen. Die Beleuchtung der Mischung führte zur Ausbildung großer Cluster, welche sich bereits qualitativ durch die Änderung der Farbe von Rot nach Violett infolge der veränderten Oberflächenplasmonenresonanz (surface plasmon resonance, SPR) der Goldnanopartikel

zeigte. Um die lichtgetriebene Assemblierungsreaktion der Photorezeptor-Nanopartikel-Konjugate genauer zu charakterisieren, wurden zeitaufgelöste Absorptionsspektren in Abwesenheit und unter Blaulichtbeleuchtung aufgenommen (Abbildung 27A).

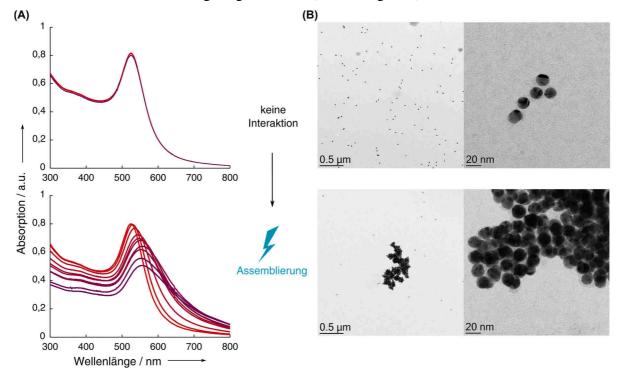


Abbildung 27: Blaulichtgetriebene Assemblierung von Goldnanopartikeln. (A) Zeitserie von UV/VIS -Spektren über 90 min von Ni²+-funktionalisierten AuNP in Anwesenheit von VIVID-His6 in Dunkelheit (oben) und während Blaulichtbestrahlung (unten). Blaulichtexposition führt zur Verschiebung und Verbreiterung der Oberflächenplasmonbande, was indikativ für die Assemblierung der Nanopartikel ist. (B) Transmissionselektronenmikroskopische Aufnahmen mit VIVID-His6 konjugierten Ni²+-NTA-AuNP in Dunkelheit (oben) und nach Blaulichtbestrahlung (unten). In Abwesenheit von Blaulicht kommt es zur gleichmäßigen Verteilung und keiner direkten Interaktion, während Blaulicht zur Assoziation und Interaktion der Partikel führt.

Die Lokalisation der SPR-Bande der AuNP gibt dabei Aufschluss über die Größe der Nanopartikelcluster (He et al. 2016). Ni²⁺-NTA funktionalisierte AuNP weisen lichtunabhängig eine definierte SPR-Bande bei rund 524 nm auf. Innerhalb dieser Arbeit konnte gezeigt werden, dass die Gegenwart von VIVID-His₆ zu keiner signifikanten Änderung der spektralen Eigenschaften führte, sofern die Proben im Dunkeln gehalten wurden. Ausschließlich bei Blaulichtbestrahlung der proteinhaltigen Proben konnte eine deutliche Rotverschiebung und Verbreiterung der SPR-Bande beobachtet werden (Abbildung 27A). Diese Veränderungen spiegeln die Ausbildung von heterogenen, ausgedehnten Nanopartikelansammlungen wider (Kundu et al. 2015, Zhang et al. 2015, Neupane et al. 2017, Chen et al. 2018). In Gegenwart von Imidazol, welches mit Histidin um die Bindung an den Ni²⁺-NTA-Linker konkurriert, konnte in keinem Fall eine Rotverschiebung beobachtet werden. Diese Ergebnisse bestärken die These, dass die blaulichtinduzierte Dimerisierung der immobilisierten LOV Proteine ausschlaggebend für die Assemblierung der Nanopartikel ist. Es konnte zudem gezeigt werden, dass eine Erhöhung bzw. Verringerung der

Menge an lichtschaltbaren Proteinen auf der Oberfläche die Beschleunigung bzw. Verlangsamung der Assemblierung bedingt und einen zusätzlichen Ansatzpunkt zur Reaktionskontrolle liefert.

Zur Bestätigung der Ergebnisse wurden die in Dunkelheit oder unter Blaulicht inkubierten Proben mittels Transmissionselektronenmikroskopie (TEM) untersucht (Abbildung 27B). Die Aufnahmen zeigen, dass die AuNP auf dem TEM-Gitter in Abwesenheit von Blaulicht monodispers und gleichmäßig verteilt vorliegen. Demgegenüber führt Blaulichtbestrahlung zur Ausbildung von stabilen, ausgedehnten Netzwerken, die eine Größe von bis zu 1,5 µm einnehmen können. Die blaulichtinduzierte Ausbildung der Cluster konnte, sobald diese in unmittelbare Nähe gebracht werden, auf Grund der starken Wechselwirkung der Nanopartikel untereinander nicht wieder ausgelöst werden (Pamies et al. 2014).

Zusammenfassend unterstreicht diese Arbeit das breite Anwendungspotential von LOV Rezeptoren auch außerhalb der Optogenetik. Die hier gezeigte Kombination von anorganischen und proteinartigen Bausteinen demonstriert ein neues Verfahren zur präzisen und nicht-invasiven Reaktionskontrolle und eröffnet die Verwendung in den Bereichen der Bio- und Materialwissenschaft.

2.5 Fazit

Die molekulare Wirkweise von LOV Rezeptoren und deren Empfindlichkeit gegenüber Parametern wie Licht und Temperatur sind vielschichtig und trotz intensiver Studien noch immer nicht vollständig aufgeklärt.

Die hier erbrachten Erkenntnisse zu einer gezielten und sequenziellen Kontrolle mittels gepulster Beleuchtung sowie die Charakterisierung der Signalweiterleitung und Sensitivität von LOV Rezeptoren erweitern das Verständnis und sind in vielen Bereichen von großem Interesse. Die Untersuchung der intrinsischen Kinetik, mit welcher ein Photorezeptor nach Anregung wieder in seinen dunkeladaptierten Zustand zurückkehrt, vermag in zahlreichen, auch bereits existierenden optogenetischen Systemen zur Verwendung gepulster, energieärmerer Beleuchtungsschemata führen. Genauere Einblicke in den Mechanismus der Signaltransduktion und die innerhalb dieser Arbeit näher untersuchten biochemischen sowieso biophysikalischen Eigenschaften helfen die Funktionsweise von LOV Rezeptoren besser zu verstehen, um diese optimieren und für (optogenetische) Zwecke einsetzten zu können. Die hier gezeigte Entwicklung weiterer blaulichtsensitiver Schalter erweitert zum einen das Spektrum an optogenetischen Werkzeugen und ebnet zum anderen den Weg für den Einsatz von lichtsensitiven biologischen Bausteinen in chemischen Bereichen.

3 Literaturverzeichnis

- Alexandre MT, van Grondelle R, Hellingwerf KJ, Kennis JT. 2009. Conformational heterogeneity and propagation of structural changes in the LOV2/Jalpha domain from Avena sativa phototropin 1 as recorded by temperature-dependent FTIR spectroscopy. Biophys J, 97(1):238–47.
- Alexandre MTA, Arents JC, van Grondelle R, Hellingwerf KJ, Kennis JTM. 2007. A Base-Catalyzed Mechanism for Dark State Recovery in the Avena sativa Phototropin-1 LOV2 Domain. Biochemistry, 46(11):3129–3137.
- Anantharaman V, Balaji S, Aravind L. 2006. The signaling helix: a common functional theme in diverse signaling proteins. Biology Direct, 1:25.
- Aravind L, Koonin EV. 2000. The STAS domain a link between anion transporters and antisigma-factor antagonists. Curr Biol, 10(2):R53-5.
- Arnon DI. 1959. Conversion of Light into Chemical Energy in Photosynthesis. Nature, 184(4679):10–21.
- Avila-Perez M, Hellingwerf KJ, Kort R. 2006. Blue light activates the sigmaB-dependent stress response of Bacillus subtilis via YtvA. J Bacteriol, 188(17):6411–4.
- Banerjee A, Herman E, Kottke T, Essen L-O. 2016. Structure of a Native-like Aureochrome 1a LOV Domain Dimer from Phaeodactylum tricornutum. Structure, 24(1):171–178.
- Bauer C, Rabl C-R, Heberle J, Kottke T. 2011. Indication for a radical intermediate preceding the signaling state in the LOV domain photocycle. Photochemistry and Photobiology, 87(3):548–553.
- Baumschlager A, Aoki SK, Khammash M. 2017. Dynamic Blue Light-Inducible T7 RNA Polymerases (Opto-T7RNAPs) for Precise Spatiotemporal Gene Expression Control. ACS Synthetic Biology, 6(11):2157–2167.
- Belli G. 1998. An activator/repressor dual system allows tight tetracycline-regulated gene expression in budding yeast [published erratum appears in Nucleic Acids Res 1998 Apr 1;26(7):following 1855]. Nucleic Acids Research, 26(4):942–947.
- Benedetti L, Barentine AES, Messa M, Wheeler H, Bewersdorf J, De Camilli P. 2018. Light-activated protein interaction with high spatial subcellular confinement. Proceedings of the National Academy of Sciences, 115(10):E2238–E2245.
- Berntsson O, Diensthuber RP, Panman MR, Björling A, Gustavsson E, Hoernke M, Hughes AJ, Henry L, Niebling S, Takala H, et al. 2017a. Sequential conformational transitions and α-helical supercoiling regulate a sensor histidine kinase. Nature Communications, 8(1):284.
- Berntsson O, Diensthuber RP, Panman MR, Björling A, Hughes AJ, Henry L, Niebling S, Newby G, Liebi M, Menzel A, et al. 2017b. Time-Resolved X-Ray Solution Scattering Reveals the Structural Photoactivation of a Light-Oxygen-Voltage Photoreceptor. Structure (London, England: 1993), 25(6):933-938.e3.
- Blankenship RE. 2010. Early Evolution of Photosynthesis. Plant Physiology, 154(2):434–438.
- Bonger KM, Rakhit R, Payumo AY, Chen JK, Wandless TJ. 2014. General method for regulating protein stability with light. ACS chemical biology, 9(1):111–115.

- Boyden ES, Zhang F, Bamberg E, Nagel G, Deisseroth K. 2005. Millisecond-timescale, genetically targeted optical control of neural activity. Nature Neuroscience, 8(9):1263–1268.
- Brown BA, Cloix C, Jiang GH, Kaiserli E, Herzyk P, Kliebenstein DJ, Jenkins GI. 2005. A UV-B-specific signaling component orchestrates plant UV protection. Proceedings of the National Academy of Sciences of the United States of America, 102(50):18225–18230.
- Cao Z, Livoti E, Losi A, Gärtner W. 2010. A blue light-inducible phosphodiesterase activity in the cyanobacterium Synechococcus elongatus. Photochemistry and Photobiology, 86(3):606–611.
- Chang X-P, Gao Y-J, Fang W-H, Cui G, Thiel W. 2017. Quantum Mechanics/Molecular Mechanics Study on the Photoreactions of Dark- and Light-Adapted States of a Blue-Light YtvA LOV Photoreceptor. Angewandte Chemie International Edition, 56(32):9341–9345.
- Chapman S, Faulkner C, Kaiserli E, Garcia-Mata C, Savenkov EI, Roberts AG, Oparka KJ, Christie JM. 2008. The photoreversible fluorescent protein iLOV outperforms GFP as a reporter of plant virus infection. Proceedings of the National Academy of Sciences of the United States of America, 105(50):20038–20043.
- Chaves I, Pokorny R, Byrdin M, Hoang N, Ritz T, Brettel K, Essen L-O, van der Horst GTJ, Batschauer A, Ahmad M. 2011. The cryptochromes: blue light photoreceptors in plants and animals. Annual Review of Plant Biology, 62:335–364.
- Chen C-H, DeMay BS, Gladfelter AS, Dunlap JC, Loros JJ. 2010. Physical interaction between VIVID and white collar complex regulates photoadaptation in Neurospora. Proceedings of the National Academy of Sciences of the United States of America, 107(38):16715–16720.
- Chen D, Gibson ES, Kennedy MJ. 2013. A light-triggered protein secretion system. The Journal of Cell Biology, 201(4):631–640.
- Chen X, Liu R, Ma Z, Xu X, Zhang H, Xu J, Ouyang Q, Yang Y. 2016. An extraordinary stringent and sensitive light-switchable gene expression system for bacterial cells. Cell Research, 26(7):854–857.
- Chen Y, Wang Z, He Y, Yoon YJ, Jung J, Zhang G, Lin Z. 2018. Light-enabled reversible self-assembly and tunable optical properties of stable hairy nanoparticles. Proceedings of the National Academy of Sciences, 115(7):E1391–E1400.
- Christie JM. 2007. Phototropin Blue-Light Receptors. Annual Review of Plant Biology, 58(1):21–45.
- Christie JM, Reymond P, Powell GK, Bernasconi P, Raibekas AA, Liscum E, Briggs WR. 1998. Arabidopsis NPH1: a flavoprotein with the properties of a photoreceptor for phototropism. Science, 282(5394):1698–1701.
- Christie JM, Swartz TE, Bogomolni RA, Briggs WR. 2002. Phototropin LOV domains exhibit distinct roles in regulating photoreceptor function. Plant J, 32(2):205–19.
- Christie JM, Arvai AS, Baxter KJ, Heilmann M, Pratt AJ, O'Hara A, Kelly SM, Hothorn M, Smith BO, Hitomi K, et al. 2012a. Plant UVR8 photoreceptor senses UV-B by tryptophan-mediated disruption of cross-dimer salt bridges. Science (New York, N.Y.), 335(6075):1492–1496.

- Christie JM, Gawthorne J, Young G, Fraser NJ, Roe AJ. 2012b. LOV to BLUF: Flavoprotein Contributions to the Optogenetic Toolkit. Molecular Plant, 5(3):533–544.
- Conrad KS, Bilwes AM, Crane BR. 2013. Light-induced subunit dissociation by a light-oxygen-voltage domain photoreceptor from Rhodobacter sphaeroides. Biochemistry, 52(2):378–391.
- Conrad KS, Manahan CC, Crane BR. 2014. Photochemistry of flavoprotein light sensors. Nature Chemical Biology, 10(10):801–809.
- Crosson S, Rajagopal S, Moffat K. 2003. The LOV domain family: photoresponsive signaling modules coupled to diverse output domains. Biochemistry, 42(1):2–10.
- Dagliyan O, Tarnawski M, Chu P-H, Shirvanyants D, Schlichting I, Dokholyan NV, Hahn KM. 2016. Engineering extrinsic disorder to control protein activity in living cells. Science, 354(6318):1441–1444.
- Deisseroth K. 2011. Optogenetics. Nat Methods, 8(1):26–29.
- Diensthuber RP, Bommer M, Gleichmann T, Möglich A. 2013. Full-length structure of a sensor histidine kinase pinpoints coaxial coiled coils as signal transducers and modulators. Structure, 21(7):1127–1136.
- Diensthuber RP, Engelhard C, Lemke N, Gleichmann T, Ohlendorf R, Bittl R, Möglich A. 2014. Biophysical, mutational, and functional investigation of the chromophore-binding pocket of light-oxygen-voltage photoreceptors. ACS synthetic biology, 3(11):811–819.
- Dikiy I, Edupuganti UR, Abzalimov RR, Borbat PP, Srivastava M, Freed JH, Gardner KH. 2019. Insights into histidine kinase activation mechanisms from the monomeric blue light sensor EL346. Proceedings of the National Academy of Sciences, 116(11):4963–4972.
- Drepper T, Eggert T, Circolone F, Heck A, Krauss U, Guterl J-K, Wendorff M, Losi A, Gärtner W, Jaeger K-E. 2007. Reporter proteins for in vivo fluorescence without oxygen. Nature Biotechnology, 25(4):443–445.
- Druhan LJ, Swenson RP. 1998. Role of Methionine 56 in the Control of the Oxidation–Reduction Potentials of the Clostridium beijerinckii Flavodoxin: Effects of Substitutions by Aliphatic Amino Acids and Evidence for a Role of Sulfur–Flavin Interactions †. Biochemistry, 37(27):9668–9678.
- Endres S, Granzin J, Circolone F, Stadler A, Krauss U, Drepper T, Svensson V, Knieps-Grünhagen E, Wirtz A, Cousin A, et al. 2015. Structure and function of a short LOV protein from the marine phototrophic bacterium Dinoroseobacter shibae. BMC Microbiology, 15(1):30.
- Engelhard C, Diensthuber RP, Möglich A, Bittl R. 2017. Blue-light reception through quaternary transitions. Scientific Reports, 7(1):1385.
- Ernst OP, Lodowski DT, Elstner M, Hegemann P, Brown LS, Kandori H. 2014. Microbial and Animal Rhodopsins: Structures, Functions, and Molecular Mechanisms. Chemical Reviews, 114(1):126–163.
- Farzadfard F, Lu TK. 2014. Synthetic biology. Genomically encoded analog memory with precise in vivo DNA writing in living cell populations. Science (New York, N.Y.), 346(6211):1256272.

- Franklin KA, Whitelam GC. 2005. Phytochromes and Shade-avoidance Responses in Plants. Annals of Botany, 96(2):169–175.
- French C, Ward JM. 1996. Production and modification of E. coli transketolase for large-scale biocatalysis. Annals of the New York Academy of Sciences, 799:11–18.
- Furuya A, Kawano F, Nakajima T, Ueda Y, Sato M. 2017. Assembly Domain-Based Optogenetic System for the Efficient Control of Cellular Signaling. ACS Synthetic Biology, 6(6):1086–1095.
- Gaidenko TA, Kim TJ, Weigel AL, Brody MS, Price CW. 2006. The blue-light receptor YtvA acts in the environmental stress signaling pathway of Bacillus subtilis. J Bacteriol, 188(17):6387–95.
- Ganguly A, Thiel W, Crane BR. 2017. Glutamine Amide Flip Elicits Long Distance Allosteric Responses in the LOV Protein Vivid. Journal of the American Chemical Society, 139(8):2972–2980.
- Gao R, Stock AM. 2017. Quantitative Kinetic Analyses of Shutting Off a Two-Component System. mBio, 8(3):e00412-17, /mbio/8/3/e00412-17.atom.
- Gatz C, Quail PH. 1988. Tn10-encoded tet repressor can regulate an operator-containing plant promoter. Proceedings of the National Academy of Sciences, 85(5):1394–1397.
- Gehring WJ. 2005. New Perspectives on Eye Development and the Evolution of Eyes and Photoreceptors. Journal of Heredity, 96(3):171–184.
- Geissendörfer M, Hillen W. 1990. Regulated expression of heterologous genes inBacillus subtilis using the Tn10 encodedtet regulatory elements. Applied Microbiology and Biotechnology, 33(6):657–663.
- Glantz ST, Carpenter EJ, Melkonian M, Gardner KH, Boyden ES, Wong GK-S, Chow BY. 2016. Functional and topological diversity of LOV domain photoreceptors. Proceedings of the National Academy of Sciences of the United States of America, 113(11):E1442-1451.
- Gomelsky M. 2011. cAMP, c-di-GMP, c-di-AMP and now cGMP: bacteria use them all! Molecular microbiology, 79(3):562–565.
- Gomelsky M, Klug G. 2002. BLUF: a novel FAD-binding domain involved in sensory transduction in microorganisms. Trends Biochem Sci, 27(10):497–500.
- Gossen M, Freundlieb S, Bender G, Muller G, Hillen W, Bujard H. 1995. Transcriptional activation by tetracyclines in mammalian cells. Science, 268(5218):1766–1769.
- Gottesfeld JM, Turner JM, Dervan PB. 2001. Chemical Approaches to Control Gene Expression. Gene Expression, 9(1):77–92.
- Grusch M, Schelch K, Riedler R, Reichhart E, Differ C, Berger W, Inglés-Prieto Á, Janovjak H. 2014. Spatio-temporally precise activation of engineered receptor tyrosine kinases by light. The EMBO journal, 33(15):1713–1726.
- Guntas G, Hallett RA, Zimmerman SP, Williams T, Yumerefendi H, Bear JE, Kuhlman B. 2015. Engineering an improved light-induced dimer (iLID) for controlling the localization and activity of signaling proteins. Proceedings of the National Academy of Sciences of the United States of America, 112(1):112–117.

- Halavaty AS, Moffat K. 2007. N- and C-terminal flanking regions modulate light-induced signal transduction in the LOV2 domain of the blue light sensor phototropin 1 from Avena sativa. Biochemistry, 46(49):14001–14009.
- Halavaty AS, Moffat K. 2013. Coiled-coil dimerization of the LOV2 domain of the blue-light photoreceptor phototropin 1 from Arabidopsis thaliana. Acta Crystallographica Section F: Structural Biology and Crystallization Communications, 69(Pt 12):1316–1321.
- Han T, Chen Q, Liu H. 2017. Engineered Photoactivatable Genetic Switches Based on the Bacterium Phage T7 RNA Polymerase. ACS Synthetic Biology, 6(2):357–366.
- Hao W, Fong HKW. 1999. The Endogenous Chromophore of Retinal G Protein-coupled Receptor Opsin from the Pigment Epithelium. Journal of Biological Chemistry, 274(10):6085–6090.
- Harada A, Sakai T, Okada K. 2003. phot1 and phot2 mediate blue light-induced transient increases in cytosolic Ca 2+ differently in Arabidopsis leaves. Proceedings of the National Academy of Sciences, 100(14):8583–8588.
- Harper SM, Christie JM, Gardner KH. 2004. Disruption of the LOV-Jalpha helix interaction activates phototropin kinase activity. Biochemistry, 43(51):16184–16192.
- He H, Feng M, Chen Q, Zhang X, Zhan H. 2016. Light-Induced Reversible Self-Assembly of Gold Nanoparticles Surface-Immobilized with Coumarin Ligands. Angewandte Chemie International Edition, 55(3):936–940.
- Heintz U, Schlichting I. 2016. Blue light-induced LOV domain dimerization enhances the affinity of Aureochrome 1a for its target DNA sequence. eLife, 5:e11860.
- Hellingwerf KJ, Hendriks J, Gensch T. 2003. Photoactive Yellow Protein, A New Type of Photoreceptor Protein: Will This "Yellow Lab" Bring Us Where We Want to Go? I. The Journal of Physical Chemistry A, 107(8):1082–1094.
- Hengge R. 2009. Principles of c-di-GMP signalling in bacteria. Nature Reviews Microbiology, 7(4):263–273.
- Henry L, Berntsson O, Panman M, Cellini A, Hughes AJ, Kosheleva I, Henning RW, Westenhoff S. 2020. New light on the mechanism of phototransduction in phototropin. Biochemistry, acs.biochem.0c00324.
- Herrou J, Crosson S. 2011. Function, structure and mechanism of bacterial photosensory LOV proteins. Nature reviews. Microbiology, 9(10):713–723.
- van der Horst MA, Hellingwerf KJ. 2004. Photoreceptor proteins, "star actors of modern times": a review of the functional dynamics in the structure of representative members of six different photoreceptor families. Acc Chem Res, 37(1):13–20.
- Hunt SM, Thompson S, Elvin M, Heintzen C. 2010. VIVID interacts with the WHITE COLLAR complex and FREQUENCY-interacting RNA helicase to alter light and clock responses in Neurospora. Proceedings of the National Academy of Sciences of the United States of America, 107(38):16709–16714.
- Iuliano JN, Collado JT, Gil AA, Ravindran PT, Lukacs A, Shin S, Woroniecka HA, Adamczyk K, Aramini JM, Edupuganti UR, et al. 2020. Unraveling the Mechanism of a LOV Domain

- Optogenetic Sensor: A Glutamine Lever Induces Unfolding of the J α Helix. ACS Chemical Biology, 15(10):2752–2765.
- Jayaraman P, Devarajan K, Chua TK, Zhang H, Gunawan E, Poh CL. 2016. Blue light-mediated transcriptional activation and repression of gene expression in bacteria. Nucleic Acids Research, 44(14):6994–7005.
- Jin X, Riedel-Kruse IH. 2018. Biofilm Lithography enables high-resolution cell patterning via optogenetic adhesin expression. Proceedings of the National Academy of Sciences of the United States of America, 115(14):3698–3703.
- Jones MA, Feeney KA, Kelly SM, Christie JM. 2007. Mutational Analysis of Phototropin 1 Provides Insights into the Mechanism Underlying LOV2 Signal Transmission. J Biol Chem, 282(9):6405–14.
- Jurk M, Dorn M, Kikhney A, Svergun D, Gärtner W, Schmieder P. 2010. The switch that does not flip: the blue-light receptor YtvA from Bacillus subtilis adopts an elongated dimer conformation independent of the activation state as revealed by a combined AUC and SAXS study. Journal of Molecular Biology, 403(1):78–87.
- Karniol B, Vierstra RD. 2003. The pair of bacteriophytochromes from Agrobacterium tumefaciens are histidine kinases with opposing photobiological properties. Proceedings of the National Academy of Sciences, 100(5):2807–2812.
- Kawano F, Aono Y, Suzuki H, Sato M. 2013. Fluorescence Imaging-Based High-Throughput Screening of Fast- and Slow-Cycling LOV Proteins. PLoS ONE, 8(12):e82693.
- Kawano F, Suzuki H, Furuya A, Sato M. 2015. Engineered pairs of distinct photoswitches for optogenetic control of cellular proteins. Nature Communications, 6:6256.
- Kawano F, Okazaki R, Yazawa M, Sato M. 2016. A photoactivatable Cre-loxP recombination system for optogenetic genome engineering. Nature Chemical Biology.
- Kennis JT, van Stokkum IH, Crosson S, Gauden M, Moffat K, van Grondelle R. 2004. The LOV2 domain of phototropin: a reversible photochromic switch. J Am Chem Soc, 126(14):4512–3.
- Kim J-Y, Ryu DDY. 1991. The effects of plasmid content, transcription efficiency, and translation efficiency on the productivity of a cloned gene protein in Escherichia coli. Biotechnology and Bioengineering, 38(11):1271–1279.
- Kobayashi I, Nakajima H, Hisatomi O. 2020. Molecular Mechanism of Light-Induced Conformational Switching of the LOV Domain in Aureochrome-1. Biochemistry, 59(28):2592–2601.
- Kolar K, Knobloch C, Stork H, Žnidarič M, Weber W. 2018. OptoBase: A Web Platform for Molecular Optogenetics. ACS Synthetic Biology, 7(7):1825–1828.
- Kong S-G, Okajima K. 2016. Diverse photoreceptors and light responses in plants. Journal of Plant Research, 129(2):111–114.
- Kottke T, Heberle J, Hehn D, Dick B, Hegemann P. 2003. Phot-LOV1: photocycle of a blue-light receptor domain from the green alga Chlamydomonas reinhardtii. Biophys J, 84(2 Pt 1):1192–1201.

- Kottke T, Xie A, Larsen DS, Hoff WD. 2018. Photoreceptors Take Charge: Emerging Principles for Light Sensing. Annual Review of Biophysics.
- Kreslavski VD, Los DA, Schmitt F-J, Zharmukhamedov SK, Kuznetsov VV, Allakhverdiev SI. 2018. The impact of the phytochromes on photosynthetic processes. Biochimica et Biophysica Acta (BBA) Bioenergetics, 1859(5):400–408.
- Kundu PK, Samanta D, Leizrowice R, Margulis B, Zhao H, Börner M, Udayabhaskararao T, Manna D, Klajn R. 2015. Light-controlled self-assembly of non-photoresponsive nanoparticles. Nature Chemistry, 7(8):646–652.
- Kutta RJ, Magerl K, Kensy U, Dick B. 2015. A search for radical intermediates in the photocycle of LOV domains. Photochemical & Photobiological Sciences, 14(2):288–299.
- Lalwani MA, Ip SS, Carrasco-Lopez C, Zhao EM, Kawabe H, Avalos JL. 2019. Optogenetic lac operon to control chemical and protein production in Escherichia coli with light. preprint. Synthetic Biology.
- Lalwani MA, Ip SS, Carrasco-López C, Day C, Zhao EM, Kawabe H, Avalos JL. 2020. Optogenetic control of the lac operon for bacterial chemical and protein production. Nature Chemical Biology.
- Lee J, Natarajan M, Nashine VC, Socolich M, Vo T, Russ WP, Benkovic SJ, Ranganathan R. 2008. Surface sites for engineering allosteric control in proteins. Science (New York, N.Y.), 322(5900):438–442.
- Li X, Zhang C, Xu X, Miao J, Yao J, Liu R, Zhao Y, Chen X, Yang Y. 2020. A single-component light sensor system allows highly tunable and direct activation of gene expression in bacterial cells. Nucleic Acids Research, 48(6):e33–e33.
- Losi A, Gärtner W. 2012. The evolution of flavin-binding photoreceptors: an ancient chromophore serving trendy blue-light sensors. Annual Review of Plant Biology, 63:49–72.
- Losi A, Gärtner W. 2017. Solving Blue Light Riddles: New Lessons from Flavin-binding LOV Photoreceptors. Photochemistry and Photobiology, 93(1):141–158.
- Losi A, Gardner KH, Möglich A. 2018. Blue-Light Receptors for Optogenetics. Chemical Reviews, 118(21):10659–10709.
- Lungu OI, Hallett RA, Choi EJ, Aiken MJ, Hahn KM, Kuhlman B. 2012. Designing photoswitchable peptides using the AsLOV2 domain. Chemistry & biology, 19(4):507–517.
- Lutz R. 1997. Independent and tight regulation of transcriptional units in Escherichia coli via the LacR/O, the TetR/O and AraC/I1-I2 regulatory elements. Nucleic Acids Research, 25(6):1203–1210.
- Magaraci MS, Veerakumar A, Qiao P, Amurthur A, Lee JY, Miller JS, Goulian M, Sarkar CA. 2014. Engineering Escherichia coli for Light-Activated Cytolysis of Mammalian Cells. ACS synthetic biology.
- Malzahn E, Ciprianidis S, Káldi K, Schafmeier T, Brunner M. 2010. Photoadaptation in Neurospora by competitive interaction of activating and inhibitory LOV domains. Cell, 142(5):762–772.

- Mathes T. 2016. Natural Resources for Optogenetic Tools. Methods in Molecular Biology (Clifton, N.J.), 1408:19–36.
- Mathony J, Niopek D. 2020. Enlightening Allostery: Designing Switchable Proteins by Photoreceptor Fusion. Advanced Biosystems, 2000181.
- Miller JH. 1972. Experiments in Molecular Genetics. Cold Spring Harbor Laboratory, Cold Spring Harbor, NY.
- Mills E, Chen X, Pham E, Wong S, Truong K. 2012. Engineering a photoactivated caspase-7 for rapid induction of apoptosis. ACS synthetic biology, 1(3):75–82.
- Möglich A. 2019. Signal transduction in photoreceptor histidine kinases. Protein Science, 28(11):1923–1946.
- Möglich A, Moffat K. 2007. Structural Basis for Light-dependent Signaling in the Dimeric LOV Domain of the Photosensor YtvA. J Mol Biol, 373(1):112–126.
- Möglich A, Moffat K. 2010. Engineered photoreceptors as novel optogenetic tools. Photochemical & Photobiological Sciences: Official Journal of the European Photochemistry Association and the European Society for Photobiology, 9(10):1286–1300.
- Möglich A, Ayers RA, Moffat K. 2009a. Structure and signaling mechanism of Per-ARNT-Sim domains. Structure, 17(10):1282–1294.
- Möglich A, Ayers RA, Moffat K. 2009b. Design and signaling mechanism of light-regulated histidine kinases. Journal of Molecular Biology, 385(5):1433–1444.
- Möglich A, Ayers RA, Moffat K. 2010a. Addition at the molecular level: signal integration in designed Per-ARNT-Sim receptor proteins. Journal of Molecular Biology, 400(3):477–486.
- Möglich A, Yang X, Ayers RA, Moffat K. 2010b. Structure and function of plant photoreceptors. Annual Review of Plant Biology, 61:21–47.
- Motta-Mena LB, Reade A, Mallory MJ, Glantz S, Weiner OD, Lynch KW, Gardner KH. 2014. An optogenetic gene expression system with rapid activation and deactivation kinetics. Nature Chemical Biology, 10(3):196–202.
- Nack J, Möglich A. 2017. Biochemie 2016: Optische Kontrolle zellulärer Prozesse. Nachrichten aus der Chemie, 65(3):309–313.
- Nagata T, Koyanagi M, Lucas R, Terakita A. 2018. An all-trans-retinal-binding opsin peropsin as a potential dark-active and light-inactivated G protein-coupled receptor. Scientific Reports, 8(1):3535.
- Nagel G. 2002. Channelrhodopsin-1: A Light-Gated Proton Channel in Green Algae. Science, 296(5577):2395–2398.
- Nakatani Y, Hisatomi O. 2015. Molecular Mechanism of Photozipper, a Light-Regulated Dimerizing Module Consisting of the bZIP and LOV Domains of Aureochrome-1. Biochemistry, 54(21):3302–3313.
- Nash AI, Ko W-H, Harper SM, Gardner KH. 2008. A conserved glutamine plays a central role in LOV domain signal transmission and its duration. Biochemistry, 47(52):13842–13849.

- Nash AI, McNulty R, Shillito ME, Swartz TE, Bogomolni RA, Luecke H, Gardner KH. 2011. Structural basis of photosensitivity in a bacterial light-oxygen-voltage/helix-turn-helix (LOV-HTH) DNA-binding protein. Proceedings of the National Academy of Sciences of the United States of America, 108(23):9449–9454.
- Navarro MVAS, De N, Bae N, Wang Q, Sondermann H. 2009. Structural Analysis of the GGDEF-EAL Domain-Containing c-di-GMP Receptor FimX. Structure, 17(8):1104–1116.
- Neupane S, Pan Y, Takalkar S, Bentz K, Farmakes J, Xu Y, Chen B, Liu G, Qian SY, Yang Z. 2017. Probing the Aggregation Mechanism of Gold Nanoparticles Triggered by a Globular Protein. The Journal of Physical Chemistry C, 121(2):1377–1386.
- Nihongaki Y, Kawano F, Nakajima T, Sato M. 2015. Photoactivatable CRISPR-Cas9 for optogenetic genome editing. Nature Biotechnology, 33(7):755–760.
- Nozaki D, Iwata T, Ishikawa T, Todo T, Tokutomi S, Kandori H. 2004. Role of Gln1029 in the photoactivation processes of the LOV2 domain in adiantum phytochrome3. Biochemistry, 43(26):8373–8379.
- Ohlendorf R, Vidavski RR, Eldar A, Moffat K, Möglich A. 2012. From dusk till dawn: one-plasmid systems for light-regulated gene expression. Journal of molecular biology, 416(4):534–542.
- Ohlendorf R, Schumacher CH, Richter F, Möglich A. 2016. Library-Aided Probing of Linker Determinants in Hybrid Photoreceptors. ACS synthetic biology, 5(10):1117–1126.
- Okajima K, Aihara Y, Takayama Y, Nakajima M, Kashojiya S, Hikima T, Oroguchi T, Kobayashi A, Sekiguchi Y, Yamamoto M, et al. 2014. Light-induced Conformational Changes of LOV1 (Light Oxygen Voltage-sensing Domain 1) and LOV2 Relative to the Kinase Domain and Regulation of Kinase Activity in Chlamydomonas Phototropin. Journal of Biological Chemistry, 289(1):413–422.
- Orth P, Cordes F, Schnappinger D, Hillen W, Saenger W, Hinrichs W. 1998. Conformational changes of the Tet repressor induced by tetracycline trapping. Journal of Molecular Biology, 279(2):439–447.
- Pamies R, Cifre JGH, Espín VF, Collado-González M, Baños FGD, de la Torre JG. 2014. Aggregation behaviour of gold nanoparticles in saline aqueous media. Journal of Nanoparticle Research, 16(4):2376.
- Pathak GP, Losi A, Gärtner W. 2012. Metagenome-based Screening Reveals Worldwide Distribution of LOV-Domain Proteins: Photochemistry and Photobiology. Photochemistry and Photobiology, 88(1):107–118.
- Pham E, Mills E, Truong K. 2011. A synthetic photoactivated protein to generate local or global Ca(2+) signals. Chemistry & Biology, 18(7):880–890.
- Polstein LR, Gersbach CA. 2012. Light-Inducible Spatiotemporal Control of Gene Activation by Customizable Zinc Finger Transcription Factors. Journal of the American Chemical Society, 134(40):16480–16483.
- Polverini E, Schackert FK, Losi A. 2020. Interplay among the "flipping" glutamine, a conserved phenylalanine, water and hydrogen bonds within a blue-light sensing LOV domain. Photochemical & Photobiological Sciences, 19(7):892–904.

- Porter ML. 2016. Beyond the Eye: Molecular Evolution of Extraocular Photoreception. Integrative and Comparative Biology, 56(5):842–852.
- Pu L, Yang S, Xia A, Jin F. 2018. Optogenetics Manipulation Enables Prevention of Biofilm Formation of Engineered Pseudomonas aeruginosa on Surfaces. ACS Synthetic Biology, 7(1):200–208.
- Pudasaini A, El-Arab KK, Zoltowski BD. 2015. LOV-based optogenetic devices: light-driven modules to impart photoregulated control of cellular signaling. Frontiers in Molecular Biosciences, 2:18.
- Purcell EB, Siegal-Gaskins D, Rawling DC, Fiebig A, Crosson S. 2007. A photosensory two-component system regulates bacterial cell attachment. Proc Natl Acad Sci U S A, 104(46):18241–18246.
- Purcell EB, McDonald CA, Palfey BA, Crosson S. 2010. An analysis of the solution structure and signaling mechanism of LovK, a sensor histidine kinase integrating light and redox signals. Biochemistry, 49(31):6761–6770.
- Raffelberg S, Mansurova M, Gärtner W, Losi A. 2011. Modulation of the Photocycle of a LOV Domain Photoreceptor by the Hydrogen-Bonding Network. Journal of the American Chemical Society, 133(14):5346–5356.
- Renicke C, Schuster D, Usherenko S, Essen L-O, Taxis C. 2013. A LOV2 domain-based optogenetic tool to control protein degradation and cellular function. Chemistry & Biology, 20(4):619–626.
- Richter F, Fonfara I, Bouazza B, Schumacher CH, Bratovič M, Charpentier E, Möglich A. 2016. Engineering of temperature- and light-switchable Cas9 variants. Nucleic Acids Research, 44(20):10003–10014.
- Richter F, Fonfara I, Gelfert R, Nack J, Charpentier E, Möglich A. 2017. Switchable Cas9. Current Opinion in Biotechnology, 48:119–126.
- Rivera-Cancel G, Motta-Mena LB, Gardner KH. 2012. Identification of natural and artificial DNA substrates for light-activated LOV-HTH transcription factor EL222. Biochemistry, 51(50):10024–10034.
- Rivera-Cancel G, Ko W, Tomchick DR, Correa F, Gardner KH. 2014. Full-length structure of a monomeric histidine kinase reveals basis for sensory regulation. Proceedings of the National Academy of Sciences of the United States of America, 111(50):17839–17844.
- Rockwell NC, Lagarias JC. 2010. A brief history of phytochromes. Chemphyschem, 11(6):1172–1180.
- Römling U, Bian Z, Hammar M, Sierralta WD, Normark S. 1998. Curli fibers are highly conserved between Salmonella typhimurium and Escherichia coli with respect to operon structure and regulation. Journal of Bacteriology, 180(3):722–731.
- Rullan M, Benzinger D, Schmidt GW, Milias-Argeitis A, Khammash M. 2018. An Optogenetic Platform for Real-Time, Single-Cell Interrogation of Stochastic Transcriptional Regulation. Molecular Cell, 70(4):745-756.e6.
- Salomon M, Lempert U, Rüdiger W. 2004. Dimerization of the plant photoreceptor phototropin is probably mediated by the LOV1 domain. FEBS Lett, 572(1–3):8–10.

- Sanford L, Palmer A. 2017. Recent Advances in Development of Genetically Encoded Fluorescent Sensors. Methods in Enzymology. 1–49, Elsevier;
- Schleicher E, Kowalczyk RM, Kay CW, Hegemann P, Bacher A, Fischer M, Bittl R, Richter G, Weber S. 2004. On the reaction mechanism of adduct formation in LOV domains of the plant blue-light receptor phototropin. J Am Chem Soc, 126(35):11067–76.
- Schmidt AJ, Ryjenkov DA, Gomelsky M. 2005. The Ubiquitous Protein Domain EAL Is a Cyclic Diguanylate-Specific Phosphodiesterase: Enzymatically Active and Inactive EAL Domains. Journal of Bacteriology, 187(14):4774–4781.
- Serra DO, Richter AM, Klauck G, Mika F, Hengge R. 2013. Microanatomy at Cellular Resolution and Spatial Order of Physiological Differentiation in a Bacterial Biofilm. mBio, 4(2):e00103-13.
- Sharma AK, Rigby AC, Alper SL. 2011. STAS Domain Structure and Function. Cellular Physiology and Biochemistry, 28(3):407–422.
- Shcherbakova DM, Shemetov AA, Kaberniuk AA, Verkhusha VV. 2015. Natural Photoreceptors as a Source of Fluorescent Proteins, Biosensors, and Optogenetic Tools. Annual Review of Biochemistry, 84(1):519–550.
- Shu X, Lev-Ram V, Deerinck TJ, Qi Y, Ramko EB, Davidson MW, Jin Y, Ellisman MH, Tsien RY. 2011. A Genetically Encoded Tag for Correlated Light and Electron Microscopy of Intact Cells, Tissues, and Organisms. PLOS Biology, 9(4):e1001041.
- Sommerfeldt N, Possling A, Becker G, Pesavento C, Tschowri N, Hengge R. 2009. Gene expression patterns and differential input into curli fimbriae regulation of all GGDEF/EAL domain proteins in Escherichia coli. Microbiology, 155(4):1318–1331.
- Sprenger WW, Hoff WD, Armitage JP, Hellingwerf KJ. 1993. The eubacterium Ectothi-orhodospira halophila is negatively phototactic, with a wavelength dependence that fits the absorption spectrum of the photoactive yellow protein. Journal of Bacteriology, 175(10):3096–3104.
- Strickland D, Moffat K, Sosnick TR. 2008. Light-activated DNA binding in a designed allosteric protein. Proceedings of the National Academy of Sciences of the United States of America, 105(31):10709–10714.
- Strickland D, Yao X, Gawlak G, Rosen MK, Gardner KH, Sosnick TR. 2010. Rationally improving LOV domain-based photoswitches. Nature Methods, 7(8):623–626.
- Studier FW, Moffatt BA. 1986. Use of bacteriophage T7 RNA polymerase to direct selective high-level expression of cloned genes. Journal of Molecular Biology, 189(1):113–130.
- Swartz TE, Corchnoy SB, Christie JM, Lewis JW, Szundi I, Briggs WR, Bogomolni RA. 2001. The photocycle of a flavin-binding domain of the blue light photoreceptor phototropin. J Biol Chem, 276(39):36493–500.
- Swartz TE, Tseng TS, Frederickson MA, Paris G, Comerci DJ, Rajashekara G, Kim JG, Mudgett MB, Splitter GA, Ugalde RA, et al. 2007. Blue-light-activated histidine kinases: two-component sensors in bacteria. Science, 317(5841):1090–1093.

- Takahashi F, Yamagata D, Ishikawa M, Fukamatsu Y, Ogura Y, Kasahara M, Kiyosue T, Kikuyama M, Wada M, Kataoka H. 2007. AUREOCHROME, a photoreceptor required for photomorphogenesis in stramenopiles. Proc Natl Acad Sci U S A, 104(49):19625–19630.
- Taylor BL, Zhulin IB. 1999. PAS domains: internal sensors of oxygen, redox potential, and light. Microbiol Mol Biol Rev, 63(2):479–506.
- Tian H, Trozzi F, Zoltowski BD, Tao P. 2020. Deciphering the Allosteric Process of the Phaeodactylum tricornutum Aureochrome 1a LOV Domain. The Journal of Physical Chemistry B, acs.jpcb.0c05842.
- Trajtenberg F, Buschiazzo A. 2020. Protein Dynamics in Phosphoryl-Transfer Signaling Mediated by Two-Component Systems. In: Eyers CE, Hrsg. Histidine Phosphorylation. 1–18, New York, NY: Springer US;
- Vaidya AT, Chen C-H, Dunlap JC, Loros JJ, Crane BR. 2011. Structure of a light-activated LOV protein dimer that regulates transcription. Science Signaling, 4(184):ra50.
- Wang X, Chen X, Yang Y. 2012. Spatiotemporal control of gene expression by a light-switch-able transgene system. Nature Methods, 9(3):266–269.
- Wilde A, Fiedler B, Börner T. 2002. The cyanobacterial phytochrome Cph2 inhibits phototaxis towards blue light: Cyanobacterial phytochrome Cph2. Molecular Microbiology, 44(4):981–988.
- Wu D, Hu Q, Yan Z, Chen W, Yan C, Huang X, Zhang J, Yang P, Deng H, Wang J, et al. 2012. Structural basis of ultraviolet-B perception by UVR8. Nature, 484(7393):214–219.
- Wu YI, Frey D, Lungu OI, Jaehrig A, Schlichting I, Kuhlman B, Hahn KM. 2009. A genetically encoded photoactivatable Rac controls the motility of living cells. Nature, 461(7260):104–108.
- Yamamoto A, Iwata T, Tokutomi S, Kandori H. 2008. Role of Phe1010 in Light-Induced Structural Changes of the neo1-LOV2 Domain of Adiantum †. Biochemistry, 47(3):922–928.
- Yee EF, Diensthuber RP, Vaidya AT, Borbat PP, Engelhard C, Freed JH, Bittl R, Möglich A, Crane BR. 2015. Signal transduction in light-oxygen-voltage receptors lacking the adduct-forming cysteine residue. Nature Communications, 6:10079.
- Zayner JP, Antoniou C, Sosnick TR. 2012. The amino-terminal helix modulates light-activated conformational changes in AsLOV2. Journal of molecular biology, 419(1–2):61–74.
- Zhang L, Dai L, Rong Y, Liu Z, Tong D, Huang Y, Chen T. 2015. Light-triggered reversible self-assembly of gold nanoparticle oligomers for tunable SERS. Langmuir: the ACS journal of surfaces and colloids, 31(3):1164–1171.
- Ziegler T, Möglich A. 2015. Photoreceptor engineering. Frontiers in Molecular Biosciences, 2:30.
- Zoltowski BD, Crane BR. 2008. Light activation of the LOV protein vivid generates a rapidly exchanging dimer. Biochemistry, 47(27):7012–7019.
- Zoltowski BD, Gardner KH. 2011. Tripping the Light Fantastic: Blue-Light Photoreceptors as Examples of Environmentally Modulated Protein–Protein Interactions. Biochemistry, 50(1):4–16.

- Zoltowski BD, Schwerdtfeger C, Widom J, Loros JJ, Bilwes AM, Dunlap JC, Crane BR. 2007. Conformational Switching in the Fungal Light Sensor Vivid. Science, 316(5827):1054–1057.
- Zoltowski BD, Vaccaro B, Crane BR. 2009. Mechanism-based tuning of a LOV domain photoreceptor. Nature Chemical Biology, 5(11):827–834.
- Zoltowski BD, Nash AI, Gardner KH. 2011. Variations in protein-flavin hydrogen bonding in a light, oxygen, voltage domain produce non-Arrhenius kinetics of adduct decay. Biochemistry, 50(41):8771–8779.
- Zoltowski BD, Motta-Mena LB, Gardner KH. 2013. Blue light-induced dimerization of a bacterial LOV-HTH DNA-binding protein. Biochemistry, 52(38):6653–6661.
- Zschiedrich CP, Keidel V, Szurmant H. 2016. Molecular Mechanisms of Two-Component Signal Transduction. Journal of Molecular Biology, 428(19):3752–3775.

4 Eigenanteil

4.1 Manuskript I

Titel: "Optogenetic Control by Pulsed Illumination"

Autoren: J. Hennemann; R. S. Iwasaki.; T. N. Grund; R. P. Diensthuber; R. Richter; A. Möglich

Veröffentlicht in: ChemBioChem (2018), vol. 19(12), pp. 1296 –1304,

DOI: 10.1002/cbic.201800030

A. Möglich, J. Hennemann, R. S. Iwasaki und R. P. Diensthuber hatten die zugrunde liegende Idee. F. Richter entwickelte den Beleuchtungssetup und J. Hennemann optimierte diesen. A. Möglich und J. Hennemann planten die darauffolgenden Experimente. A. Möglich erstellte das kinetische Model für die lichtgesteuerte Genexpression. J. Hennemann klonierte die verwendeten pDusk- und pDawn-*Ds*Red-Konstrukte und führte die entsprechenden Reportergenmessungen durch. T. N. Grund reinigte die YF1 Varianten und vollzog die spektroskopischen Analysen zur Bestimmung der Ratenkonstanten für die Rückkehr in den dunkeladaptierten Zustand. J. Hennemann wertete die Daten aus und erstellte die Abbildungen. J. Hennemann und A. Möglich verfassten und bearbeiteten das Manuskript. Der korrespondierende Autor ist A. Möglich.

4.2 Manuskript II

Titel: "Pulsatile Illumination for Photobiology and Optogenetics"

Autoren: J. Dietler; R. Stabel; A. Möglich

Veröffentlicht in: Methods in Enzymology (2019) vol. 624, pp. 227-248,

DOI: 10.1016/bs.mie.2019.04.005

A. Möglich, J. Dietler und R. Stabel hatten die zugrunde liegende Idee und planten die Experimente sowie die Weiterentwicklung des Beleuchtungssetups. J. Dietler und A. Möglich simulierten die Systemantworten zu Photorezeptoren hinsichtlich gepulster Beleuchtung. J. Dietler führte die Experimente zur Kontrolle der bakteriellen Genexpression mittels Variation der Lichtintensität und Pulsfrequenz durch. Die Erstellung und Charakterisierung photoaktivierbarer Adenylylcyklasen erfolgte durch R. Stabel. J. Dietler und R. Stabel erstellten die Abbildungen. J. Dietler und A. Möglich verfassten das Manuskript. J. Dietler, R. Stabel und A. Möglich bearbeiteten das Manuskript. Der korrespondierende Autor ist A. Möglich.

4.3 Manuskript III

Titel: "Signal Transduction in Light-Oxygen-Voltage Receptors Lacking the Active-Site Glutamine"

Autoren: J. Dietler*; R. Gelfert*; J. Kaiser*; V. Borin; C. Renzl; S. Pilsl; A. T. Ranzani; A. G. Fuentes; T. Gleichmann; R. P. Diensthuber; M. Weyand, G. Mayer; I. Schapiro und A. Möglich In *Nature Chemical Biology* eingereichtes Manuskript.

J. Dietler, R. Gelfert, J. Kaiser und A. Möglich planten die Experimente. J. Dietler führte alle YF1 und LOV-GGDEF-basierten Experimente durch, während J. Kaiser NmPAL-basierte Reportergenassays, entsprechende spektroskopische Messungen und die lichtvermittelte RNA-Bindung realisierte. A. T. Ranzani führte zusätzlich spektroskopische Messungen an NmPAL durch und analysierte ebenso dessen RNA-Bindung. AsLOV2-basierte Experimente wurden von R. Gelfert durchgeführt. A. G. Fuentes untersuchte AsLOV2 Varianten via CD-Spektroskopie. T. Gleichmann und R. P. Diensthuber entwickelten den YF1 Anisotropieassay. C. Renzl, S. Pilsl und G. Mayer führten die Experimente an NmPAL in eukaryotischen Zellen durch. V. Borin und I. Schapiro realisierten die Molekulardynamikstudien und werteten diese aus. Die Datenauswertung für alle YF1- und LOV-GGDEF-beinhaltenden Experimente erfolgte durch J. Dietler. PAL-inbegriffene Experimente wurden von J. Kaiser und sich auf AsLOV2-stützende Studien von R. Gelfert ausgewertet. M. Weyand gab Hilfestellung bei der Kristallisation und der Strukturauflösung. A. Möglich erstellte das Sequenzalignment und löste zusammen mit R. Gelfert die Kristallstruktur J. Dietler verfasste zusammen mit A. Möglich das Manuskript. Der korrespondierende Autor ist A. Möglich.

4.4 Manuskript IV

Titel: "A Light-Oxygen-Voltage Sensor Integrates Light and Temperature"

Autoren: J. Dietler; R. Schubert; T. G. A. Krafft; S. Meiler; S. Kainrath; F. Richter; K. Schweimer; M. Weyand; H. Janovjak und A. Möglich

Veröffentlicht in: Journal of Molecular Biology (2021), vol. 433(15), 167107

DOI: 10.1016/j.jmb.2021.167107

A. Möglich, R. Schubert, F. Richter und J. Dietler hatten die zugrunde liegenden Ideen. J. Dietler und A. Möglich planten die bakteriellen und biochemischen Experimente. Die Säugerzellenexperimente wurden von S. Kainrath und H. Janovjak entwickelt. R. Schubert erstellte das initiale bakterielle lichtinduzierte Expressionssystem. J. Dietler optimierte dieses, erstellte und

testete alle weiteren Konstrukte. J. Dietler erstellte und durchsuchte eine Bibliothek zur Identifizierung neuer *Rs*LOV Varianten und testete diese im bakteriellen Reportergenassay auf Lichtsowie Temperatursensitivität. PROSS-basierte *Rs*LOV Varianten wurden von J. Dietler kloniert und im TetR195-*Rs*LOV Kontext untersucht. Initiale biochemische Studien der PROSS-basierten Varianten erfolgten durch S. Meiler unter Anleitung von J. Dietler. Alle weiteren grundlegenden biochemischen Experimente wurden von J. Dietler durchgeführt. K. Schweimer realisierte zusammen mit J. Dietler die NMR-Messungen. T. G. A. Krafft kristallisierte mit Hilfe von A. Möglich und M. Weyand die *Rs*LOV-Varianten. A. Möglich löste zusammen mit T. G. A. Krafft und M. Weyand die Kristallstrukturen. S. Kainrath führte die Rezeptortyrosinkinase-experimente durch. Die Datenauswertung erfolgte durch J. Dietler für bakterielle Genexpressionsexperimente und durch S. Kainrath für eukaryotische Rezeptorsingalweiterleitungsexperimente. Biochemische Experimente wurden von J. Dietler zusammen mit A. Möglich ausgewertet. J. Dietler erstellte die Abbildungen. J. Dietler und A. Möglich verfassten das Manuskript. Der korrespondierende Autor ist A. Möglich.

4.5 Manuskript V

Titel: "Photobiologically Directed Assembly of Gold Nanoparticles"

Autoren: J. Dietler*; C. Liang*; S. Frank; A.-K. Müller; A. Greiner; A. Möglich

Veröffentlicht in: Advanced Biology

DOI: 10.1002/adbi.202000179

A. Möglich, A. Greiner, J. Dietler und C. Liang hatten die zugrunde liegenden Ideen und planten die Experimente. J. Dietler und S. Frank erstellten und charakterisierten die verwendeten Proteine. C. Liang synthetisierte und analysierte die Ni²⁺-NTA funktionalisierten Goldnanopartikel. Erste Interaktionsstudien wurden von J. Dietler, C. Liang und S. Frank umgesetzt. A.-K. Müller etablierte und nahm zusammen mit J. Dietler und C. Liang die AF4 Messungen vor. Die zeitaufgelösten Absorptionsspektren bei unterschiedlichen Proteinkonzentrationen und in Gegenwart von Imidazol wurden von J. Dietler realisiert. S. Frank und C. Liang präparierten die Proben für TEM-Messungen und C. Liang führte diese durch. Die Datenauswertung erfolgte durch J. Dietler, C. Liang, A.-K. Müller und A. Möglich. J. Dietler erstellte mit Unterstützung von C. Liang und A. Möglich die Abbildungen. J. Dietler und A. Möglich erstellten das Manuskript. Die Bearbeitung erfolgte durch J. Dietler, A. Möglich, C. Liang, A.-K- Müller und A. Greiner. Die korrespondierenden Autoren sind A. Greiner und A. Möglich.

^{*}Gleichberechtigte Erstautoren

5 Manuskripte

5.1 Manuskript



DOI: 10.1002/cbic.201800030





Optogenetic Control by Pulsed Illumination

Julia Hennemann,^[a] Roman S. Iwasaki,^[b] Tamara N. Grund,^[a] Ralph P. Diensthuber,^[b] Florian Richter,^[b] and Andreas Möglich*^[a, b]

Sensory photoreceptors evoke numerous adaptive responses in nature and serve as light-gated actuators in optogenetics to enable the spatiotemporally precise, reversible, and non-invasive control of cellular events. The output of optogenetic circuits can often be dialed in by varying illumination quality, quantity, and duration. A programmable matrix of light-emitting diodes has been devised to efficiently probe the response of optogenetic systems to intermittently applied light of varying intensity and pulse frequency. Circuits for light-regulated

gene expression markedly differed in their responses to pulsed illumination of a single color which sufficed for their sequential triggering. In addition to quantity and quality, the pulse frequency of intermittent light hence provides a further input variable for output control in optogenetics and photobiology. Pulsed illumination schemes allow the reduction of overall light dose and facilitate the multiplexing of several light-dependent actuators and reporters.

Introduction

Sensory photoreceptors elicit a wide palette of light-dependent physiological responses in nature,[1,2] for example, plant development, [3,4] phototaxis, [5-7] and vision in diverse organisms.^[8] They commonly feature modular architectures that comprise photosensor (or input) and effector (or output) modules. [9] Photon absorption by the thermodynamically most stable, dark-adapted (or resting) state D of the photosensor initiates a photocycle, that is, a series of photochemical events within and adjacent to the chromophore, leading to population of the light-adapted (or signaling) state L.[9] In a process denoted dark recovery, the metastable light-adapted state L thermally reverts to the dark-adapted state D; in photochromic photoreceptors, secondary absorption of a photon can actively drive the reversion of L to D. In case of the light-oxygen-voltage (LOV) photoreceptors, [10,11] absorption of blue light by a flavin nucleotide chromophore in its quinone form leads to population of the excited singlet state S₁, which, within nanoseconds, undergoes intersystem crossing to the triplet state T₁. Within microseconds, the T₁ state decays to the signaling state L through the formation of a covalent thioether bond between atoms C(4a) of the flavin isoalloxazine ring system and $S\gamma$ of a nearby conserved cysteine residue within the LOV photosensor. Concomitant with thioether formation, the N5 atom of the

flavin chromophore is protonated, which triggers hydrogenbond rearrangements throughout the LOV photosensor. Studies on cysteine-devoid variants of LOV receptors revealed that N5 protonation was both necessary and sufficient for downstream signal propagation.^[12] The stability of the thioether bond in cysteine-containing LOV receptors is strongly governed by temperature, solvent composition, and molecular environment of the flavin chromophore. [13,14] Certain residue exchanges within the LOV photosensor adjacent to the flavin cofactor strongly stabilize or destabilize the thioether bond and thereby alter the lifetime of the signaling state L over up to several orders of magnitude. At least for LOV receptors, the deliberate variation of the dark-recovery kinetics through residue exchanges represents the means of choice for modulating effective light sensitivity at the photostationary state under constant illumination.^[9] By contrast, the absolute light sensitivity is determined by the absorption cross section and the quantum yield for the formation of the signaling state; these are largely invariant for a given photoreceptor class.

Sensory photoreceptors generally trigger biological reactions in response to incident light with exquisite spatiotemporal precision, non-invasiveness, and full reversibility. These attractive attributes not only underpin numerous natural light-dependent processes, but they are also central to the deployment of sensory photoreceptors in optogenetics.^[15] Briefly, optogenetics denotes the (mostly) heterologous expression of sensory photoreceptors to render target cells, tissues, and organisms light-sensitive, and thus, amenable to precise control in time and space by illumination. Initially developed in the neurosciences and exclusively reliant on light-gated ion channels and pumps, [6,7,16,17] optogenetics has been empowered by the advent of additional sensory photoreceptors and now affords light-dependent control of numerous cellular parameters and processes. [9,18,19] In particular, the optogenetic repertoire has been greatly expanded by the engineering of novel sensory

This article is part of a Special Issue on the Optical Control of Biological Processes.

 [[]a] J. Hennemann, T. N. Grund, Prof. Dr. A. Möglich Lehrstuhl für Biochemie, Universität Bayreuth 95447 Bayreuth (Germany) E-mail: andreas.moeglich@uni-bayreuth.de

[[]b] R. S. Iwasaki, Dr. R. P. Diensthuber, Dr. F. Richter, Prof. Dr. A. Möglich Biophysikalische Chemie, Institut für Biologie Humboldt-Universität zu Berlin 10115 Berlin (Germany)

Supporting information and the ORCID identification numbers for the authors of this article can be found under https://doi.org/10.1002/ cbic.201800030.



photoreceptors with custom-tailored light-dependent output. As a case in point, we constructed the blue-light-repressed histidine kinase YF1 by linking the LOV photosensor of the Bacillus subtilis YtvA protein, [20] engaged in mediating the general stress response in this bacterium, [21,22] to the effector module of the FixL histidine kinase from Bradyrhizobium japonicum. [23] Together with its cognate response regulator BjFixJ, YF1 forms a light-regulated two-component system (TCS).^[24] In its darkadapted state D, YF1 readily phosphorylates BjFixJ, thus triggering the transcription of target genes from a specific promoter, which is denoted FixK2. By contrast, in its light-adapted state L, YF1 acts as a net phosphatase that removes phosphoryl groups from phospho-BjFixJ, and consequently, suspends target-gene expression. Based on the YF1/BjFixJ TCS, the plasmids pDusk and pDawn allow light-repressed and -enhanced gene expression, respectively, in Escherichia coli (Figure 1 A). The expression output of both pDusk and pDawn varies hyperbolically with the intensity of constant blue-light illumination.[25]

In optogenetics, a graded response of the system under study can often be effected through variation of the intensity and duration of constant illumination. Although this approach frequently suffices for adjusting the system response to desired

set levels, we reasoned that additional optogenetic control could be exerted by resorting to pulsed illumination applied intermittently. This reasoning is supported by previous studies that used pulsed lighting schemes to control optogenetic circuits, for example, refs. [26] and [27]. As mentioned above, even within a single photoreceptor class, the dark-recovery kinetics can greatly vary. Put another way, photoreceptor variants can substantially differ in the refractory time after photoactivation, during which they retain their signaling state L and have not fully returned to the dark-adapted state D. Accordingly, one should be able to differentially address and activate pairs of photoreceptors with pulsed illumination, if they sufficiently differ in their recovery kinetics. To test this idea, we have constructed a programmable matrix of light-emitting diodes (LEDs) that allow the parallel interrogation of numerous intensities and pulse frequencies of illumination. Using pDusk and pDawn as paradigms, we show that for certain lighting regimes the system response does not scale monotonically with the applied average light dose, but is primarily governed by the pulse frequency of illumination. We exploit the differential response to pulsed, monochromatic illumination to sequentially control gene expression for pDawn variants that only differ in their dark-recovery kinetics. Taken together, our results show

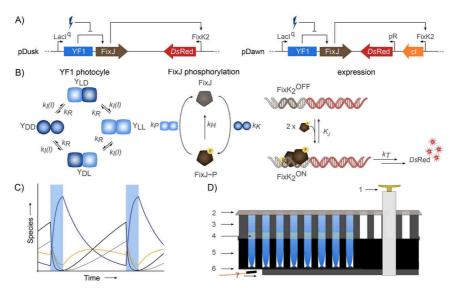


Figure 1. A) The plasmids pDusk and pDawn employ the light-responsive TCS YF1/B/FixJ to mediate light-repressed and -activated gene expression, respectively. The plasmid pDawn is derived from pDusk through insertion of a gene-inversion cassette based on the phage λ repressor cl. B) Kinetic model of YF1/B/FixJ TCS, as implemented on the pDusk plasmid. Y_{DD} , Y_{LD} , Y_{LD} , and Y_{LL} denote the diarsic YF1 receptor with its two LOV domains in the states specified by the subscript, that is, D and L for the dark- and light-adapted states, respectively. YF1 is photoactivated in a forward reaction determined by the rate constant k_1 and the intensity of applied blue light l; k_R denotes the dark-recovery rate constant. Notably, the two LOV photosensors transition between their respective states D and L independently from one another, as previously shown. Fill Fill for fully light-adapted species Y_{DD} catalyzes the phosphorylation of the response regulator B/FixJ with rate constant k_R . In its partially or fully light-adapted state (Y_{LD} , Y_{LD} , and Y_{LL}) YF1 acts as a phosphatase on phosphor-FixJ and catalyzes the hydrolysis of the phosphoryl group with rate constant k_R ; the rate of spontaneous hydrolysis is given by k_R . Once phosphorylated, B/FixJ binds as a homodimer to its cognate FixK2 promoter, governed by the affinity constant K_R , to activate transcription with a rate constant k_R C) The numerical solution of the kinetic scheme in (A) illustrates the time evolution of different molecular species (Y_{DD} , black; Y_{D}/Y_{DD} , orange; Y_{LD}) blue; phospho-B/FixJ, gray) during regimes of alternating illumination (blue shading) and darkness. D) Schematic of the Arduino-based programmable LED matrix. 1) Spring clip; 2) O₂-permeable sealing film; 3) black-wall, transparent-bottom 96-well microtiter plate (MTP); 4) bacterial culture; 5) adapter; 6) eight-by-eight LED array; 7) mounting plate.

www.chembiochem.org





that the pulse frequency of intermittent light can serve as a further control variable, in addition to light quality (i.e., color) and quantity (i.e., intensity).

TCS. To evaluate experimental data obtained for the pDawn system, we expanded the above model accordingly (see the Experimental Section).

Results

Kinetic model for light-dependent gene expression

To inform the experimental design for investigating pulsed illumination, we developed a kinetic framework for gene expression in the pDusk and pDawn systems that comprised three modules (Figure 1B). The first module accounts for the photocycle of the YF1 photoreceptor. As determined by absorption spectroscopy, the rate constant k_{-1} for the monoexponential dark recovery of YF1 after prior photoactivation amounts to $(7.4\pm0.1)\times10^{-4}\,\text{s}^{-1}$ at $37\,^{\circ}\text{C}$. Experiments had previously demonstrated that the two LOV photosensors of the homodimeric YF1 receptor recovered their dark-adapted state D independently from one another with identical microscopic rate constants, $k_{\rm R} = k_{-1}/2$. Likewise, light-induced formation of the signaling state L proceeds independently in the two LOV protomers. Because the photochemical reactions leading to the population of L are very fast, in comparison to the timescales of dark recovery and gene expression, we lumped them together into a single unimolecular reaction with rate constant k_1 , the magnitude of which depended on the intensity, l, of applied blue light, according to $k_1 = k_1 l$. The second module describes the phosphorylation and dephosphorylation of the response regulator BjFixJ. As experimentally demonstrated, [23] YF1 is only active as a net histidine kinase if both its LOV photosensors reside in their dark-adapted states; this is denoted as YDD. By contrast, if one or two LOV domains assume their lightadapted states, Y_{LD} and Y_{DL} or $Y_{LL},$ respectively, YF1 acts as a net phosphatase on phospho-BjFixJ. As borne out by experiment,^[23] the histidine kinase activity of YF1 hence recovers in sigmoidal, rather than exponential, manner after prior photoactivation. The velocities of the BjFixJ phosphorylation and dephosphorylation reactions catalyzed by YF1 are given by the rate constants $k_{\rm K}$ and $k_{\rm P}$ respectively, and the spontaneous rate of hydrolysis of phospho-BjFixJ is denoted k_H . The third module implements expression from the FixK2 promoter. Phospho-BjFixJ binds as a homodimer to this promoter with a dissociation constant of $K_{\scriptscriptstyle J}$ to initiate transcription of a target gene with a rate constant of k_T . The kinetic model was expressed as a set of ordinary differential equations (ODEs; see the Experimental Section) and numerically solved (Figure 1C). The model accurately recapitulated the experimental findings that the population of Y_{DD} decreased in exponential manner during phases of blue-light illumination, but recovered sigmoidally, that is, with a lag phase, during dark periods. Because the degree of phosphorylation of the response regulator BiFixJ is governed by the relative concentrations of YDD, YLD, YDL, and Y₁₁, it also varies as a function of light over time.

In pDawn, target genes are expressed from the p_R promoter, which is controlled by the phage λ repressor cl. $^{\!\![25]}$ The expression of cl, in turn, occurs from the FixK2 promoter and is hence subject to light-dependent control by the YF1/BjFixJ

Pulsed illumination for graded control of gene expression

Next, we devised a setup for illuminating samples at defined light qualities, quantities, and pulse frequencies (Figure 1D and Figure S1 in the Supporting Information). To this end, we constructed a programmable matrix of eight-by-eight threecolor LEDs for illumination from below of individual wells of 96-well microtiter plates (MTPs). The setup employs opensource Arduino microcontrollers and commercially available electronics. A custom-made adapter piece and a mounting frame allow placement of the entire setup on a shaker platform. The light output of the LED matrix was calibrated with a lamp power meter. To facilitate the programming of the LED matrix, we developed a Python-based graphical user interface (cf. Figure S1). Our setup is similar to the light-plate apparatus (LPA) previously constructed by the Tabor laboratory. [29] In contrast to the LPA, our setup works with 96-well, rather than 24well, plates, and its assembly does not require any soldering. On the downside, in our setup, the LEDs are presently fixed to wavelengths of \approx 470, 525, and 620 nm, whereas the LPA can be variably outfitted with a range of different LEDs.

We employed the programmable LED matrix to systematically interrogate the response of the pDusk and pDawn systems to lighting regimes of different intensity and pulse frequency. To readily gauge the system output, we used a DsRed Express2 fluorescence reporter gene. [30] E. coli cultures harboring pDusk-DsRed or pDawn-DsRed were incubated in black-wall, clearbottom MTPs at 37 °C for 16 h while being exposed to alternating cycles of darkness and blue-light illumination. The illumination period was fixed at 30 s, whereas the dark period ranged from 0 to 65 min. For different samples, the light intensity varied between 0 and 130 $\mu W\, cm^{-2}$. Following incubation, the DsRed fluorescence and optical density at $\lambda = 600 \text{ nm}$ (OD₆₀₀) were measured. Notably, the OD₆₀₀ values of the cultures were independent of illumination; this indicated that phototoxicity did not significantly affect the experimental results. A contour plot of the results for the pDusk-DsRed system shows that for a given light intensity reporter-gene output increases monotonically with the duration of the dark period (Figure 2A); likewise, for a given dark period, the reporter output decreases monotonically with increasing light intensity. As expected, [25] the pDawn-DsRed system exhibited an inverted signal response with reporter-gene output monotonically decreasing with dark period, but increasing with light intensity. Consistent with previous findings,[25] the maximum expression output for the pDawn-DsRed system was around 3.6-fold times that for the pDusk-DsRed system. To further characterize the system response of pDawn-DsRed, we evaluated the expression output as a function of the applied light dose averaged over the entire experiment (Figure 2B). Overall, the data can be described by a hyperbolic relation with a half-maximal light dose (LD₅₀) of (4.1 \pm 0.8) μW cm⁻². For comparison, we previously obtained a value for LD_{50} of (12 \pm 3) $\mu W\,cm^{-2}$ for the pDawn-



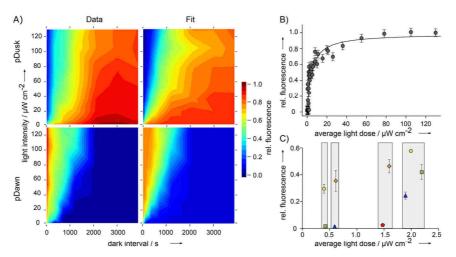


Figure 2. Control of gene expression from pDusk (upper row) and pDawn (lower row) with illumination of varying intensity and pulse frequency. A) (left column) Steady-state expression of DsRed from the pDusk and pDawn plasmids during incubation under pulsed illumination. Samples were alternately illuminated for 30 s at λ = 470 nm at variable intensities, followed by incubation in the dark for variable time periods. The contour plots show the dependence of reporter-gene expression on the duration of the dark period (x axis) and intensity of applied pulsed light (y axis). The fluorescence data are shown as a color code and represent averages of three replicates \pm standard deviation (s.d.), normalized to the maximum fluorescence value of either pDusk-DsRed or pDawn-DsRed. (right column) The experimental data were globally fitted to the numerical solution of the kinetic scheme depicted in Figure 1 B. B) Overall, the DsRed reporter-gene expression for the pDawn plasmid increased hyperbolically with time-averaged light dose. C) However, at low average light doses between 0 and $2.5 \,\mu$ W cm⁻², the system output greatly varied with the pulse frequency of light. In particular, higher gene expression output was systematically obtained if the light dose was distributed across several pulses of lower intensity, rather than a single pulse of high intensity. The colored symbols denote data obtained for different intensities of applied light (=: 2, •: 8, =: 55, \pm : 78, and •: 105 μ W cm⁻²).

DsRed system at constant illumination, albeit for quite different culture volumes and geometry of illumination. [25] Interestingly, at average light doses well below saturation, the system response did not scale monotonically with the overall dose, but rather depended on the pulse frequency of illumination (Figure 2C). In particular, nearly identical overall input doses could result in quite different expression output, as prominently seen in the dose regime $0-2.5 \mu \text{W} \, \text{cm}^{-2}$. For example, a particularly pronounced differential effect was observed at an average light dose of around 0.6 μW cm⁻². Application of strong light pulses of 78 $\mu\text{W}\,\text{cm}^{-2}$ every 65 min did not result in significant activation of gene expression, but, if pulses of 8 µW cm⁻² were applied every 6 min, gene expression was activated to around 40% of maximum extent. In general, for a given average dose, systematically higher gene expression output was obtained if light application was evenly distributed over several weaker pulses, rather than concentrated in a single strong pulse. Likewise, a desired expression output level could be obtained by different lighting schemes and overall light doses. For example, half-maximal activation of the pDawn-DsRed system could either be achieved through continuous illumination at around $4\;\mu\text{W}\,\text{cm}^{-2}$ (cf. above) or by applying light pulses of 30 s duration and $8\;\mu\text{W}\,\text{cm}^{-2}$ intensity at 6 min intervals, corresponding to a 70% reduction of overall light dose. More generally, by using optimized illumination conditions, the applied light dose can hence be deliberately reduced to minimize detrimental phototoxic effects, which, to first approximation, are expected to scale linearly with applied light dose. These findings also

confirmed one of our initial premises, namely, that, in addition to light color and intensity, pulse frequency governs system output.

Sequential expression control with monochromatic light

To assess if the kinetic framework (cf. Figure 1B) adequately accounted for the experimental results, we globally fitted the data for pDusk-DsRed and pDawn-DsRed to the numerical solution of the model (Figure 2A). Altogether, the model described the experimental data well, and the fitted parameters assumed realistic values. For example, the YF1 kinase turnover (rate constant k_K) amounted to around 1.0 min⁻¹, which compared to an experimental value of around 0.9 min⁻¹ determined at 22°C.[23] Moreover, the YF1 phosphatase turnover was fitted to be 15 min⁻¹, which agreed with the experimental finding that dephosphorylation of BjFixJ proceeded much faster than its phosphorylation. Having corroborated our kinetic model, we predicted how system output varied if the underlying YF1/BjFixJ TCS was modified. Specifically, we reasoned that modulation of the dark-recovery kinetics k_R of YF1 through mutagenesis should strongly affect the system response to pulsed illumination. To this end, we exchanged the residue valine at position 28 for either threonine (V28T) or isoleucine (V28I) in the YF1 receptor because corresponding exchanges in the LOV2 domain of Avena sativa phototropin 1 had strongly accelerated and decelerated, respectively, dark-recovery kinetics. [31] The YF1 variants V28T and V28I were hetero-

ChemBioChem 2018, 19, 1296 - 1304

www.chembiochem.org

1299

© 2018 Wiley-VCH Verlag GmbH & Co. KGaA, Weinheim



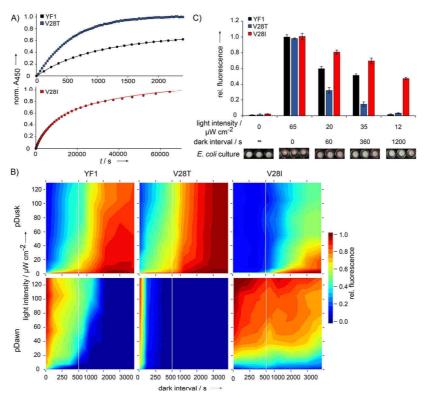


Figure 3. Modulating the intensity/pulse frequency response of light-regulated gene expression. A) Introduction of the residue exchanges V28T (\blacksquare) and V28I (\blacksquare) caused acceleration or deceleration, respectively, of the YF1 dark-recovery kinetics (K_R). Absorption data were recorded at 37 °C of purified proteins following saturating illumination with blue light, and were fitted to single-exponential functions. The bottom panel shows the very slow recovery kinetics for the V28I variant. B) DsRed expression in the pDusk and pDawn variants YF1, V28T, and V28T as a function of pulse frequency and intensity of blue light. The contour plots show DsRed reporter-gene expression normalized to the maxima obtained for pDusk-DsRed or pDawn-DsRed, respectively, as a function of light intensity and duration of dark period. To better visualize data at short dark periods, the x axis was split at 500 s, as indicated by the vertical white line. Fluorescence values are shown as color code and represent averages of three replicates \pm s.d. \bigcirc Individual control of several light-dependent gene-expression systems by varying intensity and frequency of pulsed illumination. E coli cultures harboring the YF1 (\blacksquare), V28T (\blacksquare), and V28I (\blacksquare) variants of pDawn-DsRed were incubated under different lighting protocols, as indicated. Resultant reporter-gene expression was determined as the average of three biological replicates \pm s.d. and normalized as before. Bottom row shows photographs of the corresponding cultures grown in MTPs.

logously expressed, purified, and their dark-recovery kinetics were monitored by absorption spectroscopy at 37 °C (Figure 3 A). Whereas the rate constant of dark recovery for V28T of $k_{-1} = (1.7 \pm 0.1) \times 10^{-3} \text{ s}^{-1}$ was around twice as large as that for the original YF1, in the case of V28I the recovery reaction was slowed down by around tenfold, relative to that of YF1, to $k_{-1} = (5.3 \pm 0.1) \times 10^{-5} \text{ s}^{-1}$. The residue exchanges V28T and V28I were also introduced into the pDusk-DsRed and pDawn-DsRed systems, and the gene expression output was monitored at different light intensities and pulse frequencies (Figure 3 B). Consistent with the altered dark-recovery kinetics, the variants V28T and V28I showed decreased and increased light sensitivity, respectively, in both the pDusk and pDawn contexts. In particular, the V28I variants were efficiently switched, even at low light doses and extended dark periods. Inspection of the gene expression output for the YF1, V28T, and V28I variants in the pDawn-DsRed context revealed areas in the intensity/pulse frequency space in which a subset of variants was efficiently switched, whereas the other variants barely responded. Based on these data, we reran the gene expression experiments for the pDawn-DsRed variants YF1, V28T, and V28I at five discrete intensity/pulse frequency settings. By choosing extended dark periods (20 min) and moderate blue-light intensities (12 μW cm⁻²), the V28I variant of the system could be activated to around half-maximal extent without significantly activating either of the other two systems. At somewhat higher intensity (35 µW cm⁻²) and shorter dark period (6 min), the original YF1 system could be more strongly activated than the V28T variant. In regimes of high light intensity (constant illumination at 65 µW cm⁻²), all three variants were activated to similar extents. Notably, the use of pulsed illumination was required for individual activation of the systems, whereas con-



stant illumination (i.e., a dark period of 0 in Figure 3B) did not suffice for discriminating between the different systems. Evidently, pulsed illumination affords enhanced control, for example, to enable the parallel use of several photoreceptor systems and their consecutive activation with monochromatic light.

Response of derivative gene expression systems to pulsed illumination

Using the programmable LED matrix, we also interrogated the intensity/pulse frequency response of derivative pDusk and pDawn systems that harbored YF1 variants with altered functional properties (Figure 4). The single-residue exchanges D21V and H22P, both situated at the dimer interface of homodimeric YF1, have been shown to invert the response to light.[32,33] We introduced these mutations into the pDusk-DsRed and pDawn-DsRed contexts and measured gene expression output as a function of intensity and pulse frequency of illumination. In the pDusk-DsRed setting, both the D21V and H22P variants showed the inverted response to illumination relative to YF1, in that reporter output decreased with increasing dark period and increased with light intensity. Whereas reporter-gene expression in the H22P variant was upregulated by up to 14-fold, in the D21V variant a maximum upregulation of only sixfold was achieved. For reference, in the original pDusk-DsRed, light induced a downregulation of reporter-gene expression by up to 11-fold. Within the pDawn-DsRed context, both D21V and H22P variants also displayed inverted behavior, relative to the original YF1, with reporter-gene expression that increased with dark period and decreased with light intensity. Again, the maximum degree of light regulation for D21V was less pronounced than that obtained for H22P.

Next, we assessed the response to intensity and pulse frequency of illumination in pDusk and pDawn systems harboring YF1 variants that lacked the conserved adduct-forming Cvs62 inside the LOV photosensor (Figures 4 and S2). We previously showed that such cysteine-devoid LOV receptors could still retain light sensitivity and downstream signal transduction because, in the absence of the conserved cysteine, blue-light absorption promotes reduction of the flavin chromophore to the neutral semiquinone state (NSQ).[12] Notably, formation of the NSQ entails protonation of the flavin N5 atom, which is key to triggering downstream responses. Introduction of the C62A substitution substantially impaired the regulation of reportergene expression in both the pDusk-DsRed and pDawn-DsRed contexts, relative to the original YF1-based variants, in agreement with previous observations (Figure S2).[12] Although the difference between minimum and maximum reporter expression was attenuated due to cysteine removal, the sensitivity to light of different pulse frequencies and intensities remained largely invariant. These data indicate that inside bacterial cells the cysteine-devoid variants possess similar kinetics for the formation and depletion of the signaling state as the cysteinecontaining variants. We also introduced the C62A substitution in the background of the signal-inverted D21V and H22P variants. In the pDusk-DsRed context, light responsiveness was retained for both D21V:C62A and H22P:C62A (Figures 4 and S2). Remarkably, although pDusk-DsRed H22P:C62A suffered a slight reduction in light sensitivity compared with the H22P variant, it displayed essentially the same maximum degree of regulation. In the pDawn-DsRed context, regulation by light was largely abolished for the D21V:C62A variant, whereas the H22P:C62A variant retained light responsiveness, albeit to lesser extent than that of the H22P variant.

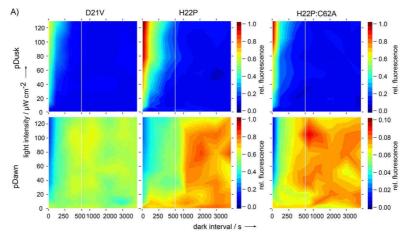


Figure 4. Intensity/pulse frequency response of variant gene-expression systems to intermittent illumination. In both pDusk–DsRed and pDawn–DsRed contexts, the YF1 variants D21V and H22P showed inverted gene expression output relative to the original YF1 system. Fluorescence data represent the average±s.d. of three biological replicates, and are normalized to the maximum output of the pDusk–DsRed and pDawn–DsRed systems, respectively, shown as color code. Responsiveness to light was retained in pDusk–DsRed and pDawn–DsRed variants, despite replacement of the adduct-forming cysteine residue 62 in the YF1 photoreceptor by alanine, as most clearly seen for the pDusk–DsRed H22P:C62A variant that fully conserved the light-dependent regulation of gene expression.

www.chembiochem.org 1301

© 2018 Wiley-VCH Verlag GmbH & Co. KGaA, Weinheim





Discussion

Genetically encoded, light-gated circuits enable the control and analysis of cellular processes and parameters with unprecedented spatiotemporal accuracy, reversibility, and noninvasiveness. A cohort of natural and engineered sensory photoreceptors underpin a multitude of optogenetic applications in many areas of basic and applied science, including biotechnology, synthetic biology, and cell biology. [9,18] Of particular benefit, the output of optogenetic circuits can often be adjusted in a graded manner by altering the quality (color), quantity (intensity), and duration of illumination. Herein, we have explored the use of pulsed illumination schemes for enhanced optogenetic control. Employing as paradigms setups for lightregulated gene expression in prokaryotes, [25] we demonstrate that variation of the pulse frequency of illumination provides an additional input variable for controlling the output of lightgated systems. Specifically, we exploit that sensory photoreceptors retain their signaling state for a refractory time after illumination ceases before eventually resuming their dark-adapted resting state. As a consequence, the physiological effect induced by light persists for a period, the length of which is strongly governed by the dark-recovery kinetics of the underlying photoreceptor. In addition, processes downstream of the actual photoreceptor may also persist, and hence, contribute to the overall dark-recovery kinetics of the entire system under study. By analyzing the response function of a given optogenetic circuit to varying intensities and pulse frequencies of light, optimized illumination protocols may be devised that maximize the biological effect, but minimize the overall light dose and detrimental phototoxic processes. Although the precise outcome will differ between scenarios, we expect the maximum effect for pulse frequencies on the timescale of the recovery kinetics of the system under study. We note that pulsed illumination also provides an avenue towards temporally synchronizing optogenetic circuits, for example, across a cell culture population.[34] Moreover, pulsed illumination is suitable for separately addressing pairs of photoreceptors, even if they respond to the same light quality (cf. Figure 3). In particular, for LOV and rhodopsin photoreceptors, [8,14] and, to lesser extent, for cryptochrome photoreceptors, [35] molecular determinants that govern the dark-recovery process have been identified. The kinetics of dark recovery can often be deliberately modulated over a wide range by substitution of certain protein residues near the chromophore. In this manner, the response of the photoreceptor to pulsed illumination can thus be adjusted as demanded by a given application. The ability to differentially control several photoreceptor systems with a single light color can reduce the required number of independent input channels; this particularly benefits experiments in which photoreceptor systems are multiplexed and/or are combined with fluorescent proteins. Evidently, pulsed illumination schemes extend to more than one light color, which is of particular utility for bimodally switchable, photochromic photoreceptors. [9,36]

To unravel the response of optogenetic circuits to pulsed light in a facile manner, we have developed a versatile, programmable LED matrix for the parallel illumination of individu-

al wells of MTPs at varying intensity and pulse frequency. We deployed this setup to characterize the response of the pDusk and pDawn systems for light-regulated gene expression in prokaryotes.[25] Introduction of the residue exchanges V28T or V28I in YF1 sped up or down, respectively, the recovery kinetics of both the pDusk and pDawn systems and, accordingly, decreased or increased, respectively, their effective light sensitivities (cf. Figure 3 A, B). Judiciously chosen pulsed illumination enabled the differential optogenetic control of gene expression for pDawn variants, even with a single light color (cf. Figure 3 C). The LED matrix also served to analyze, in more detail, the response to illumination of pDusk and pDawn variants in which the YF1 photoreceptor lacks the conserved, active-site cysteine residue.[12] At least in some variants, essentially intact light response was retained, even after removal of this cysteine (cf. Figures 4 and S2). In the absence of the cysteine residue, blue light promotes the reduction of the flavin chromophore to the NSO radical state, which, owing to its protonation at the N5 atom, can still elicit downstream signaling processes.^[12] The present data show that under physiological conditions this process can be as efficient as signal transduction by the original cysteine-containing LOV receptors.

In general, the programmable LED matrix, and related devices for automated illumination, [29,37-41] stand to facilitate the analysis and application of optogenetic circuits and other light-responsive systems. These lighting setups directly pertain to the optogenetic regulation of gene expression in prokaryotes [25,39,42-49] and eukaryotes, [36,50-52] and readily extend to additional optogenetic experiments. [53,27,54] More generally, setups for programmable, parallelized illumination may also benefit the analysis of other light-sensitive biological and chemical processes, for example, the cultivation of photoautotrophic organisms, such as cyanobacteria. [55]

Experimental Section

Assembly of the programmable LED matrix: To examine, in a facile manner, light-dependent biological processes at varying intensities and pulse frequencies of illumination, we constructed a programmable matrix of LEDs. A commercially available circuit board with an eight-by-eight array of three-color LEDs (Adafruit NeoPixel, Adafruit industries, New York, USA) was outfitted with a custom-made adapter, upon which a standard 96-well MTP could be placed (cf. Figures 1 D and S1). The adapter thus enabled the illumination of 64 individual wells of an MTP from below. To achieve optical isolation between adjacent wells, the adapter featured recessed holes into which the individual LEDs were embedded. In addition, MTPs with transparent bottom and black walls were used (Greiner BioOne, Frickenhausen, Germany). The entire assembly was encased in a mounting frame to allow placement on a standard MTP shaker (Figure S1). Although these parts were originally shaped by subtractive manufacturing, we also supply templates for additive manufacturing, that is, 3D printing (available for download at http://www.moeglich.uni-bayreuth.de/en/software). A programmable Arduino Uno microcontroller was used to set the color, intensity, and pulse frequency of illumination for the individual pixels of the LED matrix (part list and circuit layout are available from the above URL). Each LED pixel comprised three color channels (470, 525, and 620 nm, respectively) that could be controlled through

1302



pulse-width modulation in 256 brightness steps (8 bit). We developed a Python-based graphical user interface to facilitate the configuration of the LED matrix (Figure S1; also available at the above URL). As output, the user interface generates an Arduino sketch file to be uploaded to the Arduino microcontroller. To improve the temporal accuracy of the Arduino microcontroller, optionally a real-time clock (RTC D53221 Precision, Adafruit industries, New York, USA) could be implemented. Actual light intensities for each LED matrix were calibrated with a power meter (model 842-PE, Newport, Darmstadt, Germany) and a silicon photodetector (model 918D-IIV-OD3. Newport).

Light-dependent gene expression at varying intensity and pulse frequency of illumination: Variants of YF1 were generated by sitedirected mutagenesis in the background of the reporter plasmids pDusk-DsRed and pDawn-DsRed, according to the QuickChange protocol (Invitrogen, Life Technologies). [25] The identity of all constructs was confirmed by DNA sequencing (GATC Biotech). All experiments were performed in the E. coli CmpX13 strain in lysogeny broth (LB) plus kanamycin (50 µg mL⁻¹).^[56] To determine the dependence of gene expression on varying lighting schemes, starter cultures (5 mL) were inoculated from freshly transformed plates and grown at 37 °C to an OD₆₀₀ of 0.3 under noninducing conditions (i.e., in the dark for pDawn-DsRed or at 100 µW cm-2 470 nm light for pDusk-DsRed constructs). Aliquots (10 μL) of these cultures were used to inoculate LB medium (15 mL), and this solution (200 µL) was added to 64 wells of a black-wall, transparent-bottom 96-well MTP (Greiner BioOne, Frickenhausen, Germany). The MTP plate was sealed with gas-permeable sealing film BF-400-S (Corning, New York, USA) and placed on top of the LED-array setup. The assembly was mounted on an MTP shaker (PMS-1000i Microplate Shaker, Grant Instruments, Cambridge, UK) and incubated at 37°C and 600 rpm for 16 h (HN-2 Herp Nursery II, Lucky Reptile, Waldkirch, Germany). Dark conditions were achieved by covering the windows of the incubator and all displays with black plastic foil. During incubation, each well was repeatedly illuminated by light of $\lambda = (470 \pm 5)$ nm, of which the intensity varied between 0 and $130 \,\mu\text{W}\,\text{cm}^{-2}$. Pulses of blue light (30 s) were followed by dark periods of between 0 and 65 min. Following incubation, OD₆₀₀ and DsRed fluorescence were measured for each well in a Tecan Infinite M200 PRO plate reader (Tecan Group Ltd., Männedorf, Switzerland) by using excitation and emission wavelengths of (554 ± 9) and (591 ± 20) nm, respectively. Fluorescence data were normalized to $\ensuremath{\mathsf{OD}}_{\ensuremath{\mathsf{600}}}$ and represent the averages of three biological replicates \pm

Kinetic model for light-dependent gene expression: Experimental data were represented as contour plots as a function of the duration of the dark interval and intensity of pulsed illumination. To quantitatively evaluate the experimental data for pDusk–DsRed, the kinetic model shown in Figure 1B was cast as a set of ODEs [Eqs. (1), (2), (3), (4), (5), (6), (7)]:

$$d[Y_{DD}]/dt = -2 k_I I[Y_{DD}] + k_R([Y_{LD}] + [Y_{DL}])$$
 (1)

$$d[Y_{LD}]/dt = -(k_R + k_I I)[Y_{LD}] + k_I I[Y_{DD}] + k_R[Y_{LL}]$$
 (2)

$$d[Y_{DL}]/dt = -(k_R + k_I I)[Y_{DL}] + k_I I[Y_{DD}] + k_R[Y_{LL}]$$
 (3)

$$d[Y_{LL}]/dt = -2\,k_R[Y_{LL}] + k_I I([Y_{LD}] + [Y_{DL}]) \eqno(4)$$

$$d[J]/dt = -k_{K}[Y_{DD}][J] + k_{H}[J_{P}] + k_{P}([Y_{LD}] + [Y_{DL}] + [Y_{LL}])[J_{P}]$$
 (5)

$$d[R]/dt = k_{T}[J_{P}]^{2}/(K_{J} + [J_{P}]^{2})$$
(7)

In Equations (1)–(7), $[Y_{DD}]$, $[Y_{LD}]$, $[Y_{DL}]$, and $[Y_{LL}]$ denote the concentrations of YF1 with its two LOV photosensors in the states indicated by the subscripts (i.e., D, dark-adapted, and L, light-adapted); [J] and $[J_{P}]$ denote the concentrations of the response regulator B_{J}^{F} FixJ in dephosphorylated and phosphorylated states, respectively; and [R] denotes the concentration of DsRed reporter protein. The microscopic rate constants k_{J} and k_{R} describe photoactivation and dark recovery processes of the LOV photosensors, in which I is the applied light intensity; k_{K} and k_{R} denote the rate constants for phosphorylation and dephosphorylation, respectively, of B_{J}^{F} FixJ; K_{J} is the dissociation constant for binding of phospho- B_{J}^{F} FixJ to the FixK2 promoter; and k_{T} is the rate transcription from said promoter upon activation by phospho- B_{J}^{F} FixJ. For the evaluation of pDawn, Equation (7) was replaced by Equations (8) and (9):

$$d[\lambda]/dt = k_{T}[J_{P}]^{2}/(K_{J} + [J_{P}]^{2}) - k_{D}[\lambda]$$
(8)

$$d[R]/dt = k_{\lambda}K_{\lambda}/(K_{\lambda} + [\lambda]^{4})$$
(9)

In Equations (8) and (9), $[\lambda]$ denotes the concentration of the phage λ cl repressor that forms part of the pDawn system; K_{λ} and k_{λ} are the dissociation constant of λ cl from the pR promoter and the basal transcription rate from this promoter, respectively; and $k_{\rm D}$ denotes the rate constant for degradation of λ cl destabilized by appendage of a C-terminal LVA tag. Notably, these models are approximations of the experimental systems under study. For example, growth and dilution of the culture are not taken into account

By using a Python program, the experimental data for the pDusk and pDawn systems were globally fitted to the numerical solution of the ODE system defined in Equations (1)–(9). During periods of darkness, intensity I, and hence, the rate constant $k_1=k_II$ were set to zero. To reduce the number of floating parameters and achieve a better fit convergence, several parameters were held constant. Specifically, the rate constant for the dark recovery of YF1 at 37 °C, $k_{\rm R}$, was fixed at a value of $3.7\times10^{-4}~{\rm s}^{-1}$, as experimentally determined by absorption spectroscopy. The rate constant for spontaneous hydrolysis of phospho-BJFixI $k_{\rm H}$ was fixed at a low value of $1~{\rm h}^{-1}$; the rate constants for transcription from the FixK2 and pR promoters were arbitrarily restrained at $1~{\rm s}^{-1}$. The remaining parameters were fitted as $k_{\rm I}=1.2\times10^{-4}~{\rm \mu W}^{-1}{\rm cm}^2{\rm min}^{-1}$, $k_{\rm K}=1.0~{\rm min}^{-1}$, $k_{\rm F}=1.5~{\rm min}^{-1}$, $K_{\rm J}=35$, $k_{\rm D}=2~{\rm min}^{-1}$, and $K_{\rm A}=0.02$.

Protein expression and purification: Variants of YF1 were generated by site-directed mutagenesis in the background of the expression plasmid pET-41a-YF1 through the QuikChange protocol (Invitrogen, Life Technologies GmbH). Purification of YF1 and its variants V281 and V28T was performed as described previously. Briefly, expression in *E. coli* CmpX13 cells was induced by adding isopropyl β-D-1-thiogalactopyranoside (1 mm), and cells were then incubated for 4 h at 37°C. Cells were harvested by centrifugation and lysed by ultrasound. Proteins were purified by Ni:NTA affinity chromatography and dialyzed into storage buffer (10 mm Tris-HCI pH 8.0, 10 mm NaCl, 10% (w/v) glycerol). Protein concentration was determined by absorption measurements with an Agilent 8453 UV/Vis spectrophotometer (Agilent Technologies, Santa Clara, USA) by using an extinction coefficient of 12500 m⁻¹ cm⁻¹ at λ = 450 nm.

Spectroscopic analysis: Absorption spectra of YF1 and its variants V28T and V28I were collected on an Agilent 8453 diode-array spectrophotometer as a function of time at a controlled temperature of 37 °C. To photoactivate the samples, they were illuminated for 10 s with an LED (450 nm, 30 mWcm⁻²), and dark recovery was fol-

 $\mathrm{d}[J_{\mathrm{P}}]/\mathrm{d}t = k_{\mathrm{K}}[Y_{\mathrm{DD}}][J] - k_{\mathrm{H}}[J_{\mathrm{P}}] - k_{\mathrm{P}}([Y_{\mathrm{LD}}] + [Y_{\mathrm{DL}}] + [Y_{\mathrm{LL}}])[J_{\mathrm{P}}]$

(6)





lowed by continuously recording absorption spectra. Spectra were corrected for baseline drift by subtracting the absorbance reading at $\lambda = 600$ nm. Time-dependent absorption at $\lambda = 450$ nm was fitted to a single-exponential function to determine the rate constant k_{-1} for dark recovery.

Acknowledgements

Discussions with Dr. Philipp Sasse (University of Bonn), Dr. Harald Janovjak (EMBL Australia) and members of the Möglich lab are greatly appreciated. Financial support through a Sofja-Kovalevskaya Award by the Alexander-von-Humboldt Foundation and project MO2192/3-1 by the Deutsche Forschungsgemeinschaft are gratefully acknowledged.

Conflict of Interest

The authors declare no conflict of interest.

Keywords: gene expression \cdot optogenetics \cdot photobiology \cdot sensors \cdot synthetic biology

- [1] P. Hegemann, Annu. Rev. Plant Biol. 2008, 59, 167-189.
- [2] A. Möglich, X. Yang, R. A. Ayers, K. Moffat, Annu. Rev. Plant Biol. 2010, 61, 21–47.
- [3] J. Hughes, Annu. Rev. Plant Biol. 2013, 64, 377-402.
- [4] J. M. Christie, L. Blackwood, J. Petersen, S. Sullivan, *Plant Cell Physiol.* 2015, 56, 401–413.
- [5] T. W. Engelmann, Pflüger, Arch. für die Gesammte Physiol. des Menschen und der Thiere 1883, 30, 95 – 124.
- [6] G. Nagel, D. Ollig, M. Fuhrmann, S. Kateriya, A. M. Musti, E. Bamberg, P. Hegemann, Science 2002, 296, 2395 – 2398.
- [7] G. Nagel, T. Szellas, W. Huhn, S. Kateriya, N. Adeishvili, P. Berthold, D. Ollig, P. Hegemann, E. Bamberg, Proc. Natl. Acad. Sci. USA 2003, 100, 13940–13945.
- [8] O. P. Ernst, D. T. Lodowski, M. Elstner, P. Hegemann, L. S. Brown, H. Kandori, Chem. Rev. 2014, 114, 126–163.
- [9] T. Ziegler, A. Möglich, Front. Mol. Biosci. 2015, 2, 30.
- [10] J. M. Christie, P. Reymond, G. K. Powell, P. Bernasconi, A. A. Raibekas, E. Liscum, W. R. Briggs, Science 1998, 282, 1698–1701.
- [11] K. S. Conrad, C. C. Manahan, B. R. Crane, Nat. Chem. Biol. 2014, 10, 801 809
- [12] E. F. Yee, R. P. Diensthuber, A. T. Vaidya, P. P. Borbat, C. Engelhard, J. H. Freed, R. Bittl, A. Möglich, B. R. Crane, Nat. Commun. 2015, 6, 10079.
- [13] M. T. Alexandre, J. C. Arents, R. van Grondelle, K. J. Hellingwerf, J. T. Kennis, Biochemistry 2007, 46, 3129–3137.
- [14] A. Pudasaini, K. K. El-Arab, B. D. Zoltowski, Front. Mol. Biosci. 2015, 2, 18.
- [15] K. Deisseroth, Nat. Methods 2011, 8, 26-29.
- [16] E. S. Boyden, F. Zhang, E. Bamberg, G. Nagel, K. Deisseroth, Nat. Neurosci. 2005, 8, 1263 – 1268.
- [17] F. Zhang, L.-P. Wang, M. Brauner, J. F. Liewald, K. Kay, N. Watzke, P. G. Wood, E. Bamberg, G. Nagel, A. Gottschalk, K. Deisseroth, *Nature* 2007, 446, 633–639.
- [18] N. A. Repina, A. Rosenbloom, A. Mukherjee, D. V. Schaffer, R. S. Kane, Annu. Rev. Chem. Biomol. Eng. 2017, 8, 13–39.
- [19] Q. Liu, C. L. Tucker, Curr. Opin. Chem. Biol. 2017, 40, 17–23.
- [20] A. Losi, E. Polverini, B. Quest, W. Gärtner, Biophys. J. 2002, 82, 2627–2634.
- [21] S. Akbar, T. A. Gaidenko, C. M. Kang, M. O'Reilly, K. M. Devine, C. W. Price, J. Bacteriol. 2001, 183, 1329 1338.
 [22] M. Avila-Perez, K. J. Hellingwerf, R. Kort, J. Bacteriol. 2006, 188, 6411 –
- 6414.
- [23] A. Möglich, R. A. Ayers, K. Moffat, J. Mol. Biol. 2009, 385, 1433 1444.

- [24] E. J. Capra, M. T. Laub, Annu. Rev. Microbiol. 2012, 66, 325-347.
- [25] R. Ohlendorf, R. R. Vidavski, A. Eldar, K. Moffat, A. Möglich, J. Mol. Biol. 2012, 416, 534 – 542.
- [26] L. J. Bugaj, A. T. Choksi, C. K. Mesuda, R. S. Kane, D. V. Schaffer, Nat. Methods 2013, 10, 249 – 252.
- [27] J. E. Toettcher, O. D. Weiner, W. A. Lim, Cell 2013, 155, 1422-1434.
- [28] R. P. Diensthuber, C. Engelhard, N. Lemke, T. Gleichmann, R. Ohlendorf, R. Bittl, A. Möglich, ACS Synth. Biol. 2014, 3, 811–819.
- [29] K. P. Gerhardt, E. J. Olson, S. M. Castillo-Hair, L. A. Hartsough, B. P. Landry, F. Ekness, R. Yokoo, E. J. Gomez, P. Ramakrishnan, J. Suh, D. F. Savage, J. J. Tabor, Sci. Rep. 2016, 6, 35363.
- [30] R. L. Strack, D. E. Strongin, D. Bhattacharyya, W. Tao, A. Berman, H. E. Broxmeyer, R. J. Keenan, B. S. Glick, *Nat. Methods* 2008, *5*, 955–957.
 [31] F. Kawano, Y. Aono, H. Suzuki, M. Sato, *PLoS One* 2013, *8*, e82693.
- [32] R. P. Diensthuber, M. Bommer, T. Gleichmann, A. Möglich, Structure 2013, 21, 1127 – 1136.
- [33] T. Gleichmann, R. P. Diensthuber, A. Möglich, J. Biol. Chem. 2013, 288, 29345—29355
- [34] H. E. Johnson, Y. Goyal, N. L. Pannucci, T. Schüpbach, S. Y. Shvartsman, J. E. Toettcher, *Dev. Cell* **2017**, *40*, 185–192.
- [35] A. Taslimi, B. Zoltowski, J. G. Miranda, G. P. Pathak, R. M. Hughes, C. L. Tucker, Nat. Chem. Biol. 2016, 12, 425 430.
- [36] K. Müller, R. Engesser, S. Schulz, T. Steinberg, P. Tomakidi, C. C. Weber, R. Ulm, J. Timmer, M. D. Zurbriggen, W. Weber, Nucleic Acids Res. 2013, 41, e124.
- [37] F. Richter, U. S. Scheib, J. Mehlhorn, R. Schubert, J. Wietek, O. Gernetzki, P. Hegemann, T. Mathes, A. Möglich, *Photochem. Photobiol. Sci.* 2015, 14, 270–279.
- [38] Á. Inglés-Prieto, E. Reichhart, M. K. Muellner, M. Nowak, S. M. B. Nijman, M. Grusch, H. Janovjak, Nat. Chem. Biol. 2015, 11, 952–954.
- [39] E. J. Olson, L. A. Hartsough, B. P. Landry, R. Shroff, J. J. Tabor, Nat. Methods 2014, 11, 449–455.
- [40] V. Agus, H. Janovjak, *Curr. Opin. Biotechnol.* **2017**, *48*, 8–14.
- [41] A. M. Chagas, L. L. Prieto-Godino, A. B. Arrenberg, T. Baden, PloS Biol. 2017, 15, e2002702.
- [42] A. Levskaya, A. A. Chevalier, J. J. Tabor, Z. B. Simpson, L. A. Lavery, M. Levy, E. A. Davidson, A. Scouras, A. D. Ellington, E. M. Marcotte, C. A. Voigt, *Nature* 2005, 438, 441 442.
- [43] J. J. Tabor, A. Levskaya, C. A. Voigt, J. Mol. Biol. 2011, 405, 315–324.
- [44] X. Chen, R. Liu, Z. Ma, X. Xu, H. Zhang, J. Xu, Q. Ouyang, Y. Yang, Cell Res. 2016, 26, 854–857.
- [45] T. Han, Q. Chen, H. Liu, ACS Synth. Biol. 2017, 6, 357 366.
- [46] A. Baumschlager, S. K. Aoki, M. Khammash, ACS Synth. Biol. 2017, 6, 2157–2167.
- [47] P. Ramakrishnan, J. J. Tabor, ACS Synth. Biol. 2016, 5, 733 740.
- [48] M. S. Magaraci, J. G. Bermudez, D. Yogish, D. H. Pak, V. Mollov, J. Tycko, D. Issadore, S. G. Mannickarottu, B. Y. Chow, ACS Synth. Biol. 2016, 5, 781-785.
- [49] M. S. Magaraci, A. Veerakumar, P. Qiao, A. Amurthur, J. Y. Lee, J. S. Miller, M. Goulian, C. A. Sarkar, ACS Synth. Biol. 2014, 3, 944–948.
- [50] L. B. Motta-Mena, A. Reade, M. J. Mallory, S. Glantz, O. D. Weiner, K. W. Lynch, K. H. Gardner, Nat. Chem. Biol. 2014, 10, 196–202
- Lynch, K. H. Gardner, *Nat. Chem. Biol.* **2014**, *10*, 196–202. [51] X. Wang, X. Chen, Y. Yang, *Nat. Methods* **2012**, *9*, 266–269.
- [52] G. P. Pathak, J. I. Spiltoir, C. Höglund, L. R. Polstein, S. Heine-Koskinen, C. A. Gersbach, J. Rossi, C. L. Tucker, *Nucleic Acids Res.* 2017, 45, e167.
- [53] J. E. Toettcher, D. Gong, W. A. Lim, O. D. Weiner, Nat. Methods 2011, 8, 837–839.
- [54] A. A. Kaberniuk, A. A. Shemetov, V. V. Verkhusha, Nat. Methods 2016, 13, 591–597.
- [55] A.-M. Reimers, H. Knoop, A. Bockmayr, R. Steuer, Proc. Natl. Acad. Sci. USA 2017, 114, E6457 – E6465.
- [56] T. Mathes, C. Vogl, J. Stolz, P. Hegemann, J. Mol. Biol. 2009, 385, 1511– 1518.

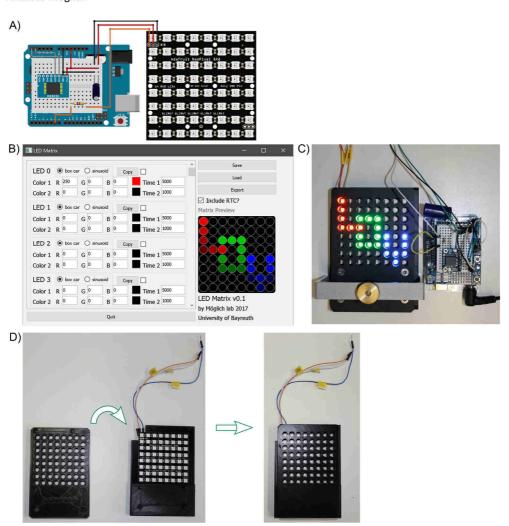
Manuscript received: January 14, 2018
Accepted manuscript online: February 14, 2018

Version of record online: April 14, 2018

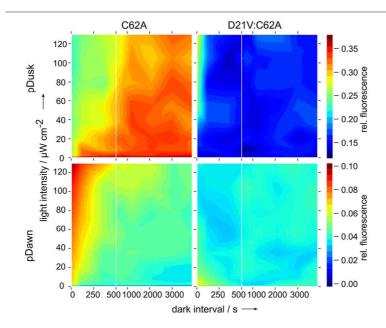
Supplementary Material

Optogenetic Control by Pulsed Illumination

Julia Hennemann, [a] Roman S. Iwasaki, [b] Tamara N. Grund, [a] Ralph P. Diensthuber, [b] Florian Richter, [b] and Andreas Möglich*(a, b)



Supplementary Figure 1. Arduino-based programmable LED matrix. A) Wiring scheme for the LED matrix. For enhanced temporal precision, a real-time clock can optionally be included. B) A Python-Qt-based user interface facilitates the configuration of the programmable LED matrix. As output, the interface generates Arduino program code ready to be compiled and uploaded to the microcontroller. C) Exemplary configuration of the programmable LED matrix. D) Adapter pieces for the programmable LED matrix can be 3D-printed, e.g., on an Anycubic i3 Mega printer using PLA (polylactic acid) filament.



Supplementary Figure 2. Intensity/pulse frequency response to intermittent illumination of gene-expression systems lacking the adduct-forming cysteine in the YF1 photoreceptor. Responsiveness to light was retained in pDusk-*Ds*Red and pDawn-*Ds*Red variants despite replacement of cysteine residue 62 in YF1 by alanine in YF1. Although the maximum degree of regulation of gene expression was diminished in most cases, the sensitivity to different intensities and pulse frequencies of light was barely affected. Fluorescence data represent the average ± s.d. of three biological replicates, are normalized to the maximum output of pDusk-*Ds*Red or pDawn-*Ds*Red, and are shown as color code.

5.2 Manuskript II



Pulsatile illumination for photobiology and optogenetics

Julia Dietler^{a,†}, Robert Stabel^{a,†}, Andreas Möglich^{a,b,c,d,*,†}

^aLehrstuhl für Biochemie, Universität Bayreuth, Bayreuth, Germany

Contents

1.	Introduction	228
2.	Programmable arrays of light-emitting diodes	231
	2.1 Arrays with red/green/blue-emitting diodes	231
	2.2 Arrays with custom light-emitting diodes	233
	2.3 Housing and adapters for the LED arrays	234
	2.4 Configuration and calibration of the LED arrays	235
3.	Control of bacterial gene expression by varying light intensity and pulse	
	frequency	236
	3.1 Materials	238
	3.2 Protocol	238
4.	Engineering and characterization of photoactivated adenylyl cyclases	240
	4.1 Materials	240
	4.2 Protocol A	242
	4.3 Protocol B	243
5.	Summary and conclusion	244
Acknowledgments		245
References		245

Abstract

Living organisms exhibit a wide range of intrinsic adaptive responses to incident light. Likewise, in optogenetics, biological systems are tailored to initiate predetermined cellular processes upon light exposure. As genetically encoded, light-gated actuators, sensory photoreceptors are at the heart of these responses in both the natural and engineered scenarios. Upon light absorption, photoreceptors enter a series of generally rapid photochemical reactions leading to population of the light-adapted signaling

Methods in Enzymology, Volume 624 ISSN 0076-6879 https://doi.org/10.1016/bs.mie.2019.04.005 © 2019 Elsevier Inc. All rights reserved.

227

^bResearch Center for Bio-Macromolecules, Universität Bayreuth, Bayreuth, Germany

^cBayreuth Center for Biochemistry & Molecular Biology, Universität Bayreuth, Bayreuth, Germany

^dNorth-Bavarian NMR Center, Universität Bayreuth, Bayreuth, Germany

^{*}Corresponding author: e-mail address: andreas.moeglich@uni-bayreuth.de

[†] ORCID identifiers: J.D. 0000-0002-0418-0796; R.S. 0000-0002-9159-0004; A.M. 0000-0002-7382-2772.

state of the receptor. Notably, this state persists for a while before thermally reverting to the original dark-adapted resting state. As a corollary, the inactivation of photosensitive biological circuits upon light withdrawal can exhibit substantial inertia. Intermittent illumination of suitable pulse frequency can hence maintain the photoreceptor in its light-adapted state while greatly reducing overall light dose, thereby mitigating adverse side effects. Moreover, several photoreceptor systems may be actuated sequentially with a single light color if they sufficiently differ in their inactivation kinetics. Here, we detail the construction of programmable illumination devices for the rapid and parallelized testing of biological responses to diverse lighting regimes. As the technology is based on open electronics and readily available, inexpensive components, it can be adopted by most laboratories at moderate expenditure. As we exemplify for two use cases, the programmable devices enable the facile interrogation of diverse illumination paradigms and their application in optogenetics and photobiology.

1. Introduction

Numerous organisms employ sensory photoreceptor proteins to derive spatial and temporal cues from incident light for the adjustment of physiology, behavior and lifestyle (Hegemann, 2008; Möglich, Yang, Ayers, & Moffat, 2010). Photoreceptors double as genetically encoded, light-gated actuators in optogenetics (Deisseroth et al., 2006) to enable the non-invasive optical manipulation of diverse cellular processes with exquisite spatiotemporal resolution (Losi, Gardner, & Möglich, 2018). In the absence of light, sensory photoreceptors assume their thermodynamically most stable, dark-adapted state, denoted D in the following; absorption of light initiates a cyclic series of photochemical reactions, denoted photocycle, as part of which the light-adapted signaling state L is populated (Ziegler & Möglich, 2015). This photocycle is generally reversible, and the metastable state L persists for a while before passively, i.e., thermally, decaying to D in a process called dark recovery over the course of seconds to days, depending on photoreceptor. Based on the chromophore used for light absorption and the photochemistry exhibited, sensory photoreceptors divide into around 10 families. As one family, light-oxygen-voltage (LOV) receptors bind flavin-nucleotide chromophores and respond to blue light (Christie et al., 1998; Salomon et al., 2001; Yee et al., 2015). Of note, the light-adapted state L of LOV receptors reverts to D in a strongly temperature-dependent, base-catalyzed reaction (Alexandre, Arents, van Grondelle, Hellingwerf, & Kennis, 2007), the kinetics of which can be deliberately varied over several orders of magnitude via modification of certain amino acids adjacent to the flavin chromophore (Pudasaini, El-Arab, &

Zoltowski, 2015). Phytochromes (Phys) constitute a large receptor family sensitive to red and far-red light that occur in plants, (cyano)bacteria and fungi (Rockwell & Lagarias, 2010). In conventional Phys, red light drives the transition of D to the light-adapted state L which returns to D either thermally or through absorption of a second light quantum of far-red color.

Experiments in the neurosciences aside, optogenetic applications often take place on comparatively long time scales and frequently involve the prolonged exposure to light of the system under study. The underlying photoreceptors hence repeatedly transition between their dark-adapted and light-adapted states D and L, and under constant illumination a photostationary state is assumed. Rather than continuously illuminating throughout the experiment, light may also be applied intermittently in pulsatile manner. By reducing the overall light dose (cf. below), this approach can mitigate phototoxicity, photobleaching and sample heating. In addition, pulsed illumination can enable the multiplexing of several light-sensitive systems and their selective activation (Hennemann et al., 2018). We illustrate these aspects by means of two numerical simulations (Fig. 1). In the first and conceptually simplest scenario, a given photoreceptor be monomeric and assume either the D or L state. The forward transition $D \rightarrow L$ proceed with a unimolecular rate constant k_1 , dependent on the applied light intensity, and the backward reaction $L \rightarrow D$, i.e., the dark recovery, with a lightindependent unimolecular rate constant k_{-1} . As shown in Fig. 1B, during a train of light pulses the system repeatedly cycles between the D and L states as determined by the relative magnitudes of the microscopic rate constants k_1 and k_{-1} and of the applied pulse frequency. At least two points are of note: first, lighting schemes with the same overall light dose may activate the photoreceptor to rather different average levels, depending upon the timing of successive light pulses (left and right panels in Fig. 1B); second, two photoreceptor systems may be discriminated in the pulse-frequency domain, albeit to limited extent, given the single-exponential recovery kinetics. A second, more complex scenario considers a homodimeric photoreceptor subjected to the same light-pulse sequence as before (Fig. 1C). For simplicity, we assume that the two subunits of the receptor undergo the $D \leftrightarrow L$ transition independently of another with microscopic rate constants of k_1 and k_{-1} . As a consequence, the reaction from the fully darkadapted state DD to the fully light-adapted state LL, and vice versa, proceeds via the mixed-state intermediates DL and LD, therefore giving rise to sigmoidal reaction kinetics instead of single-exponential ones. For the present scope, we further assume that the receptor be cooperative (Monod,

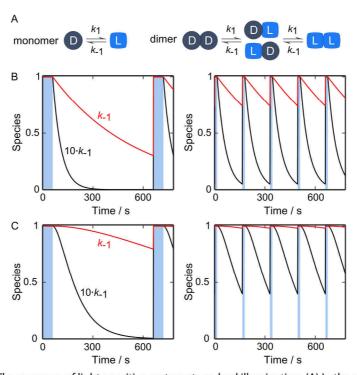


Fig. 1 The response of light-sensitive systems to pulsed illumination. (A) In the simplest scenario, light drives the transition of a monomeric photoreceptor from its darkadapted state (D) to its light-adapted signaling state (L) with a unimolecular rate constant k_1 that depends on illumination intensity. Once in the signaling state, the receptor thermally reverts to state D with a unimolecular rate constant k_{-1} . In a somewhat more complex scenario, the photoreceptor be dimeric and capable of populating an intermediate state with one protomer in the D, and the other in the L state. For simplicity, the protomers are assumed to transition between the two photochemical states D and L independently of another with the rate constants k_1 and k_{-1} , respectively. (B) The kinetic scheme for the monomer scenario was numerically solved in time for the indicated regime of periodic illumination. Blue bars mark periods where light is applied and the D

L transition is hence promoted; at other times, light is off, and the monoexponential $L \rightarrow D$ reversion predominates. The ordinate denotes the fraction of the receptor in the L state. Two simulations for slow and fast dark recovery with rate constants $k_{-1} = 0.01 \,\mathrm{s}^{-1}$ and $10 \cdot k_{-1}$ are shown as red and black lines, respectively. Compared to the left panel, in the righthand one the frequency of pulsing is increased fourfold and the duration of each light period reduced by the same factor, thus retaining the same overall light dose. (C) The two panels report corresponding simulations for the dimer scenario, where the ordinate shows the sum of the species DL, LD and LL. In contrast to (B), the recovery reaction is of sigmoidal functionality.

Wyman, & Changeux, 1965) in that the LL, DL and LD states have the same output activity, a situation that has been experimentally demonstrated for at least one photoreceptor system (Möglich, Ayers, & Moffat, 2009). As illustrated in Fig. 1C, the homodimeric scenario also exhibits higher average extents of light activation if a given light dose is spread over several shorter pulses rather than concentrated in infrequent but longer pulses. In addition, the simulations show that the sigmoidal reaction course enables a much better discrimination between two systems with different recovery kinetics, thus allowing the sequential addressing of these systems by light of varying pulse frequency and intensity (Hennemann et al., 2018). While, evidently, other and more complex photoreceptor reaction schemes are conceivable, even the simple simulations compellingly show that the response to light may drastically differ between systems. We note that during optogenetic deployment, reaction steps downstream of photoreceptor activation, often nonlinear and cooperative, may additionally contribute to complex recovery kinetics and response dynamics to pulsatile light (Ziegler & Möglich, 2015).

To efficiently probe and subsequently exploit the response of optogenetic systems to intermittently applied light, we built programmable arrays of light-emitting diodes (LEDs) that allow the testing and application of multiple lighting regimes in parallel (Hennemann et al., 2018; Stüven et al., 2019). Here, we recapitulate the construction of these arrays (Section 2) and their deployment to two photoreceptor systems (Sections 3 and 4).



2. Programmable arrays of light-emitting diodes

2.1 Arrays with red/green/blue-emitting diodes

In this section, we detail the assembly of a programmable matrix of red/green/blue (RGB) three-color LEDs based on an open-source Arduino microcontroller and commercially available electronics (Hennemann et al., 2018). The setup allows the illumination from below of 64 wells of a standard 96-well microtiter plate (MTP) with programmable light signals of adjustable intensity, timing and color (peak wavelengths of 470, 525 and 620 nm) (Fig. 2). The wiring scheme (Fritzing file) of the three-color LED setup can be obtained at http://www.moeglich.uni-bayreuth.de/en/software.

2.1.1 Materials

- Arduino Uno microcontroller (Arduino, Turin, Italy)

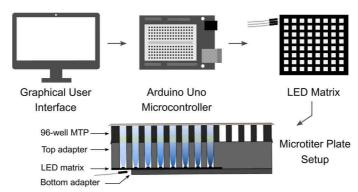


Fig. 2 Schematic illustrating the application of programmable lighting in microtiter-plate (MTP) format. A graphical user interface, implemented in Python/Qt, facilitates the configuration of the programmable array of 64 light-emitting diodes (LED). The configuration file is uploaded to an Arduino circuit board which controls the timing and intensity of the single LEDs in the array. The array is encased in a 3D-printed housing and an MTP mounted on top to allow illumination of individual wells from below (Hennemann et al., 2018; Stüven et al., 2019).

- Adafruit NeoPixel NeoMatrix 8×8 (Adafruit Industries, New York, USA)
- jumper wires (EXP GmbH, Saarbrücken, Germany)
- resistor 470Ω (EXP GmbH)
- electrolytic capacitor 4700 μF, 10 V (EXP GmbH)
- breadboard (EXP GmbH)
- solder and soldering iron
- AC power supply 5 V, 4 A (EXP GmbH)
- optional: real-time clock DS3221 (Adafruit Industries)

2.1.2 Protocol

- i. Optionally, a real-time clock (RTC) for enhanced temporal precision can be used. If so, place the RTC on the breadboard and connect it to the 5 V power (5 V) and ground (GND) pins of the Arduino board using jumper wires. Further, connect the SCL (serial clock line) and SDA (serial data line) pins of the RTC to the analog inputs 4 and 5, respectively, of the Arduino board.
- ii. Connect the 5V and GND pins of the Arduino board to the "+" and "-" rows of the breadboard. Now, any pin/wire inserted into these rows will also be connected to power or ground, respectively.
- **iii.** Connect the electrolytic capacitor by attaching its cathode (short leg) to the "-" row and its anode (long leg) to the "+" row of the board.

- iv. Place the $470\,\Omega$ resistor on the breadboard and connect it to the digital pin 6 of the Arduino microcontroller.
- **v.** Connect the 5V and GND pins of the NeoPixel LED matrix to "+"/"—" on the breadboard; connect the DIN pin to the resistor. To secure the connections, the jumper wires can be soldered in place.

2.2 Arrays with custom light-emitting diodes

Here, we describe a dual-color array that uses custom LEDs (Stüven et al., 2019). The setup allows the illumination from below of 64 wells of a standard 96-well MTP with programmable light signals of adjustable intensity, timing and two custom colors. In the example detailed here, LEDs with peak wavelengths of 655 and 850 nm are used, but the design also applies to other LEDs of diverse colors.

2.2.1 Materials

- Arduino Uno microcontroller (Arduino)
- ITEAD Full Color RGB LED Matrix Driver Shield (Itead, Shenzhen, China)
- jumper wires (EXP GmbH)
- resistor 470Ω (EXP GmbH)
- electrolytic capacitor 4700 μF, 10 V (EXP GmbH)
- breadboard (EXP GmbH)
- solder and soldering iron
- AC power supply 5 V, 4 A (EXP GmbH)
- 64×3 -mm LED color #1 [e.g., Kingbright WP908A8SRD, (655 \pm 20) nm, Mouser Electronics, Munich, Germany]
- 64 × 3-mm LED color #2 [e.g., Harvatek HE1-120AC-XXXX (850 ± 42) nm, Conrad Electronic SE, Hirschau, Germany]
- printed circuit board (PCB) [Eagle template file (.brd) and wiring scheme (.sch) are available at http://www.moeglich.uni-bayreuth.de/ en/software]
- optional: real-time clock DS3221 (Adafruit Industries)

2.2.2 Protocol

i. Print the custom circuit board according to the Eagle template file (.brd). Electronics shops or dedicated companies, such as PCBA-Store (http://www.pcbastore.com), EasyEDA (http://easyeda.com), Pad2pad (http://www.pad2pad.com), or ExpressPCB (http://www.expresspcb.com), can routinely do this for a small fee.

ii. Position the two sets of 64 LEDs on the PCB according to the wiring scheme (.sch) and solder them in place.

- **iii.** Connect the LED driver shield to the Arduino microcontroller such that the pins on both elements line up.
- **iv.** Use jumper wires to connect the assembled PCB and the LED driver shield according to the wiring scheme.

2.3 Housing and adapters for the LED arrays

The above LED arrays need to be embedded in a custom-made mounting adapter that reduces light contamination between adjacent LEDs and allows positioning of an MTP on top such that it can be illuminated from below. As one option, the required adapter pieces may be obtained by subtractive manufacturing, which is offered by various companies. As described below, alternatively the pieces can be obtained by 3D printing.

2.3.1 Materials

- template files for the base plate and mounting adapter (.stl files available at http://www.moeglich.uni-bayreuth.de/en/software)
- 3D printer, e.g., Anycubic I3 MEGA (GearBest, China)
- polylactic acid (PLA) print filament, ideally in black (available from diverse suppliers)

2.3.2 Protocol

- i. There are separate versions of the adapter pieces for the RGB (cf. Section 2.1) and the custom LED arrays (cf. Section 2.2); ensure to use the correct one. Prior to printing, the template file for the adapter pieces can be further adjusted to accommodate individual needs (e.g., different MTPs, incubator platforms, etc.). To this end, free software for computer-aided design, e.g., TinkerCAD (http://www.tinkercad.com) can be used.
- ii. Print bottom and top piece of the adapter using PLA filament, a fill factor between 25% and 50%, and a precision of 100 μm. Use of ABS filament is not recommended as it is prone to warping. We found that the print precision of consumer-grade printers is fully sufficient for the task. Alternatively, printing can be done by 3D-printing services, such as Proto Labs (http://www.protolabs.com), i.materialise (http://all3dp.com) or 3D Hubs (http://www.3dhubs.com).
- **iii.** Remove residual filament from the printed pieces using pliers and scissors.

iv. Place LED array on bottom adapter piece, then cover with top piece.

2.4 Configuration and calibration of the LED arrays

To facilitate the configuration of the programmable LED matrices, we supply a Python-based graphical user interface (GUI). As output, the interface generates an Arduino sketch file (.ino) that needs to be compiled and uploaded to the Arduino board. Optionally, a light power meter may be used to calibrate the intensity of the programmable LED arrays.

2.4.1 Materials

- USB-A to USB-B cable
- Python-based LED controller interface (available at http://www.moeglich.uni-bayreuth.de/en/software)
- Arduino Integrated Development Environment (IDE) (available at http://www.arduino.cc)
- optional: light power meter (model 842-PE, Newport, Darmstadt, Germany)
- optional: silicon photodetector (model 918D-UV-OD3, Newport)

2.4.2 Protocol

- i. Identify the version of the GUI applicable to the LED matrix you are using (RGB, cf. Section 2.1; or custom LEDs, cf. Section 2.2) and download the corresponding Python file. The program can be executed with Python version 3 on Windows, Linux and OS X platforms. Alternatively, for Windows platforms, we supply a stand-alone binary file.
- **ii.** Use the GUI to configure the timing scheme and brightness of each LED individually. Note that the brightness of the LEDs is set by pulsewidth modulation (PWM) on an 8-bit scale.
- **iii.** *optional*: To enhance the temporal accuracy of the Arduino board (which can be quite modest), an RTC module (cf. above) may be included. If so, a checkbox in the GUI should be activated.
- **iv.** Once the configuration is completed, the current settings can be saved as a configuration file (.cfg). Export the configuration as an Arduino sketch file (.ino), close the GUI.
- v. Start the Arduino IDE and open the (.ino) file generated in the previous step. At first use, Arduino driver libraries for the RTC and, in case of the RGB LED matrix (cf. Section 2.1), the NeoPixel matrix need to be installed. To this end, select "Manage Libraries" from

the "Sketch→Include Library" pull-down menu. Locate the "RTClib" and "Adafruit NeoMatrix" entries and install the libraries as required.

- **vi.** Advanced users may optionally wish to directly modify the Arduino sketch file rather than use the GUI. Connect the Arduino board to the computer via the USB cable, compile the program code and upload it to the board.
- **vii.** Provided no errors occurred, the LED array should now start lighting up as configured.
- viii. optional: The actual light output of the LED matrix for given intensity settings may be calibrated with a lamp power meter. To this end, place the detector of the lamp power meter directly atop the upper piece of the LED assembly and measure the emitted light output for several software intensity settings. Owing to the use of PWM, we found the set and actual light intensities to be linearly correlated. Variations between different LEDs of the matrix were found to be negligible. Note that the light output may depend on the power supply attached to the LED matrix; hence, the calibration should be done for the power supply to be used in the actual experiment.



3. Control of bacterial gene expression by varying light intensity and pulse frequency

We deployed the programmable RGB LED matrix (cf. Section 2.1) to systematically chart the response of the YF1/BjFixJ two-component system (TCS) (Hennemann et al., 2018), as implemented on the pDusk plasmid (Ohlendorf, Vidavski, Eldar, Moffat, & Möglich, 2012), to intermittently applied blue light of varying intensity (Fig. 3A). Briefly, the LOV receptor YF1 derives from the fusion of the photosensor module of Bacillus subtilis YtvA and the effector module of the Bradyrhizobium japonicum BjFixL histidine kinase (Möglich et al., 2009). Provided both LOV sensors of the homodimeric YF1 reside in their dark-adapted states (denoted DD), the receptor readily phosphorylates the so-called response regulator (RR) BjFixJ. In its phosphorylated form, the RR drives the expression from cognate promoters, e.g., of the red-fluorescent reporter DsRed (Strack et al., 2008). Upon blue-light absorption by the LOV modules, YF1 assumes the photochemically mixed states DL and LD or the fully light-adapted state LL, all of which act as a phosphatase on phospho-BjFixJ (Möglich et al.,

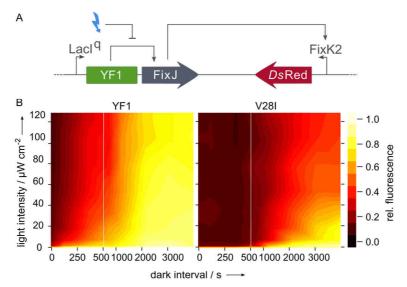


Fig. 3 Optogenetic control of the pDusk system by pulsed blue light. (A) The pDusk-DsRed plasmid wires the blue-light-inhibited two-component system YF1/BjFixJ to the expression of the red-fluorescent reporter DsRed (Möglich et al., 2009; Ohlendorf et al., 2012). (B) Escherichia coli bacteria harboring pDusk-DsRed were cultivated under different lighting regimes as controlled by the programmable LED array. In periodic manner, illumination for 30s at different intensities (denoted on the ordinate) was followed by dark intervals of variable duration (abscissa). For each parameter setting, the reporter fluorescence of three replicate bacterial cultures was averaged and is plotted as color code. Data for the original pDusk system (left) are juxtaposed to data for a derivative pDusk system (right) which employs the V28I variant of YF1 that features much decelerated recovery kinetics and is hence effectively more light-sensitive (Hennemann et al., 2018).

2009). As for other LOV receptors, the light-adapted state thermally returns to the dark-adapted state in the dark recovery reaction. Certain residue exchanges placed near the flavin chromophore of the LOV sensor can strongly modulate the kinetics of dark recovery (Pudasaini et al., 2015). Specifically, within the pDusk context, we replaced valine 28 of YF1 by isoleucine which resulted in greatly decelerated recovery kinetics (Hennemann et al., 2018; Kawano, Aono, Suzuki, & Sato, 2013). As explained in the below protocol, we assessed the impact of different blue-light regimes on DsRed reporter expression from pDusk plasmids encoding the original YF1 receptor or its V28I variant.

3.1 Materials

 plasmid pDusk encoding a fluorescent reporter such as DsRed (plasmid pDusk available from Addgene, plasmid 43795)

- Escherichia coli expression strain, e.g., BL21 or CmpX13 (Mathes, Vogl, Stolz, & Hegemann, 2009)
- lysogeny broth medium supplemented with $50 \,\mu g \, mL^{-1}$ kanamycin (LB/Kan)
- programmable RGB LED matrix (cf. Sections 2.1 and 2.3)
- black-wall clear-bottom 96-well MTPs (Greiner BioOne, Frickenhausen, Germany)
- black 96-well MTPs (e.g., Greiner)
- transparent 96-well MTPs (e.g., Greiner)
- gas-permeable sealing film (BF-410400-S, Corning, New York, USA)
- incubator, e.g., HN-2 Herp Nursery II (Lucky Reptile, Waldkirch, Germany)
- MTP shaker, e.g., PMS-1000i (Grant Instruments, Cambridge, UK)
- multimode MTP reader, e.g., Tecan Infinite M200 PRO (Tecan Group Ltd., Männedorf, Switzerland)

3.2 Protocol

- i. Transform between 10 pg and 100 ng of the pDusk-DsRed plasmid into E. coli CmpX13 cells, plate on LB/Kan agar and incubate over night at 37 °C. (Note that here and in the following experimental steps, we assume that the DsRed reporter and E. coli CmpX13 cells are used. However, other fluorescent proteins and E. coli BL21 strains may be used instead.)
- **ii.** Inoculate a 5-mL LB/Kan starter culture with a single clone from a freshly transformed plate and incubate at 37 °C until an optical density at 600 nm (OD₆₀₀) of 0.3 is reached.
- iii. Take 10 µL of the starter culture and inoculate 15 mL of pre-warmed LB/Kan medium.
- iv. Mix thoroughly and dispense $200\,\mu\text{L}$ each to 64 wells (use rows A–H and columns 1–8) of a black-wall, clear-bottom 96-well MTP using a multichannel pipette.
- **v.** Seal the MTP with a gas-permeable film to allow sufficient air circulation during subsequent incubation.

- vi. Configure the LED matrix according to Section 2. For the study of light-dependent gene expression in pDusk, we varied the intensity of blue light (470 nm) between 0 and 130 μW cm⁻² and used a periodic illumination scheme where individual wells were exposed to light for 30s before incubation in the dark for periods between 0 and 65 min. The alternating dark/light cycles continued until the end of the incubation (Hennemann et al., 2018).
- **vii.** Place the sealed MTP plate on top of the configured LED-array setup. If necessary, fix the plate in position with duct tape.
- viii. Mount the assembly on an MTP shaker, place inside a suitable incubator and incubate at 37 °C and 600 rpm for 16 h. Continuous shaking throughout the entire experiment promotes aeration of the cultures and ensures their homogenous mixing and illumination. Ensure that the incubator is tightly sealed against stray light from the outside and stays closed for the entire experiment.
 - ix. Remove the sealing film. Using a multi-channel pipette, transfer $40\,\mu\text{L}$ of each culture to a transparent MTP and add $210\,\mu\text{L}$ H_2O . Measure OD_{600} of each well in an MTP reader. If absorbance falls outside the interval 0.1–1.0, prepare another solution of the bacterial cultures at an appropriate dilution factor.
 - **x.** Using a multi-channel pipette, transfer $40\,\mu\text{L}$ of the diluted solutions from the previous step to a black MTP and add $210\,\mu\text{L}$ H₂O. Measure reporter fluorescence of each well in an MTP reader. To monitor DsRed fluorescence, we used excitation and emission wavelengths of (554 ± 9) and (591 ± 20) nm, respectively. For optimal results, adjust the gain and focal height of the MTP reader. To allow comparison between experiments on different days, these settings must be left unchanged.
 - **xi.** Normalize fluorescence data to OD_{600} and plot as 2D contours plots as a function of the duration of the dark period and the intensity of pulsed illumination (Fig. 3B).
- **xii.** As the expected result, the *Ds*Red reporter-gene output for either YF1 or V28I should decrease monotonically with light intensity (ordinate in Fig. 3B) but increase monotonically with the length of the dark period (abscissa). In comparison to the original YF1, the V28I variant with slower dark-recovery kinetics is toggled by lower overall light doses, i.e., it is more light-sensitive.



4. Engineering and characterization of photoactivated adenylyl cyclases

We originally developed the programmable arrays with custom LEDs (cf. Section 2.2) to probe the response of certain photoactivated adenylyl cyclases (PAC) to red/far-red light regimes of varying intensity and timing (Stüven et al., 2019). Briefly, PACs mediate the production of the versatile second messenger 3', 5' cyclic adenosine monophosphate (cAMP) in a lightstimulated manner. Several naturally occurring, mostly blue-light-sensitive PACs (Blain-Hartung et al., 2018; Iseki et al., 2002; Raffelberg et al., 2013; Ryu, Moskvin, Siltberg-Liberles, & Gomelsky, 2010; Schröder-Lang et al., 2007; Stierl et al., 2011) have been supplemented by engineered PACs that respond to red and far-red light (Etzl, Lindner, Nelson, & Winkler, 2018; Ryu et al., 2014; Stüven et al., 2019). These PACs are based on bacteriophytochrome (BPhy) sensor units and can be bidirectionally toggled between two functional states by red and far-red light, respectively, thus potentially enhancing the precision in time and space of optogenetic applications (Ziegler & Möglich, 2015). Moreover, red and far-red light exhibit deeper penetration of biological tissue than blue light (Weissleder, 2001), thus rendering BPhy-based PACs attractive for optogenetics in vivo. To rapidly assess the light-dependent activity of PACs, we established the pCyclR reporter-gene assay in E. coli, as illustrated in Fig. 4A (Stüven et al., 2019). In this assay, the functional expression of PACs, followed by stimulation with light of suitable quality and quantity, prompts the intracellular production of cAMP. In turn, the endogenous E. coli catabolite activator protein binds cAMP and activates the expression of the redfluorescent reporter DsRed. By resorting to this assay, we engineered the photoreceptor DdPAC which displays cAMP production that is elevated and diminished by exposure to red and far-red light, respectively. The two protocols below illustrate the application of the pCyclR reporter system to record the response of DdPAC to red and far-red light of varying intensity (protocol A, Fig. 4B) and timing (protocol B, Fig. 4C).

4.1 Materials

- pCyclR reporter plasmid (kanamycin resistance marker; available from the authors)
- pCDF plasmid harboring expression cassettes for *Dd*PAC and *Synechocystis* sp. heme oxygenase (streptomycin resistance marker; available from the authors)

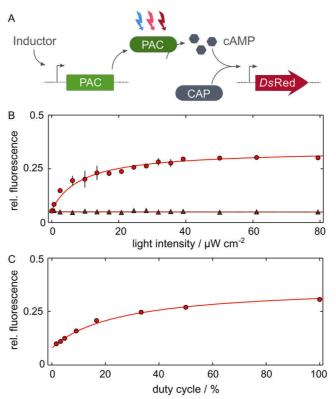


Fig. 4 Characterization of the red-light-responsive adenylyl cyclase *Dd*PAC (Stüven et al., 2019). (A) The pCyclR test bed for photoactivated adenylyl cyclases (PAC) relies on the inducible expression of PACs in *Escherichia coli*. Upon stimulation with light, PACs ramp up the production of the second messenger 3′, 5′ cyclic adenosine monophosphate (cAMP) which associates with the endogenous catabolite activator protein (CAP) to enable upregulation of the expression of a *Ds*Red reporter gene. (B) Using the pCyclR system and programmable lighting, we probed the response of *Dd*PAC to constant illumination of varying intensity and wavelengths of 655 (circles) and 850 nm (triangles), respectively. *E. coli* cultures harboring pCyclR and *Dd*PAC were grown at the different light settings, and *Ds*Red fluorescence of four biological replicates \pm standard deviation is reported. (C) As in (B), but cultures were intermittently illuminated with 655-nm light at 40 μW cm⁻². The abscissa denotes the fraction of time for which light was applied.

- adenylyl-cyclase-deficient *E. coli* strain CmpX13 $\Delta cyaA$ (available from the authors)
- lysogeny broth medium supplemented with 50 µg mL⁻¹ kanamycin and 100 µg mL⁻¹ streptomycin (LB/Kan+Strep)
- isopropyl β-D-1-thiogalactopyranoside (IPTG; 1 M stock solution)
- programmable matrix with 655 and 850-nm LEDs (cf. Sections 2.2 and 2.3)

- black-wall clear-bottom 96-well MTPs (Greiner)
- black 96-well MTPs (e.g., Greiner)
- transparent 96-well MTPs (e.g., Greiner)
- gas-permeable sealing film (BF-410400-S, Corning)
- incubator, e.g., HN-2 Herp Nursery II (Lucky Reptile)
- MTP shaker, e.g., PMS-1000i (Grant Instruments)
- multimode MTP reader, e.g., Tecan Infinite M200 PRO (Tecan Group Ltd.)

4.2 Protocol A

- i. Transform between 10 pg and 100 ng each of the pCyclR reporter and the pCDF expression plasmids into *E. coli* CmpX13 ΔcyaA cells, plate on LB/Kan + Strep agar and incubate over night at 37 °C. If efficiency is insufficient, transform the two plasmids sequentially. (Note that here and in the following experimental steps, we assume that the pCDF DdPAC expression plasmid and *E. coli* CmpX13 ΔcyaA cells are used. However, other PAC proteins and cyclase-deficient *E. coli* BL21 strains may be used instead.)
- **ii.** Inoculate a 5-mL LB/Kan+Strep starter culture with a single clone from a freshly transformed plate and incubate over night at 37 °C.
- iii. Dispense $180\,\mu\text{L}$ LB/Kan + Strep each to 64 wells (use rows A–H and columns 1–8) of a black-wall, clear-bottom 96-well MTP using a multichannel pipette. Inoculate each well with $2\,\mu\text{L}$ of the over-night culture.
- **iv.** Seal the MTP with a gas-permeable film to allow sufficient air circulation during subsequent incubation.
- **v.** Place the MTP on a shaker and incubate at 37 °C and 800 rpm for 1 h in darkness.
- vi. Add 60 μL of 0.2 mM IPTG in LB/Kan+Strep to each well. The resultant final IPTG concentration of 50 μM proved ideal for *Dd*PAC; however, other PACs may require different inductor concentrations.
- vii. Configure the LED matrix according to Section 2. For the study of *Dd*PAC activation by constant illumination, we varied the intensity of red (peak emission 655 nm) and far-red light (850 nm) between 0 and 80 μW cm⁻² (Stüven et al., 2019).
- **viii.** Place the sealed MTP plate on top of the configured LED-array setup. If necessary, fix the plate in position with duct tape.

- **ix.** Mount the assembly on an MTP shaker, place inside a suitable incubator and incubate at 37 °C and 800 rpm for 22 h. Ensure that the incubator is tightly sealed against stray light from the outside and stays closed for the entire experiment.
- **x.** Remove the sealing film. Using a multi-channel pipette, transfer $25\,\mu\text{L}$ of each culture to a transparent MTP and add $225\,\mu\text{L}$ H₂O. Measure OD₆₀₀ of each well in an MTP reader. If absorbance falls outside the interval 0.1–1.0, prepare another solution of the bacterial cultures at an appropriate dilution factor.
- **xi.** Using a multi-channel pipette, transfer $50\,\mu\text{L}$ of the diluted solutions from the previous step to a black MTP and add $200\,\mu\text{L}$ H₂O. Measure reporter fluorescence of each well in an MTP reader. To monitor DsRed fluorescence, we used excitation and emission wavelengths of (554 ± 9) and (591 ± 20) nm, respectively. For optimal results, adjust the gain and focal height of the MTP reader. To allow comparison between experiments on different days, these settings must be left unchanged.
- **xii.** Normalize fluorescence data to OD_{600} and plot as a function of the intensity of red/far-red illumination, e.g., using the open-source Fit-o-mat software (Möglich, 2018) (Fig. 4B).
- **xiii.** As the expected result, the *Ds*Red reporter-gene output should increase hyperbolically with red-light intensity but should stay constant at a basal level for far-red illumination.

4.3 Protocol B

- i. Follow steps i-vi as described for protocol A.
- ii. Configure the LED matrix according to Section 2. For the study of *Dd*PAC activation by pulsed illumination, we used a red-light (peak emission 655 nm) intensity of 40 μW cm⁻². In periodic manner, illumination for 60 s was followed by incubation in darkness for between 0 and 3600 s. The alternating dark/light cycles continued until the end of the incubation (Stüven et al., 2019).
- iii. Follow steps viii-xii as described for protocol A.
- **iv.** As the expected result, the *Ds*Red reporter-gene output should increase hyperbolically with the duty cycle of red-light exposure (Fig. 4C), where the duty cycle denotes the fraction of time during which light was applied.

5. Summary and conclusion

Beyond variation of light quantity (intensity) and quality (color), the timing of intermittently applied light affords an additional input dial for adjusting the output of optogenetic systems. Pulsatile illumination offers at least two principal advantages (Hennemann et al., 2018): first, carefully chosen lighting sequences can significantly lower the required overall light dose, thus reducing phototoxicity, photobleaching and heat input, but retaining the desired optogenetic output. Second, intermittent light facilitates the parallel deployment of several light-regulated circuits even when they are sensitive to the same light quality (i.e., wavelength), as long as they differ in their response to pulsatile light. As exemplified for the pDusk variants YF1 and V28I (cf. Section 3), a single light color suffices for successively actuating two systems, thus freeing up optical input channels that may be used for other optogenetic actuators and fluorescent reporters. The exact response to pulsed illumination is primarily governed by the reversal kinetics of the system in question, i.e., how fast is the dark-adapted state regained after prior light exposure, but other aspects matter as well. Whereas in simple scenarios these kinetics are of single-exponential form (cf. Fig. 1B), the output of other systems may be governed by oligomeric species and cooperative effects, thus giving rise to non-exponential and more complex reversal kinetics (cf. Fig. 1C). This type of cooperativity has indeed been observed for certain homodimeric photoreceptors (Möglich et al., 2009) and is generally expected to at least some extent for light-mediated reactions that involve two or more light-responsive entities. As a case in point, the plant cryptochrome 2 is known to undergo light-dependent homo-oligomerization which has been amply exploited for optogenetic intervention in different cellular processes (Bugaj, Choksi, Mesuda, Kane, & Schaffer, 2013; Bugaj et al., 2015; Losi et al., 2018; Taslimi et al., 2014). Moreover, reaction sequences downstream of the photoreceptor and en route to the eventual optogenetic output may entail nonlinear and thresholding effects, thus further altering the response dynamics of the system to (pulsed) illumination. Taken together, the relevant response kinetics may be challenging to gauge upfront and should ideally be assessed on a case-by-case basis for each optogenetic system.

Against this backdrop, the advent of affordable, customizable, parallelizable and programmable illumination devices appears particularly relevant. Numerous light intensities and timing schemes can be interrogated

in parallel and facile manner, thus allowing the response characteristics of a given light-sensitive system to be precisely mapped. Provided two such systems sufficiently differ in that regard, they can be sequentially activated by a single light color (cf. Fig. 3; Hennemann et al., 2018). To fully capitalize on the enhanced throughput for light-mediated actuation, the recording of the system response should support commensurate throughput. On the one hand, reporter-gene assays, as demonstrated here (cf. Sections 3 and 4), apply as they efficiently report on the activity of the light-responsible system, even if only in indirect manner. On the other hand, one may directly monitor the desired optogenetic response of the system under study if it gives rise to a readily recordable phenotype.

The programmable arrays of light-emitting diodes used here are entirely based on open electronics and commercially available parts. Hence, most laboratories will be able to assemble them at moderate expenditure of time and cost. Our setups (Hennemann et al., 2018; Stüven et al., 2019) and a host of related ones for programmable illumination (Chen, Mertiri, Holland, & Basu, 2012; Davidson, Basu, & Bayer, 2013; Gerhardt et al., 2016; Heo, Cho, Ramanan, Oh, & Kim, 2015; Lee, Lee, Kim, & Lee, 2013; Olson, Hartsough, Landry, Shroff, & Tabor, 2014; Pilizota & Yang, 2018; Richter et al., 2015; Szymula et al., 2018) now allow the routine testing of multiple lighting settings and efficient exploration of the accessible parameter space. As discussed above, this methodology particularly benefits optogenetics but it also extends to other light-dependent biological and even chemical phenomena, with pertinent examples being the growth dynamics of photoautotrophic organisms (Reimers, Knoop, Bockmayr, & Steuer, 2017), the activity of light-driven enzymes (Sorigué et al., 2017), and the photocatalysis of diverse chemical conversions (König, 2013; Romero & Nicewicz, 2016).

Acknowledgments

We thank our colleagues in the Möglich laboratory for discussion; Dr. Markus Lippitz for advice on the design of the programmable LED arrays; and the electronics shop at the University of Bayreuth for help with the assembly. This work was supported by Grant MO2192/4-1 (to A.M.) by the Deutsche Forschungsgemeinschaft.

References

Alexandre, M. T. A., Arents, J. C., van Grondelle, R., Hellingwerf, K. J., & Kennis, J. T. M. (2007). A base-catalyzed mechanism for dark state recovery in the Avena sativa phototropin-1 LOV2 domain. *Biochemistry*, 46(11), 3129–3137. https://doi.org/ 10.1021/bi062074e.

Blain-Hartung, M., Rockwell, N. C., Moreno, M. V., Martin, S. S., Gan, F., Bryant, D. A., et al. (2018). Cyanobacteriochrome-based photoswitchable adenylyl cyclases (cPACs)

for broad spectrum light regulation of cAMP levels in cells. *Journal of Biological Chemistry*, 293(22), 8473–8483. https://doi.org/10.1074/jbc.RA118.002258.

- Bugaj, L. J., Choksi, A. T., Mesuda, C. K., Kane, R. S., & Schaffer, D. V. (2013). Optogenetic protein clustering and signaling activation in mammalian cells. *Nature Methods*, 10(3), 249–252. https://doi.org/10.1038/nmeth.2360.
- Bugaj, L. J., Spelke, D. P., Mesuda, C. K., Varedi, M., Kane, R. S., & Schaffer, D. V. (2015). Regulation of endogenous transmembrane receptors through optogenetic Cry2 clustering. *Nature Communications*, 6, 6898. https://doi.org/10.1038/ncomms7898.
- Chen, M., Mertiri, T., Holland, T., & Basu, A. S. (2012). Optical microplates for high-throughput screening of photosynthesis in lipid-producing algae. *Lab on a Chip*, 12(20), 3870–3874. https://doi.org/10.1039/c2lc40478h.
- Christie, J. M., Reymond, P., Powell, G. K., Bernasconi, P., Raibekas, A. A., Liscum, E., et al. (1998). Arabidopsis NPH1: A flavoprotein with the properties of a photoreceptor for phototropism. *Science*, 282(5394), 1698–1701.
- Davidson, E. A., Basu, A. S., & Bayer, T. S. (2013). Programming microbes using pulse width modulation of optical signals. *Journal of Molecular Biology*, 425(22), 4161–4166. https://doi.org/10.1016/j.jmb.2013.07.036.
- Deisseroth, K., Feng, G., Majewska, A. K., Miesenböck, G., Ting, A., & Schnitzer, M. J. (2006). Next-generation optical technologies for illuminating genetically targeted brain circuits. *Journal of Neuroscience*, 26(41), 10380–10386. https://doi.org/10.1523/JNEUROSCI.3863-06.2006.
- Etzl, S., Lindner, R., Nelson, M. D., & Winkler, A. (2018). Structure-guided design and functional characterization of an artificial red light–regulated guanylate/adenylate cyclase for optogenetic applications. *Journal of Biological Chemistry*, 293(23), 9078–9089. https://doi.org/10.1074/jbc.RA118.003069.
- Gerhardt, K. P., Olson, E. J., Castillo-Hair, S. M., Hartsough, L. A., Landry, B. P., Ekness, F., et al. (2016). An open-hardware platform for optogenetics and photobiology. *Scientific Reports*, 6, 35363. https://doi.org/10.1038/srep35363.
- Hegemann, P. (2008). Algal sensory photoreceptors. *Annual Review of Plant Biology*, 59, 167–189. https://doi.org/10.1146/annurev.arplant.59.032607.092847.
- Hennemann, J., Iwasaki, R. S., Grund, T. N., Diensthuber, R. P., Richter, F., & Möglich, A. (2018). Optogenetic control by pulsed illumination. *Chembiochem*, 19(12), 1296–1304. https://doi.org/10.1002/cbic.201800030.
- Heo, J., Cho, D.-H., Ramanan, R., Oh, H.-M., & Kim, H.-S. (2015). PhotoBiobox: A tablet sized, low-cost, high throughput photobioreactor for microalgal screening and culture optimization for growth, lipid content and CO2 sequestration. *Biochemical Engineering Journal*, 103, 193–197. https://doi.org/10.1016/j.bej.2015.07.013.
- Iseki, M., Matsunaga, S., Murakami, A., Ohno, K., Shiga, K., Yoshida, K., et al. (2002). A blue-light-activated adenylyl cyclase mediates photoavoidance in *Euglena gracilis*. *Nature*, 415(6875), 1047–1051. https://doi.org/10.1038/4151047a.
- Kawano, F., Aono, Y., Suzuki, H., & Sato, M. (2013). Fluorescence imaging-based high-throughput screening of fast- and slow-cycling LOV proteins. *PLoS One*, 8(12). e82693. https://doi.org/10.1371/journal.pone.0082693.
- König, B. (2013). Chemical photocatalysis. Berlin, Boston: De Gruyterhttps://doi.org/10.1515/9783110269246.
- Lee, J. M., Lee, J., Kim, T., & Lee, S. K. (2013). Switchable gene expression in Escherichia coli using a miniaturized photobioreactor. *PLoS One*, 8(1), e52382. https://doi.org/10.1371/journal.pone.0052382.
- Losi, A., Gardner, K. H., & Möglich, A. (2018). Blue-light receptors for optogenetics. *Chemical Reviews*, 118(21), 10659–10709. https://doi.org/10.1021/acs.chemrev. 8b00163.

- Mathes, T., Vogl, C., Stolz, J., & Hegemann, P. (2009). In vivo generation of flavoproteins with modified cofactors. *Journal of Molecular Biology*, 385(5), 1511–1518. https://doi.org/10.1016/j.jmb.2008.11.001.
- Möglich, A. (2018). An open-source, cross-platform resource for nonlinear least-squares curve fitting. *Journal of Chemical Education*, 95(12), 2273–2278. https://doi.org/10.1021/acs.jchemed.8b00649.
- Möglich, A., Ayers, R. A., & Moffat, K. (2009). Design and signaling mechanism of light-regulated histidine kinases. *Journal of Molecular Biology*, 385(5), 1433–1444. https://doi.org/10.1016/j.jmb.2008.12.017.
- Möglich, A., Yang, X., Ayers, R. A., & Moffat, K. (2010). Structure and function of plant photoreceptors. *Annual Review of Plant Biology*, 61, 21–47. https://doi.org/10.1146/annurev-arplant-042809-112259.
- Monod, J., Wyman, J., & Changeux, J. P. (1965). On the nature of allosteric transitions: A plausible model. *Journal of Molecular Biology*, 12, 88–118. https://doi.org/10.1016/S0022-2836(65)80285-6.
- Ohlendorf, R., Vidavski, R. R., Eldar, A., Moffat, K., & Möglich, A. (2012). From dusk till dawn: One-plasmid systems for light-regulated gene expression. *Journal of Molecular Biology*, 416(4), 534–542. https://doi.org/10.1016/j.jmb.2012.01.001.
- Olson, E. J., Hartsough, L. A., Landry, B. P., Shroff, R., & Tabor, J. J. (2014). Characterizing bacterial gene circuit dynamics with optically programmed gene expression signals. *Nature Methods*, 11(4), 449–455. https://doi.org/10.1038/nmeth.2884.
- Pilizota, T., & Yang, Y.-T. (2018). "Do it yourself" microbial cultivation techniques for synthetic and systems biology: Cheap, fun, and flexible. *Frontiers in Microbiology*, 9, https://doi.org/10.3389/fmicb.2018.01666.
- Pudasaini, A., El-Arab, K. K., & Zoltowski, B. D. (2015). LOV-based optogenetic devices: Light-driven modules to impart photoregulated control of cellular signaling. Frontiers in Molecular Biosciences, 2, 18. https://doi.org/10.3389/fimolb.2015.00018.
- Raffelberg, S., Wang, L., Gao, S., Losi, A., Gärtner, W., & Nagel, G. (2013). A LOV-domain-mediated blue-light-activated adenylate (adenylyl) cyclase from the cyanobacterium Microcoleus chthonoplastes PCC 7420. *Biochemical Journal*, 455(3), 359–365. https://doi.org/10.1042/BJ20130637.
- Reimers, A.-M., Knoop, H., Bockmayr, A., & Steuer, R. (2017). Cellular trade-offs and optimal resource allocation during cyanobacterial diurnal growth. *Proceedings of the National Academy of Sciences of the United States of America*, 114, E6457–E6465. https://doi.org/10.1073/pnas.1617508114.
- Richter, F., Scheib, U. S., Mehlhorn, J., Schubert, R., Wietek, J., Gernetzki, O., et al. (2015). Upgrading a microplate reader for photobiology and all-optical experiments. *Photochemical & Photobiological Sciences*, 14(2), 270–279. https://doi.org/10.1039/c4pp00361f.
- Rockwell, N. C., & Lagarias, J. C. (2010). A brief history of phytochromes. *Chemphyschem*, 11(6), 1172–1180. https://doi.org/10.1002/cphc.200900894.
- Romero, N. A., & Nicewicz, D. A. (2016). Organic photoredox catalysis. *Chemical Reviews*, 116(17), 10075–10166. https://doi.org/10.1021/acs.chemrev.6b00057.
- Ryu, M.-H., Kang, I.-H., Nelson, M. D., Jensen, T. M., Lyuksyutova, A. I., Siltberg-Liberles, J., et al. (2014). Engineering adenylate cyclases regulated by near-infrared window light. Proceedings of the National Academy of Sciences of the United States of America, 111(28), 10167–10172. https://doi.org/10.1073/pnas.1324301111.
- Ryu, M.-H., Moskvin, O. V., Siltberg-Liberles, J., & Gomelsky, M. (2010). Natural and engineered photoactivated nucleotidyl cyclases for optogenetic applications. *Journal* of *Biological Chemistry*, 285(53), 41501–41508. https://doi.org/10.1074/jbc.M110. 177600.

Salomon, M., Eisenreich, W., Dürr, H., Schleicher, E., Knieb, E., Massey, V., et al. (2001). An optomechanical transducer in the blue light receptor phototropin from Avena sativa. *Proceedings of the National Academy of Sciences of the United States of America*, 98(22), 12357–12361. https://doi.org/10.1073/pnas.221455298.

- Schröder-Lang, S., Schwärzel, M., Seifert, R., Strünker, T., Kateriya, S., Looser, J., et al. (2007). Fast manipulation of cellular cAMP level by light in vivo. *Nature Methods*, 4(1), 39–42. https://doi.org/10.1038/nmeth975.
- Sorigué, D., Légeret, B., Cuiné, S., Blangy, S., Moulin, S., Billon, E., et al. (2017). An algal photoenzyme converts fatty acids to hydrocarbons. *Science*, *357*(6354), 903–907. https://doi.org/10.1126/science.aan6349.
- Stierl, M., Stumpf, P., Udwari, D., Gueta, R., Hagedorn, R., Losi, A., et al. (2011). Light-modulation of cellular cAMP by a small bacterial photoactivated adenylyl cyclase, bPAC, of the soil bacterium beggiatoa. *Journal of Biological Chemistry*, 286(2), 1181–1188. https://doi.org/10.1074/jbc.M110.185496.
- Strack, R. L., Strongin, D. E., Bhattacharyya, D., Tao, W., Berman, A., Broxmeyer, H. E., et al. (2008). A noncytotoxic DsRed variant for whole-cell labeling. *Nature Methods*, 5(11), 955–957. https://doi.org/10.1038/nmeth.1264.
- Stüven, B., Stabel, R., Ohlendorf, R., Beck, J., Schubert, R., & Möglich, A. (2019). Characterization and engineering of photoactivated adenylyl cyclases. *Biological Chemistry*, 400, 429–441. https://doi.org/10.1515/hsz-2018-0375.
- Szymula, K. P., Magaraci, M. S., Patterson, M., Clark, A., Mannickarottu, S. G., & Chow, B. Y. (2018). An open-source plate reader. *Biochemistry*, 58, 468–473. https://doi.org/10.1021/acs.biochem.8b00952.
- Taslimi, A., Vrana, J. D., Chen, D., Borinskaya, S., Mayer, B. J., Kennedy, M. J., et al. (2014). An optimized optogenetic clustering tool for probing protein interaction and function. *Nature Communications*, *5*, 4925. https://doi.org/10.1038/ncomms5925.
- Weissleder, R. (2001). A clearer vision for in vivo imaging. Nature Biotechnology, 19, 316–317. https://doi.org/10.1038/86684.
- Yee, E. F., Diensthuber, R. P., Vaidya, A. T., Borbat, P. P., Engelhard, C., Freed, J. H., et al. (2015). Signal transduction in light-oxygen-voltage receptors lacking the adduct-forming cysteine residue. *Nature Communications*, 6, 10079. https://doi.org/10.1038/ncomms10079.
- Ziegler, T., & Möglich, A. (2015). Photoreceptor engineering. Frontiers in Molecular Biosciences, 2, 30. https://doi.org/10.3389/fimolb.2015.00030.

5.3 Manuskript III

Signal Transduction in Light-Oxygen-Voltage Receptors 1 **Lacking the Active-Site Glutamine** 2 3 Julia Dietler^{1,#}, Renate Gelfert^{1,#}, Jennifer Kaiser^{1,#}, Veniamin Borin², Christian Renzl³, Sebastian Pilsl³, Américo 4 Tavares Ranzani¹, Andrés García de Fuentes¹, Tobias Gleichmann⁴, Ralph P. Diensthuber⁴, Michael Weyand¹, 5 6 Günter Mayer^{3,5}, Igor Schapiro², and Andreas Möglich^{1,4,6,7,1,*} 7 8 ¹ Department of Biochemistry, University of Bayreuth, 95447 Bayreuth, Germany 9 ² Institute of Chemistry, The Hebrew University of Jerusalem, Jerusalem, Israel 10 ³ Life and Medical Sciences (LIMES), University of Bonn,53121 Bonn, Germany 11 ⁴ Biophysical Chemistry, Humboldt-University Berlin, 10115 Berlin, Germany ⁵ Center of Aptamer Research & Development, University of Bonn, 53121 Bonn, Germany 12 ⁶ Bayreuth Center for Biochemistry & Molecular Biology, Universität Bayreuth, 95447 Bayreuth, Germany 13 14 ⁷ North-Bavarian NMR Center, Universität Bayreuth, 95447 Bayreuth, Germany 15 16 # These authors contributed equally. 17 † ORCID identifiers: J.D. 0000-0002-0418-0796; R.G. 0000-0002-2677-5774; J.K. 0000-0003-3029-3505; V.B. 18 0000-0001-7832-1443; C.R. 0000-0003-2296-1825; S.P. 0000-0003-1063-1407; A.T.R. 0000-0002-6203-9467; 19 A.G.F. 0000-0002-0072-4725; R.P.D. 0000-0002-4864-7001; M.W. 0000-0002-7499-1324; G.M. 0000-0003-20 3010-4049; I.S. 0000-0001-8536-6869; A.M. 0000-0002-7382-2772 21 * To whom correspondence should be addressed. Tel: +49-921-55-7835; Email: andreas.moeglich@uni-bay-22 reuth.de 23 24 **Abstract** In nature as in biotechnology, light-oxygen-voltage (LOV) photoreceptors perceive blue light to elicit spatio-25 temporally defined cellular responses. Photon absorption drives thioadduct formation between a conserved 26 27 cysteine and the flavin chromophore. An equally conserved, proximal glutamine processes the resultant fla-28 vin protonation into downstream hydrogen-bond rearrangements. Here, we report that this glutamine, long 29 deemed essential, is generally dispensable. In its absence, several LOV receptors invariably retained produc-30 tive, if often attenuated, signaling responses. Structures of a LOV paradigm at around 1 Å resolution revealed 31 highly similar light-induced conformational changes, irrespective of whether the glutamine is present. Naturally occurring, glutamine-deficient LOV receptors likely serve as bona fide photoreceptors, as we showcase 32 33 for a diguanylate cyclase. We propose that without the glutamine, water molecules transiently approach the 34 chromophore and thus propagate flavin protonation downstream. Signaling without glutamine appears in-35 trinsic to LOV receptors, which pertains to biotechnological applications and suggests evolutionary descend-36 ance from redox-active flavoproteins. 37

Keywords

glutamine; hydrogen bond; light-oxygen-voltage; optogenetics; photoreception; signal transduction

39 40 41

42 43

44 45

46

47

48 49

50

51

52

53

54 55

56

57 58

59

60

61 62

63 64

65

38

Introduction

Light-oxygen-voltage (LOV) proteins form a sensory photoreceptor class that elicit a wide palette of physiological responses to blue light across archaea, bacteria, protists, fungi, and plants ¹⁻³. Complementing their eminent role in nature, LOV receptors also serve as genetically encoded actuators in optogenetics ⁴ for the spatiotemporally precise control by light of cellular state and processes ⁵. At the heart of these responses lies the flavin-binding LOV photosensor module which belongs to the Per-ARNT-Sim superfamily ⁶ and comprises several α helices (denoted $C\alpha$, $D\alpha$, $E\alpha$, and $E\alpha$) arranged around a five-stranded antiparallel $E\alpha$ sheet (strands Aβ, Bβ, Gβ, Hβ, and Iβ) ^{7,8} (Suppl. Fig. S1). Light absorption by the flavin triggers a well-studied photocycle ^{2,9-} 11, as part of which an initial electronically excited singlet state (S1) decays within nanoseconds to a triplet state (T₁) (Fig. 1a). Likely via radical-pair mechanism ¹², T₁ reacts within microseconds to the signaling state, characterized by a covalent thioadduct between a highly conserved cysteine residue in the LOV photosensor and the C4a atom of the flavin isoalloxazine ring system. Once illumination ceases, the signaling state passively reverts to the resting state in the base-catalyzed dark-recovery reaction ¹³. Thioadduct formation entails a hybridization change of the flavin C4a atom from sp^2 to sp^3 and concomitant protonation of the adjacent N5 atom. The resultant conversion of the N5 position from a hydrogen bond acceptor to a donor serves as the principal trigger ¹⁴ for a raft of conformational and dynamic transitions, that depending upon LOV receptor, culminate in order-disorder transitions ¹⁵, oligomerization ¹⁶, or other quaternary structural changes ¹⁷. A strictly conserved glutamine residue in strand Iβ is situated immediately adjacent to the flavin and has been identified as instrumental in reading out the flavin N5 position and eliciting the downstream transitions. Supported by spectroscopy, structural and functional data, chemical reasoning, and molecular simulations 8,18-23, the glutamine is widely held to rotate its amide sidechain to accommodate N5 protonation in the signaling state. As a corollary, additional hydrogen-bond rearrangements permeate the LOV photosensor and propagate towards the β -sheet scaffold. As recently proposed 24 , glutamine reorientation and signal propagation may be aided by transient rearrangements of two conserved asparagine residues that coordinate the pteridin portion of the flavin.

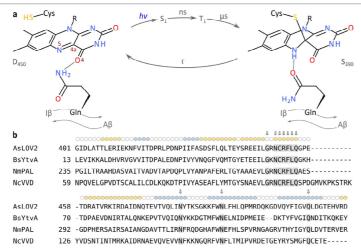


Fig. 1 - **a**, Photocycle of light-oxygen-voltage (LOV) receptors. Absorption of blue light by the dark-adapted state (D₄₅₀) prompts the LOV receptor to traverse short-lived excited singlet (S₁) and triplet (T₁) states before assuming the light-adapted state (S₃₉₀) which is characterized by a thioadduct between the flavin atom C4a and the sidechain of a conserved cysteine. Adduct formation goes along with protonation of the N5 atom which entails changes in hydrogen bonding within the LOV receptor, particularly of a conserved glutamine residue situated in strand Iβ of an antiparallel β pleated sheet. The light-adapted state passively decays to the dark-adapted state over a matter of seconds to hours, depending on the flavin surroundings. **b**, Multiple sequence alignment of *A. sativa* phototropin 1 LOV2 (*As*LOV2) ¹⁵, *B. subtilis* YtvA LOV (*Bs*YtvA) ²⁵, *N. multipartita* PAL LOV (*Nm*PAL) ²⁶, and *N. crassa* Vivid LOV (*Nc*VVD) ²⁷. The secondary structure, as observed in *As*LOV2 ²⁸, is indicated on top, with α helices in tan and β strands in blue. Residues conserved across LOV receptors ²⁹ are highlighted by arrows and grey shading.

Notwithstanding the strict conservation of the glutamine residue and its established role in LOV receptors, recent reports indicate that at least in certain proteins, productive signaling responses to blue light may occur without the glutamine $^{30-32}$. Potentially, these responses harness steric interactions rather than hydrogen-bonding changes as a means of signal transduction 30,33 . By contrast, reports on other LOV receptors considered the glutamine essential for eliciting blue-light responses 21,34 . To rationalize these conflicting findings and to provide further insight into signal transduction, we systematically investigated the role of the conserved glutamine in several model LOV receptors (Fig. 1b and Suppl. Fig. S1). Unexpectedly, the glutamine residue is not essential in LOV signaling as productive blue-light responses were generally maintained even in its absence. Almost all other amino acids could functionally substitute for the conserved glutamine, with notable exceptions. High-resolution crystal structures of the paradigm *Avena sativa* phototropin 1 LOV2 (*AsL*OV2) domain revealed that after glutamine substitution by leucine, closely similar structural changes are evoked by light as in the wild type. Based on structural data, chemical reasoning, and molecular simulations, we propose that in the absence of the glutamine, water molecules relay hydrogen-bonding signals from the flavin N5 position to the LOV β sheet. The ability to transduce light signals without the glutamine appears to

be an inherent, general trait of LOV receptors and may reflect their evolutionary origin. This notion finds support in the existence in nature of numerous LOV receptors that lack the conserved glutamine and presumably serve as blue-light receptors, as we confirm for a glutamine-deficient, proteobacterial LOV-diguanylate cyclase.

Results

Signal transduction in LOV receptors lacking the active-site glutamine.

To evaluate if and how LOV photosensors can transduce light signals to associated effector units in the absence of the conserved glutamine, we initially resorted to the histidine kinase YF1, as it allows the efficient assessment of signaling responses ^{35–37}. Together with the response regulator *Bj*FixJ, the engineered LOV receptor YF1 forms a light-sensitive two-component system (TCS) (Fig. 2a). *E. coli* cultures harboring the pDusk-*Ds*Red plasmid ³⁵, which encodes the YF1/*Bj*FixJ TCS, exhibited strong expression of the red-fluorescent reporter *Ds*Red as YF1 acts as a net kinase in darkness ³⁷. Blue light converts YF1 to a net phosphatase, and accordingly the *Ds*Red fluorescence decreased by around 12-fold (Fig. 2b).

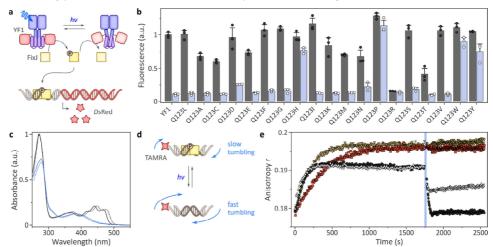


Fig. 2 - Activity and light response of YF1 variants. **a**, The net kinase activity of the variants was assessed in the pDusk-*Ds*Red setup ³⁵, where alongside the response regulator *Bj*FixJ, YF1 drives the expression of the red-fluorescent reporter *Ds*Red in blue-light-repressed manner. **b**, Normalized *Ds*Red fluorescence of *E. coli* cultures harboring pDusk plasmids encoding different YF1 variants. Cells were cultivated in darkness (black dots and grey bars) or under constant blue light (white dots and blue bars). Data represent mean ± s.d. of three biologically independent replicates. **c**, Absorbance spectra of YF1 Q123L (solid lines) in its dark-adapted (black) and light-adapted states (blue), compared to the corresponding spectra of YF1 (dotted lines). **d**, Schematic of the coupled fluorescence anisotropy assay to probe YF1 activity. Once phosphorylated in light-dependent manner (see panel a), *Bj*FixJ homodimerizes and binds to its cognate DNA operator sequence. Said operator is embedded in a TAMRA-labelled double-stranded DNA molecule, and *Bj*FixJ binding can be detected as an increase in fluorescence anisotropy due to decelerated rotational tumbling. **e**, YF1 (black dots), YF1 Q123L (white diamonds), YF1

Q123H (yellow triangles), or YF1 Q123P (red squares) were incubated in darkness together with *Bj*FixJ and the TAMRA-labelled DNA. At time zero, the reaction was initiated by ATP addition and fluorescence anisotropy was recorded for 30 min. Samples were then illuminated for 30 s with blue light (blue bar), and the measurement continued. All experiments were repeated at least twice with similar results.

To probe the role of the active-site glutamine (position Q123) in signal transduction, we substituted this residue for all 19 other canonical amino acids. Strikingly, most of the resultant glutamine-deficient YF1 variants prompted a blue-light-induced reduction of reporter gene fluorescence, similar to the original YF1 and almost regardless of which residue replaced the glutamine. These data clearly indicate that at least in the pDusk setup, the majority of residue substitutions, including alanine, cysteine, glutamic acid and leucine, leave light-dependent signal transduction largely unimpaired. Merely, the substitution by proline and the bulky aromatic amino acids His, Trp, and Tyr abolished responsiveness and resulted in high reporter expression independently of light. Similarly, the Q123R variant did not react to light but exhibited constitutively low reporter fluorescence.

To glean additional insight, we expressed and purified the variants Q123H, Q123L, Q123P, and Q123R alongside YF1. Absorbance spectroscopy revealed flavin incorporation, as indicated by a three-pronged peak around 450 nm, for all variants but Q123R which failed to incorporate the chromophore and was prone to aggregation (Fig. 2c and Suppl. Fig. S2). As indicated by circular dichroism (CD) spectroscopy, the variants Q123H, Q123L, and Q123P were folded and adopted secondary and by inference, tertiary structure similar to YF1 (Suppl. Fig. S2). Upon blue-light exposure, YF1 and its variants Q123L and Q123P underwent the canonical LOV photocycle and adopted the thioadduct state with a characteristic absorption maximum near 390 nm (Fig. 2c and Suppl. Fig. S2). By contrast, the Q123H variant failed to form the adduct state despite incorporating the flavin cofactor, in line with earlier reports on AsLOV2 38. Only at high blue-light doses, the flavin absorption band slightly decreased in intensity but no band at 390 nm was formed. As reported earlier ^{20,21,38}, replacement of the glutamine residue incurred a hypsochromic shift by around 8 nm of the flavin absorbance peak in both the dark-adapted and light-adapted states. This spectral shift can tentatively be attributed to the loss of hydrogen bonding to the flavin O4 atom (see Fig. 1a) and is reminiscent of a bathochromic shift of similar magnitude during the photocycle of the so-called 'sensors of blue light using flavin adenine dinucleotide' (BLUF) 39,40. Taken together, the absorbance data account for the absent light responses in the pDusk context (see Fig. 2b) of the Q123H (no photocycle) and Q123R variants (no chromophore).

We next recorded the dark recovery after blue-light exposure and found the return to the dark-adapted state 10-fold decelerated in Q123L relative to YF1 (Suppl. Fig. S2). The Q123P variant exhibited even slower kinetics that were not completed even after several days. Given that the Q123L variant principally retained the capability of transducing signals (see Fig. 2b), we reasoned that modification of the active-glu-

tamine provides an additional, little tapped means of altering recovery kinetics ⁴¹ and thus modulating photosensitivity at photostationary state ⁴². To explore this effect, we assessed the response of YF1 Q123L to pulsatile blue-light illumination ⁴³ in the pDawn system that derives from pDusk but exhibits inverted response to blue light ³⁵. The Q123L variant was toggled by much lower light doses than YF1, fully consistent with its retarded dark recovery (Suppl. Fig. S3). Compared to the V28I substitution, which also decelerates dark recovery by around 10-fold ^{41,43,44}, the Q123L exchange was somewhat less sensitive to blue light. Combining the substitutions V28I and Q123L did not provide a further gain but slightly reduced the effective light sensitivity.

As the pDusk and pDawn systems only indirectly report on the molecular activity of the receptors, we probed the catalytic activity and response to light of purified YF1 and its variants in a coupled fluorescence anisotropy assay (Fig. 2d). In darkness and in the presence of ATP, YF1 phosphorylates its cognate response regulator BjFixJ, thus prompting its homodimerization and binding of the FixK2 DNA operator sequence 14,45. Phosphorylation-induced binding of BjFixJ to a short, double-stranded DNA molecule slows its rotational diffusion and causes an increase in fluorescence anisotropy of a 5'-attached tetramethylrhodamine (TAMRA) moiety. As noted above, blue light converts YF1 into a net phosphatase, thus promoting BjFixJ dephosphorylation, DNA dissociation and a decrease of fluorescence anisotropy. Upon ATP addition, the dark-adapted YF1 and the Q123H, Q213L, and Q123P variants all exhibited increasing fluorescence anisotropy, albeit with somewhat differing kinetics and amplitude. Whereas Q123L showed similar response as YF1, the Q123H and Q123P variants reached higher anisotropy values which likely reflects a higher degree of BjFixJ phosphorylation than the roughly 50% achieved for YF1 ³⁷. The intrinsic equilibrium between the elementary histidine kinase and phosphatase activities of the TCS thus appears tilted towards the kinase state for Q123H and Q123P compared to YF1 and Q123L ^{46,47}. Upon blue-light application, the Q123L variant responded with a rapid fluorescence anisotropy decay of around half the amplitude seen for YF1, indicating that light signals are transduced by this variant but less efficiently so (Fig. 2e). Consistent with the pDusk reporter assay (see Fig. 2b), neither the Q123H nor the Q123P variant showed any response in their catalytic activities to blue light. In case of Q123H, these observations are readily explained by its inability to undergo light-induced adduct formation and flavin N5 protonation. By contrast, the absorbance measurements unequivocally showed that Q123P can progress through the canonical LOV photocycle (see Suppl. Fig. S2). As the LOV photochemistry hence remains intact, signal transduction in the Q123P variant must be interrupted further downstream.

184 185 186

187

188

189 190

155

156

157 158

159

160

161162

163

164

165166

167168

169

170

171

172

173174

175

176

177178

179

180 181

182

183

LOV signal transduction can generally occur in the absence of the active-site glutamine.

We next addressed whether the unexpected ability to transduce light signals without the conserved glutamine residue is specific for YF1 or more widely shared across LOV receptors. To this end, we examined light-dependent signaling responses in *Nakamurella multipartita* PAL ²⁶, as a naturally occurring LOV receptor, and the *A. sativa* phototropin 1 LOV2 domain, as the arguably best-studied and optogenetically most widely used

LOV module 5,15,28,48. Notably, NmPAL differs from YF1 by an unusual C-terminal arrangement of its LOV photosensor and binds a small RNA aptamer sequence-specifically and in light-activated manner ²⁶. By embedding this aptamer directly upstream of the Shine-Dalgarno sequence in an mRNA encoding the fluorescent DsRed protein, NmPAL activity and response to light can be assessed in a bacterial reporter assay (Fig. 3a). In its dark-adapted state, wild-type NmPAL has little affinity for the aptamer, and DsRed is readily expressed. Light-induced binding by NmPAL interferes with expression, presumably at the translational level, and reporter fluorescence is diminished by 10-fold (Fig. 3b). Using this assay, we tested the effect of replacing the active-site glutamine (residue Q347 in NmPAL) by histidine, leucine, or proline. Consistent with the findings for YF1, the resultant Q347H and Q347P variants no longer exhibited light-induced changes in reporter fluorescence. As in the YF1 case, the proline variant had constitutive activity similar to the dark-adapted parental wild-type NmPAL. Conversely, for Q347H we observed constitutively low fluorescence values, indicative of RNA binding and thus corresponding to light-adapted wild-type NmPAL. This contrasts with YF1 where the corresponding histidine variant functionally corresponded to the dark-adapted state of the parental receptor. The Q347L variant exhibited a light-induced decrease of DsRed fluorescence by around 17-fold, thus even surpassing the value for wild-type NmPAL. Taken together, the results from the NmPAL reporter assay are broadly consistent with the findings for YF1 in that the leucine substitution supported light responses to significant extent whereas the histidine and proline substitutions incurred a loss of light-dependent signal transduction.

191 192

193

194

195

196

197

198

199 200

201

202

203

204

205

206

207

208

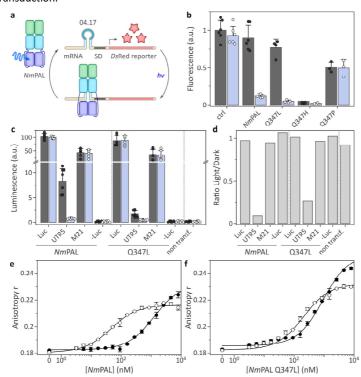


Fig. 3 - Activity and light response of NmPAL variants. a, By embedding a specific aptamer (denoted 04.17) near the Shine-Dalgarno sequence (SD) of an mRNA encoding DsRed, the expression of the fluorescent reporter can be modulated with NmPAL as a function of blue light 26. In darkness, NmPAL shows little affinity for the aptamer, and expression ensues. Under blue light, NmPAL binds and thus attenuates expression. b, E. coli cultures harboring different NmPAL variants and the reporter system depicted in panel a were cultivated in darkness (black dots and grey bars) or under blue light (white dots and blue bars). Normalized DsRed fluorescence represents mean ± s.d. of at least three biologically independent samples. c, NmPAL variants were expressed in HeLa cells to translationally repress expression of a luciferase reporter, conceptually similar to the setup shown in panel a but using the 53.19 aptamer 26 . Bars represent mean \pm s.d. of luminescence acquired for six biologically independent samples incubated in darkness (black dots and grey bars) or under blue light (white dots and blue bars). UTR5 refers to the intact reporter system giving rise to NmPAL-mediated light responses ²⁶; in M21, NmPAL binding is disrupted by a mutation in the target aptamer, and light responsiveness is abolished. As positive and negative controls, luciferase was constitutively expressed (Luc) or left out altogether (-Luc). d, Ratio of the luminescence values obtained under light and dark conditions. e, The interaction of wild-type NmPAL with the TAMRA-labeled 04.17 aptamer was assessed in its dark-adapted (black dots) and light-adapted states (white dots) by fluorescence anisotropy 26. The line represents a fit to a single-site binding isotherm. f, As in panel e but for NmPAL Q347L. Experiments in panels e and f were repeated twice with similar results.

We next tested whether the ability of *Nm*PAL Q347L to transduce light signals extends to applications in eukaryotic cells. To this end, we harnessed an approach based on the translational repression of a luciferase reporter in HeLa cells ²⁶ (Fig. 3c). Under blue light, wild-type *Nm*PAL can bind to an aptamer sequence embedded in the 5'-untranslated region of an mRNA and thereby represses luciferase expression by 10-fold relative to darkness (Fig. 3d). Upon introduction of the Q347L substitution into *Nm*PAL, blue-light-induced downregulation of reporter expression was maintained, albeit at reduced, 4-fold efficiency.

To investigate photochemistry and RNA binding in detail, we expressed and purified NmPAL wild-type and Q347L. In line with the reporter assays (see Fig. 3b-d), the Q347L variant retained flavin chromophore binding and underwent canonical LOV photochemistry upon blue-light exposure (Suppl. Fig. S4). As in YF1, replacement of the glutamine entailed a hypsochromic shift of the flavin absorption. Recovery kinetics after blue-light illumination were however only slowed down by 1.2-fold in the Q347L variant, rather than the 10-fold slowdown in YF1. Far-UV CD spectroscopy showed that NmPAL and its Q347L variant adopt closely similar secondary structure (Suppl. Fig. S4c). We next assessed the binding of NmPAL wild-type and Q347L to a TAMRA-labelled RNA aptamer by fluorescence anisotropy 26 (Fig. 3e, f). Wild-type NmPAL bound the RNA with an affinity of (45.4 ± 5.4) nM in its light-adapted state but showed much reduced interaction in darkness [(1200 \pm 93) nM]. Under the same conditions, NmPAL Q347L interacted with the aptamer somewhat less strongly under blue light [(202.5 \pm 8.5) nM] but exhibited more pronounced residual binding in darkness with an affinity of around (930 ± 70) nM. Thus, light-dependent signal transduction is principally retained in NmPAL Q347L but is impaired compared to the wild-type receptor, similar to the observations made for YF1.

We next turned to the LOV2 domain from A. sativa phototropin 1 (AsLOV2) as a widely studied paradigm ^{15,28,38,49,50} that underpins manifold applications in optogenetics ^{5,51,52}. Whereas AsLOV2 wild-type, Q513H, and Q513L could all be produced with good yield and purity, the Q513P variant suffered from poor expression and severe aggregation, thus precluding its further analysis. The Q513H and Q513L variants incorporated flavin cofactors and exhibited a hypsochromically shifted absorbance spectrum compared to wild-type AsLOV2 (Suppl. Fig. S5), as seen for YF1 and NmPAL. Under blue light, the Q513L variant populated the thioadduct state which recovered to the resting state in darkness with kinetics around 22-fold slower than those of the wild-type domain (Suppl. Fig. S5). By contrast, the Q513H variant failed to undergo the canonical LOV photochemistry, consistent with the YF1 and NmPAL scenarios. The dark-adapted wild-type, Q513H, and Q513L proteins showed closely similar far-UV CD spectra, characterized by two minima of the molar ellipticity per residue, $[\Theta]_{MRW}$, at around 208 nm and 220 nm, and consistent with the mixed $\alpha\beta$ fold of AsLOV2 28 (Fig. 4 and Suppl. Fig. S5). Exposure to blue light diminished the amplitude of the minima by around 30-35% for both AsLOV2 wild-type and Q513L, reflecting the unfolding of the N-terminal A' α and the C-terminal Jα helices ⁵⁰. However, given the relatively fast recovery of AsLOV2 wild-type (see Suppl. Fig. S5), significant return to the dark-adapted state is expected during the spectral scan (taking around 1 min). We hence monitored the α -helical CD signal at (208 \pm 5) nm immediately after withdrawal of blue light (Fig. 4b, d). The kinetic measurements revealed that the initial amplitude of the light-induced CD change in AsLOV2 Q513L was only half that in the wild-type protein. For both variants, the CD spectra fully recovered to their original states (Fig. 4) with kinetics matching those of the photochemical recovery probed by absorbance measurements (see above and Suppl. Fig. S5). In agreement with our findings, an earlier study reported lightinduced CD changes for the Q513L variant but at much reduced amplitude compared to wild-type AsLOV2 21. Taken together, our CD measurements suggest that glutamine replacement by leucine (but not by histidine) qualitatively, if not quantitatively, preserves light-induced signaling responses, fully consistent with the results on the other LOV receptors.

248

249250

251

252

253254

255

256

257

258259

260

261

262

263

264265

266267

268

269

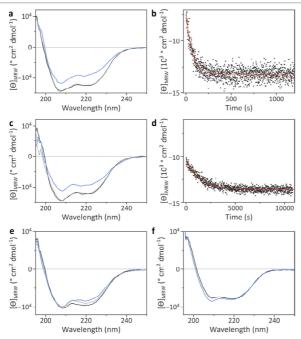


Fig. 4 - Light response of *As*LOV2 variants. **a**, Far-UV circular dichroism (CD) spectra of *As*LOV2 in its dark-adapted (black) and light-adapted states (blue), and after dark recovery (grey dotted). **b**, Recovery reaction of *As*LOV2 following blue-light exposure, as monitored by the CD signal at (220 ± 5) nm. Data were fitted to a single-exponential decay (red line), yielding a recovery rate constant k_{-1} of (1.43 ± 0.05) × 10⁻² s⁻¹. **c**, As panel a but for *As*LOV2 Q513L. **d**, As panel b but for *As*LOV2 Q513L, with k_{-1} amounting to (6.61 ± 0.15) × 10⁻⁴ s⁻¹. **e**, As panel a but for *As*LOV2 C450A:Q513D. **f**, As panel a but for *As*LOV2 C450A:Q513D Δ A'α Δ Aα. Experiments were repeated at least twice with similar results.

A previous investigation showed that LOV receptors can trigger productive signaling responses even when devoid of their active-site cysteine ¹⁴. Blue light then promotes photoreduction of the flavin chromophore from its oxidized quinone form to the partially reduced neutral semiquinone (NSQ), which shares with the thioadduct state a protonated N5 atom and is thus capable of intact signal transduction ¹⁴. We consequently wondered whether these aspects also hold true for LOV receptors that lack both the conserved cysteine and glutamine residues. As cysteine-deficient LOV receptors can efficiently sensitize molecular oxygen ⁵³, pertinent experiments may be complicated by reactive oxygen species (ROS) which potentially disrupt or obscure genuine signaling responses to blue light. We therefore opted to assess the effect of combined cysteine and glutamine removal by CD spectroscopy in the isolated AsLOV2 module, as a comparatively well-defined and tractable experimental setup. Replacement of the active-site cysteine (residue 450) in wild-type AsLOV2 by alanine abolished canonical photochemistry but the NSQ yield was poor, even at prolonged illumination and in the presence of the reductant TCEP (Suppl. Fig. S5). Nor did additional introduction of the Q513L exchange significantly enhance NSQ formation. We thus capitalized on the recent finding that replacement of the active-site glutamine by aspartate in an *Arabidopsis thaliana* phototropin LOV domain greatly

promoted photoreduction to the NSQ ⁵⁴. Given that the corresponding Q123D substitution in YF1 retained signaling capability (see Fig. 2b), we generated AsLOV2 Q513D and the doubly substituted C450A:Q513D variant. Absorbance spectroscopy revealed that the Q513D variant underwent the canonical LOV photochemistry and formed the thioadduct state (Suppl. Fig. S5). CD spectroscopy showed a light-induced 25% loss of $[\theta]_{MRW}$, indicating that the Q513D variant can indeed transduce blue-light signals (Suppl. Fig. S5). In case of AsLOV2 C450A:Q513D, blue light drove rapid conversion to the NSQ state even without addition of reductants, as determined by absorbance spectroscopy (Suppl. Fig. S5). Analysis by CD spectroscopy identified an around 10% loss in α -helical content upon blue-light exposure (Fig. 4e). Notably, the underlying conformational change was reversible, and upon slow reoxidation of the NSQ to the quinone state, the CD signal recovered over time. To ascertain that the change in helical content truly involves the A' α and J α helices as in wild-type AsLOV2, we generated the AsLOV2 C450A:Q513D ΔA'α ΔJα derivative with these helices truncated. Consistent with the removal of A' α and J α , this variant exhibited a 20% reduction in [θ]_{MRW} at 220 nm (Fig. 4f). Rather than a decrease, blue light elicited a small signal gain around 208 nm which we tentatively ascribe to flavin photoreduction, given that both the quinone and NSQ states strongly absorb in the far-UV region. By contrast, we did not observe any loss in α -helical structure from which we concluded that the light-induced structural changes in AsLOV2 C450A:Q513D are likely caused by partial unfolding of the terminal A' α and J α helices. Although the amplitude of the structural response is greatly reduced compared to wild type, it is striking that light-induced responses can be elicited in the absence of two strictly conserved active-site residues.

313 314

315

316317

318

319320

321

322 323

324

325326

327

328

294

295296

297

298299

300

301

302

303

304305

306

307

308

309310

311

312

Molecular bases of LOV signal transduction without the active-site glutamine.

The above findings compellingly show that several LOV receptors transduce light signals in the absence of the active-site glutamine, long considered essential. To arrive at a molecular understanding, we solved the crystal structures of *As*LOV2 wild-type and Q513L in the dark-adapted states to resolutions of 1.00 Å and 0.90 Å, respectively. Notably, both *As*LOV2 variants formed crystals at the previously published solution conditions ²⁸ and adopted the same space group with closely similar cell dimensions (Suppl. Tables S1 and S2). To additionally acquire information on the light-adapted state, we pursued a freeze-trapping strategy. Dark-grown crystals were exposed to blue light and rapidly cryo-cooled, X-ray diffraction was recorded, and structures were refined to resolutions of 1.09 Å (wild type) and 0.98 Å (Q513L) (Suppl. Tables S1 and S2). Although the crystal lattice stands to influence any structural rearrangements, in the past light-induced conformational transitions could thus be resolved for several LOV receptors ^{8,19,28,55}, if likely at reduced amplitude and extent than in solution. Overall, the dark- and light-adapted states of *As*LOV2 wild-type and Q513L exhibited closely similar structures with pairwise root mean-square displacement (rmsd) values of 0.33 to 0.36 Å for the mainchain atoms of residues 404-546 (Suppl. Fig. S6). Differences among the four structures were subtle and concentrated on the chromophore-binding pocket and its surroundings (Fig. 5). Notably, these differences

Fig. 5 - Structural analyses of *As*LOV2 variants. **a**, Chromophore-binding pocket of wild-type *As*LOV2 in its dark-adapted state as revealed by a 1.00 Å crystal structure. **b**, Chromophore-binding pocket of wild-type *As*LOV2 in its light-adapted state as revealed by a 1.09 Å crystal structure. **c**, Chromophore-binding pocket of *As*LOV2 Q513L in its dark-adapted state as revealed by a 0.90 Å crystal structure. **d**, Chromophore-binding pocket of *As*LOV2 Q513L in its light-adapted state as revealed by a 0.98 Å crystal structure. For clarity, helices Cα and Dα are not shown in panels a-d. The Jα helix is drawn in orange, and the flavin mononucleotide cofactor and key amino acids are highlighted in stick representation. Minor conformations of residues and the flavin nucleotide are drawn in narrower diameter. Dashed lines denote hydrogen bonds. **e**, Water density in the interior of dark-adapted *As*LOV2 Q513L derived from a 300 ns classical molecular dynamics simulation. The red mesh denotes a density level of 0.3 water molecules per ų. **f**, As panel e but for light-adapted *As*LOV2 Q513L.

The structure of dark-adapted AsLOV2 wild type (Fig. 5a) well agreed with a previous determination at 1.4 Å (PDB entry 2v0u, mainchain rmsd 0.13 Å) 28 . As observed before, the active-site cysteine 450 adopted a major (80%) conformation a, pointing away from the flavin C4a atom, and a minor (20%) one b, oriented towards C4a (Suppl. Fig. S7). The flavin pteridin moiety was coordinated by the asparagines N482 and N492, and the flavin O4 atom hydrogen-bonded to the amide NEH2 group of the conserved Q513. Via its N δ H2 group, N414 at the start of strand A β entered hydrogen bonds with the backbone carbonyl oxygen of Q513 and the carboxylate group of D515, situated at the tip of strand I β and part of the conserved PAS DIT motif 6 . At the present high resolution, an alternate conformation could be resolved for the terminal turn of the J α helix (residues 543-546), possibly reflecting the inherent equilibrium between folded and unfolded helical states 15,56

343

344

345

346

347348

349

350

351

352

353354

355

356

357 358

359

360

361362

363

364

365366

367

368 369

370

371

372

373

374375

376

377

The light-adapted state of AsLOV2 wild type (Fig. 5b) exhibited a series of conformational differences consistent with a previous report at 1.7 Å resolution (PDB entry 2v0w, mainchain rmsd 0.21 Å) 28. Given the higher resolution achieved presently, additional structural transitions could be pinpointed as summarized below. The sidechain of C450 reoriented towards the flavin C4a, thus shifting the ratio of the conformations a and b to 40%:60% (Suppl. Fig. S7). As in other structures of photoactivated LOV receptors, e.g., 8,28, little electron density for the cysteinyl-flavin thioadduct was observed, likely owing to X-ray radiolysis of the metastable thioether bond. Beyond the altered conformation of C450, the population of the light-adapted state was indicated by a ~ 6.9° tilt of the isoalloxazine plane towards the cysteine (Suppl. Fig. S8) 8,19. Based on earlier reports 8,19,28,55,57, chemical reasoning and spectroscopic evidence 18,20, the sidechain of the conserved glutamine Q513 was modelled to undergo a 180° flip in response to enable hydrogen bonding between the amide Oε atom and the newly protonated flavin N5 position. Upon reorientation, the Q513 amide NεH₂ group hydrogen-bonded with the backbone carbonyl O of N414. The asparagine 414 in turn rotated, thus breaking contact to D515 and enabling a new hydrogen bond between its amide O δ atom and NeH $_2$ of Q513 (Suppl. Fig. S7). Notably, the dark-adapted state conformations of both Q513 and N414 were retained as a minor population (20%) in the light-adapted state, potentially due to incomplete photoactivation in the crystal. The reorientation of N414 correlated with a 0.4 Å shift of its $C\alpha$ atom, thereby prompting the entire A' α segment to dislodge and move away from Q513 (Suppl. Fig. S9). Crucially, the $A'\alpha$ helix is interlocked with the C-terminal part of J α via the hydrophobic residues L408, I411, I539, A542, and L546. The displacement of A' α thus went along with an outward movement of the last 1.5 helical turns of $J\alpha$, which could potentially promote its unfolding 15. Support for this notion derives from the well-documented detrimental effect of the I539E substitution at the A'a:Ja interface 48 and from a recent study on circularly permuted AsLOV2 which pinpointed the J α C terminus as pivotal for light-dependent signaling, whereas the N-terminal part could be dispensed with 32. In addition to the above differences, the light-adapted state also exhibited enhanced flexibility of the Aβ-Bβ and Gβ-Hβ loops, consistent with a global gain of mobility upon light absorption in AsLOV2 and other LOV domains 15,58.

In dark-adapted AsLOV2 Q513L (Fig. 5c), the flavin plane was displaced by around 0.4 Å relative to the wild-type protein, arguably due to steric interactions between the flavin O4 and the Cδ2 methyl group of L513. Notably, no ordered water molecules entered the space vacated by the glutamine removal. The resultant loss of hydrogen bonds at the flavin O4 atom may account for the hypsochromic absorbance shift evidenced above across the different LOV receptors with replaced glutamine. C450 adopted the orientations a and b, pointed away and towards the flavin C4a atom, respectively, at a ratio of 70%:30% (Suppl. Fig. S7). The Q513L replacement notwithstanding, the crucial N414 residue assumed the conformation seen in darkness for the wild type, i. e. engaged in hydrogen bonds with D515 and the backbone carbonyl O of residue 513. Interestingly, the Q513L dark state showed alternate conformations for the Aβ-Bβ and Gβ-Hβ loops, in case of the wild-type receptor only seen upon light exposure. Despite lacking the conserved glutamine, the AsLOV2 Q513L variant displayed structural responses in its light-adapted state structure remarkably similar to the wild type, in line with the above functional assays that invariably demonstrated qualitatively intact light responses after leucine introduction. Specifically, C450 adopted the conformations a and b at a 40%:60% ratio, and the flavin ring plane tilted towards the cysteine by around 4.6°. Strikingly, L513 did not exhibit any dark-light differences, implying that its sidechain is inert and not actively participating in signal relay. This notion is supported by the observation that most of the canonical amino acids with diverse sidechains supported productive light responses in the YF1 receptor (see Fig. 2b). Intriguingly, the crucial N414 assumed the light-adapted conformation to 40% extent; signals were evidently transduced from the flavin to this site even in the absence of the intermediary glutamine, if at reduced efficiency compared to wild-type AsLOV2. Rotation of the asparagine sidechain was accompanied by the same structural transitions evidenced in the wild-type receptor, most importantly an outward shift of the N414 C α atom and the complete A' α segment (Suppl. Fig. S9).

Collectively, the data reveal at high resolution how light stimuli propagate from the flavin to the LOV β -sheet interface and the terminal A' α and J α helices, structural elements generally associated with downstream signal transduction across LOV domains ^{15,26,27,36,59,60}. Strikingly, the Q513L variant underwent the same qualitative responses as wild type which raises the question how signal relay to N414 and beyond can be rationalized in the absence of the glutamine? As candidate mechanisms, we principally considered electrostatic interactions through space and water-mediated rearrangement of hydrogen-bonding networks. To assess the validity of these proposals, we resorted to molecular simulations. Electrostatics calculations revealed that in wild-type AsLOV2 the light-induced formation of the cysteinyl-flavin thioadduct and accompanying flavin N5 protonation prompt changes in the electrostatic potential that are small in size, largely confined to the chromophore itself and not extending far in space (Suppl. Fig. S10). Highly similar electrostatic potentials resulted for the corresponding AsLOV2 Q513L structures, and we thus deem signal transduction through space via altered electrostatics unlikely. Although the light-state structures of AsLOV2 wild-type and Q513L did not exhibit ordered water molecules in the immediate vicinity of position 513, we hypothesized that water might transiently enter the chromophore-binding pocket and thus relay the N5 protonation

change in the light-adapted state. This notion finds support in classical molecular dynamics (MD) simulations that indicate water penetration into the flavin binding pocket upon light exposure (Fig. 5e, f). Whereas in the simulations of dark-adapted *As*LOV2 Q513L only two significant water clusters were observed inside the protein, the light-adapted state seemed to "soak" up water from the bulk solvent and displayed nine clusters in the protein interior. Closely similar results were obtained in simulations on *As*LOV2 wild type (Suppl. Fig. 11a, b). This striking phenomenon can be rationalized by reduced rigidity of the protein backbone upon formation of the cysteinyl adduct (Suppl. Fig. 11c, d). The pairwise root mean square deviation between snapshots from the MD trajectory was below 1.8 Å for dark-adapted *As*LOV2 Q513L but lay in the region of 2.4 Å and higher for the light-adapted state. We note that these findings concur with the above-mentioned increase in general protein mobility evidenced in LOV receptors upon thioadduct formation ^{15,58}.

Signal transduction in natural glutamine-deficient LOV receptors.

Given that LOV signal transduction evidently does not strictly depend on the conserved glutamine, we wondered whether LOV-like receptors exist in nature that lack this residue. To address this question, we conducted sequence searches and identified around 350 putative LOV receptors, denoted LOV^{AQ} in the following, that possess several residues highly conserved across LOV domains ²⁹ but lack the active-site glutamine (Fig. 6a and Suppl. Fig. S12). Interestingly, these receptors featured a range of other amino acids in lieu of the active-site glutamine, predominantly the hydrophobic amino acids leucine and isoleucine, but also polar residues as serine or threonine, and even histidine and cysteine. By contrast, large aromatic residues (phenylal-anine, tyrosine, and tryptophan) were largely absent, as were proline and charged amino acids (Suppl. Fig. S13).

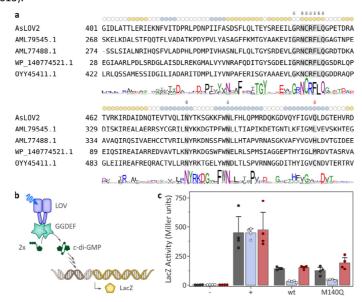


Fig. 6 - Naturally occurring, glutamine-deficient LOV^{ΔQ} receptors. **a**, Sequence searches identify around 350 receptors that have homology to *bona fide* LOV receptors but lack the conserved active-site glutamine. The multiple sequence alignment shows *As*LOV2 as a reference and four selected glutamine-deficient receptors. The sequence logo below the alignment was calculated for the entire set of glutamine-deficient LOV receptors (see Suppl. Fig. S12). Coloring, shading, and arrows as in Fig. 1, with the position of the conserved glutamine residue indicated by a red arrow. **b**, Activity and light response of the LOV^{ΔQ}-GGDEF fragment of WP_140774521.1 were assessed in an *E. coli* reporter strain harboring a *dgcE* knockout and a translational fusion between the cyclic-di-GMP-controlled *csgB* and *lacZ*. Light-dependent diguanylate cyclase activity can hence be assessed by measuring β-galactosidase levels. **c**, Bacteria expressing the wild-type LOV^{ΔQ}-GGDEF receptor or the M140Q variant were cultivated in darkness (black dots and grey bars), under blue light (white dots and blue bars), or under red light (red dots and bars). '-' refers to an empty-vector negative control, and '+' denotes a strain expressing the major diguanylate cyclase DgcE that served as the positive control. β-galactosidase activity is reported in Miller units and represents mean \pm s.d. of four biologically independent replicates. The experiment was repeated twice with similar outcome.

The sheer existence of LOV $^{\Delta Q}$ proteins in nature raises the tantalizing prospect that they can truly serve as blue-light receptors. To principally address this possibility, we selected for further analysis a LOV^{ΔQ}-GGDEF-EAL receptor from the proteobacterium Mesorhizobium loti which features a methionine at position 140 instead of the conserved glutamine (Genbank entry WP_140774521.1, see Fig. 6a). GGDEF and EAL domains antagonistically synthesize and degrade, respectively, the ubiquitous bacterial second messenger cyclic-di-(3'-5')-guanosine monophosphate (c-di-GMP) 61. To assess potential light responses, we expressed the C $terminally\ truncated\ LOV^{\Delta Q}-GGDEF\ receptor\ in\ the\ \textit{E.\ coli}\ reporter\ strain\ KN78\ which\ lacks\ the\ major\ diguanyl-like the coline of the$ ate cyclase DgcE and carries a translational fusion between the c-di-GMP-controlled csqB locus and β -galactosidase 62 (Fig. 6b). Bacteria were cultivated in darkness, under blue light, or under red light, and β -galactosidase activity was determined. As a positive control, a strain expressing DgcE exhibited constitutively high activity of around 450 Miller units (M.u.), irrespective of illumination (Fig. 6c). The KN78 strain carrying an empty plasmid served as a negative control and showed low activity of around 2 M.u., again independent of light. LOV^{AQ}-GGDEF expression resulted in 145 M.u. in darkness but only 30 M.u. under blue light. Conversely, red light had no effect on the detectable activity. Replacement of M140 by glutamine yielded activity levels and light responses similar those of the wild-type protein. Taken together, the results suggest that the M. loti $LOV^{\Delta Q}\text{-}GGDEF\ acts\ as\ a\ blue-light-repressed\ diguany late\ cyclase\ despite\ lacking\ the\ conserved\ glutamine\ respectively. The properties of the conserved of th$ idue.

Discussion

Mechanism of signal transduction sans glutamine.

Following the description of light-oxygen-voltage receptors as blue-light-receptive flavoproteins 1 , optical and nuclear magnetic resonance spectroscopy identified formation of the cysteinyl-flavin adduct in the signaling state 10,18 . Owing to a hybridization change of the flavin C4a atom from sp^2 to sp^3 in the adduct, the adjacent

N5 atom is protonated and thus converted from a hydrogen-bond acceptor in the dark-adapted state to a donor in the signaling state (Suppl. Fig. S14). N5 protonation is an essential step in signal transduction as not least evidenced by reconstitution of LOV receptors with 5-deaza-FMN 63. Despite retaining the ability to form the thioadduct under blue light, these receptors are incapable of downstream signaling responses, arguably due to a lack of hydrogen bonding at the C5 position. Further support for the pivotal role of N5 protonation derives from cysteine-deficient LOV receptors that undergo photoreduction to the NSQ state which is protonated at N5 and thus elicits intact signaling responses 14. Three-dimensional structures of phototropin LOV domains early on pinpointed the conserved glutamine residue close-by the flavin chromophore and in hydrogen-bonding distance to the O4 and N5 atoms ^{7,8,19}. Supported by spectroscopic evidence ^{18,20,64}, the glutamine is generally held to rotate its sidechain upon N5 protonation to satisfy hydrogen bonding 8,19. Possibly, this rotation is aided by transient rearrangements of two conserved asparagines (residues N482 and N492 in AsLOV2, see Fig. 5) that coordinate the flavin nucleotide chromophore ^{24,63}. Reorientation of the glutamine residue in turn provokes a cascade of hydrogen-bonding and structural changes, as for instance revealed in the past ²⁸ and present structures of light-adapted AsLOV2 (see Fig. 5). Photochemical reactions within the flavin chromophore, i.e. thioadduct formation or reduction to the NSQ state 14, are thus coupled to the protein scaffold, in particular the LOV β sheet and elements contacting it, e.g., N- and C-terminal extensions to the core domain. In AsLOV2 specifically, asparagine 414 responds with a sidechain flip, accompanied by a shift of the protein backbone. Signals are thus channeled to the $A'\alpha$ and $J\alpha$ helices and likely drive their lightdependent unfolding.

 Irrespective of the strong conservation of the glutamine and its central involvement in canonical LOV signal transduction, its removal unexpectedly does not abolish light-dependent signaling responses. Intriguingly, this effect spans LOV receptors of distant phylogenetic origin and with disparate associated output modules (see Figs. 2-5), that invariably retained intact responses upon replacement of the glutamine, if to different and often reduced quantitative extent. In line with these observations, two recent reports revealed that the LOV domains from *Vaucheria frigida* aureochrome 1 and *A. thaliana* ZTL also elicited intact downstream responses after replacement of the glutamine by leucine or other residues ^{30,31}. Taken together, we propose that the conserved glutamine, long considered essential for LOV signal transduction, is in fact generally dispensable. This view is corroborated by the existence of hundreds of glutamine-deficient LOV^{AQ} proteins in nature (see Fig. 6a, Suppl. Fig. S12 and ³⁰), which presumably serve as blue-light receptors, as we presently demonstrate for a proteobacterial LOV^{AQ}-GGDEF protein (see Fig. 6b).

Our functional and structural data suggest a potential mechanism for signal transduction in glutamine-deficient LOV receptors. The observation that most amino acids can stand in for the glutamine and support intact signal transduction (see Figs. 2 and 5) immediately argues against a direct involvement of the sidechain of these residues. Strikingly, the crystal structures of AsLOV2 wild-type and Q513L revealed highly similar light-induced conformational changes that culminated in reorientation and altered hydrogen bonding of N414 and translocation of the $A'\alpha$ segment. The problem of signal transduction in glutamine-deficient LOV

receptors thus reduces to the question of how signals are relayed across 10 Å from the newly protonated N5 atom to the LOV β sheet, and specifically to N414 in AsLOV2. In the following, we principally consider and discuss in turn as potential mechanisms i. steric rearrangements near the chromophore; ii. altered electrostatics in the thioadduct state; and iii. water-mediated hydrogen-bonding changes. First, as recently proposed for A. thaliana ZTL ³⁰, steric rearrangements upon adduct formation, i.e. bond strain, $sp^2 \rightarrow sp^3$ hybridization change of the C4a atom, and tilting of the isoalloxazine heterocyclic system 8,19, might underpin signal propagation. However, the light-state Q513L structure did not reveal substantial conformational changes of residues immediately next to the flavin. Moreover, as previously demonstrated 14, cysteine-deficient LOV receptors can elicit canonical signaling responses when photoreduced to their NSQ state which is protonated at the N5 position like the thioadduct but experiences different steric constraints. Taken together, we thus regard steric effects as an unlikely general mechanism for signal propagation in glutamine-deficient receptors but note that for specific LOV proteins they plausibly play a crucial role ³⁰. Second, formation of the thioadduct evidently modifies the electronic structure of the flavin and gives rise to an altered electrostatic potential. However, molecular simulations revealed (see Fig. 5) that such changes in electrostatics are comparatively small and of short reach. We hence deem it unlikely that electrostatic interactions transmitted through space are causative for signal transduction. Rather, we favor the third option of water-mediated hydrogenbonding rearrangements, as illustrated in Fig. 7.

510

511

512

513

514

515 516

517

518

519 520

521 522

523

524

525

526

527 528

529

530

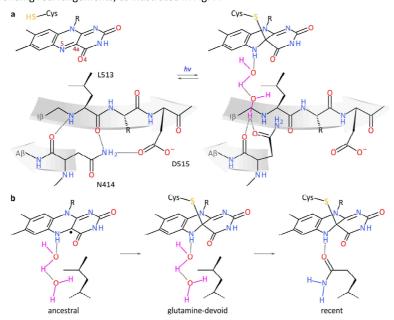


Fig. 7 - Signal transduction in light-oxygen-voltage (LOV) receptors lacking the conserved glutamine, exemplified for the *A. sativa* phototropin 1 LOV2 domain. **a**, Lewis formulae show the flavin nucleotide chromophore and surrounding residues of the glutamine-deficient leucine variant in the dark-adapted (left) and light-adapted states (right). As revealed by X-ray crystallography (see Fig. 5), qualitatively

similar structural responses to light-induced N5 protonation (see Fig. 1) are observed in both the absence of the conserved glutamine Q513 and in its presence (see Suppl. Fig. S14). Without the glutamine, water molecules might transiently enter the chromophore-binding pocket, thereby stand in for the glutamine, and relay the signal as changes in hydrogen bonding to the Iβ and Aβ strands of the central β pleated sheet (involving residues N414 and 513). Notably, signals are thus also propagated to the LOV C terminus (D515) that is frequently engaged in signal transduction and often exhibits a conserved DIT motif ⁶. **b**, The observation that LOV receptors can transduce signals without either or both of their strictly conserved cysteine and glutamine residues suggests a potential origin from redox-active flavoproteins ¹⁴. LOV signal transduction in a primordial LOV ancestor lacking the Cys and Gln residues would have relied on flavin photoreduction to the NSQ radical and on water mediation. Both the Cys and Gln residues would be secondary acquisitions that minimize side reactions (Cys); enhance the fidelity of signal transduction (Cys and Gln); bathochromically shift the action spectrum (Gln); accelerate the dark recovery and thereby benefit temporal resolution (Cys and Gln); and render the signaling state less susceptible to the cellular environment (Cys). Note that we have no evidence in which sequential order the Gln and Cys residues may have been acquired.

We propose that water molecules transiently enter the flavin-binding pocket, occupy the space vacated by glutamine removal, and form hydrogen bonds to the protonated flavin N5 and N414. Water would thus substitute for the glutamine side chain of canonical LOV receptors and relay hydrogen-bonding changes originating at the chromophore to the LOV β sheet, and N414 in case of AsLOV2. We note that neither the dark-adapted nor the light-adapted structures of AsLOV2 Q513L revealed direct evidence for ordered water molecules near the flavin N5 atom. However, support for our model derives from MD simulations suggesting that water dynamically enters this region of the light-adapted receptor. Moreover, the model would explain why, as one of only few amino acids, proline cannot functionally substitute for glutamine, despite leaving chromophore binding and LOV photochemistry intact. In the imino acid proline, the $C\gamma$ and $C\delta$ methylene groups of the sidechain loop back onto the amide nitrogen atom, thus sterically interfering with the proposed water-mediated hydrogen bonding. Alternatively, we cannot however rule out that proline fails to convey light signals because of its restricted conformational freedom or its lack of an amide proton. Lastly, the proposed mechanism would rationalize the near-identical conformational changes elicited by light in both AsLOV2 wild-type and Q513L. Regardless of the presence of the glutamine, light signals would initially be converted into altered flavin N5 protonation and a subsequent hydrogen-bonding cascade that propagates to N414 at the LOV β -sheet interface 28 . Concomitant with formation of new hydrogen bonds, N414 would break or weaken the hydrogen bonds formed in darkness between its backbone oxygen and the amide proton of residue 513, and between its $N\delta H_2$ amide and the sidechain of D515, respectively. The resultant weakening of the LOV β sheet would then transmit to the A' α and J α helices that interact with the outer face of the sheet.

Although residue N414 is not strictly conserved (see, e.g., Fig. 1 and Suppl. Fig. S1), the proposed mode of signal transmission principally extends to other LOV receptors. Even in the absence of a polar residue at the position equivalent to N414, hydrogen-bond rearrangements could still be relayed to the β sheet and

beyond, as for instance evidenced in *Neurospora crassa* Vivid ^{22,57}. Across several LOV receptors, the outer β-sheet face and the adjacent DIT motif ⁶ recurringly take center stage in signal transduction ^{15,26,27,37,60,65}. Once relayed there, signals are then channeled into disparate structural responses in individual LOV receptors, including order-disorder transitions, association reactions, and quaternary structural transitions ⁵. It is worth noting that our mechanistic proposal is not in contradiction to common models advanced for signal transition in the presence of the glutamine, for instance a recent suggestion that two conserved asparagine residues crucially contribute ²⁴. Rather, by principally rationalizing how signal transduction occurs in the absence of the glutamine, our model reinforces the central roles of N5 protonation and hydrogen bonding in LOV signal transduction, which likely also applies to receptors with intact glutamine.

578579580

581

582

583

584 585

586

587

588 589

590

591

592 593

594

595596

597

598

599

600

601 602

603

604

570

571572

573

574

575

576

577

LOV passes the QC

Our data demonstrate that LOV receptors can evidently transduce light signals without the conserved glutamine. As qualitatively intact light responses are evoked upon glutamine replacement across all systems tested, we consider signaling in the absence of the glutamine a general and inherent, yet dormant trait of LOV receptors. This view is borne out by the existence of numerous glutamine-deficient LOV $^{\Delta Q}$ receptors in nature that could potentially serve as bona fide blue-light receptors. In a similar vein, we previously showed that LOV^{AC} receptors devoid of the conserved cysteine exist in nature and can elicit productive light responses owing to photoreduction to the NSQ state which is protonated at the flavin N5 atom 14. We show presently that the paradigm AsLOV2 domain perplexingly retains signaling capability, if at greatly attenuated efficiency, even when both the conserved cysteine and glutamine are replaced. Building on our earlier proposal 14, these observations jointly raise the prospect that LOV receptors arose during evolution from originally light-inert flavoproteins, e.g., enzymes involved in redox processes (Fig. 7b). The question then begs, if signal transduction can take place in the absence of the cysteine and glutamine, why are these residues so prevalent in recent LOV receptors. Our data provide clues as to the potential driving forces underlying the strong glutamine conservation. First, introduction of the glutamine generally enhances the fidelity and degree of the light response. Second, glutamine induces a bathochromic absorbance shift of approximately 10 nm, thus expanding light sensitivity to longer wavelengths. Third, glutamine accelerates the base-catalyzed dark recovery reaction ⁶⁴, thus enhancing temporal resolution of light-dependent physiological responses. Similarly, the cysteine may have prevailed as its introduction minimizes side reactions (fluorescence and photosensitizing), desensitizes the light-adapted signaling state against environmental influences (e.g., partial oxygen pressure and redox conditions), and enhances the fidelity of the signaling response 14.

Beyond implications for the potential origin of LOV receptors, our data directly pertain to applications in optogenetics and biotechnology. First, replacement of the conserved glutamine residue generally decelerated the dark recovery kinetics but preserved signaling responses to substantial extent. Targeted modification of the glutamine residue thus provides a so-far little explored avenue towards modulating these kinetics

and thus the effective light sensitivity at photostationary state (see Suppl. Fig. S3) ^{41,42}. In a similar vein, glutamine substitution may serve to deliberately attenuate the light response as demanded by application. Second, substitutions of either the conserved cysteine or glutamine residues have often been used as presumably light-insensitive, unresponsive negative controls. Our data however illustrate that even when these residues are replaced, LOV receptors can principally transduce light signals, although likely with reduced amplitude. These considerations transcend the optogenetic deployment of LOV receptors and also concern the widespread applications of cysteine-deficient (and often additionally glutamine-deficient ⁶⁶) LOV modules as fluorescent proteins ^{67,68} and photosensitizers for molecular oxygen ⁵³.

612613614

615

616617

618619

620

621622

623

624

625 626

627

628 629

630

631

632633

605

606 607

608

609

610

611

Methods

Molecular biology

YF1 variants with residue Q123 replaced were constructed in the background of the pDusk-DsRed and pDawn-DsRed reporter plasmids 35, or the expression plasmid pET-41a-YF1 36 according to the QuikChange protocol (Agilent Technologies). The gene of the cognate response regulator BjFixJ from Bradyrhizobium diazoefficiens, formerly designated B. japonicum, was amplified from an earlier expression construct 37, subcloned onto the pET-19b vector (Novagen) and thus furnished with an N-terminal His₆-SUMO tag. Substitutions of residue Q347 in the NmPAL receptor were performed via QuikChange in either the pCDF-PALopt reporter plasmid or the pET-28c-PALopt expression plasmid 26. For the expression of AsLOV2, a gene encoding residues 404-546 of A. sativa phototropin 1 (Uniprot O49003) was synthesized with an N-terminal GEF extension 15,28 and codon usage adapted to E. coli (GeneArt), and was cloned into the pET-19b vector. Notably, AsLOV2 was thus equipped with an N-terminal His₆-SUMO tag and its expression put under the control of a T7-lacO promoter. Replacements of the active-site residues Q513 and C450 were generated by QuikChange. Deletions of the N- and C-terminal A' α and J α helices were prepared by PCR amplification and blunt-end ligation of the vector; the resultant truncated AsLOV2 variant comprised residues 411-517. The gene encoding residues 1-326 of the glutamine-deficient LOV-GGDEF receptor (ANN58260.1/WP_140774521.1) was amplified by PCR from genomic DNA of the proteobacterium Mesorhizobium loti NZP2037 (purchased from Deutsche Sammlung für Mikroorganismen und Zellkulturen, DSMZ no. 2627) and cloned into the pQE-30 vector (Qiagen) via Gibson cloning 69. Residue replacements were prepared by QuikChange. All oligonucleotide primers were purchased from Integrated DNA Technologies. All constructs were verified by Sanger sequencing (Microsynth AG, Göttingen).

634635636

637

638

639

Protein expression and purification

Protein expression and purification were carried out as previously described for YF1 ³⁶ and *Nm*PAL ²⁶. To express and purify the response regulator *Bj*FixJ, the above pET-19b *Bj*FixJ expression plasmid was transformed into *E. coli* BL21 CmpX13 cells ⁷⁰. Bacteria were grown at 37°C in Luria broth (LB) medium to an optical

density at 600 nm (OD_{600}) of around 0.6-0.8, at which point the temperature was lowered to 16°C and expression induced by addition of 1 mM isopropyl β -D-1-thiogalactopyranoside (IPTG). Following incubation overnight at 16°C, cells were lysed by sonication, and the supernatant was cleared by centrifugation and purified by Ni²⁺ immobilized metal ion affinity chromatography (IMAC). The His₆-SUMO tag was cleaved off by the SUMO protease Senp2, followed by a second IMAC purification. *Bj*FixJ protein was dialyzed into storage buffer [20 mM tris(hydroxymethyl)aminomethane (Tris)/HCl pH 8.0, 250 mM NaCl, 10% (w/v) glycerol], and the concentration was determined using an extinction coefficient of 4860 M-1 cm⁻¹ at 280 nm⁻³⁷.

For production of AsLOV2 variants, the pET-19b expression plasmid (see above) was transformed into $E.\ coli$ BL21 CmpX13 or LOBSTR cells 71 . Protein expression was induced by addition of 1 mM IPTG and conducted at 16°C overnight. When using the CmpX13 strain, the medium was supplemented with 50 μ M riboflavin. The cleared bacterial cell lysate was purified by Co²⁺ IMAC, Senp2 cleavage of the His₆-SUMO tag and a second IMAC step, as described for BjFixJ. Depending on purity, AsLOV2 variants were further purified by anion-exchange chromatography. Purified protein was dialyzed into storage buffer [20 mM Tris/HCl pH 7.4, 20 mM NaCl, 20% (v/v) glycerol], and its concentration was determined spectroscopically using an extinction coefficient of 13,800 M⁻¹ cm⁻¹ for the flavin absorption maximum around 447 nm 10 .

Spectroscopic analyses

UV/vis absorbance spectra were recorded on an Agilent 8435 diode-array spectrophotometer at 22°C, as controlled by an Agilent 89090A Peltier thermostat. Absorbance spectra were acquired for the dark-adapted LOV receptors and after saturating illumination with a 455-nm light-emitting diode (LED) (30 mW cm⁻²). Throughout the study, all light intensities were determined with a power meter (model 842-PE, Newport) and a silicon photodetector (model 918D-UV-OD3, Newport). The recovery to the dark-adapted state was monitored by recording spectra over time. The resultant kinetics were corrected for baseline drift and evaluated by nonlinear least-squares fitting to exponential functions using the Fit-o-mat software 72. Absorbance spectroscopy on YF1 variants was conducted at 37°C in 20 mM Tris/HCl pH 8.0, 20 mM NaCl; to accelerate the recovery in the Q123L variant, up to 1 M imidazole was added 13, and the resulting rate constants for dark recovery were extrapolated to 0 M imidazole. UV/vis-spectroscopic analysis of NmPAL was performed in 12 mM 4-(2-hydroxyethyl)-1-piperazineethanesulfonic acid (HEPES)/HCl pH 7.7, 135 mM KCl, 10 mM NaCl, 1 mM MgCl₂, 10% (v/v) glycerol ²⁶. AsLOV2 variants were analyzed in 10 mM sodium phosphate pH 7.5, 10 mM NaCl; to aid solubility, for the Q513D variant 20% (v/v) glycerol was added. To promote photoreduction in the cysteine-devoid AsLOV2 C450A variant, 1 mM tris(2-carboxyethyl)phosphine (TCEP) was added. Secondary structure and light-induced changes were assessed by circular dichroism (CD) spectroscopy on a JASCO J710 spectrophotometer equipped with a PTC-348WI Peltier element. CD spectra were recorded at 22°C in a 1-mm cuvette for the dark-adapted state and following saturating blue-light illumination for the light-adapted state. All spectra were corrected by blank spectra and represent the average of at least 4 scans. In case of the faster-recovering AsLOV2 variants, blue light was applied before each scan. Buffers were as above except for NmPAL where 12 mM HEPES/HCl pH 7.7, 135 mM KCl, 10 mM NaCl, 1 mM MgCl₂, 10% (v/v) glycerol was used instead. In case of the AsLOV2 variants, the return to the dark-adapted state after blue-light exposure was monitored over time at a wavelength of (208 \pm 5) nm and evaluated by fitting to exponential functions using Fit-o-mat 72 .

YF1 functional assays

The net kinase activity of YF1 variants and its dependence on blue light were assessed in the pDusk-DsRed reporter setup 35,73. To this end, pDusk-DsRed plasmids harboring different YF1 variants were transformed into E. coli CmpX13. Individual wells of a 96-deep-well microtiter plate (P-DW-11-C-S, Corning, New York) containing 400 μ L LB supplemented with 50 μ g mL $^{-1}$ kanamycin were inoculated with a given YF1 variant. Plates were sealed with a gas-permeable film (BF-410400-S, Corning) and incubated for 16 h at 37 °C and 700 rpm in either darkness or under constant blue light (470 nm, 100 μ W cm $^{-2}$). Following incubation, OD_{600} and the fluorescence of the DsRed Express2 reporter 74 were measured with a Tecan Infinite M200 PRO plate reader (Tecan Group Ltd. Männedorf, Switzerland). For the fluorescence measurements, the excitation wavelength was (554 \pm 9) nm and that of the emission (591 \pm 20) nm. Fluorescence data were divided by OD_{600} and normalized to the value for YF1 under dark conditions. Data represent the mean ± s.d. of three biologically independent samples. The response to trains of blue-light pulses was assessed for pDawn-DsRed systems harboring different YF1 variants as previously described 43. Briefly, bacterial cultures were grown in sealed, black-walled 96-well microtiter plates (Greiner BioOne, Frickenhausen, Germany) for 16 h at 37°C and 600 rpm. The transparent bottom of the plates allowed illumination from below with a programmable matrix of light-emitting diodes. Following incubation, OD_{600} and DsRed fluorescence were measured and evaluated as above.

Activity and light response of purified YF1 variants were characterized in a coupled assay that reports on the phosphorylation-induced binding of BjFixJ to a fluorescently labeled, double-stranded DNA (dsDNA). To this end, a dsDNA substrate with the sequence 5'-GAG CGA TAT CTT AAG GGG GGT GCC TTA CGT AGA ACC C-3' and labeled at its 5' end with (5-and-6)-carboxytetramethylrhodamine (TAMRA) was prepared as described before ¹⁴. The underlined portion of the sequence corresponds to the BjFixK2 operator site that BjFixJ binds to ⁴⁵. To assess light-dependent catalytic activity, 2.5 μ M of each YF1 variant in its dark-adapted state were incubated at 25°C with 1.25 μ M BjFixK2 dsDNA substrate and 25 μ M BjFixJ in buffer containing 10 mM HEPES/HCl pH 7.6, 80 mM KCl, 2.5 mM MgCl₂, 0.1 mM ethylenediaminetetraacetic acid (EDTA), 111 μ g mL⁻¹ bovine serum albumin (BSA), 10% (v/v) glycerol, 4% (v/v) ethylene glycol and 20 mM TCEP. The solution was transferred to a black 96-well microtiter plate (FluoroNunc). Upon starting the reaction by addition of 1 mM ATP, the kinetics were followed by measuring TAMRA fluorescence anisotropy with a multi-mode microplate reader (CLARIOstar, BMG Labtech) over 30 min. Fluorescence was recorded at excitation and emission wavelengths of (540 \pm 10) nm and (590 \pm 10) nm, respectively, and using a 566-nm long-pass beam splitter. After

30 min, the microtiter plate was ejected, the samples illuminated for 30 s with a 470-nm LED (30 mW cm⁻²), and the measurement continued for another 12 min.

NmPAL functional assays

The light-dependent binding of *Nm*PAL variants to their RNA target was assessed in a bacterial reporter-gene system 26 . Briefly, *E. coli* CmpX13 cells 70 were transformed with the arabinose-inducible pCDF-PALopt expression and the pET-28c-*Ds*Red-SP reporter plasmids 26 . Notably, the reporter plasmid contains the *Nm*PAL aptamer 04.17 upstream of the Shine-Dalgarno (SD) sequence of the *Ds*Red gene; *Nm*PAL binding to this site thus reduces reporter expression at the mRNA level. Bacterial starter cultures were grown at 37°C overnight, transferred to individual wells of a 96-deep-well microtiter plate, and diluted to an OD_{600} of 0.03 in 700 μ L LB medium supplemented with 4 mM arabinose, 50 μ g mL⁻¹ kanamycin, and 100 mg mL⁻¹ streptomycin. Following 2 h incubation at 37°C and 600 rpm, cultures were supplemented with 1mM IPTG to induce *Ds*Red expression. Cultures were then split into two samples which were incubated for 16 h at 29°C in darkness or under blue light (470 nm, 40 μ W cm⁻²), respectively. OD_{600} and DsRed fluorescence were determined as described above. Data represent the mean \pm s.d. of four biologically independent replicates.

For the quantitative analysis of NmPAL binding to RNA, we recorded its interaction with 4 nM TAMRA-labeled 04.17 aptamer by fluorescence anisotropy as described before 26 . Experiments were carried out in reaction buffer containing 12 mM 4-(2-hydroxyethyl)-1-piperazineethanesulfonic acid (HEPES)/HCl pH 7.7, 135 mM KCl, 10 mM NaCl, 1 mM MgCl₂, 10% (v/v) glycerol, 100 μ g mL⁻¹ BSA. Fluorescence anisotropy was recorded with a multi-mode microplate reader (CLARIOstar) at (540 \pm 10) nm excitation, (590 \pm 10) nm emission, and using a 566-nm long-pass beam splitter. Data obtained in the presence of rising concentrations of either dark-adapted or light-adapted NmPAL (obtained by illumination with 455 nm, 50 mW cm⁻², 60 s) were fitted to single-site binding isotherms using Fit-o-mat 72 according to eq. (1).

$$r = r_0 + r_1 \times [PAL]/([PAL] + K_d) \tag{1}$$

To probe the light-dependent activity of *Nm*PAL variants in eukaryotic cells, 50,000 Hela cells per well were seeded in 24-well plate format 26 . Following 24 h incubation at 37°C, cells were transfected. In brief, the medium was aspirated, and 500 μ L OptiMem medium were added to each well. In parallel, the transfection mix was prepared by combining 450 ng plasmid encoding an mCherry-tagged *Nm*PAL variant and 50 ng reporter plasmid encoding *Metridia* secreted luciferase in 50 μ L OptiMem plus 2 μ L lipofectamin 2000. Upon incubation for 20 min at room temperature, 50 μ L of the transfection mix were added to each well, followed by incubation for 4 h at 37°C in either darkness or under blue light (100 μ W cm $^{-2}$, 465 nm, 60 s dark intervals followed by 30 s light intervals). The cell supernatant was then replaced by full medium (DMEM, supplemented with 10% fetal calf serum), and incubation continued at 37°C. At 19 h post transfection, the luciferase expression was assessed by transferring 50 μ L of the cell supernatant to a fresh 96-well white plate (Lumitrac 200, Greiner). 5 μ L of the luciferase reagent (Ready-To-Glow secreted luciferase, Takara Clontech) were

added to each well, and the plate was incubated for 25 min at room temperature. Chemiluminescence was then measured using an EnSpire plate reader (Perkin Elmer) with an integration time of 5 s.

747 748 749

750751

752 753

754

755

756757

758

759

746

Diguanylate cyclase assay

The activity of the LOV-GGDEF protein was assessed in the *E. coli* strain KN78 which carries a knockout of the major diguanylate cyclase DgcE and encodes in its genome a translational fusion between the nucleator protein csgB involved in curli formation and the β -galactosidase $lacZ^{62,75}$. To this end, a pQE-30 vector encoding a given LOV-GGDEF variant was transformed into *E. coli*. An empty pQE-30 plasmid served as negative control; as positive control, the empty pQE-30 plasmid was transformed into strain AR1100 which expresses a functional copy of DgcE. Bacterial starter cultures were grown overnight at 37°C in 5 mL LB medium supplemented with 50 µg mL⁻¹ ampicillin. Cultures were then diluted 100-fold, 1 mM IPTG was added, and growth continued for 24 h at 28°C and 550 rpm in either darkness, under constant blue light (450 nm, 40 µW cm⁻²), or under constant red light (660 nm, 40 µW cm⁻²). LacZ activity was then determined according to Miller ⁷⁶ using the chromogenic substrate *ortho*-nitrophenyl- β -galactoside. Data represent mean \pm s.d. of three separate experiments comprising four biologically independent replicates each.

760761762

763

764

765

766 767

768 769

770

771772

773

774

775 776

777 778

779

780

Structure determination of AsLOV2 variants

The expression vectors for the AsLOV2 variants were intentionally designed such that upon Senp2 cleavage during purification (see above) the same N-terminal GEF cloning artifact resulted as in a previous structural study 28. Crystallization was conducted by sitting-drop vapor diffusion at solvent conditions adapted from the previous report ²⁸. Orthorhombic crystals were obtained at protein concentrations between 10 and 20 mg mL⁻¹ in 0.1 M sodium acetate pH 4.6-5.0, 6-8% (w/v) PEG 4000, 30% (v/v) glycerol. Crystal growth and handling were generally performed in darkness or under dim red light, respectively. To characterize the darkadapted state, single crystals were mounted in loops and rapidly cryo-cooled by immersion in liquid nitrogen. To assess the light-adapted state, crystals were exposed to blue light (470 nm, 20 mW cm⁻², 1 min) prior to cryo-cooling. Diffraction data were collected at the BESSY (beamlines 14.1 and 14.2) synchrotron 77 to resolutions between 0.90 Å and 1.09 Å (Suppl. Tables S1 and S2). Indexing and integration were performed with XDS ⁷⁸, and scaling was done with Pointless ⁷⁹, all through the XDSapp interface ⁸⁰. Structures were solved by molecular replacement using the previously determined structure of dark-adapted AsLOV2 as search model (PDB entry 2v0u ²⁸). Model building was done in Coot ⁸¹, and restrained refinement with anisotropic *B* factors was conducted in Refmac 82. Occupancies of residues with multiple conformations were manually refined. Due to the absence of electron density for the covalent thioadduct in the light-adapted structures, the cofactors were generally modelled as noncovalently bound oxidized flavin mononucleotides. Atom coordinates and structure-factor amplitudes were deposited in the Protein Data Bank under accession codes 7pgx (wildtype, dark), 7pgy (wild-type, light), 7pgz (Q513L, dark), and 7ph0 (Q513L, light). Molecular graphics were

prepared with PyMOL (Schrodinger LLC). Root mean square deviation between the structures was calculated with LSQKAB ⁸³.

Molecular simulations

The simulations were performed using the crystal structures obtained in this work. Missing hydrogen atoms were added to the initial structures using the *tleap* program of AMBER 18. The protonation states of all titratable residues were considered at a pH of 7.0. The protein was solvated in a truncated octahedral box of TIP3P water molecules with a distance of at least 15 Å between the atoms and the boundaries of the box. The system was neutralized by adding K⁺ and Cl⁻ ions. The SHAKE algorithm was used to constrain the bonds involving hydrogen atoms in all classical MD simulations, allowing a time step to be 2 fs. A Langevin thermostat with a collision frequency of 1 ps⁻¹ was used for temperature control in all simulations. The VMD plugin VolMap served to analyze the water density inside the protein. The MM parameters for FMN and the FMN-Cys adduct were obtained from ⁸⁴.

Initially, the solvent was minimized in 100,000 steps with restraints of 100 kcal mol⁻¹ Å⁻² on all protein atoms and FMN. The system was then gradually heated from 100 K to 300 K within 50 ns with restraints on protein and FMN in NVT ensemble. The density of the solvent was then gradually equilibrated for another 20 ns under NPT conditions. The equilibration was extended for another 20 ns with weaker restraints of 10 kcal mol⁻¹ Å⁻². Then, MD of 20 ns each was conducted with weakened restraints of 1 kcal mol⁻¹ Å⁻² and 0.1 kcal mol⁻¹ Å⁻², respectively, on the protein backbone. Finally, an unrestrained MD production run of 300 ns was carried out.

Sequence analysis of LOV receptors lacking the active-site glutamine

As in a previous analysis ¹⁴, a BLAST search was performed with *Bacillus subtilis* YtvA (*Bs*YtvA ²⁵, residues 1-127) as the query sequence and with an *E*-value cutoff of 10. Using custom Python scripts, the results were filtered for entries that possess at least eight out of nine residues (residue positions Gly59, Asn61, Cys62, Arg63, Phe64, Leu65, Gln66, Asn94 and Asn104 in *Bs*YtvA), which are conserved across LOV receptors ²⁹, but lack the active-site glutamine (position Gln123 in *Bs*YtvA). Corresponding entries were aligned to the sequences of *Bs*YtvA and *As*LOV2 using ClustalX ⁸⁵. A sequence logo was generated with WebLogo version 3.7 ⁸⁶.

Acknowledgements

We thank U. Jenal for discussion; R. Hengge for discussion and supplying the *E. coli* reporter strains harboring the genomic *csgB::lacZ* integration; and C. Feiler and F. Lennartz for assistance with data acquisition at the BESSY synchrotron. Funding by the Deutsche Forschungsgemeinschaft (grants MO2192/6-1/2 and MO2192/8-1 to A.M.; grants MA3442/5-1/2 to G.M.) and the Alexander-von-Humboldt Foundation (Sofja-Kovalevskaya Award to A.M.) is gratefully acknowledged.

O	1	7

Authors' contributions

- 819 J.D. performed all experiments on the YF1 and LOV^{AQ}-GGDEF variants. R.G. performed all experiments on the
- 820 isolated AsLOV2 domain and refined crystal structures. J.K. analyzed NmPAL in bacterial reporter assays and
- 821 by absorbance spectroscopy, and she studied its RNA interaction by fluorescence anisotropy. V.B. and I.S.
- 822 conducted and evaluated molecular simulations. C.R., S.P., and G.M. did experiments on NmPAL in eukaryotic
- 823 cells. A.T.R. performed spectroscopy on NmPAL and analyzed RNA binding. A.G.F. analyzed AsLOV2 variants
- 824 by CD spectroscopy. T.G. and R.P.D. developed the fluorescence anisotropy assay for YF1. M.W. advised on
- 825 crystallization and structure refinement. A.M. conducted sequence analyses, refined crystal structures, and
- 826 conceived and coordinated the research. J.D. and A.M. wrote the manuscript with input from all authors.

827 828

Conflict of interest

829 The authors declare no conflict of interest.

830 831

Data availability

- 832 Atom coordinates and structure-factor amplitudes have been deposited in the Protein Data Bank under ac-
- 833 cession codes 7pgx (AsLOV2 wild-type, dark), 7pgy (wild-type, light), 7pgz (Q513L, dark), and 7ph0 (Q513L,
- 834 light). Other data are available from the authors upon request.

835

836 References

- 837 1. Christie, J. M. *et al.* Arabidopsis NPH1: a flavoprotein with the properties of a photoreceptor for phototropism. 838 *Science* **282**, 1698–1701 (1998).
- 839 2. Conrad, K. S., Manahan, C. C. & Crane, B. R. Photochemistry of flavoprotein light sensors. *Nat. Chem. Biol.* **10**, 801–840 809 (2014).
- 841 3. Möglich, A., Yang, X., Ayers, R. A. & Moffat, K. Structure and function of plant photoreceptors. *Annu. Rev. Plant Biol.* 842 61, 21–47 (2010).
- 843 4. Deisseroth, K. Optogenetics. *Nat Methods* **8**, 26–29 (2011).
- 844 5. Losi, A., Gardner, K. H. & Möglich, A. Blue-Light Receptors for Optogenetics. Chem. Rev. 118, 10659–10709 (2018).
- 845 6. Möglich, A., Ayers, R. A. & Moffat, K. Structure and signaling mechanism of Per-ARNT-Sim domains. *Structure* 17, 846 1282–1294 (2009).
- 847 7. Crosson, S. & Moffat, K. Structure of a flavin-binding plant photoreceptor domain: insights into light-mediated sig-848 nal transduction. *Proc Natl Acad Sci U A* **98**, 2995–3000 (2001).
- 849 8. Fedorov, R. *et al.* Crystal structures and molecular mechanism of a light-induced signaling switch: The Phot-LOV1 domain from Chlamydomonas reinhardtii. *Biophys J* **84**, 2474–82 (2003).
- 851 9. Kottke, T., Heberle, J., Hehn, D., Dick, B. & Hegemann, P. Phot-LOV1: photocycle of a blue-light receptor domain from the green alga Chlamydomonas reinhardtii. *Biophys J* **84**, 1192–1201 (2003).

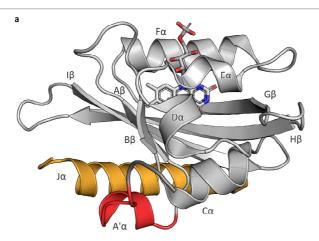
- 853 10. Salomon, M., Christie, J. M., Knieb, E., Lempert, U. & Briggs, W. R. Photochemical and mutational analysis of the FMN-binding domains of the plant blue light receptor, phototropin. *Biochemistry* **39**, 9401–10 (2000).
- 855 11. Pfeifer, A. *et al.* Time-resolved Fourier transform infrared study on photoadduct formation and secondary structural changes within the phototropin LOV domain. *Biophys. J.* **96**, 1462–1470 (2009).
- 857 12. Schleicher, E. et al. On the reaction mechanism of adduct formation in LOV domains of the plant blue-light receptor
 858 phototropin. J Am Chem Soc 126, 11067–76 (2004).
- Alexandre, M. T. A., Arents, J. C., van Grondelle, R., Hellingwerf, K. J. & Kennis, J. T. M. A Base-Catalyzed Mechanism for Dark State Recovery in the Avena sativa Phototropin-1 LOV2 Domain. *Biochemistry* 46, 3129–3137 (2007).
- Yee, E. F. *et al.* Signal transduction in light-oxygen-voltage receptors lacking the adduct-forming cysteine residue.
 Nat. Commun. 6, 10079 (2015).
- 863 15. Harper, S. M., Neil, L. C. & Gardner, K. H. Structural basis of a phototropin light switch. *Science* **301**, 1541–1544 864 (2003).
- Zoltowski, B. D. & Crane, B. R. Light activation of the LOV protein vivid generates a rapidly exchanging dimer. *Bio-chemistry* 47, 7012–7019 (2008).
- 867 17. Berntsson, O. et al. Sequential conformational transitions and α-helical supercoiling regulate a sensor histidine
 868 kinase. Nat. Commun. 8, 284 (2017).
- 869 18. Salomon, M. *et al.* An optomechanical transducer in the blue light receptor phototropin from Avena sativa. *Proc.* 870 *Natl. Acad. Sci.* 98, 12357–12361 (2001).
- 871 19. Crosson, S. & Moffat, K. Photoexcited structure of a plant photoreceptor domain reveals a light-driven molecular switch. *Plant Cell* **14**, 1067–1075 (2002).
- 873 20. Nozaki, D. *et al.* Role of Gln1029 in the Photoactivation Processes of the LOV2 Domain in Adiantum Phytochrome3. 874 *Biochemistry* **43**, 8373–8379 (2004).
- 21. Nash, A. I., Ko, W.-H., Harper, S. M. & Gardner, K. H. A conserved glutamine plays a central role in LOV domain signal transmission and its duration. *Biochemistry* **47**, 13842–13849 (2008).
- 22. Ganguly, A., Thiel, W. & Crane, B. R. Glutamine Amide Flip Elicits Long Distance Allosteric Responses in the LOV
 Protein Vivid. J. Am. Chem. Soc. 139, 2972–2980 (2017).
- 879 23. Freddolino, P. L., Dittrich, M. & Schulten, K. Dynamic Switching Mechanisms in LOV1 and LOV2 Domains of Plant 880 Phototropins. *Biophys. J.* **91**, 3630–3639 (2006).
- 24. Iuliano, J. N. *et al.* Unraveling the Mechanism of a LOV Domain Optogenetic Sensor: A Glutamine Lever Induces
 Unfolding of the Jα Helix. *ACS Chem. Biol.* 15, 2752–2765 (2020).
- 25. Losi, A., Quest, B. & Gärtner, W. Listening to the blue: the time-resolved thermodynamics of the bacterial blue-light receptor YtvA and its isolated LOV domain. *Photochem Photobiol Sci* **2**, 759–66 (2003).
- 885 26. Weber, A. M. *et al.* A blue light receptor that mediates RNA binding and translational regulation. *Nat Chem Biol* **15**, 886 1085–1092 (2019).
- 887 27. Zoltowski, B. D. et al. Conformational Switching in the Fungal Light Sensor Vivid. Science 316, 1054–1057 (2007).
- 28. Halavaty, A. S. & Moffat, K. N- and C-terminal flanking regions modulate light-induced signal transduction in the LOV2 domain of the blue light sensor phototropin 1 from Avena sativa. *Biochemistry* **46**, 14001–14009 (2007).
- 890 29. Crosson, S., Rajagopal, S. & Moffat, K. The LOV domain family: photoresponsive signaling modules coupled to diverse output domains. *Biochemistry* **42**, 2–10 (2003).
- 892 30. Pudasaini, A. *et al.* Steric and Electronic Interactions at Gln154 in ZEITLUPE Induce Reorganization of the LOV Domain Dimer Interface. *Biochemistry* **60**, 95–103 (2021).

- 894 31. Kobayashi, I., Nakajima, H. & Hisatomi, O. Molecular Mechanism of Light-Induced Conformational Switching of the LOV Domain in Aureochrome-1. *Biochemistry* **59**, 2592–2601 (2020).
- 896 32. He, L. *et al.* Circularly permuted LOV2 as a modular photoswitch for optogenetic engineering. *Nat. Chem. Biol.* **17**, 915–923 (2021).
- 898 33. Polverini, E., Schackert, F. K. & Losi, A. Interplay among the "flipping" glutamine, a conserved phenylalanine, water and hydrogen bonds within a blue-light sensing LOV domain. *Photochem. Photochem. Sci.* **19**, 892–904 (2020).
- 900 34. Zayner, J. P., Antoniou, C., French, A. R., Hause, R. J., Jr & Sosnick, T. R. Investigating models of protein function and allostery with a widespread mutational analysis of a light-activated protein. *Biophys. J.* **105**, 1027–1036 (2013).
- 902 35. Ohlendorf, R., Vidavski, R. R., Eldar, A., Moffat, K. & Möglich, A. From dusk till dawn: one-plasmid systems for light-903 regulated gene expression. *J. Mol. Biol.* 416, 534–542 (2012).
- 904 36. Diensthuber, R. P., Bommer, M., Gleichmann, T. & Möglich, A. Full-length structure of a sensor histidine kinase pinpoints coaxial coiled coils as signal transducers and modulators. *Structure* 21, 1127–1136 (2013).
- Möglich, A., Ayers, R. A. & Moffat, K. Design and signaling mechanism of light-regulated histidine kinases. *J. Mol.* Biol. 385, 1433–1444 (2009).
- 908 38. Zayner, J. P. & Sosnick, T. R. Factors That Control the Chemistry of the LOV Domain Photocycle. *PLoS ONE* **9**, e87074 (2014).
- 910 39. Iseki, M. *et al.* A blue-light-activated adenylyl cyclase mediates photoavoidance in *Euglena gracilis*. *Nature* **415**, 911 1047–1051 (2002).
- 912 40. Gomelsky, M. & Klug, G. BLUF: a novel FAD-binding domain involved in sensory transduction in microorganisms.
 913 Trends Biochem Sci 27, 497–500 (2002).
- 914 41. Pudasaini, A., El-Arab, K. K. & Zoltowski, B. D. LOV-based optogenetic devices: light-driven modules to impart photoregulated control of cellular signaling. *Front. Mol. Biosci.* **2**, 18 (2015).
- 916 42. Ziegler, T. & Möglich, A. Photoreceptor engineering. Front. Mol. Biosci. 2, 30 (2015).
- 917 43. Hennemann, J. et al. Optogenetic Control by Pulsed Illumination. Chembiochem 19, 1296–1304 (2018).
- 918 44. Kawano, F., Aono, Y., Suzuki, H. & Sato, M. Fluorescence Imaging-Based High-Throughput Screening of Fast- and Slow-Cycling LOV Proteins. *PLoS ONE* **8**, e82693 (2013).
- 920 45. Nellen-Anthamatten, D. *et al.* Bradyrhizobium japonicum FixK2, a crucial distributor in the FixL1-dependent regulatory cascade for control of genes inducible by low oxygen levels. *J Bacteriol* **180**, 5251–5255 (1998).
- 922 46. Russo, F. D. & Silhavy, T. J. The essential tension: opposed reactions in bacterial two-component regulatory systems.
 923 Trends Microbiol 1, 306–310 (1993).
- 924 47. Möglich, A. Signal transduction in photoreceptor histidine kinases. Protein Sci. 28, 1923–1946 (2019).
- 48. Harper, S. M., Christie, J. M. & Gardner, K. H. Disruption of the LOV-Jalpha helix interaction activates phototropin
 kinase activity. *Biochemistry* 43, 16184–16192 (2004).
- 49. Harper, S. M., Neil, L. C., Day, I. J., Hore, P. J. & Gardner, K. H. Conformational changes in a photosensory LOV
 domain monitored by time-resolved NMR spectroscopy. *J Am Chem Soc* 126, 3390–1 (2004).
- 929 50. Zayner, J. P., Antoniou, C. & Sosnick, T. R. The amino-terminal helix modulates light-activated conformational changes in AsLOV2. *J. Mol. Biol.* **419**, 61–74 (2012).
- 931 51. Wu, Y. I. *et al.* A genetically encoded photoactivatable Rac controls the motility of living cells. *Nature* **461**, 104–108 (2009).
- 933 52. Strickland, D., Moffat, K. & Sosnick, T. R. Light-activated DNA binding in a designed allosteric protein. *Proc. Natl.* 934 *Acad. Sci. U. S. A.* 105, 10709–10714 (2008).

- 935 53. Shu, X. *et al.* A Genetically Encoded Tag for Correlated Light and Electron Microscopy of Intact Cells, Tissues, and Organisms. *PLOS Biol.* **9**, e1001041 (2011).
- 937 54. Kopka, B. *et al.* Electron transfer pathways in a light, oxygen, voltage (LOV) protein devoid of the photoactive cysteine. *Sci. Rep.* **7**, 13346 (2017).
- 939 55. Möglich, A. & Moffat, K. Structural Basis for Light-dependent Signaling in the Dimeric LOV Domain of the Photosen-940 sor YtvA. *J Mol Biol* **373**, 112–126 (2007).
- 941 56. Yao, X., Rosen, M. K. & Gardner, K. H. Estimation of the available free energy in a LOV2-J alpha photoswitch. *Nat. Chem. Biol.* **4**, 491–497 (2008).
- 943 57. Vaidya, A. T., Chen, C.-H., Dunlap, J. C., Loros, J. J. & Crane, B. R. Structure of a light-activated LOV protein dimer that regulates transcription. *Sci. Signal.* **4**, ra50 (2011).
- 945 58. Dietler, J. et al. A Light-Oxygen-Voltage Receptor Integrates Light and Temperature. J. Mol. Biol. 433, 167107 (2021).
- 946 59. Conrad, K. S., Bilwes, A. M. & Crane, B. R. Light-induced subunit dissociation by a light-oxygen-voltage domain photoreceptor from Rhodobacter sphaeroides. *Biochemistry* **52**, 378–391 (2013).
- 948 60. Rivera-Cancel, G., Ko, W., Tomchick, D. R., Correa, F. & Gardner, K. H. Full-length structure of a monomeric histidine 949 kinase reveals basis for sensory regulation. *Proc. Natl. Acad. Sci. U. S. A.* **111**, 17839–17844 (2014).
- 950 61. Jenal, U., Reinders, A. & Lori, C. Cyclic di-GMP: second messenger extraordinaire. *Nat. Rev. Microbiol.* **15**, 271–284 951 (2017).
- 952 62. Serra, D. O., Richter, A. M., Klauck, G., Mika, F. & Hengge, R. Microanatomy at Cellular Resolution and Spatial Order 953 of Physiological Differentiation in a Bacterial Biofilm. *mBio* **4**, (2013).
- 954 63. Kalvaitis, M. E., Johnson, L. A., Mart, R. J., Rizkallah, P. & Allemann, R. K. A Noncanonical Chromophore Reveals 955 Structural Rearrangements of the Light-Oxygen-Voltage Domain upon Photoactivation. *Biochemistry* **58**, 2608– 956 2616 (2019).
- 957 64. Alexandre, M. T., van Grondelle, R., Hellingwerf, K. J. & Kennis, J. T. Conformational heterogeneity and propagation 958 of structural changes in the LOV2/Jalpha domain from Avena sativa phototropin 1 as recorded by temperature-959 dependent FTIR spectroscopy. *Biophys J* **97**, 238–47 (2009).
- 960 65. Nash, A. I. *et al.* Structural basis of photosensitivity in a bacterial light-oxygen-voltage/helix-turn-helix (LOV-HTH) DNA-binding protein. *Proc. Natl. Acad. Sci. U. S. A.* **108**, 9449–9454 (2011).
- 962 66. Remeeva, A. *et al.* Insights into the mechanisms of LOV domain color tuning from a set of high-resolution X-ray structures. *bioRxiv* 2021.02.05.429969 (2021) doi:10.1101/2021.02.05.429969.
- 964 67. Drepper, T. et al. Reporter proteins for in vivo fluorescence without oxygen. Nat. Biotechnol. 25, 443–445 (2007).
- 965 68. Chapman, S. *et al.* The photoreversible fluorescent protein iLOV outperforms GFP as a reporter of plant virus infection. *Proc. Natl. Acad. Sci. U. S. A.* **105**, 20038–20043 (2008).
- 967 69. Gibson, D. G. *et al.* Enzymatic assembly of DNA molecules up to several hundred kilobases. *Nat. Methods* **6**, 343–968 345 (2009).
- 969 70. Mathes, T., Vogl, C., Stolz, J. & Hegemann, P. In vivo generation of flavoproteins with modified cofactors. *J. Mol.* 970 *Biol.* 385, 1511–1518 (2009).
- 971 71. Andersen, K. R., Leksa, N. C. & Schwartz, T. U. Optimized E. coli expression strain LOBSTR eliminates common contaminants from His-tag purification. *Proteins Struct. Funct. Bioinforma.* 81, 1857–1861 (2013).
- 973 72. Möglich, A. An Open-Source, Cross-Platform Resource for Nonlinear Least-Squares Curve Fitting. *J. Chem. Educ.* 95,
 974 2273–2278 (2018).

- 975 73. Ohlendorf, R., Schumacher, C. H., Richter, F. & Möglich, A. Library-Aided Probing of Linker Determinants in Hybrid Photoreceptors. *ACS Synth. Biol.* **5**, 1117–1126 (2016).
- 977 74. Strack, R. L. et al. A noncytotoxic DsRed variant for whole-cell labeling. Nat. Methods 5, 955–957 (2008).
- 978 75. Sommerfeldt, N. *et al.* Gene expression patterns and differential input into curli fimbriae regulation of all GGDEF/EAL domain proteins in Escherichia coli. *Microbiology,* **155**, 1318–1331 (2009).
- 980 76. Miller, J. H. Experiments in Molecular Genetics. (Cold Spring Harbor Laboratory, Cold Spring Harbor, NY, 1972).
- 981 77. Mueller, U. *et al.* The macromolecular crystallography beamlines at BESSY II of the Helmholtz-Zentrum Berlin: Current status and perspectives. *Eur. Phys. J. Plus* **130**, 141 (2015).
- 983 78. Kabsch, W. XDS. Acta Crystallogr. D Biol. Crystallogr. 66, 125–132 (2010).
- 984 79. Evans, P. R. An introduction to data reduction: space-group determination, scaling and intensity statistics. *Acta Crystallogr. D Biol. Crystallogr.* **67**, 282–292 (2011).
- 986 80. Krug, M., Weiss, M. S., Heinemann, U. & Mueller, U. XDSAPP: a graphical user interface for the convenient processing of diffraction data using XDS. *J. Appl. Crystallogr.* **45**, 568–572 (2012).
- 988 81. Emsley, P. & Cowtan, K. Coot: model-building tools for molecular graphics. *Acta Crystallogr. D Biol. Crystallogr.* **60**, 2126–2132 (2004).
- Murshudov, G. N., Vagin, A. A. & Dodson, E. J. Refinement of macromolecular structures by the maximum-likelihood
 method. Acta Crystallogr Biol Crystallogr 53, 240–255 (1997).
- 992 83. Kabsch, W. A solution for the best rotation to relate two sets of vectors. Acta Cryst A 32, 922–923 (1976).
- 84. Bocola, M., Schwaneberg, U., Jaeger, K.-E. & Krauss, U. Light-induced structural changes in a short light, oxygen,
 voltage (LOV) protein revealed by molecular dynamics simulations—implications for the understanding of LOV photoactivation. *Front. Mol. Biosci.* 2, 55 (2015).
- 996 85. Larkin, M. A. *et al.* Clustal W and Clustal X version 2.0. *Bioinformatics* **23**, 2947–2948 (2007).
- 997 86. Crooks, G. E., Hon, G., Chandonia, J.-M. & Brenner, S. E. WebLogo: A Sequence Logo Generator. *Genome Res.* **14**, 998 1188–1190 (2004).

1	Supplementary Information
2	
3	Signal Transduction in Light-Oxygen-Voltage Receptors
4	Lacking the Active-Site Glutamine
5	
6	Julia Dietler ^{1,#} , Renate Gelfert ^{1,#} , Jennifer Kaiser ^{1,#} , Veniamin Borin ² , Christian Renzl ³ , Sebastian Pilsl ³ , Améric
7	Tavares Ranzani¹, Andrés García de Fuentes¹, Tobias Gleichmann⁴, Ralph P. Diensthuber⁴, Michael Weyand
8	Günter Mayer ^{3,5} , Igor Schapiro ² , and Andreas Möglich ^{1,4,6,7,†,*}
9	
10	st To whom correspondence should be addressed. Tel: +49-921-55-7835; Email: andreas.moeglich@uni-bay
11	reuth.de



b	Key residues	AsLOV2	<i>Nm</i> PAL	YF1 (BsYtvA)
		N414	A248	G26
		C450	C284	C62
		N482	N316	N94
		N492	N326	N104
		Q513	Q347	Q123
		D515	D349	D125

Fig. S1 - Overview of tertiary structure and key residues in model light-oxygen-voltage (LOV) receptors. **a**, Three-dimensional structure of AsLOV2 in its dark-adapted state (PDB 7pgx, this work). Secondary structure elements are labeled, and the terminal helices $A'\alpha$ and $J\alpha$ are highlighted in red and orange, respectively. **b**, The table lists key residues in AsLOV2 ¹⁵ and the structurally equivalent residues in the NmPAL ²⁶ and YF1 ³⁷ receptors (see Fig. 1b). Note that the chimeric receptor YF1 comprises the BsYtvALOV domain ²⁵.

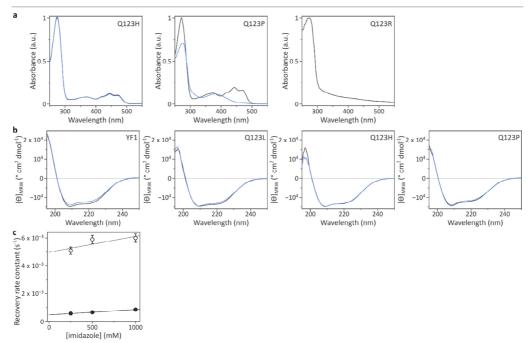


Fig. S2 - Spectral analysis of YF1 variants. **a**, Absorbance spectra of the YF1 variants Q123H, Q123P, and Q123R in their dark-adapted states (black) and light-adapted states (blue). **b**, Far-UV circular dichroism spectra of YF1 and its variants Q123L, Q123H, and Q123P in their dark-adapted (black) and light-adapted states (blue). **c**, Rate constants for dark recovery of YF1 (open circles) and the Q123L variant (filled circles) determined at 37°C and varying imidazole concentrations ¹³. Extrapolated to zero imidazole, recovery rate constants k_{-1} of $(5.05 \pm 0.05) \times 10^{-3}$ s⁻¹ and $(4.91 \pm 0.09) \times 10^{-4}$ s⁻¹ are obtained for YF1 and Q123L, respectively.

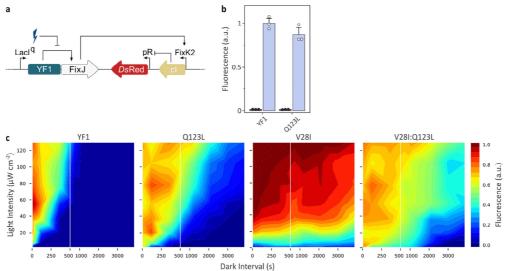


Fig. S3 - Activity and light response of YF1 variants, assessed in the pDawn-*Ds*Red system ³⁵. **a**, The pDawn plasmid derives from pDusk (see Fig. 2a) and harbors an additional inversion cassette based on the lambda phage repressor cl. Expression of the *Ds*Red reporter is hence promoted by blue light rather than repressed. **b**, Normalized *Ds*Red fluorescence of *E. coli* cultures harboring pDawn plasmids encoding YF1 or the Q123L variant. Cells were cultivated in darkness (black dots and grey bars) or under constant blue light (white dots and blue bars). Data represent mean ± s.d. of three biologically independent replicates. **c**, *E. coli* cultures harboring pDawn plasmids encoding different YF1 variants were exposed to pulsatile blue light of varying intensity (ordinate) ⁴³. Half-minute periods of illumination alternated with dark intervals of differing duration (abscissa). Normalized fluorescence value represent mean ± s.d. of three biologically independent replicates. The experiments were repeated at least twice with similar outcome.

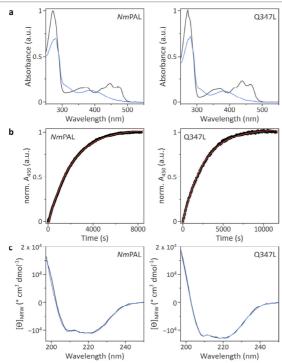


Fig. S4 - Spectral analysis of *Nm*PAL variants. **a**, Absorbance spectra of *Nm*PAL wild-type and Q347L in their dark-adapted states (black) and light-adapted states (blue). **b**, Dark recovery of *Nm*PAL wild-type and Q347L after blue light ceases, monitored at a wavelength of 450 nm, respectively. Data were fitted to a single-exponential decay (red lines), yielding recovery rate constants k_{-1} of (4.86 \pm 0.02) \times 10⁻⁴ s⁻¹ and (3.92 \pm 0.02) \times 10⁻⁴ s⁻¹ for *Nm*PAL wild-type and Q347L, respectively. **c**, Far-UV circular dichroism spectra of *Nm*PAL wild-type and Q347L in their dark-adapted (black) and light-adapted states (blue).

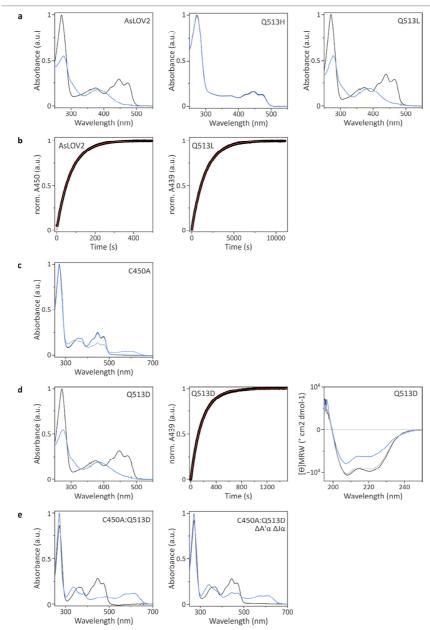


Fig. S5 - Spectral analysis of AsLOV2 variants. **a**, Absorbance spectra of AsLOV2 wild-type, Q513H, and Q513L in their dark-adapted states (black) and light-adapted states (blue). **b**, Dark recovery of AsLOV2 wild-type and Q513L after blue light ceases, monitored at wavelengths of 450 nm and 439 nm, respectively. Data were fitted to a single-exponential decay (red lines), yielding recovery rate constants k_{-1} of $(1.41 \pm 0.01) \times 10^{-2} \, \text{s}^{-1}$ and $(6.37 \pm 0.01) \times 10^{-4} \, \text{s}^{-1}$ for AsLOV2 wild-type and Q513L, respectively. **c**, Absorbance spectra of AsLOV2 C450A in the presence of 1 mM TCEP in its dark-adapted state and after illumination (470 nm, 20 mW cm⁻²) for 30 s (solid blue line) and 5 min (dotted blue line). **d**, As in panels a and b, absorbance spectra and recovery kinetics for the AsLOV2 Q513D variant; the recovery rate

constant k_{-1} amounted to $(5.67 \pm 0.01) \times 10^{-3}$ s⁻¹. (right) Far-UV circular dichroism spectra of AsLOV2 Q513D in its dark-adapted (black) and light-adapted states (blue). **e**, Absorbance spectra of AsLOV2 C450A:Q513D in its dark-adapted state and after illumination (as in panel c) with no reductant added.

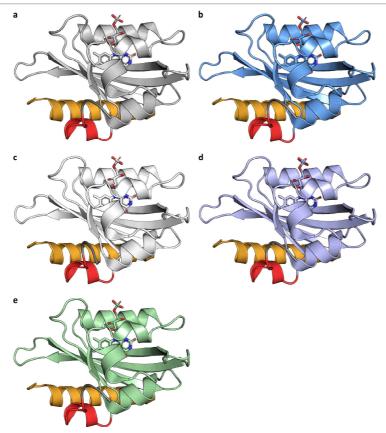


Fig. S6 - Structural analyses of *As*LOV2 variants. **a**, Wild-type *As*LOV2 in its dark-adapted state as revealed by a 1.00 Å crystal structure. **b**, Wild-type *As*LOV2 in its light-adapted state as revealed by a 1.09 Å crystal structure. **c**, *As*LOV2 Q513L in its dark-adapted state as revealed by a 0.90 Å crystal structure. **d**, *As*LOV2 Q513L in its light-adapted state as revealed by a 0.98 Å crystal structure. **e**, The previously determined crystal structure of wild-type AsLOV2 (PDB 2v0u²⁸). The flavin mononucleotide cofactors are shown in stick representation, and the A' α segment and the J α helix are drawn in red and orange, respectively; N-terminal tags resulting from purification are shown in dark grey.

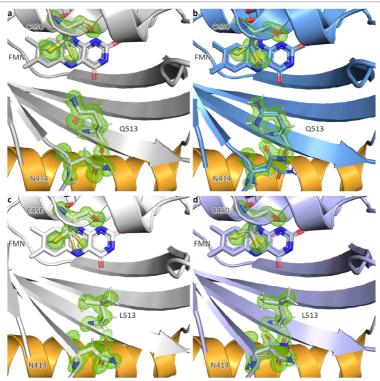


Fig. S7 - F_0 - F_0 omit maps calculated upon setting the occupancy of residues N414, C450, and Q513 to zero. The green mesh denotes a contour level of +3.0 σ . **a**, Wild-type *As*LOV2 in its dark-adapted state. **b**, Wild-type *As*LOV2 in its light-adapted state. **c**, *As*LOV2 Q513L in its dark-adapted state. **d**, *As*LOV2 Q513L in its light-adapted state.

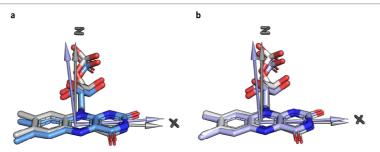


Fig. S8 - Tilting of the flavin cofactor in the light-adapted state. **a**, Structures of the dark-adapted (grey) and light-adapted states (blue) of AsLOV2 wild type were superposed. The flavin isoalloxazine plane tilts by around $\sim 6.9^{\circ}$ in the light-adapted state relative to the dark-adapted one. **b**, As in a but for AsLOV2 Q513L and with a plane tilt of $\sim 4.6^{\circ}$.

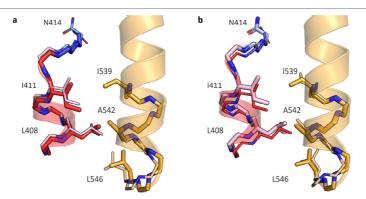


Fig. S9 - Conformational transitions in AsLOV2 wild type (panel a) and Q513L (panel b), as observed in the structures of the respective light-adapted states. Selected sidechains and the backbone of the A' α segment and the J α helix are shown in stick representation. Minor conformations are drawn with narrower diameter. The A' α conformation corresponding to the dark-adapted state is shown in light pink.

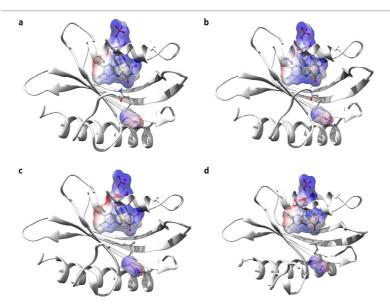


Fig. S10 - Electrostatic potential for *As*LOV2 wild-type and Q513L. **a**, Electrostatic potential acting on the flavin chromophore and residue N414 in the dark-adapted state of wild-type *As*LOV2. **b**, As panel a but for light-adapted *As*LOV2 wild-type. **c**, As panel a but for dark-adapted *As*LOV2 Q513L. **d**, As panel a but for light-adapted *As*LOV2 Q513L.

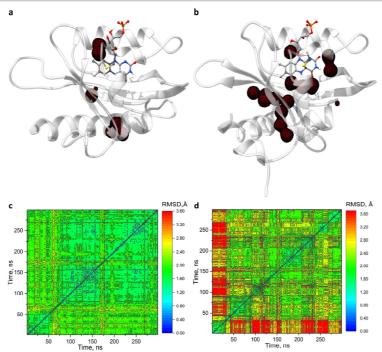


Fig. S11 - **a-b**, Internal water density maps of *As*LOV2 wild-type derived from a 300 ns classical molecular dynamics (MD) run. The red mesh denotes a density level of 0.3 water molecules per \mathring{A}^3 . Panels a and b show maps for the dark-adapted and light-adapted states of *As*LOV2 wild-type, respectively. **c**-**d**, Pairwise root mean square deviation between snapshots from a 300 ns MD trajectory of *As*LOV2 Q513L in the dark-adapted (panel c) and light-adapted states (panel d).

	00000000000000000000000000000000000000			_
AsL0V2	401 GIDLATTLERIEKNFVITDPRLPD-NPIIFAS-DSFLOLTEYSREEILGRNCRFLOGPE			_
AHZ63804.1	917 GIDLATTLERIGQSFVISDPRLPD-NPIIFAS-DQFLELTEYSREEVLGINCRFLQGRD	The state of the s		
ANC96854.1	186DMATTVERIQQNFCICDPNLPD-IPIVFVS-DAFLELTEYAREEVLGRNCRFLQGPA			
PRW56520.1	190 QLDLGTTMERMQHNFVVSDPTLPD-CPIVFAS-DGFLELTGYRREEVLGHNCRFLQGPD	TDRAEVERLKAAINNW-	-EEVTVKLLNYNKSGKPFWNLLTVAPILDGKGHPRLLVGVLVDVTNIS	E 311
XP_005644455.1	5WGFLLLQVCFAISSARDPD-MPIIFAS-PSFYELTGYTPEEVLGSNCRFLHGPD			
AML77588.1	14 DQKLESALGAFDFAFVVTDPSQRD-NPIRFAS-EAFYDLTGYSPNEVLNRNCRFLQGPE		The state of the s	
AML79545.1	268 SKELKDALSTFQQTFLVADATKPD-YPVLYAS-AGFFKMTGYAAKEVIGRNCRFLQGAG			
AML76562.1	117 SEELRAALSAFQQTFVVSDATRPD-HPILYAS-AGFFNMTGYSSSEVVGRNCRFLQGSG			
ANC96846.1	54 KAELRDALTAFQQTFVMVDATKPD-HPIMFAS-EGFYQLTGYTALETIGRNPRFLQGAD			
AML76832.1 WP_131196670.1	181YNRMDSLDHTFVVSDPTLPD-CPIVFAS-ERFFHLTGFEKEEVLGRNCRFLQGPR 95 HDAFAAAFRSIRTAIIMTDPTLPD-NPIVFAN-DAFLQLTGYASHDVVGRNCRFLQGPE			
WP_085852941.1	17SFPTSMVLSDPHLPD-NPLVFVN-GAFEKLTLYPSDVVIGRNCRFLQCDD			
API61829.1	281 -FSLVTALQSAQKSFVITDPALSD-NPIVFAS-PKFLQMTGYTSDQVVGRNCRFLQGPK			
AML77488.1	274 -SSLSIALNRIHQSFVLADPHLPD-MPIVHAS-NLFLQLTGYSRDEVLGRNCRFLQGRD	TDKAAVAQIRQSIVAE-	-HCCTVRILNYRKDNSSFWNLLHTAPVRNASGKVAFYVGVHLDVTGID	E 394
AML77466.1	272 -SSLTIALSRIQQSFVLVDPYLPD-MPIVHAS-DSFLHLTGYSRDEVLGKNCRILQGQD	TNQEDISKIRQSIEAE-	-QPCTVRILNYRKDGNPFWNLLHTAPVRNASGKVAFYVGVHLDVTGME	N 392
AML76778.1	19 -SSLMVSLTRIQQSFVLSDPNLPD-MPIVYAS-DLFCDLTGYSRDEVVGRNCRFLQGPD			
XP_010096336.1	243 -SSLTISLGRIKQSFVLIDPHLPD-MPIVYAS-DAFLKLTGYTRHEVLGCNCRFLNGAD			
AML78103.1	247 CSSLNISLGRIKQSFVLTDPHLHD-TPIVYAS-VEFLRLTGYTADEVLGHNCRFLSGND			
XP_021685402.1 AML78131.1	234 -SSLNISLGRIKQSFVLTDPHLPD-MPIVYAS-DAFLKLTGYARDEVLGRNCRFLSGVE 177 GSALHISLGRIKQSFVLTDAYQTD-MPIVYAS-DAFLSLTGYSRHEVLGRNCRFLCGPS		The state of the s	
AML79165.1	277 -SSLSIALGRINQSFVLTDPHLPN-MPIVYAS-DAFLNLTGYARHEVLGHNCRFLQGPG			
AML76533.1	73 SSSLNLSLGRIKHSFVLTDPHLPD-MPIVYAS-DCFLRLTGYLRHEVLGRNCRFLNGGG			
AML77625.1	188 PCSLESSLLNIPQPFVLVDANLPD-MPVVFAS-DAFVQLTGYSRCEVVGKNCRFLQGDA			
OTB05271.1	171 PQHLTVLSEALAEGFYLTDPSKPD-NPVILASQGESPPCPPYDTNYAIGQNCRFLQGVP			
KAF2858525.1	216AEAFCLADPSRAD-TPLVFIS-EEFARMTQYSPSFLIGKNCRFLQGPA	TNKATDAAKRRMAEACSCS-	-KEITELVLNFRRDGSPFMNLITIAPLVDSRGALKYFLGVÄTDVSHLL	T 329
WP_140774521.1	28 EGIAARLPDLSRDGLAISDLREKG-MALVYVN-RAFQDITGYSGDELIGRNCRFLQGS			
WP_136618668.1	32 ESIKARLLDLSRDGVAISDLREKS-MALVYVN-RAFQDITGYSSGELLGRNCRFLQGN			
WP_140642020.1	39TNRLPDLSRDGVAISDLRDKD-CALVYVN-RAFQEITGYVSSELVGKNCRFLQGS			
WP_082613883.1	31DLTSLLDLSTDGVLVGDLHDND-CALIYVN-PAFERITGYTKSEAIGKNCRYLQGG 64 -AAYGLALDHVGDGVVVADMRQRG-HPIVKVN-AAFEAITGYAAAEAIGKNCRYLQGS			
WP_117351238.1 RZI74485.1	36 -LASSLAVDHGSDGVLIADMRMRG-QPIVHVN-PAFELITGYAADEAIGKNCRYLQGS			
PZ071755.1	1MALDHISDGVLIADMRMRG-HPIVQVN-SAFEAITGYSPDEALGKNCRHLQGS			
HCB79621.1	29ENSCEGVLISDMAARG-QPIIHVN-HAFEMITGYPTAEAIGKNCRYLQGS			
WP_048879934.1	71 LSVCARALAAIDEGVLLSNVCAPG-MPLIHVN-PAFERITGYTAKEAIGKNCRYLQGA	DRLQPQVAQIRAAVENG-	-KEVRVTLRNYRKDGSLFWNDLHLIPITGVDGKYQYSMGIIRDVTEYRI	
MAW86729.1	51 TEALGLVIEEIDEGVLIADAQDPQ-MRLIHVN-RAFETITGYSRDEAIGKNCRYLQGT	DRLQPEIAKIGEAIANL-	-KPIAVTLRNYRKDGRLFWNSIRLFPLPGPDSMTYIVGLIKDVTDLY	S 171
WP_161138949.1	1MGILVADIRSAD-SRIVYVN-NTFEAITGYSRKEAIGKNCRYLQGS			
WP_159872891.1	24 EWRSRAIVDCAQEGILVADICAPD-APIVYVN-RAFEAITGYSCDEAVGKNCRYLQGS	DHLQPEIGVMRHALKAG-	-VATQVRLRNYRKDGSLFWNELHLVPLGEASSPTHYVGFIRDVTEQI	T 144
WP_052213940.1	1MQD-HPLVYVN-SAFERISGYRREELLGRNCRFLQGT	ERTQPAVREMASAIAEG-	-RDSTVVLRNFRRDGTPFWSEVRLRPLRDAEGRVTHYLGTTRDVTEFRI	V 101
WP_090564534.1	23 LALNEQTLEGFSDGIAVADLSMPD-YPLVYVN-SAFERISGYQRGELLGRNCRFLQGD	ERQQPAIEAMAQAIAER-	-RDATVVLRNYRRDGTPFWNELRLCPLRNADGKVTHYLGNMRDVTSIR	L 144
RYH95782.1	43ESFSDGVAIADISLPD-TPVIYVN-SAIGRITGYDVAELLGHNCRFLQGT	1977		
A0Y00296.1	691 ISLLASVIEASSLGVLIVDANADD-LPLIFVN-TAFEQMTGYARHEVLGKNCRFLQGR			
WP_018698921.1				
	206 PSLKEQALNSIREGVLVVDMTVGT-QPVIYVN-EGFLRLSGYDENEVLGRNCRFLQAS	DRNQPAVGLVRDAIAQE-	-RAVRVTLRNYRKNGTMFWNELSLTPIHGHDGILTHYAGVAHDVTEAV	G 327
HAT31873.1	151 LQLSNRALAASLNGVLISDASQAS-FPIMYAN-PAFCRMTGYDLIEVMGRNCRFLQND	DRNQPAVGLVRDAIAQE- DREQPAVAAIRSAIDAR-	-RAVRVTLRNYRKNGTMFWNELSLTPIHGHDGILTHYAGVAHDVTEAVN -ESVHVVLRNYRKDGSLFWNELFISPVPDERGDITHYIGILNDITAFKN	G 327 N 272
WP_132137257.1	151 LQLSNRALAASLNGVLISDASQAS-FPIMYAN-PAFCRMTGYDLIEVMGRNCRFLQND 54 PQLSARALAASSNGVLIADARQPS-CPIVYAN-PAFCRMTGYALDELLGRNCRFLQGQ	DRNQPAVGLVRDAIAQE- DREQPAVAAIRSAIDAR- DREQAAVAVLRHAIARG-	-RAVRVTLRNYRKNGTMFWNELSLTPIHGHDGILTHYAGVÄHDVTEAVI -ESVHVVLRNYRKDGSLFWNELFISPVPDERGDITHYIGILNDITAFKI -EDAHVVLRNYRKDGSLFWNDLFLSPVPDQHGELAHYIGIVTDITELKI	G 327 N 272 R 175
WP_132137257.1 WP_093555924.1	151 LQLSNRALAASLNGVLISDASQAS-FPIMYAN-PAFCRMTGYDLIEVMGRNCRFLQND 54 PQLSARALAASSNGVLIADARQPS-CPIVYAN-PAFCRMTGYALDELLGRNCRFLQGQ 28 DALSNRALSACSNGVMIADAAAPD-MPIMYAN-PAFCAMTGYPLGELLGRNCRFLQGD	DRNQPAVGLVRDAIAQE- DREQPAVAAIRSAIDAR- DREQAAVAVLRHAIARG- DQDQPALAALRQAIAAR-	-RAVRVTLRIVYRKINGTMFNWELSLTPIHGHDG	G 327 N 272 R 175 Q 149
WP_132137257.1 WP_093555924.1 PKL98247.1	151 LQLSNRALAASLNGVLISDASQAS-FPIMYAN-PAFCRMTGYDLIEVMGRNCRFLQND 54 PQLSARALAASSNGVLIADARQPS-CPIVYAN-PAFCRMTGYALDELLGRNCRFLQGQ	DRNQPAVGLVRDAIAQE- DREQ	-RAVRVTLRIVYRKINGTMFWIELSLTPIHGHDG	G 327 N 272 R 175 Q 149 Q 162
WP_132137257.1 WP_093555924.1	151 LQLSIRALAASLINGVLISDASQAS-FPIMYAN-PAFCRMTGYDLIEVMGRINCRFLQND 54 PQLSARALAASSINGVLIDAARQPS-CPILYAN-PAFCRMTGYALDELLGRINCRFLQGG 28 DALSIRALSACSSINGVIIADAAAPD-MPIMYAN-PAFCAMTGYPUGELLGRINCRFLQGG 41 MRLLERAIENSHSAVLIADARQPD-FPAIYIN-HAFEGMTGYTVDECLGRINCRFLQGG	DRNQ	-RAVRVTLRNYRKINGTMFWNELSLTPIHGHDGILTHYAGVÄHDVTEAVI -ESVHVVLRNYRKDGSLFWNELFISPVPDERGDITHYIGILNDITAFKI -EDAHVVLRNYRKDGSLFWNDLFLSPVPDHGELAHYIGIYTDITELK -GDAHVVVRNYRKDGTFFWNDLFISPVPDALGVVTHYVGIÄTDVTALKI -EDCHVVLRNYKKDGTLFWNELTLSPVRDAGGWITHYLGISTDITVEVI -QSVQAVLRNYRKDGEAFWNELTLVPLLDAEDSLVFYMGVSRDATREAI	G 327 N 272 R 175 Q 149 Q 162 L 130
WP_132137257.1 WP_093555924.1 PKL98247.1 WP_126799631.1	151 LQLSIRALAASLINGVLISDASQAS-FPIMYAN-PAFCRMTGYDLIEWMGRICRFLQND 54 PQLSARALAASSINGVLIDAARQPS-CPILYMAN-PAFCRMTGYALDELLGRICGRELQGG 52 BALSIRKALSACSINGWITADAAAPD-MPIMYAN-PAFCAMTGYDLGELLGRINGRELQGG 41 MRLLERAIENSHSAVLIADARQPD-FPAIYIN-HAFEGMTGYTVDECLGRINCRFLQGG 10 -ASHWGALDAMPSVITIADAKYAD-MPILYTIN-PAFEALTGYTSDEARGRINCRFLQGG 539EASLPILICDARQAD-MPILYM-PSFERLTGYMATEAMGRINCHFLQGG 11 PQLLSQATAACTWGVWTDARQHD-HPILYWN-PAFEALSGYTADETLGHINGRFLQGG	DRNQ	-RAVRVTLRIVYRKINGTMFWIELSLTPIHGHDG ILTHYAGVÄHDVTEAVI -ESVHVVLRIVYRKÖGSLFWIELFISPVPDERG DITHYIGILINDITARKI -EDAHVVLRIVYRKOGSLFWIDLFLSPVPDDHG ELAHYIGIVTDITELKI -QOAHVVVRIVYRKOGTPFWIDLFISPVPDALG VVTHYVGIATDVTALKI -EDCHVVLRIVYRKOGTLFWIELTLSPVRDAGG NVTHYLGISTDITVEVI -QSVQAVLRIVYRKOGEAFWIELTLVPLLDAED SLLYFYMGVSRDATREAH -ESTTVTLRIVIYRKOGGAFLINELHLTPVRDAED QLTHYMAVLSDQTERHI -RSTTVTLRIVYRKOGGAFLISELSLSPVHDASG TLTHYLGFLINDVTAREI	G 327 N 272 R 175 Q 149 Q 162 L 130 Q 651 A 132
WP_132137257.1 WP_093555924.1 PKL98247.1 WP_126799631.1 TXH46092.1 WP_161883475.1 TAN70402.1	151 LQLSIRALAASLINGVLISDASQAS-FPINYAN-PAFCRMTGYDLIEVMGRINCRFLQND 54 PQLSARALAASSINGVLIADARQPS-CPIJYAN-PAFCRMTGYALDELLGRINCRFLQGD 28 DALSIRALSACSNGWILADAAPD-MPINYAN-PAFCAMTGYPLGELLGRINCRFLQGD 41 MRLLERAIENSHSAVLIADARQPD-FPAIYIN-HAFEGMTGYTVDECLGRINCRFLQGD 10 -ASMVGALDAMPVSVIIADAKVAD-MPIJYAN-PSFERLTGYTSDEARGRINCRFLQGD 539EASLPILLCDARQAD-MPIJYAN-PSFERLTGYMATEAMGRINCHFLQGD 11 PQLLSQAIAACTVGVWTDARQHD-HPIJYAN-PSFERLTGYTADELIGHINGRELQG 406 IRILFRAVFASASSTSMADAINKPD-MPITYVN-PAFEALSGYTADELIGHINGRINGHELQGG 406 IRILFRAVFASASSTSMADAINKPD-MPITYVN-PAFEALSGYSRDEVIGRINCRFLQGG	DRNQ	RAVRVTLRIVYRKINGTMFWIELSLTPIHGHDG ILTHYAGVÄHDVTEAVI ESVHVVLRIVYRKÖGSLFWIELFISPVPDERG DITHYIGILINDITAFKI EDAHVVLRIVYRKÖGSLFWIDLFLSPVPDQHG ELAHYIGIVTDITELKI -QOAHVVVRIVYRKOGTPFWIDLFISPVPDALG VVTHYVGIATDVTALKI -EDCHVVLRIVYKKOGTLFWIELTLSPVRDAGG NVTHYLGISTDITVEVI -QSVQAVLRIVYRKÖGEAFWIELTLVPLLDAED SLYFYMGVSRDATREAH -EACTVLMRIVYRKÖGGAFLINELHLTPVRDAEDQLTHYMAVLSDQTERHI -ERSTTVTLRIVYRKÖGTLFWIELSLSPVHDASG TLTHYLGFLINDVTAREI -RVGFVI VHINYRKÖGTPFWIDI RTAPVHDEQG RI THFIGTSDDVTERHI -RVGFVI VHINYRKÖGTPFWIDI RTAPVHDEQG RI THFIGTSDDVTERHI	G 327 N 272 R 175 Q 149 Q 162 L 130 Q 651 A 132 A 527
WP_132137257.1 WP_093555924.1 PKL98247.1 WP_126799631.1 TXH466092.1 WP_161883475.1 TAN70402.1 WP_051906796.1	151 LQLSHRALAASLNGVLISDASQAS-FPIMYAN-PAFCRMTGYDLIEVMGRNCRFLQND 54 PQLSARALAASSNOVLTADARQPS-CPIVYAN-PAFCRMTGYALDELLGRNCRFLQGG 28 DALSHRALSACSNGVMIADAAPD-MPIMYAN-PAFCAMTGYPLGELLGRNCRFLQGG 41 MRLLERAIENSHSAVLTADARQPD-FPATYIN-HAFEGMTGYTVDECLGRNCRFLQGG 10 -ASMVGALDAMPVSVIIADAKVAD-MPIVYIN-PAFEALTGYTSDEARGRNCRFLQGG 539EASLPTLICDARQAD-MPITYAN-PSFERLTGYMATEAMGRNCHFLQGG 11 PQLLSQAIAACTVGVVMTDARQHD-HPIVYVN-PAFEALSGYTADELIGHNCRFLQGG 66 LRILFRAVFASASSTSMADAUKPD-MPITYWN-PAFERITGYSRDEVIGRNCRFLQGG 517 LRLLQRAVAASNNGITIADVQQKD-MPLIYVN-PSFERITGFSREEAVGRNCRFLQGG	- DRNQ	-RAVRVTLRIVYRKINGTMFNWELSLTPIHGHDG ILTHYAGVÄHDVTEAVI -ESVHVVLRIVYRKOGSLFWILLFISPVPDERG DITHYTGILINDITARKI -EDAHVVLRIVYRKOSLFWILLFISPVPDHAG LEAHYIGITVDITELKI -QDAHVVVRIVYRKOGTLFWILLTISPVPDALG VVTHYVGIÄTDVTALKI -EDCHVVLRIVYKKOGTLFWILLTISPVRDAGG HIVTHYLGISTDITTEVE -GOSVQAVLRIVRKOGEAFWILLTIVLLIDAED SLLYFMKYSYRDATERAI -EACTVLMRIVYRKOGAFLHILLTIPVRDAED QLTHYMAVLSDQTERHI -RSTTYLRIVYHKOGTLFWILLSLSPVHDAGG TLTHYLGFLINDYTARRI -RSTTYLRIVYHKOGTLFWILLSLSPVHDAGG RITHETGTSDNYTERRI -RGFUYLNIVRKOGTLFWILLSLSPVHDAGG QVTHTGITEDVSERLI -KGTRALLRIVYRKNGELFWILLIAPVHDERG QVTHTGITEDVSERLI	G 327 N 272 R 175 Q 149 Q 162 L 130 Q 651 A 132 A 527 A 638
WP_132137257.1 WP_093555924.1 PKL98247.1 WP_126799631.1 TXH46092.1 WP_161883475.1 TAN70402.1 WP_051906796.1 WP_125218592.1	151 LQLSIRALAASLINGVLISDASQAS-FPIMYAN-PAFCRMTGYDLIEWMGRNCRFLQND 54 PQLSARALAASSINGVLIDAARQFS-CPITYAN-PAFCRMTGYALDELLGRICGREQGG 42 BALSINGLASCSNOWITADAAAPD-MPIMYAN-PAFCAMTGYDLGELLGRINGRFLQGG 41 MRLLERAIENSHSAVLIADARQPD-FPAIYIN-HAFEGMTGYTVDECLGRINGRFLQGG 10 -ASMYGALDAMYSVITADAKYAD-MPIMYTN-PAFEALTGYTSDEARGRINGRFLQGG 139	DRNQ	-RAVRVTLRIVYRKINGTMFWIELSLTPIHGHDG ILTHYAGVÄHDVTEAVI -ESVHVVLRIVYRKOGSLFWIELFISPVPDERG DITHYIGILINDITARKI -EDAHVVLRIVYRKOGSLFWIDLFLSPVPDQHG ELAHYIGILYTDITELKI -QOAHVVVRIVYRKOGTFFWIDLFLSPVPDALG VYTHYVGIATDVTALKI -EDCHVVLRIVYRKOGTFFWIELTLSPVRDAGG HVTHYLGISTDITVEVI -EDCHVVLRIVYRKOGTFFWIELTLVPLLDAED SLVFYMGVSRDATREAI -EACTVLMRIVYRKOGAFLWELTLVPLLDAED SLVFYMGVSRDATREAI -EACTVLMRIVYRKOGAFLWELHLTPVRDAED QLTHYMAVLSOQTERHI -RSTTVTLRIVYHKOGTLFYWELSLSPVHDASG TLTHYLGFLINDVTAREI -RUGEVI VHINYRKOGTPRWIDL RIADVHDERG RI THFIGTSDDVTFRRI -KGTRALLKINYRKOELFWINDLHTAPVHDERG OVTHFIGTIEDVSERLI -EKVEGVLRIVYRKOGSMFWIELRIAPVHDERG NLTHFIGIIKDVSERVI	G 327 N 272 R 175 Q 149 Q 162 L 130 Q 651 A 132 A 527 A 638 S 638
WP_132137257.1 WP_093555924.1 PKL98247.1 WP_126799631.1 TXH46092.1 WP_161883475.1 TAN70402.1 WP_051906796.1 WP_125218592.1 OYY92272.1	151 LQLSIRALAASLINGVLISDASQAS-FPIMYAN-PAFCRMTGYDLIEWMGRICRFLQND 54 PQLSARALAASSINGVLIDAARQPS-CPIJYAN-PAFCRRMTGYALDELLGRICRFLQGG 28 DALSIRALSACSINGVITADAAAPD-MPIJYAN-PAFCAHTGYDYDEGLLGRICRFLQGG 41 MRLLERAIENSHSAVLIADARQPD-FPAIYIN-HAFEGMTGYTVDECLGRICRFLQGG 10 -ASHVGALDAMVSVITADAKVAD-MPIJYYN-PSFERLTGYMATEAMGRINCRFLQGG 139EASLPJLICDARQAD-MPIJYAN-PSFERLTGYMATEAMGRINCRFLQGG 1406 LRILERAVFASASSTSMADAIKPD-MPLTYWI-PAFEALSGYTADETLGHINGRFLQGG 1517 LRLLQRAVAASINGSTTADVQQKO-MPLTYWI-PAFERTTGYSREDEVIGRICRFLQGG 1517 LKLLGRAVAASTNGSTTADVQQKO-MPLTYWI-PSFERTTGFSREDAVGRICRFLQGG 1518 LKLGRAVAASTNGSTTADVQQKO-MPLTYWI-PSFERTTGFSREDAVGRICRFLQGG 1519 LKLLGRAVAASTNGSTTADVQQKO-MPLTYWI-PSFERTTGFSREDAVGRICRFLQGG 1510 LKLTRAVASTSTGTADATAPOT-PTIN-KAPERTTGYSREGLIGKNGSTGTANG 1511 KALTGRAVASTSTGTADATAPOT-PLTYIN-PAFERTTGYASAEVLGRICRFLUSS 1512 KALTGRAVASTSTGTADATAPOT-PLTYIN-PAFERTTGYASAEVLGRICRFLUSS 1513 LAYRRAMEASSVSMSTADATAPOT-PLTYIN-PAFERTTGYASAEVLGRICRFLQGG	DRNQ	RAVRVTLRIVYRKINGTMFWIELSLTPIHGHDG ILTHYAGVÄHDVTEAVI ESVHVVLRIVYRKÖGSLFWIELFISPVPDERG DITHYIGILINDITARKI EDAHVVLRIVYRKÖGSLFWIDLFLSPVPDDHG ELAHYIGIVTDITELKI QOAHVVVRIVYRKÖGTFPWIDLFISPVPDALG VVTHYVGIATDVTALKI EDCHVVLRIVYRKÖGTLFWIELTLSPVRDAGG NVTHYLGISTDITVEVI QOSVQAVLRIVYRKÖGEAFWIELTLVPLLDAED SLLYFYMGVSRDATREAH -RSTTVTLRIVYRKÖGGAFLINELHLTPVRDAED QLTHYMAVLSDOTERHH -RSTTVTLRIVYRKÖGTFPWIDLSLSPVHDASG TLTHYLGFLINDYTAREI -RVGFU VHIVYRKÖGTPPWIDL RIAPVHDERG RI THFIGTSDNYTFRRI KGTRALLRIVYRKÖGSFWIELTRIVHDERG QVTHFIGITEDVSERLI -EKVEGVLRIVYRKÖGSFWIELTAPVHDERG MLTHFIGITKOVSERVI -ROGRALLRIVYRKÖGSFPWIELTIAPVHDERG KLTHFIGITSUVSERVI -ROGRALLRIVYRKÖGSFPWIELTIAPVHDERG KLTHFIGITSUVSERVI -ROGRALLRIVYRKÖGSFPWIELTIAPVHDERG KLTHFIGITSUVSERVI	G 327 N 272 R 175 Q 149 Q 162 L 130 Q 651 A 132 A 527 A 638 S 638 M 524
WP_132137257.1 WP_093555924.1 PKL98247.1 WP_126799631.1 TXH46092.1 WP_161883475.1 TAN76402.1 WP_051906796.1 WP_125218592.1 OYY92272.1 WP_112183883.1	151 LQLSIRALAASLINGVLISDASQAS-FPIMYAN-PAFCRMTGYDLIEVMGRINCRFLQND 54 PQLSARALAASSINGVLIADARQPS-CPIJVYAN-PAFCRMTGYALDELLGRINCRFLQGD 28 DALSIRALSACSNGWILADAAPD-MPIMYAN-PAFCAMTGYPLGELLGRINCRFLQGD 41 MRLLERAIENSHSAVLIADARQPD-FPAIYIN-HAFEGMTGYTVDECLGRINCRFLQGD 10 -ASMVGALDAMPVSVIIADAKVAD-MPIJYYM-PAFEALTGYTSDEARGRINCRFLQGD 13 - EASLPILICDARQAD-MPIJYM-PAFEALTGYTSDEARGRINCRFLQGG 46 IRI LFRAVFASASSTSMADAIKPD-MPIJYWI-PAFEALTGYSRDEVIGRINCRFLQGG 46 IRI LFRAVFASASSTSMADAIKPD-MPIJYWI-PAFEALTGYSRDEVIGRINGRFLQGG 517 LRLLQRAVASNINGITIADVQQKD-MPLIYWI-PSFERITGYSREELIGKNICRFLUGG 517 LKLLERAVEASTSGIVIADANQYD-MPLIYMI-PSFERITGYSREELIGKNICRFLUGS 61 LALYRRAMEASSSYSMSTADATAPD-LPLIYIN-PAFEALTGYSREELIGKNICRFLGGG 61 DAALPIVVADATQPD-LPVVYN-PAFEATTGYSASEVLGRINGRFLQGG 63 DAALPIVVADATQPD-LPVYVN-PAFEATTGYSASEVLGRINGRFLQGG	- DRNQ	RAVRVTLRIVYRKINGTMFNWELSLTPIHGHDG ILTHYAGVÄHDVTEAVI ESVHVVLRIVYRKOGSLFNWELFISPVPDERG DITHYTGILINDITARKI EDAHVVLRIVYRKOSLFNWELFISPVPDHAG ELAHYIGITVDITELKI -QDAHVVVRIVYRKOGSLFNWELFISPVPDALG VVTHYVGIÄTDVTALKI -EDCHVVLRIVYKKOGTLFNWELTISPVRDAGG HIVTHVLGIÄTDITALKI -EDCHVVLRIVYKKOGAFHNELTIJPLLDLAED SLLYFNWSYRBATERAI -EACTVLIMRIVYRKOGAFHNELTIJPLLDLAED QLTHYMAVLSDQTERHI -RSTTYLRIVYHKOGTLFVINLESLSPVHDAGG TLTHTGISTDNITFERN -KGTRALLRIVYRKOGSH-WELTIAPVHDEGG QVTHFIGITEDVSERLI -EKVEGVU NIVNSKOGSPNWELRIAPVHDERG QVTHFIGITEDVSERLI -EKVEGVU NIVNSKOGSPNWELRIAPVHDERG HLTHFIGITSDVSERLI -EKVEGVU NIVNSKOGSPNWELRIAPVHDEGG HLTHFIGISDVSERLI -EKVEGURINNSKOGSPNWELRIAPVHDEGG HTHFIGISDVSCRULEKCTVLLRIVRROGSPPWELLIYPPVHDGGG HTHFIGISDVSORUL -EACTVLLRINNSKOGSPPWELLIYPPVHDGGG HTTYQTGVUQDVSGRUL -EACTVLLRINNSKOGSPPWELLIYPPVHDGGG HTTQTGVUQDVSGRUL -EACTVLLRINNSKOGSPPWELLIYPPVHDGGG HTTQTGVUQDVSGRUL	G 327 N 272 R 175 Q 149 Q 162 L 130 Q 651 A 132 A 527 A 638 S 638 M 524 A 620
WP_132137257.1 WP_093555924.1 PKL98247.1 WP_126799631.1 TXH46092.1 WP_161883475.1 TAN70407.1 WP_051906796.1 WP_125218592.1 OYY92272.1 TXC65962.1	151 LQLSIRALAASLINGVLISDASQAS-FPIMYAN-PAFCRMTGYDLIEWMGRNCRFLQND 54 PQLSARALAASSINGVLIDAARQFS-CPITYAN-PAFCRMTGYALDELLGRICGREQGG 42 ROLSINGALSACSNOWITADAAAPD-MPIMYAN-PAFCAMTGYDLGELLGRINGRELGGG 43 MRILERAIENSHSAVLIADARQPD-FPAIYIN-HAFEGMTGYTVDECLGRINGRFLQGG 44 MRILERAIENSHSAVLIADARQPD-FPAIYIN-HAFEGMTGYTVDECLGRINGRFLQGG 539 ——EASLPILICADARQAD-MPITYYN-PAFEALTGYTSDEARGRINGRFLQGG 54 PQLLSQAIAACTVGVWTTDARQHD-HPITYVN-PAFEALTGYTSDEARGRINGRFLQGG 55 RILFRAVFASASSISMADMIKPD-MPITYVN-PAFEATTGYSRDEVI,GRINGRFLQGG 56 RILFRAVEASHSTADATAPD-LPITYN-PAFEATTGYSREEVAGNINGRFLQGG 57 LKLLERAVEASTSGIVIADAIQYD-MPLIFTN-KAFERITGYSREELIGKNCRFLNSN 58 ——DAALPIWADATQPD-LPYWN-PAFERITGYSASEVLGRINGRFLQGG 58 ——DAALPIWADATQPD-LPWYN-AAFERITGYARDEVJGRINGRFLQGG 56 ——DAALPIWADATQPD-LPWYN-AAFERITGYARDEVJGRINGRFLQGD 57 ——DAAMPIWYDSTQPD-RPIVYN-AAFERITGYARDEVJGRINGRFLQGD	- DRNQ	RAVRVTLRIVYRKINGTMFWIELSLTPIHGHDG ILTHYAGVÄHDVTEAVI ESVHVVLRIVYRKOGSLFWIELFISPVPDERG DITHYIGILINDITARKI EDAHVVLRIVYRKOGSLFWIDLFISPVPDENG ELAHVIGIVTDITELKI QDAHVVRINYRKOGTFFWIDLFISPVPDALG VYTHYVGIÄTDVTALKI EDCHVVLRIVYKKOGTLFWIELTLSPVPDAGG HVTHVLGISTDITVEVI ECHVULRIVYRKOGGAFIWELTLVPLLDAED SLVFYMGVSRDATREAI EACTVLMRIVYRKOGGAFIWELTLVPVLDAEG QLTHYMAVLSDOTERHI ERSTTVLRIVYHKOGTLFYWELSLSPVHDASG TLTHYLGFLINDVTAREI RRYGEVI VHINYRKOGTPFWIDL RIAPVHDERG RI THFIGTSDDYTFRRI EKYGEVLRIVYRKOGSPRWIDLRIAPVHDERG VYTHFIGTIEVSERLI EKVEGVLRIVYRKOGSPRWIELTVTPVHDGGG KLTHFIGTSDOVSGRI ECACTVLLERIKROGTSPFWIELTVTPVHDGGG KLTHFIGTSDOVSGRI ECACTVLLERIKROGTSPFWIELTVTPTPVHDGGG KLTHFIGTSDOVSGRI ECACTVLLERIKROGTSPFWIELTVTPTPVHDGGG KLTHFIGTSDOVSGRI ECACTVLLERIKROGTSPWIELTVTPTPVHDGGG KLTHFIGTSDOVSGRI ECACTVLLERIKROGTSPWIELTVTPTPVHDGGG KLTHFIGTSDOVSGRI ECACTVLLERIKROGTPMTPMTPVTPVHDGGG KLTHFIGTSDOVSGRI ECACTVLLERIKROGTPMTPMTPVTPVHDGGG KLTHFIGTSDOVSGRI ECACTVLLERIKROGTPMTPMTPVTPVHDGGG KLTHFIGTSDOVSGRI ECACTVLLERIKROGTPMTPMTPVTPVHDGGG KLTHFIGTSDOVSGRI ECACTVLLERIKROGTPMTPMTPMTPVTPVHTPVTPVHTPVTPVHTPVTPVHTPVTPVHTP	G 327 N 272 R 175 Q 149 Q 162 L 130 Q 651 A 132 A 527 A 638 S 638 M 524 A 620 A 363
WP_132137257.1 WP_093555924.1 PKL98247.1 WP_126799631.1 TXH46092.1 WP_161883475.1 TAN70402.1 WP_051906796.1 WP_125218592.1 OYY92272.1 WP_112183883.1 TXC65962.1 WP_140625868.1	151 LQLSIRALAASLINGVLISDASQAS-FPIMYAN-PAFCRMTGYDLIEVMGRINCRFLQND 54 PQLSARALAASSINGVLIADARQPS-CPIJVYAN-PAFCRMTGYALDELLGRINCRFLQGD 28 DALSIRALSACSNGWILADAAPD-MPIMYAN-PAFCAMTGYPLGELLGRINCRFLQGD 41 MRLLERAIENSHSAVLIADARQPD-FPAIYIN-HAFEGMTGYTVDECLGRINCRFLQGD 10 -ASMVGALDAMPVSVIIADAKVAD-MPIJYYM-PAFEALTGYTSDEARGRINCRFLQGD 13 - EASLPILICDARQAD-MPIJYM-PAFEALTGYTSDEARGRINCRFLQGG 46 IRI LFRAVFASASSTSMADAIKPD-MPIJYWI-PAFEALTGYSRDEVIGRINCRFLQGG 46 IRI LFRAVFASASSTSMADAIKPD-MPIJYWI-PAFEALTGYSRDEVIGRINGRFLQGG 517 LRLLQRAVASNINGITIADVQQKD-MPLIYWI-PSFERITGYSREELIGKNICRFLUGG 517 LKLLERAVEASTSGIVIADANQYD-MPLIYMI-PSFERITGYSREELIGKNICRFLUGS 61 LALYRRAMEASSSYSMSTADATAPD-LPLIYIN-PAFEALTGYSREELIGKNICRFLGGG 61 DAALPIVVADATQPD-LPVVYN-PAFEATTGYSASEVLGRINGRFLQGG 63 DAALPIVVADATQPD-LPVYVN-PAFEATTGYSASEVLGRINGRFLQGG	DRNQ	RAVRVTLRIVYRKINGTMFWIELSLTPIHGHDG ILTHYAGVÄHDVTEAVI ESVHVVLRIVYRKOGSLFWIELFISPVPDERG DITHYIGILINDITARKI EDAHVVLRIVYRKOGSLFWIDLFLSPVPDOHG ELAHYIGIYTDITELKI QOAHVVVRIVYRKOGTFPWIDLFISPVPDALG VVTHYVGIATDVTALKI EDCHVVLRIVYRKOGTLFWIELTLSPVRDAGG INTHYLGISTDITVEVI QSVQAVLRIVYRKOGAFLNEHLITPVPLDAED SLYFTMOVSRDATREAH EACTVJMRIVRKOGAFLNEHLITPVRDAED QLTHYMAVLSOOTERH RSTTVTLRIVYHKOGTFPWIDLSLSPVHDASG TLTHYLGFLINDVTAREI RRGTRALLRIVYRKOGSFPWIDLSTAPVHDERG QVTHFIGITSDDVTFRAH EKGTRALLRIVYRKOGSFPWIELTMPVHDERG QVTHFIGITSDVSFRAH EKGTRALLRIVYRKOGSFPWIELTAPVHDERG MLTHFIGITSOVSERVI ROGRALLRIVYRKOGSPFWIELTAPVHDERG MLTHFIGITSOVSERVI ROGRALLRIVYRKOGSPFWIELTMPVHDERG MLTHFIGITSOVSERVI ROGRALLRIVYRKOGSPFWIELTMPVHDERG HTVYVICTUROVSERVI RACTVLLRIMRROGSFPFWIELTMPVHDGGG HTVYVICTUROVSERVI RACTVLLRIMRROGSFPFWIELTMPVHDAGG HTVYVICTUROVSERVI RACTVLLRIMRROGSFPFWIELTMPVHDAGG HTVYVICTUROVSERVI RACTVLLRIMRROGSFPFWIELTMPVHDAGG HTVYVICTUROVSERVI RACTVLLRIMRROGSFPFWIELTMPVHDAGG HVYVICTUROVSERVI RACTVLLRIMRROGSFPFWIELTMPVHDAGG HVYVICTUROVSERVI RACTVLLRIMRROGSFPFWIELTMPVHDAGG HVYVICTUROVSERVI RACTVLLRIMRROGSFPFWIELTMPVHDAGG HVYVICTUROVSERVI RACTVLLRIMRROGSFPMIELTMPVHDAGG HVYVICTUROVSERVI RACTVLLRIMRROGSFP	G 327 N 272 R 175 Q 149 Q 162 L 130 Q 651 A 132 A 527 A 638 S 638 M 524 A 620 A 363 A 430
WP_132137257.1 WP_093555924.1 PKL98247.1 WP_126799631.1 TXH46092.1 WP_161883475.1 TAN70407.1 WP_051906796.1 WP_125218592.1 OYY92272.1 TXC65962.1	151 LQLSIRALAASLINGVLISDASQAS-FPIMYAN-PAFCRMTGYDLIEWMGRNCRFLQND 54 PQLSARALAASSNOVLIDAARQPS-CPIVYAN-PAFCRMTGYALDELLGRNCRFLQGG 48 DALSINGALSACSNOVITADAAAPD-MPIWYAN-PAFCAMTGYDVGGLLGRNCRFLQGG 41 MRLLERAIENSHSAVLIADARQPD-FPAIYIN-HAFEGMTGYTVDECLGRNCRFLQGG 40 -ASHWGALDAMPSVYITADAKVAD-MPILYYN-PAFEALTGYTSDEARGRNCRFLQGG 41 PQLLSQATAACTVGVWMTDARQND-MPILYYN-PAFEALTGYTADEAMGRNCRFLQGG 406 IRI FRAVFASASSTSWADAMKPD-MPILYVN-PAFEALSGYTADETLGHNCRFLQGG 417 LRLLGRAVAASNNGITIADVQNCD-MPLITYN-PAFERITGYSRGEVIGRNCRFLQGG 418 LRLGRAVASSNSTADATAPD-LPITYN-RAFERITGYSRGEVIGRNCRFLQGG 419 LRLGRAVASSNSTADATAPD-LPLYVN-PAFERITGYSRGEVIGRNCRFLQGG 401 LALGRAVASSNSTADATAPD-LPLYVN-PAFERITGYSRGEVIGRNCRFLQGG 410 LALGRAVASSNSTADATAPD-LPLYVN-PAFERITGYSRGEVIGRNCRFLQGG 411 PQLDAMPTVYNDSTQPD-RPTVYN-PAFERITGYSRGEVIGRNCRFLQGG 412 LALGRAVASSNSTADATAPD-LPVYVN-PAFERITGYSRGEVIGRNCRFLQGG 413 LALYRRAMEASSVSMSIADATAPD-LPVYVN-PAFERITGYSRGEVIGRNCRFLQGG 414 DAAMPTVYNDSTQPD-RPTVYN-PAFERITGYSRGEVIGRNCRFLDD 415 DAAMPTVYNDSTQPD-RPTVYN-PAFERITGYSRGEVIGRNCRFLINGG	- DRNQ	RAVRVTLRIVYRKINGTMFNWELSLTPIHGHDG ILTHYAGVÄHDVTEAVI ESVHVVLRIVYRKOGSLFNWELFISPVPDERG DITHYTGILINDITARKI ESDHAVVLRIVYRKOSSLFNWELFISPVPDERG ELAHYIGITVDITELKI -QDAHVVVRIVYRKOSLFNWELFISPVPDALG ELAHYIGITVDITELKI -QDAHVVVRIVYRKOGTFFNWELFISPVPDAGG WITHYLGISTDITVEVI -GDCHAVVLRIVYRKOGAFHNELTIJPULDAED SLYFYMSVSRADIFRAH -EACTVLIMRIVYRKOGAFHNELTIJPLELDAED GLTHYMAVLSDQTERHI -RSTTYLRIVYHKOGTLFVINELSLSPVHDAGG ILTHTGISTDITVERKI -KGTRALLRIVYRKOGAFHNELHLTPVRDAED QLTHYMAVLSDQTERHI -KSTTAVLRIVYRKOGTLFVMELSLSPVHDAGG ILTHTGISTDNYTERRI -KGTRALLRIVYRKOGSHPMIELTAPVHDERG QVTHFIGITEDVSERLI -EKVEGVU NINYRKOGSHPMIELTAPVHDERG UTHFIGITEDVSERLI -EKVEGVU NINYRKOGSHPMIELTYPYHDGGG KLTHFIGISTDVSPRI -EACTVLLRINRRROGSFPINELLVPYLVDAAG HTVQVIGVULDVTEGVI -EACTVLLRINRRROGSFFINELSVYPIRDARG HVQVIGVULDVTEGVI -RSTYLLARINRROGSFFINELHVAPIVDAAG RVTHFIGITUTVERTI -RECSVVINNYRKOGSFPFINELHVAPIVDAAG RVTHFIGITHOVTERTI -RECSVVINNYRKOGSFFFINELHVAPIVDAAG SVTHFIGITHOVTERTI -RECSVVINNYRKOGSFFFINELHVAPIVDAAG SVTHFIGITHOVTERTI -RECSVVINNYRKOGSFFFINELHVAPIVDAAG SVTHFIGITHOVTERTI -RECSVVINNYRKOGSFFFINELHVAPIVDAAG GLSHFIGVHDVTERTI	G 327 N 272 R 175 Q 149 Q 162 L 130 Q 651 A 132 A 527 A 638 S 638 M 524 A 620 A 363 A 430 A 672
WP_132137257.1 WP_093555924.1 PKL98247.1 WP_126799631.1 TXH46092.1 WP_161883475.1 TAN70402.1 WP_051906796.1 WP_125218592.1 OYY92272.1 WP_112183883.1 TXC65962.1 WP_140625868.1 WP_085751094.1	151 LQLSHRALAASLNGVLISDASQAS-FPIMYAN-PAFCRMTGYDLIEWMGRNCRFLQND 54 PQLSARALAASSNGVLIDAARQPS-CPIVYAN-PAFCRMTGYALDELLGRNCRFLQGG 48 DALSHRALAASSNGVILDAARQPS-CPIVYAN-PAFCRMTGYDLGELLGRNCRFLQGG 41 MRLLERAIENSHSAVLIADARQPD-FPAIYIN-HAFEGMTGYTVDECLGRNCRFLQGD 40 -ASHWGALDAMPSVITIADAKYAD-MPIVYTN-PAFEALTGYTSDEARGRNCRFLQGG 41 PQLLSQATAACTVGVWTDARQHD-HPIVYWN-PAFEALTGYTADEAMGRNCRFLQGG 466 IRLIFRAVEASASSTSMADAIKPD-MPITYWN-PAFEALSGYTADETLGHNCRFLQGG 475 TLRLQRAVAASHNGITIADVQKD-MPLTYWN-PAFEALTGYTSRDEVLGRNCRFLQGG 476 TLRLQRAVAASHNGITIADVQKD-MPLTYWN-PAFEALTGYSRDEVLGRNCRFLQGG 477 TLRLQRAVAASHNGITIADVQKD-MPLTYNN-PAFEALTGYSRDEVLGRNCRFLQGG 483 IALYRRAMEASSVSMSIADATAPD-LPLYTIN-PAFEATTGYSRDEVLGRNCRFLQGG 484 TLBRAVEASTSGVTADANQYD-MPLTYNN-PAFEATTGYSRDEVLGHNCRFLQGG 485 TLBRAVEASTSGVTADANQYD-MPLTYNN-PAFERTTGYSRDEVLGHNCRFLQGG 486 TLBRAVEASTSGVTADANQYD-MPLTYNN-PAFEATTGYSRDEVLGHNCRFLQGG 487 TLBRAVEASTSGVTADANQYD-MPLTYNN-PAFEATTGYSRDEVLGHNCRFLQGG 488 TLBRAVEASTSGVTADANQYD-MPLTYNN-PAFEATTGYSRDEVJGHNCRFLUNGG 489 TLBRAVEASTSGVTADANQYD-MPLTYNN-PAFEATTGYARDEAVGRNCRFLUNGG 489 TLBRAVEAGAGAGAGAGAGAGAGAGAGAGAGAGAGAGAGAGAGA	- DRNQ	RAVRVTLRIVYRKINGTMFWIELSLTPIHGHDG ILTHYAGVÄHDVTEAVI ESVHVVLRIVYRKOGSLFWIELFISPVPDERG DITHYIGILINDITARKI ESVHVVLRIVYRKOGSLFWIELFISPVPDERG ELAHYIGILVTDITELKI QOAHVVVRIVYRKOGSLFWIELTISPVPDALG VVTHYVGIATDVTALKI QOAHVVVRIVYRKOGTFWIELTISPVPDALG VVTHYVGIATDVTALKI EDCHVVLRIVYRKOGAFNWELTLVPLLDAED SLVFYMGVSRDATREAI EACTVLMRIVYRKOGAFNWELTLVPLLDAED SLVFYMGVSRDATREAI EACTVLMRIVYRKOGAFNWELTLVPLDAEG QLTHYMAVLSOOTERH ERSTTVTLRIVYHKOGIFFWIELSSPVHDASG TLTHYLGFLINDVTAREI RRISTRULRIVYRKOGSPFWIELTAPVHDERG QVTHFIGITEDVSERLI EKVEGVLRIVYRKOGSPFWIELTAPVHDERG MLTHFIGITEDVSERLI EKVEGVLRIVYRKOGSPFWIELTAPVHDERG HLTHFIGITEDVSERLI ERCTVLLRIVRRKOGSPFWIELTAPVHDERG HTVYGISLQDVSERVI EACTVLLRIVRRKOGSPFWIELTVPVHDGGG HTVYGISLQDVSERVI EACTVLLRIVRRKOGSFPWIELTVPVHDGGG HTVYGISLQDVSERVI RASTVLLRIVRRKOGSFPWIELTVPVHDGGG HTVYGISLQDVSERVI RASTVLLRIVRRKOGSFPWIELTVPVHDGGG HTVYGISLQDVSERVI RASTVLLRIVRRKOGSFPWIELTVPVHDAGG HTVYGISLQDVSERVI RASTVLLRIVRRKOGSFPWIELTVPVHDAGG HTVYGISLQDVSERVI RRECSVULRIVRRKDGSFFVINLHVAPIRDAAG SCHFIGVLHDVTERTI RECSVULRIVRRKDGSSFYWELTSVPTRAFGSEGG DLTHFIGVETDVTREVI RRYVEYTVRIVRRKOGSFPWIALSLAPVRDETG AVSHFVGLTTDVTERHI RSCSVELRIVRRADGSFFVINLSLAPVRDETG AVSHFVGLTTDVTERHI RSCSVELRIVRRADGSFFVINLSLA	G 327 N 272 R 175 Q 149 Q 162 L 130 G 651 A 132 A 527 A 638 S 638 M 524 A 620 A 363 A 430 A 672 M 97 L 322
WP_132137257.1 WP_093555924.1 PKL98247.1 WP_126799631.1 TXH46092.1 WP_161883475.1 TAN70402.1 WP_051906796.1 WP_125218592.1 OYY92272.1 WP_112183883.1 TXC65962.1 WP_140625868.1 WP_085751094.1 RME97112.1 WP_158540843.1	151 LQLSIRALAASLINGVLISDASQAS-FPIMYAN-PAFCRMTGYDLIEWMGRICRFLQND 54 PQLSARALAASSINGVLIDAARQPS-CPIJYAN-PAFCRMTGYDLIEUMGRICRFLQGG 48 DALSIRALAASSINGVILDAARQPS-CPIJYAN-PAFCRMTGYALDELLGRICRFLQGG 44 MRLLERAIENSHSAVLIADARQPD-FPAIYIN-HAFEGMTGYTVDECLGRICRFLQGG 55 - ASHWGALDAMPSVYLTADAKVAD-MPIJYYNI-PAFEALTGYTSDEARGRICRFLQGG 56 - EASLPILICDARQAD-MPIJYYNI-PAFEALTGYTATEAMGRINCRFLQGG 57 - EASLPILICDARQAD-MPIJYYNI-PAFEALTGYTADEAMGRICRFLQGG 58 - EASLPILICDARQAD-MPIJYWI-PAFEALTGYTADEAMGRICRFLQGG 59 - TRLLQRAVAASINGSTIADVQQKD-MPLIYWI-PAFEALTGYTADEAMGRICRFLQGG 50 - LRLLGRAVAASINGSTIADVQQKD-MPLIYWI-PAFERTTGYSREDAVGRICRFLQGG 50 - DAALPIVADANQYD-MPLITYNI-PAFERTTGYSREDAVGRICRFLUSH 50 - DAALPIVADATQPD-LPLYVVII-PAFERTTGYBADEAVGRICRFLQGG 50 - DAAMPIVATDSTQPD-RPIVYWI-PAFERTGYBADEAVGRICRFLQGG 51 - DAAMPIVATDSTQPD-RPIVYWI-PAFERTGYBADEAVGRICRFLQGG 55 - MPKKRGVEAAAALPMCVCDATQPD-LPLYVWI-PAFERTGYBADEAVGRICRFLQGG 56 - DAALPITYDATTLPD-QPLIYWI-PAFERTGYBADEAVGRICRFLQGG 57 - MYKKRGVEAAAALPMCVCDATQPD-LPLYWI-PAFERTGYBADEAVGRICRFLQGG 58 - MYKKRGVEAAAALPMCVCDATQPD-LPLYWI-PAFERTGYTGAVGRICRFLQGG 59 - QURLKAATEATDVGVTYADARARD-FPLYWI-PAFERTGYTGAQAGRICRFLQGG 59 - QURLKAATEATDVGVTYADARARD-FPLYWI-PAFERTGYTGAQAGRICRFLQGG 51 - QURLKAATEATDVGVTYADARARD-FPLYWI-PAFERTGYTGAQAGGRICRFLQGG 51 - QURLKAATEATDVGVTYADARARD-FPLYWI-PAFERTGYTGAQAGGRICRFLQGG 51 - QURLKAATEATDVGVTYADARARD-FPLYWI-PAFTERTGYTAAQALGGRICRFLQGG 51 - QURLKAATEATDVGVTYADARARD-FPLYWI-PAFTERTGYTAAQALGGRICRFLQGG	- DRNQ	RAVRVTLRIVYRKINGTMFNWELSLTPIHGHDG ILTHYAGVÄHDVTEAVI ESVHVVLRIVYRKOGSLFNWELFISPYPDERG DITHYTGILINDITARKI ESDHAVVLRIVYRKOSSLFNWELFISPYPDERG DITHYTGILINDITARKI EDCHAVVLRIVYRKOSSLFNWELFISPYPDALG VYTHYVGIÄTDVTALKI "QDAHVVVRIVYRKOGTFFNWELFISPYRDAGG HVTHYGIÄTDVTALKI "EDCHAVVLRIVYRKOGAFHNELTIJPLEDAED SLYFYMKYSYRDATERAI "EACTVLIMRIVYRKOGAFHNELTIJPLEDAED OLTHYMAVLSDOTERHI "RSTTYTLRIVYHKOGTFVIELSLSPYHDAGG TILTHYAGFLINDYTARRI "RSTTYTLRIVYHKOGTLFWÜLSLSPYHDAGG RI THFTGTSDYTFRRI "RKGEVI VHINYRKOFSPHWELTIPPHDEGG QVTHFTGITEOVSERLI "EKVEGVU KNYRKOGSPHWELTIPPHDEGG MILTHFTGTSDVTFSRI "EKVEGVU KNYRKOGSPHWELTIPPHDEGG MILTHFTGTSDVTSPRI "EKVEGVU KNYRKOGSPHWELTIPPHDEGG MILTHFTGTSDVSPRIL "EKVEGVU KNYRKOGSPHWELTIPPHDEGG MILTHFTGTSDVSSRIL "EKVEGVU KNYRKOGSPHWELTIPPHDEGG MILTHFTGTSDVSSRIL "EKVEGVU KNYRKOGSPHWELTIPPHDEGG MILTHFTGTSDVSSRIL "ERGGRALLENNROGSPFFINLENLSVYPTRDARG HVYQYLGVLIDVTERWI "RESTYLLANRRKOGSFFINLEHVAPIVDAAG RVTHFTGVTTVTERTI "RESSYUTINNRKOGSFFNEWILHAPPROAAG GLSHFTGVLHDVTEQTI "RESSYUTINNRKOGSFPNEWILAPPROEAG AVSHFVGLTTVTERHI "RSCSVELRINNRADGSFPNIKLSLAPVRGEAG AVSHFVGLTTVTERHI "RSCSVELRINNRADGSFPNIKLSLAPVRGEAG ATITHVOLINDVSARHI "RSCSVELRINNRADGSFPNIKLALPVRGEAG ATITHVOLINDVSARHI "RSCSVELRINNRADGSFPNIKALPVRGEAG ATITHVOLINDVSARHI "RSCSVELRINNRADGSVFNIKENSLAPVRGEAG ATITHVOLINDVSARHI "RSCSVELRINVADGSFPNIKALPVRGEAG ATITHVOLINDVSARHI "RSCSVELRINVADGSFPNIKALPVRGEAG ATITHVOLINDVSARHI "RSCSVELRINVADGSFPNIKALPVRGEAG ATITHVOLINDVSARHI "RSCSVELRINVADGSFPNIKALPVRGEAG ATITHVOLINDVSARHI "RSCSVELRINVADGSFPNIKALPVRGEAG ATITHVOLINDVSARHI "ROTHT RATIVATE	G 327 N 272 R 175 Q 149 Q 162 L 130 Q 651 A 132 A 527 A 638 S 638 M 524 A 620 A 363 A 430 A 470 M 97 L 322 L 303
WP_132137257.1 WP_093555924.1 PKL98247.1 WP_126799631.1 TXH46092.1 WP_161883475.1 TAN70402.1 WP_051906796.1 WP_125218592.1 WP_112183883.1 TXC65962.1 WP_140625868.1 WP_085751094.1 RME97112.1 0ZB44497.1 WP_1518840843.1 WP_051848818.1	151 LQLSIRALAASLINGVLISDASQAS-FPIMYAN-PAFCRMTGYDLIEWMGRICRFLQND 54 PQLSARALAASSINGVLIDAARQB-CPITYAN-PAFCRMTGYDLIELWMGRICRFLQNG 54 PQLSARALAASSINGVLIDAARQB-CPITYAN-PAFCAMTGYDLDELLGRICRFLQGG 41 MRLLERAIENSHSAVLIADARQPD-FPAIYIN-HAFEGMTGYTVDECLGRICRFLQGG 40 - ASMYGALDAMPYSVITJADAXQAD-MPITYTIN-PAFEALTGYTSDEARGRICRFLQGG 539 EASLPILICDARQAD-MPITYTIN-PAFEALTGYTSDEARGRICRFLQGG 11 PQLLSQAIAACTVGVWMTDARQHD-HPIVYWN-PAFEALTGYTSDEAUGRICRFLQGG 406 IRI JERAVEASASSTSMADAIKDP-MPITYWN-PAFEATTGYSRDEVI GRICRFLQGG 517 LRLLGRAVAASSINGTIADAVQYQK-MPLTYWN-PAFEATTGYSRDEVI GRICRFLQGG 518 LIERAVEASTSGIVIADAVQYD-MPLIFTIN-KAFERITGYSREELIGKICRFLINGN 608 DAALPTWADATQPD-LPYVWN-PAFEATTGYSAEVLGRICRFLQGG 519 DAALPTWADATQPD-LPYVWN-PAFEATTGYGASEVLGRICRFLQGG 5201 DAAMPIVYTDSTQPD-RPIVYWN-PAFEATTGYGAEVGHICRFLINGD- 511 MWRKGVEAAAALPMCVCDATQPD-LPYVWN-PAFEATTGYGAEVGHICRFLINGD- 512 LYMKRGVEAAAALPMCVCDATQPD-LPYVWN-PAFEATTGYTAEVGAEVGHICRFLINGG- 513 PASLPTTVTDATLPD-QPLYVWN-PAFEATTGYTAEVGAEVGHICRFLINGG- 514 LYMKRGVEAAAALPMCVCDATQPD-LPYVWN-PAFEATTGYTAEVGAEVGHICRFLQGG- 515 LYMKRGVEAAAALPMCVCDATQPD-LPYVWN-PAFEATTGYTAEVGAEVGRICRFLQGG- 516 LYMLKAAITEATDVGVTVADARARD-FPLYVWN-PAFEATTGYTAEQAGRICRFLQGG- 517 LKLLKAAMEATEVGSVVDAQSGD-YPLVYWN-PAFEATTGYTAEQALGRICRFLQGG- 518 LYMLKAAITEATGVGSVVDAQSGD-YPLVYWN-PAFEATTGYTAEQALGRICRFLQGG-	- DRNQ	RAVRVTLRIYRKINGTMFNWELSLTPIHGHDG ILTHYAGVÄHDVTEAVI ESVHVVLRIYRKOGSLFNWILELTSPYPDERG DITHYTGILINDITARKI EDAHVVLRIYRKOGSLFNWILELTSPYPDERG ELAHYIGITVDITELKI QDAHVVWRIYRKOGSLFNWILETLSPYPDDALG VYTHYVGIÄTDVTALKI EDCHVVLRIYKKOGTLFNWILETLSPYRDAGG NVTHYLGIÄTDVTALKI EDCHVVLRIYKKOGTLFNWILETLSPYRDAGG STUPTVAGSTDITVEV ECKTVLPRIYRKOGGAFNWELTLVPLLDAED SLVFYWOVSRDATREA EACTVLPRIYRKOGGAFNWELTLVPVLDAGG CLTHTWAVLSDOTERHI ERSTTVTLRIYHKOGTLFVNLESLSPVHDAGG TLTHYLGFLINDVTAREI KGTRALLRIYRKOGSFPNWELTAPVHDERG VTHFIGITEDVSERLI EKVEGVIVRIYRKOGSPRWILELTAPVHDERG VTHFIGITEDVSERLI EKVEGVIVRIYRKOGSPRWILELTAPVHDERG HITTPIGITEDVSERLI EKVEGVILRIYRKOGSPRWILELTAPVHDERG HITTPIGITEDVSERLI EKVEGVILRIYRKOGSPRWILELTAPVHDERG HITTPIGITEDVSERLI EKVEGVILRIYRKOGSPRWILELTAPVHDERG HITTPIGITEDVSERLI ERCTVILRIKRRROGTFPYNELHVAPTVDAAG HITTPIGVULDDVSERVI ERCTVILLRIKRROGSFFLINELIVYPIRDAGG HIVOHLGVLIDVTERVI RASTVILLRINARKOGSFELNELSVYPIRDARG HIVOHLGVLIDVTERVI RECSVYLINKYRKOTFTPTNALHVAPVEDAAG SCHIFTLEVIDVTETTE RECSVYLINKYRKOTFTPTNALHVAPVEDAAG SCHIFTLEVIDVTETTE RECSVYLINKYRKOTFTPTNALHVAPVEDAAG ALSHFIGVLIDVTETTE RECSVYLINKYRADGSPPWILSLAPVRSESG DLTHFIGVETDVTREVI RECSVYLERVARDAGGVFRWIENSLAPVRSESG ATTHYVOLIDVTEAVI RECSVYLERVARDAGGVFRWIENSLAPVRSESG ATTHYVOLIDVTSRVI	G 327 N 272 R 175 Q 159 Q 162 L 130 Q 651 A 132 A 527 A 638 S 638 M 524 A 620 A 630 A 430 A 672 M 97 L 303 L 303
WP_132137257.1 WP_093555924.1 PKL98247.1 WP_126799631.1 TXH46092.1 WP_161883475.1 TAN70402.1 WP_051906796.1 WP_125218592.1 OYY92272.1 WP_112183883.1 TXC65962.1 WP_140625868.1 WP_085751094.1 RME97112.1 UP_158540843.1 WP_051848818.1 WP_051848818.1	151 LQLSIRALAASLINGVLISDASQAS-FPIMYAN-PAFCRMTGYDLIEWMGRNCRFLQND 54 PQLSARALAASSINGVLIDAARQPS-CPIJYAN-PAFCRMTGYALDELLGRICGR-LQGG 42 DALSINGLASCSINGWITADAAAPD-MPIHYAN-PAFCAHTGYPLGELLGRINGGR-LQGG 43 MRILERAIENSHSAVLIADARQPD-FPAIYIN-HAFEGMTGYTVDECLGRINCRFLQGD 44 MRLLERAIENSHSAVLIADARQPD-FPAIYIN-HAFEGMTGYTVDECLGRINCRFLQGD 45 - ASMYGALDAMPYSYITADAKYAD-MPILYYNI-PAFEALTGYTSDEARGRINCRFLQGD 46 IRI FRAVFASASSTSMADAINCPI-MPITYAN-PAFEALTGYTADEALGRINCRFLQGG 466 IRI FRAVFASASSTSMADAINCPI-MPITYAN-PAFEALTGYTADEALGRINCRFLQGG 517 LRLLGRAVAASNINGITIADVQNCD-MPLITYNI-PAFERITGFSREEAVGRINCRFLQGG 518 LLERAVEASTSGIVIADAINQYD-MPLITYNI-PAFERITGFSREEAVGRINCRFLQGG 519 LLLERAVEASTSGIVIADAINQYD-MPLITYNI-PAFERITGFSREEAVGRINCRFLQGG 510 DAALPIVVADATQPD-LPLYTNI-PAFERITGYSRDEVLGRINCRFLQGD 510 DAALPIVVADATQPD-LPLYYVNI-PAFERITGYBDEVLGRINCRFLQGD 511 DAALPIVADATQPD-LPLYYVNI-PAFERITGYBDEVLGRINCRFLQGD 512 DAALPIVADATQPD-LPLYYVNI-PAFERLSGYRDEVIGHICRFLINGG 513 DASLPITYTDATLPD-QPLIYWI-PAFERLTGYBDEVGRINCRFLINGG 514 NYMKRGVEAAAALPHCVCDATQPD-LPLYYWI-PAFERLSGYTAGAELGRINCRFLQGG 515 LQMLKAAIEASTGGYTVADARARD-FPLYYWI-PAFERITGYTAGAELGRINCRFLQGG 516 LQMLKAAIEASTGGYTVADARARD-FPLYYWI-PAFERITGYTAAQALGRINCRFLQGG 517 LGMLKAAIEASTGGYTVADARARD-FPLYYWI-PAFERITGYTAAQALGRINCRFLQGG 518 LQMLKAAIEASTGGYTVADARARD-FPLYYWI-PAFERITGYTAAQALGRINCRFLQGG 519 LHLLKAAMEATEVGYSVVDAQSGD-YPLYYWI-PAFERITGYTAAQALGRINCRFLQGG 511 LARAMLAMEASPLGYTTADARQAD-LPLYYNI-PAFTSLGGYTAAQALGRINCRFLQGG 511 LARAMLAMEASPLGYTTADARQAD-LPLYYNI-PAFTSLGGYTAAQALGRINCRFLQGG 512 LARAMLAMEASPLGYTTADARQAD-LPLYYNI-PAFTSLGGYTAAQALGRINCRFLQGG 513 LARAMLAMEASPLGYTTADARQAD-LPLYYNI-PAFTSLGGYTAAQALGRINCRFLQGG	- DRNQ	RAVRVTLRIVYRKINGTMFWIELSLTPIHGHDG ILTHYAGVÄHDVTEAVI ESVHVVLRIVYRKOGSLFWIELFISPVPDERG DITHYIGILINDITARKI ESVHVVLRIVYRKOGSLFWIELFISPVPDERG ELAHYIGILVTDITELKI QDAHVVVRINYRKOGSLFWIDLFISPVPDALG VYTHYVGIATDVTALKI QDAHVVVRINYRKOGTFFWIDLFISPVPDALG VYTHYVGIATDVTALKI EDCHVVLRIVYRKOGTFFWIELTLSPVRDAGG HVTHYLGSTDITVEVI ESCHVVLRIVYRKOGAFIWELTLVPLLDAED SLVFYYMGVSRDATREAI EACTVLMRIVYRKOGAFIWELTLVPLLDAED QLTHYMAVLSOQTERHI RSTTVTLRIVYHKOGTFPWIDLSLSPVHDASG TLTHYLGFLINDVTAREI RRIGEVI VHINYRKOGSPFWIDLTAPPVHDERG RI THFIGTSDDVTFRRI EKGTRALLKNIVRKOELFWIDLHAPPVHDERG VYTHFIGTIEDVSERLI EKVEGVLRIVYRKOGSPFWIELTVTPVHDGGG KLTHFIGTSDDVSERVI RPCTVVLLRIMRROGSFFWIELTSVPTRDAGG HTVQVIGVLQDVSERVI RPCTVVLLRIMRROGSFFWIELTSVPTRDAGG HVVQHLCVLHDVTERVI RASTVLLRIMRROGSFFINELHVAPTRDAAG RVTHFIGVHTDVTERTI RPCSVVTININVRKOGSPFWIALSLAPVRDEGG ALTHVOLVLHDVTERVI RPCSVTYRININVRKOGSFFWIALSLAPVRDEGG ALTHVOLVTTERVI RPCSVLERNIVRROGSFFWIALSLAPVRDETG AVSHFVGLTTDVTERTI RPCSVLERNIVRROGSFFWIALSLAPVRDETG AVSHFVGLTTDVTERTI RPCSVLERNIVRROGSFFWIALSLAPVRDETG AVSHFVGLTTDVTERTI RSCSVLERNIVRADGSFFWIALSLAPVRDETG ALTHVOLKNIDVSARMI RSCSVLERNIVRADGSFFWIALSLAPVRDETG ALTHVOLKNIDVSARMI RSCSVLERNIVRADGSFFWIALSLAPVRDETG ALTHVOLKNIDVSARMI RSCSVLERNIVRADGSFFWIALSLAPVRDETG ALTHVOLKNIDVSARMI RSCSVLERNIVRADGSFFWIALSLAPVRDETG ALTHVOLKNIDVSARMI RSCSVLERNIVRADGSFFWIMLSLAPVRDETG STHFVGLHHDVTQNIV	G 327 N 272 R 175 Q 149 Q 162 L 130 Q 651 A 132 A 527 A 638 S 638 M 524 A 620 A 630 A 430 A 672 M 97 L 322 L 303 L 302 L 332
WP_132137257.1 WP_093555924.1 PKL98247.1 WP_126799631.1 TXH46092.1 WP_161883475.1 TAN70402.1 WP_051906796.1 WP_125218592.1 0YY92272.1 WP_112183883.1 TXC65962.1 WP_085751094.1 RWE97112.1 WP_140625868.1 WP_085751094.1 WP_15844847.1 WP_1584484818.1 WP_051848818.1 WP_051848818.1 WP_024306487.1 WP_051959502.1	151 LQLSIRALAASLINGVLISDASQAS-FPIMYAN-PAFCRMTGYDLIEWMGRICRFLQND 54 PQLSARALAASSINGVLIDAARQPS-CPILYVAN-PAFCRMTGYALDELLGRICRFLQGG 428 DALSIRALSACSINGWITADAAAPD-MPIWYAN-PAFCAMTGYDLGELLGRICRFLQGG 44 MRLLERAIENSHSAVLIADARQPD-FPAIYIN-HAFEGMTGYTVDECLGRICRFLQGD 45 -ASHWGALDAMWSVITADAKVAD-MPIWYTN-PAFEALTGYTSDEARGRICRFLQGG 46 -CASHWGALDAMWSVITADAKVAD-MPIWYAN-PSFERLTGYMATEAMGRINCRFLQGG 47 -CASHWGALDAMWSVITADARQHD-MPIWYAN-PSFERLTGYMATEAMGRINCHFLQGG 48 - LRILERAWFASASSTSMADAIKND-MPIWYM-PAFEALSGYTADETLGHINCRFLQGG 48 - LRILERAWFASASSTSMADAIKND-MPIWYM-PAFEALSGYTADETLGHINCRFLQGG 49 - LRILERAWFASASSTSMADAIKND-MPIWW-PAFEALSGYTADETLGHINCRFLQGG 40 - LRILERAWFASASSTSMADAIND-MPIWW-PAFEALSGYTADETLGHINCRFLQGG 40 - LRILERAWFASTSGYLADANQYO-MPILTYNN-PAFERTTGYSREELIGKINGRFLQGG 41 - DAAMPIWWTDSTQPD-RPIWWW-PAFERTTGYBAEDAWGRICRFLIND-PAMPIWWTDSTQPD-RPIWWW-PAFERTGYBAEDAWGRICRFLIND-PASELTGWTGAEVLGRICRFLQGG 42 - DAAMPIWWTDSTQPD-RPIWWW-PAFERTGYBAEDAWGRICRFLIND-PASELTGWTGAEVLGRICRFLQGG 43 - LOHLKAAIEATDWGWTWADARAB-FPLWWW-PAFERTTGYTEAQAMGRICRFLQGG 44 - LOHLKAAIEATDWGWTWADARAB-FPLWWW-PAFFRITGYTEAQAMGRICRFLQGG 45 - LOHLKAAIEATDWGWTWADARAB-FPLWWW-PAFFRITGYTEAQAMGRICRFLQGG 46 - LRILKAMEATEWGWSWWADASGD-YPLWWW-PAFFRITGYTEAQAMGRICRFLQGG 47 - LHILKAAMEATEWGWSWWADASGD-YPLWWW-PAFFRITGYTEAQAMGRICRFLQGG 48 - LARANLAMBEASPLGWTJADARQAD-LPLYVN-PAFFRITGYTEAQAMGRICRFLQGG 48 - LARANLAMBEASPLGWTJADARQAD-LPLYVN-PAFFRITGYTEAQAMGRICRFLQGG 49 - LARANLAMBEASPLGWTJADARQAD-LPLYVN-PAFFRITGYTEAQAMGRICRFLQGG 40 - LARANLAMBEASPLGWTJADARQAD-LPLYVN-PAFFRITGYTEAQAMGRICRFLQGG 41 - LARANLAMBEASPLGWTJADARQAD-PLYPLYYN-PAFFRITGYTEAQAMGRICRFLQGG 42 - LARANLAMBEASPLGWTJADARQAD-PLYPLYYN-PAFFRITGYTEAQEVLGRICRFLQGG	- DRNQ	RAVRVTLRIVYRKINGTMFNWELSLTPIHGHDG ILTHYAGVÄHDVTEAVI ESVHVVLRIVYRKOGSLFNWELFISPVPDERG DITHYTGILINDITARKI ESDHAVVLRIVYRKOSSLFNWELFISPVPDERG DITHYTGILINDITARKI EDCHAVVLRIVYRKOSSLFNWELFISPVPDALG VVTHYVGIÄTDVTALKI "QDAHVVVRIVYRKOGTFFNWELFISPVPDALG VVTHYVGIÄTDVTALKI "EDCHAVVLRIVYRKOGAFMELTILYPLEDAED BLYFTMKYSYRATREAL "EACTVLIMRIVYRKOGAFMELTILYPLEDAED GLTHYMAVLSDQTERHI "RSTTYTLRIVYHKOGTFVPIKLSLSPVHDAGG TILTHTGISTDNTYFERI "RKGEVI VHINYRKOFTFPWILSLSPVHDAGG RI THFTGISTDNTYFERI "RKGEVI VHINYRKOFTFPWILSLSPVHDAGG RI THFTGISTDNTYFERI "ERVGEVI VLINYRKOFTFPWILSLSPVHDERG RI THFTGISTDNTYFERI "ERVGEVI VLINYRKOGSPHWILELTYPVHDEGG RI THFTGISTDNTYFERI "ERGRALLRIVYRKOSPHWELTTPVHDGGG RITHTGISTDVSERLI "ERVGEVI LANNROGSPFFWILSTVPHDAGG HTVQVTGVLQDVSERVI "RASTVLLARRROGSFFENLELSVYPTRDAAG HTVQVTGVLQDVSERVI "RASTVLLARRROGSFFINLEHVAPIVDAAG HTVQVTGVLQDVSERVI "RESTVLARRROGSFFINLEHVAPIVDAAG RVTHFTGVHTDVTERTI "RECSVVINNYRKOGSFFNEVHTAPVRESGS GLSHFTGVLHDVTEQTI "RECSVVILRIVRROGSFFNEVHTAPVRESGS ATHTVQLIRDVTGVTFHT "RSCSVELRIVRADGGSFNEWELSLAPVRGEAG ATHTVQLIRDVSARHI "RSCSVELRIVRADGGSFNMENLSLAPVRGEAG ATHTVQLIRDVSARHI "RSCGAVLRIVRADGGGPFMIMESLAPVRGEAG ATHTVQLIRDVSARHI "RSCGAVLRIVRROGSFFINLSLSVSPVRIDAG VLTHFVGLIRTDVSARHI "RSCGAVLRIVRROGSFFNMLSLSPVRROEAG SISHFVGLIHDVTERVI "RSCGAVLRIVRROGSFFMIMLSVSSPVRIDAG VLTHFVGLIRTDVSARHI "RSCGAVLRIVRROGSFFMIMLSVSSPVRIDAG SISHFVGLIHDVTGNT "EFCQAVLRIVRROGSFFMIMLSVSSPVRIDAG SISHFVGLIHDVTGNT "EFCQAVLRIVRROGSFFMILSVLAPPREDAG SISHFVGLIHDVTGNT "EFCQAVLRIVRROGSFFMIMLSVSSPVRIDAG SISHFVGLIHDVTGNT "EFCQAVLRIVRROGSFFMIMLSVSSPVRIDAG SISHFVGLIHDVTGNT "EFCQAVLRIVRROGSFFMIMLSVSSPVRIDAG SISHFVGLIHDVTGNT "EFCQAVLRIVRROGSFFMIMLSVSSPVRIDAG SISHFVGLIHDVTGNT "EFCQAVLRIVRROGSFFMIMLSVSSPVRIDAG SISHFVGLIHDVTGNT "EFCQAVLRIVRROGSFFMIMLSVSSPVRIDAG SISHFVGLIHDVTGNT	G 327 N 272 R 175 Q 149 Q 162 L 130 Q 651 A 132 A 527 A 638 S 638 M 524 A 620 A 363 A 430 A 430 A 430 A 430 A 363 A 430 A 430 A 527 L 322 L 303 L 322 L 303 L 322 L 343 A 343
WP_132137257.1 WP_093555924.1 PKL98247.1 WP_126799631.1 TXH46092.1 WP_161883475.1 TAN70402.1 WP_051906796.1 WP_125218592.1 OYY92272.1 WP_112183883.1 TXC65962.1 WP_140625868.1 WP_085751094.1 RME97112.1 UP_158540843.1 WP_051848818.1 WP_051848818.1	151 LQLSIRALAASLINGVLISDASQAS-FPIMYAN-PAFCRMTGYDLIEWMGRNCRFLQND 54 PQLSARALAASSINGVLIDAARQPS-CPIJYAN-PAFCRMTGYALDELLGRICGR-LQGG 42 DALSINGLASCSINGWITADAAAPD-MPIHYAN-PAFCAHTGYPLGELLGRINGGR-LQGG 43 MRILERAIENSHSAVLIADARQPD-FPAIYIN-HAFEGMTGYTVDECLGRINCRFLQGD 44 MRLLERAIENSHSAVLIADARQPD-FPAIYIN-HAFEGMTGYTVDECLGRINCRFLQGD 45 - ASMYGALDAMPYSYITADAKYAD-MPILYYNI-PAFEALTGYTSDEARGRINCRFLQGD 46 IRI FRAVFASASSTSMADAINCPI-MPITYAN-PAFEALTGYTADEALGRINCRFLQGG 466 IRI FRAVFASASSTSMADAINCPI-MPITYAN-PAFEALTGYTADEALGRINCRFLQGG 517 LRLLGRAVAASNINGITIADVQNCD-MPLITYNI-PAFERITGFSREEAVGRINCRFLQGG 518 LLERAVEASTSGIVIADAINQYD-MPLITYNI-PAFERITGFSREEAVGRINCRFLQGG 519 LLLERAVEASTSGIVIADAINQYD-MPLITYNI-PAFERITGFSREEAVGRINCRFLQGG 510 DAALPIVVADATQPD-LPLYTNI-PAFERITGYSRDEVLGRINCRFLQGD 510 DAALPIVVADATQPD-LPLYYVNI-PAFERITGYBDEVLGRINCRFLQGD 511 DAALPIVADATQPD-LPLYYVNI-PAFERITGYBDEVLGRINCRFLQGD 512 DAALPIVADATQPD-LPLYYVNI-PAFERLSGYRDEVIGHICRFLINGG 513 DASLPITYTDATLPD-QPLIYWI-PAFERLTGYBDEVGRINCRFLINGG 514 NYMKRGVEAAAALPHCVCDATQPD-LPLYYWI-PAFERLSGYTAGAELGRINCRFLQGG 515 LQMLKAAIEASTGGYTVADARARD-FPLYYWI-PAFERITGYTAGAELGRINCRFLQGG 516 LQMLKAAIEASTGGYTVADARARD-FPLYYWI-PAFERITGYTAAQALGRINCRFLQGG 517 LGMLKAAIEASTGGYTVADARARD-FPLYYWI-PAFERITGYTAAQALGRINCRFLQGG 518 LQMLKAAIEASTGGYTVADARARD-FPLYYWI-PAFERITGYTAAQALGRINCRFLQGG 519 LHLLKAAMEATEVGYSVVDAQSGD-YPLYYWI-PAFERITGYTAAQALGRINCRFLQGG 511 LARAMLAMEASPLGYTTADARQAD-LPLYYNI-PAFTSLGGYTAAQALGRINCRFLQGG 511 LARAMLAMEASPLGYTTADARQAD-LPLYYNI-PAFTSLGGYTAAQALGRINCRFLQGG 512 LARAMLAMEASPLGYTTADARQAD-LPLYYNI-PAFTSLGGYTAAQALGRINCRFLQGG 513 LARAMLAMEASPLGYTTADARQAD-LPLYYNI-PAFTSLGGYTAAQALGRINCRFLQGG	- DRNQ	RAVRVTLRIYRKINGTMFNWELSLTPIHGHDG ILTHYAGVÄHDVTEAVI ESVHVVLRIVRRKOGSLFNWILELTSPYPDERG DITHYTGILINDITARKI ESVHVVLRIVRRKOGSLFNWILELTSPYPDERG ELAHYIGITVDITELKI - EDAHVVLRIVRKOGSLFNWILETLSPYPDDALG ELAHYIGITVDITELKI - QDAHVVVRINYRKOGTFPNWILETLSPYPDDAG EVTHYVGIÄTDVTALKI - EDCHVVLRIVRKOGTLFNWILETLSPVRDAGG INTHYLGISTDITVEVI - ECHVVLRIVRKOGTAFNWILETLLVPLLDAED SLVFYMOVSRDATREAI - EACTVLURNIVRKOGAFNWELTLVPVLDAGG ILTHYMAVISDOTERHI - ERSTTVTLRIVYRKOGTFPNWILSLSSPVHDAGG ITTHYLGFLINDVTAREI - KRYGFU VHINYRKOGTFPNWILSLSPVHDAGG INTHYLGITEDVSERLI - EKVGFU VHINYRKOGSPRWILETLAPVHDERG INTHYLGITEDVSERLI - EKVGFU VLNIVRRKOGSPRWILELTAPVHDERG INTHYLGITEDVSERLI - EKVGFU VLNIVRRKOGSPRWILELTAPVHDERG INTHYLGITEDVSERLI - EKVGFU VLNIVRRKOGSPRWILELTAPVHDERG INTHYLGITEDVSERLI - ERCTVLLRINRRROGSFELNELTVPLTDAGG HVVQHLOVLHDVTERVI - RASTVLLRINRRKOGSFELNELTVPLTDAGG HVVQHLOVLHDVTERVI - RASTVLLRINRRKOGSFELNELSVVPLRDAGG HVVQHLOVLHDVTERVI - RRECSVVINNWRKOFTPTNALHVAPVFDAAG INTHTIGVHDVTERVI - RRECSVVINNWRKOFTPTNALHVAPVFDAAG SLSHFLGVHDVTETTI - RRECSVSURNARDGOFFPNIKLSLAPVRDETG AVSHFVGLTTOTTERMI - RRSCSVELRIVRADGGFFNIKLSLSVPVRIDAG VLTHFVGLHDVSARH - RSCSVELRIVRADGGFFNIKLSLSVPVRIDAGG ATTHYVGLHDVSARH - RSCSVELRIVRADGGFFNIKLSLSVPVRIDAGG STHYVGLHDVSARH - RSCSVELRIVRADGGFFNIKLSLSVPVRIDAGG STHYVGLHDVSARH - RSCSVELRIVRADGGFFNIKLSLSPVRIDAGG STHYVGLHDVSARH - RSCSVELRIVRADGGFFNIKLSLSPVRIDAGG STHYVGLHDVSARH - RSCSVELRIVRADGGFFNIKLSLSPVRIDAGG STHYVGLHDVSARH - RSCSVELRIVRADGGSFNIKLSLSPVRIDAGG STHYVGLHDVSARH - RSCSVELRIVRADGGSFNIKLSLSPVRIDAGG STHYVGLHDVSARH - RSCSVELRIVRADGGSFNIKLSLSPVRIDAGG STHYVGLHDVSARH - RSCSVELRIVRADGGSFNIKLSLSPVRIDAGG STHYVGLHDVSARH - RSCSVELRIVRADGGSFNIKLSLAPVRDEGG STHYVGLHDVSARH - RSCSVELRIVRADGGSFNIKLSLAPVRDEGG STHYVGLHDVSARH - RSCSVELRIVRADGGSFNIKLSLAPVRDEGG STHYVGLHDVSARH - RSCSVELRIVRADGGSFNIKLSLAPVRDEGG STHYVGLHDVSARH - RSCSVELRIVRADGSLFNIKETLAPVRDAGG STHYVGLHDVSARH - RSCSVELRIVRADGSLFNIKETLAPVRDAGG STHYVGLHDVAGGT	G 327 N 272 R 175 Q 149 Q 162 L 130 Q 651 A 132 A 132 A 132 A 132 A 638 G 638 M 524 A 630 A 630 A 672 M 97 L 303 L 302 L 303 L 302 L 433 A 434 A 582
WP_132137257.1 WP_093555924.1 PKL98247.1 WP_126799631.1 TXH46092.1 WP_161883475.1 TAN70402.1 WP_051906796.1 WP_125218592.1 WP_112183883.1 TXC65962.1 WP_140625868.1 WP_085751094.1 RNE97112.1 OZB44497.1 WP_158540843.1 WP_051848818.1 WP_051848818.1 WP_051848818.1 WP_051848818.1 WP_051848818.1 WP_051848818.1	151 LQLSIRALAASLINGVLISDASQAS-FPIMYAN-PAFCRMTGYDLIEWMGRNCRFLQND 54 PQLSARALAASSINGVLIDAARQPS-CPIVYAN-PAFCRMTGYDLIEUMGRNCRFLQGG 48 DALSINKALSACSINGWITADAAAPD-MPIWYNN-PAFCRMTGYDLGELLGRNCRFLQGG 41 MRLLERAIENSHSAVLIADARQPD-FPAIYIN-HAFEGMTGYTVDECLGRNCRFLQGD 53	- DRNQ PAVGLVRDATAQE DREQ - PAVAATRSATDAR DREQ - AAVAVLRHATARG DODQ - PALAALRQATARA DREC - PETAVWRNAL ERN DRAD - PESAMROALAKG DRDQ - PGVGETRQALVEQ FILD - PG I DGTRAVI REG DRDQ - PGVGETRQALVEQ FILD - PG I DGTRAVI REG DRDQ - PGLDHVRSALSKG DRDQ - PGLDHVRSALSKG DRDQ - PGLDHVRSALSKG DRDQ - TGLQTLRAALARG ERDQ - AGLVETRAALARG FTAQ - PGLPELRAALAGE FTAQ - PGLTRLREATAG ERDQ - PALDEVRAALREG ERDQ - PALDEVRAALREG DRAQ - LELQPLRAALARG DRAQ - LELQPLRAALARG DRAQ - LELQPLRAALARG DRAQ - PALDELRAALARG DRAQ - PALDELRAAVRAG DTAQ - PALDELRAAVRAG DRAQUETRNAVQKG DRADQUETRNAVQKG DRADQUETRNAVQKG DRADQUETRNAVQKG DRADGUETRNAVQKG DRADGUETRNAVAG DRADGUETRNAVAG DRADGUETRNAVAG DRADGUETRNAVAG DRADGUETRNAVAG DRADGUE	RAVRVTLRIVYRKINGTMFNWELSLTPIHGHDG ILTHYAGVÄHDVTEAVI ESVHVVLRIVYRKOGSLFNWIELFISPVPDERG DITHYIGILINDITARKI ESVHVVLRIVYRKOGSLFNWIELFISPVPDERG DITHYIGILINDITARKI -EDCHVVLRIVYRKOGSLFNWIELFISPVPDALG ELAHYIGILYDTIELKI -EDCHVVLRIVYRKOGTFPNWIELTISPVPDAGG WYTHYVGIĀTDYTALKI -EDCHVVLRIVYRKOGAFINBELTLVPLLDAED SLVFYMGVSRDATREAI -EACTVLMRIVYRKOGAFINBELTLVPLLDAED SLVFYMGVSRDATREAI -EACTVLMRIVYRKOGAFINBELTLVPLLDAED QLTHYMAVLSDQTERHI -RSTTYLRIVYHKOGTLFYNBELSLSPVHDASG TLTHYLGFLINDYTAREI -RSTTYLLRIVYRKOGSPPNWIELTLYPUHDGG RI THFIGTSDDYTFRRI -KSTRALLRIVYRKOGELFNWIELTLAPVHDERG VYTHFIGTIEDVSERLI -EKVEGVLRIVYRKOGSPRWIELTLYPVHDGGG KLTHFIGTSDDVSRENI -EKVEGVLRIVYRKOGSPPNWIELTLYPVHDGGG KLTHFIGTSDDVSRENI -RECTVLLRIMRROGSFYNIELTLAPVHDERG HTVYOTSQLQVSERVI -RPCTVLLRIMRROFFYNIELTLAPVATDAAG HTVYOTSQLQVSERVI -RPCTVLLRIMRROFFYNIELTLAPVATDAAG HTVYOTSQLQVSTEVI -RPCSVSTURIVRROGSPFNWIELTLAPVRSESG DLTHFIGVETDVTERTI -RPCSVSTURIVRROGSFPNWIELSLAPVROEGG ALTHVOLHDVTEOTI -RPCSVSTURIVRROGSFPNWIELSLAPVROEGG ALTHVOLHDVTEOTI -RPCSVSTURIVRROGSFPNWIELSLAPVROEGG ALTHVOLHDVTEOTI -RPCSVSTURIVRROGSFPNWIELSLAPVROEGG ALTHVOLHDVTEOTI -RPCSVSTURIVRROGSFPNWIELSLAPVROEGG ALTHVOLHDVTEOTI -RPCSVSTURIVRROGSFPNWIELSLAPVROEGG ALTHVOLHDVTEOTI -RPCSVSTURIVRROGSFPNWIELSLAPVROEGG ALTHVOLHDVSSARH -HSGQAVVRIVYRKOGSPPNWIELSLAPVROEGG SHFVGLHDVTONSAHHSGQAVVRIVYRKOGSPPNWIEVVLAPMRDELG SHFVGLHDVTONSAHHSGQAVVRIVYRKOGAPPNWIEVSLAPWRDELG SHFVGLHDVTONSAHHSGQAVVRIVYRKOGAPPNWIEVSLAPWRDELG SHFVGLHDVTONVI -EPCQAVLRIVRROGAFRIMESLSLSPNRDAEG CLSHTVGLABOTTTNV -KYCKVLIRIVRKOGAFRIMELSLSPNRDAEG CLSHTVGLABOTTRIV	G 327 N 272 R 175 Q 149 Q 162 L 130 Q 162 L 130 Q 163 A 132 A 527 A 638 S 527 A 620 A 363 A 430 A 430 A 672 M 97 L 322 L 302 L 302 L 303 L 302 L 303 L 302 L 303 L 303 L 304 G 304 G 304 G 304 G 305 G 306 G
WP_132137257.1 WP_093555924.1 PKL98247.1 WP_126799631.1 TXH46092.1 WP_161883475.1 TAN70402.1 WP_051906796.1 WP_15218592.1 0YY92272.1 WP_112183883.1 TXC65962.1 WP_140625868.1 WP_085751094.1 RME97112.1 0ZB44497.1 WP_158540843.1 WP_051846818.1 WP_051059592.1 WP_08157253.1 WP_081617253.1 WP_145246018.1	151 LQLSIRALAASLINGVLISDASQAS-FPIMYAN-PAFCRMTGYDLIEWMGRNCRFLQND 54 PQLSARALAASSINGVLIDAARQPS-CPIJYAN-PAFCRMTGYALDELLGRICGRLQGG 48 DALSINGLASCSINGWITADARAPD-MPIHYMN-PAFCAMTGYDLGELLGRINGRFLQGG 41 MRLLERAIENSHSAVLIADARQPD-FPAIYIN-HAFEGMTGYTVDECLGRNCRFLQGG 40 -ASMVGALDAMPVSVITADAKYAD-MPILYVIN-PAFEALTGYTSDEARGRNCRFLQGG 41 PQLLSQAIAACTVGVWTDARQHD-HPILYWN-PAFEALTGYTSDEARGRNCRFLQGG 406 IRI FRAVPASASSISMADAINCPD-MPILYWN-PAFEALSGYTADETLGHNCRFLQGG 410 IRI FRAVPASASSISMADAINCPD-MPILYWN-PAFEALTGYRASEEAVGRNCRFLQGG 517 LRLLGRAVAASSINGTITADVQNCD-MPILYWN-PAFEATTGYSRDEVLGRNCRFLQGG 518 LLCRAVEASTSGYUTADANQYD-MPILYWN-PAFEATTGYSRDEVLGRNCRFLQGG 519 LCLLGRAVEASTSGYUTADANQYD-MPILYWN-PAFEATTGYSRDEVLGRNCRFLQGG 510 DAALPIWADATQPD-LPLYVIN-PAFEATTGYSRDEVLGRNCRFLQGG 511 MDAAMPIWADATQPD-PHIYWN-PAFEATTGYARDEAVGRNCRFLQGG 512 LQMLKAATEASTGAPCVATQPD-LPLYVN-PAFEATTGYARDEAVGRNCRFLUNGD 513 DASLPITYTDATUPD-QPLYWN-PAFEATTGYARDEAVGRNCRFLUNGD 514 MYMKRGVEAAAALPMCVCDATQPD-LPLYVN-PAFEATTGYARDEAVGRNCRFLUNGD 515 LQMLKAATEASTGARGWCVADAQAPD-YPLYVNI-PAFEATTGYARDEAVGRNCRFLUNGG 516 LQMLKAATEASTGARGWCVADAQAPD-YPLYVNI-PAFEATTGYTAAQALGRNCRFLQGG 517 LGMLKAATEASTGARGWCVADAQAPD-YPLYVNI-PAFTSTGYTAAQALGRNCRFLQGG 518 LQMLKAATEASTGARGWCVADAQAPD-YPLYVNI-PAFTSTGYTFAAQALGRNCRFLQGG 519 LHLKAATEASTGARGWCVADAQAPD-LPLYVNI-PAFTSTGYTFAAQALGRNCRFLQGG 510 LHLKAATEASTGARGWCVADAQAPD-LPLYVNI-PAFTSTGYTFAAQALGRNCRFLQGG 511 LALTGRATAGARGATGARGAD-LPLYVNI-PAFTSTGYTGAAGAGRNCRFLQGG 512 LATTGRATAGARGATGARGAD-LPLYVNI-PAFTSTGYGADAGRNCRFLQGG 513 LATTGRATAGARGATGARGAD-LPLYYNI-PAFTSTGYGADAGARGAGNCRFLQGG 514 LALTGRATAGARGAGADAGAD-LPLYYNI-PAFTSGYGADGADAGAGAGAGAGAGAGAGAGAGAGAGAGAGAGAG	- DRNQ	RAVRVTLRIVYRKINGTMFNWELSLTPIHGHDG ILTHYAGVAHDVTEAVI ESVHVVLRIVYRKOGSLFWIDLFLSPYPDERG DITHYTGILINDITARKI ESVHVVLRIVYRKOSSLFWIDLFLSPYPDERG DITHYTGILINDITARKI EDCHVVLRIVYRKOSSLFWIDLFLSPYPDALG VVTHYVGIATDVTALKI "QDAHVVVRIVYRKOGTFFNWIDLFLSPYPDALG VVTHYVGIATDVTALKI "EDCHVVLRIVYRKOGAFWILETLSPVRDAGG INTHYLGISTDITVEVI "EDCHVVLRIVYRKOGAFWILETLYPULDAED SLYFYMKYSYRATREAI "EACTVLIMRIVYRKOGAFWILELLSPVHDAGG TLTHYAGFLINDVTAREI "ERKGEVI VHINYRKOFAFWIDLFLABPVHDERG RI THFTGTSDVTFRRI "KGTRALLRIVYRKINGELFNWOLHTAPVHDERG QVTHFIGITEDVSERLI "ERKGEVI VHINYRKOFSPHWILELTPYPHDEGG RI THFTGTSDVTFRRI "KGTRALLRIVYRKOGSHPMIELTPYPHDEGG RI THFTGTSDVTFRRI "KGTRALLRIVRRKOSFPHWILENTPYPHDGGG RITHTGTSDVSERVI "ERKGEALLRIVYRKOSPHWILELTPYPHDGGG RITHTGTSDVSSRVI "ERCTVLLAINRRDGFPFINLELSVYPTRDARG HTVQYIGVLDDVTERVI "REASTVLLRIMRRKOGSFPHIMLAHPAPTRDAAG RIVTHTGVTTVTTERT "RESTVLRIMRRKOGAFTNEHLHAPTRDAAG RIVTHTGVTTVTTERT "RECSVELRINYRADGGFPMILALSVPROFAG AVSHYGLTVTVTERT "RECSVELRINYRADGGPPMILASVSPVRIDAG VTHTFVGLHTDVTSARH "RSCSVELRINYRADGGPPMILSVSSPVRIDAG VTHTFVGLHTDVSARH "RSCSVELRINYRADGGPPMILSVSSPVRIDAG VTHTFVGLHTDVSARH "RSCSVELRINYRADGGPPMILSVSSPVRIDAG THTFVGLHTDVSARH "RSCSVELRINYRADGGPPMILSVSSPVRIDAG SHYNGLHTDVSARH "RSCSVELRINYRADGGPPMILSVSSPVRIDAG SHYNGLHTDVSARH "RSCSVELRINYRKOGSFSMILSVSSPVRIDAG SHYNGLHTDVSARH "RSCSVELRINYRKOGSFSMILSVSSPVRIDAG SHYNGLHTDVSARH "RSCSVELRINYRKOGSFSMILSVSSPVRIDAG SHYNGLHTDVSARH "RSCSVELRINYRKOGSFSMILSVSSPVRIDAG SHYNGLHTDVSARH "RSCSVELRINYRKOGSFSMILSVSSPVRIDAG SHYNGLHTDVSARH "RSCSVELRINYRKOGSFSMILSSSPVRIDAG	G 327 N 272 R 175 Q 149 Q 162 L 130 Q 651 A 132 A 527 A 638 M 524 A 638 M 524 A 630 A 430 A 430 A 672 M 97 L 322 L 303 L 322 L 303 L 322 L 433 Q 434 A 585 H 381
WP_132137257.1 WP_093555924.1 PKL98247.1 WP_126799631.1 TXH46092.1 WP_161883475.1 TAN70407.1 WP_051906796.1 WP_125218592.1 0YY92272.1 WP_112183883.1 TXC65962.1 WP_085751094.1 RWE97112.1 WP_140625868.1 WP_085751094.1 WP_158540843.1 WP_051848818.1 WP_051846818.1 WP_051059502.1 WP_081617253.1 WP_01524648.1	151 LQLSIRALAASLINGVLISDASQAS-FPIMYAN-PAFCRMTGYDLIEWMGRNCRFLQND 54 PQLSARALAASSINGVLIDAARQPS-CPITYAN-PAFCRMTGYALDELLGRICGRLQGG 48 DALSINGLASCSINGWITADARAPD-MPIMYAN-PAFCAMTGYDLGELLGRINGRFLQGG 41 MRLLERAIENSHSAVLIADARQPD-FPAIYIN-HAFEGMTGYTVDECLGRINGRFLQGG 40 -ASMVGALDAMPVSVITADAKYAD-MPIMYTIN-PAFEALTGYTSDEARGRINGRFLQGG 51 PQLLSQAIAACTVGVWTDARQHD-HPIMYAN-PSFERLTGYMATEAMGRINGRFLQGG 406 IRI FRAMFASASTSMADAINCPD-MPIMYAN-PAFEALSGYTADETLGHINGRFLQGG 407 IRI FRAMFASASTSMADAINCPD-MPIMYAN-PAFEALTGYSRDEVI GRNCRFLQGG 517 LKLLGRAVAASNINGTITADVQNCD-MPLIMYN-PSFERITGFSREEAVGRINGRFLQGG 518 LLGRAVAASNINGTITADVQNCD-MPLIMYN-PSFERITGFSREEAVGRINGRFLQGG 519 LLGRAVAASNINGTITADVQNCD-MPLIMYN-PAFEALTGYSRDEVI GRNCRFLQGG 510 LDALPIWADATQPD-LPLYTIN-PAFEATTGYSRDEVI GRNCRFLQGG 511 LWARAMEASSYSMITADATAPD-LPLYTIN-PAFEATTGYSRDEVIGRINGRFLQGG 512 LQMLKAATEASTGATUMTDATUPD-CPLYWN-PAFERLTGYARDEAVGRINGRFLUGG 513 DASALPITYDTATUPD-OPLYWN-PAFERLTGYARDEAVGRINGRFLUGG 514 LWARGWEAAAALPMCVCDATQPD-LPLYVN-PAFERLTGYARDEAVGRINGRFLUGG 515 LYMKRGVEAAAALPMCVCDATQPD-LPLYVN-PAFERLTGYARDEAVGRINGRFLUGG 516 LQMLKAATEASGAGCVADAQAPD-YPLYVNI-PAFERTTGYTAAQALGRINGRFLQGG 517 LURLGAAMEATEVGSVYDAOSGG-YPLVYWI-PAFERTTGYTAAQALGRINGRFLQGG 518 LQMLKAATEASGAGCVADAQAPD-YPLYVWI-PAFTSRTGYTAAQALGRINGRFLQGG 519 LURLGAATEASGAGCVADAQAPD-PLPLYVN-PAFTSRTGYTAAQALGRINGRFLQGG 510 LHLKAATEASGAGCVADAQAPD-LPLTYVN-PAFTSRTGYGADEGGNIGGRINGRFLQGG 511 LATGRATDASFOXCTADARQPD-LPLTYVN-PAFTSRTGYGADGAGNIGGRINGRFLQGG 512 LTALTGAATGATATADARQPD-LPLTYVN-PAFTSRTGYGAAGCRINGRFLQGG 513 LATGRATAGAGGAGCAGAGAGADARD-MPLTYN-PAFFSRTGYGAAGEVLGRINGRFLQGG 514 LSTRTQAIEALQVGGATADARQPD-LATVYN-PAFTSRTGYGAAGEVLGRINGRFLQGG 515 LLGRINGATEAGSSGALTADARQPD-LATVYN-PAFTSRTGYGAAGEVLGRINGRFLQGG 516	- DRNQ PAVGLVRDAIAQE DREQ - PAVAAIRSAIDAR DREQ - AAVAVLRHAIARG DRDQ - PALAALRQAIAARA DRED - PELAVWRNALERN DRDQ - PELAVWRNALERN DRDQ - PGVQEIRQALVEQ FILD - PG LOTRAVIARG DRDQ - PGVQEIRQALVEQ FILD - PG LOTRAVIARG DRDQ - PGLTRAAIAG DRDQ - PGLTRAAIAG DRDQ - PGLTRAAIAG DRDQ - TGLQTIRAALERG FROQ - AGLVEIRAALERG FTAQ - PGLTRAAIAG DRDQ - PALDELRAAIRG DRDQ - PGLTRAAIRG DRDQ - PGLTTRAAIRG DRDQ - PG	RAVRVTLRIVYRKINGTMFNWELSLTPIHGHDG ILTHYAGVÄHDVTEAVI ESVHVVLRIVYRKOGSLFNWELFISPVPDERG DITHYIGILINDITARKI ESVHVVLRIVYRKOGSLFNWELFISPVPDERG DITHYIGILINDITARKI EDCHVVLRIVYRKOGSLFNWELFISPVPDERG ELAHYIGILYTDITELKI QDAHVVVRINYRKOGFPFNWELFISPVPDALG VYTHYVGIATDYTALKI EDCHVVLRIVYRKOGFFNWELTLSPVRDAGG HVTHYLGISTDITVEVL ESCHVVLRIVYRKOGFFNWELTLSPURDAGG BLYFTYMGVSRDATREAI EACTVLMRIVYRKOGGAFINELHLTPVRDAED QLTHYMAVLSDOTERHI ERSTYLTRIVYHKOGTLFYNELSLSPVHDASG TLTHYLGFLINDVTAREI RRSTYLVRIVYRKOGSPRWELTLYPURDAGG RVTHFIGTSDDVTFRRI EKVEGVLRIVYRKOGSPRWELTLYPVHDGGG RVTHFIGTSDDVTFRRI EKVEGVLRIVYRKOGSPRWELTLYPVHDGGG RVTHFIGTSDVSPRIH EKVEGVLRIVYRKOGSPRWELTYPVHDGGG RVTHFIGTSDVSPRIH EKCTALLRIVYRKOGSPRWELTYPVHDGGG RVTHFIGTSDVSPRIH ERCTVLLRIRARROFFYPHELHVAPYDAAG RVTHFIGVDVSFRIV RRCTVLLRIRARROFFYPHELHVAPYDAAG RVTHFIGVHTOVTERTI RRCSVVINIVRKOGSPRWILLSVPVRDAGG RVTHFIGVHTOVTERTI RRCSVVINIVRKOGSFFNWELHVAPVRSESG DLTHFIGVETDVTREVI RRCSVVELRIVRADGSPFNWELSLAPVRDEGG AVSHFVGLITDVTERM RSCSVELRIVRADGSPRWIALSLAPVRDETG AVSHFVGLITDVTERM RSCSVELRIVRADGSPRWIALSLAPVRDETG AVSHFVGLITDVTERM RSCSVELRIVRADGSPRWIALSLAPVRDETG AVSHFVGLITDVTSRMH -RSCSVELRIVRADGSPRWIALSLAPVRDETG STHFVGLHNDVSARH -HSGQAVVRIVYRKOGSPRWIALSLAPVRDEGG SIHFVGLHNDVSARH -HSGQAVVRIVYRKOGSPRWIALSLAPVRDEGG SIHFVGLHDVSARH -HSGQAVVRIVYRKOGSPRWIALSLAPVRDEGG SIHFVGLHDVSARH -HSGQAVVRIVYRKOGAPRWIELSLSPPRDAGG GLSHTIGVATDVTDRV -EPCQAVLRIVRROGALFWIELSLSPPRDAGG GLSHTIGVATDVTDRV -EPCCAVLRIVRROGALFWIELSLSPPRDAGG GLSHTIGVATDVTDRV -EPCCAVLRIVRROGAFRWIGLTLAPVRDAGG GLSHTIGVATDVTDRV -EPCCAVLRIVRROGAFRWIGLTLAPVRDAGG GLSHTIGVTOTTDRV -EPCCAVLRIVRROGAFRWIGLTLAPVRDAGG GLSHTIGVTOTTDRV -EPCCAVLRIVRROGAFRWIGLTLAPVRDAGG GLSHTIGVTOTTDRV -EPCCAVLRIVRROGAFRWIGLTLAPVRDAGG GLSHTIGVTOTTDRV -EPCCAVLRIVRROGAFRWIGLTSPRIVGG GLSHTIGVGTOTTDRV -EPCCAVLRIVRROGAFRWIGLTSPRIVGG GLSHTIGVGTOTTDRV -EPCCAVLRIVRROGAFRWIGLTSPRIVGG GLSHTIGVGTOTTDRV -EPCCAVLRIVRROGAFRWIGLTSPRIVGG GLSHTIGVGTOTTDRV -EPCCAV	G 327 N 272 R 175 Q 149 Q 162 L 162 L 163 A 132 A 577 A 638 A 430 A 630 A 363 A 430 A 572
WP_132137257.1 WP_093555924.1 PKL98247.1 WP_126799631.1 TXH46092.1 WP_161883475.1 TAN76407.1 WP_051906796.1 WP_125218592.1 0YY92272.1 WP_112183883.1 TXC65962.1 WP_085751094.1 RWE97112.1 WP_158540843.1 WP_051848818.1 WP_051846818.1 WP_051846818.1 WP_051846818.1 UP_061817253.1 WP_07436481.1 WP_07436481.1 UP_07436481.1 UP_151846018.1 UP_15184618.1 UP_15184618.1 UP_15184618.1	151 LQLSIRALAASLINGVLISDASQAS-FPIMYAN-PAFCRMTGYDLIEWMGRNCRFLQND 54 PQLSARALAASSINGVLIDAARQPS-CPILYVAN-PAFCRMTGYALDELLGRICGR-LQGG 48 DALSINGLASCSINGWITADAAAPD-MPIWYNN-PAFCRMTGYDLGELLGRINGGR-LQGG 41 MRLLERAIENSHSAVLIADARQPD-FPAIYIN-HAFEGMTGYTVDECLGRINCRFLQGD 40 -ASHWGALDAMPSVITIADAKYAD-MPILYVIN-PAFEALTGYTSDEARGRINCRFLQGD 41 PQLLSQATAACTVGVWTDARQHD-HPILYVNI-PAFEALTGYTSDEARGRINCRFLQGD 436 IRLIFRAVEASASSISMADAINCPD-MPILYVNI-PAFEALTGYTADEALGHINCRFLQGG 446 IRLIFRAVEASASSISMADAINCPD-MPILYVNI-PAFEALTGYTASEEAVGRINCRFLQGG 557 LRLLCRAVAASINGITIADVQNCD-MPILYVNI-PAFEATTGYSRDEVIGRINCRFLQGG 568	- DRNQ - PAVGLVRDAIAQE DREQ - PAVAAIRSAIDAR DREQ - AAVAVLRHAIARG DRQ - PALAALRQAIAARG DRDQ - PALAALRQAIAARG DREQ - PETAVWRNALERN DRDQ - PGSERWRDALAKG DRDQ - PGVQEIRQALVEQ FILD - PGI DGTRAVI REG DRDQ - PGLTERAAIAAG EADQ - TGLQTLRAALARG FTAQ - PGLTRLRAIAAG DTGQ - PALAEVRAALRG ERDQ - PALAEVRAALRG ERDQ - PALAEVRAALRG DRQ - LELQPLRAALRG DRQ - LELQPLRAALRG DRQ - LELQPLRAALRG DRQ - DRQ - DRQ DRQ - PGLTRLRAIAGR DRQ - PGLTRLRAIAG DRQ - PGLTRAIACHG PGLTTAIACHG PGLTTAIACHG PGLTTAIACHG	RAVRVTLRIVYRKINGTMFNWELSLTPJHGHDG ILTHYAGVÄHDVTEAVI ESVHVVLRIVYRKOGSLFNWIELFISPVPDERG DITHYIGILINDITARKI ESVHVVLRIVYRKOGSLFNWIELFISPVPDERG DITHYIGILINDITARKI QDAHVVVRINYRKOGSLFNWIELFISPVPDENG ELAHYIGILYDITELKI QDAHVVVRINYRKOGTFPNWIELTISPVPDALG VYTHYVGJATDVTALKI EDCHVVLRIVYRKOGTFPNWIELTLVPLLDAED SLVFYYMGVSRDATREAI EACTVLMRIVYRKOGGAFLWELHLTPVRDAED SLVFYYMGVSRDATREAI EACTVLMRIVYRKOGAFLWELHLTPVRDAED QLTHYMAVLSOQTERHI RSTTVTLRIVYHKOGTLFYWELSLSPVHDASG TLTHYLGFLINDVTAREI RRIVERU VHINVRKOGTPRWIDL RTAPVHDERG RI THFIGTSDDVTFRRI EKSTRALLRIVYRKOELFNWIDL HAPPHDERG OVTHFIGTIEDVSERLI EKVEGVLRIVYRKOGSPRWIELTVTPVHDGGG KLTHFIGTSDDVSTRRI EACTVLLRINRROGSFFWIELTVTPVHDGGG KLTHFIGTSDDVSTRRI RPCFLVLRINRROGSFFWIELTVTPVHDGGG KLTHFIGTSDDVSTRRI RPCTVVLLRINRROGSFFNIELLVAPTIDAAG HVVQHLCVLHDVTERVI RRSCSVELRIVRAROGSFFNIELSVYPTRDARG HVVQHLCVLHDVTERVI RRSCSVELRIVRADGSFFWIELSVYPTRDAGG SLHFIGVLHDVTERVI RSCSVELRIVRADGSFFWIELSVPPROBAGG ALTHVOLHDVTETVI RSCSVELRIVRADGSFFWIELSLPVROBEGG ALTHVOLHDVTEATVI RSCSVELRIVRADGSFFWIELSLPVROBEGG ALTHVOLHDVTEATVI RSCSVELRIVRADGSFFWIELSLPVROBEGG ALTHVOLHDVTEATVI RSCSVELRIVRADGSFFWIELSLPVROBEGG ALTHVOLHDVSARHI HSGQAVVRIVYRKOGSFFWIELSLPVROBEGG SHFVGLLTDVTERHI HSGCAVVRIVYRKOGSFFWIELSLSPVROBGG SHFVGLLTDVTGRIV EPCQAVLRIVYRKOGSFFWIELSLSPVROBGG SHFVGLLTDVTORVI EPCQAVLRIVYRKOGSLFWIELSLSPVROBGG SHF	G 327 N 272
WP_132137257.1 WP_093555924.1 PKL98247.1 WP_126799631.1 TXH46092.1 WP_161883475.1 TAN70402.1 WP_051906796.1 WP_125218592.1 OYY92272.1 WP_112183883.1 TXC65962.1 WP_085751094.1 RWE97112.1 02844497.1 WP_168540843.1 WP_05184818.1 WP_09510959502.1 WP_081617253.1 WP_145246618.1 00U47901.1 0YY45411.1 MAU11331.1 WP_121277549.1 WP_162909382.1	151 LQLSIRALAASLINGVLISDASQAS-FPIMYAN-PAFCRMTGYDLIEWMGRICRFLQND 54 PQLSARALAASSINGVLIDAARQPS-PPIMYAN-PAFCRMTGYALDELLGRICRFLQGG 48 DALSINGLASCSINGVILDAARQPS-PETVYAN-PAFCRMTGYALDELLGRICRFLQGG 41 MRLLERAIENSHSAVLIADARQPD-FPAIYIN-HAFEGMTGYTVDECLGRICRFLQGD 53 — — EASLPILICOARQAD-MPITYYIN-PAFEALTGYTSDEARGRICRFLQGG 54 PQLLSQALAACTVGVWMTDARQHD-HPIVYWI-PAFEALTGYTSDEARGRICRFLQGG 55 — — EASLPILICOARQAD-MPITYWI-PAFEALTGYTSDEARGRICRFLQGG 66 IRI FRAVFASASSTSMADAINCPD-MPITYWI-PAFEALTGYTSGNEVI GRICRFLQGG 67 PQLLSQALAACTVGVWMTDARQHD-HPIVYWI-PAFEALTGYTSGNEVI GRICRFLQGG 68 IRI FRAVFASASSTSMADAINCPD-HPITYWI-PAFEATTGYSREEVI GRICRFLQGG 69 TLXLLERAVEASTSGIVIADANQYD-MPLIFTIN-KAFERITGYSREELIGKNCRFLINGN 60 DAALPIVADATOPD-LPITYWI-PAFEATTGYFASAEVLGRICRFLQGG 60 DAALPIVADATOPD-LPITYWI-PAFEATTGYFOASAEVLGRICRFLQGG 61 DAAMPIVATDSTQPD-RPIVYWI-PAFEATSGYFROEVIGHNCRFLINGD 62 DAALPIVADATOPD-LPITYWI-PAFEATSGYFROEVIGHNCRFLINGD 63 DAALPIVADATOPD-LPITYWI-PAFEATSGYFROEVIGHNCRFLINGD 64 DAALPIVADATOPD-LPITYWI-PAFEATSGYFROEVIGHNCRFLINGG 65 DAALPIVADAAALPFU-YWI-PAFEATSGYFROEVIGHNCRFLINGG 66 DAALPIVADAARAD-PPU-YWI-PAFEATSGYFROEVIGHNCRFLQGG 67 LHILKAAITEATDWGYTVADARARD-FPU-YWI-PAFEATSGYFROEVIGHNCRFLQGG 68 LRICKAATEATDWGYTVADARARD-FPU-YWI-PAFEATSGYFROEVIGHNCRFLQGG 68 LRICKAATEASEAGMCADAQPD-PU-YWI-PAFEATSGYFROEVIGHNCRFLQGG 69 LHILKAAITEASEAGMCADAQPD-PU-YWI-PAFEATSGYFROEVIGHNCRFLQGG 60 LHILKAAITEASEAGMCADAQPD-PU-YWI-PAFEATSGYFROEVIGHNCRFLQGG 61 LARIKAAMEASPLOVTTADARQAD-PU-YWIN-PAFEATSGYFROEVIGHNGRFLQGG 61 LARIKAAMEASPLOVTTADARQAD-PU-YWIN-PAFEATSGYFROEVIGHNGRFLQGG 62 LTGSSAMESSIGGILTADARQPD-LPLYVNI-PAFEATSGYFROEVIGHNGRFLQGG 63 LARIKAATSGASGASGASD-TPLYWI-PAFEATSGYFROEVIGHNGRFLQGG 64 LTRATEATSGASGASGASGASGASGASGASGASGASGASGASGASGAS	- DRNQ - PAYGLVRDAIAQE DREQ - PAYAAIRSAIDAR DREQ - AAVAVE,HAILARG DODQ - PALAALRQAIAAR DREO - PETAYWRNALERN DREO - PETAYWRNALERN DRDQ - PGETRYRNALHAG DRDQ - PGSEMPROALAKG DRDQ - PGUSETROALVEQ ELDQ - PGLDGTRAVI REG DRDQ - PGLTELRAAIAAG DRRO - PGLTELRAAIAAG EQDQ - AGLVEIRAALAEA EADQ - TGLQTLRAALRKG TREQ - PGLPELRAALAEA TREQ - PGLPELRAALAEA TREQ - PGLPELRAALAEA TREQ - PGLEEIRNAIASK EPPQ - ASMEEVRAALREG PGLDQ - AGLDEVRAALREG ERDQ - PALDELRAALREG ERDQ - PALDELRAALREG ERDQ - DRAQUENRAALREG DRAQ - LELQPLRAALREG DRHQ - DRHQ - SELHGRAALARG DRHQ -	RAVRVTLRIVYRKINGTMFNWELSLTPIHGHDG ILTHYAGVÄHDVTEAVI ESVHVVLRIVYRKOGSLFNWELFISPVPDERG DITHYTGILINDITARKI ESVHVVLRIVYRKOGSLFNWELFISPVPDERG LELAHYIGITYDTTELKI EDAHVVLRIVYRKOSLFNWELFISPVPDHAG ELAHYIGITYDTTELKI -QDAHVVVRIVYRKOGTFPNWELFISPVPDHAG VVTHYVGIÄTDVTALKI -QDAHVVVRIVYRKOGTFPNWELFISPVPDHAG VVTHYVGIÄTDVTALKI -EDCHVVLRIVYRKOGAFNWELTISPVRDAGG NEVTHYLGISTDITTEVE -EACTVUPRIVYRKOGAFNWELTISPVRDAGG LITHYMAVISDOTERHI -EACTVUPRIVYRKOGAFNWELTISPVRDAGG TLITHYLGFLINDVTAREI -EACTVUPRIVYRKOGTFPNWELSISPVHDAGG TLITHYLGFLINDVTAREI -ERVGEVI VHINYRKOGTFPNWELSISPVHDAGG TLITHYLGFLINDVTAREI -KGTRALLRIVYRKOGSPRWELETAPVHDERG TLITHIGTSDDVTERNI -ERVGEVI VHINYRKOGSPRWELETAPVHDERG TLITHIGTSDVSERVI -ERCYVLLRIVYRKOGSPRWELETAPVHDERG HTVQVICUQUDSERVI -EACTVLLRIVRRROGSFPRWELLTYPVHDGGG KLTHFIGTSDVSGRUF -EACTVLLRIVRRROGSFPRHELIVTPVHDGGG HVTQVICUQUDSERVI -RECTVLLRIVRROGSFPRHELIVTPVHDAGG HVTQVICUQUDSERVI -RECSVITINIVRROGSFPRHELHVAPTVDAAG HVTQVICUQUDSERVI -RECSVITINIVRROGSFPRHELHVAPTVDAAG HVTQVICUQUDSERVI -RECSVITINIVRROGSFPRHELHVAPTVBAGG SATIHGVHIDVTERTI -RECSVITINIVRROGSFPRHALSLAPVREDEG AVSHFVGLITDVTERNI -RECSVILRIVRROGSFPRHALSLAPVREDEG AVSHFVGLITDVTERNI -RECSVILRIVRROGSFPRHEVLAPPREDGG SATIHFVGLHIDVSARHI -RSCSVELRIVRROGSFPRHEVLAPPREDGG SATIHFVGLHIDVSARHI -RSCSVELRIVRROGSFPRHEVLAPPREDGG SHTPVGLHIDVSARHI -RSCSVELRIVRROGSFPRHEVLAPPREDGG - SHTPVGLHIDVSARHI -RSCSVELRIVRROGSFPRHEVLAPPREDGG - SHTPVGLHIDVSTENTIRECVSALLRIVRROGSLAPHWELSSSPPREDGG - SHTPVGLHIDVSTENTIRECVSALLRIVRROGSLAPHWELSSSPPREDGG - STHTPVGLHIDVSTENTIREVSALLRIVRROGSLAPHWELSSSPPREDGG - HTTHTVGVILDVTENTIREVSALLRIVRROGSLAPHWELSSSPPREDGG - HTTHTVGVILDVTENTI	G 327 N 272
WP_132137257.1 WP_093555924.1 PKL98247.1 WP_126799631.1 TXH46092.1 WP_161883475.1 TAN70402.1 WP_051906796.1 WP_125218592.1 WP_112183883.1 TXC65962.1 WP_140625868.1 WP_085751094.1 RME97112.1 0ZB44497.1 WP_1518540843.1 WP_051848818.1 WP_051848818.1 WP_051848818.1 WP_051848818.1 WP_051848818.1 WP_051848818.1 WP_051859592.1 WP_145246018.1 0DU47901.1 MAU11331.1 WP_1212777549.1 WP_162090382.1 WP_162090382.1 WP_162090382.1	151 LQLSIRALAASLINGVLISDASQAS-FPIMYAN-PAFCRMTGYDLIEWMGRNCRFLQND 54 PQLSARALAASSINGVLIDAARQPS-PEIDYVAN-PAFCRMTGYALDELLGRICGREQGG 41 MRLLERAIENSHSAVLIADARQPD-FPAIYIN-HAFEGMTGYTVDECLGRICGREQGGGGGGGGGGGGGGGGGGGGGGGGGGGGGGGGGGG	- DRNQ - PAYGLVRDATAQE DREQ - PAVAAIRSATDAR DREQ - AAVAVE,HATLARG DODO - PALAALRQATAAR DREO - PETAYWRNALERN DRAO - PESENRNDALAKG DRAO - PGVQETRQALVEG ELDO - PG LOGTRQALVEG ELDO - PG LOGTRAVI REG DRAO - PGLERAATAAG DRHQ - PGLDHYRSALSKG EDDO - AGLVETRAALAKG EDDO - AGLVETRAALAKG TREO - PGLDHYRSALSKG EDDO - AGLVETRAALAKG TREO - PGLPELRAALAGG YRRO - AALDELRHALAEG YRRO - AALDELRHALAEG FTAQ - PGLTELRAALAKG FTAQ - PGLEERNATASK EPPO - ASWEEVRAALREG ERDQ - PALAEVRAALREG ERDQ - PALAEVRAALREG DRAO - LELQPLRAALRAG DRHO - SELHGLRAALARG DRHO - SELHGLRAALARG DRHO - DARQQTRNAVQKG DROO - EALRTVRETLAKG DRRO - BALRTVRETLAKG DRRO - PGLETIRAFRAFRO DRRO - GELVATREGLARN DRRO - EGLVATREGLARN DRRO - EGLVATREGLARN DROO - EGLVATREGLARN-	RAVRVTLRIVYRKNGTMFNWELSLTPIHGHDG ILTHYAGVÄHDVTEAVI ESVHVUVRIVYRKOGSLFNWILELTSPYPOERG DITHYIGILINDITARKI ESVHVUVRIVYRKOGSLFNWILELTSPYPOERG ELAHYIGITVOITELK -QDAHVUVRIVYRKOGSLFNWILETSPYPOERG ELAHYIGITVOITELK -QDAHVUVRIVYRKOGSLFNWILETSPYPODALG VYTHYVGIÄTDVTALKI -QDAHVUVRIVYRKOGTFPNWILETSPYPODALG VYTHYVGIÄTDVTALKI -EDCHVUVRIVYRKOGTFPNWILETLVPLLDAED SLVFYWGVSRDATREAI -EACTVULPRIVYRKOGGAFINELHLTPVRDAED GLTHTWAVLSDOTERHI -EACTVULPRIVYRKOGTFPNWILSLSSPYHDASG TLTHYLGFLINDVTAREI -RSTTYTLRIVYHKOGTFPNWILSLSSPYHDASG TLTHYLGFLINDVTAREI -RSTTYTLRIVYRKOGSPPNWILLTAPVHDERG NLTHFIGTSDDVTFRRI -EKYGEVI VNIVYRKOGSPRWILLTAPVHDERG WYTHFIGTIEDVSERLI -EKVEGVLRIVYRKOGSPRWILLTAPVHDERG NLTHFIGTSDUVSERVI -RECTALLRINYRKOGSPRWILLTYPYHDGGG KLTHFIGTSDUVSGRVI -RPCTVVLAINRRROGSFFLINELSVYPIRDARG HVVQHLGVLHDVTERVI -RASTVLLRIVARKOGSAFNWILLTAPVRDAAG RVTHFIGVHTDVTERVI -RRSCSVELRIVRADGSPFNWILSLSSPVPIRDARG HVVQHLGVLHDVTERVI -RPCSVSVLNIVRKOGSPPNWILSLSSPVPIRDAGG ALTHYVGLHUDVSTEVI -RPCSVSVLNIVRKOGSPFNWILSLSSPVPIRDAGG ALTHYVGLHUDVSARHI -RSCSVELRIVRADGSPFNWILSLSSPVPIRDAGG ALTHYVGLHUDVSARHI -RSCSVELRIVRADGSPFNWILSLSSPVPIRDAGG ALTHYVGLHUDVSARHI -RSCSVELRIVRADGSPFNWILSLSSPVPIRDAGG TISHFVGLHTDVTREVI -RPCSVSVLNIVRKOGSFFNWILSLSSPVPIRDAGG SISHFVGLHTDVTREVI -RPCSVSVLNIVRKOGSFFNWILSLSSPVPIRDAGG SISHFVGLHTDVTREVI -RPCSVSVLNIVRKOGSFFNWILSLSSPVPRIDAGG SISHFVGLHTDVTREVI -RPCSVSVLNIVRKOGSLFNWILSLSSPVRIDAGG SISHFVGLHTDVTREVI -RPCVSVLNIVRKOGSLFNWILSLSSPVRIDAGG SISHFVGLHTDVTREVI -RPCVSVLNIVRKOGSLFNWILSLSSPVRIDAGG SISHFVGLHTDVSARHI -RSCTVLTRIVYRKOGALFNWILSLSSPVRIDAGG SITHYTGVGNDVTERTI -RECVSVLNIVRKOGALFNWILSLSSPVRIDAGG SITHYTGVGNDVTENTI -RECVSVLNIVRKOGALFNWILSLSSPVRIDAGG SITHYTGVGNDVTENTI -RECVSALLRIVYRKOGALFNWILSLSSPVRIDAGG SITHYTGVGNDVTENTI -REVSALLRIVYRKOGALFNWILSLSSPVRIDAGG HTTHHTAVVSINOVTEUT -REVSALLRIVYRKOGALFNWILSLTAPVPDAGG SITHYTGVCNDVTENTIREVSALLRIVYRKOGALFNWILSLTAPVPDAGG SITHYTGVCNDVTENTIREVSALLRIVYRKOGALFNWILSLSSPVRIDAGG SITHYTGVCNDVTENTIREVSALLRIVYRKOGALFNWILSTAPVPDAGG SITHYTGVCNDVTENTIREVSALLRIVYRKOGALFNWILSTAPVPDAGG SITHYTGVCNDVTENTI	G 327 N 272
WP_132137257.1 WP_093555924.1 PKL98247.1 WP_126799631.1 TXH46092.1 WP_161883475.1 TAN76407.1 WP_051906796.1 WP_125218592.1 0YY92727.1 WP_112183883.1 TXC65962.1 WP_160625868.1 WP_085751094.1 RME97112.1 WP_158540843.1 WP_051848818.1 WP_051846818.1 WP_051846818.1 WP_051846818.1 UP_061817253.1 WP_0418411.1 WP_151854018.1 ODU47901.1 OYY45411.1 WP_121277549.1 WP_121277549.1 WP_1212083303.1 WP_121283303.3	151 LQLSIRALAASLINGVLISDASQAS-FPIMYAN-PAFCRMTGYDLIEWMGRNCRFLQND 54 PQLSARALAASSINGVLIDAARQPS-PPIMYAN-PAFCRMTGYALDELLGRICGR-LQGG 48 DALSINGLASCSINGWITADAAAPD-MPIMYAN-PAFCAMTGYDLGELLGRINGGR-LQGG 41 MRLLERAIENSHSAVLIADARQPD-FPAIYIN-HAFEGMTGYTVDECLGRINCRFLQGD 43 -ASHWGALDAMPYSVITADAKYAD-MPIMYTIN-PAFEALTGYTSDEARGRINCRFLQGD 45 -EASLPILICDARQAD-MPIMYAN-PSFERLTGYMATEAMGRNCRFLQGD 46 IRI FRAMFASASTSMADAINCPD-MPIMYAN-PAFEALTGYTADEAUGNICHFLQGD 47 - LRLQRAMAASINGTITADVQNCD-MPLITYM-PAFEALTGYTASDETLGHINCRFLQGG 57 - LRLLGRAWAASINGTITADVQNCD-MPLITYM-PAFEATTGYSRDETLGRINCRFLQGG 58 - LOAAMPIMYADATQPD-LPLYTIN-PAFEATTGYSRDETLGRINCRFLQGG 59 - DAAMPIMYDTSTQPD-PRIMYM-AAFEALTGYARDEAWGRNCRFLQGG 50 - DAAMPIMYDTSTQPD-PRIMYM-PAFEATTGYARDEAWGRNCRFLQGD 51 - DAAMPIMYDTSTQPD-RPIMYM-PAFEATTGYARDEAWGRNCRFLUDGD 521 - DAAMPIMYDTSTQPD-PRIMYM-PAFEATTGYARDEAWGRNCRFLUDGD 551 MYMKRGWEANAALPMCVCDATQPD-LPLYVM-PAFEATTGYARDEAWGRNCRFLUDGD 551 MYMKRGWEANAALPMCVCDATQPD-LPLYVM-PAFEATTGYARDEAWGRNCRFLUDGD 61 LQMLKAAIEASEAGMCVADAQAPD-YPLYVM-PAFEATTGYARDEAWGRNCRFLQGG 61 LQMLKAAIEASEAGMCVADAQAPD-YPLYVM-PAFEATTGYARDEAWGRNCRFLQGG 61 LGMLKAAIEASEAGMCVADAQAPD-YPLYVM-PAFEATTGYGTAAQALGRNCRFLQGG 61 LALTGRATDASFNOVLTADARQAD-LPLYVCN-PAFEATTGYTSRDEAWGRNCRFLQGG 61 LALTGRATDASFNOVLTADARQAD-LPLYVCN-PAFEATTGYTSRDEAWGRNCRFLQGG 61 LALTGRATDASFNOVLTADARQAD-LPLYVCN-PAFEATTGYTSRDEAWGRNCRFLQGG 61 LALTGRATDASFNOVLTADARQAD-LPLYVCN-PAFEATTGYTSRDEAWGRNCRFLQGG 61 LALTGRATDASTNOVLTADARQAD-LPLYVCN-PAFEATTGYTSRDEAWGRNCRFLQGG 62 AFESSKSGMLIADARSAD-LATVYM-PAFARTTGYGNAEFUGGNICRFLQGG 63 AFESSKSGMLIADARSAD-LATVYM-PAFARTTGYGNAEFUGGNICRFLQGG 64 LATGRATDASVIATATDARQAD-LPLYVN-PAFARTTGYGNAEFUGGNICRFLQGG 65 AFESSKSGMLIADARSAD-LATVYM-PAFARTTGYGNAEFUGGNICRFLQGG 66 AFESSKSGMLIADARSAD-LATVYM-PAFARTTGYGNAEFUGGNICRFLQGG 67 LLTRIGATGASPGSTATDARAPD-MPLTYM-PAFARTTGYGNAEFUGGNICRFLQGG 68 LRQGRALDASVINATUTHQWING-DUTYYAN-PAFARTTGYGTHEVIGKORGRCGGCRCRQD 68 LRQGRALDASVINATUTHQWING-DUTYYAN-PAFARTTGYGTHEVIGKORGRCGRCGRD 68 LRQGRALDASVINATUTHQWING-DUTYYAN-PAFARTTGYGTHEVIGKORGRCGRCGRD 68 LRQGRALDASVINATUTHQWING-DUTYYAN-PAFAR	- DRNQ - PAYGLVRDATAQE DREC - PAYAAIRSATDAR DREC - PAYAAIRSATDAR DREC - PAYAAIRSATDAR DREC - PETAYMRIALERA DREC - PETAYMRIALERA DREC - PETAYMRIALERA DREC - PETAYMRIALERA DRDQ - PGSERMRDALAKG DRDQ - PGSERMRDALAKG DRDQ - PGLTGRAV REG DRDQ - PGLTGRAV REG DRDQ - PGLDHYRSAL KSG DRDQ - PGLDHYRSAL KSG ECODO - AGLVEIRAALAEA EADQ - TGLDHYRSAL KSG TREC - PGLPEIRAALAEA FTAQ - PGLTEIRAALAEA FTAQ - PGLTEIRAALAEA FTAQ - PGLTEIRAALAEA FTAQ - PGLTEIRAALAEA FTAQ - PGLEIRNATASK EPPQ - ASMEEVRAALREG ERDQ - PALAEVRAALREG DRAQ - LELQPLRAALREG DRAQ - LELQPLRAALREG DRAQ - PGLEIRAAVRAG DRAQ - PGLEIRAAVRAG DRAQ - PGLEIRAAVRAG DRAQ - PGLEIRAAVRAG DRAQ - PGLEIRAAFGG DRAQ - PGLEIRAAFGA DRAQ - PGLEIRAAFGA DRAQ - PGLIVLROALOTN DRAQ - EGLYLLROALOTN DRAQ - EGLYLLROALOTN-	RAVRVTLRIVYRKINGTMFNWELSLTPIHGHDG ILTHYAGVAHDVTEAVI ESVHVVLRIVYRKOGSLFWIDLFLSPYPDERG DITHYTGILINDITARKI ESVHVVLRIVYRKOSSLFWIDLFLSPYPDERG DITHYTGILINDITARKI EDCHVVLRIVYRKOSSLFWIDLFLSPYPDALG VVTHYVGIATDVTALKI QDAHVVVRIVYRKOGTFFNWIDLFLSPYPDALG VVTHYVGIATDVTALKI EDCHVVLRIVYRKOGTAPHIELTLYPULDAED SLYFMKYSYRSPATEAI EACTVLIWRIVYRKOGAFLINELHLTPVRDAED OLTHYMAVLSDQTERHI ERKTTVTLRIVYHKOGAFLWELHLTPVRDAED QLTHYMAVLSDQTERHI ERSTTVTLRIVYHKOGTLFWILELSPYHDAGG TLTHTGTSDVTFRRI KGTRALLRIVYRKINGELFWIQLHIAPVHDERG QVTHFIGITEDVSERLI EKVEGVU NINYRKOGSPHWIELTPYPHDEGG QVTHFIGITEDVSERLI EKVEGVU NINYRKOGSPHWIELTPYPHDGGG MLTHFIGISDVSFRIJ EKVEGVU NINYRKOGSPHWIELTPHPHDGGG MLTHFIGISDVSFRIJ EKCSTULLRIWRRDGFFFINLELSVYPIRDARG HTVQYIGVLQDVSERVI ERSTYLLRIWRKOGSFFNIELHAPPIRDAAG HTVQTIGVLDDVTERVI RESTYLLRIWRKOGSFFNIELHAPPIRDAAG AVSHFVGLITVTTERHI RESCSVELRIWRADGGFFMILGUSPWIDLSVFRIGGG AVSHFVGLITVTFEHH RSCSVELRIWRADGGFFWINLSVSPVRIDAG VLTHFVGLHTDVSARHI RSCSVELRIWRADGGFFWINLSVSPVRIDAG VLTHFVGLHTDVSARHI RSCGVELRIWRADGGPFWINEVLAPWROELG SHFVGLHTDVSARHI RSCGVELRIWRROGSFFWILLSVSPVRIDAG LTHFVGLHTDVSARHI EFCQAVLNIWRKOGALFWINEVLAPWROELG SHFVGLHTDVSARHI EFCQAVLNIWRKOGAFFWIELSLSPWRDAEG GLHFVGVATDVTDKY EFCCQAVLNIWRKOGAFFWIELSLSPWRDAEG GLHFVGVATDVTDKY EFCCAVLLRIWRKOGAFFWIELSLSPWRDAEG GLHFVGVATDVTDKY EFCCAVLLRIWRKOGAFFWIELSLSPWRDAEG GLHFVGVATDVTDKY EFCCAVLLRIWRKOGAFFWIELSLSPWRDAEG GLHFVGVATDVTDKY EFCCSVELRIWRKOGAFFWIELSLSPWRDAEG GLHFVGVATDVTDKY EFCSVALLRIWRKOGAFFWIELSLSPWRDAEG GLHFVGVATDVTDKY EFCSVALLRIWRKOGAFFWIELSLSPWRDAEG GLHFVGVATDVTDKY EFCSVALLRIWRKOGAFFWIELSLSPWRDAEG GLHFVGVATDVTDKY EFCSVALLRIWRKOGAFFWIELSLSPWRDAEG HTTHHVGVINDVTEUT ERCYSAVLRIWRKOGAFFWIELSLSPWRDAEG HTTHHVGVINDVTEUT ERCYSAVLRIWRKOGAFFWIELSLAPPVDADG HTTH	G 327 N 272
WP_132137257.1 WP_093555924.1 PKL98247.1 WP_126799631.1 TXH46092.1 WP_161883475.1 TAN70402.1 WP_051906796.1 WP_125218592.1 WP_112183883.1 TXC65962.1 WP_140625868.1 WP_085751094.1 RME97112.1 0ZB44497.1 WP_1518540843.1 WP_051848818.1 WP_051848818.1 WP_051848818.1 WP_051848818.1 WP_051848818.1 WP_051848818.1 WP_051859592.1 WP_145246018.1 0DU47901.1 MAU11331.1 WP_1212777549.1 WP_162090382.1 WP_162090382.1 WP_162090382.1	151 LQLSIRALAASLINGVLISDASQAS-FPIMYAN-PAFCRMTGYDLIEWIGRICRELQIGD 54 PQLSARALAASSINGVLIDAARQPS-PPIMYAN-PAFCRMTGYDLIEWIGRICRELQIGG 42 DALSIRKALSACSINGVILIDAARQPS-PETVYAN-PAFCRMTGYDLEGLIGRICRELQIGG 43 RALSIRALSACSINGVITADARQPD-FPAIYIN-HAFEGMTGYTVDECLGRICRERLQIGG 44 MRLLERAIENSHSAVLIADARQPD-FPAIYIN-HAFEGMTGYTVDECLGRICRERLQIGG 55	- DRNQ PAVGLVRDATAQE DREQ PAVAAIRSATDAR DREQ PAVAAIRSATDAR DREQ PALAALRQATAAR DREQ PALAALRQATAAR DREQ PETAVWRNALERN DRAD PGETAVWRNALERN DRAD PGSERMRDALAKG DRAD PGSERMRDALAKG DRAD PGUTETRAALARG DRAD PGLDATARAALRG EDDQ AGLVEIRAALARA EDRO PGLTELRAATAAG EQDQ AGLVEIRAALARA EADD TGLQTLRAALRKG TREQ PGLTELRAALARG YRDQ AALDELRAALARG YRDQ AALDELRAALARG TTGU PGLTELRAALARG TTGU PGLTELRAALARG FTAO PGLTELRAALARG ETAO PGLTELRAALRG ERDQ AALDELRAALRG ERDQ AALDELRAALRG ERDQ PALDELRAALRG DRAQ LELQPLRAALRG DRAQ LELQPLRAALRG DRHQ PALDELRAAVRG DRHQ PALDELRAAVRG DRHQ PALDELRAAVRG DRHQ PGLETTREGLAN DRGQ PGLETTREGLAN DRQQ PGLETTREGLAN DRQQ PGLETTREGLAN DRQQ PGLETTREGLAN DRQQ EGLYALRSAARAN DRQQ EGLYALRSAALRTE DRQQ EGLYALRSAARAN DRQQ EGLYALRSAARA	RAVRVTLRIVYRKINGTMFNWELSLTPIHGHDG ILTHYAGVÄHDVTEAVI ESVHVVLRIVYRKOGSLFNWELFISPVPDERG DITHYTGILINDITARKI ESVHVVLRIVYRKOGSLFNWELFISPVPDERG DITHYTGILINDITARKI EDCHVVLRIVYRKOGSLFNWELFISPVPDENG ELAHYIGITVDITELKI QDAHVVVRIVYRKOGSLFNWELFISPVPDHAG VVTHYVGIÄTDVTALKI EDCHVVLRIVYRKOGTFPNWELFISPVPDALG VVTHYVGIÄTDVTALKI EDCHVVLRIVYRKOGTAFNELTISPVRDAGG BIVTHVLGISTDITTEVE ESCHVELVRIVYRKOGAFNELTILYPLLDAED SLYFYMGVSRDATREAL EACTVUMENTRKOGAFNELTILYPLLDAED GLTHYMAVISDOTERHI RSTTYTLRIVYHKOGTFPNWELSISPVHDAGG RITHETGISDDVTFRRI KGTRALLRIVYRKOGSPFNWELTAPVHDERG QVTHTIGITEDVSERLI EKVEGUVLRIVYRKOGSPFNWELTAPVHDERG QVTHTIGITEDVSERLI EKVEGVLRIVYRKOGSPFNWELTAPVHDERG HITHFIGITEDVSERLI EKVEGVLRIVYRKOGSPFNWELTAPVHDERG HITHFIGITEDVSERLI EKVEGVLRIVYRKOGSPFNWELTAPVHDERG HITHFIGITEDVSERLI EKVEGVLRIVYRKOGSPFNWELTAPVHDERG HITHFIGITEDVSERLI EKVEGVLRIVYRKOGSPFNWELTHAPPVDAAG HITHVOTVLQUDVSERVI RACTVLLRINYRKOGSPFNWELTHAPPVDAAG HITHVOTVLQUDVSERVI RRCTVLLRINRRKOGSFFNWELHTAPVSDAAG HITHVOTVLQUDVSERVI RRCTVLLRINRRKOGSFFNWELHTAPVSESG DITHFIGVHDVTEOTT RECSVYLINNYRKOGSPFNWELSLAPVREGGG AXSHFVGLITDVTERH RSCSVELRINVRADGGVFNWERSLAPVRGEAG AXSHFVGLITDVTERH RSCSVELRINVRADGGVFNWERSLAPVRGEAG AXSHFVGLITDVTERH RSCSVELRINVRADGGVFNWENSLAPVRGEAG AXSHFVGLITDVTERH RSCSVELRINVRADGGVFNWENSLAPVRGEAG AXSHFVGLITDVTERH RSCSVELRINVRADGGVFNWENSLAPVRGEAG ATHTVOSLINDVSARH RSCSVELRINVRADGGVFNWENSLAPVRGEAG ATHTVOSLINDVSARH RSCSVELRINVRADGGFNMILSLSPPRDAGG SHFVGLITDVTERH RSCSVELRINVRROGSLFNMILSLSPPRDAGG SHFVGLITDVTERH RSCSVELRINVRROGSLFNMILSLSPPRDAGG SHFVGLITDVTERH RSCSVELRINVRROGSLFNMILSLSPPRDAGG SHFVGLITDVTERH RSCSVELRINVRROGSLFNMILSLSPPRDAGG SHFVGLITDVTERH RSCSVELRINVRROGSLFNMILSLAPVRDEGG SHTHFIGITSTOTTERW RSCSVELRINVRROGSLFNMILSLAPVRDEGG SHTHFIGITSTOTTERW RSCSVELRINVRROGSLFNMILSLAPVRDEGG SHTHFIGITSTOTTERW RSCSVELRINVRROGSLFNMILSLAPVRDEGG SHTHFIGITSTOTTERW RSCSVELRINVRROGSLFNMILSLAPVRDAGG SHTHFIGITSTOTTERW RSCSVELRINVRROGSLFNMILSLAPVRDAGG	G 327 N 272
WP_132137257.1 WP_093555924.1 PKL98247.1 WP_126799631.1 TXH46092.1 WP_161883475.1 TAN70402.1 WP_051906796.1 WP_125218592.1 OYY92272.1 WP_112183883.1 TXC65962.1 WP_140625868.1 WP_085751094.1 RWE97112.1 WP_158540843.1 WP_051848818.1 WP_024306447.1 WP_051846818.1 WP_024306447.1 WP_051840818.1 WP_05184083.1 WP_061850550.2 WP_121803303.1 WP_107142356.1 WP_107142356.1	151 LQLSIRALAASLINGVLISDASQAS-FPIMYAN-PAFCRMTGYDLIEWMGRNCRFLQND 54 PQLSARALAASSINGVLIDAARQPS-PPIMYAN-PAFCRMTGYALDELLGRICGR-LQGG 48 DALSINGLASCSINGWITADAAAPD-MPIMYAN-PAFCAMTGYDLGELLGRINGGR-LQGG 41 MRLLERAIENSHSAVLIADARQPD-FPAIYIN-HAFEGMTGYTVDECLGRINCRFLQGD 43 -ASHWGALDAMPYSVITADAKYAD-MPIMYTIN-PAFEALTGYTSDEARGRINCRFLQGD 45 -EASLPILICDARQAD-MPIMYAN-PSFERLTGYMATEAMGRNCRFLQGD 46 IRI FRAMFASASTSMADAINCPD-MPIMYAN-PAFEALTGYTADEAUGNICHFLQGD 47 - LRLQRAMAASINGTITADVQNCD-MPLITYM-PAFEALTGYTASDETLGHINCRFLQGG 57 - LRLLGRAWAASINGTITADVQNCD-MPLITYM-PAFEATTGYSRDETLGRINCRFLQGG 58 - LOAAMPIMYADATQPD-LPLYTIN-PAFEATTGYSRDETLGRINCRFLQGG 59 - DAAMPIMYDTSTQPD-PRIMYM-AAFEALTGYARDEAWGRNCRFLQGG 50 - DAAMPIMYDTSTQPD-PRIMYM-PAFEATTGYARDEAWGRNCRFLQGD 51 - DAAMPIMYDTSTQPD-RPIMYM-PAFEATTGYARDEAWGRNCRFLUDGD 521 - DAAMPIMYDTSTQPD-PRIMYM-PAFEATTGYARDEAWGRNCRFLUDGD 551 MYMKRGWEANAALPMCVCDATQPD-LPLYVM-PAFEATTGYARDEAWGRNCRFLUDGD 551 MYMKRGWEANAALPMCVCDATQPD-LPLYVM-PAFEATTGYARDEAWGRNCRFLUDGD 61 LQMLKAAIEASEAGMCVADAQAPD-YPLYVM-PAFEATTGYARDEAWGRNCRFLQGG 61 LQMLKAAIEASEAGMCVADAQAPD-YPLYVM-PAFEATTGYARDEAWGRNCRFLQGG 61 LGMLKAAIEASEAGMCVADAQAPD-YPLYVM-PAFEATTGYGTAAQALGRNCRFLQGG 61 LALTGRATDASFNOVLTADARQAD-LPLYVCN-PAFEATTGYTSRDEAWGRNCRFLQGG 61 LALTGRATDASFNOVLTADARQAD-LPLYVCN-PAFEATTGYTSRDEAWGRNCRFLQGG 61 LALTGRATDASFNOVLTADARQAD-LPLYVCN-PAFEATTGYTSRDEAWGRNCRFLQGG 61 LALTGRATDASFNOVLTADARQAD-LPLYVCN-PAFEATTGYTSRDEAWGRNCRFLQGG 61 LALTGRATDASTNOVLTADARQAD-LPLYVCN-PAFEATTGYTSRDEAWGRNCRFLQGG 62 AFESSKSGMLIADARSAD-LATVYM-PAFARTTGYGNAEFUGGNICRFLQGG 63 AFESSKSGMLIADARSAD-LATVYM-PAFARTTGYGNAEFUGGNICRFLQGG 64 LATGRATDASVIATATDARQAD-LPLYVN-PAFARTTGYGNAEFUGGNICRFLQGG 65 AFESSKSGMLIADARSAD-LATVYM-PAFARTTGYGNAEFUGGNICRFLQGG 66 AFESSKSGMLIADARSAD-LATVYM-PAFARTTGYGNAEFUGGNICRFLQGG 67 LLTRIGATGASPGSTATDARAPD-MPLTYM-PAFARTTGYGNAEFUGGNICRFLQGG 68 LRQGRALDASVINATUTHQWING-DUTYYAN-PAFARTTGYGTHEVIGKORGRCGGCRCRQD 68 LRQGRALDASVINATUTHQWING-DUTYYAN-PAFARTTGYGTHEVIGKORGRCGRCGRD 68 LRQGRALDASVINATUTHQWING-DUTYYAN-PAFARTTGYGTHEVIGKORGRCGRCGRD 68 LRQGRALDASVINATUTHQWING-DUTYYAN-PAFAR	- DRNQ - PAYGLVRDATAQE DREQ - PAVAAIRSATDAR DREQ - AAVAVE,HATLARG DODO - PALAALRQATAAR DREO - PETAYWRNALERN DRAO - PESERWROALAKG DRAO - PGSERWROALAKG DRAO - PGVQETRQALVEG ELDO - PG LDGTRAVI REG DRAO - PGLTERAATAAG DRHO - PGLDHYRSALSKG EQDO - AGLVEIRAALAKG EQDO - AGLVEIRAALAKG ERDO - PGLTELRAATAAG FRAO - TGLOTLRAALRKG TREO - PGLPELRAALAEG YRRO - AALDELRHALAEG YRRO - AALDELRHALAEG FTAO - PGLEEIRNATASK EPPO - ASWEEVRAALREG ERDQ - PALAEVRAALREG ERDQ - PALAEVRAALREG DRAO - LELOPLRAALRHG DRHO - SELHGLRAALARG DRHO - DARQOIRNAVKG DRHO - DARQOIRNAVKG DRHO - BALRYWRETLAKO DRAO - PGLEIRRAALRGG DRHO - BALRYWRETLAKO DRAO - PGLEIRRAALRGG DRHO - BALRYWRETLAKO DRAO - BELVAIRRGLARN DROO - EGLVAIRRGLARN DROO - DGLREIRNALN DROO - DGLREIRNAIN DROO - DGLREIRNALN DROO - DGLREIRNALN DROO - DGLRE	RAVRVTLRIYRKINGTMFNWELSLTPIHGHDG ILTHYAGVÄHDVTEAVI ESVHVVLRIVRROGSLFNWILELTSPYPOERG DITHYIGILINDITARKI ESVHVVLRIVRROGSLFNWILELTSPYPOERG LELAHYIGITYDTITELK -QDAHVVLRIVRKOGSLFNWILETLSPYPOERG ELAHYIGITYDTITELK -QDAHVVVRINYRKOGSLFNWILETLSPYPODAG LEVTHYVGIÄTDVTALKI -QDAHVVVRINYRKOGTFPNWILETLSPYPODAG LIVTHYVGIÄTDVTALKI -EDCHVVLRIVRKOGTLFNWILETLSPVRDAGG LIVTHYLGISTDITVEV -ECHVVLRIVRKOGTAFNWILETLVPILLDAED SLVFYMGVSRDATREAI -EACTVLMRIVRROGAFNWELHLTPVRDAED CLTHYMAVLSDOTERHI -ERSTYTLRIVHKOGTLFVWILESLSPVPDAGG RITHFIGTSDIDVTARRI -KROFALLRIVRROGTFPNWILELTAPVHDERG RITHFIGTSDIDVTARRI -KGTRALLRIVRKOGSPFNWILELTAPVHDERG VYTHFIGTIEDVSERLI -EKVEGVLRIVRROGSPFNWILELTAPVHDERG NLTHFIGTSDOVSGRLI -ERVEGVLRIVRROGSFFNWILELTAPVHDERG HVVQHLGVLHDVTERVI -RECTVLLRIMRROGSFFNWELTVAPVDAGG HVVQHLGVLHDVTERVI -RECTVLLRIMRROGSFFNWELTVAPVDAGG HVVQHLGVLHDVTERVI -RASTVLLRIMRROGSFFNWELTVAPVRDAGG HVVQHLGVLHDVTERVI -RECSVSTURNWROGTFPTNALHAPVFDAAG RVTHFIGVHTDVTERVI -RECSVSTURNWROGTFPTNALHAPVFDAAG SLSHFIGVLHDVTGVT -RPSCSVSLRIVRADGSFPNWALSLAPVRGEGG ALTHVVGLHDVSAHH -RSCSVSLRIVRADGSFPNWALSLAPVROEGG SLSHFIGVLHDVTGANI -RSCSVELRIVRADGSFPNWELSLAPVROEGG ATTHVGLHDVSAHH -RSCSVELRIVRADGSFPNWELSLAPVROEGG SLSHFIGVLHDVTGANI -RECSVSLRIVRADGSFPNWELSLAPVROEGG STHYGLHTDVSAHH -RSCSVELRIVRADGSFPNWELSLAPVROEGG STHYGLHTDVSAHH -RSCSVELRIVRADGSFPNWELSLAPVROPAG STHYGLHTDVSAHH -RSCSVELRIVRADGSFFNWELTLAPPROAGG STHYGLHTDVSAHH -RSCAVLRIVRKOGALFNWELSLAPVROPAG SCHTHYGVSTDUTDRV -KYCKULTRIVRKOGALFNWELSLAPVROPAG SCHTHYGVSTDUTDRV -KYCKULTRIVRKOGALFNWELSLAPVROPAG SCHTHYGVSTDUTDRV -REVSAVLRIVRROGALFNWELSLAPVROPAG SCHTHYGVSTDUTDRV -REVSAVLRIVRROGALFNWELSLAPVROPAG SCHTHFIGVATOVTORV -REVSAVLRIVRKOGALFNWELSLAPVROPAG SCHTHFIGVATOVTORV -REVSAVLRIVRKOGALFNWELSLAPVROPAG SCHTHHIGVATINOTTENVI -REVSAVLRIVRKOGALFNWELSLAPVROPAG SCHTHHIGVATINOTTENVI -REVSAVLRIVRROGALFNWELSLAPVROPAG SCHTHHIGVATINOTTENVI -REVSAVLRIVRROGALFNWELDGALFNWELSLAPVROPAG SCHTHHIGVATINOTTENVI -REVSAVLRIVRROGALFNWELSLAPVROPAGG SCHTHHIGVATINOTTENVI -REVSAVLRIVRROGALFNWELSLAPVROPAGG SCHTHHIGVATINOTTENVI -REVSAVLRIVRROGALFNWELSLAPVROPAGG SCH	G 327 N 272

WP 052452293.1	336 LRLKNRAIQASVNAIIITDLEGNIEYAN-PAFENITGYSVTEAVGCNCRFLQGN	DRAQAGVARLRNAIRQREESSVLLRNYRKDGRLFWNDVHIAPVRGPDGEVTHFVGVLNDISD	KHY 454
WP_151634712.1	338QASVNAIIITDLEGNIEYAN-PAFERMTGYSVRETLGKNCRFLQAG	DRNQAGIAAIRHSIAMREESSALLRNYRKDGEMFWNDVHIAPVRGQDDEVTHFVGVLNDISA	KQY 448
RZI42720.1	337 LRLSNRALQASVNAIIITDLEGNIEYAN-PAFERITGYGLDEAIGQNCRFLQGS	DTEQPGVDAIRSAIQRQSEVSVLLRNYRKDGALFWNDVHIAPVRGPDGAVTHFVGVLNDITE	KHY 455
NEX62298.1		DSEQPGILSIRRAIRMQEEGNALLRNYRKDGTLFWNDLHIAPVPNADGEVTHFVGVLNDVTG	
RJF96104.1		DTEQAGIAVLRNAIAQRQEVSALLRNYRKDGTLFWNEMHIAPVRDPYGVVTHFVGVLNDISA	
OHC61749.1		DTDQPALENIRAALRENKKGRALLRNYRKDGSLFWNDLHLAPVQGDGGVVTHFIGILNDVTD	
WP_135209473.1		DTEQPALADLRRALHEERAITVVLRNYRKDGSLFWNELRVAPVRDAQGAVTHWVGILNDITA	
WP_110399911.1 OHC49289.1		ESEQPALREIAAAVREEREGHGVFRNRRKDGSAFWNELHIAPVRDAEGAVTHFVGVLNDVTAI EQDQPALDAIRRALRGQEEGGAILRNYRKDGSAFWNDLKVAPVVNDRGKYSHFVGILHDITE	
ARD68205.1		-EQUQPALDAIRNALNOQEEGSAQLRNYRKDGSEFWNDLTVTPVVNDRGKISHFVGILHDITE	
WP_147173937.1	SPECIAL SERVICE DE PRODUCTION DE LA CASA DE CASA DE LA CASA DEL CASA DE LA CASA DEL CASA DE LA CASA DEL CASA DE	ETEOPELASVRALQAEEEGRAVLRNYRKDGSAFWNELRLAPVVNDRGRVSHFVGILNDITE	
WP 052679321.1	STATES AND SECURITION OF THE PROPERTY OF THE P	DRDQIDLIGIRQALOTEQEGSAVLRNYRKDGSEFWNELNISPVVNDRGKISHFVGILHDITE	
WP 008900325.1		DRHQPGLDSIRRAIRNNCKGNAELLNYRKDGSSFWNDLTLAPVVNDRGHTSHFVGILRDITES	
WP 127700725.1		AQDQPGLDLIRRLLKNHEHGKAELLNFRKDGSAFWNELTLAPVVNDRGQTSHFVGILRDITQ	
WP 020410026.1	508EASVNAVVITDYNQKD-NPIVYVN-PAFERITGYTKEEVLGTNCRFLQKD	DRNQIGIASIKRAVSSGEPGSALLRNYHKDGTLFWNELQVAPVKDAAGKINHFVGVLNDVTE	KRY 621
WP_094711329.1	501 LILRTRAVEASINAVVITDTSLPD-NPIVYVN-PAFERITGYRKEEALGKNCRFLQND	DRNQLGIASIRRAIDSGDKGGALLRNYRKDGSLFWNDLQIAPVRDQAGNISHYVGVVNDVTE	KRY 622
WP_110189015.1		DREQRJLESIRRALRNGSEGAALLRNYRKDGSLFWNELRVAPVRDDQGRIRHFVGVLNDVTE	
WP_072430140.1		DQDQPALSSIRLALQLGQEGKALLRNYRKDGSMFWNELRVTPTLDSQGGISHFVGVLNDVTE	
WP_014088122.1	Change Indicated a second control of the sec	DTAQPELTAIRRALENRHEGKALLRNYRKDGSMFWNELRVAPVRDSQGEVSHYIGVLNDVTE	
WP_084089384.1		DLDQPELMAVRRALEQGTDGRALLRNYRKDGSMFWNDLRLSPSRDAEGRISHFVGVLNDITE	
WP_148714457.1		DRDQPDLVFIRRAVAQGTEGKALLRNYRKDGSMFWNALHVLPAPDAQGRITHYVGVIDDVTA	
WP_159672521.1		DHDQPGLLAIRRAVAQGIEGKAVLRNYRRDGSMFWNDLRVAPSFDGEGNVSHFVGVLSDISD	
0ZB62968.1		DNAQPELDKIRAAIRERRAATAVLRNYRKDGSLFLNELHIAPVHDPRHGKVTHYVGIMHDITQ	
WP_112991931.1		DTDQGAGHFVGVLYDVTQ:	
WP_156962941.1 WP 152331449.1		DREQAAVDAIRSALQSERDVRVTLRNYRRDGSLFWINDLHLTPLRAPDGVVTHHVAIVNDVTEG ERDQPARADIRDAIAQTREIRVQVRNYRRDGSPFWNELRMAPVRDQDGVLTHFVGILNDISDF	
WP_162301427.1		DRDQPGIDIIRNALRESHEVRTLLRNYRKDGTLFWNEVYIAPVRDDRGALTHFVGILNDVSEF	
WP_182301427.1		DRDOAGLDAIRRGIREAHEVRTLLRNYRKDGSLFWNEVYMAPVRDERGALTHFVGILHDVSEF	
WP_159017065.1		DQAQPGIEAVRGALREQREARVLLRNYRKDGALFWNDFHVAPVSDENGVLSHFVGVISDVSEF	
0GT59526.1		DRYQAGLDAVRTAIHGNYENQSLLRNYRKNGEMFYNQLSISPVRDDNGQLTHFVGVLNDVSDF	
KFL37100.1		ETRQPELKILRRSLAEGRESNVILRNFRKDGELFWNHLFTSPVRDEQGTITHFVGILNDLTEF	
OHE81221.1	249 LLLLQRAVESSMNGIVIADAQAPD-MPIIYVN-PSFERMTGYTTEQVIGRNCRFLQGE	ERNQPELEILRRTLRDAGDCNVMLRNFRSDGELFWNHLFISPVRDEAGRLTHFVGILNDLTER	RQV 370
WP_139448749.1	385 LQLLERAVESSINGVAITDANAPD-LPLIYVN-PAFESMTGYSAQEVVGRNCRFLQGP	LRAQPELDVLREALRQQTDCNVILSNQRKDGSLFWNHLFVSPVRDDRGRVTHYVGVLNDLTER	RQV 506
WP_146474684.1		QRDDQALAPLREALREGRTAHVVLKNYRKDRTPFWNELLVSPVRDDHGRLTHYVGVLNDVTQF	
WP_146472278.1		ETDQPELHELRKALREGRDCEVVLRNYRKDGTVFWNQLAISPVRDGDGVVTHLVGIVSDVTE	
WP_088708545.1	SHADOW DEFINITION OF THE PROPERTY AND THE PROPERTY OF THE PROP	DRDQPGLEELRAALQEEREVHVVLRNYRKDGSRFWNELSVSPVRDANGAVTHFVSEMVDVTAF	
WP_161812444.1		DHEQEGLEKIRTALRQGVSVQTTLRNYRKDGTMFWNEVTIQPLRDGNGNVTHFAGFHREGGDF	
WP_121440657.1	34 GRLKQAALDISTTAVVLVDYRQSD-QPVVYVN-RAFEMLTGYAAAEVVGRNCRFLQGNG	/DVDARELDKIRQALNEGDEGWAILANQCKDGTPFWNELQIAPLRDDRGAITHYVGYLSDITQI	KSN 157
AMD00610.1	409 AGGTERSVEASTNGTVTADATEAD-CPTTYAN-SAFOVMTGYREFEI MGRNCREI OGE	FTDPFTVALLRSRLAFDRECHVTLRNYRKDGSAFWNALYVSPVPDSDGRVTHEVGVLNDVSE)AY 530
AMD00610.1 WP 010627231.1		ETDP	
WP_010627231.1	594 LRVLERSVQASINGIVITDASQHD-LPISYVN-EAFLALTGYREEEVLGRNCRMLQGV	ETDP	HAY 715
	594 LRVLERSVQASINGIVITDASQHD-LPISYVN-EAFLALTGYREEEVLGRNCRMLQGV 304 LRTLQRGVEASVNGVVIADAREPD-MPIVYAN-ATFMKMTGYREDEILGRNCRFMQGE	ETEPDAVAWLRRCVVERRDCHVTLLNYRKDGSTFWNALYVSPVLDGDGGVTHFVGELRDVSE	HAY 715 KAY 425
WP_010627231.1 WP_102627940.1	594 LRVLERSVQASINGIVITDASQHD-LPISYVN-EAFLALTGYREEEVLGRNCRMLQGV 304 LRTLQRGVEASVNGVVIADAREPD-MPIVYAN-ATFMKNTGYREDEILGRNCRFMQGE 776 LRILERSVEASVHGVLIVDANQTD-MPIIFAN-HAFSRISGYSNAEIKGRNCRFLQGH	ETEPGAVAWLRRCVVERRDCHVTLLNYRKDGSTFWNALYVSPVLDGDGGVTHFVGELRDVSE ETDPEAVAMIRRHLAEQREVLVTLRNYRKDGTPFWNDAFISPVRDGEGRVTHFVGVLHDISE	HAY 715 KAY 425 IAD 897
WP_010627231.1 WP_102627940.1 WP_112054571.1 WP_161423473.1 WP_159341723.1	594 LRVLERSVQASINGIVITDASQHD-LPISYVN-EAFLALTGYREEEVLGRNCRMLQGV 304 LRTUCRGVEASVHGVYLADAREPD-MFIVYAN-ATFMKHTGYREDETLGRNCRFMQGE 776 LRILERSVEASVHGVLIVDANQTD-MPIIFAN-HAFSRISGYSNAEIKGRNCRFLQGH 774 LLTLERSVEASINGVTIVDATOPG-MPLIFWN-QAFSRITGYKEEVQGRNCRFLQGP	ETEPDAVAWLRRCVVERRDCHVTLLI\YRKDGSTFW\\\ALYVSPVLDGDGGVTHFVGELRDVSE\\\ ETDPEAVAMIRRHLAEQREVLVTLR\\\YRKDGTPFW\\\\\\\\\\\\\\\\\\\\\\\\\\\\\\\\\\\\	HAY 715 KAY 425 IAD 897 IED 895
WP_010627231.1 WP_102627940.1 WP_112054571.1 WP_161423473.1	594 LRVLERSVQASINGIVITDASQHD-LPISYVN-EAFLALTGYREEEVLGRNCRMLQGV 304 LRTLQRGVEASVNGVVIADAREPD-MPIVYAN-ATFMKNTGYREDEILGRNCRFMQGE 776 LRILERSVEASVNGVIVDANIQT-MPIIFAN-HAFSRISGYSNAETKGRNCRFLQGH 774 LLTLERSVEASINGVITVDATDPG-MPLIFVN-QAFSRITGYGKEEVQGRNCRFLQGP 767 LRIFGRSLEASSNGVLICEANIDD-FPIIFVN-PAFVEITGYPGDVRHRNCRFLQGP 600 LRIYQRSLEASSNGVICEALQDD-YPILYVN-PAFVAITGYQLDDKGLNCRFLNGQ	ETEP	HAY 715 KAY 425 IAD 897 IED 895 KDH 888 RDH 721
WP_010627231.1 WP_102627940.1 WP_112054571.1 WP_161423473.1 WP_159341723.1 WP_146875715.1 TVP44179.1	594 LRVLERSVQASINGIVITDASQHD-LPISYVN-EAFLALTGYREEEVLGRNCRMLQGV 304 LRTLGRGVEASVNGWYIADAREPD-MPIVYAN-ATFIKHTGYREDEILGRNCRFMQGE 776 LRILERSVEASVNGVLIVADNQTD-MPIIFAN-HAFSRISGYNBALEKGRNCRFLQGH 774 LLTLERSVEASINGVTIVDATQPG-MPLIFVN-QAFSRITGYGKEEVQGRNCRFLQGP 767 LRIFGRSLEASSNGVLICEAQNDD-FPIIFVN-PAFVAITGYQDDVRRRNCRFLQGP 600 LRIYQRSLEASSNGIVICEALQDD-YPILYVN-PAFVAITGYQLDIKGRLGKRFLNGG 600 LRIYQRSLEASSNGILICEALQDD-YPIIFVN-PAFVAITGYPLEEVKGHNCRRLLQGK	ETEP- DAVAWLRRCVVERRDCHVTLLNYRKDGSTFWNALYVSPVLDGDG GFTHFVGELRDVSEI ETDP- EAVAMIRRHLAEQREVLVTLRNYRKDGTFFWNDAFISPVRDGEG FFTHFVGVLHDISEI ETDP- OTYQEIRQGLDQG - ROVOTLGNYRKNGERFWNDAFISPVRDGEG FFTHFVGVWNDVTQ ETDP- EAVPMIRRSLVARREVSVTLRNYRKNGESFWNELKISPVSNRHG FTHFVGVWNDVTQ ETDP- KGVQEICDALLQQRDISLITRNYRKNGGAFWNNVFISPVRAQDG GFTHFVGIINDISEI ETDP- KNIDALQQALEQQ -QDITLTIRNYRKNGQAFWNNVFISPVRAQDG VVTHFVASINDISEI ETDP- KGUADIQAFEQQRDISLITRNYRKNGQAFWNNVFISPVRAPDG VVTHFVASINDISEI ETDP- KGIADIQAFEQQRDIALTIRNYRKNGQAFWNNLFLSPVKSHNG GFTHFVASINDISEI	HAY 715 KAY 425 IAD 897 IED 895 KDH 888 RDH 721 RDH 721
WP_010627231.1 WP_102627940.1 WP_112054571.1 WP_161423473.1 WP_159341723.1 WP_146875715.1 TVP44179.1 WP_100821604.1	594 LRVLERSVQASINGIVITDASQHD-LPISYVN-EAFLALTGYREEEVLGRNCRMLQGV 304 LRTLQRGVEASVNGVYLADAREPD-MFIVYAN-ATFRKHTGYREDETLGRNCRFNQGE 776 LRILERSVEASVHGVLIVDANIQTD-MFIIFAN-HAFSRISGYSNAEIKGRNCRFLQGH 774 LLTLERSVEASINGVTIVDATQPG-MPLIFVN-DAFSRLTGYKEEVQGRNCRFLQGP 767 LRIFQRSLEASSNGVLICEAQNDD-FPIIYVN-PAFVEITGYDFDDVRHRNCRFLQGP 660 LRIYQRSLEASSNGIVICEALQDD-YPILYWN-PAFVAITGYQLDIKGLNCRFLNGQ 600 LRIYQRSLEASSNGIVICEALQDD-YPILYWN-PAFVAITGYPLEVKGHNCRLLQGK 33 RYLFQRSLEASSNGIVISAIWPE-LPILYTN-PAFVAITGYPFEDVKGLSCRFLQGM	ETEP	HAY 715 KAY 425 IAD 897 IED 895 KDH 888 RDH 721 RDH 721 KHQ 154
WP_010627231.1 WP_102627940.1 WP_112054571.1 WP_161423473.1 WP_159341723.1 WP_146875715.1 TVP44179.1 WP_100821604.1 WP_075879636.1	594 LRVLERSVQASINGIVITDASQHD-LPISYVN-EAFLALTGYREEEVLGRNCRMLQGV 304 LRTUCRGVEASVNGVYLADAREPD-HPIVYAN-ATFIKKHTGYREDEILGRNCRFNQGE 776 LRILERSVEASVHGVLIVDAIQTD-MPIIFAN-HAFSRISGYSNAEIKGRNCRFLQGH 774 LLTLERSVEASINGVTLOPATOPG-MPLIFWN-DAFSRITGYKEEVQGRNCRFLQGP 767 LRIFQRSLEASSNGVLICEAQNDD-FPIIFVN-PAFVEITGYDFDDVRHRNCRFLQGP 600 LRIYQRSLEASSNGIVICEALQDD-YPILFVN-PAFVAITGYQLDDIKGLNCRFLNGG 33 RYLFQRSLEASSNGILICEALQDD-YPIIFVN-PAFVAITGYPLEEVKGHNCRLLQGK 33 RYLFQRSLEASSNGVIISQATWPE-LPILFYN-PAFVAITGYPLEEVKGHNCRLLQGC 240 LHIFERSLQASSNGVLIADATQTD-QPIYYAN-PAFVAITGYPLEEVKGRNCRFLQGP	ETEP- DAVAWLRRCVVERRDCHVTLLNYRKDGSTFWNALYVSPVLDGDG GFTHFVGELRDVSEI ETDP- EAVAMIRRHLAEQ REVLVTLRNYRKDGTFFWNDAFISPVRDGEG RVTHFVGVLHDISEI ETDP- QTVQEIRQGLDDQ RDVQVTLCNYRKNGEFFWNDAFISPVRDEHG SFTHFUGVNDVTQ ETDP- EAVHKIRSLVAR REVSVTLRNYRKNGEFFWNELKISPVSNRHG EITHFVGVANDVTQ DTDP- KQVQEICDALLQQ RDISLTIRNYRKNGAFFWNNVFISPVRAQDG QATHFVGIINDISEI DTDP- KNIDAIQQALEQQ QOITLTIRNYRKNGQAFWNNVLFISPVRAPDG VVTHFVASINDISEI DTDP- KQIADIQLAFEQQ RDIALTIRNYRKNGQAFWNNVLFISPVRAPDG QVTHFVGSITDISEI DTDP- GQVEALRQALKHG KOISLTIRNYRKNGQAFWNNVLFISPVKSHNG RVTHFIGILNDISEI DTPP- EQVEALRQALKHG KOISLTIRNYRKNGAFWNNVLFISPVRADG VCHTHFUGILNDISEI DTPP- EQVEALRQALKHG KOISLTIRNYRKNGAFWNNVLFISPVRADG VCHTHFIGILNDISEI	HAY 715 KAY 425 IAD 897 IED 895 KOH 888 RDH 721 RDH 721 KHQ 154 KNH 361
WP_010627231.1 WP_102627940.1 WP_1112054571.1 WP_161423473.1 WP_159341723.1 WP_146875715.1 TVP44179.1 WP_100821604.1 WP_075879636.1 WP_083517734.1	594 LRVLERSVQASINGIVITDASQHD-LPISYVN-EAFLALTGYREEEVLGRNCRMLQGV 304 LRTLQRGVEASVMGVYIADAREPD-MPIVYAN-ATFMKHTCYREDEILGRNCRFMGGE 776 LRILERSVEASVMGVLYDANGTO-MPILFAN-HAFSRISGYNALEKGRNCRFMGGH 774 LLTLERSVEASINGVTIVDATQPG-MPLIFVN-QAFSRITGYGKEEVQGRNCRFLQGP 767 LRIFGRSLEASSMGVLICEAQNDD-FPILYWN-PAFVALTGYDDDVRRHNCRFLQGP 600 LRIVGRSLEASSMGVILGEAQDD-YPILYWN-PAFVALTGYDLDIKGLKGRELNGG 600 LRIVGRSLEASSMGVILGALQDD-YPILYWN-PAFVALTGYPLEEVKGHNCRFLLQGK 33 RYLFGRSLEASSMGVILGALTWG-LPILYTN-PAFTOLTGYPFEDVKGLSGRFLQGM 240 LHIFERSLQASSMGVLIADATTQTD-QPIVYAN-PAFTOLTGYPEEVKGRNCRFLQGP 291 LRLLGRGIEASPMGVLHADATTQTD-MPLYYAN-EAFSQLTGYALLGNUCKRFLQGP	ETEP- DAVAWLRRCVVER - RDCHVTLLNYRKDGSTFWNALYVSPVLDGDG GFTHFVGELRDVSEI ETDP - EAVAMTRRHLAEQ - REVLVTLRNYRKDGTFFWNDAFISPVRDGEG RVTHFVGVLHDISEI ETDP - OTYQETRGGLDOG - RDVQVTLGNKDGTFFWNDAFISPVRDGEG - RVTHFVGVANDVTQ ETDP - EAVMKIRRSLVAR - REVSVTLRNYRKNGESFWNELKISPVSNRHG - EITHFVGVÄNDVTQ DTDP - KGVQEICDALLQQ - RDISLITRNYRKDGRAFWNNVFISPVRAQDG - QATHFVGINDISEI DTDP - KKIDAIQQALEQQ - QOITLTRNYRKNGAFWNNVFISPVRAQDG - VYTHFVASINDISEI DTDP - KQIADIQLAFEQQ - RDIALTRNYRKNGQAFWNNLFISPVRSHG - QVTHFVGSITDISEI DTOP - EQVEALRQALKHG - KDISLITRNYRKDGRAFWNNLFISPVRDNAG - RVTHFIGILNDISEI DTOP - EQVEALRQALKHG - KOTSLITRNYRKDGRAFWNNLFISPVRDNAG - QVTHFIGILNDISEI DTHP - EPVAQNHQALSEG - RVODLTVRNYRKDGRPFWNQVFISPVHASDG - QVTHFIGILNDISEI DTRP - GOVEATRQALSSC - NSVQVILVNYRKDGTPFWNNLAISPVPEGTG - SCSHFIGTWDITTR	HAY 715 KAY 425 IAD 897 IED 895 KDH 888 RDH 721 RDH 721 KHQ 154 KNH 361 RNQ 412
WP_010627231.1 WP_102627940.1 WP_112054571.1 WP_112054571.1 WP_161423473.1 WP_159341723.1 WP_146875715.1 TVP44179.1 WP_00821604.1 WP_075879636.1 WP_083517734.1 SEF71116.1	594 LRVLERSVQASINGIVITDASQHD-LPISYVN-EAFLALTGYREEEVLGRNCRMLQGV 304 LRTLQRGVEASVHGVLADAREPD-MFIVYAN-ATFHKHTGYREDEILGRNCRFMQGE 776 LRILERSVEASVHGVLIVDATQPG-MPLIFAN-HAFSRISGYSNAEIKGRNCRFLQGH 774 LLTLERSVEASINGVITVDATQPG-MPLIFVN-DAFSRITGYKEEVQGRNCRFLQGP 767 RIFQRSLEASSNGVLICEAQNDD-FPIIYVN-PAFVATTGYKEEVQGRNCRFLQGP 600 LRIYQRSLEASSNGVILCEALQDD-YPILYVN-PAFVATTGYQLDDIKGLNCRFLNGG 600 LRIYQRSLEASSNGVILCEALQDD-YPIIYVN-PAFVATTGYQLEDHKGRHLQGC 33 RYLFQRSLEASSNGVILGALQDD-YPIYVN-PAFVATTGYPLEVKGHKCRFLNGG 240 LHIFERSLQASSNGVILADATQTD-0PIVYAN-PAFTQNTGYPIEEVKGRNCRFLQGP 291 LRLLQGRGSSPNGIHADATQTD-MPLVYAN-EAFSQLTGYALDEVLGRNCRFLQGN 292 LRLLQGRGSSPNGIHADATRHD-LPLYAN-EAFSQLTGYALDEVLGRNCRFLQGN	ETEP- DAVAWLRRCVVERRDCHVTLLNYRKDGSTFWNALYVSPVLDGDG GFTHFVGELRDVSEI ETDP EAVAMIRRHLAEQ - REVLVTLRNYRKDGTFFWNDAFISPVRDGEG RVTHFVGVLHDISEI ETDP QTVQEIRQGLDDQ - RDVQVTLCNYRKNGERFWNDLHISPVRDEHG AVSHFIGVVNDVTQ ETDP EAVMKIRRSLVAR - REVSVTLRNYRKNGESFWNELKISPVSNRHG EITHFVGVANDVTQ DTDP KGVQEICDALLQQ - RDISLTIRNYRKNGERFWNNVFISPVRADDG QATHFVGIINDISEI DTDP KNIDAIQQALEQQ - QDITLTIRNYRKNGGAFWNNVFISPVRADDG VVTHFVASINDISEI DTDP KQIADTQLAFEQQ - RDIALTIRNYRKNGAFWNNVFISPVRADDG VVTHFVGSITDISEI DTDP EQVEALRQALKHG - KDISLTIRNYRKNGAFWNNVFISPVRADGG RVTHFVGSITDISEI DTPP EPVAQMHQALSEA - RAVDLTVRNYRKDGRFWNQVFISPVRADGG VTHFVGSITDISEI DTHP EPVAQMHQALSEA - RAVDLTVRNYRKDGRFFWNQVFISPVHASDG VTHFVGILNDISEI DTHP GDVEAIRQALSEA - RAVDLTVRNYRKDGRFFWNQVFISPVHASDG SCSHFIGTNNDTRI	HAY 715 KAY 425 IAD 897 IED 895 KDH 888 RDH 721 RDH 721 KHQ 154 KNH 361 RNQ 412 KNQ 419
WP_010627231.1 WP_102627940.1 WP_112054571.1 WP_161423473.1 WP_159341723.1 WP_146875715.1 TVP44179.1 WP_00821604.1 WP_075879636.1 WP_083517734.1 SEF71116.1 WP_141320011.1	594 LRVLERSVQASINGIVITDASQHD-LPISYVN-EAFLALTGYREEEVLGRNCRMLQGV 304 LRTLQRGVEASVNGVYLADAREPD-MFIVYAN-ATFIKHTGYREDETLGRNCRFNQGE 776 LRILERSVEASVHGVLIVDAIDYD-MFIIFAN-HAFSRISGYSNAEIKGRNCRFLQGH 774 LLTLERSVEASINGVTIVDATOPG-MPLIFVN-DAFSRITGYKEEVQGRNCRFLQGP 767 LRIFQRSLEASSNGVLICEAQNDD-FPIIFVN-PAFVEITGYDEDVRHRNCRFLQGP 608 LRIYQRSLEASSNGIVICEALQDD-YPILYVN-PAFVAITGYQLDDIKGLNCRFLNGG 33 RYLFGRSLEASSNGILICEALQDD-YPIIFVN-PAFVAITGYPLEEVKGHNCRLLQGK 34 RYLFGRSLEASSNGVLIADATQTD-DEIVYAN-PAFVAITGYPLEVKGHNCRFLQGH 291 LRLLQRGIGASPNGVLNADATQPD-MPLVYAN-EAFTQITOPPDUKGLSCRFLQGN 292 LRLLQRGIGSSPNGLNADATRID-LPLYVAN-EAFTQITOPPDUKGLNCRFLQGN 298 LRLLQRGIGSSPNGLNADATRID-LPLYVAN-EAFTQITOPPDUKGLNCRFLQGN	ETEP- DAVAWLRRCVVERRDCHVTLLNYRKDGSTFWNALYVSPVLDGDG GFTHFVGELRDVSEI ETDP EAVAMTRRHLAEG -REVLVTLRNYRKDGTFFWNDAFISPVRDGEG RVTHFVGVLHDISE ETDP GTVGEIRQGLDDG -RDVQVTLCNYRKNGEFFWNDAFISPVRDEHG AVSHFIGVVNDVTQ ETDP EAVMKIRRSLVAR -REVSVTLRNYRKNGESFWNELKISPVSNRHG EITHFVGVANDVTQ DTDP KQVQEICDALLQQ -RDISLTIRNYRKNGAFFWNNVFISPVRAQDG QATHFVGIINDISE DTDP KNIDAIQQALEQQ -QDTILTIRNYRKNGQAFWNNVFISPVRAQDG VVTHFVASINDISE DTDP KQIADIQLAFEQQ -RDIALTIRNYRKNGQAFWNNLFISPVRAPDG VVTHFVASINDISE DTDP KQIADIQLAFEQQ -RDIALTIRNYRKNGQAFWNNLFISPVRANDG RVTHFIGILNDISE DTDP EQVEALRQALKHG -KDISLTIRNYRKNGGAFWNNVFISPVRANDG RVTHFIGILNDISE DTHP EPVAQMHQALSEA -RAVDLTVRNYRKDGRFWNQVFISPVBASDG QVTHFIGILNDISE DTHP GOVEAIRQALSSC -NSVQVTLVNYRKDGFFWNQVFISPVFDETG SCSHFIGTWDVITR ETDP - AAIGKTRGSVVOR -TEVQVILNYRKDGFFWNNLAISPVFDETG RCTHFIGILEDTE ETDP - ASIDTIRDALRRC -SAVEVTILNYRGDGSTFWNNLISPVPDETG KCTHFIGILEDTE ETDP - ASIDTIRDALRC -SAVEVTILNYRGDGSTFWNNLISPVPDETG KCTHFIGILEDTE	HAY 715 KAY 425 IAD 897 IED 895 KDH 888 RDH 721 RDH 721 KHQ 154 KNH 361 RNQ 412 KNQ 419 LEQ 419
WP_010627731.1 WP_102627940.1 WP_112054571.1 WP_161423473.1 WP_159341723.1 WP_146875715.1 TVP44179.1 WP_100821604.1 WP_075879636.1 WP_083517734.1 SEF71116.1 WP_141320011.1	594 LRVLERSVQASINGIVITDASQHD-LPISYVN-EAFLALTGYREEEVLGRNCRMLQGV 304 LRTLQRGVEASVNGWYIADAREPD-MPIVYAN-ATFRKHTGYREDEILGRNCRFMQGE 776 LRILERSVEASVNGVLYDANQHOT-MPIITAN-HAFSTSISONALEKGRNCRFMQGE 774 LLTLERSVEASINGVTIVDATQPG-MPLIFVN-QAFSRITGYGKEEVQGRNCRFLQGP 767 LRIFQRSLEASSNGVLICEAQNDD-PFILYWN-PAFVEITGYDFDDVRRRNCRFLQGP 600 LRIYQRSLEASSNGVILGEAQNDD-YPILYWN-PAFVAITGYDLEEVKGHNCRFLNGG 600 LRIYQRSLEASSNGVILGALQDD-YPILYWN-PAFVAITGYPLEEVKGHNCRFLLQGK 33 RYLFGRSLEASSNGVILGATWPE-LPILYTN-PAFVAITGYPLEEVKGHNCRFLQGM 294 LRLLQRGIEASPNGVLADATOTD-OPIVYAN-PAFVAITGYPLEEVKGRNCRFLQGP 295 LRLLQRGIEASPNGVLADATOTD-HPLYAN-LAFSQLTGYALDEVLGNNCRFLQGN 298 LRLLQRGIEASPNGVLADATOTD-D-MPLYYAN-LAFSQLTGYALDEVLGNNCRFLQGN 298 LRLLQRGIEASPNGVLADATOTD-D-MPLYYAN-LAFSQLTGYALDEVLGNNCRFLQGN 298 LRLLQRGIEASPNGVLADATOTD-D-MPLYYAN-LAFSQLTGYALDEVLGNNCRFLQGN 298 LRLLQRGIEASPNGVLADATOTD-D-MPLYYAN-LAFSQLTGYALDEVLGNNCRFLQGS 298 LKLLRSIESSPSGFLLADAGSPD-LPVYAN-PAFTANTGYDDEITGRNCRFLQGS	ETEP- DAVAWLRRCVVER - RDCHVTLLNYRKDGSTFWNALYVSPVLDGDG GFTHFVGELRDVSEI ETDP - EAVAMTRRHLAEQ - REVLVTLRNYRKDGTFFWNDAFTSPVRDGEG RVTHFVGVLHDISEI ETDP - OTYQETRGDLDQ - RDVQVTLCNYRKNGERFWNDAFTSPVRDGEG - RVTHFVGVLHDISEI ETDP - EAVMKIRRSLVAR - REVSVTLRNYRKNGESFWNELKISPVSNRHG - EITHFVGVÄNDVTQ ETDP - KRUDALQQ - RDISLITRNYRKNGGAFWNNVFTSPVRAQDG - QATHFVGINDISEI DTDP - KKIDALQQALEQQ - QDITLTIRNYRKNGQAFWNNLFTSPVRADDG - VYTHFVASINDISEI DTDP - KQIADIQLAFEQQ - RDIALTIRNYRKNGQAFWNNLFTSPVRSHNG - QVTHFVGSITDISEI DTDP - EQVEALRQALKHG - KDISLITRNYRKNGGAFWNNLFTSPVRSHNG - QVTHFVGSITDISEI DTPP - EPVAQMHQALSEG - RAVDLTVRNYRKDGRAFWNNLFTSPVRSHNG - QVTHFIGILNDISEI DTRP - GOVEATRQALSGS - KNSQUTLVNYRKDGTPFWNRLATSPVPEGTG - SCSHFIGTWDITTR ETDP - AAIGKTRGSVVDR - TEVQVTLLNYRKDGTFFWNRLATSPVPEGTG - RCTHFIGILEDITE ETDP - AAIGKTRGSVVDR - TEVQVTLLNYRKDGTFFWNRLATSPVVDETG - KCTHFIGILEDITE ETDP - AAIGKTRGSTAH - TDVNVLLNYRKDGTFFWNRLATSPVVDETG - KCTHFIGILEDITE ETDP - AATIKTRGGTKAH - TDVNVLLNYRKDGSTFWNNLSTSPVVDETG - KCTHFIGILEDITE	HAY 715 KAY 425 IAD 897 IED 895 KOH 888 RDH 721 RDH 721 KHQ 154 KNH 361 RNQ 412 KNQ 419 LEQ 419
WP_010627231.1 WP_102627940.1 WP_112054571.1 WP_161423473.1 WP_159341723.1 WP_146875715.1 TVP44179.1 WP_100821604.1 WP_07587963.1 SEF71116.1 WP_141320011.1 WP_110200210.1 WP_100690146.1	594 LRVLERSVQASINGIVITDASQHD-LPISYVN-EAFLALTGYREEEVLGRNCRMLQGV 304 LRTLGROVEASVNGVYLADAREPD-MPIVYAN-ATFRKHTCYREDEILGRNCRFMQGE 776 LRILERSVEASVHGVLIVDANQTD-MPIIFAN-HAFSRISGYSNAEIKGRNCRFLQGH 774 LLTLERSVEASINGVITVDATQPG-MPLIFVN-QAFSRITGYREEVQGRNCRFLQGP 767 RIFQRSLEASSNGVLICEAQNDD-FPIIFVN-PAFVAITGYREEVQGRNCRFLQGP 600 LRIYQRSLEASSNGVILCEALQDD-YPILYVN-PAFVAITGYQLDDIKGLNGRFLNGG 600 LRIYQRSLEASSNGVILCEALQDD-YPILYVN-PAFVAITGYPLEEVKGHNCRFLNGG 33 RYLFQRSLEASSNGVILGEALQDD-YPILYVN-PAFVAITGYPLEEVKGHNCRFLUGG 240 LHIFERSLQASSNGVILADATQTD-QPIVYAN-PAFVAITGYPLEEVKGNCRFLUGGP 291 LRLLQRGIGASPNGVINADATQPD-MPLVYAN-EAFSQLTGALDEVLGNNCRFLUGGN 298 LRLLQRGIQSSPNGILMADATRHD-LPLVYAN-EAFSQLTGRNCRFLUGN 298 LRLLQRGIQSSPNGILMADATRHD-LPLVYAN-GAFSCHTGFFGSVTGRNCRFLUGG 298 LKLLKRSIESSPSGFLLADAGSPD-LPVVYAN-PAFTAMTGYQDDEIIGRNCRFLUGG 298 LKLLKRGIEASPNGVINADATGP	ETEP- DAVAWLRRCVVERRDCHVTLLNYRKDGSTFWNALYVSPVLDGDG GTHFVGELRDVSEI ETDP- EAVAMIRRHLAEQREVLVTLRNYRKDGTFFWNDAFISPVRDGEG RVTHFVGVLHDISE ETDP- OTVQEIRQGLDDQRDVQVTLCNYRKNGEFFWNDAFISPVRDGEG STHFUGVVNDVTQ ETDP- EAVMKIRRSLVARREVSVTLRNYRKNGEFFWNDLKISPVSNRHG EITHFVGVANDVTQ DTDP- KGVQEICDALLQQRDISLITANYRKNGGRAFWNNVFISPVRADDGQATHFVGIINDISE DTDP- KNIDAIQQALEQQQDIILTIRNYRKNGQAFWNNVFISPVRADDG VVTHFVASINDISE DTDP- KGIADIQAFEQQRDIALTIRNYRKNGQAFWNNLFISPVRADDG RVTHFVGSITDISE DTQP- EQVEALRQALKHGKDISLITANYRKNGQAFWNNLFISPVRADDG RVTHFVGSITDISE DTQP- EQVEALRQALKHGKDISLITANYRKNGQAFWNNLFISPVRADDG RVTHFVGSITDISE DTQP- EQVEALRQALKHGKDISLITANYRKNGQAFWNNLFISPVRADGG RVTHFVGILNDISE DTRP- GOVEATRQALSSCNSVQTTLVNYRKDGTPFWNNVFISPVHASDGQVTHFVGILNDISE ETDP- AAIGKIRQSVVDRTEVQVTLLNYRKDGTPFWNRLAISPVFDETG SCSHFIGTMYDTIRE ETDP- AAIGKIRQSVVDRTEVQVTLLNYRKDGTPFWNRLAISPVFDEGG RCTHFIGILEDITEFTAP AASTOTTRDAL RRCSAVEVTI LNYRRDGSFFWNNI STSPVVDFTG	HAY 715 KAY 425 IAD 897 IED 895 KOH 888 ROH 721 ROH 721 KHQ 154 KNH 361 RNH 419 KEQ 419 REQ 420
WP_010627231.1 WP_102627940.1 WP_112054571.1 WP_161423473.1 WP_159341723.1 WP_159341723.1 WP_10687515.1 TVP44179.1 WP_008317734.1 SEF71116.1 WP_141320011.1 WP_110200210.1 WP_00990146.1 WP_0255109.1	594 LRVLERSVQASINGIVITDASQHD-LPISYVN-EAFLALTGYREEEVLGRNCRMLQGV 304 LRTLQRGVEASVNGVYLADAREPD-MFIVYAN-ATFRKHTGYREDEILGRNCRFNQGE 776 LRILERSVEASVHGVLIVDANIQTD-MFIIFAN-HAFSRISGYSNAEIKGRNCRFLQGH 774 LLTLERSVEASINGVTIVDATQPG-MPLIFVN-DAFSRITGYKEEVQGRNCRFLQGP 767 LRIFQRSLEASSNGVLICEAU,DD-FPIIYVN-PAFVAITGYQLDIKKLNCRFLUGG 608 LRIYQRSLEASSNGIVLCEAL,DD-YPILYVN-PAFVAITGYQLDIKKLNCRFLUGG 33 RYLFQRSLEASSNGIVLGAL,DD-YPILYVN-PAFVAITGYPLEVKGKNGKFLQGG 240 LHIERSLGASSNGVLIADATQTD-OPIVYAN-PAFTGNTGYPIEEVKGRNCRFLQGG 291 LRLQRGIGASPNGVLMADATQPD-MPLVYAN-EAFSQLTGYALDEVLGRNCRFLQGN 292 LRLLQRGIGASPNGVLMADATGPD-MPLVYAN-EAFSQLTGYALDEVLGRNCRFLQGN 298 LRLLQRGIGASPNGVLMADATGPD-MPLVYAN-BAFVRITGYPDDVLGRNCRFLQGN 298 LRLLQRGIGASPNGVLMADATGPD-MPLVYAN-BAFVRITGYPDDVLGRNCRFLQGN 298 LRLLQRGIGASPNGVLMADATGPD-MPLVYAN-PAFTANTGYQDOETIGRNCRFLQGS 298 LKLLKRSIESSPSGFLLADAGSPD-LPVVYAN-PAFTANTGYQDOETIGRNCRFLQGG 299 LHLLRRGLEANPNGMLMVDARSPD-MPVVYAN-PAFTENTGYPHDVGGRNCRFLQGG 399 LHLLRRGLEANPNGMLMVDARSPD-MPVVYAN-PAFTENTGYPHEVIGRNCRFLQGG 399 LHLLRRGLEANPNGMLMVDARSPD-MPVVYAN-PAFTENTGYPHEVIGRNCRFLQGG	ETEP- DAVAWLRRCVVERRDCHVTLLNYRKDGSTFWNALYVSPVLDGDG GTHFVGELRDVSEI ETDP EAVAMIRRHLAEQ - REVLVTLRNYRKDGTFFWNDAFISPVRDGEG RVTHFVGVLHDISE ETDP QTVQEIRQGLDDQ - RDVQVTLCNYRKNGERFWNDLHISPVRDEHG AVSHFIGVVNDVTQ ETTDP EAVMKIRRSLVAR - REVSVTLRNYRKNGERFWNDLHISPVRDEHG EITHFVGVANDVTQ DTDP KQVQEICDALLQQ - RDISLTIRNYRKDGRFWNNLFISPVRAQDG QATHFVGIINDISE DTDP KQVQEICDALLQQ - RDISLTIRNYRKDGAFWNNLFISPVRAQDG QATHFVGIINDISE DTDP KQIADQLAEQQ - RODITLTIRNYRKDGAFWNNLFISPVRAPDG VVTHFVASINDISE DTDP EQVEALRQALKHG - KDISLTIRNYRKDGAFWNNLFISPVRAPDG VTHFVGSITDISE DTOP EQVEALRQALKHG - KDISLTIRNYRKDGRFWNDVFISPVRAPDG VTHFVGSITDISE DTHP EPVAQNHQALSEA - RAVDLTVRNYRKDGRFWNDVFISPVRAPDG VTHFIGILNDISE DTHP GOVEAIRQALSGA - RAVDLTVRNYRKDGRFFWNDVFISPVBASDG VTHFIGILNDISE ETDP AAIGKTRGSVVDR - TEVQVTLLNYRKDGTFFWNNLAISPVFDETG SCSHFIGTNVDITR ETDP AASIDTIRDALRC - SAVEVTLLNYRKDGTFFWNNLAISPVFDETG KCTHFIGILEDITE ETAP ASIDTIRDALRC - SAVEVTLLNYRQDGSTFWNNLSISPVVDETG KCTHFIGILEDITE ETAP ATIKKTRDGIKAH - TDVNVVLLNYRKDGTFFWNNLAISPVFDGGG NCSHFTGSLQDITW DTDAP EALETIRQGLHHQ - TEVNVELINYRKDGTFFWNNLAISPVFDGGG RCTHLIGTHQDITY ETDP AAVAKTRAALSON - REIDVLQNTRKDGTFFWNNLAISPVFDHDG RCTHLIGTHQDITY ETDP AAVAKTRAALSON - REIDVLQNTRKDGTFAWNLAISPVFDHDG RCTHLIGTHQDITY ETDP AAVAKTRAALSON - REIDVLQNTRKDGTFAWNLAISPVFDHGG RCTHLIGTHQDITY ETDP AAVAKTRAALSON - REIDVLQNTRKDGTFAWNLAISPVFDHDG RCTHLIGTHQDITY ETDP AAVAKTRAALSON - REIDVLQNTRKDGTFAWNLAISPVFDHDG RCTHLIGTHQDITY ETDP AAVAKTRAALSON - REIDVLQNTRKDGTFAWNLAISPVFDHDG RCTHLIGTHQDITY	HAY 715 KAY 425 IAD 897 IED 895 KOH 888 ROH 721 ROH 721 KHQ 154 KNH 361 RNIQ 412 KNQ 419 LEQ 419 REQ 420 KKI 1116
WP_010627231.1 WP_102627940.1 WP_112054571.1 WP_161423473.1 WP_159341723.1 WP_146875715.1 TVP44179.1 WP_100821604.1 WP_07587966.1 WP_083517734.1 SEF71116.1 WP_141320011.1 WP_110200210.1 WP_100690146.1	594 LRVLERSVQASINGIVITDASQHO-LPISYVN-EAFLALTGYREEEVLGRNCRMLQGV 304 LRTLQRGVEASVIKGVIXDAREPO-MPIVYAN-ATFIKHTGYREDEILGRNCRFMGGE 776 LRILERSVEASVIKGVLYDANGTO-MPILFWN-QAFSRITGYGKEEVQGRNCRFLQGH 774 LLTLERSVEASINGVTIVDATQPG-MPLIFWN-QAFSRITGYGKEEVQGRNCRFLQGP 767 LRIFGRSLEASSKGVLICEAQNOD-FPILYWN-PAFVAITGYDEDVRRNCRFLQGP 600 LRIYQRSLEASSKGVLICEAQNOD-YPILYWN-PAFVAITGYDLDIKGLKGREHLGGG 600 LRIYQRSLEASSKGVIIGALQDD-YPILYWN-PAFVAITGYPLEEVKGHNCRLLQGK 33 RYLFGRSLEASSKGVIIGATWPE-LPILYTN-PAFTOITGYPFEDVKGLSGRFLQGM 294 LRILGRGIEASPHGVIMADATQTO-OPIVYAN-PAFTANTGYPLEEVKGHNCRFLQGP 295 LRLLGRGIEASPHGVIMADATRID-LPLVYAN-EAFSQLTGYALDEVLGRNCRFLQGN 298 LRLLGRGIESSPGGFLLADAGSPD-LPVYAN-PAFTANTGYPDEVLGRNCRFLQGS 298 LKLLKRSIESSPGGFLLADAGSPD-LPVYYAN-PAFTANTGYQDETIGRNCRFLQGS 299 LHLKRGIEASPHGVIMDATTQD-MPLVYAN-PAFTANTGYQDETIGRNCRFLQGG 299 LHLKRSIESSPGGFLLADAGSPD-LPVYYAN-PAFTANTGYQDETIGRNCRFLQGG 299 LHLLKRSIESSPGGFLLADAGSPD-LPVYYAN-PAFTANTGYQDETIGRNCRFLQGG 299 LHLLKRSIESSPGGFLLADAGSPD-LPVYYAN-PAFTANTGYQDETIGRNCRFLQGG 290 LHLKRSIESSPGGFLADAGSPD-LPVYYAN-PAFTANTGYGNHEVGRNCRFLQGG 297 LHLLGRSGMEASAKGVIIADAKTD-PE-FPLIYNN-PAFTANTGYKHEVGRNCRFLQGG 277 LHLLSRSMEASAKGVIIADAKTD-PE-FPLIYNN-PAFTANTGYKHEVGRNCRFLQGG	ETEP- DAVAWLRRCVVERRDCHVTLLNYRKDGSTFWNALYVSPVLDGDG GTHFVGELRDVSEI ETDP- EAVAMIRRHLAEQREVLVTLRNYRKDGTFFWNDAFISPVRDGEG RVTHFVGVLHDISE ETDP- OTVQEIRQGLDDQRDVQVTLCNYRKNGEFFWNDAFISPVRDGEG STHFUGVVNDVTQ ETDP- EAVMKIRRSLVARREVSVTLRNYRKNGEFFWNDLKISPVSNRHG EITHFVGVANDVTQ DTDP- KGVQEICDALLQQRDISLITANYRKNGGRAFWNNVFISPVRADDGQATHFVGIINDISE DTDP- KNIDAIQQALEQQQDIILTIRNYRKNGQAFWNNVFISPVRADDG VVTHFVASINDISE DTDP- KGIADIQAFEQQRDIALTIRNYRKNGQAFWNNLFISPVRADDG RVTHFVGSITDISE DTQP- EQVEALRQALKHGKDISLITANYRKNGQAFWNNLFISPVRADDG RVTHFVGSITDISE DTQP- EQVEALRQALKHGKDISLITANYRKNGQAFWNNLFISPVRADDG RVTHFVGSITDISE DTQP- EQVEALRQALKHGKDISLITANYRKNGQAFWNNLFISPVRADGG RVTHFVGILNDISE DTRP- GOVEATRQALSSCNSVQTTLVNYRKDGTPFWNNVFISPVHASDGQVTHFVGILNDISE ETDP- AAIGKIRQSVVDRTEVQVTLLNYRKDGTPFWNRLAISPVFDETG SCSHFIGTMYDTIRE ETDP- AAIGKIRQSVVDRTEVQVTLLNYRKDGTPFWNRLAISPVFDEGG RCTHFIGILEDITEFTAP AASTOTTRDAL RRCSAVEVTI LNYRRDGSFFWNNI STSPVVDFTG	HAY 715 KAY 425 LAD 897 LED 895 KOH 888 ROH 721 ROH 721 ROH 721 ROH 721 ROH 741 ROH 741 ROH 412 ROH 419 LEO 419 REQ 419 REQ 410 KKI 1116 LDI 248
WP_010627731.1 WP_1102637940.1 WP_11054571.1 WP_161423473.1 WP_159341723.1 WP_146875715.1 TVP44179.1 WP_075879536.1 WP_083517734.1 SEF71116.1 WP_141320611.1 WP_141320611.1 WP_142051109.1 WP_142051109.1	594 LRVLERSVQASINGIVITDASQHD-LPISYVN-EAFLALTGYREEEVLGRNCRMLQGV 304 LRTLQRGVEASVIKGVYLADAREPD-MPIVYAN-ATFRKHTCYREDETLGRNCRFMQGE 776 LRILERSVEASVIKGVLYADAIQTD-MPILTAN-HAFSRISGYNBALKKERKICKELQGH 774 LLTLERSVEASINGVTIVDATQPG-MPLIFVN-QAFSRITGYGKEEVQGRNCRFLQGP 767 LRIFQRSLEASSINGVLICEAQNDD-FPILTVN-PAFVATTGYQLDDIKGINGRFLQGP 600 LRIYQRSLEASSNGVILICEALQDD-YPILYVN-PAFVATTGYQLDDIKGINGRFLUGG 33 RYLFQRSLEASSNGVILICEALQDD-YPILYVN-PAFVATTGYPLEEVKGHNCRFLUGG 240 LHIFERSLQASSNGVLIADATQTD-QPLYYAN-PAFVATTGYPLEEVKGHNCRFLQGP 291 LRLLQRGICASPNGVLIADATQTD-MPLYYAN-EAFSQLTGYALDEVLGNNCRFLQGP 298 LRLLQRGIGSSPNGILMADATRDD-LPLYYAN-EAFSQLTGYALDEVLGNNCRFLQGP 298 LRLLQRGIGSSPNGILMADATGD-MPLYYAN-EAFSQLTGYALDEVLGNNCRFLQGN 298 LRLLQRGIGSSPNGILMADATGD-MPLYYAN-PAFFANTGYDDOETIGRNCRFLQGN 299 LHLLKRGIEANPNGMLMVDARSPD-MPVYYAN-PAFFANTGYDDOETIGRNCRFUGGE 299 LHLLKRGIEANPNGMLMVDARSPD-MPVYYAN-PAFFANTGYDDOETIGRNCRFUGGE 299 LHLLKRGIEANPNGMLMVDARSPD-MPVYYAN-PAFFANTGYDOETIGRNCRFUGGE 291 LHLLRSSLACYMAVTIADATDGE	ETEP- DAVAWLRRCVVER - RDCHVTLLNYRKDGSTFWNALYVSPVLDGDG GTHFVGELRDVSEI ETDP - EAVAMTRRHLAEQ - REVLVTLRNYRKDGTFFWNDAFTSPVRDGEG RVTHFVGVLHDISE ETDP - OTVQETRGDLDQ - RDVQVTLCNYRKNGERFWNDAFTSPVRDGEG RVTHFVGVINDTG ETDP - EAVMKIRRSLVAR - REVSVTLRNYRKNGESFWNELKISPVSNRHG ETHFVGVÄNDVTQ ETDP - KKQVQETCDALLQQ - RDISLITRNYRKNGGAFWNNVFTSPVRAQDG QATHFVGITNDISE DTDP - KKIDATQQALQQQ - ODITLTRNYRKNGAFWNNVFTSPVRAQDG QVTHFVGSITNDISE DTDP - KQIADIQLAFEQQ - RDIALTIRNYRKNGGAFWNNLFTSPVRADGG QVTHFVGSITDISE DTDP - KQIADIQLAFEQQ - RDIALTIRNYRKNGGAFWNNLFTSPVRANAG RVTHFIGILNDISE DTDP - EQVEALRQALKHG - KOTSLITRNYRKDGRAFWNNLFTSPVRANAG QVTHFIGILNDISE DTPP - EPVAQNHQALSEA - RAVDLTVRNYRKDGRFFWNNLFTSPVRANAG QVTHFIGILNDISE DTRP - GOVEATRQALSSC - INSVQVITLNYRKDGTPFWNRLATSPVFDETG SCSHFIGTWDITTR ETDP - AAIGKTRQSVVDR - TEVQVTLLNYRKDGTFFWNRLATSPVFDETG KCTHFIGILEDITE ETDP - AASIDITRDAI RRC SAVEVTLLNYRKDGTFFWNRLATSPVFDGG RCTHFIGTLEDITE FTAP ATIKKTRGGIKAH - TDVNVLLNYRKDGTFFWNNLATSPVFDGG RCTHFIGTLEDITE TTDP - ATIKKTRGGIKAH - TDVNVLLNYRKDGTFFWNNLATSPVFDGG RCTHFIGTLEDITE TTDP - AAIGKTRAGSVDR - TEVWELTNYRKDGTFFWNNLATSPVFDGG RCTHFIGTLEDITE TTDP - AAIGKTRAGSUDHG - TEVWELTNYRKDGTFFWNNLATSPVFDGG RCTHFIGTLEDITE TTDP - AAIGKTRAGSUDHG - TEVWELTNYRKDGTFFWNNLATSPVFDGG RCTHFIGTLEDITE TTDP - AAIGKTRAGSUDHG - TEVWELTNYRKDGTFFWNNLATSPVFDGG RCTHLIGTNOOTTY ETDP - AAVAKTRALSDD - REIDIVLQNTRKDGTFFWNNLATSPVFDGG RCTHLIGTNOOTTY ETDP - AAVAKTRALSDD - REIDIVLQNTRKDGTFFWNLATSPVFDGG RVENFIGTLNDTQ ETDA - GVVDMTRAGLERE - KQVSVTLLNYRKDGTFFWNLATSPVFDGTG - QVTHFIGTIDDITQ ETDA - GVVDMTRAGLERE - KQVSVTLLNYRKDGTFFWNLATSPVFDGTG - QVTHFIGTIDDITQ	HAY 715 KAY 425 LAD 897 LED 895 KRDH 721 ROH 721 ROH 721 KHQ 154 KNH 361 RNH 419 LEQ 419 KEQ 419 REQ 420 KKKI 1116 LITI 248 KRY 490
WP_010627231.1 WP_102627940.1 WP_112054571.1 WP_112054571.1 WP_161423473.1 WP_159341723.1 WP_146875715.1 TVP44179.1 WP_100821604.1 WP_075879663.1 SEF71116.1 WP_141320011.1 WP_110200210.1 WP_100690146.1 WP_142051109.1 WP_126775935.1 WP_028239827.1	594 LRVLERSVQASINGIVITDASQHD-LPISYVN-EAFLALTGYREEEVLGRNCRMLQGV 304 LRTLQRGVEASVHGVLADAREPD-MPIVYAN-ATFRKHTGYREDEILGRNCRFMQGE 776 LRILERSVEASVHGVLIVDAIQTD-MPIIFAN-HAFSRISGYSNAEIKGRNCRFLQGH 774 LLTLERSVEASINGVITVDATQPG-MPLIFVN-QAFSRITGYKEEVQGRNCRFLQGP 767 RIFQRSLEASSNGVLICEAQNDD-FPIIFVN-PAFVATTGYKEEVQGRNCRFLQGP 600 LRIYQRSLEASSNGVILCEALQDD-YPILYVN-PAFVATTGYQLDDIKGINGRFLNGG 600 LRIYQRSLEASSNGVILCEALQDD-YPIIYVN-PAFVATTGYQLDDIKGINGRFLNGG 600 LRIYQRSLEASSNGVILGEALQDD-YPIIYVN-PAFVATTGYPLEEVKGHNCRFLLQGC 33 RYLFQRSLEASSNGVIIGAATWPE-LPILYTN-PAFTQTTGYPLEEVKGHNCRFLQGG 240 LHIERSLQASSNGVIIADATGTD-OPIVYAN-PAFTQNTGYPLEEVKGRNCRFLQGD 291 LRLLQRGIGASPNGVIHADATGPD-MPLVYAN-EAFSQLTGYALDEVLGRNCRFLQGN 292 LRLLQRGIGSSPNGIIHANDATRHD-LPLYYAN-EAFSQLTGYALDEVLGRNCRFLQGN 293 LRLLKRGIEASPNGVVINADATGPD-MPLVYAN-AFFXRTTGYPDDVLGRNCRFLQGN 294 LRLLKRGIEANPNGHLWDARSPD-MPVVYAN-PAFTANTGYQDDEIIGRNCRFLQGP 295 LHLLKRGIEANPNGHLWDARSPD-MPVVYAN-PAFTANTGYQNDEIIGRNCRFLQGP 296 LHLLKRGIEANPNGHLWDARSPD-MPVYAN-PAFTANTGYQNDEIIGRNCRFLQGP 297 LHLLKRGIEANPNGHLWDARSPD-MPVYAN-PAFTANTGYYMFEVIGRNCRFLQGP 298 LRLLKRSLEASFNGVXIVADARD-HBIYTN-PAFTANTGYAKHEVIGRNCRFLQGP 298 LRLLKRSLEASFNGVXIVADARD-HBIYTN-PAFTANTGYAKHEVIGRNCRFLQGP 298 LRLLKRSLEASFNGVXIVADARD-HBIYTN-PAFFTANTGYTHEVIGRNCRFLQGP 298 LRLLKRSLEASFNGVXIVALADH-PHIYXN-PAFFTANTGYTHFEVIGRNCRFLQGP	ETEP- DAVAMLRRCVVERRDCHVTLLNYRKDGSTFWNALYVSPVLDGDG- GYTHFVGELRDVSEI ETDP- EAVAMIRRHLAEQREVLVTLRNYRKDGTFFWNDAFISPYRDGEG- RVTHFVGVLHDISE ETDP- OTYQELRQGLDQ- RNOVYTLNYRKNGERFWNDAFISPYRDGEG- AVSHFIGVYNDVTQI ETDP- EAVMKIRRSLVARREVSVTLRNYRKNGESFWNELKISPYSNRHG- EITHFVGVÄNDVTQI ETDP- KGVQELCDALLQQRDISLITRNYRKNGGAFWNNVFISPYRADDG- VATHFVGIINDISE ETDP- KKJUALQQALEQQQDIILTIRNYRKNGQAFWNNVFISPYRADDG- VVTHFVASINDISE ETDP- KKJUALQQALEQQQDIILTIRNYRKNGQAFWNNLFLSPYKSHNG- QVTHFVGSITDISE ETDP- EQVEALRQALKHGKDISLITRNYRKNGQAFWNNLFLSPYKSHNG- QVTHFVGSITDISE ETDP- EPVAQWHQALSEARAVDLTVRNYRKDGRAFWNNLFLSPYKSHNG- QVTHFIGIINDISE ETTPP- GOVEALRQALKHGKDISLITRNYRKNGGAFWNNLFLSPYKSHNG- QVTHFIGIINDISE ETTPP- AAIGKIRQSVVDRTEVQVTLNYRKDGTFFWNRLAISPYFDETG- SCSHFIGTWDITTN ETDP- AAIGKIRQSVVDRTEVQVTLNYRKDGTFFWNRLAISPYFDETG- SCSHFIGTWDITTN ETDP- AAIGKIRQSVVDRTEVQVTLNYRKDGTFFWNRLAISPYFDETG- KCTHFIGILEDITE ETAP- AATIKKIRDGKAHTOWNVLLNYRKDGTFFWNNLSTSPYVDFTG- KCTHFIGILEDITE ETAP- ATIKKIRDGKAHTOWNVLLNYRKDGTFFWNNLSTSPYVDFTG- KCTHFIGTIFETTQ- DTAP- EALETIRQGLHHQTEVNVELINYRKDGTFFWNNLSTSPYFDHDG- RCTHLIGTHQDITY ETDP- AAVAKIRAALSONREIDIVLQNTRKDGTFFWNNLSTSPYFDHDG- RVENFIGIILDDITQ- ETDA- GVUDMRAGLRERKQVSVTILNYRKDGTFFWNNLSTSPYFDGGG- MCSHFTGSLIDDITQ- ETDA- GVUDMRAGLRERKQVSVTILNYRKDGTFFWNNLSTSPYFDGGG- RCTHLIGTHQDITY- ETDA- GVUDMRAGLRERKQVSVTILNYRKDGTFFWNDLVISPYFSGSG- RSTHFVGVLNIDITQ- DREQ- RGLEDTRGSLPQEREVHLVLNYNKDGTFFWNDLVISPYFSGSG- RSTHFVGVLNIDISP	HAY 715 KAY 425 IAD 897 IED 895 KOH 888 ROH 721 ROH 721 KKHQ 154 KKHQ 154 KKHQ 412 KKNQ 412 KKQ 419 KEQ 419 KEQ 420 KKI 1116 IDI 248 KKY 496 KKY 151
WP_010627231.1 WP_102627940.1 WP_112054571.1 WP_112054571.1 WP_161423473.1 WP_159341723.1 WP_146875715.1 TVP44179.1 WP_00821604.1 WP_075879636.1 WP_141320011.1 WP_1112000210.1 WP_1141320011.1 WP_110200210.1 WP_126775935.1 HCP_02833827.1 HCT41415.1	594 LRVLERSVQASINGIVITDASQHO-LPISYVN-EAFLALTGYREEEVLGRNCRMLQGV 304 LRTLQRGVEASVIKGVIXDAREPO-MPIVYAN-ATFIKHTGYREDEILGRNCRFMGGE 776 LRILERSVEASVIKGVIXDANGTO-MPITAN-HAFSTGSYDANELKGRNCRFMGGE 774 LLTLERSVEASINGVITVDATQPG-MPLIFVN-QAFSRITGYGKEEVQGRNCRFLQGP 767 LRIFGRSLEASSKIGVILCEAU,DO-YPILYWN-PAFVAITGYDEDVRRHRCRFLQGP 600 LRIYQRSLEASSKIGVILCEAU,DO-YPILYWN-PAFVAITGYDLDIKGLIKGRFLGGG 600 LRIYQRSLEASSKIGVILGAL,DOD-YPILYWN-PAFVAITGYPLEEVKGHNCRLLQGK 33 RYLFGRSLEASSKIGVILGAL,DOD-YPILYWN-PAFVAITGYPLEEVKGHNCRLLQGK 294 LHLURGIEASPNGVLMADATQPO-MPLVYAN-EAFSOLTGYEEVKGHNCRFLQGP 295 LRLLQRGIEASPNGVLMADATQPO-MPLVYAN-EAFSOLTGYEEVKGHNCRFLQGN 298 LRLLGRGIEASPNGVLMADATQPO-MPLVYAN-EAFSOLTGYNGRFLGGN 298 LKLLKRSIESSPSGFLLADAGSPO-LPVVYAN-PAFTANTGYQDEIIGRNCRVLQGP 299 LHLLKRGIEAPWNGMLMVDARSPO-MPVVYAN-PAFTANTGYQDEIIGRNCRVLQGP 299 LHLLKRSIEASYNGTVATADATGPE-FPLTYWN-PAFFANTGYFTHEVGTRNCRFLQGE 127 LHLLRSSLEACYNAVTIADATGPE-FPLTYWN-PAFFANTGYGTRACRFTLQGE 1369 LRLLGRSBASANGVITDALAPO-HPITYTN-PAFFANTGYGASTFTALGRNCRFLQGP 369 LRLLKRSLEASYNGTVADLAPO-HPITYTN-PAFFANTGYFGSEVIGKNCRFLQGP 369 LRLLKRSLEASYNGTVADLAPO-HPITYTN-PAFFANTGYFGSEVIGKNCRFLQGP 360 LRLLGRSLEASYNGTVADLAPO-HPITYTN-PAFFANTGYFGSEVIGKNCRFLQGG 360 LRLLGRSLEASYNGTVADLAPO-HPITYTN-PAFFANTGYFGSEVIGKNCRFLQGG 360 LRLLGRSLEASYNGTVADLAPO-HPITYTN-PAFFANTGYFGSEVIGKNCRFLQGG	ETEP- DAVAWLRRCVVERRDCHVTLLNYRKDGSTFWNALYVSPVLDGDG GYTHFVGELRDVSEI ETDP- EAVAMIRRHLAEQ - REVLVTLRNYRKDGTFFWNDAFISPYRDGEG RYTHFVGVLHDISE ETDP- QTVQEIRQGLDDQ - RDVQVTLCNYRKNGERFWNDLHISPYRDEHG AVSHFIGVVNDVTQ ETTDP- EAVAMIRRHSLVAR - REVSYTLRNYRKNGESFWNLELKISPYSNRHG EITHFVGVANDVTQ DTDP- KGVQEICDALLQQ - RDISLTIRNYRKNGGAFWNNVFISPYRADDG QATHFVGIINDISE DTDP- KNIDAIQQALEQQ - QDITLTIRNYRKNGGAFWNNVFISPYRADDG VYTHFVASINDISE DTDP- KQIADTQLAFEQQ - RDIALTIRNYRKNGGAFWNNLFISPYRADDG VYTHFVGSITDISE DTQP- EQVEALRQALKHG - KDISLTIRNYRKNGGAFWNNLFISPYRADDG RYTHFVGSITDISE DTQP- EQVEALRQALKHG - KDISLTIRNYRKNGGAFWNNLFISPYRDADG RYTHFVGSITDISE DTQP- EQVEALRQALKHG - KDISLTIRNYRKNGGAFWNNLFISPYRDADG RYTHFVGSITDISE DTQP- EQVEALRQALKHG - KDISLTIRNYRKDGRFFWNQVFISPYHASDG SCHFIGTNDITRI ETDP- GDVEAIRQALSSC - RAVDLTVRIVRKDGRFFWNQVFISPYHASDG RTHFIGILNDISE ETDP- AAIGKIRGSVVDR - TEVQYTLLNYRKDGTFFWNNLAISPYFDETG SCSHFIGTNDITRI ETDP- AATIKKRDGIKAH - TDVNVVLLNYRKDGTFFWNNLAISPYFDEGG RCTHFIGILEDITE FTAP - AATIKKRDGIKAH - TDVNVVLLNYRKDGTFFWNNLAISPYFDHOG RCTHFIGSLDDITW DTAP - EALETTRQGLHHO - TEVNVELINYRKDGTFFWNNLAISPYFDHOG RCTHIGTHDOTTY ETDP - AAVAKIRAALSDN - REIDIVLQNTRKDGTFFWNNLAISPYFDHOG RCTHIGTHDOTTY ETDP - GRUEDTRGSCPC - REVIELLYNTRKDGTFFWNDLVISPYSGSG RITHFVGVLNDISE ETDA - GVENDTRAGLRER - KQVSVTILNYRKDGTFFWNDLVISPYSGSG RITHFVGVLNDISE ETDA - MLVEERCGLVQA - RDVHVVLNIYRKDGVLFWNDLVISPISFEQG - VTNFVGVINDITE	HAY 715 KAY 425 LAD 897 LED 895 KOH 888 ROH 721 ROH 721 KKHQ 154 KKHQ 154 KKHQ 1419 LEQ 419 KKQ 419 LEQ 420 KKI 1116 LOII 248 KKRY 499 KKY 151 KKY 489
WP_010627231.1 WP_102627940.1 WP_112054571.1 WP_112054571.1 WP_161423473.1 WP_159341723.1 WP_146875715.1 TVP44179.1 WP_00821604.1 WP_075879636.1 WP_141320011.1 WP_111320011.1 WP_110200210.1 WP_126759935.1 WP_126759935.1 HCT41415.1 WP_090447691.1 WP_127329474.1 WP_127329474.1 WP_127329474.1	594 LRVLERSVQASINGIVITDASQHD-LPISYVN-EAFLALTGYREEEVLGRNCRMLQGV 304 LRTLQRGVEASVHGVYLADAREPD-MPIVYAN-ATFRKHTCYREDEILGRNCRFMQGE 776 LRILERSVEASVHGVLIVDANQTD-MPIIFAN-HAFSRISGYSNAEIKGRNCRFLQGH 777 LRILERSVEASINGVITVDATQPG-MPLIFVN-QAFSRITGYKEEVQGRNCRFLQGP 767 RIFQRSLEASSNGVLICEAQNDD-FPIIFVN-PAFVEITGYDFDDWRRRHCRFLQGP 600 LRIYQRSLEASSNGVILCEALQDD-YPILYVN-PAFVAITGYQLDDIKGLNGRFLNGG 600 LRIYQRSLEASSNGVILCEALQDD-YPILYVN-PAFVAITGYQLDDIKGLNGRFLNGG 33 RYLFQRSLEASSNGVILGEALQDD-YPILYVN-PAFVAITGYQLEDKKGNKGRFLQGG 240 LHIFERSLQASSNGVILGADATQTD-QPIVYAN-PAFVAITGYPLEVKGNKGRFLQGD 291 LRLLQRGIGASPNGVINADATQPD-MPLYVAN-EAFSVLTGYDLEVLGNGNCRFLQGN 292 LRLLQRGIGSSPNGILMADATRHD-LPLYYAN-EAFVAITGYQNDEVIGRNCRFLQGN 293 LRLLKRSIEASPNGVINADATQPD-MPLYVAN-PAFTANTGYQNDEVIGRNCRFLQGN 294 LRLLKRSIEASPNGVINADATQPD-MPLYVAN-PAFTANTGYQNDEVIGRNCRFLQGP 295 LHLLKRSIEASPNGVINADATQPD-MPLYVAN-PAFTANTGYQNDEVIGRNCRFLQGP 296 LRLLKRGIEANPNGMINDOASPD-LPVVYAN-PAFTANTGYQNDEVIGRNCRFLQGP 297 LHLLKRSIEASPNGVINADTQPD-MPLYVYAN-PAFTANTGYQNDEVIGRNCRFLQGP 298 LRLLKRSIEASPNGVVINADATQPD-MPLYYN-PAFTANTGYAKHEVIGRNCRFLQGP 298 LRLLKRSIEASSNGVITADAKKTD-QPLIYWN-PAFTENTGYSKTEVAGRNCRFLQGP 298 LRLLKRSIEASSNGVITADAKKTD-QPLIYWN-PAFTENTGYSKEVETEVLGRNCRFLQGP 298 LRLLKRSIEASSNGVVINDALAPD-HFIYWN-PAFTENTGYSKEVETEVLGRNCRFLQGP	ETEP- DAVAWLRRCVVER-RDCHVTLLNYRKDGSTFWNALYVSPVLDGDG GVTHFVGELRDVSEI ETDP EAVAMIRRHLAEQ - REVLVTLRNYRKDGTFFWNDAFISPYRDGEG RYTHFVGVLHDISE ETDP OTVQEIRQGLDDQ - RDVQVTLCNYRKNGEFFWNDAFISPYRDGEG AVSHFIGVYNDVTQ ETTDP EAVAMIRRHLAEQ - REVSYTLRNYRKNGEFFWNDLHISPYRDEHG AVSHFIGVYNDVTQ ETTDP EAVMCIRSSLVAR - REVSYTLRNYRKNGESFWNLELISPYSNRHG EITHFVGVANDVTQ DTDP KGVQEICDALLQQ - RDISLITIRNYRKNGGAFWNNVFISPYRADDG VYTHFVASINDISE DTDP KNIDAIQQALEQQ - QDITLITIRNYRKNGAFWNNVFISPYRADDG VYTHFVASINDISE DTDP KQIADTQLAFEQQ - RDIALTIRNYRKNGAFWNNVFISPYRAPDG VYTHFVGSITDISE DTQP EQVEALRQALKHG - KDISLITIRNYRKNGAFWNNVFISPYRADDG RYTHFIGILNDISE DTQP EQVEALRQALKHG - KDISLITIRNYRKNGAFWNNVFISPYRADDG RYTHFIGILNDISE DTQP GOVEATRQALSSC - NSVQTLYNYRKDFFFWNNVFISPYHASDG SCHIGTMVDITR ETDP AAIGKIRQSVVDR - TEVQVTLLNYRKDFFFWNNLAISPYVDETG SCSHIGTMVDITR ETDP AAIGKIRQSVVDR - TEVQVTLLNYRKDGFFWNNLSISPYVDFTG RCTHFIGILEDITE FTAP ASTDTTRDAL RRC - SAVEVTL NYRKDGSFFWNNL STSPYVDFTG RCTHFIGILEDITE FTAP AAIGKIRQSVADR - TEVQVTLLNYRKDGFFWNNLAISPYVDFTG RCTHFIGILEDITE FTAP AAIGKIRQSKAH - TDVNVVLLNYRKDGFFWNNLAISPYVDFDGG NCSHFTGSLQDITW TOTAP EALETTRQGLHHO - TEVNVELINYRKDGTFFWNNLAISPYVDFDGG RCTHLIGTHQDITY ETDP AAVAKIRAALSON - REIDIVLQNTRKDGTFFWNNLAISPYVPDEGG RCTHLIGTHQDITY ETDA GVVDMTRAGLRER - KQVSVTLLNYRKDGTFFWNNLYSPYPDEGG RVFNIFGILINDITQ ETDA GVGVDMTRAGLRER - KQVSVTLLNYRKDGTFFWNDLYISPYFSGSG RTTHFVGVLNDISE FTAP MLVEEIRCGLVQA - RDVHVVLRNYRKDGSFFWNDLYISPYFSGSG RTITHFVGVLNDISE ERDP MLVEEIRCGLVQA - RDVHVVLRNYRKDGSFFWNDLYISPYFSGG VTINFVGVINDITE ERDP NBGALDEIREGLKKQ - SPVKVVLRNYRKDGSFFWNDLYLSPTRDQG OVTHFIGUINDISD	HAY 715 KAY 425 LAT 25 KAY 425 LAT 26 KAY 426 LAT 26 KAY 419 LAT 2
WP_010627231.1 WP_102627940.1 WP_110264571.1 WP_161423473.1 WP_159341723.1 WP_164875715.1 TVP44179.1 WP_00821604.1 WP_075879636.1 WP_083517734.1 SEF71116.1 WP_114206110.1 WP_1142061109.1 WP_142051109.1 WP_142051109.1 WP_126775935.1 WP_028239827.1 HCT41415.1 WP_090447691.1 WP_127329474.1 WP_1066944265.1 WP_106694265.1 WP_1066694265.1	594 LRVLERSVQASINGIVITDASQHO-LPISYVN-EAFLALTGYREEEVLGRNCRMLQGV 304 LRTLQRGVEASVIKGVIXDAREPO-MPIVYAN-ATFIKHTGYREDEILGRNCRFMGGE 776 LRILERSVEASVIKGVIXDANGTO-MPITAN-HAFSTGSYDANELKGRNCRFMGGE 777 LLTLERSVEASINGVITVDATQPG-MPLIFVN-QAFSRITGYGKEEVQGRNCRFLQGP 778 LRIFGRSLEASSKIGVICCEAUDO-PFILYWN-PAFVAITGYDEDVRRHRCRFLQGP 600 LRIYQRSLEASSKIGVICCEAU,OD-YPILYWN-PAFVAITGYDLDIKGLKGREKHGGO 600 LRIYQRSLEASSKIGVITGALQOD-YPILYWN-PAFVAITGYPLEEVKGHNCRLLQGK 33 RYLFGRSLEASSKIGVITGALTGP-LPILYWN-PAFVAITGYPLEEVKGHNCRLLQGK 294 LHIFERSLQASSKIGVILADATGTO-PILYWN-PAFVAITGYPLEEVKGHNCRLGGM 295 LRLLQRGIEASPNGVLMADATGPO-HPLYYAN-EAFSQLTGYBLEWGRNCRFLQGN 298 LRLLGRGIEASPNGVLMADATGPO-HPLYYAN-EAFSQLTGYRGREFLQGN 298 LRLLGRGIEASPNGVLMADATGPO-HPLYYAN-EAFSQLTGYRGRFLGGN 298 LKLLKRSIESSPSGFLADAGSPO-LPVYYAN-PAFTANTGYQDEITGRNCRFLQGN 299 LHLLKRSIESSPSGFLADAGSPO-LPVYYAN-PAFTANTGYQDEITGRNCRFLQGP 299 LHLLRSSLBASYNGTUNDARSPO-MPVYYAN-PAFTANTGYGNGTRIGRFLQGG 295 LHLLRSSLBASYNGTVTDALAPO-HPITYTN-PAFEANTGYAREVIGNRCRFLQGP 369 LRLLGRSCHASANGVITDALAPO-HPITYTN-PAFEANTGYAREVIGNRCRFLQGP 369 LRLLGRSCHASSNYGTUNDALAPO-HPITYTN-PAFEANTGYAREVIGNRCRFLQGP 360 LRLLGRSLBASYNGTUNDALAPO-HPITYTN-PAFEANTGYAREVIGNRCRFLQGP 361 LRLGRSLBASYNGTUNDALAPO-HPITYTN-PAFEANTGYAREVIGNRCRFLQGP 362 LRLLGRSLBASYNGTUNDALAPO-HPITYTN-PAFEANTGYAREVIGNRCRFLQGG 363 LRLKRSIESTTNGTVANHAND-LPITYWN-PAFEANTGYSABETTGNRCRFLQGG 255 LKLLKRSIESTNGUNTANHAND-LPITYWN-PAFEANTGYSABETTGNRCRFLQGG 257 LKLLKRGIESSSNGUNTDALAED-MPLYYWN-PAFEANTGYSABETTGNRCRFLQGG	ETEP- DAVAWLRRCVVER - RDCHVTLLNYRKDGSTFWNALYVSPVLDGDG GVTHFVGELRDVSEI ETDP - EAVAMTRRHLAEQ - REVLVTLRNYRKDGTFFWNDAFTSPVRDGEG RVTHFVGVLHDISE ETDP - OTYQETRGDLDO - RDVQVTLCNYRKNGERFWNDLHTSPVRDEHG AVSHTGVVNDVTQ ETDP - EAVHKIRRSLVAR - REVSVTLRNYRKNGESFWNELKISPVSNRHG EITHFVGVÄNDVTQ ETDP - KKQVGETCDALLQQ - RDISLITRNYRKNGGAFWNELFSPVRAQDG QATHFVGITNDISE DTDP - KKQIADLQQ ODTITLTRNYRKNGGAFWNNLFISPVRAQDG QVTHFVGSITDISE DTDP - KQIADIQLAFEQQ - RDIALTIRNYRKNGGAFWNNLFISPVRADDG QVTHFVGSITDISE DTDP - KQIADIQLAFEQQ - RDIALTIRNYRKNGGAFWNNLFISPVRANAG RVTHFIGILNDISE DTDP - EQVEALRQALKHG - KOISLITRNYRKNGGAFWNNLFISPVRANAG RVTHFIGILNDISE DTPP - EPVAQHNAGLSEA - RAVDLTVRNYRKDGFFWNNLFISPVRDNAG RVTHFIGILNDISE DTRP - GOVEALRQALKHG - KOISLITRNYRKNGGAFWNNLFISPVRDNAG RVTHFIGILNDISE DTRP - GOVEALRQALKHG - KOISLITRNYRKNGGAFWNNLFISPVRDNAG RVTHFIGILNDISE DTRP - GOVEALRQALKHG - KOISLITRNYRKNGGFFWNNLFISPVFDETG SCSHFIGTNVDITR ETDP - AAIGKTRQSVVDR - TEVQVTLLNYRKDGTPFWNRLAINPVFDEAG RCTHFIGILDITE FTAP - AAIGTRABA RC SAAVEVTLINYRDGTFFWNNLSTSPVVFDETG SCHFIGTNVDITR HTDP - ATIKKRDGIKAH - TDVNVVLLNYRKDGTPFWNLSTSPVVFDGG NCSHFTGSLQDITW HTDP - AAIAKTRABLSDN - REIDIVLQNTRKDGTFFWNLLSTSPVFDHDG RVCHFIGTNDITQ ETDP - AAVAKTRAALSDN - REIDIVLQNTRKDGTFFWNLLSTSPVFDHDG RVCHFIGTNDITQ ETDP - AAVAKTRAALSDN - REIDIVLQNTRKDGTFFWNLLSTSPVFDHG RVCHFIGTNDITQ ETDA - GVVDMTRAGLRER - KQVSVTLLNYRKDGTFFWNLLVISPVFSGSG RITHFVGVLNDISE ETDA - GVVDMTRAGLERE - KQVSVTLLNYRKDGTFFWNLLVISPVFSGSG RITHFVGVLNDISE ETDA - GVVDMTRAGLERE - KQVSVTLLNYRKDGTFFWNLLVISPVFSGSG RITHFVGVLNDISE ETDA - GVVDMTRAGLERE - KQVSVTLLNYRKDGTFFWNLLVISPVFSGG VTTNFVGVINDITE ETDA - GRUEDTRGLLQQ - ROTHVVLNIFKNDGTFFWNLDLYISPVFSGG RSHFICVLNNISE ETDP - MLVEEIRCGLVQA - ROVHVVLRNYRKDGTFFWNLDLYISPVFSGG VTTNFVGVINDITE ETDA - GVJDATRAGLERE - KQVSVVLLNYRKDGTFFWNLDLYISPVFSGG - VTTNFVGVINDITE ETDA - GVJDATRAGLERE - KQVSVVLLNYRKDGTFFWNLDLYISPVFSGG - VTTNFVGVINDITE ENDP - NDGALLEREGLKXQ - SPSVVVLNYRKDGTFFWNLDLYISPVFDGG - VTTNFVGVINDISE ENDD - TTTLATRGGLETR - QQLHVLLNYRKDGTFFWNLDLYISPFRDDDG - TTTHFVGVLNDISE ENDS - NEGALLGIRKGLERE - QQLSV	HAY 715 KAY 425 LAT 25 KOH 888 ROH 721 KHQ 154 KHQ 154 KHQ 419 LEQ 419 KEQ 419 KEQ 419 KEQ 419 KEQ 429 KKY 490 KKY 489 KSA 382 KSA 382 KSS 381 REY 281
WP_010627231.1 WP_102627940.1 WP_112054571.1 WP_161423473.1 WP_159341723.1 WP_146875715.1 TVP44179.1 WP_00821604.1 WP_075879636.1 WP_083517734.1 SEF71116.1 WP_141320011.1 WP_106690146.1 WP_142051109.1 WP_106890146.1 WP_142051109.1 WP_028239827.1 HCT41415.1 WP_090447691.1 WP_127329474.1 WP_106694265.1 WP_127329474.1 WP_106694265.1 WP_127329476.1	594 LRVLERSVQASINGIVITDASQHO-LPISYVN-EAFLALTGYREEEVLGRNCRMLQGV 304 LRTLQRGVEASVNGWYIADAREPO-MPIVYAN-ATFRKHTGYREDEILGRNCRFMQGE 776 LRILERSVEASVNGVLYDANQTO-MPILTAN-HAFSRISGYNAELKGRNCRFMQGE 777 LLTLERSVEASINGVTIVDATQPG-MPLIFVN-QAFSRITGYGKEEVQGRNCRFLQGP 767 LRIFQRSLEASSNGVLICEAQNDO-PPILYWN-PAFVATTGYDDDVRRRNCRFLQGP 600 LRIYQRSLEASSNGVILCEALQDD-YPILYWN-PAFVATTGYQLDIKGLKGRFLNGG 600 LRIYQRSLEASSNGVILGEALQDD-YPILYWN-PAFVATTGYPLEEVKGHNCRFLQGC 33 RYLFQRSLEASSNGVILGEALQDD-YPILYWN-PAFVATTGYPLEEVKGHNCRFLQGG 240 LHIFERSLQASSNGVILGDATQTD-QPIVYAN-PAFVATTGYPLEEVKGHNCRFLQGG 291 LRLLQRGIEASPHGVJHADATQPD-MPLYYAN-EAFSQLTGYALDEVLGNNCRFLQGG 292 LRLLQRGIEASPHGVJHADATQPD-MPLYYAN-EAFSQLTGYALDEVLGNNCRFLQGG 293 LRLLQRGIEASPHGVJHADATQPD-MPLYYAN-PAFTANTGYQDEITGRNCRFLQGG 294 LKLLKRSIESSPSGFLLADAGSPD-LPVYAN-PAFTANTGYQDEITGRNCRFLQGG 295 LHLLKRGIEASPHGVJHADATDPD-FPLIYVN-PAFEANTGYQDEITGRNCRFLQGG 296 LKLLKRSIEASYNGVIYDALSPD-HPVYYAN-PAFEANTGYQDEITGRNCRFLQGG 297 LHLLRSSMEASANGVITDALAPD-HPILYTN-PAFEANTGYAHEVIGRNCRFLQGG 360 LRLLGRSLASYNGTVADAKTD-QPLYVN-PAFEANTGYAHEVIGRNCRFLQGG 361 LRLLGRSLASYNGTVADAKD-LPILYWN-PAFEANTGYAHEVIGRNCRFLQGG 362 LRLLGRSLASYNGTVADAKD-LPILYWN-PAFEANTGYAKHEVIGRNCRFLQGD 253 LKLLKRSIESSTNGTVADAKD-HPILYTN-PAFEATTGYAREVIGRNCRFLQGD 254 LKLLKRSIESSTNGTVADAKD-LPILYWN-PAFEATTGYAREVIGRNCRFLQGD 255 LKLLKRSIESSTNGTVADALAED-MPLVYN-PAFEATTGYAREVIGRNCRFLQGG 256 LKLLKRSIESSTNGTVADALAED-MPLVYN-PAFEATTGYAREVIGRNCRFLQGG 257 LKLLKRSIESSTNGTVADALAED-MPLVYN-PAFEATTGYAREVIGRNCRFLQGG 257 LKLLKRSIESSTNGTVADALAED-MPLVYN-PAFEATTGYAREVIGRNCRFLQGG	ETEP- DAVAWLRRCVVER - RDCHVTLLNYRKDGSTFWNALYVSPVLDGDG GYTHFVGELRDVSEI ETDP - EAVAMIRRHLAEQ - REVLVTLRNYRKDGTFFWNDAFISPVRDGEG RVTHFVGVLHDISE ETDP - OTYQEIRQGLDQ - RNOVTLKINYRKDGTFFWNDAFISPVRDGEG - RVTHFVGVLHDISE ETDP - EAVMKIRRSLVAR - REVSVTLRNYRKNGESFWNELKISPVSNRHG EITHFVGVÄNDVTQ ETDP - EAVMKIRRSLVAR - REVSVTLRNYRKNGGSFWNELKISPVSNRHG - EITHFVGVÄNDVTQ DTDP - KKQVQEICDALLQQ - RDISLITRNYRKNGGAFWNNVFISPVRAQDG - VATHFVGIINDISE DTDP - KKQIADIQAFEQQ - QDITLTIRNYRKNGQAFWNNLFISPVRAPDG - VYTHFVGSITDISE DTDP - KQIADIQAFEQQ - RDIALTIRNYRKNGGAFWNNLFISPVRAPDG - VYTHFVGSITDISE DTDP - EQVEALRQALKHG - KDISLITRNYRKDGAFWNNLFISPVRAPDG - QVTHFIGILNDISE DTPP - EPVAQMHQALSEA - RAVDLTVRNYRKDGRFFWNNLFISPVRAPDG - QVTHFIGILNDISE DTPP - GOVEAIRQALSG - NSVQVILVINYRKDGTFFWNRLAINPVFDETG - SCSHFIGTNDISTE ETDP - AAIGKIRQSVVDR - TEVQVTLLNYRKDGTFFWNRLAINPVFDEAG - RCTHFIGILEDITE ETDP - AASIDITIRDALRG - SAVEVTIL NYRQDGSTFWNNLSISPVVDETG - KCTHFIGTLEFITQ NTTDP - ATIKKIRDGIKAH - TDVNVULLNYRKDGTFFWNHLAISPVFDGG - NCSHFTGSLQDITW DTAP - EALETIRQGLHHG - TEVWVELTNYRKDGTFFWNHLAISPVFDGG - RVENFIGTINDITQ ETDP - AAVAKIRAALSDN - REIDIVLQNTRKDGTFFWNHLLSPVPNDEG - RVENFIGTINDITQ ETDP - AAVAKIRAALSDN - REIDIVLQNTRKDGTFFWNDLLISPVFDGG - RVENFIGTINDITQ DTAP - EALETIRQGLHG - TEVWVELTNYRKDGTFFWNDLYISPVFDGG - RVENFIGTINDITQ DTAP - GVOMTRAGLERE - KQVSVTILNYRKDGTFFWNDLYISPVFDGG - RVENFIGTINDITQ DREQ - RGLEDIRQSLPQE - REVHLVLRNYRKDGTFFWNDLYISPVFSGG - RITHFVGVLNDISE ETDD - MCCHERGGLQQ - RDITVLRNYRKDGTFFWNDLYISPTFSGG - VITNFVGVLNDITE ETDA - GVOMTRAGLERE - KQVSVTILNYRKDGTFFWNDLYISPTFSGG - VITNFVGVLNDITE ETDA - GVOMTRAGLERE - KQVSVTLLNYRKDGTFFWNDLYISPTFSGG - VITNFVGVLNDITE ETDA - GVOMTRAGLERE - KQVSVTLLNYRKDGTFFWNDLYISPTFSGG - VITNFVGVLNDITE ETDA - GVOMTRAGLERE - KQVSVTLLNYRKDGSFFWNDLYLSPTFSGG - VITNFVGVLNDITE ETDA - GVOMTRAGLERE - KQVSVTLLNYRKDGSFFWNDLYLSPTFSGG - VITNFVGVLNDITE ETDA - GVOMTRAGLERE - KQVSVTLLNYRKDGSFFWNDLYLSPTFSGG - VITNFVGVLNDISE TADPF - NDGALNEIREGLKQ - SPVKVVLRNYRKDGSFFWNDLYLSPTRDQN - VTTHFGVLNDISD THREST - TRENTRAGTER - TRANSPROTTER TRANSPLOTTER TRANSPLOTTE	HAY 715 KAY 425 IAD 895 KOH 888 ROTH 721 ROH 721 ROH 721 ROH 741 ROH 7
WP_010627231.1 WP_102627940.1 WP_112054571.1 WP_112054571.1 WP_161423473.1 WP_159341723.1 WP_146875715.1 TVP44179.1 WP_00821604.1 WP_008517734.1 SEF71116.1 WP_141320011.1 WP_110200210.1 WP_10690146.1 WP_142051109.1 WP_126775935.1 WP_028239827.1 HCT41415.1 WP_098239827.1 HC741415.1 WP_106694265.1 WP_134847999.1 WP_137840462.1	594 LRVLERSVQASINGIVITDASQHD-LPISYVN-EAFLALTGYREEEVLGRNCRMLQGV 304 LRTLQRGVEASVIKGVYLADAREPD-MPIVYAN-ATFRKHTCYREDEILGRNCRFMQGE 776 LRILERSVEASVIKGVLIVDANQTD-MPIIFAN-HAFSRISGYSNAEIKGRIKGRELQGH 777 LLTLERSVEASINGVITVDATQPG-MPLIFWN-QAFSRITGYGKEEVQGRNCRFLQGP 767 LRIEGRSLEASSINGVLICEAQNDD-FPIIFWN-PAFVEITGYDFDDWRRRIKGRELQGP 600 LRIYQRSLEASSNGVLICEAQNDD-FPIIFWN-PAFVAITGYQLDDIKGINGRFLNGG 600 LRIYQRSLEASSNGVILICEALQDD-YPILYWN-PAFVAITGYQLDDIKGINGRFLNGG 33 RYLFQRSLEASSNGVILICEALQDD-YPILYWN-PAFVAITGYPLEEVKGHKCRELQGG 240 LHIFERSLQASSNGVLIADATQTD-QPIVYAN-PAFVAITGYPLEEVKGHKCRELQGG 291 LRLLQRGIGASPNGVLIMADTQPD-MPLYVAN-EAFSQLTGYALDEVLGWNCRFLNGG 292 LRLLQRGIGASPNGVLIMADTQPD-MPLYVAN-EAFSQLTGYALDEVLGWNCRFLQGN 293 LRLLKRSIESSPSGFLANDATQPD-MPLYVAN-PAFFVAITGYPDDVLGRNCRFLQGN 294 LRLLKRSIESSPSGFLANDASPD-MPVYYAN-PAFFVAITGYDDQDEITGRNCRFLQGN 295 LHLLKRGIEANPNGNILMVDARSPD-MPVVYAN-PAFFVAITGYDDQDEITGRNCRFLQGC 296 LRLLKRSIESSPSGFLANDASPD-MPVVYAN-PAFFVAITGYDDQDEITGRNCRFLQGC 297 LHLLKRSLEASYNGVIVDALSPD-HPVVYAN-PAFFARTTGYSTEVLGRNCRFLQGC 30 LHLKRSLEASYNGVIVDALSPD-HPIYVN-PAFERTTGYSTEVLGRNCRFLQGG 30 LRLKRSLEASSNGVVIDALAPD-HPIYYN-PAFERTTGYSTGVEUNGKRELQGG 30 LHLKRSLEASYNGVIVDALSPD-HPVYN-PAFERTTGYSTGVEUNGKRELQGG 30 LHLKRSLEASYNGVIVDALSPD-HPIYVN-PAFERTTGYSTGVEUNGKRELQGG	ETEP- DAVAMLRRCVVER-RDCHVTLLNYRKDGSTFWNALYVSPVLDGDG GVTHFVGELRDVSEI ETDP- EAVAMIRRHLAEO - REVLVTLRNYRKDGTFFWNDAFISPYRDGEG RYTHFVGVILHDISE ETDP- OTVQETRGGLDQO - ROVQVTLCNYRKNGEFFWNDAFISPYRDGEG - RYTHFVGVILHDISE ETDP- EAVAMIRRHLAEO - REVLVTLRNYRKNGEFFWNDLHISPYRDGEG - AVSHFIGVYNDVTQ ETDP- EAVEKTRRSLVAR - REVSYTLRNYRKNGESFWNLEKISPYSNRHG EITHFVGVÄNDVTQ DTDP- KGVQETCDALLQO - ROISLITRNYRKNGGAFWNNVFISPYRADDG - QATHFVGITNDISE DTDP- KNIDAIQQALEQO - QDITLTIRNYRKNGQAFWNNLFLSPYKASHIG - QVTHFVGSITDISE DTDP- KQUALOFQQ - ROISLITRNYRKNGQAFWNNLFLSPYKSHHG - QVTHFVGSITDISE DTDP- EQVEALRQALKHG - KOISLITRNYRKNGQAFWNNLFLSPYKSHHG - QVTHFVGSITDISE DTDP- EQVEALRQALKHG - KOISLITRNYRKNGQAFWNNLFLSPYKSHHG - QVTHFIGILNDISE DTDP- EQVEALRQALKHG - KOISLITRNYRKNGQAFWNNLFISPYRDNAG RYTHFIGILNDISE DTDP- GOVEATRGALSSC - NSVQVTLNYRKDGTPFWNQFISPYHASDG - QVTHFIGILNDISE ETDP- AAIGKIRQSVVDR - TEVQVTLLNYRKDGTPFWNRLAISPYPDETG - SCSHFIGTMVDITR ETDP- AAIGKIRQSVVDR - TEVQVTLLNYRKDGTPFWNRLAISPYPDETG - KCTHFIGILEDITE ETDP- AAIKTRGGKAH- TOWNVLLNYRKDGTPFWNNLSTSPYDFDGG - NCSHFTGSLQDITW DTAP- EALETIRQGLHHQ - TEVNVELINYRKDGTPFWNNLTSPYVDFTG - RCTHLIGTHQDITY DTAP - EALETIRQGLHHQ - TEVNVELINYRKDGTFPWNHLFISPYFDHDG - RCTHLIGTHQDITY ETDA - GVVDMTRAGLRER - KQVSVTILNYRKDGTFPWNLVISPYFSSGG - RITHFVOVLNDISE ETDA - GVVDMTRAGLRER - KQVSVTILNYRKDGTFPWNDLYISPYFSSGG - RTHFIGUINDITQ DREQ - RGLEDTRQSLPQE - REVHLVLRNYRKDGTFPWNDLYISPYFSSGG - RYTHFIGVINDISE ERDP - MLVEETRGGLVQA - ROVHVVLRNYRKDGTFPWNDLYISPYFDSGG - RVSHFIGVINDISE ERDP - MCDALLETREGLQQ - ROVHVVLRNYRKDGTFPWNDLYISPYFDSGG - RYTHFIGVINDISE ERDD - PGLTETRIG.QQ - ROVHVVLRNYRKDGTFPWNDLYISPYFDDG - RVSHFIGVINDISE ERDD - MLVEETRGGLVQA - ROVHVVLRNYRKDGTFPWNDLYISPYFDSGG - RVSHFIGVINDISE ERDD - PGLTETRIG.QQ - ROVHVVLRNYRKDGTFPWNDLYISPYFDGG - TTTHFVGVLNDISE ERDD - PGALTERIG.QQ - ROVHVVLRNYRKDGTFPWNDLYLSPPDDGG - TTTHFVGVLNDISE ERDD - GALAURGAGR - DDISVVLRNYRKDGTFPWNDLYLSPPDDGG - TTTHFVGVLNDISE EFDLS - NEQALDQIRGLARG - DDISVVLRNYRKDGTFPWNDLYLSPFDDGG - TTTHFVGVLNDISE	HAY 715 KAY 425 LAT 25 KAY 425 LAT 26 KAY 425 LAT 26 KAY 425 LAT 26 KAY 425 LAT 26 KAY 426 KAY 496 KKY 486 KKY 486 KKY 496 KKY 486 KKY
WP_010627231.1 WP_112054571.1 WP_112054571.1 WP_116423473.1 WP_159341723.1 WP_159341723.1 WP_10821604.1 WP_075879636.1 WP_10821604.1 WP_083517734.1 SEF71116.1 WP_1112000210.1 WP_114132011.1 WP_110200210.1 WP_126775935.1 WP_108239827.1 HCT41415.1 WP_028239827.1 HCT41415.1 WP_1273229474.1 WP_1273229474.1 WP_1273229474.1 WP_137340462.1 WP_137840462.1 WP_137840462.1 WP_009553309.1	594 LRVLERSVQASINGIVITDASQHD-LPISYVN-EAFLALTGYREEEVLGRNCRMLQGV 304 LRTLQRGVEASVINGVIADAREPD-MPIVYAN-ATFRKHTGYREEULGRNCRFNQGE 776 LRILERSVEASVINGVLIVDAIQTD-MPIIFAN-HAFSRISGYSNAEIKGRNCRFLQGH 776 LRILERSVEASVINGVLIVDAIQTG-MPIIFAN-HAFSRISGYSNAEIKGRNCRFLQGF 767 LRIEGRSLEASSINGVLICEAQNDD-FPIIFVN-PAFVEITGYDEDWRRRIKGRFLQGP 600 LRIYQRSLEASSINGVLICEAQNDD-FPIIFVN-PAFVAITGYQLEDDIKGNCRFLNGG 600 LRIYQRSLEASSINGVLICEALQDD-YPILYVN-PAFVAITGYQLEDDIKGNCRFLNGG 81 RYLFQRSLEASSINGVLICEALQDD-YPILYVN-PAFVAITGYQLEDWRGNCRFLQGG 240 LHIERSLQASSINGVLIADATOTD-OPIVYAN-PAFVAITGYPLEVKGNCRFLNGG 291 LRLLQRGIGASPNGVLMDATGPD-MPLVYAN-EAFSQLTGYALDEVLGNNCRFLQGN 292 LRLLQRGIGASPNGVLMDATGPD-MPLVYAN-EAFSQLTGYALDEVLGNNCRFLQGN 298 LRLLQRGIGASPNGVLMDATGPD-MPLVYAN-EAFSVRITGYPDDVLGNNCRFLQGN 299 LHLLKRGIEASPNGVLMDATGPD-MPLVYAN-PAFTANTGYPDDEVLGNNCRFLQGN 299 LHLLKRGIEASPNGVLMDATGPD-MPLVYAN-PAFTANTGYPDDEVLGNNCRFLQGD 299 LHLLKRGIEASPNGVLMDATGPD-MPLVYAN-PAFTANTGYQNDETIGRNCRFLQGP 360 LRLLGRGIASSPNGVLMDATGPD-MPLYYNN-PAFTANTGYQNDETIGRNCRFLQGP 370 LRLLKRSLEASFNGVJTDALPD-HPITYNN-PAFTANTGYPHEVIGRNCRFLQGP 371 LRLKRSLEASFNGVJTDALPD-HPITYNN-PAFFENTGYSAAETIGRNCRFLQGP 258 LRLLKRSLEASFNGVJTDALPD-HPITYNN-PAFFENTGYSAAETIGRNCRFLQGD 258 LRLLKRSLEASFNGVJTDALPD-HPITYNN-PAFFENTGYSAAETIGRNCRFLQGD 258 LRLLKRSLEASFNGVJTVDALSHD-LPITYNN-PAFFENTGYSAAETIGRNCRFLQGD 258 LRLLKRSLESSSNGVTVDALSHD-LPITYNN-PAFFENTGYSAEETIGNCRFLQGG 257 LKLLKRGIESSSNGVTVDALSHD-LPITYNN-PAFFENTGYFREEVLGRNCRFLQGG	ETEP- DAVAWLRRCVVER-RDCHVTLLNYRKDGSTFWNALYVSPVLDGDG GYTHFVGELRDVSEI ETDP EAVAMIRRHLAEQ - REVLVTLRNYRKDGTFFWNDAFISPYRDGEG RYTHFVGVLHDISE ETDP QTVQEIRQGLDDQ - RDVQVTLCNYRKNGEFFWNDAFISPYRDGEG AVSHFIGVVNDVTQ ETTDP EAVAMIRRHLAEQ - REVSYTLRNYRKNGEFFWNDAFISPYRDGEG AVSHFIGVVNDVTQ ETTDP EAVMCIRSSLVAR - REVSYTLRNYRKNGESFWNLELISPYSNRHG EITHFVGVANDVTQ DTDP KGVQEICDALLQQ - RDISLITIRNYRKNGGAFWNNVFISPYRADDG QATHFVGIINDISE DTDP KNIDAIQQALEQQ - QDITLITIRNYRKNGGAFWNNVFISPYRADDG VVTHFVGSITDISE DTDP KQIADTQLAFEQQ - RDIALTIRNYRKNGGAFWNNLFISPYRADDG RYTHFVGSITDISE DTDP EQVEALRQALKHG - KDISLITIRNYRKNGGAFWNNLFISPYRADDG RYTHFVGSITDISE DTDP EQVEALRQALKHG - KDISLITIRNYRKNGGAFWNNLFISPYRDADG RYTHFVGSITDISE DTDP EQVEALRQALKHG - KDISLITIRNYRKNGGAFWNNLFISPYRDADG RYTHFIGILNDISE DTDP GOVEAIRQALSSC - RAVDLITVRNYRKDGRFFWNQVFISPYHASDG RYTHFIGILNDISE DTRP GOVEAIRQALSSC - NSVQVTLVNYRKDGTFFWNNLAISPYFDETG SCSHFIGTNDITR ETDD AAIGKTRGSVVDR - TEVQVTLLNYRKDGTFFWNNLAINPYFDEAG RCTHFIGILEDITE FTAP ASTOTTRDA IRRC - SAVEVTILNYRKDGFFFWNNLAINPYFDEAG RCTHFIGILEDITE FTAP ASTOTTRDA IRRC - SAVEVTILNYRKDGFFFWNNLAISPYFDHOG RCTHFIGILDITQ DTAP EALETIRGGLHHO - TEVNVELINYRKDGTFFWNNLAISPYFDHOG RCTHFIGILDITQ ETDD AAVAKIRAALSDN - REIDIVLQNTRKDGTFFWNNLAISPYFDHOG RCTHFIGILDITQ ETDD AAVAKIRAALSDN - REIDIVLQNTRKDGTFFWNNLAISPYFDHOG RCTHFIGILDITQ ETDD GVGWIRAGLRER - KQVSVTILNYRKDGTFFWNDLVISPYFSGG RITHFVGVLNDISE ETDD BAQALRIERGLAGQ - RDVHVVLRNYRKDGSFFWNDLVISPYFSGG RITHFVGVLNDISE ERDP MLVEEIRCGLVQA - RDVHVVLRNYRKDGSFFWNDLVISPYFDGG VITNFVGVINDISE ERDP MLVEEIRCGLVQA - RDVHVVLRNYRKDGSFFWNDLVISPTPDNGG VITNFVGVINDISE ERDP NDGALDEIREGLKKQ - SPVKVVLRNYRKDGSFFWNDLVISPTPDNGG VITNFVGVINDISE ERDD - NDGALDEIREGLKKQ - SDVKVVLRNYRKDGSFFWNDLVISPTPDNGG VITNFVGVINDISE EFDLS NBQALDEIREGLKG - SOSSNVVNNINYRKDGSFFWNDLVISPTDONON TITHFUGVLNDISA NDD - ETRLAIRQGLETR - QQLHVTLRNYRKDGTFFWNDLVISPYDSGG VITNFVGVINDISA NDD - ETRLAIRQGLETR - QQLHVTLRNYRKDGTFFWNDLVISPYDSGG VITNFVGVINDISA NDD - ETRLAIRQGLETR - QQLHVTLRNYRKDGTFFWNDLVISPYDSGG VITNFVGVINDISA NDD - ETRLAIRQGLETR - QQLHVTLRNYRKDGTFFWNDLVISPYDSGG VITNFVGVI	HAY 715 KAY 425 LAT 25 KAY 425 LAT 26 KAY 425 KAY 425 KAY 425 KAY 425 KAY 425 KAY 419
WP_010627231.1 WP_102627940.1 WP_110265471.1 WP_1161423473.1 WP_159341723.1 WP_164875715.1 TVP44179.1 WP_00821604.1 WP_075879636.1 WP_083517734.1 SEF71116.1 WP_141320011.1 WP_106690146.1 WP_142051109.1 WP_028239827.1 HCT41415.1 WP_127329474.1 WP_127329474.1 WP_106694265.1 WP_137844799.1 WP_137844799.1 WP_137844799.1 WP_137844799.1 WP_137844799.1 WP_137844799.1 WP_13784946462.1 WP_137849645.1 WP_108533399.1 WP_127996758.1	594 LRVLERSVQASINGIVITDASQHO-LPISYVN-EAFLALTGYREEEVLGRNCRMLQGV 304 LRTLQRGVEASVIKGVYLADAREPO-MPIVYAN-ATFIKHTGYREDEILGRNCRFMQGE 776 LRILERSVEASVIKGVLYADAREPO-MPIVYAN-ATFIKHTGYREDEILGRNCRFMQGE 777 LLTLGRSLEASSINGVITUDATQPG-MPLIFVN-QAFSRITGYGKEEVQGRNCRFLQGP 767 LRIFQRSLEASSINGVILTGEAUDD-PFILYWN-PAFVATTGYDDDVRRRNCRFLQGP 600 LRIYQRSLEASSINGILTGEALQDD-YPILYWN-PAFVATTGYDDDVRRRNCRFLQGP 33 RYLFQRSLEASSINGILTGEALQDD-YPILYWN-PAFVATTGYPLEEVKGHNCRFLLQGK 34 RYLFQRSLEASSINGVILTGATUTO-QPIVYAN-PAFVATTGYPLEEVKGHNCRFLLQGK 290 LRLLQRGIGASPHGVUHADATQTD-QPIVYAN-PAFVATTGYPLEEVKGHNCRFLQGP 291 LRLLQRGIGASPHGVUHADATQPD-MPLYYAN-EAFSQLTGYALDEVLGNNCRFLQGP 292 LRLLQRGIGASPHGVUHADATQPD-MPLYYAN-EAFSQLTGYALDEVLGNNCRFLQGG 293 LRLLQRGIGASPHGVUHADATQPD-MPLYYAN-PAFTANTGYQDEITGRNCRFLQGG 294 LRLLRSSIESSPSGFLLADAGSPD-LPVYAN-PAFTANTGYQDEITGRNCRFLQGG 295 LHLLKRSIESSPSGFLADAGSPD-LPVYAN-PAFTANTGYQDEITGRNCRFLQGG 296 LRLLRSSMEASAHGVITADAKKTD-QPLYVAN-PAFTANTGYQDEITGRNCRFLQGG 297 LHLLRSSMEASAHGVITADAKKTD-QPLYVN-PAFEANTGYATEVGRNCRFLQGG 306 LRLLGRSGLASYHGTLVGADAGA	ETEP- DAVAWLRRCVVER - RDCHVTLLINYRKDGSTFWNALYVSPVLDGDG - GVTHFVGELRDVSEI ETDP - EAVAMIRRHLAEQ - REVLVTLRINYRKDGTFFWNDAFISPVRDGEG - RVTHFVGVLHDISEI ETDP - OTYQEIRGGLDQ - RNOVTLCINYRKDGERFWNDAFISPVRDGEG - RVTHFVGVLHDISEI ETDP - EAVAMIRRHLAEQ - REVSVTLRINYRKDGSFFWNDLLISPVRDGHG - AVSHFIGVYNDVTOL ETDP - EAVAMIRRSLVAR - REVSVTLRINYRKDGSFWNELKISPVSNRHG - EITHFVGVÄNDVTQ ETDP - KKQVQEICDALLQQ - RDISLITRINYRKDGAFWNNVFISPVRAQDG - QATHFVGIINDISEI DTDP - KKQIADIQAFEQQ - QDITLTIRINYRKDGAFWNNVFISPVRAQDG - VYTHFVGSITDISEI DTDP - KQIADIQAFEQQ - RDIALTIRINYRKDGAFWNNLFISPVRADGG - VYTHFVGSITDISEI DTDP - EQVEALRQALKHG - KOISLITRINYRKDGAFWNNLFISPVRADGG - QVTHFIGILNDISEI DTOP - EQVEALRQALKHG - KOISLITRINYRKDGAFWNNLFISPVRADGG - QVTHFIGILNDISEI DTPP - EPVAQMHQALSEA - RAVDLIVRINYRKDGRFFWNNLLISPVRDAGG - QVTHFIGILNDISEI DTPP - GOVEATRQALSSC - INSQVITLINYRKDGTFFWNRLAINPVFDEGG - SCSHFIGTWDITRI ETDP - AAIGKTRQSVVDR - TEVQVTLLINYRKDGTFFWNRLAINPVFDEAG - RCTHFIGILEDITE ETDP - AAIGKTRQSVVDR - TEVQVTLLINYRKDGTFFWNRLAINPVFDEAG - RCTHFIGILEDITE ETDP - AAIGKTRQSCHAH - TOWIVLLINYRKDGFFFWNRLAINPVFDEGG - NCSHFTGSLQDITW DTAP - EALETTRQGLHHG - TEVWVELTINYRKDGTFFWNILLISPVFDEGG - RCHILIGTHQDITY ETDP - AAVAKIRAALSDN - REIDIVLQNTRKDGTFFWNILLISPVFDEGG - RVENFIGIINDITQ ETDP - AAVAKIRAALSDN - REIDIVLQNTRKDGTFFWNDLYISPVFDEGG - RVENFIGIINDITQ ETDP - AAVAKIRAALSDN - REIDIVLQNTRKDGTFFWNDLYISPVFDEGG - RVENFIGIINDITQ ETDP - AAVAKIRAALSDN - REIDIVLQNTRKDGTFFWNDLYISPVFDEGG - VITNFVGVINDITE ETDP - GVODRITAGLERE - KQVSVTLLNYRKDGTFFWNDLYISPVFDEGG - VITNFVGVINDITE ETDA - GVODRITAGLERE - KQVSVTLLNYRKDGTFFWNDLYISPYFDEGG - VITNFVGVINDITE ETDA - GVODRITAGLERE - KQVSVTLLNYRKDGTFFWNDLYISPYFDEGG - VITNFVGVINDITE ETDA - GVODRITAGLERE - KQVSVTLLNYRKDGSFFWNDLYLSPIFSEGG - VITNFVGVINDITE ETDA - GVODRITAGLERE - KQVSVTLLNYRKDGSFFWNDLYLSPIFSEGG - VITNFVGVINDISE ERDD - PQLTETILG LOQQ - RDIHVURNFRKDGSFFWNDLYLSPIFSEGG - VITNFVGVINDISE ERDD - PGLTETLAGLOQU - SDISVVURNFRKDGSFFWNDLYLSPIFDDDON - TITHFVGVINDISE TADPF - NDGALNEIREGLKQ - SPVKVVLRNYRKDGSFFWNDLYLSPIRDDON - TITHFVGVINDISE TADPF - NDG	HAY 715 KAY 425 IAD 897 IED 895 KOH 888 ROH 721 ROH 721 ROH 721 KHO 154 KKHO 419 LEG 419 KKE 419 LEG 419 KKKI 1116 KKKI 1116 KKKY 490 KKKI 1116 KKKY 490 KKKY 151 KKKY 490 KKKY 382 KKKY 489 KKY 489 KKKY 489 KKY 489 K
WP_010627231.1 WP_102627940.1 WP_112054571.1 WP_112054571.1 WP_161423473.1 WP_159341723.1 WP_146875715.1 TVP44179.1 WP_00821604.1 WP_075879663.1 WP_10821604.1 WP_10821604.1 WP_141320011.1 WP_141320011.1 WP_140690146.1 WP_142051109.1 WP_126775935.1 WP_126775935.1 WP_126775935.1 WP_090447691.1 WP_127329474.1 WP_106694265.1 WP_1318447099.1 WP_137840462.1 WP_09553309.1 WP_137840462.1 WP_127896758.1 WP_127896758.1 WP_145061629.1	594 LRVLERSVQASINGIVITDASQHO-LPISYVN-EAFLALTGYREEEVLGRNCRMLQGV 304 LRTLQRGVEASVIKGVYLADAREPO-MPIVYAN-ATFRKHTCYREDEILGRNCRFMQGE 776 LRILGRSVEASVIKGVLYADAREPO-MPIVYAN-ATFRKHTCYREDEILGRNCRFMQGE 777 LLTLGRSVEASVIKGVLYADATOPG-MPLIFVN-QAFSRITGYGKEEVQGRNCRFLQGP 767 LRIFQRSLEASSINGVLICEAQNDO-FPILYVN-PAFVAITGYQLDDIKGINCRFLQGP 600 LRIYQRSLEASSINGVLICEAQNDO-FPILYVN-PAFVAITGYQLDDIKGINCRFLQGG 600 LRIYQRSLEASSINGVILGEALQDO-YPILYVN-PAFVAITGYQLDDIKGINCRFLQGG 33 RYLFQRSLEASSINGVILGALTOPO-PPILYVN-PAFVAITGYPLEEVKGHNCRFLQGG 240 LHIFERSLQASSINGVLIADATQTO-OPIVYAN-PAFVAITGYPLEEVKGHNCRFLQGP 291 LRLLQRGIGASSPNGVLIADATQTO-MPIVYAN-EAFSQLTGYALDEVLGNNCRFLQGP 292 LRLLQRGIGASSPNGVLIADATQTO-MPIVYAN-EAFSQLTGYALDEVLGNNCRFLQGP 293 LRLLQRGIGSSPNGILMADATROP-MPIVYAN-EAFSQLTGYALDEVLGNNCRFLQGP 294 LRLLQRGIGASSPNGVUTMADATPO-MPIVYAN-EAFSQLTGYALDEVLGNNCRFLQGP 295 LHLLKRSIESSSPGGLLADAGSPO-LPVVYAN-PAFTANTGYODEITGRICKGFLQGG 296 LRLLKRSIESSSPGGLLADAGSPO-LPVVYAN-PAFTANTGYODEITGRICKGFLQGG 297 LHLLRSSLEASYNGVUTMALADATDPCPPLTYVN-PAFERTTGYSRTEALGRICKFLQGG 36 LRLLGRSLEASSNGVITDALAPO-HPITYVN-PAFERTTGYATEVLGRNCRFLQGG 37 LHLERSLEASYNGVUTDALAPO-HPITYVN-PAFERTTGYATEVLGRNCRFLQGG 38 LRLLGRSLEASYNGVUTDALAPO-HPITYVN-PAFERTTGYATEVLGRNCRFLQGG	ETEP- DAVAWLRRCVVER - RDCHVTLLNYRKDGSTFWNALYVSPVLDGDG - GVTHFVGELRDVSEI ETDP - EAVAMIRRHLAEQ - REVLVTLRNYRKDGTFFWNDAFISPVRDGEG - RVTHFVGVLHDISE ETDP - OTYQETRGGLDQ - RDVQVTLGNKRDGEFMOLLISPVRDGEG - RVTHFVGVLHDISE ETDP - EAVMKIRRSLVAR - REVSVTLRNYRKNGESFWNDELTSPVRDGHG - AVSHFIGVYNDVTQ ETDP - EAVMKIRRSLVAR - REVSVTLRNYRKNGESFWNDELTSPVRADDG - GATHFVGITNDISE DTDP - KROVGETCDALLQQ - RDISLITRNYRKNGGAFWNNVFISPVRADDG - VYTHFVGSINDISE DTDP - KNIDAIQQALEQQ - QDITLTIRNYRKNGGAFWNNVFISPVRADDG - VYTHFVGSINDISE DTDP - KOJADIQAFEQQ - RDIALTIRNYRKNGGAFWNNLFLSPVKSHNG - QVTHFVGSINDISE DTDP - EQVEALRQALKHG - KOISLITRNYRKNGGAFWNNLFLSPVRADDG - QVTHFVGSITDISE DTOP - EQVEALRQALKHG - KOISLITRNYRKNGGAFWNNLFLSPVRADDG - QVTHFIGIILNDISE DTOP - EQVEALRQALSSC - RNSVQTLVNYRKDGTFFWNRLAISPVPDBTG - SCSHFIGTWDITTR ETDP - AAIGKIRQSVVDR - TEVQVTLLNYRKDGTFFWNRLAISPVPDBTG - SCSHFIGTWDITTR ETDP - AAIGKIRQSVVDR - TEVQVTLLNYRKDGTFFWNRLAISPVFDBTG - KCTHFIGILEDITE ETAP - ASTDITRDAL RRC - SAVEVTL INVRRDGSTFWNNL ISSPVVDFTG - KCTHFIGILEDITE ETAP - ATIKKIRDGKAH - TOWINVLLNYRKDGTFFWNNLLSPVPDBTG - KCTHFIGILEDITE ETDA - ATIKKIRDGKAH - TOWINVLLNYRKDGTFFWNNLLSPVPDBTG - RCTHLIGTHQDITY DTAP - EALETIRQGLHHQ - TEVNVELINYRKDGTFFWNNLLSPVPDBTG - RCTHLIGTHQDITY ETDA - GVVDMIRAGLRER - KQVSVTILNYRKDGTFFWNDLYISPVPDBTG - RTHFIGILIDITQ DTAP - EALETIRQGLHQ - REVNLVLNYRKDGTFFWNDLYISPVPDBGG - NCSHFIGILDDITQ DTAP - BAVAKIRALSON - REIDIVLQNTRKDGTFFWNDLYISPVPDBGG - RTHFVGVLNDISE ETDA - GVVDMIRAGLRER - KQVSVTILNYRKDGTFFWNDLYISPVPDBGG - RTHFVGVLNDISE ETDA - GVDMIRAGLRER - KQVSVTILNYRKDGTFFWNDLYISPVPDBGG - RVSHFIGILDDITQ DREQ - RGLEDTRGSLPQQ - RDHVVLRNYRKDGFFFWNDLYISPVPDBGG - RVSHFIGVLNDISE ERDD - MLVEETRGGLYQA - RDHVVLRNYRKDGFFFWNDLYLSPTPSGGG - RVSHFIGVLNDISE ERDD - MLVEETRGGLYQA - RDHVVLRNYRKDGFFFWNDLYLSPTPDNGG - VTTHFIGVLNDISE EFDLS - NEQALDQIRKGLARG - DDISVVLRNYRKDGFFFWNDLYLSPTPDNGG - VTTHFIGVLNDISE EFDLS - NEQALDQIRKGLARG - DDISVVLRNYRKDGFFFWNDLYLSPTPDDQG - VTTHFIGVLNDISE EFDLS - NEQALDQIRKGLARG - DDISVVLRNYRKDGFFFWNDLYLSPTPDGGG - VVTHFIGVLNDISE DNDQ - GIAVRDAIREG - RACQUVVRNYRKSGE	HAY 715 KAY 425 LAT 25 KAY 425 LAT 26 KAY 425 KAY 425 LAT 21 KAY 425 LAT 26 KAY 490 KA
WP_010627231.1 WP_102627940.1 WP_112054571.1 WP_112054571.1 WP_161423473.1 WP_159341723.1 WP_146875715.1 WP_100821604.1 WP_075879636.1 WP_1083517734.1 SEF71116.1 WP_1112000210.1 WP_1141320011.1 WP_1142051109.1 WP_126775935.1 HCT41415.1 WP_0262339827.1 HCT41415.1 WP_026339827.1 HC741415.1 WP_127329474.1 WP_147340462.1 WP_1474061629.1 WP_1474061629.1 WP_1561636744.1	594 LRVLERSVQASINGIVITDASQHD-LPISYVN-EAFLALTGYREEEVLGRNCRMLQGV 304 LRTLQRGVEASVINGVIADAREPD-MPIVYAN-ATFRWITCYREDEILGRNCRFMQGE 776 LRILERSVEASVINGVILTVDATQPG-MPIIFAN-HAFSRISGYSNAEIKGRNCRFLQGH 776 LRILERSVEASVINGVILTVDATQPG-MPIIFAN-AFSRITGYKEEVQGRNCRFLQGP 767 RIFQRSLEASSINGVILTCEAUQDD-PPIIFVN-PAFVATTGYKEEVQGRNCRFLQGP 600 LRIYQRSLEASSINGVILCEAUQDD-YPILYVN-PAFVATTGYLDDINGSLNGRFLNGG 600 LRIYQRSLEASSNGVILCEAUQDD-YPILYVN-PAFVATTGYLEEVKGHNCRFLNGG 33 RYLFQRSLEASSNGVILGEAUQDD-YPILYVN-PAFVATTGYLEEVKGHNCRFLNGG 240 LHIFERSLQASSNGVILTADATQTD-OPIVYAN-PAFVATTGYPLEEVKGHNCRFLNGG 291 LRLLQRGIGASPNGILHADATQPD-MPIVYAN-EAFSVLTGYDLEVLGRNCRFLNGG 292 LRLLQRGIGASPNGILHADATRHD-LPLYYAN-EAFVATTGYTDDVLGRNCRFLNGGN 293 LRLLQRGIGASPNGILHADATRHD-LPLYYAN-EAFVATTGYTDDVLGRNCRFLNGGN 294 LRLLKRSIEASPNGVVINDAATGPDMPIVYAN-PAFTAHTGYQNDETIGRNCRFLNGG 295 LHLLKRGIEANPNGHINDARSPD-MPVYAN-PAFTAHTGYQNDETIGRNCRFLNGG 296 LRLLKRGIEANPNGHINDARSPD-MPVYAN-PAFTAHTGYQNDETIGRNCRFLNGG 297 LHLLKRGIEANPNGHINDARSPD-MPVYAN-PAFTENTGYFRETVGRNCRFLNGG 306 LRLLKRSLEASYNGVVINDALAPG-HBIYYN-PAFETATGYAKHEVIGRNCRFLNGG 307 LRLLKRSLEASYNGVVINDALAPG-HBIYYN-PAFETATGYSAKETEVLGRNCRFLNGG 308 LRLLKRSLEASYNGVVINDALAPG-HBIYYN-PAFETTGYSKEESLGGNCRFLNGG 308 LRLLKRSLEASYNGVVINDALAPG-HBIYYN-PAFETTGYSKEESLGGNCRFLNGG 309 LRLLKRSLEASYNGVVINDALAPG	ETEP- DAVAWLRRCVVER-RDCHVTLLNYRKDGSTFWNALYVSPVLDGDG GVTHFVGELRDVSEI ETDP EAVAMIRRHLAEQ - REVLVTLRNYRKDGTFFWNDAFISPYRDGEG RYTHFVGVLHDISE ETDP OTVQEIRQGLDDQ - RDVQVTLCNYRKNGEFFWNDAFISPYRDGEG AVSHFIGVYNDVTQ ETTDP EAVAMIRRHLAEQ - REVSYTLRNYRKNGEFFWNDAFISPYRDGEG AVSHFIGVYNDVTQ ETTDP EAVAMIRRSLVAR - REVSYTLRNYRKNGESFWNLELISPYSNRHG EITHFVGVANDVTQ ETTDP KGVQEICDALLQQ - RDISLITIRNYRKNGGAFWNNVFISPYRADDG VYTHFVASINDISE DTDP KNIDAIQQALEQQ - QDITLITIRNYRKNGGAFWNNVFISPYRADDG VYTHFVASINDISE DTDP KQUQEICDALLQQ - RDISLITIRNYRKNGGAFWNNVFISPYRADDG VYTHFVASINDISE DTDP EQVALRQALKHG - KDISLITIRNYRKNGGAFWNNLFISPYRADDG VYTHFVASINDISE DTDP EQVALRQALKHG - KDISLITIRNYRKNGGAFWNNLFISPYRADDG VYTHFVGSITDISE DTDP EQVALRQALKHG - KDISLITIRNYRKNGGAFWNNLFISPYRDADG RYTHFIGILNDISE DTDP EQVALRQALKHG - KDISLITIRNYRKNGGAFWNNLFISPYRDADG RYTHFIGILNDISE DTPP GOVEAIRQALSEA - RAVDLITVRNYRKDGFPFWNRLAISPYPDETG SCSHFIGTMYDITR ETDP AAIGKIRQSVVDR - TEVQVTLLNYRKDGTPFWNRLAISPYPDETG SCHFIGTMYDITR ETDP AAIGKIRQSVVDR - TEVQVTLLNYRKDGTPFWNRLAISPYPDEAG RCTHFIGILEDITE FTAP ASTDTTRDALRC - SAVEVTLLNYRKDGTFFWNNLISTSPYDDFTG KCTHFIGTLEDITE FTAP ASTDTTRDALRC - SAVEVTLLNYRKDGTFFWNNLISTSPYDDFTG KCTHFIGTLEDITE FTAP AAIGKIRQGLHHO - TEVNVELLINYRKDGTFFWNNLISTSPYDDFTG RCTHLIGTHQDITV ETDP AAVAKIRAALSDN - REIDIVLQNTRKDGTFFWNNLISTSPYDDFTG RCTHLIGTHQDITV ETDA GVOWNTRAGLERG - KQVSVTILNYRKDGTFFWNDLVISPYFSGSG RTTHFVGVLNDISE FTAD GVOWNTRAGLERG - KQVSVTILNYRKDGTFFWNDLVISPYFSGSG RTTHFVGVLNDISE FTAD MLVEEIRCGLVQA - RDVHVVLRNYRKDGSFFWNDLVIAPYPDEGG VTHFIGILNDITQ ETDA GVOWNTRAGLERG - ROUNVVLRNYRKDGSFFWNDLVIAPYPDEGG VTHFVGVLNDISE FROD MLVEEIRCGLVQA - RDVHVVLRNYRKDGSFFWNDLVIAPYPDEGG VTHFVGVLNDISE FTDD SONGWARGALBRG - ROUNVVLRNYRKDGSFFWNDLVIAPYPDEGG VTHFVGVLNDISE FTDD SONGWARGALBRG - ROUNVVLRNYRKDGSFFWNDLVIAPYPDEGG VTHFVGVLNDISE FTDD SONGWARGALBRG - ROUNVVRNYRKDGFFFWNDLVIAPYPDEGG VTHFVGVLNDISE FTDD SONGWARGALBRG - ROUNVVRNYRKDGFFFWNDLVIAPYPDEGG VTHFVGVLNDISE FTDD SONGWARGALBRG - ROUNVVRNYRKDGFFFWNDLVIAPYPDDGG SONGWARGALBRG - RUNNVGVLNDISE FTDD SONGWARGALBRG - RAUNTVRNGTGFFFWNDLVIAPYPDDGG SONGWARGAL	HAY 715 KAY 425 LAT 25 KAY 425 LAT 26 KAY 425 KOH 888 ROH 721 KHQ 154 KHQ 154 KHQ 154 KHQ 419 LEO 419 KEQ 420 KKI 1116 LOII 248 KKY 490 KKY 151 KRY 489 KKY 151 KRY 489 KRY 490 KRY 254 KRY 490 KRY 264 KRY 490 KRY 264 KRY 490 KRY 499 KRY 499 KRY 499 KRY 499 KRY 499 KRY 499 KRY 490 KRY 500 KRY 50
WP_010627731.1 WP_102627940.1 WP_112054571.1 WP_1161423473.1 WP_159341723.1 WP_146875715.1 TVP44179.1 WP_075879636.1 WP_075879636.1 WP_083517734.1 SEF71116.1 WP_141320011.1 WP_106090145.1 WP_142051109.1 WP_142051109.1 WP_126775935.1 WP_028239827.1 HCT41415.1 WP_142051109.1 WP_127329474.1 WP_106694265.1 WP_1378447999.1 WP_137844799.1 WP_137849799.1 WP_137849799.1 WP_157996758.1 WP_145961629.1 WP_151636744.1 WP_066818302.1	594 LRVLERSVQASINGIVITDASQHO-LPISYVN-EAFLALTGYREEVLGRNCRMLQGV 304 LRTLQRGVEASVIKGVIXADAREPO-MPIVYAN-ATFIKHTGYREDEILGRNCRFMQGE 776 LRILERSVEASVIKGVIXDANGTO-MPITAN-HAFSRISGYSNAELKGRNCRFMQGE 777 LLTLERSVEASINGVITVDATQPG-MPLIFVN-QAFSRITGYGKEEVQGRNCRFLQGP 767 LRIFQRSLEASSKGVILCEAU,DD-FPITYN-PAFVATTGYDDDVRRRNCRFLQGP 600 LRIYQRSLEASSKGVILCEAU,DD-YPILYWN-PAFVATTGYDDDVRRRNCRFLQGP 33 RYLFQRSLEASSKGVILCEAU,DD-YPILYWN-PAFVATTGYPLEEVKGHNCRFLLQGK 33 RYLFQRSLEASSKGVILGEAU,DD-YPILYWN-PAFVATTGYPLEEVKGHNCRFLLQGK 290 LRILGRGIEASPHGVUMADATQPD-MPLYYAN-EAFSQLTGYALDEVLGNNCRFLQGP 291 LRILGRGIEASPHGVUMADATQPD-MPLYYAN-EAFSQLTGYALDEVLGNNCRFLQGP 292 LRILGRGIEASPHGVUMADATQPD-MPLYYAN-EAFSQLTGYALDEVLGNNCRFLQGG 293 LRILGRGIEASPHGVUMADATQPD-MPLYYAN-PAFTANTGYQDEITGRNCRFLQGG 294 LRILGRGIEASPHGVUMADATQPD-MPLYYAN-PAFTANTGYQDEITGRNCRFLQGG 295 LHLIKRSIESSPSGFLIADAGSPD-LPVYAN-PAFTANTGYQDEITGRNCRFLQGG 296 LKLLKRSIESSPSGFLIADAGSPD-LPVYAN-PAFTANTGYQDEITGRNCRFLQGG 297 LHLLRSGLASYNGTVADAKTD 298 LRILGRGIEASPHGVUMADATRDD	ETEP- DAVAWLRRCVVER - RDCHVTLLINYRKDGSTFWNALYVSPVLDGDG - GVTHFVGELRDVSEI ETDP - EAVAMIRRHLAEQ - REVLVTLRINYRKDGTFFWNDAFISPVRDGEG - RVTHFVGVLHDISE ETDP - OTYQETRGDLDQ - RDVQVTLGVTLGVRKNGERFWNDLISFSVRDGEG - RVTHFVGVLHDISE ETDP - EAVMKIRRSLVAR - REVSVTLRINYRKDGSFWNDLISFSVRDGHG - AVSHFIGVYNDVTQ ETDP - EAVMKIRRSLVAR - REVSVTLRINYRKDGSFWNELKISPVSNRHG - EITHFVGVÄNDVTQ DTDP - KKQVQETCDALLQQ - RDISLITRINYRKDGAFWNNVFISPVRAQDG - QATHFVGIINDISE DTDP - KKIDAIQQALEQQ - QDITLITRINYRKDGAFWNNVFISPVRAQDG - VYTHFVASINDISE DTDP - KQIADTQLAFEQQ - RDIALTIRNYRKDGAFWNNLFISPVRAPDG - VYTHFVASINDISE DTDP - EQVEALRQALKHG - KOTSLITRINYRKDGAFWNNLFISPVRAPDG - QVTHFIGILNDISE DTOP - EQVEALRQALKHG - KOTSLITRINYRKDGAFWNNLFISPVRADDG - QVTHFIGILNDISE DTPP - EPVAQMHQALSEA - RAVDLIVRNYRKDGTFFWNNLLISPVRDADG - QVTHFIGILNDISE ETDP - AAIGKTRQSVVDR - TEVQVTLLINYRKDGTFFWNRLAINPVFDETG - SCSHFIGTWDITTR ETDP - AAIGKTRQSVVDR - TEVQVTLLINYRKDGTFFWNRLAINPVFDEAG - RCTHFIGILEDITE ETDP - AAIGKTRQSVVDR - TEVQVTLLINYRKDGTFFWNRLAINPVFDEAG - RCTHFIGILEDITE ETDP - AAIGKTRQSCVDR - TEVQVTLLINYRKDGTFFWNRLAINPVFDEAG - RCTHFIGILEDITE ETDP - AAIGKTRQSLAHD - TOWVVLLINYRKDGTFFWNNLLISPVVDETG - KCTHFIGILEDITE ETDP - AAIGKTRQSLAHD - TEVWVLLINYRKDGTFFWNNLLISPVVDETG - KCTHFIGILEDITE ETDP - AAIGKTRQSLAHD - TEVWVLLINYRKDGTFFWNNLLISPVFDEGG - NCSHTGSLQDITW DTAP - EALETTRQGLHHD - TEVWVLLINYRKDGTFFWNNLLISPVFDEGG - RVENFIGIINDITQ ETDP - AAVAKIRAALSDN - REIDIVLQNTRKDGTFFWNDLYISPVFDEGG - RVENFIGIINDITQ DREQ - RGLEDIRQSLPQE - REVHLVLRINYRKDGTFFWNDLYISPVFDEGG - RVENFIGIINDITQ DREQ - RGLEDIRQSLPQE - REVHLVLRINYRKDGTFFWNDLYISPVFDEGG - RVENFIGIINDITQ DREQ - RGLEDIRQSLPQE - REVHLVLRINYRKDGTFFWNDLYISPVFDEGG - RVSHFIGVINDISE ETDD - MDGALNEIREGLKQ - SPVKVVLRINYRKDGSFFWNDLYLSPTFSEGG - VITTHFVGVLNDISE TADPF - NDGALNEIREGLKQ - SPVKVVLRINYRKDGSFFWNDLYLSPTFDDDON - TITHFVGVLNDISE TADPF - NDGALNEIREGLKQ - SPVKVVLRINYRKDGSFFWNDLYLSPTPDDOD - TITHFVGVLNDISE TADPF - NDGALNEIREGLKQ - SPVKVVLRINYRKDGSFFWNDLYLSPTPDDOD - TITHFVGVLNDISE TODOG - ASHTLARAGRE - RACQVVVRINYRKSGELFYNDLYISPRDDOD - TVTHFVGVLNDISE DDEQP -	HAY 715 KAY 425 IAO 895 KOH 888 ROH 721 ROH 721 ROH 721 ROH 412 ROH 419 LEG 419 KKEQ 4
WP_010627731.1 WP_110264794.1 WP_112054571.1 WP_1161423473.1 WP_159341723.1 WP_146875715.1 TVPA4179.1 WP_00821604.1 WP_075879636.1 WP_083517734.1 SEF71116.1 WP_141320611.1 WP_110200210.1 WP_100690146.1 WP_142651109.1 WP_126775935.1 WP_028239827.1 HCT41415.1 WP_0928239827.1 HCT41415.1 WP_126775935.1 WP_127329474.1 WP_106694265.1 WP_137840462.1 WP_137840462.1 WP_137840462.1 WP_137840462.1 WP_1516367658.1 WP_145061629.1 WP_151636744.1 WP_1688302.1 TAL86525.1	594 LRVLERSVQASINGIVITDASQHO-LPISYVN-EAFLALTGYREEEVLGRNCRMIQGV 304 LRTLGROVEASVIKGVYLADAREPO-MPIVYAN-ATFRKHTCYREDEILGRNCRFMIQGE 776 LRILERSVEASVIKGVLYADAREPO-MPIVYAN-ATFRKHTCYREDEILGRNCRFMIQGE 777 LLTLGRSVEASVIKGVLYADARTOP-MPLIFVN-QAFSRITGYGKEEVQGRNCRFLIQGP 767 LRIFGRSLEASSIKGVLICEAU,DO-PPILYVN-PAFVAITGYGKEEVQGRNCRFLIQGP 600 LRIYQRSLEASSNGVLICEAU,DO-YPILYVN-PAFVAITGYQLDDIKGLKGRFLIGGG 600 LRIYQRSLEASSNGVILICEAU,DO-YPILYVN-PAFVAITGYQLDDIKGLKGRFLIGGG 33 RYLFGRSLEASSNGVILICEAU,DO-YPILYVN-PAFVAITGYPLEEVKGHNCRFLIQGF 240 LHIFERSLQASSNGVLIADATQTO-OPIVYAN-PAFVAITGYPLEEVKGHNCRFLIQGP 291 LRILGRGIGASPNGVLHADATQFO-MPLYVAN-EAFSQLTGYALDEVLGNNCRFLIQGP 292 LRILLGRGIGASPNGVLHADATQFO-MPLYVAN-EAFSQLTGYALDEVLGNNCRFLIQGP 293 LRILGRGIGASPNGVINADATRDHPLYVAN-EAFSQLTGYALDEVLGNNCRFLIQGP 294 LRILGRGIGASPNGVINADATGPMPLYVAN-PAFVAITGYDDVLGRNCRFLIGGS 295 LHLIKRSIESSSPGGLLADAGSPO-LPVYVAN-PAFTANTGYODEITGRNCRFLIGGS 296 LRILKRSIESSSPGGLADAGSPO-LPVYNAN-PAFTANTGYODEITGRNCRFLIGGS 297 LHLLKRGIEANPNGMLHVDARSPO-MPVVYAN-PAFTANTGYODEITGRNCRFLIGGS 298 LRILKRSIESSSPGGLADAKKTO-OPLTVN-PAFTANTGYODEITGRNCRFLIGGG 30 LHLKRSLEASYNGVIVDALSHO-LPITYN-PAFERTTGYSAETGKRGFLIGGP 31 LILGRGIEASSNGVYYDALSHO-LPITYN-PAFERTTGYSAETGKRGFLIGGF 32 LRILKRSIESSTNGVYTDALAPO-HPITYTN-PAFERTTGYSAETIGKNGRFLIGGG 257 LKLLKRSIESSTNGVYTADALABO-HPITYN-PAFERTTGYSAETIGKNGRFLIGGG 257 LKLLKRSIESSSNGVVYDTRLED-DPISYNN-PAFERTTGYSAETGKNGRFLIGGG 257 LKLLKRSIESSNGVVYDTRLED-DPISYNN-PAFERTTGYSKEESLGONGRFLIGGG	ETEP- DAVAWLRRCVVER - RDCHVTLLINYRKDGSTFWNALYVSPVLDGDG - GVTHFVGELRDVSEI ETDP - EAVAMIRRHLAEQ - REVLVTLRINYRKDGTFFWNDAFISPYRDGEG - RVTHFVGVLHDISE ETDP - OTYQETRGGLDQ - RNOVPTLGNYRKDGEFMOLLISPYRDGEG - RVTHFVGVLHDISE ETDP - EAVAMIRRHLAEQ - REVSVTLRINYRKDGSFFWNDLTSPYRDGGG - RVTHFVGVANDVTQ ETDP - EAVAMIRRSLVAR - REVSVTLRINYRKDGSFWNELKISPVSNRHG - EITHFVGVÄNDVTQ DTDP - KKQVQETCDALLQQ - RDISLITRINYRKDGAFWNNVFISPVRAQDG - QATHFVGITNDISE DTDP - KNIDAIQQALEQQ - QDITLTIRINYRKDGAFWNNVFISPVRAQDG - VYTHFVGSITDISE DTDP - KOLADDIQAFEQQ - RDIALTIRINYRKNGQAFWNNLFLSPVKSHHG - QVTHFVGSITDISE DTDP - EQVEALRQALKHG - KOISLITRINYRKDGAFWNNLFLSPVKSHHG - QVTHFVGSITDISE DTOP - EQVEALRQALKHG - KOISLITRINYRKDGAFWNNLFLSPVRSHHG - QVTHFIGILNDISE DTOP - EQVEALRQALKHG - KOISLITRINYRKDGAFWNNLFLSPVRDADG - QVTHFIGILNDISE DTPP - GOVEALRQALSSC - NSVQVTLINYRKDGFFFWNRLAISPYPDETG - SCSHFIGTWDITRI ETDP - AAIGKIRQSVVDR - TEVQVTLLNYRKDGFFFWNRLAISPYPDETG - SCSHFIGTWDITRI ETDP - AAIGKIRQSVVDR - TEVQVTLLNYRKDGFFFWNRLAISPYPDETG - KLTHFIGILEDITE ETAP - ASTDITRDAI RRC - SAVEVTL INYRKDGFFFWNRLAISPYPDEGG - RCTHFIGILEDITE ETAP - ATIKKIRDGKAH - TDVINVLLNYRKDGFFFWNNLLSFSPVDETG - KLTHFIGILEDITE ETDP - AAVAKIRAALSON - REIDIVLQNTRKDGTFFWNNLSTSPYDEGG - RVSHFIGILNDITQ DTAP - EALETIRQGLHHQ - TEVNVELINYRKDGFFFWNNLSTSPYDEGG - RVSHFIGILNDITQ DTAP - EALETIRQGLHQ - TEVNVELINYRKDGFFFWNDLYSPYFSGG - RTHFVGVINDISE ETDA - GVVDNTRAGRER - KQVSVTLINYRKDGTFFWNDLYSPYFSGG - RTHFVGVINDISE ETDA - GVVDNTRAGRER - KQVSVTLINYRKDGTFFWNDLYSPYFSGG - VITHFVGVINDISE ERDP - MLVEETRGGLVQA - RDVHVVLRNYRKDGFFFWNDLYSPYFSGG - VITHFVGVINDISE ERDP - MLVEETRGGLVQA - RDVHVVLRNYRKDGFFFWNDLYSPYFSGG - VYTHFVGVINDISE ERDD - PGITEIRLGLQQQ - RDIHVVLRNYRKDGFFFWNDLYSPYFDDGO - TYTHFIGVINDISE ERDD - FINDALARGARG - SONVVVLRNYRKDGSFFWNDLYSPYFDDGO - TYTHFIGVINDISE ERDD - GIAVRDAIRGG - RACHVVLVRNYRKDGSFFWNDLYSPYFDDGO - TYTHFIGVINDISE ERDD - GIAVRDAIRGG - RACHVVLVRNYRKDGSFFWNDLYSPYFDDGO - TYTHFIGVINDISE EFDLS - NGGALDETRGLAKG - SSPWVVLRNYRKDGSFFWNDLYSPTRDDON - TITHFVGVINDISE EFDLS - NDGALWETRGLKKG - SSPWVVLRNYRKDGSFFWNDLYSPTR	HAY 715 KAY 425 LAD 897 LED 895 KOH 888 ROH 721 ROH
WP_010627231.1 WP_102627940.1 WP_112054571.1 WP_112054571.1 WP_161423473.1 WP_159341723.1 WP_146875715.1 TVP44179.1 WP_100821604.1 WP_075879636.1 WP_141326011.1 WP_110200210.1 WP_10699146.1 WP_110200210.1 WP_126775935.1 WP_12675935.1 WP_028239827.1 HCT41415.1 WP_090447691.1 WP_12675995.1 WP_127329474.1 WP_106694265.1 WP_137840462.1 WP_09553309.1 WP_127996758.1 WP_151636744.1 WP_066816302.1 TAL86525.1 WP_1668040027.1	594 LRVLERSVQASINGIVITDASQHD-LPISYVN-EAFLALTGYREEEVLGRNCRMLQGV 304 LRTLQROVEASVINGVIADAREPD-MPIVYAN-ATFRWITCYREDEILGRNCRFMQGE 776 LRILERSVEASVHGVLIVDANQTD-MPIIFAN-HAFSRISGYSNAEIKGRNCRFLQGH 776 LRILERSVEASVHGVLIVDANQTD-MPIIFAN-HAFSRISGYSNAEIKGRNCRFLQGH 767 LRIEQRSLEASSINGVLICEAUQDD-PPIIFVN-PAFVAITGYREEVQGRNCRFLQGP 600 LRIYQRSLEASSINGVILCEAUQDD-YPILYVN-PAFVAITGYQLDDIKGINGRFLNGG 600 LRIYQRSLEASSNGVILCEAUQDD-YPILYVN-PAFVAITGYQLDDIKGINGRFLNGG 33 RYLFQRSLEASSNGVILGEAUQD-YPILYVN-PAFVAITGYPLEEVKGHNCRFLLQGH 240 LHIERSLQASSNGVILGAAUDTOTD-OPIVYAN-PAFVAITGYPLEEVKGHNCRFLLQGH 291 LRLLQRGIGASSPNGVIADATOTD-OPIVYAN-EAFSVAITGYQLDEVLGNCRFLNGG 298 LRLLQRGIGASSPNGVIADATOTD-HOPIVYAN-EAFSVAITGYTDDVLGRNCRFLQGH 298 LRLLQRGIGASSPNGVIADATOTD-HOPIVYAN-EAFSVAITGYCHDEVLGRNCRFLQGH 298 LKLLKRSIEASSPNGVIADATOTD-HOPIVYAN-PAFTANTGYQDEDIGRNCRFLQGH 299 LHLLKRGIEANPHOGHINDOASPD-LPVVYAN-PAFTANTGYQDEDIGRNCRFLQGH 299 LHLLKRGIEANPHOGHINDOASPD-HOVYAN-PAFTANTGYQDEDIGRNCRFLQGG 290 LHLLKRGIEANPHOGHINDOASPD-HOVYAN-PAFTANTGYQDEDIGRNCRFLQGG 291 LRLLGRGIEASSPNGVIADATORD	ETEP- DAVAWLRRCVVER-RDCHVTLLNYRKDGSTFWNALYVSPVLDGDG GVTHFVGELRDVSEI ETDP EAVAMIRRHLAEQ - REVLVTLRNYRKDGTFFWNDAFISPYRDGEG RYTHFVGVLHDISE ETDP OTVQEIRQGLDDQ - RDVQVTLCNYRKNGEFFWNDAFISPYRDGEG RYTHFVGVLHDISE ETDP EAVAMIRRHLAEQ - REVLVTLRNYRKNGEFFWNDAFISPYRDGEG STHFUGVINDVTQ ETDP EAVAMIRRSLVAR - REVSYTLRNYRKNGESFWNDLKISPYSNRHG EITHFVGVANDVTQ DTDP EAVAMIRRSLVAR - REVSYTLRNYRKNGGAFWNNVFISPYRADDG OTATHVGIINDISE DTDP KGVQEICDALLQQ - RDISLITIRNYRKNGGAFWNNVFISPYRADDG VYTHFVASINDISE DTDP KKJUADIQALEQQ - QDIILTIRNYRKNGGAFWNNVFISPYRADDG OTATHVGIINDISE DTDP KKJUADIQAFEQQ - RDIALTIRNYRKNGGAFWNNLFISPYRADDG OTATHVGSITNDISE DTDP EQVEALRQALKHG KDISLITIRNYRKNGGAFWNNLFISPYRADDG RYTHFVGSITNDISE DTDP EQVEALRQALKHG KDISLITIRNYRKNGGAFWNNLFISPYRDNAG RYTHFIGILNDISE DTDP EQVEALRQALKHG KDISLITIRNYRKNGGAFWNNLFISPYRDNAG RYTHFIGILNDISE DTDP EQVEALRQALKHG KDISLITIRNYRKNGGAFWNNLFISPYRDDAG RYTHFIGILNDISE DTDP AAIGKIRQSVVDR - TEVQVTLLNYRKDGTPFWNRLAISPYPDETG SCSHIGTMYDITR ETDP AAIGKIRQSVVDR - TEVQVTLLNYRKDGTPFWNRLAISPYVDETG KCTHIGTHEDITE ETDP AAIGKIRQSVVDR - TEVQVTLLNYRKDGTPFWNRLAISPYVDFGG NICSHFTGSLQDTIW DTAP EALETIRGGLHHQ - TEVNWELINYRKDGTPFWNNLISPYVDFGG NICSHFTGSLQDTIW DTAP EALETIRGGLHHQ - TEVNWELINYRKDGTFFWNNLISPYVDFGG RYCHIGTIDDITQ DTAP EALETIRGGLHHQ - TEVNWELINYRKDGTFFWNNLISPYVDFGG QVTHFIGITQDITQ DTAP EALETIRGGLHQ - ROVHVULNIYRKDGTFFWNDLYISPYPGSG RITHFVGVINDISE ETDA GVVDMIRAGLRER - KQVSVTILNYRKDGTFFWNDLYISPYPGSG RITHFVGVINDISE ETDA GVVDMIRAGLRER - KQVSVTILNYRKDGTFFWNDLYISPYPGSG RITHFVGVINDISE ERDP MLVEEIRCGLVQA - RDVHVVLRNYRKDGTFFWNDLYISPYPGSG RITHFVGVINDISE ERDP MLVEEIRCGLVQA - RDVHVVLRNYRKDGFFFWNDLYISPYPDEGG VTTNFVGVINDISE ERDD - MGALLETREGLQQA - RDSHVVLRNYRKDGFFFWNDLYISPYPDEGG RVSHFIGVINDISE EFDLS - NIEQALDQIRKGLARG - DDISVVLRNYRKDGSFFWNDLYISPYPDEDG TVTHFIGVINDISE EFDLS - NIEQALDQIRKGLARG - DDISVVLRNYRKDGSFFWNDLYISPYDDGDG TVTHFIGVINDISE EFDLS - NIEQALDQIRKGLARG - DDISVVLRNYRKDGSFFWNDLYISPYDDGDG TVTHFIGVINDISE EFDLS - NIEQALDQIRKGLARG - DDISVVLRNYRKDGSFFWNDLYISPYDDGG SVRHYVGVINDISE EFDLS - NIEQALDQIRKGLARG - DDISVVLRNYRKDGSFFWNDLYISPYDDGG S	HAY 715 KAY 425 KAY 425 KAY 425 KAY 425 KOH 888 RADH 721 RRDH 721 RRHQ 154 KHQ 154 KHQ 154 KHQ 419 REQ 420 KKI 1116 LDI 248 KKY 490 KKY 151 KKY 489 KKY 151 KKY 490 KKY 151 KK
WP_010627231.1 WP_102627940.1 WP_110264571.1 WP_1161423473.1 WP_159341723.1 WP_159341723.1 WP_16875715.1 TVP44179.1 WP_00821604.1 WP_075879636.1 WP_083517734.1 SEF71116.1 WP_141320011.1 WP_106090146.1 WP_142051109.1 WP_106090145.1 WP_142051109.1 WP_126775935.1 WP_028239827.1 HCT41415.1 WP_127329474.1 WP_10669447691.1 WP_127329474.1 WP_10669447691.1 WP_1373840462.1 WP_1373840462.1 WP_09553309.1 WP_127996758.1 WP_145061629.1 WP_151636744.1 WP_068618302.1 TAL86525.1 WP_168840027.1 WP_1688441486.1	594 LRVLERSVQASINGIVITDASQHO-LPISYVN-EAFLALTGYREEVLGRNCRMLQGV 304 LRTLQRGVEASVIKGVIXADAREPO-MPIVYAN-ATFIKHTGYREDEILGRNCRFMQGE 776 LRILERSVEASVIKGIVLYADAIGO-MPILTWN-DAFFRITGYGKEEVQGRNCRFLQGH 774 LLTLERSVEASINGVITVDATQPG-MPLIFWN-QAFSRITGYGKEEVQGRNCRFLQGP 767 LRIFGRSLEASSKIGVILCEAUDO-PPILYWN-PAFVEITGYDFDDVRRRNCRFLQGP 600 LRIYQRSLEASSKIGVILCEAUDO-YPILYWN-PAFVALTGYDLDIKGLKGRELNGG 600 LRIYQRSLEASSKIGVILGALQDO-YPILYWN-PAFVALTGYDLEEVKGRNCRFLQGK 33 RYLFGRSLEASSKIGVILGALQDO-YPILYWN-PAFVALTGYPLEEVKGRNCRFLQGK 294 LRILGRGIEASPHGVUHADATQTO-OPILYVAN-PAFTANTGYPLEEVKGRNCRFLQGP 295 LRLLGRGIEASPHGVUHADATQTO-DPILYYAN-EAFSQLTGYALDEVLGNNCRFLQGG 298 LRLLGRGIEASPHGVUHADATQTD-MPLYYAN-EAFSQLTGYALDEVLGNNCRFLQGG 298 LRLLGRGIEASPHGVUHADATQTD-MPLYYAN-EAFSQLTGYALDEVLGNNCRFLQGG 299 LHLKRSIESSPSGFLLADAGSPO-LPVYAN-PAFTANTGYQDEITGRNCRFLQGG 299 LHLKRSIESSPSGFLADAGSPO-LPVYAN-PAFTANTGYQDEITGRNCRFLQGG 299 LHLLKRSIESSPSGFLADAGSPO-LPVYAN-PAFTANTGYQDEITGRNCRFLQGG 290 LRLLGRSEASHGVITDALAPO-HPILYYN-PAFEANTGYATEVGRNCRFLQGG 369 LRLLGRSEASHGVITDALAPO-HPILYYN-PAFEANTGYATEVGRNCRFLQGG 369 LRLLGRSEASHGVITDALAPO-HPILYYN-PAFEANTGYATEVGRNCRFLQGG 369 LRLLGRSLEASYNGTUCDAGAKO-LPILYWN-PAFEANTGYATEVGRNCRFLQGG 369 LRLLGRSLEASYNGTUCDAGAKO-LPILYWN-PAFEANTGYATEVGRNCRFLQGG 369 LRLLGRSLEASYNGTUCDAGAKO-LPILYWN-PAFEATTGYATETVGARCRFLQGG 360 LRLLGRSLEASYNGTUCDAGAKO-LPILYWN-PAFEATTGYATETVGARCRFLQGG 370 LRLKGRSLEASYNGTUCDAGAKO-LPILYWN-PAFEATTGYATETVGARCRFLQGG 258 LRLLGRSLEASYNGTUCDAGAKO-LPILYWN-PAFEATTGYATEVGARCRFLQGG 371 LRLGRSLEASYNGTUCDAGAKO-LPILYWN-PAFEATTGYATEVGARCRFLQGG 372 LRLGRSLEASYNGTUCDAGAKO-LPILYWN-PAFEATTGYATEVGARCRFLQGG	ETEP- DAVAWLRRCVVER - RDCHVTLLNYRKDGSTFWNALYVSPVLDGDG - GVTHFVGELRDVSEI ETDP - EAVAMIRRHLAEQ - REVLYTLRNYRKDGTFFWNDAFISPYRDGEG - RVTHFVGVLHDISE ETDP - OTYQETRGDLDQ - RDVQVTLGVKTKOREFFWNDAFISPYRDGEG - RVTHFVGVLHDISE ETDP - EAVMKIRRSLVAR - REVSVTLRNYRKDGSFWNDLHSPYRDGEG - RTHFVGTNDVTDF ETDP - EAVMKIRRSLVAR - REVSVTLRNYRKDGSFWNELKISPVSNRHG - EITHFVGVÄNDVTQ ETDP - KKQVQETCDALLQQ - RDISLITRNYRKDGAFWNNVFISPYRAQDG - QATHFVGIINDISE DTDP - KKQIADIQLAFEQQ - RDIALITRNYRKNGQAFWNNLFISPYRAPDG - VYTHFVGSITDISE DTDP - KQIADIQLAFEQQ - RDIALITRNYRKNGQAFWNNLFISPYRSHNG - QYTHFVGSINDISE DTDP - EQVEALRQALKHG - KOTSLITRNYRKDGAFWNNLFISPYRSHNG - QYTHFVGSITDISE DTDP - EQVEALRQALKHG - KOTSLITRNYRKDGRAFWNNLFISPYRDNAG - RVTHFIGILNDISE DTPP - EPVAQMHQALSEA - RAVDLIVRNYRKDGRFFWNNLAISPYRDBG - QYTHFIGILNDISE DTRP - GOVEATRQALSSC - MSVQVTLLNYRKDGTFFWNRLAIBPYFDETG - SCSHFIGTWDITRI ETDP - AAIGKTRQSVVDR - TEVQVTLLNYRKDGTFFWNRLAIBPYFDETG - SCSHFIGTWDITRI ETDP - AAIGKTRQSVVDR - TEVQVTLLNYRKDGTFFWNRLAIBPYFDETG - KCTHFIGTLEFITQ NTTDP - ATIKKTRGGIKAH - TDVNVVLLNYRKDGFFFWNRLAIBPYFDETG - KCTHFIGTLEFITQ DTAP - EALETTRQGLHHG - TEVWVELTINYRKDGFFFWNLLSISPYVDETG - KCTHFIGTLEFITQ DTAP - EAVAKIRAALSDN - REIDIVLQNTRKDGTFFWNLLSISPYFDEGG - RVENFIGILNDITQ ETDP - AAVAKIRAALSDN - REIDIVLQNTRKDGTFFWNDLVISPYFDEGG - RVENFIGILNDITQ ETDP - AAVAKIRAALSDN - REIDIVLQNTRKDGTFFWNDLVISPYFDEGG - RVENFIGILNDITQ DREQ - RGLEDTRQSLPQE - REVHLVLRNYRKDGTFFWNDLVISPYFDEGG - RVENFIGILNDITQ DREQ - RGLEDTRQSLPQE - REVHLVLRNYRKDGTFFWNDLVISPYFDEGG - VITHFVGVINDISE ERDP - MLVEETRGLVQA - RDVHVVLRNYRKDGFFFWNDLVISPYFDEGG - RVSHFIGVINDISE TADPF - NDGALNEIREGLKQ - SPVKVVLRNYRKDGFFFWNDLVISPYFDEGG - VITHFVGVINDITE EFDD - ARVENTAGERER - KQVSVTLLNYRKDGFFFWNDLVISPYFDEGG - VITHFVGVINDITE ERDP - MLVEETRGLVQA - RDVHVVLRNYRKDGFFFWNDLVISPYFDEGG - VITHFVGVINDITE ERDP - MILVEETRGLVQA - RDVHVVLRNYRKDGFFFWNDLVISPYFDEGG - VYTHFVGVINDITE ERDD - STRLATRQGETRAG - SOSSVVVVLRNYRKDGFFFWNDLVISPYFDEGG - VYTHFVGVINDISE TADPF - NDGALNEIREGLKQ - SPVKVVLRNYRKDGFFFWNDLVISPYDDEGG - VVTHFVGVINDISE TADPF - NDGALNEIREGLKQ - SPVKV	HAY 715 KAY 425 IAO 895 KOH 888 ROH 721 ROH 721 ROH 721 ROH 721 ROH 419 LEG 419 KKE
WP_010627231.1 WP_102627940.1 WP_112054571.1 WP_112054571.1 WP_161423473.1 WP_159341723.1 WP_146875715.1 TVP44179.1 WP_100821604.1 WP_075879636.1 WP_141326011.1 WP_110200210.1 WP_10699146.1 WP_110200210.1 WP_126775935.1 WP_12675935.1 WP_028239827.1 HCT41415.1 WP_090447691.1 WP_12675995.1 WP_127329474.1 WP_106694265.1 WP_137840462.1 WP_09553309.1 WP_127996758.1 WP_151636744.1 WP_066816302.1 TAL86525.1 WP_1668040027.1	594 LRVLERSVQASINGIVITDASQHO-LPISYVN-EAFLALTGYREEVLGRNCRMIQGV 304 LRTLGROVEASVIKGVYLADAREPO-MPIVYAN-ATFRKHTCYREDEILGRNCRFMIQGE 776 LRILERSVEASVIKGVLYADAREPO-MPIVYAN-ATFRKHTCYREDEILGRNCRFMIQGE 777 LLTLGRSLEASSINGVITUDATQPG-MPLIFVN-QAFSRITGYGKEEVQGRNCRFLIQGP 767 LRIFGRSLEASSINGVITUDATQPG-MPLIFVN-QAFSRITGYGKEEVQGRNCRFLIQGP 600 LRIYQRSLEASSINGVITUDATQPG-MPLIFVN-PAFVAITGYQLDDIKGINGRFLIQGP 800 LRIYQRSLEASSINGVITUDATQPG-MPLIFVN-PAFVAITGYQLDDIKGINGRFLIQGC 33 RYLFQRSLEASSINGVITUDALTQDYPILYVN-PAFVAITGYPLEEVKGHNCRFLIQGC 240 LHIFERSLQASSINGVILADATQTO-QPIVYAN-PAFVAITGYPLEEVKGHNCRFLIQGP 291 LRILGRGIGASPNGVLHADATQPO-MPLYVAN-EAFSQLTGYALDEVLGNNCRFLIQGP 292 LRILLGRGIGASPNGVLHADATQPO-MPLYVAN-EAFSQLTGYALDEVLGNNCRFLIQGC 293 LRILGRGIGASPNGVLHADATQPO-MPLYVAN-EAFSQLTGYALDEVLGNNCRFLIQGC 294 LRILGRGIGASPNGVLHADATQPO-MPLYVAN-EAFSQLTGYALDEVLGNNCRFLIQGC 295 LHLIKRSIESSPSGFLHADAGSPO-LPVVYAN-PAFTANTGYODEITGRNCRFLIQGG 296 LRILKRSIESSPSGFLHADAGSPO-LPVVYAN-PAFTANTGYODEITGRNCRFLIQGG 297 LHLLKRGIEANPNGMLHVDARSPO-MPVVYAN-PAFTANTGYODEITGRNCRFLIQGG 298 LRILKRSIESSPSGFLHADAGSPO-LPVYAN-PAFTANTGYODEITGRNCRFLIQGG 30 LHLKRSLEASYNGTUADATRD	ETEP- DAVAWLRRCVVER-RDCHVTLLNYRKDGSTFWNALYVSPVLDGDG GVTHFVGELRDVSEI ETDP EAVAMIRRHLAEQ - REVLVTLRNYRKDGTFFWNDAFISPYRDGEG RYTHFVGVLHDISE ETDP OTVQEIRQGLDDQ - RDVQVTLCNYRKNGEFFWNDAFISPYRDGEG RYTHFVGVLHDISE ETDP EAVAMIRRHLAEQ - REVLVTLRNYRKNGEFFWNDAFISPYRDGEG STHFUGVINDVTQ ETDP EAVAMIRRSLVAR - REVSYTLRNYRKNGESFWNDLKISPYSNRHG EITHFVGVANDVTQ DTDP EAVAMIRRSLVAR - REVSYTLRNYRKNGGAFWNNVFISPYRADDG OTATHVGIINDISE DTDP KGVQEICDALLQQ - RDISLITIRNYRKNGGAFWNNVFISPYRADDG VYTHFVASINDISE DTDP KKJUADIQALEQQ - QDIILTIRNYRKNGGAFWNNVFISPYRADDG OTATHVGIINDISE DTDP KKJUADIQAFEQQ - RDIALTIRNYRKNGGAFWNNLFISPYRADDG OTATHVGSITNDISE DTDP EQVEALRQALKHG KDISLITIRNYRKNGGAFWNNLFISPYRADDG RYTHFVGSITNDISE DTDP EQVEALRQALKHG KDISLITIRNYRKNGGAFWNNLFISPYRDNAG RYTHFIGILNDISE DTDP EQVEALRQALKHG KDISLITIRNYRKNGGAFWNNLFISPYRDNAG RYTHFIGILNDISE DTDP EQVEALRQALKHG KDISLITIRNYRKNGGAFWNNLFISPYRDDAG RYTHFIGILNDISE DTDP AAIGKIRQSVVDR - TEVQVTLLNYRKDGTPFWNRLAISPYPDETG SCSHIGTMYDITR ETDP AAIGKIRQSVVDR - TEVQVTLLNYRKDGTPFWNRLAISPYVDETG KCTHIGTHEDITE ETDP AAIGKIRQSVVDR - TEVQVTLLNYRKDGTPFWNRLAISPYVDFGG NICSHFTGSLQDTIW DTAP EALETIRGGLHHQ - TEVNWELINYRKDGTPFWNNLISPYVDFGG NICSHFTGSLQDTIW DTAP EALETIRGGLHHQ - TEVNWELINYRKDGTFFWNNLISPYVDFGG RYCHIGTIDDITQ DTAP EALETIRGGLHHQ - TEVNWELINYRKDGTFFWNNLISPYVDFGG QVTHFIGITQDITQ DTAP EALETIRGGLHQ - ROVHVULNIYRKDGTFFWNDLYISPYPGSG RITHFVGVINDISE ETDA GVVDMIRAGLRER - KQVSVTILNYRKDGTFFWNDLYISPYPGSG RITHFVGVINDISE ETDA GVVDMIRAGLRER - KQVSVTILNYRKDGTFFWNDLYISPYPGSG RITHFVGVINDISE ERDP MLVEEIRCGLVQA - RDVHVVLRNYRKDGTFFWNDLYISPYPGSG RITHFVGVINDISE ERDP MLVEEIRCGLVQA - RDVHVVLRNYRKDGFFFWNDLYISPYPDEGG VTTNFVGVINDISE ERDD - MGALLETREGLQQA - RDSHVVLRNYRKDGFFFWNDLYISPYPDEGG RVSHFIGVINDISE EFDLS - NIEQALDQIRKGLARG - DDISVVLRNYRKDGSFFWNDLYISPYPDEDG TVTHFIGVINDISE EFDLS - NIEQALDQIRKGLARG - DDISVVLRNYRKDGSFFWNDLYISPYDDGDG TVTHFIGVINDISE EFDLS - NIEQALDQIRKGLARG - DDISVVLRNYRKDGSFFWNDLYISPYDDGDG TVTHFIGVINDISE EFDLS - NIEQALDQIRKGLARG - DDISVVLRNYRKDGSFFWNDLYISPYDDGG SVRHYVGVINDISE EFDLS - NIEQALDQIRKGLARG - DDISVVLRNYRKDGSFFWNDLYISPYDDGG S	HAY 715 KAY 425 KAY 425 KAY 425 KAY 425 KAY 425 KAY 425 KAY 485 KAY 486 KAY 48
WP_010627231.1 WP_102627940.1 WP_110264571.1 WP_1161423473.1 WP_159341723.1 WP_146875715.1 TVP44179.1 WP_00821604.1 WP_075879636.1 WP_083517734.1 SEF71116.1 WP_141320611.1 WP_110200210.1 WP_100690146.1 WP_142651109.1 WP_10690146.1 WP_126775935.1 WP_028239827.1 HCT41415.1 WP_090447691.1 WP_127329474.1 WP_106694265.1 WP_137840462.1 WP_137840462.1 WP_090553309.1 WP_137840462.1 WP_109553301.1 WP_151636740.1 WP_151636740.1 TAL86525.1 WP_160840027.1 WP_088341486.1 WP_0958341486.1	594 LRVLERSVQASINGIVITDASQHO-LPISYVN-EAFLALTGYREEVLGRNCRMIQGV 304 LRTLGRCVEASVIKGVYLADAREPO-MPIVYAN-ATFRKHTCYREDETLGRNCRFMIQGE 776 LRILGRSVEASVIKGVLYDANIQTO-MPILTAN-HAFSRISGYSNAETKGRNCRFLQGH 777 LLTLGRSVEASVIKGVLYDANIQTO-MPILTAN-HAFSRISGYSNAETKGRNCRFLQGH 778 LRICRSVEASVIKGVLYDATQPG-MPLIFVN-QAFSRITGYGKEEVQGRNCRFLQGP 767 LRIFQRSLEASSIKGVLICEAU,DD-FPILYVN-PAFVAITGYGLDDIKGINGRFLIGG 600 LRIYQRSLEASSKIGVLICEAU,DD-YPILYVN-PAFVAITGYQLDDIKGINGRFLIGG 600 LRIYQRSLEASSKIGVLICEAU,DD-YPILYVN-PAFVAITGYPLEEVKGHNCRFLLQGK 33 RYLFGRSLEASSKIGVLISQAIVPE-LPILYTN-PAFVAITGYPLEEVKGHNCRFLLQGH 240 LHIFERSLQASSKIGVLISDAITQTD-QPIVYAN-PAFVAITGYPLEEVKGHNCRFLLQGH 251 LRLLQRGIGSSPNGVLIADATQTD-MPILYAN-EAFSQLTGYALDEVLGRNCRFLLQGH 252 LRLLQRGIGSSPNGVLIADATQTD-MPILYAN-EAFSQLTGYALDEVLGRNCRFLLQGH 253 LRLLQRSIGSSPNGVLIADATQTD-MPILYAN-EAFSQLTGYALDEVLGNCRFLLQGH 254 LRLLKRSIESSSFGFLUADASPD-LPVYAN-PAFFANTGYDDEUTGRNCRFLLQGH 255 LHLLKRGIEANPNGMLHVDARSPD-MPVYYAN-PAFFANTGYDQDETLGRNCRFLLQGH 256 LRLLKRSIESSSFGGVLADASPD-LPVYYAN-PAFFANTGYDQDETLGRNCRFLLQGH 257 LKLLKRSLEASYNGVYTDALAPD-HPILYYN-PAFERTTGYSTETLALGRNCRFLQGH 36 LRLLGRSLEASYNGVYTDALAPD-HPILYYN-PAFERTTGYATEVLGRNCRFLQGH 37 LNLFRSLEASYNGVYTDALAPD-HPILYYN-PAFERTTGYATEVLGRNCRFLQGH 257 LKLLKRSLEASYNGVYTDALAPD-HPILYYN-PAFERTTGYATEVLGRNCRFLQGH 258 LRLLKRSIESSSNGVYTDALAPD-HPILYYN-PAFERTTGYATEVLGRNCRFLQGH 257 LKLLKRGIESSSNGVYTDALAD-HPILYYN-PAFERTTGYATEVLGRNCRFLQGH 258 LRLLKRSIESSSNGVYTDALAD-HPILYYN-PAFERTTGYATEVLGRNCRFLQGH	ETEP- DAVAMLRRCVVER - RDCHVTLLINYRKDGSTFWNALYVSPVLDGDG - GVTHFVGELRDVSEI ETDP - EAVAMIRRHLAEQ - REVLVTLRINYRKDGTFFWNDAFISPVRDGEG - RVTHFVGVLHDISE ETDP - OTYQETRGLDDQ - RDVQVTLGNKROEFFWNDAFISPVRDGEG - RVTHFVGVLHDISE ETDP - EAVAMIRRHLAEQ - REVSVTLRINYRKDGTFFWNDAFISPVRDGEG - RVTHFVGVLHDISE ETDP - GYDQETRGDLDQ - RDVGTLTIRNYRKDGSFWNDLTISPVRDGG - GYTHFVGINDISE DTDP - KGVQETCDALLQQ - RDISLITRNYRKDGAFWNNVFISPVRAQDG - QATHFVGINDISE DTDP - KKIDALQQALEQQ - QDITLTIRNYRKDGAFWNNVFISPVRAQDG - VYTHFVGSINDISE DTDP - KKIDALQQALEQQ - RDISLITRNYRKDGAFWNNVFISPVRADDG - VYTHFVGSINDISE DTDP - EQVEALRQALKHG - KOISLITRNYRKDGAFWNNLFISPVRADDG - QVTHFVGSINDISE DTOP - EQVEALRQALKHG - KOISLITRNYRKDGAFWNNLFISPVRADDG - QVTHFIGILNDISE DTOP - EQVEALRQALKHG - KOISLITRNYRKDGAFWNNLFISPVRADGG - QVTHFIGILNDISE DTP - GOVEALRQALSGS - NSVQVITLNYRKDGTFFWNRLAISPVPDETG - SCSHFIGTWDITRI ETDP - AAIGKIRQSVVDR - TEVQVTLLNYRKDGTFFWNRLAISPVPDETG - SCSHFIGTWDITRI ETDP - AAIGKIRQSVVDR - TEVQVTLLNYRKDGTFFWNRLAISPVPDETG - SCSHFIGTWDITRI ETDP - AAIGKIRQSVVDR - TEVQVILLNYRKDGTFFWNRLAISPVPDEGG - RCTHFIGILEDITE ETAP - ASTDITRDAL RRC - SAVEVTI LIYRRDGSTFWNNL ISTPVPDETG - KLTHFIGILEDITE ETAP - AATRIKTRDGKAH - TDVINVELINYRKDGTFFWNRLAISPVPDEGG - RCTHLIGTHQDITY ETDP - AAVAKIRAALSON - REIDIVLQNTRKDGTFFWNNLAFSPVDHEGG - RVSNFIGILNDITQ DTAP - EALETIRQGLHQ - TEVINVELINYRKDGTFFWNDLYSPVPDEGG - RVSNFIGILNDITQ ETDD - AAVAKIRAALSON - REIDIVLQNTRKDGTFFWNDLYSPVPSGGG - RITHFVGVLNDISE ETDA - GVVONTRAGRER - KOVSVTLINYRKDGTFFWNDLYSPYPSGGG - RITHFVGVLNDISE EENDP - MLVEEIRGGLVQA - RDVHVVLRNYRKDGTFFWNDLYSPYPSGGG - RVSHFIGVLNDISE EENDP - MLVEEIRGGLVQA - RDVHVVLRNYRKDGSFFWNDLYSPYPSGGG - VITNFVGVINDITE EENDD - PGLTEIRGLQQQ - RD LHVVLRNYRKDGSFFWNDLYSPYPDEGG - VYTHFIGVLNDISE EFDLS - NDGALUEIRGGLKKQ - SPVKVVLRNYRKDGSFFWNDLYSPYPDEGG - VYTHFIGVLNDISE EFDLS - NDGALUEIRGGLKKQ - SPVKVVLRNYRKDGSFFWNDLYSPYPDEGG - VYTHFVGVLNDISE EFDLD - GETVLRDALSNG - GSSNVVVRNYRKDGSFFWNDLYSPYPDEGG - VYTHFVGVLNDISE EFDLS - NDGALUEIRGGLKKG - SPVKVVLRNYRKDGSFFWNDLYSPYPDEGG - VYTHFVGVLNDISE EFDLS - NDGALUEIRGGLKKG - SPVKVVLRNY	HAY 715 KAY 425 KAY 425 KAY 426 KAY 419 KAY 419 KAY 419 KAY 420 KAY 419 KAY 420 KAY 419 KAY 430 KAY 43
WP_010627231.1 WP_102627940.1 WP_11205491.1 WP_112054571.1 WP_161423473.1 WP_159341723.1 WP_164875715.1 TVP44179.1 WP_00821604.1 WP_075879636.1 WP_083517734.1 SEF71116.1 WP_1413206111.1 WP_1140200210.1 WP_106090146.1 WP_142051109.1 WP_106990146.1 WP_126775935.1 WP_028239827.1 HCT41415.1 WP_028239827.1 HCT41415.1 WP_127329474.1 WP_106694265.1 WP_137840462.1 WP_099533309.1 WP_137840462.1 WP_09953309.1 WP_151636744.1 WP_066818302.1 TAL86525.1 WP_160840027.1 WP_088341486.1 WP_051861776.1 WP_1646415482.1 WP_051861776.1 WP_16939838.1 HBB33017.1	594 LRVLERSVQASINGIVITDASQHO-LPISYVN-EAFLALTGYREEVLGRNCRMIQGV 304 LRTLQRGVEASVIKGVIXADAREPO-MPIVYAN-ATFIKHTGYREDEILGRNCRFMIQGE 776 LRILERSVEASVIKGIVLONIQTO-MPIITWN-DAFFRITGYGKEEVQGRNCRFLIQGH 777 LLTLGRSLEASSINGVITUDATQPG-MPLIFVN-QAFSRITGYGKEEVQGRNCRFLIQGP 767 LRIFQRSLEASSINGVITUGALQDG-MPLIFVN-QAFSRITGYGKEEVQGRNCRFLIQGP 768 LRIVQRSLEASSINGVITUGALQDD-YPILYVN-PAFVAITGYQLDDIKGLKGRFLIGGG 600 LRIYQRSLEASSINGITICEALQDD-YPILYVN-PAFVAITGYQLDDIKGLKGRFLIGGG 33 RYLFQRSLEASSINGVITGATUPG-LPILYVN-PAFVAITGYPLEEVKGHNCRFLIQGG 240 LHIFERSLQASSINGVIXADATQTD-QPIVYAN-PAFVAITGYPLEEVKGHNCRFLIQGG 291 LRILGRGIGASPHGVIMADATQTD-DPILYVAN-EAFSQLTGYALDEVLGNNCRFLIQGG 292 LRILGRGIGASPHGVIMADATRID-LPLYVAN-EAFSQLTGYALDEVLGNNCRFLIQGG 293 LRILGRGIFASPHGVIMADATRID-LPLYVAN-EAFSQLTGYALDEVLGNNCRFLIQGG 294 LRILGRGIFASPHGVIMADATRID-PLVYAN-PAFTANTGYQDETIGRNCRFLIGGS 295 LHLIKRSIESSPSGFLIADAGSPD-LPVYAN-PAFTANTGYQDETIGRNCRFLIGGS 296 LKLIKRSIESSPSGFLIADAGSPD-HPVYYAN-PAFTANTGYQDETIGRNCRFLIGGS 297 LHLLKRSIEASYNGTLVADATRID-HPILYYN-PAFTANTGYQDETIGRNCRFLIGGS 298 LKLIKRSIESSPSGFLIADAGSPD-HPVYYAN-PAFTANTGYQDETIGRNCRFLIGGS 298 LKLIKRSIESSPSGFLIADAGSPD-HPVYYAN-PAFTANTGYQDETIGRNCRFLIGGS 299 LHLIKRSIEASYNGTLVADATDPD-HPILYTN-PAFTANTGYQDETIGRNCRFLIGGS 30 LHLIKRSIEASYNGTLVADATDPD-HPILYTN-PAFERTTGYFDREVLGRNCRFLIGGF 36 LRILGRSLEASYNGTLVADALSHD-HPILYTN-PAFERTTGYFDSEVIGNKGRFLIGGT 257 LKLIKRCIESSSNGVVYDTALSHD-HPILYN-PAFERTTGYFAEEVLGRNCRFLIGGG 258 LRILGRSLEASYNGTLVADALABC	ETEP	HAY 715 KAY 425 KAY 425 KAY 425 KAY 425 KAY 425 KAY 425 KAY 485 KAY 485 KAY 481 KAY 48
WP_010627231.1 WP_102627940.1 WP_110264571.1 WP_1161423473.1 WP_159341723.1 WP_159341723.1 WP_16875715.1 TVP44179.1 WP_00821604.1 WP_075879636.1 WP_083517734.1 SEF71116.1 WP_141320011.1 WP_100690145.1 WP_142051109.1 WP_126775935.1 WP_028239827.1 HCT41415.1 WP_127329474.1 WP_106694425.1 WP_127329474.1 WP_10669405.1 WP_1373840462.1 WP_1373840462.1 WP_145061629.1 WP_13786744.1 WP_068618302.1 TAL86525.1 WP_16863002.1 TAL86525.1 WP_168614027.1 WP_088341486.1 WP_088341486.1 WP_088093898.1	594 LRVLERSVQASINGIVITDASQHO-LPISYVN-EAFLALTGYREEVLGRNCRMIQGV 304 LRTLQRGVEASVIKGVIXADAREPO-MPIVYAN-ATFIKHTGYREDEILGRNCRFMIQGE 776 LRILERSVEASVIKGIVLONIQTO-MPIITWN-DAFFRITGYGKEEVQGRNCRFLIQGH 777 LLTLGRSLEASSINGVITUDATQPG-MPLIFVN-QAFSRITGYGKEEVQGRNCRFLIQGP 767 LRIFQRSLEASSINGVITUGALQDG-MPLIFVN-QAFSRITGYGKEEVQGRNCRFLIQGP 768 LRIVQRSLEASSINGVITUGALQDD-YPILYVN-PAFVAITGYQLDDIKGLKGRFLIGGG 600 LRIYQRSLEASSINGITICEALQDD-YPILYVN-PAFVAITGYQLDDIKGLKGRFLIGGG 33 RYLFQRSLEASSINGVITGATUPG-LPILYVN-PAFVAITGYPLEEVKGHNCRFLIQGG 240 LHIFERSLQASSINGVIXADATQTD-QPIVYAN-PAFVAITGYPLEEVKGHNCRFLIQGG 291 LRILGRGIGASPHGVIMADATQTD-DPILYVAN-EAFSQLTGYALDEVLGNNCRFLIQGG 292 LRILGRGIGASPHGVIMADATRID-LPLYVAN-EAFSQLTGYALDEVLGNNCRFLIQGG 293 LRILGRGIFASPHGVIMADATRID-LPLYVAN-EAFSQLTGYALDEVLGNNCRFLIQGG 294 LRILGRGIFASPHGVIMADATRID-PLVYAN-PAFTANTGYQDETIGRNCRFLIGGS 295 LHLIKRSIESSPSGFLIADAGSPD-LPVYAN-PAFTANTGYQDETIGRNCRFLIGGS 296 LKLIKRSIESSPSGFLIADAGSPD-HPVYYAN-PAFTANTGYQDETIGRNCRFLIGGS 297 LHLLKRSIEASYNGTLVADATRID-HPILYYN-PAFTANTGYQDETIGRNCRFLIGGS 298 LKLIKRSIESSPSGFLIADAGSPD-HPVYYAN-PAFTANTGYQDETIGRNCRFLIGGS 298 LKLIKRSIESSPSGFLIADAGSPD-HPVYYAN-PAFTANTGYQDETIGRNCRFLIGGS 299 LHLIKRSIEASYNGTLVADATDPD-HPILYTN-PAFTANTGYQDETIGRNCRFLIGGS 30 LHLIKRSIEASYNGTLVADATDPD-HPILYTN-PAFERTTGYFDREVLGRNCRFLIGGF 36 LRILGRSLEASYNGTLVADALSHD-HPILYTN-PAFERTTGYFDSEVIGNKGRFLIGGT 257 LKLIKRCIESSSNGVVYDTALSHD-HPILYN-PAFERTTGYFAEEVLGRNCRFLIGGG 258 LRILGRSLEASYNGTLVADALABC	ETEP- DAVAWLRRCVVER - RDCHVTLLNYRKDGSTFWNALYVSPVLDGDG - GVTHFVGELRDVSEI ETDP - EAVAMIRRHLAEQ - REVLYTLRNYRKDGTFFWNDAFISPYRDGEG - RVTHFVGVLHDISE ETDP - OTYQETRGDLDQ - RDVQVTLGVTLGVRKNGERFWNDAFISPYRDGEG - RVTHFVGVLHDISE ETDP - EAVMKIRRSLVAR - REVSVTLRNYRKDGSFWNDLTSPYRDGEG - RVTHFVGVLNDVTQ ETDP - EAVMKIRRSLVAR - REVSVTLRNYRKDGSFWNELKISPVSNRHG - EITHFVGVÄNDVTQ ETDP - KKQVQETCDALLQQ - RDISLITRNYRKDGRAFWNNVFISPYRAQDG - QATHFVGIINDISE DTDP - KKQIADIQLAEQQ - QOTITITRNYRKDGAFWNNVFISPYRAQDG - QVTHFVGSINDISE DTDP - KKQIADIQLAEQQ - RDIALTIRNYRKDGAFWNNLFISPYRDADG - QVTHFVGSINDISE DTDP - KQIADIQLAFEQQ - RDIALTIRNYRKDGAFWNNLFISPYRDNAG - RVTHFIGILNDISE DTDP - EQVEALRQALKHG - KOISLITRNYRKDGAFWNNLFISPYRDNAG - QVTHFVGSINDISE DTPP - EQVEALRQALKHG - KOISLITRNYRKDGRAFWNNLFISPYRDNAG - RVTHFIGILNDISE DTRP - GOVEATRQALSSC - MSVQVITLNYRKDGRFFWNNLAISPYRDBGG - QVTHFIGILNDISE ETDP - AAIGKTRQSVVDR - TEVQVTLLNYRKDGTFFWNRLAIBPYFDETG - SCSHFIGTWDITTR ETDP - AAIGKTRQSVVDR - TEVQVTLLNYRKDGTFFWNRLAIBPYFDEGG - RCTHFIGTLEDITE ETDP - AAIGKTRQSVVDR - TEVQVTLLNYRKDGTFFWNRLAIBPYFDEGG - RCTHFIGTLEDITE ETDP - AAIGKTRQSLAH - TOWNVLLNYRKDGGFFWNNLRISPYFDEGG - RCTHFIGTLEDITE ETDP - AAVAKIRALSDN - REIDIVLQNTRKDGTFFWNNLLSPYFDEGG - RCTHLIGTNDITY DTAP - EALETTRQGLHHQ - TEVWELTNYRKDGTFFWNDLVISPYFDEGG - RVENFIGINDITQ ETDA - GVVDNTRAGLRER - KQVSVTLLNYRKDGTFFWNDLVISPYFSGSG - RITHFVGVLNDISE ETDA - GVVDNTRAGLRER - KQVSVTLLNYRKDGTFFWNDLVISPYFSGGG - VITNFVGVINDITE ETDA - GVVDNTRAGLRER - KQVSVTLNYRKDGTFFWNDLVISPYFSGGG - VITNFVGVINDITE ETDA - GVVDNTRAGLRER - KQVSVTLNYRKDGTFFWNDLVISPYFSGGG - VITNFVGVINDISE ENDD - PROGALDQIRKGLARG - DDISVVLRNYRKDGTFF	HAY 715 KAY 425 KAY 425 KAY 425 KAY 425 KAY 425 KAY 425 KAY 485 KAY 485 KAY 481 KAY 48

WP 015201020.1	535 I RI RORAI AASTNGTTTTDARI PN-I PTVYVN-OSFEKTTGYSACEVTGRNSREI OKS	-DHNQPALEELQTAIDTHQCCTVLLRNYRKDGVLFWNELSISPVFDVKQKLTHYIGIINDVSDRK	OS 656
WP 082218446.1		-ERNOPDLDKLRAAIREGRDCTVVLRNYRKDGSLFWNELSVSPIYDASGNLTHFIGIITDITERK	5
WP 038083769.1		-ETDQPGLLEIRQALKDGRECQVVVRNFRKDGTSFWNELKISPVYDAAGNLTNFIGVLKDISKRL	
WP 015184119.1	7.7	-DREOPALTELRTALOOERECRVVLRNYRKDGSLFWNEFSISPVRNSAGILTHYIGVHRDITELK	
WP 157730878.1		-DRNQPEIAFMSKAIGHGSSCRVLIRNYSKDGILFWNDLFITPLYDQDQKLTHFIGVLNDVTEIQ	Section Production
WP 085496934.1		-DRDQ	
WP_123897049.1		-DRDQTAVTTMNHAIKNGQSCEVILRNYKKDGSLFYNELTITPIYNDQQKLTHFIGASNDVTNRF	
WP 158775729.1		-DKDQEEINTIRAALQIGEPCKVKLRNYKKDGSLFWNELTITPVRNGKDELTHYIAIINDITHQK	
		-DKDQFEIKLMSEAIRNGEDCRVVLRNYRKDGSLFWNEVSITPIYNEKVLTHFVGVHNDVTAHK	
WP_013995172.1			
WP_055436897.1		-DLDQVLTHFIGVHKNVTARK	
WP_051219122.1		-DHDQVMTHFIGVLNDVTLRK	
WP_136842813.1	The state of the s	-DKQQKAITKLKNAVNNGKSCRATLRNYKKDGTLFWNDLQITPIKNKKGVVTHFIGILNDITRTK	
WP_109680952.1		-DRQQEAINKLQNAIKNGERCQVTLRNYKKDGTLFWNDLHITPIKDSNGIVTNYIGILNDITNKK	
GAJ72486.1		-DKDQBGLEAIREALKNNSSISVILRNYRKDGTLFYNNLRIDPVFDDENKITHFIGIITDITEIK	
WP_095572772.1		-DRDQPGIDTLRSAVSNQESCSVVLRNYRKDGTLFYNNLKIDPAFNDDGVMTHYIGVLTDVTEMK	
OHD80347.1		-DHDQQETREIRNGLKERQSTQSLIRNYRKDGTPFWNDIRIAPVWSEEGQLTHFIGVCNVVDKL-	
PXW92864.1		-DRNQPGLAQMRQALANRQGCRVLLRNYRKDGSLFWNEVTLAPII-EEGRFTHVVGMLRDITARL	
0JV88243.1	726 FWLLEQAIDASSSGVLITDANQVD-NPIIYAN-KGFEKISGFLREEVIGKNCRFLQGD	-DRPQKVEYFVGILNDVTDQVKVEYFVGILNDVTDQV	KA 847
WP_117392628.1	17 IELLKKAMDASISGIIITDNNQPD-NPIIYCN-AAFEQIAGYSRAEIIGHNCRFLQKD	-DRNQGVDYFIGVRMT	131
01016719.1	24SISPTIITNPNEDD-NHIIYAN-NAFIELFEYTFEEVVGHNCRFLHSD	-DTEQLALDEVRDAIHEKKSITVNLHNYTHSGALIYNEVTISPIFDKKSGKLKYYLGIYKDVTTTQ	RL 136
WP_135482946.1	28 MQLYEGALNATSTAVCIALADAEQDDPIIYVN-PAFESITGYNREQVLGRNCRFLQGN	-DRDQPSLDLVRKALREHCSCRAVLRNYRQNGDLFWNRIYISPIRTEAETISHFIAVCEDITLQK	/A 150
AHF03511.1	465 LNLRDRAIEAASCGILITDARRAD-NPLVYVN-PEFERITGYRASEVVGHNCRLLQAG	-DSDQPGVKMLREGLGGROPVTVLLRNYRKDGSLFWNQISIAPVFDSDGELVHFVGIVTDVTERI	RA 586
WP 115939012.1	478 LHLLTRAIESASCGIIITDAVSAD-NGLOYVN-PAFERITGYEAAEVLGMNCRFLOGD	-ETDPDMVMVLEKAVKNEEPVKVRLQNYRKDGVPFWNEVSISPVRDSRGRLINFVGVINDVTEQI	NS 599
TVR81987.1		-DTDDTATHFIGTLSDVSVLK	
WP_083685458.1		-DRDQPGIALIRHAVEHAEISTALLRÑYRKDGSLFWSRMHLFPVREDGAAPTHFVAFLQDVTEVV	
TQK10308.1		-DTNQPGLDQLRACIADQRPCTTTLRNYRKDGTMMWVRMHIFPLHDELGRLMNFAGFLQDVTDAI	
WP 064030994.1		-GADA	
PRY12250.1		-DTLPADVAHLRDGIA0EOTVSKTILNYRODGSAFYNHVVISPVFDAEGRLTHRVGVLTDVTGOV	
		-ETGADEIETIRRSIETPAEVRVTLKNYRKDGSFFWNOLFICPAHNSSGELTHFIGVIRDASKEE	
WP_126804183.1			
0YT87052.1		-DTAPEAVTQLREALREHRPVTVELLNYRRDGSTFWCRVALAPLRNERGELTHMVGVLHDLTDEF	
WP_067563330.1		-DRDQPARWRLAGALARGEPCTVVLRNFRRDGSAFDNRIEVTPVPGVDERVTHTVAVTSDLSQRQ	
WP_075085486.1		-ETNPETVGEIGVGIRQGRATHVTVLNYRKNGEQFWNELVITPVHNDQEVLTHFIGVLFDMTEHQ	
NES04871.1		-YRNQPAISQLKKAVLHGQECHVILQNVRKDGTDFWNELFIAPVYNSYNHLTNFIGIITDITERF	
WP_068142547.1		-STDPAAVQRIRQALQDRQDCVVTLQNYRRDGTSFWNELRLAMVEDEQRNITHFVGILHDVTEQV	
TLY40875.1	THE COUNTY OF THE PROPERTY OF	-DTDPSAVAEIRQALKEERGLRIELLNYRKDGRSFWNDLTISPLRDAKGRVTHYVGIISDRTERK	
TLY40624.1	DESCRIPTION OF THE PROPERTY AND THE PROPERTY OF THE PROPERTY O	-DTDSQVTHFVGVLADITARK	
WP_010043508.1	321 LRFRERAITSADQGFVICDFLAPD-RPLIYVS-PGFERITGWAAADVTGRNCRFLQGR	-DTDRRVTHYVGVLSDVTARF	L 442
WP_010043417.1	497 LRQRDRAIHAVTQGIVITDARRPG-HPIVFVS-PGFERLTGYSAAEALGRNCRFLQGK	-DTDPRVTQFVGVLTDVTQRF	AL 618
WP_162667406.1	707 LQLRDRAVRAVTQGILIADAAQPD-NPIIYAT-PGFERMTGYGVEEVLGRNCRFLQGP	-DTDRRTVSRLREAIRVGESCSAELLNYRKDRTPFWNDLSVAPVRDETGRLTHFVGVLTDVTSRF	HL 828
WP_162667406.1 WP_010041727.1	1 1 1	-DTDRATVSRLREAIRVGESCSAELLNYRKDRTPFWNDLSVAPVRDETG	
-	511 LRLRDRAIQAVTQGILITSPALPD-NPITYAS-PGFEGVTGYPPREALGRNCRFLQGK		KL 632
WP_010041727.1	511 LRLRDRAIQAVTQGILITSPALPD-NPITYAS-PGFEGVTGYPPREALGRNCRFLQGK 144 LQWRDRAIQSLVQGLCITDPSLPD-NPIIYVN-DSFLRITGYAREDVIGQNCRLLQGP	-DSDPAAVALVREAVRAGRDCAVEVLNYRKDGTPFWNALSVSPIRDDAGELTHFVGVLVDVTDRW	KL 632 LM 265
WP_010041727.1 WP_020473798.1 HCC28399.1	511 LRLRDRAIQAVTQGILITSPALPD-NPITYAS-PGFEGVTGYPPREALGRNCRFLQGK 144 LQWRDRAIQSLVQGLCITDPSLPD-NPIIYVN-DSFLRITGYAREDVIGQNCRLLQGP 3 KMFRREILEAIGHGVVFTDPAEKITYAN-RYFCEITGYDESEVLGRTCRFLQGP	-DSDPAAVALVREAVRAGRDCAVEVLNYRKDGTPFWNALSVSPIRDDAGELTHFVGVLVDVTDRI- -KTAPSVTIIREAVRDKRTCLVELQNYRKDGTTFWNGLSLSPIRDTAGAVANFVGVLTDISPLI	KL 632 LM 265 AR 121
WP_010041727.1 WP_020473798.1 HCC28399.1 WP_067676345.1	511 LRLRDRAIQAVTQGILITSPALPD-NPITYAS-PGFEGVTGYPPREALGRNCRFLQGK 144 LQWRDRAIQSLVQGLCITDPSLPD-NPITYWH-DSFLRITGYAREDVIGQNCRLLQGP 3 KWFRREILEAIGHGVVFTDAEKITYAN-RYFCEITGYDESEVLGRTGRFLQGP 3 KUFRREVIEAIGHGVIFSDAEQLITYAN-GSFCELTGYDRSEIVGRNCGFFLQGP	-DSDP	KL 632 LM 265 AR 121 VQ 121
WP_010041727.1 WP_020473798.1 HCC28399.1 WP_067676345.1 WP_157075159.1	511 LRLRDRAIQAVTQGILITSPALPD-NPITYAS-PGFEGVTGYPPREALGRNCRFLQGK 144 LOWRDRAIQSLVQGLCITDFSLPD-NPIIVWL-DSFLRITGYAREDVIGONCRLLOGP 3 KHRRREILEAIGHGVVFTDPAEKITYAN-RYFCEITGYDESEVLGRTCRFLQGP 3 KLFRREVIEAIGHGVYFSDAEQLITYAN-GSFCELTGYDRSETVGRNCRFLQGP 14 AHLDQHVIDSIGHGVIFADTTETITYAN-RYFREITGYSNSEIVGRNCRFLQGE	-DSDP	KL 632 LM 265 AR 121 VQ 121 MH 132
WP_010041727.1 WP_020473798.1 HCC28399.1 WP_067676345.1 WP_157075159.1 WP_137733386.1	511 LRLRDRAIQAVTQGILITSPALPD-NPITYAS-PGFEGVTGYPPREALGRNCRFLQGK 144 LQWRDRAIQSLVQGLCITDPSLPD-NPIIYVN-DSFLRITGYAREDVIGQNCRLLQGP 3 KMFRREILEAIGHGVVFTDPAEKITYAN-RYFCEITGYDESEVLGRTCRFLQGP 3 KLFRREVIEAIGHGVIFSDAEQLITYAN-GSFCELTGYDRSEIVGRNCRFLQGP 14 AHLDQHVIDSIGHGVIFADTTETITYAN-RYFREITGYSNSEIVGRNCRFLQGE 459 LAISHQALQAINQGVVIANPLQDITETN-GAFCRITGYSAQVLGRNCRFLQGP	-DSDP	KL 632 LM 265 AR 121 VQ 121 MH 132 QA 577
WP_010041727.1 WP_020473798.1 HCC28399.1 WP_067676345.1 WP_157075159.1 WP_137733386.1 WP_115226150.1	511 LRLRDRAIQAVTQGILITSPALPD-NPITYAS-PGFEGVTGYPPREALGRNCRFLQGK	-DSDP	KL 632 LM 265 AR 121 VQ 121 MH 132 QA 577 NS 385
WP_010041727.1 WP_020473798.1 HCC28399.1 WP_067676345.1 WP_157075159.1 WP_137733386.1 WP_115226150.1 WP_130106758.1	511 LRLRDRAIQAVTQGILITSPALPD-NPITYAS-PGFEGVTGYPPREALGRNCRFLQGK	-DSDP	KL 632 LM 265 AR 121 VQ 121 MH 132 QA 577 NS 385 NA 609
WP_010041727.1 WP_020473798.1 HCC28399.1 WP_067676345.1 WP_157075159.1 WP_137733386.1 WP_13733386.1 WP_130106758.1 WP_126771652.1	511 LRLRDRAIQAVTQGILITSPALPD-NPITYAS-PGFEGVTGYPPREALGRNCRFLQGK 144 LOWRDRAIQSLVQGLCITDFSLPD-NPIIVWL-DSFLRITGYAREDVIGQNCRLLOGP 3 KHRRREILEAIGHGVVFTDPAEKITYAN-GSFCELTGYDRSETVGRNCRFLQGP 3 KLFRREVIEAIGHGVYFSDAEQLITYAN-GSFCELTGYDRSETVGRNCRFLQGP 44 AHLDQHVIDSIGHGVIFADTTETITYAN-RYFREITGYSNSEIVGRNCRFLQGP 459 LAISHQALQAINQGVVIANPLQDITETN-GAFCRITGYSEAQVLGRNCRFLQGP 267 LKLSDAALKAISQGVLIADANRNISVN-PPLLAITGFSSEEFIGRNCNFLQGP 491 LKLSDLILKSISQGVIITANRRIISVN-BALLSITGYGREDFINKNGFLQGP	-DSDP	KL 632 LM 265 AR 121 VQ 121 MH 132 QA 577 NS 385 NA 609 RV 524
WP_010041727.1 WP_020473798.1 HCC28399.1 WP_067676345.1 WP_157075159.1 WP_137733386.1 WP_115226150.1 WP_130106758.1 WP_126771652.1 WP_153589594.1	511 LRLRDRAIQAVTQGILITSPALPD-NPITYAS-PGFEGVTGYPPREALGRNCRFLQGK	-DSDP	KL 632 LM 265 AR 121 VQ 121 MH 132 QA 577 NS 385 NA 609 RV 524 CA 431
WP_010041727.1 WP_020473798.1 HCC28399.1 WP_067676345.1 WP_157075159.1 WP_137733386.1 WP_115226150.1 WP_130106758.1 WP_126771652.1 WP_1533889594.1 WP_153115534.1	511 LRLRDRAIQAVTQGILITSPALPD-NPITYAS-PGFEGVTGYPPREALGRNCRFLQGK	-DSDP	KL 632 LM 265 AR 121 VQ 121 MH 132 QA 577 NS 385 NA 609 RV 524 CA 431 IA 422
WP_010041727.1 WP_020473798.1 HCC28399.1 WP_067676345.1 WP_157075159.1 WP_137733386.1 WP_1520150.1 WP_130106758.1 WP_126771652.1 WP_153589594.1 WP_153115534.1 NDP38329.1	511 LRLRDRAIQAVTQGILITSPALPD-NPITYAS-PGFEGVTGYPPREALGRNCRFLQGK 144 LOWRDRAIQSLVQGLCITDPSLPD-NPITYWH-DSFLRITGYAREDVIGONCRLLQGP 3 KMFRREILEAIGHGVVFTDPAEKITYAN-RYFCEITGYDESEVLGRTCRFLQGP 4 AHLDQHVIDSIGHGVIFADTTETITYAN-RYFREITGYSNSEIVGRNCRFLQGP 459 LAISHQALQAINQGVVIANPLQDITEYN-GAFCRITGYSEAQVLGRNCRFLQGP 6 LKLSDAALKAISQGVLIADANRNIISWN-PPLLAITGFSSEEFIGRNCNFLQGP 401 LKLSDALKKISGQGVIITANRRIISWN-DALLSITGYOREDFINKNCRFLQGP 407 -KLNDLSIQSISQGVIITDANRLIISWN-EAFSTNTGYSEREIAGKNCDFLQGP 313 LRLSDAALKAVSQGVVITSHDQRILTAN-EAFLEITGYARDEVIGRNCRFLQGP 304 LRVSDSALKAVSQGVVITGDRE	.DSDP	KL 632 LM 265 AR 121 VQ 121 MH 132 QA 577 NS 385 NA 609 RV 524 CA 431 IA 422 QA 311
WP_010041727.1 WP_020473798.1 HCC28399.1 WP_067676345.1 WP_157075159.1 WP_13773386.1 WP_115226150.1 WP_130106758.1 WP_15318534.1 WP_153115534.1 NDP38329.1	511 LRLRDRAIQAVTQGILITSPALPD-NPITYAS-PGFEGVTGYPPREALGRNCRFLQGK	-DSDP	CL 632 LM 265 AR 121 VQ 121 MH 132 QA 577 NS 385 NA 609 RV 524 CA 431 IA 422 QA 311 LA 589
WP_010041727.1 WP_020473798.1 HCC28399.1 WP_067676345.1 WP_157075159.1 WP_137733386.1 WP_115226150.1 WP_130106758.1 WP_126771652.1 WP_153115534.1 NDP38329.1 0YT98746.1 WP_162084453.1	511 LRLRDRAIQAVTQGILITSPALPD-NPITYAS-PGFEGVTGYPPREALGRNCRFLQGK	-DSDP	CL 632 LM 265 AR 121 VQ 121 HH 132 QA 577 VS 385 VA 609 RV 524 CA 431 IA 422 QA 311 LA 589 QV 450
WP_010041727.1 WP_020473798.1 HCC283399.1 WP_067676345.1 WP_157075159.1 WP_137733386.1 WP_130106758.1 WP_130106758.1 WP_153589594.1 WP_153589594.1 NDP38329.1 OYT98746.1 NP_165284453.1 NBV85339.1	511 LRLRDRAIQAVTQGILITSPALPD-NPITYAS-PGFEGVTGYPPREALGRNCRFLQGK 144 LOWRDRAIQSLYQGLCITDPSLPD-NPITYWH-DSFLRITGYAREDVIGQNCRLLQGP 3 KMFRREILEAIGHGYVFTDPAEKITYAN-GSFCELITGYDRSETVGRNCRFLQGP 3 KLFRREYLEAIGHGYUFSDAEQLITYAN-GSFCELITGYDRSETVGRNCRFLQGP 14 AHLDQHVIDSIGHGYIFADTTET	-DSDP	CL 632 LM 265 AR 121 VQ 121 132 QA 577 VS 385 VA 609 RVA 609 RVA 431 IA 422 QA 311 IA 422 QA 311 IA 589 QV 450 EA 310
WP_010041727.1 WP_020473798.1 HCC28399.1 WP_067676345.1 WP_157075159.1 WP_13773386.1 WP_115226150.1 WP_130106758.1 WP_153115534.1 WP_153115534.1 WP_162084453.1 WP_162084453.1 WP_052808331.1	511 LRLRDRAIQAVTQGILITSPALPD-NPITYAS-PGFEGVTGYPPREALGRNCRFLQGK- 144 LOWROBAIQSLVQGLCITDPSLPD-NPITYWN-DSFLRITGYAREDVGQNCELLQGP 3 KWFRREILEAIGHGWYFDDAEKITYAN-RYFCEITGYDESEVLGRTGREFLQGP 14 AHLDQHYIDSIGHGVIFADTETITYAN-RYFERITGYSNSETVGRNCRFLQGP 15 LKISDALQAINQGWYIDHPLQDITEN-GAFCRITGYSEAQVLGRNCRFLQGP 16 LKLSDLIKSISQGVIISDAEQKIISWN-DALLSITGYREEDFINKORFLQGP 17 LKLDSLIKSISQGVIITDAIRLIISWN-DALLSITGYREEDFINKORFLQGP 18 LKLSDLIKSISQGVIITDAIRLIITSWN-DALLSITGYREEDFINKORFLQGP 19 LRYSDVALKAVSQGVIITGADRLIVTWN-DAFLSITGYSAAEVFGGSCRFLQGP 19 LRYSDSALKAVSQGVIITTDQCIISWN-DAFVISGYSPSETLGGNCRFLQGP 19 LRYSDSALKAVSQGVIITDDVRLIISWN-DAFVISGYSPSETLGKNCRFLQGP 19 LRYSDSALKAVSQGVIITDDVRL	-DSDP	CL 632 LM 265 AR 121 VQ 121 132 QA 577 VS 385 VA 609 RV 524 CA 431 IA 422 QA 311 IA 422 QA 311 IA 422 QA 311 IA 425 QA 310 RT 1518
WP_010041727.1 WP_020473798.1 HCC28399.1 WP_067676345.1 WP_157075159.1 WP_137733386.1 WP_115226150.1 WP_130106758.1 WP_15315534.1 NDP38329.1 UP_15315534.1 NDP38329.1 UP_162084453.1 NEV85339.1 WP_052808331.1 XP_002954518.1	511 LRLRDRAIQAVTQGILITSPALPD-NPITYAS-PGFEGVTGYPPREALGRNCRFLQGK- 144 LQWRDRAIQSLVQGLCITDPSLPD-NPITYWN-DSFLRITGYAREDVIGQNCRLLQGP 3 KWFRREILEAIGHGVVFTDPAEKITYAN-GSFCELITGYDESEVLGRTGRFLQGP 14 AHLDQWYIDSIGHGVIFADTETITYAN-GSFCELITGYDESEVGRNCRFLQGP 15 ALISHQALQAINQGVVIADPLQDITENI-GAFCRITGYSEAQVLGRNCRFLQGP 267 LKLSDAALKAISQGVVIADANRNIISVN-PPLLAITGFSSEEFIGRNCRFLQGP 27 LKLSDAALKAISQGVVIADANRNIISVN-DALLSITGYGREDFINKNCRFLQGP 281 LKLSDAALKAISQGVIITDANRLIISVN-DALLSITGYGREDFINKNCRFLQGP 381 LRLSDAALKAYSQGVITTDANRL	-DSDP	CL 632 LM 265 AR 121 VQ 121 132 QA 121 VA 524 CA 431 IA 422 QA 311 IA 422 QA 311 IA 589 QV 450 EA 310 ET 1518
WP_010041727.1 WP_020473798.1 HC2283399.1 WP_067676345.1 WP_157075159.1 WP_137733365.1 WP_130106758.1 WP_130106758.1 WP_153015534.1 NP_1538299.1 UP_1538329.1 UP_052804331.1 WP_16528043331.1 WP_0528043331.1 WP_062804453.1 WP_1646404542.1	511 LRLRDRAIQAVTQGILITSPALPD-NPITYAS-PGFEGVTGYPPREALGRNCRFLQGK	DSDP	KL 632 LM 265 AR 121 VQ 121 HH 132 QA 577 NS 385 NA 609 RV 524 CA 524
WP_010041727.1 WP_020473798.1 HCC28399.1 WP_067676345.1 WP_157075159.1 WP_13773386.1 WP_115226150.1 WP_130106758.1 WP_15318534.1 WP_15318534.1 WP_15318534.1 WP_162084453.1 WP_052808331.1 XP_002954518.1 WP_146404542.1 WP_09587894.1	511 LRLRDRAIQAVTQGILITSPALPD-NPITYAS-PGFEGVTGYPPREALGRNCRFLQGK- 144 LOWROBAIQSLVQGLCITDPSLPD-NPITYWN-DSFLRITGYAREDVGQNCELLQGP 3 KWFRREILEAIGHGWYFDAEKITYAN-GYFCEITGYDESEVLGRTGREELGGP 14 AHLDQHYIDSIGHGVIFADTETITYAN-RYFCEITGYDESEVLGRTGREFLQGP 15 KLFRREVIEAIGHGWIFSDAEQLITYAN-GSFCELTGYDRSEIVGRNCRFLQGP 16 KLKSDALKAISQGVLIADARNNIISVN-PPLLAITGFSSEEFIGRNCNFLQGP 17 KLKDSLIKSISQGVIITADARNIISVN-DALLSITGYRGEFIURKGRELQGP 18 LKLSDLIKSISQGVIITADARLIISVN-DALLSITGYRGEFIURKGRELQGP 19 LEVSDVALKAVSQGVIITGADRLILTVN-DAFLSITGYAAAEVFGGSCRFLQGP 20 LRVSDVALKAVSQGVIITTDQFC	-DSDP	KL 632 LM 265 AR 121 VQ 121 MH 132 DA 577 NS 385 NO 524 CA 431 IA 422 DA 311 IA 420 DA 311 IA 420 DA 311 IA 420 DA 311 IA 420 DA 311 DA 311
WP_010041727.1 WP_020473798.1 HC2283399.1 WP_067676345.1 WP_157075159.1 WP_137733365.1 WP_130106758.1 WP_130106758.1 WP_153015534.1 NP_1538299.1 UP_1538329.1 UP_052804331.1 WP_16528043331.1 WP_0528043331.1 WP_062804453.1 WP_1646404542.1	511 LRLRDRAIQAVTQGILITSPALPD-NPITYAS-PGFEGVTGYPPREALGRNCRFLQGK- 144 LUMRDRAIQSLVQGLCITDPSLPD-NPITYWN-DSFLRITGYAREDVIGQNCRLLQGP 3 KHFRREILEAIGHGWYFTDPAEK ITYAN-GSFCELTGYDRSEIVGRNCRFLQGP 14 AHLDQHVIDSIGHGVIFADTET ITYAN-RYFCEITGYDSSEIVGRNCRFLQGP 15 LAISHQALQAINQGVVIANPLQD ITETN-GAFCRITGYSSEIVGRNCRFLQGP 267 LKLSDAALKAISQGVLIADANRN ITSWN-PLLAITGFSSEEFIGRNCRFLQGP 491 LKLSDAALKAISQGVLIADANRN ITSWN-PLAISTGYSEEFIGRNCRFLQGP 407 -KKLDNLSIOSISQGVIITANRGW ITSWN-DALLSITGYGREDFINKKCRFLQGP 1304 LRVSDVALKAVSQGVVITGHDGR ILTAN-EAFLEITGYARDEVIGRNCRFLQGP 1304 LRVSDVALKAVSQGVVITGHDGR ITYNN-DAFLSITGYAAAEVFGGSCRFLQGP 147 LRLSDAALKAYSQGVVITGHDGR ITYNN-DAFLSITGYAAAEVFGGSCRFLQGP 148 LRVSDAALKAVSQGVITGHDGR ITYNN-DAFLSITGYAAAEVFGGSCRFLQGP 159 LRVSDSALKAVSQGVILTDDVGR ITSWN-DAFTSTGYABEAVLGRNCRFLQGP 161 LRLSDAALKYSQGVILTDDVGR ITSWN-DAFTSTGYABEAVLGRNCRFLQGP 171 LRLSDAALKYSQGVILTDDVGR ITSWN-DAFTSTGYABEAVLGRNCRFLQGP 172 AEVEGPFLQTASQGVLAGADHF ITSWN-DAFTSTTGYAAEAVLGRNCRFLQGP 173 LRLSDAALKTYSQGVILTDDVG ITSWN-DAFTSTTGYAAEAVLGRNCRFLQGP 174 LRLSDAALKTYSQGVILTDDVG ITSWN-DAFTSTTGYAAEAVLGRNCRFLQGP 175 AEVEGPFLQTASQGVLAGADHF ITSWN-DAFTSTTGYAAEAVLGRNCRFLQGP 176 S USAAMESILSSLTVSDPHEEG-NPLCYVS-PGFLSMTGYNEDECLGRNCKFLQGG 177 LRLGGSRVGAATESTDFFTPLYFNN-ERFQGFTGYSEDETLGRNCKFLQGG 178 S LSAAMESILSSLTVSDPHEEG-NPLCYVS-PGFLSMTGYNEDECLGRNCKFLQGG 178 LRLGGARGATESTDFFTPLYFNN-ERFQGFTGYSEDETLGRNCKFLQGG 178 LRLGGARGATESTDFFTPLYFNN-ERFQGFTGYSEDETLGRNCKFLQGG 178 LRLGGARGATESTDFFTPLYFNN-ERFQGFTGYSEDETLGRNCKFLQGG 178 LRLGGARGATESTDFFTPLYFNN-ERFQGFTGYSEDETLGRNCKFLQGG 178 LRLGGARGATESTDFFTPLYFNN-ERFQGFTGYSEDETLGRNCKFLQGG 178 LRLGGARGATESTDFFTPLYFNN-ERFQGFTGYSEDETLGRNCKFTLQGG 178 LRLGGARGATESTDFFTQGFTGYSEDETLGRNCKFTLQGG 178 LRLGGARGATESTDFTTPLYNTDFTTYNN-DEFLNIVGYKLEEVLGGNUFFTLQGE 178 LRLGGARGATESTDFTTPLYNTDFTYNN-DEFLNIVGYKLEEVLGGNUFFTLQGE	-DSDP	KL 632 LM 265 AR 121 VQ 121 LMH 132 QA 577 VS 385 VA 524 CA 431 IA 422 QA 311 IA 422 QA 311 IA 589 EA 310 ER 31
WP_010041727.1 WP_020473798.1 HCC28399.1 WP_067676345.1 WP_157075159.1 WP_13773386.1 WP_115226150.1 WP_130106758.1 WP_15318534.1 WP_15318534.1 WP_15318534.1 WP_162084453.1 WP_052808331.1 XP_002954518.1 WP_146404542.1 WP_09587894.1	511 LRLRDRAIQAVTQGILITSPALPD-NPITYAS-PGFEGVTGYPPREALGRNCRFLQGK- 144 LUMRDRAIQSLVQGLCITDPSLPD-NPITYWN-DSFLRITGYAREDVIGQNCRLLQGP 3 KHFRREILEAIGHGWYFTDPAEK ITYAN-GSFCELTGYDRSEIVGRNCRFLQGP 14 AHLDQHVIDSIGHGVIFADTET ITYAN-RYFCEITGYDSSEIVGRNCRFLQGP 15 LAISHQALQAINQGVVIANPLQD ITETN-GAFCRITGYSSEIVGRNCRFLQGP 267 LKLSDAALKAISQGVLIADANRN ITSWN-PLLAITGFSSEEFIGRNCRFLQGP 491 LKLSDAALKAISQGVLIADANRN ITSWN-PLAISTGYSEEFIGRNCRFLQGP 407 -KKLDNLSIOSISQGVIITANRGW ITSWN-DALLSITGYGREDFINKKCRFLQGP 1304 LRVSDVALKAVSQGVVITGHDGR ILTAN-EAFLEITGYARDEVIGRNCRFLQGP 1304 LRVSDVALKAVSQGVVITGHDGR ITYNN-DAFLSITGYAAAEVFGGSCRFLQGP 147 LRLSDAALKAYSQGVVITGHDGR ITYNN-DAFLSITGYAAAEVFGGSCRFLQGP 148 LRVSDAALKAVSQGVITGHDGR ITYNN-DAFLSITGYAAAEVFGGSCRFLQGP 159 LRVSDSALKAVSQGVILTDDVGR ITSWN-DAFTSTGYABEAVLGRNCRFLQGP 161 LRLSDAALKYSQGVILTDDVGR ITSWN-DAFTSTGYABEAVLGRNCRFLQGP 171 LRLSDAALKYSQGVILTDDVGR ITSWN-DAFTSTGYABEAVLGRNCRFLQGP 172 AEVEGPFLQTASQGVLAGADHF ITSWN-DAFTSTTGYAAEAVLGRNCRFLQGP 173 LRLSDAALKTYSQGVILTDDVG ITSWN-DAFTSTTGYAAEAVLGRNCRFLQGP 174 LRLSDAALKTYSQGVILTDDVG ITSWN-DAFTSTTGYAAEAVLGRNCRFLQGP 175 AEVEGPFLQTASQGVLAGADHF ITSWN-DAFTSTTGYAAEAVLGRNCRFLQGP 176 S USAAMESILSSLTVSDPHEEG-NPLCYVS-PGFLSMTGYNEDECLGRNCKFLQGG 177 LRLGGSRVGAATESTDFFTPLYFNN-ERFQGFTGYSEDETLGRNCKFLQGG 178 S LSAAMESILSSLTVSDPHEEG-NPLCYVS-PGFLSMTGYNEDECLGRNCKFLQGG 178 LRLGGARGATESTDFFTPLYFNN-ERFQGFTGYSEDETLGRNCKFLQGG 178 LRLGGARGATESTDFFTPLYFNN-ERFQGFTGYSEDETLGRNCKFLQGG 178 LRLGGARGATESTDFFTPLYFNN-ERFQGFTGYSEDETLGRNCKFLQGG 178 LRLGGARGATESTDFFTPLYFNN-ERFQGFTGYSEDETLGRNCKFLQGG 178 LRLGGARGATESTDFFTPLYFNN-ERFQGFTGYSEDETLGRNCKFLQGG 178 LRLGGARGATESTDFFTPLYFNN-ERFQGFTGYSEDETLGRNCKFTLQGG 178 LRLGGARGATESTDFFTQGFTGYSEDETLGRNCKFTLQGG 178 LRLGGARGATESTDFTTPLYNTDFTTYNN-DEFLNIVGYKLEEVLGGNUFFTLQGE 178 LRLGGARGATESTDFTTPLYNTDFTYNN-DEFLNIVGYKLEEVLGGNUFFTLQGE	-DSDP	KL 632 LM 265 AR 121 VQ 121 LMH 132 QA 577 VS 385 VA 524 CA 431 IA 422 QA 311 IA 422 QA 311 IA 589 EA 310 ER 31
WP_010041727.1 WP_020473798.1 HCC28399.1 WP_067676345.1 WP_157075159.1 WP_137733386.1 WP_115226150.1 WP_130106758.1 WP_153115534.1 NDP38329.1 WP_162084453.1 NPV85339.1 WP_052808331.1 XP_002954518.1 WP_1646404542.1 WP_096198794.1 WP_096198794.1	511 LRLRDRAIQAVTQGILITSPALPD-NPITYAS-PGFEGVTGYPPREALGRNCRFLQGK- 144 LQWRDRAIQSLVQGLCITDPSLPD-NPITYWN-DSFLRITGYAREDVIGQNCRLLQGP 3 KWFRREILEAIGHGVVFTDPAEKITYAN-GSFCELITGYDESEVLGRTGRFLQGP 14 AHLDQWYLDSIGHGVIFADTETITYAN-RYFGEITGYDRSETVGRNCRFLQGP 15 KLRSTQAIAGNIQGVIANPLQDITENN-GSFCELITGYDRSETVGRNCRFLQGP 16 KLSDAALKAISQGVVIADANNIISVN-PPLLAITGFSSEEFIGRNCRFLQGP 17 LKLSDAALKAISQGVVIADANNIISVN-DALLSITGYSREDFINKNCRFLQGP 18 LKLSDAALKAISQGVVIIADANNIISVN-DALLSITGYSREDFINKNCRFLQGP 19 LKLSDAALKAISQGVVIIADANNIISVN-DALLSITGYGREDFINKNCRFLQGP 19 LRVSDAALKAYSQGVVITTDANRL	-DSDP	KL 632 LM 265 AR 121 VQ 121 LMH 132 QA 577 NA 609 RV 524 CA 431 IA 422 QA 311 IA 589 QV 450 ER 310 RT 1518 RT 1518 RT 1518 RT 1518 RT 1518 RT 1518 RT 1518 RT 1518 RT 1518
WP_010041727.1 WP_020473798.1 HCC28399.1 WP_067676345.1 WP_157075159.1 WP_137733365.1 WP_130106758.1 WP_130106758.1 WP_15315534.1 NDP38329.1 WP_153115534.1 NDP38329.1 WP_052808331.1 WP_052808331.1 WP_052808331.1 WP_09687894.1 WP_099687894.1 WP_099687894.1 WP_099688786.1	511 LRLRDRAIQAVTQGILITSPALPD-NPITYAS-PGFEGVTGYPPREALGRNCRFLQGK- 144 LOWROBAIQSLVQGLCITDPSLPD-NPITYWN-DSFLRITGYAREDVGQNCELLQGP 3 KWFRREILEAIGHGWYFDAEKITYAN-GYFCEITGYDESEVLGRTGREEQGP	.DSDP	KL 632 LM 265 AR 121 V9 121 V9 121 V9 121 V9 121 V9 121 V9 524 CA 431 IA 422 QA 311 IA 422 QA 311 IA 589 QV 450 EA 310 RR 1518 RR 206 RT 661 RQ 114 ER 7 ER 1518 RR 15
WP_010041727.1 WP_020473798.1 HCC28399.1 WP_067676345.1 WP_157075159.1 WP_1157075159.1 WP_13173386.1 WP_115226150.1 WP_130106758.1 WP_153115534.1 WP_153115534.1 WP_162084453.1 WP_052808331.1 WP_052808331.1 XP_002954518.1 WP_052808331.1 XP_002954518.1 WP_06198941.1 WP_06198941.1 WP_06198876.1 RYG64144.1	111 LRLRDRAIQAVTQGILITSPALPD-NPITYAS-PGFEGVTGYPPREALGRNCRFLQGK- 114 LOWROBAIQSLVQGLCITDPSLPD-NPITYWN-DSFLRITGYAREDVIGQNCBLLQGP 3 KWFRREILEAIGHGWYFDAEKITYAN-GYFCEITGYDSSEVLGRTGRELGGP 14 AHLDQHVIDSIGHGVIFADTETITYAN-GYFCEITGYDSSEVLGRTGRELGGP 15 LAISHQALQAINQGVVIANPLQDITETN-GAFCRITGYSSEAQVLGRNCRFLQGP 16 LKLSDAALKAISQGVLIADANRNITSWN-PLLAITGFSSEEFIGRNCRFLQGP 17 LKLSDAALKAISQGVLIADANRNITSWN-PLALSITGYSEEPIGRNCRFLQGP 18 LKLSDAALKAISQGVLIADANRNITSWN-DAFLSITGYSEEPIGRNCRFLQGP 19 LRVSDVALKAVSQGVVITGADRLILYAN-EAFSLTTGYSEEPIGRNCRFLQGP 19 LRVSDVALKAVSQGVVITGADRLIVTWN-DAFLSITGYAADEVFGGSCRFLQGP 19 LRVSDVALKAVSQGVVITGADRLILYAN-DAFVAITGYAEAEVLGRNCRFLQGP 19 LRVSDSALKAVSQGVLITGADRLILYAN-DAFVAITGYAEAEVLGRNCRFLQGP 19 LRVSDSALKAVSQGVLITGADRLILSAN-DAFVAITGYAEAEVLGRNCRFLQGP 19 LRVSDSALKAVSQGVLITGADRL	-DSDP	KL 632 LM 265 AW 265 AW 121 VQ 121 VQ 121 VW 122 AW 577 VW 524 CA 311 LA 589 CV 450 EX 310 EX 311 LA 589 CV 450 EX 310 EX 311 EX 311
WP_010041727.1 WP_02047379.1 HCC28397.1 WP_067676345.1 WP_157075159.1 WP_13773338.1 WP_115226150.1 WP_130106758.1 WP_153115534.1 WP_153115534.1 WP_153115534.1 WP_152084453.1 WP_052808331.1 XP_002954518.1 WP_1646404542.1 WP_096198941.1 WP_096198941.1 WP_09658876.1 RYG64188.1	111 LRLRDRAIQAVTQGILITSPALPD-NPITYAS-PGFEGVTGYPPREALGRNCRFLQGK 114 LOWROBAIQSLVQGLCITDPSLPD-NPITYWN-DSFLRITGYAREDVGQNCRLLQGP 3 KHFRREILEAIGHGWYFDAEKITYAN-GYFCEITGYDESEVLGRTGREIGGP 14 AHLDQHVIDSIGHGVIFADTETITYAN-RYFCEITGYDESEVLGRTGREIGGP 15 KLFRREVIEAIGHGWIFSDAEQLITYAN-GSFCELTGYDRSEIVGRNCRFLQGP 16 KLKJAUAQAINQGWYIDHPLQDITEN-GAFCRITGYSEAQVLGRNGRFLQGP 17 KLKIDALQAINQGWYIDHANELIISWN-DPLLAITGYSSEEPIGRNCNFLQGP 18 IKLSDLIKSTSQGVIITADARNIISWN-DAFLSTGYSEADVLGRNGRFLQGP 19 LKLSDLIKSTSQGVIITADRR	-DSDP	KL 632 LM 265 AR 121 VQ 121 VH 132 VA 609 RV 524 CA 431 LA 422 VA 311 LA 589 VA 509 EA 310 EA
WP_010041727.1 WP_020473798.1 HCC28399.1 WP_067676345.1 WP_157075159.1 WP_137733365.1 WP_1317226150.1 WP_130106758.1 WP_153115534.1 NDP38329.1 WP_153115534.1 NDP38329.1 WP_052808331.1 WP_052808331.1 WP_052808331.1 WP_06588576.1 RY064144.1 WP_106588576.1 RY065188.1 WP_106380907.1	111 LRLRDRAIQAVTQGILITSPALPD-NPITYAS-PGFEGVTGYPPREALGRNCRFLQGK 114 LOWROBAIQSLVQGLCITDPSLPD-NPITYWN-DSFLRITGYAREDVGQNCRLLQGP 3 KHFRREILEAIGHGWYFDAEKITYAN-GYFCEITGYDESEVLGRTGREIGGP 14 AHLDQHVIDSIGHGVIFADTETITYAN-RYFCEITGYDESEVLGRTGREIGGP 15 KLFRREVIEAIGHGWIFSDAEQLITYAN-GSFCELTGYDRSEIVGRNCRFLQGP 16 KLKJAUAQAINQGWYIDHPLQDITEN-GAFCRITGYSEAQVLGRNGRFLQGP 17 KLKIDALQAINQGWYIDHANELIISWN-DPLLAITGYSSEEPIGRNCNFLQGP 18 IKLSDLIKSTSQGVIITADARNIISWN-DAFLSTGYSEADVLGRNGRFLQGP 19 LKLSDLIKSTSQGVIITADRR	-DSDP	KL 632 LM 265 AR 121 VQ 121 VH 132 VA 609 RV 524 CA 431 LA 422 VA 311 LA 589 VA 509 EA 310 EA
WP_010041727.1 WP_020473798.1 HCC28399.1 WP_067676345.1 WP_157075159.1 WP_1157075159.1 WP_13173386.1 WP_115226150.1 WP_130106758.1 WP_153115534.1 WP_153115534.1 WP_153115534.1 WP_162084453.1 WP_052808331.1 XP_002954518.1 WP_052808331.1 XP_002954518.1 WP_06588576.1 RYG64144.1 RYG65188.1 WP_106380907.1 WP_0688816174.1	111 LRLRDRAIQAVTQGILITSPALPD-NPITYAS-PGFEGVTGYPPREALGRNCRFLQGK- 114 LOWROBAIQSLVQGLCITDPSLPD-NPITYWN-DSFLRITGYAREDVIGQNCBLLQGP 3 KWFRREILEAIGHGWYFDAEKITYAN-GYFCEITGYDSSEVLGRTGRELQGP 14 AHLDQHVIDSIGHGVIFADTETITYAN-GYFCEITGYDSSEVLGRTGRELQGP 15 LAISHQALQAINQGVVIANPLQDITETN-GAFCRITGYSSEAQVLGRNCRFLQGP 16 LKLSDAALKAISQGVLIADANRNITSWN-PLLAITGFSSEEFIGRNCRFLQGP 17 LKLSDAALKAISQGVLIADANRNITSWN-PLALISTGYSEEFIGRNCRFLQGP 18 LKLSDAALKAISQGVLIADANRNITSWN-DALISTGYSEEFIGRNCRFLQGP 19 LKLSDAALKAYSQGVVITGADRLITYWN-DAFLSITGYAREVIGRNCRFLQGP 19 LRVSDVALKAVSQGVVITGADRLITVAN-DAFVLSITGYAREVIGRNCRFLQGP 19 LRVSDVALKAVSQGVLITGADRLIVTWN-DAFLSITGYAREVIGRNCRFLQGP 19 LRVSDSALKAVSQGVLITGADRLITSAN-DAFVSITGYAREVIGRNCRFLQGP 19 LRVSDSALKAVSQGVLITGADRLITSAN-DAFVSITGYAREVIGRNCRFLQGP 10 LRVSDSALKAVSQGVLITGADRLITSAN-DAFVSIGGYSPSETLGGNCRFLQGP 10 LRSDAALKTVSQGVLIADVDRLILSAN-DAFVSITGYAREVIGRNCRFLQGP 10 CSANVVITINDAE	-DSDP	KL 632 LM 265 AR 121 LVQ 121 LVQ 121 LVQ 121 LVQ 121 LVQ 121 LVQ 524 LVQ 450 L
WP_010041727.1 WP_020473798.1 HCC28399.1 WP_067676345.1 WP_157075159.1 WP_137733386.1 WP_115226150.1 WP_130106758.1 WP_126771652.1 WP_153389594.1 WP_153115534.1 NDP38329.1 WP_158208331.1 XP_002954518.1 WP_052808331.1 XP_002954518.1 WP_1668876.1 WP_096198941.1 WP_096198941.1 WP_096198941.1 RYG64144.1 RYG65188.1 WP_106380907.1 WP_068816174.1 WP_1068816174.1 WP_198816174.1	111 LRLADRAIQAVTQGILITSPALPD-NPITYAS-PGFEGVTGYPPREALGRNCRFLQGK- 114 LQWROBAIQSLVQGLCITDPSLPD-NPITYWN-DSFLRITGYAREDVIGQNCRLLQGP 3 KWFRREILEAIGHGWYFTDPAEKITYAN-GSFCELTGYDESEVLGRTGRFLQGP 14 AHLDQWYIDSIGHGVIFADTETITYAN-RYFGEITGYDRSETVGRNCRFLQGP 15 KLRREVIEAIGHGWYFADTETITYAN-RYFREITGYSNSETVGRNCRFLQGP 16 KLSDAALKAISQGVLIADANNIISVN-PPLLAITGFSSEEFIGRNCRFLQGP 17 LKLSDAALKAISQGVLIADANNIISVN-PPLLAITGFSSEEFIGRNCRFLQGP 18 LKLSDAALKAISQGVLIADANNIISVN-DALLSITGYGREDFINKORFLQGP 19 LKLSDAALKAISQGVIITDANNIISVN-DALLSITGYGREDFINKORFLQGP 10 LKLSDAALKAISQGVIITDANN	-DSDP	KL 632 LM 265 AR 121 LVQ 121 L
WP_010041727.1 WP_020473798.1 HC228399.1 WP_067676345.1 WP_157075159.1 WP_137733365.1 WP_130106758.1 WP_130106758.1 WP_153115534.1 NDP38329.1 0YT98746.1 WP_162084453.1 NBV85339.1 WP_052808331.1 WP_052808331.1 WP_09688941.1 WP_166885676.1 RYG66144.1 RYG65188.1 WP_106880907.1 WP_068816174.1 WP_18385917.1 WP_068816174.1 WP_18385917.1 WP_068816174.1 WP_18385917.1 WP_068816174.1 WP_18385917.1 WP_068816174.1 WP_18385917.1	111 LRLRDRAIQAVTQGILITSPALPD-NPITYAS-PGFEGVTGYPPREALGRNCRFLQGK- 114 LQWRDRAIQSLYQGLCITDPSLPD-NPITYWH-DSFLRITGYAREDVIGQNCRLLQGP 3 KWFRREILEAIGHGWVFTDPAEKITYAN-GSFCELTGYDESEVLGRTGRFLQGP 14 AHLDQWYLDSIGHGVIFADTETITYAN-RYFGEITGYDRSETVGRNCRFLQGP 15 KLRSAIGHGWIFADTETITYAN-RYFREITGYSNSETVGRNCRFLQGP 16 ALSHQALQAINQGVVIADHPLQDITEN-GAFCRITGYSSEQVLGRNCRFLQGP 17 LKLSDAALKAISQGVVIADANRNITSWN-PPLLAITGFSSEEFIGRNCRFLQGP 18 LKLSDAALKAISQGVVITADANRNITSWN-DALLSITGYQREDFINKNCRFLQGP 19 LKLSDAALKAISQGVVITADANRNITSWN-DALLSITGYGREDFINKNCRFLQGP 10 LRUSDVALKAVSQGVVITTGADRLITSWN-DAFSTHTOFSSEETIGRNCRFLQGP 11 LRUSDAALKAVSQGVVITTGDQCITSWN-DAFSTHTOFSSEETIGRNCRFLQGP 12 LRUSDVALKAVSQGVVITTGDQCITSWN-DAFVSIGVSPSETLGGNCRFLQGP 13 LRUSDSALKAVSQGVLITDADRL	-DSDP	KL 632 LM 265 AR 121 AVQ 121 AVH 132 CS 385 NA 609 AVX 524 CA 431 LTA 422 CS 311 LTA 422 CS 311 LTA 589 LTA 58
WP_010041727.1 WP_020473798.1 HCC28399.1 WP_067676345.1 WP_157075159.1 WP_137733365.1 WP_133106758.1 WP_130106758.1 WP_153115534.1 WP_153115534.1 WP_153115534.1 WP_15318589594.1 WP_153115534.1 WP_162084453.1 WP_052808331.1 WP_052808331.1 WP_052808331.1 WP_09687844.1 WP_099687844.1 WP_09968784.1 WP_09688576.1 RYG65188.1 WP_106380907.1 WP_068816174.1 WP_1063859117.1 WP_0683556488.1	111 LRLRDRAIQAVTQGILITSPALPD-NPITYAS-PGFEGVTGYPPREALGRNCRFLQGK 114 LOWROBAIQSLYQGLCITDPSLPD-NPITYWN-DSFLRITGYAREDYIGQNCBLLQGP 3 KWFRREILEAIGHGWYFDAEKITYAN-GYFCEITGYDSESVLGRTGKELQGP 14 AHLDQHYIDSIGHGVIFADTETITYAN-RYFCEITGYDSESVLGRTGKELQGP 15 LAISHQALQAINQGVVIANPLQDITETN-GAFCRITGYSSEIVGRNCRFLQGF 16 LAISHQALQAINQGVVIANPLQDITETN-GAFCRITGYSSEQVLGRNCRFLQGF 17 LKLSDAALKAISQGVLIADANNNITSWN-PLLAITGFSSEEFIGRNCRFLQGF 18 LKLSDAALKAISQGVIITANREWITSWN-DAFLSITGYSREDIKNCRFLQGF 19 LKLSDAALKAYSQGVVITGADRIITYWN-DAFTSITGYSREDIGNCRFLQGP 10 KKNDLSIGSISQGVITGADRIIVTWN-DAFSIGTYAAAEVFGOSCRFLQGP 11 LRLSDAALKAYSQGVVITGADRIIVTWN-DAFTSITGYAAEVFGOSCRFLQGP 12 LRSDAALKAYSQGVLITGADRIIVTWN-DAFTSITGYSAERVGSCRFLQGP 13 LRVSDSALKAVSQGVLITGADRIIVTWN-DAFTSITGYSAERVGSCRFLQGP 14 LRLSDAALRTYSQGVLIADVDRIILSAN-DAFTAITGYAEAEVLGRNCRFLQGP 15 LRSDAALKAYSQGVLIADVDRIILSAN-DAFTAITGYAEAEVLGRNCRFLQGP 16 LRSDAALKTYSQGVLIADVDRI	DSDP	KL 632 LM 265 AR 121 VQ 121 HH 132 QX 5385 VA 609 VX 524 LG 431 LG 422 QX 450 EX 1518 RR 206 RR 159 QX 450 EX 1518 RR 206 RR 159 QX 114 EX 175 EX
WP_010041727.1 WP_020473798.1 HCC28399.1 WP_067676345.1 WP_157075159.1 WP_137733386.1 WP_115226150.1 WP_130106758.1 WP_153115534.1 NDP38329.1 WP_153115534.1 NDP38329.1 WP_162084453.1 NEV85339.1 WP_052808331.1 XP_002954518.1 WP_096687894.1 WP_096189941.1 WP_096189841.1 WP_096189841.1 WP_106380907.1 WP_06881617.1 WP_106385961.1 WP_106385917.1 WP_063356489.1 WP_148339905.1 WP_148339905.1 WP_148339905.1 WP_155965919.1	111 LRLADRAIQAVTQGILITSPALPD-NPITYAS-PGFEGVTGYPPREALGRNCRFLQGK- 114 LQWROBAIQSLVQGLCITDPSLPD-NPITYWN-DSFLRITGYAREDYGQNCGLLQGP 3 KWFRREILEAIGHGWYFTDAEKTYYAN-GSFCELTGYDSESVLGRTGGRELQGP 14 AHLDQWYIDSIGHGVIFADTETITYAN-GSFCELTGYDSESVLGRTGGRELQGP 15 LKLSGLGHGWYFADTTET	DSDP	KL 632 LM 265 AR 121 AV 121 AV 121 AV 132 AV 577 AV 5 385 AV 609 AV 450
WP_010041727.1 WP_020473798.1 HC228399.1 WP_067676345.1 WP_157075159.1 WP_13773386.1 WP_131733365.1 WP_130106758.1 WP_130106758.1 WP_153115534.1 NDP38329.1 WP_153115534.1 MP_052808331.1 WP_052808331.1 WP_052808331.1 WP_052808331.1 WP_0568186.1 WP_146404542.1 WP_09687894.1 WP_106588576.1 RYG65188.1 WP_106588576.1 RYG65188.1 WP_183839097.1 WP_088816174.1 WP_138539117.1 WP_133613329.1 WP_148339005.1 WP_133613329.1 TXH39291.1	111 LRLRDRAIQAVTQGILITSPALPD-NPITYAS-PGFEGVTGYPPREALGRNCRFLQGK- 114 LQWRDRAIQSLYQGLCITDPSLPD-NPITYWN-DSFLRITGYAREDYIGQNCRLLQGP 3 KWFRREILEAIGHGWYFTDPAEKITYAN-GSFCELTGYDESEVLGRTGRFLQGP 14 AHLDQWYDSIGHGVIFADTETITYAN-RYFGEITGYDRSETVGRNCRFLQGP 15 KLRREVIEAIGHGWYFADTETITYAN-RYFREITGYSNSETVGRNCRFLQGP 16 ALISHQALQAINQGWIANPLQDITENT-GAFCRITGYSEAQVLGRNCRFLQGP 17 LKLSDAALKAISQGWIJANNNIISWN-PPLLAITGFSSEEFIGRNCRFLQGP 18 LKLSDAALKAISQGWIJANNNIISWN-DALLSITGYGREDFINKNCRFLQGP 19 LKLSDAALKAISQGWIJTDANRLIISWN-DAFSTHTOFSSEETIGRNCRFLQGP 10 LKLSDAALKAISQGWIJTBADRL	DSDPAAVALVREAVRAG - RDCAVEVLNYRKDGTPFWNALSVSPIRDDAG - ELTHFVGVLVDVTDRN -KTAP - ESVTITREAVROK - RTCLVELQNYRKDGTTFWNGLSLSPIRDTAG - AVANHFVGVLTDISPLH -ETAA - ETKWRIRQALDAR - TQPFOGDVLNYRKNGDAFWNSSITPQFGDDG - ELIGYVGITRDVTESPL -DTDP - ETRVRIRKALAVG - EPFEGEILLNYRKDGKPFWNGLSLSTPQRSKFG - RLIGFVGITRDVTESPL -DTCP - EAKKRIKQAIENG - OQFDGQILNYRKNGEAFWNDLSITPQFADDR - ELTGFVGITRDVTERN -DTCP - EAKKRIKQAIENG - OQFDGQILNYRKNGEAFWNDLSITPQFADDR - ELTGFVGITRDVTERN -DTCP - EAKKRIKQAIENG - OQFDGQILNYRKNGEAFWNDLSISPVFNEKG - ULTHFIGITBTVTERN -LSSP - ETITAIRMALNSE - KEFNGEIINYRKDGAILFWNDLSISPVFNEKG - ULTHFIGITRDTTERN -QTDL - QTISQIRSALEQG - QPFAGEIINYRKDGAILFWNDLSISPVFNEKG - ULTHFIGITRDTTERN -UTST - ESSVAIRESISNI - ENFSCKILNYRKDGVFRWNGLSISPVCDEHG - TLTHFIGITRDTTERN -LTSP - RSIDAIRAALDRG - EEFSGEILNYRKDGSFFWNDLSISPVLDEGG - RLINHFIGITRDVTERN -LTSP - RSIDAIRAALDRG - EEFSGEILNYRKDGSTFWNELTISPVRDEGG - RLINHFIGITRDVTERN -LTDP - RAVDAMRLALKNIS - AEFAGEILNYRKDGSTFWNELTISPVRDEGG - RLINHFIGITRDVTERN -LTDP - QTVEAIRHCLRQG - TEFFGEILNYRKDGSTFWNELTISPVRDEGG - QLAHFIGVTRDTTORN -LTDP - QTVEAIRHCLRQG - TEFFGEILNYRKDGSTFWNELTISPVRDEGG - QLAHFIGVTRDTTORN -LTDP - QTVEAIRHCLRGC - SEEFSGEILNYRKDGSTFWNELTISPVRDAGN - RLTHHVGITRDVTERN -LTP - KTLCAHQAIESA - TEFTGEILNYRKDGSTFWNELTISPVRDAGN - RLTHHVGITRDVTERN -LTP - KTLCAHQAIESA - TEFTGEILNYRKDGSFFWNALTITPVRDSSG - VYMFHVGIRRDVTERN -TODA - KVYEAIRHCLREC - REFSGEILNYRKDGSFFWNALTITPVRDSSG - VYMFHVGIRRDVSEN -TODA - KYVEAIRHCLREC - REFSGEILNYRKDGSFFWNALTITPVRDSSG - VYMFHVGIRRDVSEN -TODD - NITIEAIRTALNEE - ERFGGELLNYRKDGSFFWNALTITPVRDSSG - KLTHFVGWSDVSLH -ATPR - AATYDSLWDALRRG - ESWHGEFVNRRKDGSFFWSFLISPVHDRSG - KLTHFVGWSDVSLH -TEFSC - DTIKELRNAIQRR - EPVEVINRKDGKSFFWNSLHEVNSDAGD - BLLYFYGLICTTDVSVO - ETTSC - AAIMQVRRAIAEK - OPTITVKKINYKNGGFFWNSLSLEPVFGEDGA - SLLHFVGWHCDLDERS - DTDP - NTIEAIRTALNEE - ERFGGELLNYRKDGSFFWNSLTHEVNSDAG - KLTHFVGNSTDITERN - ETTSV - DTIKELRNAIQRR - EPVEVLINKNSCGFFWNSLATENVYNSGAK - ELLYFYGLICTTDVERN - ETTSV - DTIKELRNAIQRR - EPVEVLINKNSGGFFWNSLATENVYNSGAK - ELLYFYGLICTTDVEN - ETTSV - D	KL 632 LM 265 AR 121 AVQ 121 AVH 132 SASS AVA 609 AVV 524 CA 431 LIA 422 AVA 311 LIA 422 AVA 311 LIA 589 AVA 450 EA 310 E
WP_010041727.1 WP_020473798.1 HCC28399.1 WP_067676345.1 WP_157075159.1 WP_157075159.1 WP_1310336.1 WP_115226150.1 WP_13316.38.1 WP_126771652.1 WP_153115534.1 NDP38329.1 WP_153115534.1 NDP38329.1 WP_052808331.1 XP_002954518.1 WP_146404452.1 WP_096989341.1 WP_096198941.1 WP_096198941.1 WP_0658856.1 RYG64184.1 RYG65188.1 WP_106389907.1 WP_18839917.1 WP_063356489.1 WP_13613329.1 WP_13613329.1 WP_155965919.1 TXH39291.1 TXH39291.1	111 LRLRDRAIQAVTQGILITSPALPD-NPITYAS-PGFEGVTGYPPREALGRNCRFLQGK 114 LOWROBAIQSLYQGLCITDPSLPD-NPITYWN-DSFLRITGYAREDYIGQNCBLLQGP 3 KHFRREILEAIGHGWYFDAEKITYAN-GYFCEITGYDSESVLGRTGKELQGP 14 AHLDQHYIDSIGHGVIFADTETITYAN-RYFCEITGYDSESVLGRTGKELQGP 15 ALSHQALQAINQGVVIANPLQDITETN-GAFCRITGYSSEIVGRNCRFLQGP 16 LAISHQALQAINQGVVIANPLQDITETN-GAFCRITGYSSEQVLGRNCRFLQGP 17 LKLSDALKAISQGVIITANARNITSWN-PLLAITGFSSEEFIGRNCRFLQGP 18 LKLSDALKAISQGVIITANARNITSWN-DALSITGYSREDIKNKCRFLQGP 19 LKLSDALKAISQGVVITANDARNITSWN-DAFSITGYSEREIAGKNCDFLQGP 10 KKNDLSIGSISQGVITGADRLILYAN-BAFTLTGYARDEVIGRNCRFLQGP 11 LRLSDAALKAVSQGVVITGADRLILYAN-DAFVISIGYSPSETLGGNCRFLQGP 12 LRVSDVALKAVSQGVLITGADRLILYAN-DAFTTITGYAREVIGRNCRFLQGP 13 LRVSDSALKAVSQGVLITGADRLILSAN-DAFVAITGYAREVIGRNCRFLQGP 14 LRLSDAALKTVSQGVLIADVDRLILSAN-DAFVAITGYAREVIGRNCRFLQGP 15 LRSDAALKTVSQGVLIADVDRL	DSDP AAVALVREAVRAG - RDCAVEVLNYRKDGTPFWINLSVSPIRDDAG - ELTHFVGVLVDVTDRI - KTAP - ESVTITREAVROK - RTCLVELQNYRKDGTTFWIGLSLSPIRDTAG - AVANFYGVLTDISFLE - ETAM - EGALDAR - TOPFOGULYNRYKNGDAFINGSLSPIRDTAG - AVANFYGVLTDISFLE - ETAM - ETAMIRICALDAR - TOPFOGULYNRYKNGDAFWINSSTIPTORDAG - ELIGYVGTTRDVTESFLE - DTDP - ETRVRIKALAVG - EPFEGEILNYRKDGKPFWINSLSITPQRSKFG - RLIGFVGITRDVTER - DTCP - EAKKRIKQAIENG - QOFFOGULNYRKNGEAFWINLSITPQFDADR - ELTGFVGITRDVTER - GTDR - AMVAQMRQALOGR - TEFFGEVLNYRQDGEPFWINLSIAPYFGADG - QLIHFISTMRDVTERF - LSSP - ETITATRMALNSE - KEFNGEIINYRKDGSIFWINLSISPVENEKG - LITHFIGITRDITTRN - TOPTOL - OTTSQIRSALEQG - OPFAGEIINYRKDGSIFWINLSISPVENEKG - LITHFIGITRDITTRN - TSSVAIRESLSNL - ENFSGKILNYRKDGSFFWINLSISPVEDEGG - TLIHFIGITRDITTRN - LTST - ESSVAIRESLSNL - ENFSGKILNYRKDGSFFWINLSISPVEDEGG - RLINHFIGITRDVTERK - LTDP - RSIDATRAALDRG - EEFSGEILNYRKDGSFFWINLSISPVEDEGG - RLINHFIGITRDVTERK - LTDP - RAVDAMRLALKNS - AEFAGEILNYRKDGSFFWINLSISPVEDEGG - RLINHFIGITRDVTERK - LTDP - QTVEATHFLCRQ - TEFFGEILNYRKDGSFFWINLSISPVEDEGG - QLAHFIGVTRDVTERF - LTEP - KTLCAHQAIESA - TEFTGEILNYRKDGSFFWINLSTSPVEDEGG - QLAHFIGVTRDVTERF - LTEP - KTLCAHQAIESA - TEFTGEILNYRKDGSFFWINLSTSPVEDEGG - QLAHFIGVTRDVSTBV LTEP - KTLCAHQAIESA - TEFTGEILNYRKDGSFFWINLSTSPVEDEGG - QTHFWGIARDISERN - FTDA - KYVEAHTCLEC - REFSGEILNYRKDGSFFWINLSTSPVEDRGG - QTHFWGIARDISERN - FTDA - KYVEAHTCLEC - REFSGEILNYRKDGSFFWINLSTSPVEDRGG - RTHFWGIARDISERN - FTDA - STHEARSAISER - REATVEYTNFRKGGSFFWINLSTSPVEDRGG - RTHFWGIARDISERN - FTDA - STHEARSAISER - REFTGELLNYRKDGSFFWINLSTSPVEDRGG - RTHFWGIARDISERN - FTDA - STHEARSAISER - REFTGELLNYRKDGSFFWINLSTSPVEDRGG - RTHFWGIARDISERN - FTDA - LVARREMGAVAGE - RSSFOYL	KL 632 LM 265 AR 121 VQ 121 HH 132 QX 577 QX 585 VA 609 RX 524 CA 431 LA 422 QX 450 AC 431 LA 589 QV 450 AC 451 AC 451 AC 451 AC 589 QV 450 AC 71 AC 450 AC 71 AC 75 AC
WP_010041727.1 WP_020473798.1 HCC28399.1 WP_067676345.1 WP_157075159.1 WP_137733386.1 WP_137733386.1 WP_130106758.1 WP_130106758.1 WP_153115534.1 NDP8329.1 WP_153115534.1 NDP8329.1 WP_162084453.1 NDP8329.1 WP_052808331.1 XP_002954518.1 WP_1646404542.1 WP_06588576.1 RYG64144.1 WP_106588576.1 RYG64144.1 WP_063356489.1 WP_063356489.1 WP_148339005.1 WP_14833905.1 WP_15965919.1 TXH39291.1 RYG54589.1 PP_155965919.1 TXH39291.1 RYG5468.1	111 LRLRDRAIQAVTQGILITSPALPD-NPITYAS-PGFEGVTGYPPREALGRICGRFLQGK 114 LQWROBAIQSLVQGLCITDPSLPD-NPITYWN-DSFLRITGYAREDVGQNCELLQGG 3 KWFRREVIEAIGHGWYFDDAEK ITYAN-GSFCELTGYDESEVLGRTGREFLQGG- 14 AHLDQWYIDSIGHGVIFADTET ITYAN-RYFCEITGYDESEVLGRTGREFLQGG- 15 KLFRREVIEAIGHGWYFADTTET ITYAN-RYFCEITGYDESEVLGRTGREFLQGG- 16 LAISHQALQAINQGVVIANPLQD ITETN-GAFCRITGYSEAQVLGRNCRFLQGG- 17 LKLSDAALKAISQGVLIADANRN ITSWN-PLLAITGFSSEEFIGRNCRFLQGG- 18 LKLSDALKAISQGVIITANREW ITSWN-DALLSITGYSREEDIGRNCRFLQGG- 19 LKLSDAALKAYSQGVVITSHDQR ITSWN-DALSITGYAREPLIGRNCRFLQGG- 19 LRVSDSALKAYSQGVVITGADRL IVTWN-DAFLSITGYARAEVFGGSCRFLQGG- 19 LRVSDSALKAYSQGVVITGADRL IVTWN-DAFLSITGYARAEVFGGSCRFLQGG- 19 LRVSDSALKAYSQGVITGADRL IVTWN-DAFLSITGYARAEVFGGSCRFLQGG- 19 LRVSDSALKAYSQGVLTADDRUFL IISAN-DAFTAITGYAEAEVLGRNCRFLQGG- 19 LRVSDSALKAYSQGVLTADDRUFL IISAN-DAFTAITGYAEAEVLGRNCRFLQGG- 19 LRVSDSALKAYSQGVLTADDRUFL IISAN-DAFTAITGYAEAEVLGRNCRFLQGG- 32 LRLSDLALKTYSQGIIISDIHQE IIWN-DAFTTITGYAEAEVLGRNCRFLQGG- 33 LRLSDALKAYSQGVLTAGADHF ITSAN-RAYSSENTGYAAEVLGRNCRFLQGG- 36 S LSAAMESILSSLTVSDPHEEG-NPLCYVS-PGFLSMTGYNAECLLGRNCRFLQGG- 37 S LSAAMESILSSLTVSDPHEEG-NPLCYVS-PGFLSMTGYNEDECLGRNCKFLQGG- 38 S LSAAMESILSSLTVSDPHEEG-NPLCYVS-PGFLSMTGYNEDECLGRNCKFLQGG- 39 LRLQAAIESTHOGFVIADATEPG-FPLVFWN-ERFGQFTGYSEDETLGRNCKFLQGG- 50 SULVDILEVNISGWWYNDFSGPD-NPLIFWN-DEFLNIVGYKLEEVLGGNRCRFLQGG- 51 SULVDILEVNISGWWYNDFSGPD-NPLIFWN-DEFLNTYYKLEEVLGGNRCRFLQGG- 51 SULVANKLTTSVIITNPRLPD-NPLIFWN-PAFTRUTGYFAQEAELGRNCKFLQGG- 51 SULVANKLTTSVIITNPRLPD-NPLIFWN-PAFTRUTGYFAQEAELIGRNCKFLQGG- 51 SULVANKLTTSVIITNPRLPD-NPLIFWN-PAFTRUTGYFAQEAELIGRNCKFLQGG- 52 NLSLARAVASTIESSCLVITDARGS-NPLIFWN-SAFTSUTGYE-EVLGTNCKFLQGG- 53 NLSLARAVASTIESSCLVITDARGS-NPLIFWN-SAFTSUTGYE-EVLGTNCKFLQGG- 54 NLSLARAVSTIESCULTDARGS-NPLIFWN-SAFTSUTGYE-EVLGTNCKFLQGG- 56 NSLARAVSTIESCULTDARGD-VPLIFWN-AAFTEITGYTGYADELIGRNCKFLQGG- 57 NAVLASTVASVTSGVULDAHGD-VPLIFWN-AAFTEITGYTADELIGRNCKFLQGG- 38 NELATAGGRTGGRTGGTDARG-NPLIFWN-AAFTEITGYTAAELGRNCKFLQGG- 39 NALLATASSVTSGVULDATGD-VPLIFW	DSDP AAVALVREAVRAG - RDCAVEVLNYRKDGTPFWINLSVSPIRDDAG - ELTHFVGVLVDVTDRI - KTAP - ESVTITREAVROK - RTCLVELQNYRKDGTTFWIGLSLSPIRDTAG - AVANFYGVLTDISFLE - ETAA - ETKNRIRGALDAR - TOPFOGULNYRKNGDAFWINSSTIPTOGDG - ELIGYVGTTRDVTESPL - TOPP - ETRVRIRGALDAR - TOPFOGULNYRKNGDAFWINSSTIPTORDAG - ELIGYVGTTRDVTESPL - DTDP - ETRVRIRGALAVG - EPFEGEILNYRKDGKPFWINSLSITPQRSKFG - RLIGFVGTRRDVTERR - DTCP - EAKKRIKQAIENG - OQFDGQILNYRKNGGAFWINDLSITPQRDAR - ELTGFVGTRRDVTERR - GTDR - AMVAQMRQALDGR - TEFFGEVLNYRQDGEPFWINSLSIAPVFGADG - QLIHFISTMRDVTERR - LSSP - ETITARNALNSE - KEFNGEIINYRKDGSIFWINDLSISPVENEKG - LITHFIGITRDITTRR - TOPOL - OTTSQIRSALEQG - OPFAGEIINYRQDGSIFWINDLSISPVENEKG - LITHFIGITRDITTRR - LTST - ESSVAIRESLSNL - ENFSGKILNYRKDGSIFWINDLSISPVEDEGG - RLINHFIGITRDITTRR - LTDP - RSIDAIRAALDRG - EEFSGEILNYRKDGSFWINDLSISPVEDEGG - RLINHFIGITRDUTERR - LTDP - RAVDANRLALKNIS - AEFAGEILNYRKDGSTFWINELTISPVENEGG - LINHFIGITRDUTERR - LTDP - GTVAIRLALQNG - EEFSGEILNYRKDGSTFWINELTISPVENEGG - QLAHFIGVTRDTORN - LTDP - OTVEAIRHCRQQ - TEFFGGEILNYRKDGSTFWINELTISPVENEGG - QLAHFIGVTRDTORN - LTDP - OTVEAIRHCRQQ - TEFFGGEILNYRKDGSTFWINELTISPVENEGG - QLAHFIGVTRDTORN - LTDP - OTVEAIRHCRQQ - TEFFGGEILNYRKDGSFFWINELTISPVENEGG - QLAHFIGVTRDTORN - LTDP - OTVEAIRHCRQQ - TEFFGGEILNYRKDGSFFWINELTISPVENEGG - QLAHFIGVTRDTORN - LTDP - STHEALRSALSER - RFATVEVTNFRKGGSFFWINELTISPVENEGG - QVTHFVGIARDISERN - FTDA - KYVEAIRTCLREC - REFSGEILNYRKDGSFFWINELTISPVENEGG - QVTHFVGIARDISERN - KLDP - STHEALRSALSER - RFATVEVTNFRKGGSFFWINELTISPVENEGG - KLTHFVGWSTDUTERR - LTDP - NITEARTALNEE - EEFFGGELLNYRKDGSFFWINELTISPVENEGG - KLTHFVGWSTDUTERR - FTDK - SATMALRSE - SPROGULNYRKDGSFFWINELTISPVENEGG - KLTHFVGWSTDUTERR - FTSKTKKKAIDNN - EPITKEEVINYRKDGSFFWINELSTRPVODDD - ELLYFIGITTDVERN - ETDK - AAIMQVRRAIAEK - QPITIWMKNYKKDGKLFWINELSTRPVODDD - ELLYFIGITTDVERN - ETDK - EKTSRIKKAIDNN - EPITKEEVINYRKDGSFFWINELSTRPVODDD - ELLYFIGITDVERN - GTDP - VAVQURRBEAIGR - SHHECKLUNYRKDGGTPFUNELTISPVENDEGG - KLTHFVGISDITGTER - ETSP - DVIAMERAIRGR - SHHECKLUNYRKDGGTPFUNELTISPVENDEGG - ELSYPYGS	KL 632 LM 265 AR 121 AV 121 AH 132 AN 609 SVA 609 SVA 431 LIA 422 AN 450
WP_010041727.1 WP_020473798.1 HCC28399.1 WP_067676345.1 WP_157075159.1 WP_137733365.1 WP_1315265150.1 WP_130106758.1 WP_153115534.1 WP_153115534.1 WP_153115534.1 WP_153115534.1 WP_162084453.1 WP_052808331.1 WP_052808331.1 WP_052808331.1 WP_0698784.1 WP_099687844.1 WP_099687844.1 WP_106380907.1 WP_106380907.1 WP_138539117.1 WP_138539117.1 WP_138539117.1 WP_138539117.1 WP_138539117.1 WP_138539117.1 WP_138539117.1 WP_138539117.1 WP_138539117.1 WP_13853917.1 WP_13853917.1 WP_13853917.1 WP_13853917.1 WP_13853917.1 WP_13853917.1 WP_13853917.1 WP_13853917.1 WP_15965856591.1 TXH39291.1 TXH39291.1 RYG54688.1 PSQ37876.1 WP_112078485.1	111 LRLADRAIQAVTQGILITSPALPD-NPITYAS-PGFEGVTGYPPREALGRNCRFLQGK- 114 LQWROBAIQSLYQGLCITDPSLPD-NPITYWN-DSFLRITGYAREDYIGQNCRLLQGP 3 KWFRREILEAIGHGWYFTDPAEKITYAN-GSFCELTGYDESEVLGRTGRFLQGG- 3 KWFRREILEAIGHGWYFTDPAEKITYAN-GSFCELTGYDRSETVGRNCRFLQGG- 14 ANLOQWYIDSIGHGVIFADTETITYAN-RYFERITGYSNSETVGRNCRFLQGP- 14 ANLOQWYIDSIGHGVIFADTETITYAN-RYFERITGYSNSETVGRNCRFLQGP- 15 KLSDAALKAISQGVIIADANNIISWN-PPLLAITGFSSEEFIGRNCRFLQGP- 16 KLSDAALKAISQGVIIADANNIISWN-PPLLAITGFSSEEFIGRNCRFLQGP- 17 KLKDDAALKAISQGVIITDANNIISWN-DALLSITGYQREDFINKNCRFLQGP- 18 LKLSDAALKAISQGVIITDANNIISWN-DALLSITGYGREDFINKNCRFLQGP- 19 LKVSDAALKAYSQGVIITBANR	-DSDPAAVALVREAVRAG - RDCAVEVLNYRKDGTPFWINLSVSPIRDDAG - ELTHFVGVLVDVTDRN -KTAP - ESVTITREAVROK - RTCLVELQNYRKDGTFFWINGLSLSPIRDTAG - AVANHFVGVLTDISPLH -ETAA - ETKWRIRQALDAR - TQPFOGDVLNYRKNGDAFWINGSLTPROTAG - AVANHFVGVLTDISPLH -ETAA - ETKWRIRQALDAR - TQPFOGDVLNYRKNGDAFWINGSLTPROTAG - AVANHFVGVLTDISPLH -DTCP - ETRYRTKALLAVG - EPFEGELLLYRKDGGKPWINGLSITPGADKFG - ELIGFVGITRDVTERN -DTCP - EAKRIKQAIENG - OQFDGGILNYRKNGEAFWINGLSITPGADR - ELTGFVGITRDVTERN -DTCP - EAKRIKQAIENG - OQFDGGILNYRKNGEAFWINGLSITPGADR - ELTGFVGITRDVTERN -USSP - ETITATRIALINSE - KEFNGEILNYRKDGALFWINGLSISPVENEKG - ILTHFIGITRDTTERN -OTDL - QTISQIRSALEQG - QPFAGEIINYRKDGALFWINDLSISPVENEKG - ILTHFIGITRDTTERN -ITST - ESSVAIRESISNIL - ENFSCKILLYRKDGGSFFWINDLSISPVENEKG - ILTHFIGITRDTTERN -LTSP - RSIDAIRAALDRG - EEFSGEILNYRKDGGSFFWINDLSISPVENEKG - ILTHFIGITRDTTERN -LTDP - RSIDAIRAALDRG - EEFSGEILNYRKDGGSFFWINDLSISPVENEGG - RLINHFIGITRDVTERN -LTDP - RAVDANRLALKNIS - AEFAGEILNYRKDGSFFWINDLSISPVENEGG - RLINHFIGITRDVTERN -LTDP - QTVEAIRHCLRQQ - TEFFGEILNYRKDGSTFWIELTISPVENEGG - QLAHFIGUTRDTORN -LTDP - QTVEAIRHCLRQQ - TEFFGEILNYRKDGSTFWIELTISPVENEGG - QLAHFIGUTRDTORN -LTDP - QTVEAIRHCLRQQ - TEFFGEILNYRKDGSTFWIELTISPVENEGG - QLAHFIGUTRDTORN -LTDP - GYTHAFIGUTRG - TEFFGEILNYRKDGSFFWIELTISPVENEGG - QLAHFIGUTRDTORN -LTP - KTLCAHQAIESA - TEFTGEILNYRKDGSFFWIELTISPVENEGG - QLAHFIGUTRDTORN -TFDA - KYVEAIRHCLRQG - TEFFGEILNYRKDGSFFWIELTISPVENEGG - RLINHFIGUTSPRONGH - RLINHFIG	KL 632 LM 265 AR 121 AV 121 AV 121 AV 121 AV 132 AV 609 AV 524 CA 431 IA 422 AV 310 IA 422 AV 310 IA 589 AV 450 EA 310 EA
WP_010041727.1 WP_020473798.1 HCC28399.1 WP_067676345.1 WP_157075159.1 WP_157075159.1 WP_13713386.1 WP_115226150.1 WP_130106758.1 WP_153115534.1 NDP38329.1 WP_153115534.1 NDP38329.1 WP_162084453.1 NBV85339.1 WP_0629634518.1 WP_146404542.1 WP_0996398941.1 WP_06588576.1 RYG64184.1 RYG65188.1 WP_106380907.1 WP_106380907.1 WP_1063855489.1 WP_138539117.1 WP_063356489.1 WP_13853917.1 WP_163356489.1 WP_13613329.1 WP_155965919.1 TXH39291.1 RYG64698.1 PSQ37876.1 WP_112078485.1 WP_112078485.1	111 LRLRDRAIQAVTQGILITSPALPD-NPITYAS-PGFEGVTGYPPREALGRNCRFLQGK 114 LOWROBAIQSLYQGLCITDPSLPD-NPITYWN-DSFLRITGYAREDYGONCGLLQGP 3 KHFRREILEAIGHGWYFDAEKITYAN-GSFCELTGYDRSEIVGRNCRFLQGP 14 AHLDQHYIDSIGHGVIFADTETITYAN-RYFCEITGYDSSEIVGRNCRFLQGP 15 ALSHQALQAINQGVVIANPLQDITETN-GAFCRITGYSSEIVGRNCRFLQGP 16 LAISHQALQAINQGVVIANPLQDITETN-GAFCRITGYSSEQVLGRNCRFLQGP 17 LKLSDAALKAISQGVIIADANNNITSWN-PLLAITGFSSEEFIGRNCRFLQGP 18 LKLSDALKAISQGVIITANREWITSWN-DALLSITGYGREDFINKNCRFLQGP 19 LKLSDALKAISQGVVITANDRRITSWN-DAFTAITGYSEREIAGKNCDFLQGP 10 KKNDLSIQSISQGVIITGADRLIVTWN-DAFSITGYAREVIGRNCRFLQGP 11 LRLSDAALKAVSQGVVITGADRLILYAN-DAFTAITGYAREVIGRNCRFLQGP 12 LRVSDVALKAVSQGVLITGADRL	-DSDP	KL 632 LM 265 AR 121 VQ 121 HH 132 QX 577 QX 585 VX 609 RX 524 CA 431 LA 422 QX 450 EA 431 LA 589 QV 450 EA 577 EA 206 EA 114 EA 589 QV 450 EA 115 EA 1518 EA 206 EA 115 EA 175 E
WP_010041727.1 WP_020473798.1 HCC28399.1 WP_067676345.1 WP_157075159.1 WP_137733365.1 WP_1315265150.1 WP_130106758.1 WP_153115534.1 WP_153115534.1 WP_153115534.1 WP_153115534.1 WP_162084453.1 WP_052808331.1 WP_052808331.1 WP_052808331.1 WP_0698784.1 WP_099687844.1 WP_099687844.1 WP_106380907.1 WP_106380907.1 WP_138539117.1 WP_138539117.1 WP_138539117.1 WP_138539117.1 WP_138539117.1 WP_138539117.1 WP_138539117.1 WP_138539117.1 WP_138539117.1 WP_13853917.1 WP_13853917.1 WP_13853917.1 WP_13853917.1 WP_13853917.1 WP_13853917.1 WP_13853917.1 WP_13853917.1 WP_15965856591.1 TXH39291.1 TXH39291.1 RYG54688.1 PSQ37876.1 WP_112078485.1	111 LRLRDRAIQAVTQGILITSPALPD-NPITYAS-PGFEGVTGYPPREALGRNCRFLQGK- 114 LOWROBAIQSLVQGLCITDPSLPD-NPITYWN-DSFLRITGYAREDVGONCGLLQGP 3 KWFRREILEAIGHOWYFDDAEKTYYAN-GSFCELTGYDSESVLGRTGREILGGP 4 KWFREILEAIGHOWYFDDAEKTYYAN-GSFCELTGYDRSEIVGRNCRFLQGP 14 AHLDQHVIDSIGHOVIFADTETITYAN-RYFCEITGYDSSEIVGRNCRFLQGP 15 LKLSDAALKAISQGVIADAWNITSWN-PLLAITGFSSEEFIGRNCRFLQGP 267 LKLSDAALKAISQGVIITANREWITSWN-PLLAITGFSSEEFIGRNCRFLQGP 278 LKLSDAALKAISQGVIITANREWITSWN-PLAITGFSSEEFIGRNCRFLQGP 289 LKLSDAALKAISQGVIITANREWITSWN-DALSITGYAREPLIKNICKFLQGP 290 LRVSDVALKAVSQGVIITGADRLITSWN-DALSITGYAREPLIGRNCRFLQGP 301 LRVSDAALKAVSQGVIITGADRLITYWN-DAFLSITGYARAEVFGGSCRFLQGP 302 LRVSDAALKAVSQGVIITADDVRL	-DSDPAAVALVREAVRAG - RDCAVEVLNYRKDGTPFWINLSVSPIRDDAG - ELTHFVGVLVDVTDRN -KTAP - ESVTITREAVROK - RTCLVELQNYRKDGTFFWINGLSLSPIRDTAG - AVANHFVGVLTDISPLH -ETAA - ETKWRIRQALDAR - TQPFOGDVLNYRKNGDAFWINGSLTPROTAG - AVANHFVGVLTDISPLH -ETAA - ETKWRIRQALDAR - TQPFOGDVLNYRKNGDAFWINGSLTPROTAG - AVANHFVGVLTDISPLH -DTCP - ETRYRTKALLAVG - EPFEGELLLYRKDGGKPWINGLSITPGADKFG - ELIGFVGITRDVTERN -DTCP - EAKRIKQAIENG - OQFDGGILNYRKNGEAFWINGLSITPGADR - ELTGFVGITRDVTERN -DTCP - EAKRIKQAIENG - OQFDGGILNYRKNGEAFWINGLSITPGADR - ELTGFVGITRDVTERN -USSP - ETITATRIALINSE - KEFNGEILNYRKDGALFWINGLSISPVENEKG - ILTHFIGITRDTTERN -OTDL - QTISQIRSALEQG - QPFAGEIINYRKDGALFWINDLSISPVENEKG - ILTHFIGITRDTTERN -ITST - ESSVAIRESISNIL - ENFSCKILLYRKDGGSFFWINDLSISPVENEKG - ILTHFIGITRDTTERN -LTSP - RSIDAIRAALDRG - EEFSGEILNYRKDGGSFFWINDLSISPVENEKG - ILTHFIGITRDTTERN -LTDP - RSIDAIRAALDRG - EEFSGEILNYRKDGGSFFWINDLSISPVENEGG - RLINHFIGITRDVTERN -LTDP - RAVDANRLALKNIS - AEFAGEILNYRKDGSFFWINDLSISPVENEGG - RLINHFIGITRDVTERN -LTDP - QTVEAIRHCLRQQ - TEFFGEILNYRKDGSTFWIELTISPVENEGG - QLAHFIGUTRDTORN -LTDP - QTVEAIRHCLRQQ - TEFFGEILNYRKDGSTFWIELTISPVENEGG - QLAHFIGUTRDTORN -LTDP - QTVEAIRHCLRQQ - TEFFGEILNYRKDGSTFWIELTISPVENEGG - QLAHFIGUTRDTORN -LTDP - GYTHAFIGUTRG - TEFFGEILNYRKDGSFFWIELTISPVENEGG - QLAHFIGUTRDTORN -LTP - KTLCAHQAIESA - TEFTGEILNYRKDGSFFWIELTISPVENEGG - QLAHFIGUTRDTORN -TFDA - KYVEAIRHCLRQG - TEFFGEILNYRKDGSFFWIELTISPVENEGG - RLINHFIGUTSPRONGH - RLINHFIG	KL 632 LM 265 AR 121 AV 121 AH 132 AV 577 AV 588 AV 609 AV 524 AV 450 AV



Fig. S12 - Naturally occurring, glutamine-deficient LOV $^{\Delta Q}$ receptors. Sequence searches identify around 350 receptors that have homology to *bona fide* LOV receptors but lack the conserved active-site glutamine. The multiple sequence alignment shows *AsL*OV2 as a reference; coloring, shading and arrows as in Fig. 1, with the position of the conserved glutamine residue indicated by a red arrow.

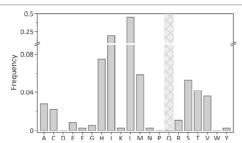


 Fig. S13 - Histogram of amino acids replacing the conserved glutamine in naturally occurring LOV $^{\Delta Q}$ receptors.

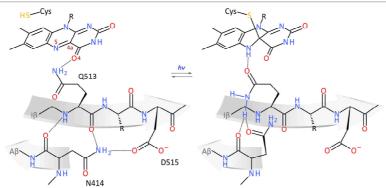


Fig. S14 - Signal transduction in light-oxygen-voltage (LOV) receptors, exemplified for the *A. sativa* phototropin 1 LOV2 domain. The Lewis formulae show the flavin nucleotide chromophore and surrounding residues of the dark-adapted (left) and light-adapted states (right). Light-induced thioadduct formation between the flavin C4a atom and the conserved cysteine (C450) residue entails flavin protonation at the N5 atom. In response, a conserved glutamine (Q513) rotates its sidechain to satisfy hydrogen bonding, thus propagating conformational changes towards the LOV β sheet. Hydrogen-bonding rearrangements involving N414, Q513, and D515 lead to a weakening of the β sheet and structural elements associating with its outer face.

Supplementary Table S1. Data collection and refinement statistics for X-ray crystallography of AsLOV2 wild
 type.

	AsLOV2 dark ^a	AsLOV2 light ^a		
Data collection				
Space group	P 2 ₁ 2 ₁ 2 ₁	P 2 ₁ 2 ₁ 2 ₁		
Cell dimensions				
a, b, c (Å)	35.5, 56.4, 66.7	35.6, 56.0, 66.5		
α, β, γ (°)	90, 90, 90	90, 90, 90		
Resolution (Å)	43.07 - 1.00 (1.06 - 1.00) ^b	42.85 – 1.09 (1.16 – 1.09)		
R_{meas}	0.081 (1.653)	0.075 (1.796)		
Ι / σΙ	13.50 (1.22)	12.04 (1.02)		
Completeness (%)	93.1 (86.5)	99.2 (98.0)		
Redundancy	7.5 (7.6)	7.0 (6.2)		
CC _{1/2}	0.999 (0.510)	0.999 (0.450)		
Refinement				
Resolution (Å)	43.07 – 1.00 (1.03 – 1.00)	42.84 – 1.09 (1.12 – 1.09)		
No. reflections	64,477 (4,481)	53,766 (4,020)		
$R_{ m work}$ / $R_{ m free}$	0.114 (0.320) / 0.148 (0.308)	0.123 (0.328) / 0.161 (0.387)		
No. atoms				
Protein	1,186	1,186		
Ligand/ion	117	89		
Water	183 195			
B-factors				
Protein	10.86	15.25		
Ligand/ion	22.05 23.78			
Water	26.26 29.75			
R.m.s deviations				
Bond lengths (Å)	0.013	0.012		
Bond angles (°)	1.80	1.82		
PDB deposition	7pgx	7pgy		

^a Data were collected from a single crystal each.

¹¹² b Values in parentheses are for highest-resolution shell.

113 Supplementary Table S2. Data collection and refinement statistics for X-ray crystallography of AsLOV2 Q513L.

	AsLOV2 Q513L darka	AsLOV2 Q513L light ^a
Data collection		
Space group	P 2 ₁ 2 ₁ 2 ₁	P 2 ₁ 2 ₁ 2 ₁
Cell dimensions		
a, b, c (Å)	35.6, 54.6, 66.5	35.3, 56.0, 66.8
α, β, γ (°)	90, 90, 90	90, 90, 90
Resolution (Å)	42.17 - 0.90 (0.95 - 0.90) ^b	42.92 – 0.98 (1.04 – 0.98)
R _{meas}	0.075 (1.908)	0.054 (2.19)
Ι / σΙ	13.81 (0.99)	14.27 (0.74)
Completeness (%)	99.0 (97.6)	99.7 (98.3)
Redundancy	7.2 (6.9)	6.9 (6.1)
CC _{1/2}	1.000 (0.371)	0.999 (0.303)
Refinement		
Resolution (Å)	42.17 - 0.90 (0.92 - 0.90)	42.92 – 0.98 (1.01 – 0.98)
No. reflections	90,644 (6,691)	72,710 (5,330)
R _{work} / R _{free}	0.115 (0.331) / 0.139 (0.328)	0.112 (0.382) / 0.136 (0.384)
No. atoms		
Protein	1,185	1,185
Ligand/ion	119	62
Water	215	217
<i>B</i> -factors		
Protein	9.30	14.50
Ligand/ion	17.22	18.54
Water	22.23	30.20
R.m.s deviations		
Bond lengths (Å)	0.013	0.013
Bond angles (°)	1.99	2.04
PDB deposition	7pgz	7ph0

^a Data were collected from a single crystal each.

^b Values in parentheses are for highest-resolution shell.



A Light-Oxygen-Voltage Receptor Integrates Light and Temperature

Julia Dietler¹, Roman Schubert², Tobias G. A. Krafft¹, Simone Meiler¹, Stephanie Kainrath³, Florian Richter², Kristian Schweimer^{4,6}, Michael Weyand¹, Harald Janovjak³ and Andreas Möglich^{1,2,5,6*}

- 1 Department of Biochemistry, University of Bayreuth, 95447 Bayreuth, Germany
- 2 Biophysical Chemistry, Humboldt-University Berlin, 10115 Berlin, Germany
- 3 Australian Regenerative Medicine Institute (ARMI), Monash University, Clayton, Victoria 3800, Australia
- 4 Biopolymers, University of Bayreuth, 95447 Bayreuth, Germany
- 5 Bayreuth Center for Biochemistry & Molecular Biology, University of Bayreuth, 95447 Bayreuth, Germany
- 6 North-Bavarian NMR Center, University of Bayreuth, 95447 Bayreuth, Germany

Correspondence to Andreas Möglich: Department of Biochemistry, University of Bayreuth, 95447 Bayreuth, Germany. andreas.moeglich@uni-bayreuth.de (A. Möglich)
https://doi.org/10.1016/j.jmb.2021.167107

Edited by Kai Zhang

Abstract

Sensory photoreceptors enable organisms to adjust their physiology, behavior, and development in response to light, generally with spatiotemporal acuity and reversibility. These traits underlie the use of photoreceptors as genetically encoded actuators to alter by light the state and properties of heterologous organisms. Subsumed as optogenetics, pertinent approaches enable regulating diverse cellular processes, not least gene expression. Here, we controlled the widely used Tet repressor by coupling to light-oxygen-voltage (LOV) modules that either homodimerize or dissociate under blue light. Repression could thus be elevated or relieved, and consequently protein expression was modulated by light. Strikingly, the homodimeric $\it RsLOV$ module from $\it Rhodobacter sphaeroides$ not only dissociated under light but intrinsically reacted to temperature. The limited light responses of wild-type $\it RsLOV$ at 37 °C were enhanced in two variants that exhibited closely similar photochemistry and structure. One variant improved the weak homodimerization affinity of 40 μM by two-fold and thus also bestowed light sensitivity on a receptor tyrosine kinase. Certain photoreceptors, exemplified by $\it RsLOV$, can evidently moonlight as temperature sensors which immediately bears on their application in optogenetics and biotechnology. Properly accounted for, the temperature sensitivity can be leveraged for the construction of signal-responsive cellular circuits.

© 2021 Elsevier Ltd. All rights reserved.

Introduction

Organisms across all kingdoms of life read out and adapt to environmental signals, e.g., light and temperature. Sensory photoreceptor proteins^{1,2} detect incident light signals and decode them into adequate physiological responses, spanning for

instance animal vision,³ plant phototropism and photomorphogenesis,⁴ and regulation of bacterial photosynthesis.⁵ Generally, these responses are self-contained, precise in time and space, and reversible. Exactly these attributes underlie the wide use of photoreceptors in optogenetics⁶ as genetically encoded actuators for the

non-invasive, on-demand control by light of cellular state and function. Conceived in the neurosciences, optogenetics has much transcended these origins and now allows the precise control of diverse cellular and organismal processes. To great extent, this development owes to the engineering of photoreceptors with custom-tailored functions. As borne out in numerous examples, the recombination of light-sensitive photosensor modules with inherently light-inert effector modules has given rise to cohorts of light-gated proteins. Notwithstanding the great diversity of engineering strategies, particularly many cellular proteins and pathways have been subjected to light control through coupling with photo associating receptors that dimerize or oligomerize under light.8 For instance, the heterodimerization of plant cryptochrome 2 with a partner protein under blue light has been harnessed to control transcription and recombination. 9-12 Likewise, homodimerizing light-oxygen-voltage (LOV) domains can similarly serve to control by blue light transcription in eukaryotes and bacteria, among many other cel-Iular processes. 13-15 Cognizant of the broad applicability of light-regulated protein:protein interactions, several groups advanced LOV receptors that heterodimerize with partners or dissociate from them, respectively, under blue light.1

The small homodimeric protein RsLOV, involved in regulating photosynthesis among processes in the purple bacterium Rhodobacter sphaeroides, 5 complements these proteins. In contrast to the above homodimeric LOV receptors that invariably associate upon illumination, RsLOV dissociates into monomers under blue light.²⁴ The dark-adapted state of RsLOV is characterized by two monomers in head-to-head orientation with a dimer interface formed by a central antiparallel β sheet, an N-terminal α -helix, and two helices, denoted $J\alpha$ and $K\alpha$, C-terminal to the LOV core domain (Figure 1(a)). In common with other LOV ²⁵⁻²⁷ blue light drives the formation of a receptors. thioether bond between a conserved cysteine residue and the C4a atom of a flavin mononucleotide (FMN) chromophore. The concomitant protonation of the flavin N5 atom^{28,29} elicits hydrogen-bonding rearrangements that generally weaken the central β-sheet and structural elements interacting with it.³⁰ In *Rs*LOV, these conformational transitions culminate in the disruption of the α -helical interface and dimer dissociation.²⁴ In R. sphaeroides, monomerization presumably allows RsLOV to interact with still-unidentified partner proteins and to trigger physiological responses. Given that RsLOV dissociates rather than associates under blue light, it is attractive for photoreceptor engineering, as it potentially enables a novel directionality in optogenetic experiments. As a case in point, we employed RsLOV to impart light sensitivity on Streptococcus pyogenes Coupling to the RsLOV module also entailed a pronounced temperature sensitivity of Cas9 activity. Though unexpected, we capitalized on this finding in the design of a temperaturesensitive variant which displayed robust activity at 29 °C but very little at 37 °C. Although the strong temperature response remains poorly understood, it could be rooted in the RsLOV module itself and indicate a general lability of the protein. Consistent with this notion, RsLOV failed to confer light regulation on receptor tyrosine kinases (RTK) whereas a photoassociating LOV domain sufficed and evoked robust optogenetic responses. 33 Likewise, RsLOV proved insufficient for controlling by light translation initiation.34 By contrast, in a recent study RsLOV served to control in response to light the homodimerization and thus repressor activity of the LexA DNAbinding domain at 37 °C. 35 The best-performing variant, dubbed eLightOn, exhibited a 500-fold transcriptional upregulation under blue light compared to darkness.

Here, we investigated the response of the RsLOV module to blue light and temperature in more detail. To this end, we designed light-regulated variants of the widely used Tet repressor (TetR), given its eminent importance in biotechnology. We Cterminally fused RsLOV to truncated TetR variants and achieved light-induced upregulation transcription at 29 °C. Replacement of RsLOV by photoassociating LOV domains yielded TetR variants activated by blue light rather than inactivated. The initial TetR-RsLOV variants were susceptible to temperature, with transcriptional repression and regulatory efficiency greatly impaired at 37 °C. Circular dichroism spectroscopy revealed that RsLOV intrinsically responds to temperature and blue light, with both cues inducing loss of α-helical structure. Two RsLOV variants, obtained by random mutagenesis and computational design, exhibited similar photochemistry, three-dimensional structures and light-induced dimer dissociation as the wild-type protein, but supported robust light-gated activity at 37 °C. Whereas one variant benefitted from thermal stabilization of its α -helical subunit interface, the other exhibited variant two-fold stronger homodimerization, which is unexpectedly weak in wild-type RsLOV with a dissociation constant around 40 µM in darkness. Coupled to different LOV modules, a suite of optimized TetR variants was generated that now enables the regulation of expression at both 29 °C and 37 °C in either lightactivated or light-repressed manner. Conjugated to a receptor tyrosine kinase, one of the enhanced RsLOV variants also conferred light sensitivity on activity where the wild-type RsLOV failed to do so.

Results

Design of light-regulated Tet repressor variants

To efficiently probe the influence of light and temperature cues, we set out to embed the

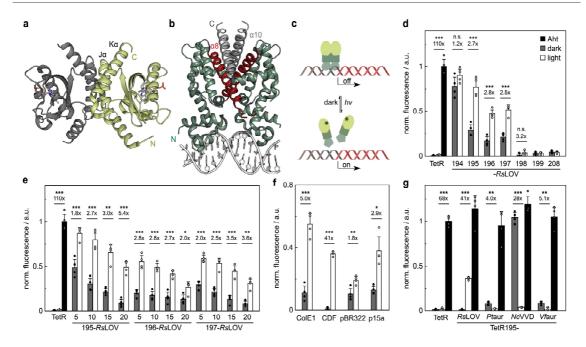


Figure 1. Design of single-chain light-regulated Tet repressor (TetR) variants. (a) The dark-adapted state of RsLOV adopts homodimeric structure, with the C-terminal J α and K α helices of the two subunits forming the dimer interface (PDB entry 4hia). (b) The homodimeric TetR comprises ten α -helices, where helices $\alpha 1-\alpha 3$ mediate DNA binding, and the C-terminal helices $\alpha 8$ and $\alpha 10$ are engaged in dimerization (PDB entry 1qpi). (c) Design rationale for the construction of light-regulated TetR variants. C-terminal truncation might render TetR monomeric and hence incapable of DNA binding. Fusion to RsLOV could rescue dimerization and DNA binding in darkness but not under blue light. Transcription initiation might hence be subjected to light control. (d) Bacterial gene expression controlled by TetR variants on a plasmid backbone with ColE1 origin of replication (ori). Expression levels were determined by DsRed reporter fluorescence normalized by optical density in darkness (grey bars), under blue light (white), or in the presence of the inducer Aht (black). TetR refers to the wild-type repressor, and the numbers denote C-terminal TetR truncations coupled to RsLOV. (e) Variation of the length (5, 10, 15, 20 residues) of the linker connecting the TetR and RsLOV moieties in the CoIE1 plasmid background. (f) Influence of the origin of replication on light-dependent gene expression for TetR195-RsLOV. (g) Replacement of RsLOV by homodimerizing LOV modules inverted the response to light of the TetR195-RsLOV variant within a pCDF plasmid. All measurements in panels d-g were conducted at 29 °C, represent mean ± s.d. of four biologically independent samples, and were normalized to the Aht-induced TetR system on the pASK (panels d-e) or the pCDF backbone (panels f-g). Asterisks denote p values from a two-sided Welch's t test (* $p \le 0.05$, ** $p \le 0.01$, *** $p \le 0.001$, n.s. not significant).

RsLOV module in a tractable and readily assayable reporter-gene system. Inspired by earlier reports harnessing photoassociating LOV receptors to control transcription, 14,36 we reasoned that the light-induced dissociation of the homodimeric RsLOV lends itself to control the activity of obligate homodimeric transcription factors. We opted for the Tn10-encoded Tet repressor (TetR, class B³⁷) because it is both well studied and widely used as a versatile tool in molecular biology. 38,39 Derived from an antibiotic resistance cassette in Gramnegative bacteria, the homodimeric TetR binds to the cognate tetO operator sequence with subnanomolar affinity and thereby represses transcription from associated promoters. The all-helical TetR protein comprises an N-terminal helix-turn-helix DNA-binding domain and a C-terminal domain that mediates dimerization and regulation (Figure 1

(b)). Binding of tetracycline (or, analogs) to the C-terminal domain induces a separation of the N-terminal domains and reduces *tetO* affinity by nine orders of magnitude. 40,41 Owing to the equally tight and stringently regulated DNA interactions, TetR underpins versatile inducible gene-expression systems for use in prokaryotes and eukaryotes.

suspected that disruption of TetR homodimerization could abolish DNA binding and transcriptional repression. If so, linkage of RsLOV to a suitably truncated TetR variant could then dimerization, tet0 binding rescue transcriptional regulation in light-dependent fashion (Figure 1(c)). Inspection of the TetR:tetO complex structure reveals that the homodimer interface is largely formed by the two long helices (residues 126–153) and α 10 (182–202) (Figure 1(b)). To experimentally validate this reasoning, we expressed a DsRed fluorescent reporter gene under TetR control from a pASK plasmid that encodes the wild-type TetR (1-208). Bacterial cultures harboring this plasmid were incubated at 29 °C with or without 0.25 μg mL-(Aht), anhydrotetracycline followed determination of the reporter fluorescence normalized to optical density. Notably, tetracycline compounds are prone to decomposition under blue light, as aptly demonstrated and exploited in the recent optochemical regulation of TetRcontrolled expression.⁴² To prevent inadvertent degradation, all experiments with Aht as an inducer were generally performed in darkness. In the absence of Aht, fluorescence levels of around 0.04 a.u. (arbitrary units) were obtained, irrespective of whether the cultures were grown in darkness or under constant blue light (470 nm, 100 μ W cm⁻²). These values were close to the background fluorescence of 0.03 a.u. determined for bacterial cultures containing a plasmid that lacked DsRed. Addition of the inducer Aht to dark-incubated cultures led to higher fluorescence (1.0 a.u.), which - correcting for background fluorescence - corresponds to around 100-fold upregulation. Using this reporter assay, we next assessed fusions between TetR and RsLOV. Appendage of RsLOV to the TetR Cterminus via a glycine-serine linker of 10 residues length did not significantly alter repression under either dark or blue-light conditions, nor did it impair inducibility by Aht (Figure 1(d)). Likewise, repression was unaffected for subsequent C-terminal truncations of the TetR helix α 10 by up to 10 residues (TetR198-10-RsLOV and TetR199-10-*Rs*LOV, where the first numbers indicate the C-terminal TetR residue and 10 refers to the linker length). More extensive truncations led to successive loss of repression, with TetR194-10-RsLOV exhibiting high reporter fluorescence, independently of light. By contrast, TetR195/196/197-10-RsLOV exhibited intermediate repression that depended on illumination. Compared to darkness, the DsRed expression was up to 2.8-fold higher under blue light, in line with the original design rationale (see Figure 1(c)).

We next sought to enhance the regulatory response to light by varying the length of the linker intervening the TetR and RsLOV moieties. Glycine-serine linkers of 5, 10, 15 and 20 residues all supported light-dependent repression in the TetR195-, TetR196and TetR197-RsLOV contexts, albeit to different extents (Figure 1(e)). Generally, repression increased (i.e. DsRed expression decreased) with linker length. Of all variants, TetR195-20-RsLOV with a 20-residue linker displayed the most pronounced light/dark expression ratio of 5.4-fold, and we focused on variant, denoted as TetR195-RsLOV subsequently. As the underlying design is based on light-modulated dimerization, its response is expected to strongly depend on repressor concentration. To assess this effect, we probed the influence of plasmid copy number on system performance. Exchange of the original ColE1 origin of replication (ori) with a copy number of 15-20 plasmids per cell for the CloDF13-derived CDF ori (copy number 20-40,43) strongly reduced expression in darkness but only moderately under blue light (Figure 1(f)). As a corollary, the degree of light induction in this system, denoted pLITR (light-inhibited Tet repressor), increased to around 41-fold (Table 1). By contrast, replacement of ColE1 by pBR322 or p15a oris of similar copy number negatively affected performance. All subsequent experiments were hence carried out in the pCDF background. In this vector context, the original TetR exhibited a 70-fold upregulation upon Aht addition, owing to higher expression levels in the induced state than for TetR195-RsLOV.

We hypothesized that the serial truncation of TetR led to a gradual weakening of its homodimeric state which could then be restored via the RsLOV module. To ascertain that the regulation of repression in TetR195-RsLOV is indeed governed by light-induced photosensor dissociation, we replaced RsLOV by the LOV domains from Neurospora crassa Vivid (NcVVD), Vaucheria frigida aureochrome1 (Vfaur), and Phaeodactylum tricornutum aureochrome (Ptaur). all of which undergo light-induced dimerization. 33,44,45 Consistent with exhibiting the opposite association response to blue light, at 29 °C these LOV domains all gave rise to TetR variants with stronger repression under light than in darkness (Figure 1(g)). In all variants, induction by the chemical inducer Aht was maintained to full extent. Notably, the TetR195-Ptaur, denoted pLATR-Pt (light-activated Tet repressor), and TetR195-Vfaur variants showed strong repression even in darkness with only moderate downregulation of expression by blue light. By contrast, the pLATR-Nc system based on NcVVD was strongly repressed under blue light, while showing full induction (as compared to Aht) in darkness, amounting to a dark/light ratio of 28-fold (Table 1). All TetR variants showed similar repression activity and response to light in a different *E. coli* strain (Suppl. Figure S1).

The RsLOV module integrates light and temperature signals

We noticed that repression and response to light of the TetR-*Rs*LOV variants were susceptible to temperature increases. Whereas at 29 °C, TetR195-*Rs*LOV (pLITR) induced expression by around 41-fold when exposed to blue light, at 37 °C repression in darkness was greatly impaired, and the overall regulatory response diminished to a mere 2-fold (Figure 2(a)). As the original TetR repressor did not suffer a similar loss of repression over the same temperature interval (Suppl. Figure S2), we tentatively ascribed the temperature response of TetR195-*Rs*LOV to the

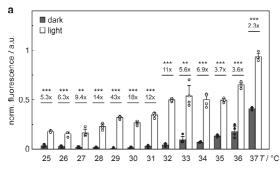
Table 1 Light-regulated gene expression by select Tet repressor variants at 29 °C and 37 °C.

		29 °C		37 °C			
Variant	Short name	Dark	Light	Fold change ^b	Dark	Light	Fold change ^b
TetR195-RsLOV	pLITR	0.009	0.362	41	0.999	0.439	2.3
TetR195-RsLOV D109G	pLITR-DG	0.001	0.016	n.d. ^c	0.040	0.484	12
TetR195-RsLOV d2	pLITR-d2	0.019	0.013	n.d. ^c	0.009	0.116	14
TetR195-NcVVD	pLATR-Nc	1.045	0.038	-28	0.949	0.921	1.0
TetR195- <i>Pt</i> aur	pLATR-Pt	0.080	0.020	-4.0	0.377	0.008	-46
TetR'(BD)196-Ptaur	pLATR-BD	0.154	0.006	-25	0.377	0.005	-75

^a Expression levels were determined by *Ds*Red reporter fluorescence normalized to the values for Aht-induced wild-type TetR.

RsLOV photosensor module. To examine this effect in more detail, we expressed and purified the isolated RsLOV protein. Using absorbance spectroscopy, we ascertained that undergoes the canonical LOV photochemistry under blue light²⁵ and recovered to its resting state in darkness with a time constant of $(5.0 \pm 0.1) \times 10^3$ s at 22 °C²⁴ (Suppl. Figure S3(a), (b)). In gel filtration experiments, conducted at an RsLOV concentration of 100 uM, the dark-adapted state eluted earlier than the light-adapted state, indicative of light-induced homodimer dissociation (Suppl. Figure S3(c)). Consistent with a previous study,²⁴ the two states showed a relatively small difference in retention time which was ascribed to the partially unfolded and hence less compact structure of the light-adapted state. We next analyzed the secondary structure of RsLOV and its response to light and temperature by circular dichroism (CD) spectroscopy. At 22 °C, the protein exhibited a far-UV CD spectrum consistent with its mixed α/β -fold. At 220 and 210 nm, the molar ellipticity per residue $[\Theta]_{MBW}$ had two minima with values of $-18,100^{\circ}$

 $cm^2 dmol^{-1} and -17,100^{\circ} cm^2 dmol^{-1}$, respectively (Suppl. Figure S3(d)). Under blue light, the CD spectrum revealed an around 40% loss of α helical secondary structure compared to darkness. These findings are consistent with earlier solution scattering measurements²⁴ that indicated lightdriven partial unfolding of RsLOV, attributed to the C-terminal $J\alpha$ and $K\alpha$ helices at the homodimer interface which together comprise around 50% of all helical residues in the protein (see Figure 1(a)). Notably, N- and C-terminal ancillary helices recur in LOV modules and frequently undergo lightinduced order-disorder transitions, as arguably best exemplified by phototropin LOV domains. The helical unfolding observed in RsLOV under blue light could hence be causative for dimer dissociation. We next assessed the thermal stability of RsLOV in its dark-adapted and light-adapted states by monitoring the α -helical CD signal at 222 nm over temperature (Figure 2(b)). Both states exhibited cooperative unfolding with nearly identical transition temperatures of $(55.8 \pm 0.1)^{\circ}$ C and $(56.0 \pm 0.1)^{\circ}$ C, respectively, suggesting that the global stability of



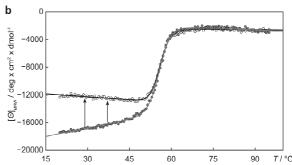


Figure 2. The RsLOV module is intrinsically responsive to both light and temperature signals. (a) Reporter-gene expression controlled by TetR195-RsLOV in darkness (grey bars) and blue light (white) at different temperatures. All measurements represent mean \pm s.d. of four biologically independent samples and were normalized to the light-induced TetR195-RsLOV at 37 °C. Asterisks denote p values from a two-sided Welch's t test (** $p \le 0.01$, *** $p \le 0.001$). (b) Thermal denaturation of RsLOV monitored by circular dichroism (CD) at 222 nm reveals cooperative unfolding transitions for both the dark-adapted (filled circles) and light-adapted (open circles) states. Below the transition region, the dark-adapted state exhibits a gradual loss of CD signal with temperature, indicative of partial α -helical unfolding. The vertical arrows denote temperatures of 29 °C and 37 °C.

^b Fold changes denote the expression ratio under dark and light conditions. Positive and negative numbers denote light-induced and light-repressed systems, respectively.

^c Not determined. Due to low expression levels no reliable fold change could be calculated.

RsLOV is unaffected by blue light. Intriguingly, between 20 and 50 °C the CD signal of the darkadapted state linearly rose with temperature [slope of $(84.1 \pm 3.3)^{\circ}$ cm² dmol⁻¹ K ¹], reflecting a successive loss of α -helical content. In marked contrast, the signal of the light-adapted state did not increase with temperature but rather slightly decreased [slope of $(-28.2 \pm 2.5)^{\circ}$ cm² dmol⁻¹ K⁻¹], which can be attributed to slow recovery to the dark-adapted state during the thermal unfolding experiment (conducted at a heating rate of 1 °C min⁻¹). Given that the temperature-driven partial unfolding of RsLOV occurs in the dark-adapted state but not in the light-adapted state, it likely also involves the very α-helical segments that become unstructured upon light absorption. Collectively, our results imply that the photoreceptor RsLOV can process and integrate both light and temperature cues.

Identification of improved RsLOV variants

Striving to amend the temperature sensitivity of the TetR195-RsLOV (pLITR) system, we next pursued a two-pronged strategy. First, we randomly introduced mutations in the RsLOV photosensor and screened for light-dependent reporter gene expression using flow cytometry. Bacteria harboring a library of TetR195-RsLOV variants were alternatingly incubated in darkness or blue light, followed by sorting based on fluorescence. After three dark-light cycles, we isolated a clone that at 37 °C exhibited a 12-fold upregulation of reporter fluorescence under blue light compared to darkness (Figure 3(a), Table 1). Sequencing revealed this clone to harbor the single residue exchange D109G. We verified that it is indeed the D109G exchange that underpins properties enhanced temperature incorporating this mutation into the original TetR195-RsLOV vector. The improvement of performance at 37 °C in the D109G variant, referred to as pLITR-DG, principally owed to stronger repression in darkness than for the wildtype RsLOV module. At the same time, gene expression under light conditions was less for D109G than for wild type, indicating more extensive residual repression at these conditions. When the temperature was varied between 25 and 37 °C, pLITR-DG consistently exhibited lower reporter gene expression than the pLITR variant based on wild-type RsLOV (Suppl. Figure S4(a)). At 29 °C, the optimum temperature for pLITR, the D109G variant promoted constitutive repression with minute light response. As the underlying design based on light-regulated homodimerization, we suspected that differences in expression levels and/or cellular stability might be causative for the differential activity displayed by the RsLOV variants. Upon overexpression of the TetR195-RsLOV variants at 29 and 37 °C, closely similar expression kinetics and overall

levels were obtained for wild type and D109G, which argues against differences in cellular concentrations (Suppl. Figure S4(b), (c)).

In a second approach, we reasoned that repression by TetR195-RsLOV at elevated enhanced temperatures might he computationally redesigning the RsLOV module. To this end, we employed the PROSS server (Protein Repair One-Stop Shop),47 which harnesses phylogenetic information and the Rosetta modeling framework⁴⁸ to vary the amino acid sequence of a protein subject such as to improve its thermodynamic and cellular stabilities, while striving to maintain protein functionality. To increase the likelihood of preserving productive photochemistry in the resultant redesigned RsLOV receptors, we excluded residues adjacent to the FMN cofactor from the redesign process. Out of the seven designs proposed by PROSS, we selected two, denoted d2 and d5, for further analysis based on the number and location of the suggested residue exchanges. Whereas variant d2 harbored six substitutions (G48D, Q49E, L77E, A90K, D92G and S157Q), design d5 comprised 13 residue exchanges (K4E, G48D, Q49E, L77E, A90K, N91D, D92G, R107E, P108D, D109G, A110N, T148A, S157H), among them the very D109G exchange we identified above. Embedded within the TetR195-RsLOV context, both the d2 and d5 variants constitutively repressed DsRed expression at 29 °C independently of illumination (Figure 3(b)). At 37 °C, the system based on d2, denoted pLITR-d2, exhibited a 14-fold upregulation of expression under blue light compared to darkness (Figure 3(a), Table 1), albeit with lower maximum levels than for pLITR and pLITR-DG. By contrast, the d5 variant lacked any light responsiveness and constitutively repressed expression (Figure 3(a)). Like for the D109G variant, stronger repression was not tied to elevated cellular concentrations of the d2 and d5 variants (Suppl. Figure S4 (b), (c)). Taken together, stabilization of the homodimeric RsLOV, be it by screening approaches, be it by computational design, appears to be a viable strategy for enhancing repression by the TetR-RsLOV fusion proteins. As a caveat, we however note that improved light responsiveness at 37 °C, as for D109G and d2, came at the cost of reduced inducibility at 29 °C.

We next assessed whether repression and the degree of light regulation of the TetR195-*Rs*LOV variant (pLITR) can also be adjusted by deliberate destabilization of the TetR entity. To this end, we replaced the original TetR module, denoted TetR (B) as it belongs to class B,³⁷ by the derivative TetR'(BD). Notably, TetR'(BD) contains the C-terminal part of the dimerization domain (residues 189–208) of the class-D TetR which exhibits reduced thermodynamic stability and dimerization compared to TetR(B).⁵⁰ Introduction of TetR'(BD) generally led to a weakening of repression for all

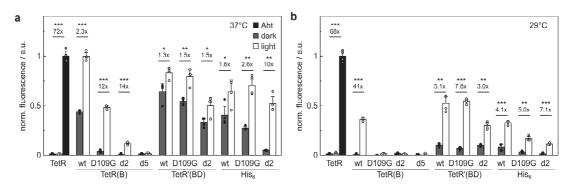


Figure 3. Identification of improved *Rs*LOV variants. **(a)** Reporter-gene expression for the *Rs*LOV variants D109G, d2, and d5 coupled to TetR195 in darkness (grey bars), under blue light (white), and in presence of Aht (black). wt refers to wild-type *Rs*LOV; TetR and TetR'(BD) denote the class-B Tet repressor and the class-B/class-D chimera; His₆ refers to the class-B TetR with C-terminally appended hexahistidine tag. All measurements were conducted at 37 °C, represent mean \pm s.d. of four biologically independent samples, and were normalized to the Aht-induced TetR system. Asterisks denote p values from a two-sided Welch's t test (* $p \le 0.05$, ** $p \le 0.01$, *** $p \le 0.001$). **(b)** As in panel a, but the temperature was 29 °C.

RsLOV variants, in both darkness and blue light, and at both 29 and 37 °C (Figure 3(a), (b)). Although in many cases this led to an overall decrease in light responsiveness, for the TetR'(BD)195-RsLOV D109G and d2 variants we obtained 7.8-fold and 3.0-fold upregulation of expression at 29 °C, where none was observed in the original TetR(B) context. In parallel, we hypothesized that the light response of TetR(B)195-RsLOV could also be modulated by appending a hexahistidine (His₆) sequence to the C-terminal Kα helix of RsLOV as, jointly with the $J\alpha$ helix, this segment contributes to light-induced dissociation. In line with this reasoning, inclusion of the C-terminal Hise tag generally incurred weakened repression, albeit to lesser extent than for the TetR'(BD) substitution (Figure 3(a), (b)). For the TetR195-RsLOV D109G and d2 variants, the His6 modification led to a moderate increase of expression in the light, corresponding to induction factors of 5.0-fold and 7.1-fold, respectively.

We expanded our studies on temperature effects to the above TetR variants that employed associating homodimeric LOV modules rather than the dissociating RsLOV. Elevating the temperature to 37 $^{\circ}\text{C}$ incurred a loss of repression for TetR195-NcVVD and abolished any light regulation (Suppl. Figure S5(a)). By contrast, the variants TetR195-Ptaur (pLATR-Pt) and TetR195-Vfaur based on aureochrome LOV domains benefitted from the temperature increase, chiefly owing to elevated reporter expression in darkness. At 37 °C, pLATR-Pt prompted downregulation of expression under blue light by 46-fold, which contrasts with only 4.0-fold at 29 °C. For TetR195-Vfaur, at 37 °C the expression was downregulated under blue light by 5.2 fold, virtually unchanged from the value of 5.1-fold at 29 °C. We wondered whether the above strategy can be applied to TetR195-Ptaur and TetR195-Vfaur to modulate

their light response. As these two variants showed overall similar properties, we focused on TetR195-Ptaur and exchanged its TetR module for the TetR'(BD) variant. Doing so entailed a weakening of repression under blue light at both 29 and 37 °C (Suppl. Figure S5(b), (c)). To counteract this effect, we successively elongated the TetR fragment from 195 to 198 residues. At 198 residues length, repression was fully restored at both temperatures, and in darkness and blue light. At lengths of 196 and 197 residues, repression was enhanced as well but primarily under blue light and less so in darkness. As a consequence, TetR'(BD)196-Ptaur, referred to as pLATR-BD, TetR'(BD)197-Ptaur exhibited regulation of gene expression at both 29 and °C (Suppl. Figure S5(b), (c), Table 1). Collectively, these data indicate that deliberate structural destabilization can weaken repression and thereby optimize the response to light and temperature.

Analysis of RsLOV variants

To better understand the temperature tolerance of the D109G and d2 variants and the lack of light response in the d5 variant, we biochemically characterized the corresponding $\it RsLOV$ domains in isolation. All three domains incorporated the FMN chromophore, underwent canonical LOV photochemistry upon blue-light absorption, and had similar kinetics of dark recovery as the wild-type $\it RsLOV$ (Suppl. Figure S6). Size-exclusion chromatography (SEC), conducted at a protein concentration of 100 μM , revealed a retention volume of 1.744 mL for dark-adapted d2, close to the value of 1.739 mL for the wild-type protein (Suppl. Figure S7) and thus suggesting overall similar shape and homodimeric state. By contrast,

the dark-adapted states of the D109G and d5 variants eluted at slightly lower retention volumes of 1.722 mL and 1.715 mL which could be due to stronger homodimerization. Under blue light, the retention volume shifted to larger values for the D109G and d2 variants (1.796 mL and 1.790 mL), resembling the findings for the wild-type protein (1.811 mL) and indicative of light-induced homodimer dissociation. By contrast, the retention volumes for *Rs*LOV d5 in darkness and blue light were nearly the same (1.715 mL and 1.721 mL), implying that light-regulated dissociation was lost. This observation directly accounts for the inability of the d5 variant to confer light sensitivity on TetR evidenced in the above experiments.

The analysis of the RsLOV variants D109G, d2 and d5 by CD spectroscopy revealed that at 22 °C they adopt similar secondary structure in darkness as the wild-type protein (Suppl. Figure S8). Differences manifested among the variants in their responses to light and temperature increases. The D109G variant exhibited thermal unfolding transitions that closely resembled those of the wild-type protein and yielded a midpoint of (56.0 ± 0) .1)°C in both darkness and blue light (Suppl. Figure S8(d)). As for the wild-type protein, at temperatures below the unfolding transition a gradual loss of α -helical structure occurred in darkness but not under blue light. Evidently, the improved temperature response of RsLOV D109G in the TetR context is not tied to a significant difference in thermodynamic stability. Whereas the d2 variant exhibited light-induced loss of α-helical content to somewhat smaller extent than for wildtype RsLOV (Suppl. Figure S8(b)), the d5 variant lacked anv comparable response (Suppl. S8(c)) **Figure** which coincides with observations made by chromatography and in the TetR context. Unexpectedly, the thermal unfolding of d2 progressed through a stable equilibrium intermediate, thus giving rise to two transitions with temperature midpoints of (43.6 ± 0.6)°C and $(58.9 \pm 0.4)^{\circ}$ C in darkness, and $(43.2 \pm 0.4)^{\circ}$ C and (59.9 ± 0.2)°C following blue-light exposure (Suppl. Figure \$8(e)). For variant d5, both the dark-adapted and light-adapted states underwent an unfolding transition resembling that of darkadapted d2 (Suppl. Figure S8(f)). As the two transitions observed for d2 and d5 each incurred a 50% loss of α -helicity, we tentatively ascribe them to successive unfolding of the C-terminal $J\alpha$ and $K\alpha$ helices, and of the *Rs*LOV domain core, respectively. In marked contrast to both RsLOV wild-type and D109G, at temperatures below the first transition hardly any α -helical signal was lost for the dark-adapted d2 and d5 variants, as reflected in a native baseline slope of (19.7 ± 14.4)° cm² dmol⁻¹ K⁻¹. Rather, the temperature-driven unfolding of α-helical elements, gradual and uncooperative in wild-type RsLOV, gained cooperativity and thus occurred at somewhat higher temperatures. These differences in thermal stability and light response are consistent with the enhanced temperature tolerance exhibited by d2 in the pLITR-d2 context and may directly account for it.

For molecular insight into the D109G and d2 variants, we determined the three-dimensional structure of their dark-adapted states by X-ray crystallography at 2.0 Å and 1.9 Å resolution. Monoclinic RsLOV D109G crystals were obtained by vapor diffusion at solvent conditions adapted from those reported for the wild-type protein.² Overall, this variant adopted a similar structure as the wild-type protein (PDB entry 4hj424) with a root mean square deviation (rmsd) of 0.5 Å for the backbone of residues 4-175 (Figure 4(a)). As revealed by the structure, introduction of the D109G substitution locally altered the conformation of the loop between the strands H β and I β (Figure 4(b), (c)). Owing to the absence of a side chain, glycine allowed the adoption of a type-II turn rather than the type-I turn in wild-type RsLOV.51 Beyond the immediate vicinity of the mutation site, the structure of the D109G variant closely resembled that of the wild-type protein. In case of the d2 variant, starting from primary screens, solution conditions were determined that yielded orthorhombic crystals. Again, the structure of this variant closely resembled the one of wild-type RsLOV with a rmsd of 0.5 Å for the backbone of residues 4–175 (Figure 4 (d)). Inspection of the substituted residue positions revealed that the exchanges Q49E and A90K jointly furnished a new salt bridge between the $G\beta$ -H β loop and helix $D\alpha$ (Figure 4(e), (f)). Notably, a glutamate: lysine salt bridge at this position is conserved across many LOV receptors and has long been ascribed relevance in signal transduction.5 larly, the S157Q exchange within the $K\alpha$ helix introduced a hydrogen bond to residue E80 situated before the G β strand (Figure 4(g), (h)). Contrariwise, replacement of D92 in the Gβ-Hβ loop by glycine removed a salt bridge to K60 in the $E\alpha$ - $F\alpha$ loop. Lastly, the substitutions G48D and L77E introduced negative charges on the protein surface.

To further compare D109G to wild-type RsLOV. we recorded ¹H-¹⁵N heteronuclear single-quantum coherence (HSQC) spectra for 250 μM uniformly ¹⁵N-labeled protein. At 29 °C in darkness, both wild-type and D109G RsLOV showed well resolved and dispersed resonance peaks that indicate folded structure (Suppl. Figure S9(a)). Consistent with the crystallographic analysis, the HSQC spectra of the wild type and D109G were closely similar, except for a few resonance peaks which we ascribe to the mutated residue and its immediate surroundings. ¹H-¹⁵N HSQC spectra acquired at 37 °C for dark-adapted RsLOV wildtype and D109G closely matched those at 29 °C (Figure 5(a)), which implies that at the used concentration of 250 µM both proteins adopted similar structures at both temperatures. To assess

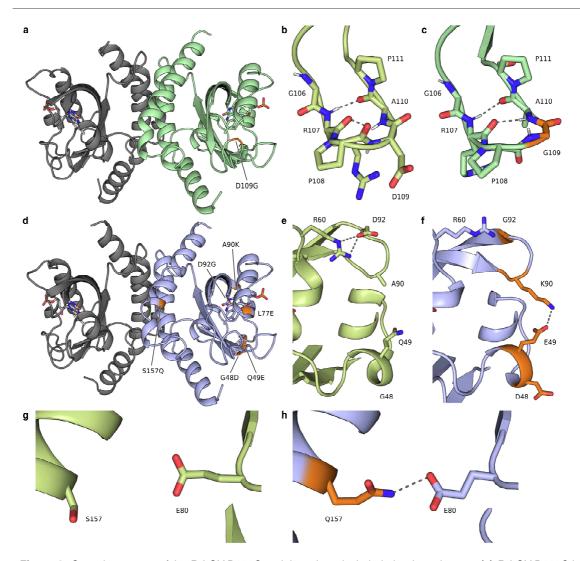


Figure 4. Crystal structures of the RsLOV D109G and d2 variants in their dark-adapted states. (a) RsLOV D109G in the same orientation as wild-type RsLOV in Figure 1(A). The mutated residue position 109 is highlighted in orange. (b) Hβ-Iβ loop in wild-type RsLOV (PDB entry 4hia). (c) Hβ-Iβ loop in RsLOV D109G. (d) RsLOV d2 with the substituted positions shown in orange and labeled. (E) Gβ-Hβ loop and vicinity in wild-type RsLOV. (f) Gβ-Hβ loop and vicinity in RsLOV d2. (g) Interface between Rs and Rs in wild-type RsLOV. (h) Interface between Rs and Rs in RsLOV d2. The dashed lines in panels b-h denote hydrogen bonds and salt bridges.

the oligomeric state, we determined amide proton transversal relaxation times T_2 , from which we estimated rotational correlation times τ_c of 17 ns at 29 °C for both proteins, consistent with a homodimeric state. Likewise, at 37 °C τ_c amounted to 16 ns for both proteins, which again suggests a homodimeric state. We also conducted $^1\text{H-}^{15}\text{N}$ HSQC measurements at 37 °C while applying saturating blue light (455 nm). Both wild type and D109G showed drastically different spectra with much reduced peak dispersion and the majority of peaks shifting position or vanishing altogether (Figure 5(b), Suppl. Figure S10). At the

same time, several broad resonance peaks appeared at 1 H chemical shifts between around 7.5 and 8.5 ppm which can be attributed to partial unfolding of protein segments. A more detailed analysis was precluded by slow protein precipitation after illumination. Taken together, these findings point toward similar light-induced conformational changes in RsLOV wild-type and D109G. These changes were profound and affected the entire RsLOV protein, consistent with the extensive α -helical unfolding evidenced by CD spectroscopy (see above). The pervasive light-induced changes seen for RsLOV wild-type and

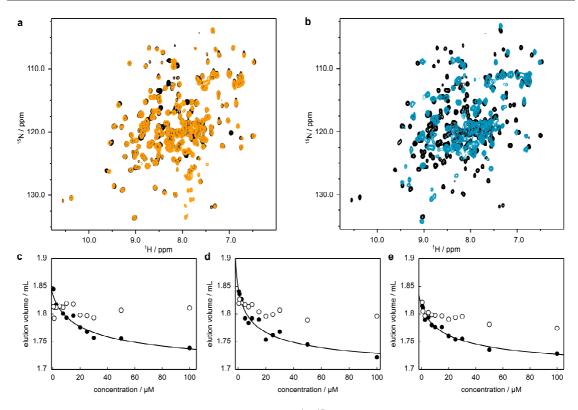


Figure 5. Biochemical analyses of *Rs*LOV variants. **(a)** ¹H-¹⁵N HSQC spectra of wild-type *Rs*LOV (black) and D109G (orange) in darkness at 37 °C. **(b)** ¹H-¹⁵N HSQC spectra of wild-type *Rs*LOV at 37 °C in its dark-adapted (black) and light-adapted (cyan) states. **(c-e)** Retention volumes from size-exclusion chromatography for *Rs*LOV wild-type (panel c), D109G (d), and d2 (e) in their dark-adapted (filled circles) and light-adapted states (open circles). The lines denote fits of the data for the dark-adapted states to homodimerization isotherms.

D109G are reminiscent of measurements on AsLOV2 that also displayed diminished spectral dispersion and extensive peak shifts under light.⁴⁶

Given the overall similar structure of wild-type and D109G RsLOV, we suspected that the improved temperature tolerance may well be rooted in differences in homodimer affinity. Notwithstanding repeated use of RsLOV in optogenetics, at a quantitative level its homodimerization has to date only been studied cursorily. A recent report⁵ employed chemical labeling to study RsLOV dimerization by fluorescence and determined a dissociation constant (K_d) for the dark-adapted state on the order of 3-7 µM at ambient temperature. To verify this measurement and to compare the K_d values of wild type, D109G and d2, we analyzed the different RsLOV variants at concentrations between 0.5 and 100 µM in their dark-adapted and lightadapted states by SEC at 4 °C. The retention times of the light-adapted state showed little variation with protein concentration (Figure 5(c)-(e)). By contrast, the retention times of the dark-adapted state hyperbolically decreased with protein concentration, indicative of monomer-dimer association over the tested concentration range. We evaluated the dependence of the retention times on protein concentration according to a reversible homodimerization reaction and obtained an apparent K_d for the dark-adapted state of RsLOV of (41 ± 12) μM, somewhat higher than the previous K_d estimation. 53 By comparison, the apparent K_d values for homodimerization of the d2 and D109G variants amounted to (36 \pm 13) μ M and (21 \pm 6) μ M. The tighter homodimerization of the D109G variant is the likely origin of its enhanced performance in the pLITR context. As revealed by the crystal structure, the site of the mutation is distal from the dimer interface, and the precise molecular details giving rise to enhanced dimerization are unclear. By contrast, d2 differs from wild-type RsLOV less in homodimer affinity, and its enhanced performance can be tied to its altered response to temperature changes, see above.

Improving light sensitivity in a receptor tyrosine kinase

Lastly, we reasoned that the improved D109G variant might benefit other approaches based on *Rs*LOV. As noted above, a previous study generated light-activated receptor tyrosine kinases (RTKs), among them the fibroblast growth factor

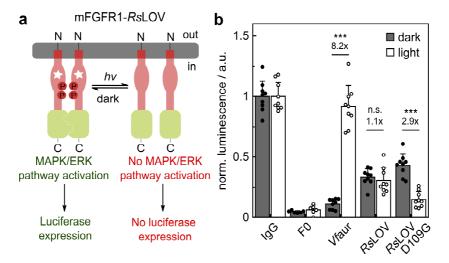
receptor 1 from mouse (mFGFR1), via C-terminal fusion to aureochrome LOV domains such as the one from V. frigida (Vfaur).33 Under blue light, these domains associate and thereby activate the RTKs and the downstream signaling pathways (Figure 6 (a)). Attempts to achieve the opposite response to blue light, i.e. pathway inactivation, by C-terminally coupling RsLOV to mFGFR1 were only partially successful as they gave rise to constitutive pathway activation with minimal downregulation under blue light. We tested the D109G variant in the context of the chimeric mFGFR1-RsLOV receptor and assessed the activation of the downstream MAPK/ ERK pathway as a function of light. At 37 °C, neither the wild-type RsLOV nor the mutant variant conferred substantial light sensitivity on mFGFR1, resulting in constitutive pathway activation with a minute light-dependent drop of ~ 20%, consistent with earlier studies³³ (Suppl. Figure S10). However, upon lowering the temperature to 29 °C, *Rs*LOV D109G prompted a clear-cut downregulation of the pathway under blue light (~70%) whereas wildtype RsLOV did not (Figure 6(b)). Thus, the D109G variant rescued the light response of mFGFR1-RsLOV and yielded a previously unavailable blue-light-inhibited RTK that now complements a green-light-inhibited RTK.54 Evidently, the beneficial effect of the D109G substitution can manifest in conjunction with very different effector modules,

and in both prokaryotes and eukaryotes. These findings lend strength to the assertion that the enhancement is indeed rooted within the *Rs*LOV module itself.

Discussion

Light-regulated Tet repressor variants in optogenetics and synthetic biology

Light-mediated dimerization has proven particularly adept at imparting photosensitivity on choice biological processes.8 This effectiveness owes as much to the frequent intrinsic reliance of such processes on oligomerization as to the availability in nature of self-contained protein modules that undergo light-induced changes in quaternary structure. As a case in point, numerous target proteins were separated into two, either by disruption of the subunit interface in case of dimeric targets, or by severing the polypeptide chain in case of monomeric targets. Whereas the isolated protein parts are (largely) devoid of activity, dimerization can reconstitute the original structure and regain activity. Associating photoreceptors that form homo- or heterooligomers under light have been widely used to bestow light sensitivity on reconstitution and to thus subject diverse cellular activities to optogenetic control. By comparison, dissociating



photoreceptors that gain monomeric state upon light exposure have been harnessed less, not least because they are comparatively rare in nature,54 although they can be constructed artificially. 16.17 We here employed the homodimeric dissociating RsLOV receptor to equip the widely used Tn10encoded class-B Tet repressor with photosensitivity, with the dual aim of furnishing new optogenetic implements and of further exploring the suitability of this LOV module for the design of light-gated proteins. Serial C-terminal truncation successively rendered TetR incapable of repression at its cognate tetO site. Fusion with RsLOV rescued repression by TetR in a light-inhibited manner, thus permitting to activate expression under blue light. Replacement of RsLOV with associating LOV modules inverted the light response and yielded TetR variants with weaker repression and stronger expression in darkness compared to light. Variation of both the LOV photosensor and the TetR effector gave rise to an optimized set of TetR variants for use at either 29 or 37 °C, to either raise or lower expression of target genes by around up to 40-fold under blue light (see Table 1). Of advantage, the resultant pLITR and pLATR systems have in common that they require a single polypeptide component only which contrasts for example with the light-sensitive two-component systems widely deployed in bacteria.

As remarked above, a design rationale similar to ours was recently employed by Yang and colleagues. 35 Through fusion of a monomerized LexA fragment to RsLOV, a chimeric transcription factor was obtained that supported light-induced expression at 37 °C with up to an impressive 500fold dynamic range. Although the LexA-RsLOV system, dubbed eLightOn, thus appears superior to our efforts in terms of sheer regulatory efficiency, we consider the newly generated light-regulated TetR variants a useful and versatile addition to the repertoire of synthetic transcriptional regulation systems. As previously noted,7 the dynamic range of the response to a signal is strongly governed by how well basal activity can be shut off in the lowactivity state of a given receptor. Hence, the maximally regulatory effect achievable in the TetR derivatives should be gauged against the efficiency of repression in the wild-type TetR, which amounted to 70-fold for Aht addition. Against this backdrop, several of the present TetR variants exhibited responses to light that were of similar magnitude, albeit somewhat smaller, as that of wild-type TetR following Aht induction. While a previous study generated a light-regulated 'upgrade' for TetRmediated gene expression, it operated at the level of transcription initiation rather than DNA binding and repression per se. 58 As the presently generated light-regulated TetR variants directly affect repression, and by inference, DNA binding, they offer a wider application scope in both prokaryotes and eukaryotes. Beyond serving as one of the most common agents for inducible gene expression.³⁹ the TetR has been amply used in synthetic biology for the construction of genetic circuits. As just one the TetR particularly prominent example, 59,60 underpins the so-called repressilator, a network of mutually interacting bacterial and viral repressors that generate oscillations in time and space. The availability of compact light-regulated TetR variants now augurs the construction of photo-entrainable oscillatory networks. Moreover, RNA aptamers have been selected that bind to TetR with high sequence specificity and affinity in lieu of DNA. Biochemical and recent crystallographic analyses reveal that the aptamer occupies the same binding region as the tetO DNA would, despite adopting utterly different structure. 49,61 Given that RNA binding is abolished by Aht addition, we expect that the TetR variants generated here will establish a means of controlling TetR:RNA interactions by light. This in turn paves the way towards novel optoribogenetic applications, as recently pioneered on the back of the natural LOV receptor PAL which binds a specific RNA hairpin under blue light.6

Signal integration by the RsLOV module

Our work also provides mechanistic insight into RsLOV and its response to signals, with implications for the design and application of lightregulated proteins. Purely based on first principles, it is evident that any process entailing changes in oligomeric state must have a pronounced dependence on the concentration of the components involved. A system is maximally responsive to perturbation, e.g., light stimuli, for component concentrations near the relevant midpoint of oligomerization. By contrast, if these concentrations are much lower or higher, responses are strongly attenuated or altogether abrogated, because the system constantly dwells in its monomeric or oligomeric states, respectively. For the design and implementation of approaches relying on signal-responsive (dis)assembly reactions, knowledge of the underlying signaldependent association process is hence important. A previous investigation⁵³ put the dimerization equilibrium constant of dark-adapted RsLOV on the low micromolar range but depended on invasive chemical labeling of the protein. Using size-exclusion chromatography, we now examined the unmodified protein and determined a somewhat higher dissociation constant of about 40 µM in darkness. Although quantitative data on the light-dependent oligomerization of photoreceptors are generally scarce, compared to a few well-studied systems, 64-66 the homodimer affinity of RsLOV appears unexpectedly weak, which has several implications. First, as detailed above, applications based on RsLOV must hence operate at relatively high effective in situ concentrations and/or enhance the dimer affinity, e.g., by appendage of other interaction domains or, possibly, by domain duplication.⁶⁷ Should the concentration drop, be it by accident, be it by design, light responsiveness will be degraded. Second, the weak dimer affinity of RsLOV might explain why at least in some cases efforts to engineer light-responsive systems on its basis failed. 33,34 Third, as pointed out by Magerl & Dick,53 the weak affinity equally calls into question whether the physiological responses inside the host organism R. sphaeroides truly rely on light-dependent RsLOV dissociation at all. Fourth, given the inherently modest affinity, there is scope for improvement by protein design, as successfully implemented for other LOV receptors. 20,64,68 However, care must be exerted, lest light responsiveness be impaired en route to stronger dimerization, as arguably the case for the d5 variant.

Several of the TetR-RsLOV variants generated presently exhibited a strong temperature response over a narrow interval between 29 °C and 37 °C. Biochemical analyses revealed the temperature sensitivity to be rooted to considerable extent in the photosensor itself and to thus represent an inherent property of RsLOV. It is worth noting that R. sphaeroides is a mesophilic bacterium with a growth optimum near 25 °C, thus putting 37 °C outside the temperature interval this organism likely ever encounters. However, the remarkable success of the eLightOn design clearly reveals that RsLOV can principally be quite effective at 37 °C.35 While even the initial eLightOn design exhibited robust light responses, their extent was significantly boosted by variation of the linker connecting the LexA and RsLOV moieties that underpin the approach. To improve performance and to specifically overcome the temperature lability of the TetR variants, we instead focused on modifying the RsLOV module itself via two principal avenues. On the one hand, we harnessed computational design to predict receptor variants with elevated thermal and cellular stabilities.⁴⁷ We thus developed the variant d2 with altered thermal unfolding which likely underpins its improved light responsiveness at higher temperatures. On the other hand, we identified the D109G substitution that likewise enhanced the light response of TetR variants at higher temperatures. Despite sharing closely similar structure and thermal stability with the wildtype RsLOV, the D109G variant exhibited enhanced dimer affinity which presumably accounts for its improved performance. We fully note that the light and temperature responses of RsLOV are evidently context-dependent and not solely determined by the properties of the light-sensitive photosensor but also by those of the effector, as evidenced by the variation of the TetR moiety, and in fact the linker, as probed currently and by Yang and coworkers.³⁵ That notwithstanding, the elevated stability incurred by the D109G modification transcends the TetR setting and extends to lightregulated RTKs in mammalian cells. Although the

D109G variant could not evoke a light response at 37 °C, it did so at 29 °C, while the wild-type *Rs*LOV failed at either temperature. We thereby also furnished a blue-light-inhibited RTK, an optogenetic tool previously unavailable.

Understanding the interplay of light, temperature, receptor concentration, ligands, and possibly other signals benefits the development and deployment of regulatable proteins. Our investigation reveals that temperature sensitivity is an inherent trait of RsLOV that may be challenging to remove. That notwithstanding, properly accounting for this aspect, systems can be configured, and experimental regimes be identified, in which the response is primarily governed by the desired stimulus (e.g., light), with minimal crosstalk from other signals (e.g., temperature). Moreover, the thermosensitivity can be valuable in its own right as it could be exploited for thermogenetics to trigger by temperature physiological responses. The sensitivity to multiple signals physiological needs not necessarily be a bane but can be deliberately leveraged for constructing logic gates and elaborate genetic circuits. For instance, certain of the presently generated TetR variants not only followed light cues but responded to temperature changes and the addition of the ligand Aht. Although not exploited here, these properties lend themselves to building systems that integrate two or more of these inputs with AND or OR Boolean logic. In a similar vein, the sensitivity to several signals can be used for sequential activation (e.g., by light) and rapid inactivation (e.g., by ligand addition). By contrast, systems responding to a sole signal can be limited by slow inactivation kinetics, for example in the case of photoreceptors due to slowly paced dark recovery once illumination ceases. In closing, we note that the integration of light and temperature cues might be more widely shared among sensory photoreceptors.71 This is not least evidenced by plant phytochromes, long known as sensors of red and far-red light, which can double as temperature sensors.

Materials and methods

Molecular biology

The gene encoding R. sphaeroides LOV (Uniprot M1E1F8_RHOS5, residues 1-176) was provided in the pET-28(a) vector by K. Conrad and B. Crane (Cornell University).²⁴ As reported previously²⁴, the gene sequence differs from the Uniprot entry by featuring a leucine residue at position 32 rather than a valine. A fusion between the Tn10-encoded TetR and RsLOV, separated by a GTGTAGGTGS linker, was constructed by Gibson cloning⁷³ in the pASK-IBA43plus vector (IBA Lifesciences). Unless stated otherwise, all subsequent cloning steps were performed by Gibson cloning. To allow assessment light-dependent TetR variants, the

DsRed-Express 2⁷⁴ reporter gene was inserted into the multiple-cloning site of the vector under TetR transcriptional control. Within this context, the TetR was successively shortened C-terminally via plasmid amplification and religation. TetR-RsLOV variants with linkers of 5, 15 and 20 amino acids, respectively, were prepared likewise (linkers GTGTAGGTGSGSGTA GTGTA, GTGTAGGTGSGSGTAGTGTA). The ColE1 origin of replication of the vector was exchanged for CoIDF13, pBR322 and p15a origins, amplified from pCDF-Duet (Novagen), pET-28(c) (Novagen) and pACYC plasmids (New England Biolabs), respectively. To furnish light-activated TetR variants, the RsLOV module was exchanged for LOV domains from N. crassa Vivid (Uniprot Q9C3Y6_NEUCS, residues 37-186, including the mutations C71V and N56K), P. tricornutum aureochrome 1a (Uniprot A0A140UHJ0_PHATR, residues 1-142) and V. frigida aureochrome1 (Uniprot A8QW55_VAUFR, residues 201-348). To modulate the repression strength of light-regulated TetR variants, the TetR moiety was C-terminally truncated. Further variants were generated by entirely replacing the TetR by TetR'(BD) which denotes a fusion of residues 1-188 of TetR(B) and residues 189-208 of TetR (D). 38,49 All constructs were verified by Sanger sequencing (Microsynth, Göttingen, Germany).

Bacterial TetR reporter-gene assay

Reporter-gene assays were performed in E. coli DH10b cells. To this end, bacteria harboring plasmids encoding a given TetR variant were cultivated in lysogeny broth (LB) medium containing 50 μg mL $^{-1}$ ampicillin (LB/Amp) in either darkness or under constant blue light (470 nm, 100 μW cm²). Light intensities were measured with a silicon photodetector (model 918D-UV-OD3, Newport). Cultures were grown in 400 μL LB/Amp in 96-deep well plates, sealed with a gas-permeable film. Plates were incubated at 29 or 37 °C under constant shaking at 700 rpm. Control cultures incubated in darkness were induced with 0.25 $\mu g\ mL^{-1}$ anhydrotetracycline. The optical density at 600 nm (OD600) and the DsRed fluorescence in the cultures measured post incubation with a Tecan Infinite M200 pro multimode plate reader fluorescence excitation and emission wavelengths of (554 \pm 9) nm (591 \pm 20) nm. Fluorescence data were normalized to OD_{600} and represent mean ± s.d. of four biologically independent replicates. Background fluorescence of bacteria harboring a plasmid without DsRed was subtracted. Each experiment was performed in triplicate with similar results.

Screening for stabilized TetR-RsLOV variants

To introduce random mutations, the *Rs*LOV domain was subjected to error-prone PCR. To this

end, the RsLOV gene was PCR-amplified using Tag polymerase (ThermoFisher Scientific), with the replication fidelity impaired by addition of 5 mM MgCl₂, 50 μ M MnCl₂, 1 M betaine, 0.8 mM dCTP and dTTP. The resultant gene library was inserted into the TetR195-20-RsLOV background via Gibson cloning and transformed into DH5 α cells. Bacterial cultures were grown in LB/Amp for 16 h at 37 °C in darkness or under constant blue light (470 nm, 100 μW cm⁻²). Following incubation, the cultures were diluted 1000-fold into phosphatebuffered saline (PBS) and sorted using an S3e Cell sorter (Bio-Rad, Germany). Events were gated based on forward and side scattering, and DsRed fluorescence was detected at (615 ± 15) nm. For cultures grown in darkness, cells were isolated that exhibited relative fluorescence units (RFU) less than 6.3×10^2 , and for cultures grown under blue light, cells with RFU values exceeding 1.4×10^5 were isolated. The sorted cells were further cultured under alternating dark and light conditions for a total of five cycles. Cells were then streaked on LB/Amp, and individual clones were selected and tested in the above reporter-gene setup. DNA sequencing of a clone displaying robust light-regulated activity at 37 °C identified the D109G substitution. To ascertain that this substitution is causative for the enhanced behavior, it was introduced by sitedirected mutagenesis into the original TetR195-20-RsLOV plasmid.

Stabilized RsLOV versions were calculated using the PROSS server. The algorithm suggested seven RsLOV variants with up to 18 mutations. Two variants, denoted d2 and d5, were selected and synthesized with E. coli-adapted codon usage (Gene Art, Germany). For reference, the wild-type RsLOV was also synthesized with the same codon usage. Resulting genes were cloned into the TetR195-20-RsLOV plasmid and tested for light-dependent activity as described above.

Expression analysis of TetR-RsLOV variants

For analyzing bacterial expression of light-regulated TetR variants, we subcloned the TetR195-20-RsLOV construct and the D109G, d2 and d5 variants into a pET-41(a) vector with a C-terminal hexahistidine tag. CmpX13 cells⁷⁶ harboring these plasmids were grown at either 29 °C or 37 °C in LB medium supplemented with 50 μ g mL⁻¹ kanamycin. At an OD_{600} of 0.6, expression was induced by adding 1 mM isopropyl β -thiogalactopyranosid (IPTG). Samples were drawn at different time points, separated by denaturing polyacrylamide gel electrophoresis, and analyzed by Coomassie staining.

Expression and purification of RsLOV variants

The RsLOV gene and its D109G, d2 and d5 variants were cloned into the expression plasmid pET-19b (Novagen) and thereby equipped with an

N-terminal His₆-SUMO tag. Plasmids were transformed into E. coli CmpX13 cells, 76 and bacteria were incubated at 37 °C in LB/Amp medium supplemented with 50 μ M riboflavin. When an OD_{600} of 0.6-0.8 was reached, the temperature was lowered to 16 °C, 1 mM IPTG was added, and incubation continued for 18 h. Cells were harvested by centrifugation (6,000 rpm) and resuspended in lysis buffer (50 mM Tris/HCl pH 8.5, 300 mM NaCl, 10 mM imidazole). Cells were lysed by ultrasound, and debris was removed by centrifugation (18,000 rpm). The soluble supernatant was purified by nickel immobilized metal-ion affinity chromatography (IMAC). To cleave off the His6-SUMO tag, the protein was incubated with Senp2 protease over night at 4 °C and again purified by IMAC. Fractions containing pure protein were pooled, dialyzed into storage buffer [50 mM Tris/HCl pH 8.5, 300 mM NaCl, 10% (w/v) glycerol] and concentrated via spin filtration. Protein concentration was determined by absorbance measurements using an extinction coefficient at 450 nm of 12,500 M⁻¹ cm⁻¹. ¹⁵N-labelled samples for analysis by NMR spectroscopy were produced likewise, except that growth was conducted in M9 minimal medium (42 mM Na₂HPO₄, 22 mM KH₂PO₄, 9 mM NaCl, 0.4 % glucose, 1 mM MgSO₄, 0.3 mM CaCl₂, 1 μg biotin, 1 μg thiamin, 134 μM EDTA, 31 μM FeCl₃, 6.2 μM ZnCl₂, 760 nM CuCl₂, 420 nM CoCl₂, 1.6 μ M H₃BO₃, 81 nM MnCl₂) supplemented with 0.5 g L⁻¹ ¹⁵NH₄Cl.

Absorbance spectroscopy

Ultraviolet-visible absorbance spectra of *Rs*LOV variants were measured on an Agilent 8453 UV-vis spectrophotometer at 22 °C. To populate the light-adapted state, samples were illuminated with blue light (470 nm, 30 mW cm ²). To analyze the dark recovery, spectra were recorded at 60-s intervals after blue-light exposure. Recovery rate constants were determined by nonlinear least-squares fitting to single-exponential functions using Fit-o-mat.⁷⁷

Circular dichroism spectroscopy

Purified *Rs*LOV protein and the D109G, d2 and d5 variants were dialyzed into 20 mM Tris/HCl pH 8.0, 20 mM NaCl. Circular dichroism (CD) spectroscopy was performed on a Jasco J-715 spectropolarimeter equipped with a PTC-348Wl Peltier element. Buffer-corrected CD spectra were recorded at a protein concentration of 10 μ M in cuvettes with 1 mm path length at a temperature of 22 °C for dark-adapted samples and samples exposed to saturating illumination with blue light (450 nm, 30 mW cm⁻²). To assess the thermal stability of the variants, the CD signal was continuously monitored in cuvettes of 1 cm path length at (222 \pm 5) nm while increasing the temperature from 15 or 20 °C to 95 °C at a rate of 1 °C min⁻¹. Measurements were conducted for

both dark-adapted and light-adapted samples. The temperature-induced unfolding transition was evaluated according to two-state or three-state models by nonlinear least-squares fitting with the Fit-o-mat software 77 to determine the unfolding midpoint $\mathcal{T}_{\rm m}$.

$$\Delta G = \Delta H - T/T_m \times \Delta H \tag{1}$$

Size-exclusion chromatography

Analytical size exclusion chromatography (SEC) was performed on an ÄKTA pure system using a Superdex 200 Increase 3.2/300 analytical column at 4 °C. The column was equilibrated with buffer (50 mM Tris/HCl pH 8.5, 150 mM NaCl). RsLOV and its D109G and d2 variants were injected in 25-μL aliquots at concentrations from 0.5 to 100 μM and analyzed at 0.05 mL min⁻¹ flow rate. The elution of the samples from the column was tracked by absorbance at 280 nm. Dark-adapted samples were handled under dim red light, and the chromatography was performed under light exclusion. Light-adapted samples were generated by saturating irradiation with blue light (450 nm, 30 mW cm⁻²) immediately prior to injection; during the run, the samples and the column were constantly exposed to blue light. As determined by the absorbance signal of the elution peaks of dark-adapted samples, the chromatography run entailed a 1.3-fold dilution of the proteins on the column. Apparent dissociation constants (K_d) for the dark-adapted samples were determined by evaluating the retention time $t_{\rm ret}$ as a function of protein concentration P_0 according to Eqs. (2) and

$$t_{\text{ret}} = t_{\text{mono}} \times t_{\text{ret,mono}} + (1 - t_{\text{mono}}) \times t_{\text{ret,di}}$$
 (2)

$$f_{\text{mono}} = -K_d/4 + \sqrt{K_d^2/16 + P_0 \times K_d/2}$$
 (3)

Nonlinear least-squares fitting was done with Fito-mat. 77

Structure determination of RsLOV D109G and d2

For crystallization, the *Rs*LOV D109G protein was dialyzed into 50 mM Tris/HCl pH 8.5, 300 mM NaCl, as reported for wild-type *Rs*LOV.²⁴ Crystallization of *Rs*LOV D109G was conducted by sitting-drop, vapor diffusion in darkness at 20 °C and a concentration of 12.0 mg mL⁻¹, starting from the reported conditions that had yielded crystals of wild-type *Rs*LOV²⁴ (100 mM HEPES/HCl pH 7.5, 4.3 M NaCl). Monoclinic crystals appeared within a few days and were optimized by variation of the solution conditions (100 mM HEPES/HCl pH 7.4, 3.44 M NaCl, 20 mM spermidine phosphate) and protein concentration (6.6 mg mL⁻¹). Single crystals were mounted in loops and rapidly cryocooled in liquid nitrogen. Diffraction data were recorded at the BESSY synchrotron (beamline 14.1) to a

resolution of 2.0 Å, and the resultant data were indexed with XDS⁷⁸ in space group P2₁, followed by integration and scaling with pointless⁷⁹ via the XDSapp interface.⁸⁰ The structure was solved by molecular replacement with *Rs*LOV L32V (PDB entry 4hia²⁴ as search model and yielded six *Rs*LOV D109G monomers in the asymmetric unit. Model building and refinement were performed with Coot.⁸¹ Refmac.⁸² and Phenix.⁸³ respectively.

The RsLOV d2 variant was dialyzed into 50 mM Tris/HCl pH 8.5, 300 mM NaCl. As in preliminary experiments RsLOV d2 could not be crystallized at the conditions established for wild-type RsLOV, we resorted to sparse-matrix screens (JCSG core I-IV, NeXtal Biotech) to identify a crystallization lead in 100 mM imidazole/HCl pH 8.0, 20% (w/v) PEG 1000, 200 mM calcium acetate. Conditions were optimized by elevating the PEG 1000 concentration to 22%, and orthorhombic crystals were obtained at 20 °C by sitting-drop vapor diffusion for a d2 concentration of 10.5 mg mL⁻¹. Data were collected using a MAR_µX Incoatc sealed-tube source and a MARdtb/MAR345 image plate system to a resolution of 1.9 Å and were indexed in space group P2₁2₁2₁. Structure solution and refinement were done as for D109G.

Data collection and refinement parameters for both structures are summarized in Supplementary Table S1. Atomic coordinates and structure-factor amplitudes for the structures of *Rs*LOV D109G and d2 have been deposited in the Protein Data Bank under accession numbers **70BZ** and **70B0**, respectively. The root mean square displacement of the backbone atom positions in *Rs*LOV D109G and d2, respectively, relative to those in the wild-type protein (4hj4²⁴) was calculated with LSQKAB.⁸⁴

Nuclear magnetic resonance spectroscopy

NMR experiments were performed on a Bruker Avance IIIHD 700 MHz spectrometer equipped with a cryogenically cooled probe. Spectra were processed using in-house software and visualized and analyzed by NMRViewJ (One Moon Scientific, Inc., Westfield, NJ, USA). Measurements were conducted at either 29 °C or 37 °C using 200 µL of 250 μM dark-adapted protein in 50 mM Na₂HPO₄/NaH₂PO₄ pH 8.0, 100 mM NaCl, 10% D₂O in 3-mm NMR tubes. Measurements on the light-adapted protein were conducted likewise, but the sample was continuously illuminated via a fiber-coupled LED with 455 nm peak emission (Prizmatix) inserted in the NMR tube. Transverse relaxation rates of amide protons were determined **HSQC**-based а two-point spin-echo measurement.⁶

Receptor tyrosine kinase assays

The previously described chimeric tyrosine kinase mFGFR1_RsLOV, 33 consisting of a myris-

toylation anchor, the murine FGFR1 kinase domain, and the RsLOV domain encoded in pcDNA3.1(-), was modified by mutagenesis PCR to introduce the D109G substitution, thus yielding the construct mFGFR1_RsLOV_D109G. HEK293T cells were maintained in complete medium (DMEM supplemented with 10% fetal bovine serum [FBS], 100 U penicillin and 0.1 mg mL⁻¹ streptomycin) at 37 °C in a humidified incubator with 5% CO2. All transfections were carried out in transfection medium (DMEM supplemented with 5% FBS) using polyethyleneimine (PEI).54 Experiments were conducted in 96-well clear-bottom plates coated with poly-L-ornithine. Activation of the MAPK/ERK pathway was assessed with the PathDetect Elk1 trans-Reporting System (Agilent, Vienna, Austria) containing firefly luciferase. A constitutively dimerized and active kinase domain (termed mFGFR1_lgG) was employed as a positive control, and a monomeric, membrane-anchored kinase domain alone (termed F0) was employed as negative control.⁵⁴ Additionally, a blue-light-activated RTK based on (termed V. frigida aureochrome 1 of mFGFR1_Vfaur) was employed as a control for blue-light induction. 33 In brief, 5×10^4 HEK293T cells per well were transfected with 211 ng DNA (200 ng trans-activator, 10 ng trans-reporter, 1 ng receptor) and 1000 ng PEI per well. After 6 h, the transfection medium was changed to starve medium (CO₂-independent medium with 0.5 % FBS). Plates were placed in custom incubators set to 37 °C or 29 °C and illuminated with blue light at 200 μW cm⁻² intensity for 16 h, with an additional dark control plate for each temperature condition (wrapped in aluminum foil). After 16 h, luciferase expression was assessed with a homemade luciferase assay reagent^{54,86} and measured in a microplate reader (CLARIOstar Plus, BMG Labtech).

Data availability and accession numbers

Primary data underlying the manuscript are available from the authors upon reasonable request. Atomic coordinates and structure factors for the reported crystal structures have been deposited with the Protein Data bank under accession number 7OBZ and 7OB0.

CRediT authorship contribution statement

Julia Dietler: Conceptualization, Investigation, Visualization, Writing - original draft, Writing - review & editing. Roman Schubert: Investigation. Tobias G.A. Krafft: Investigation. Simone Meiler: Investigation. Stephanie Kainrath: Investigation, Visualization, Writing - original draft. Florian Richter: Conceptualization. Kristian Schweimer: Methodology, Resources. Michael

Weyand: Methodology, Resources. Harald Janovjak: Writing - review & editing, Supervision. Andreas Möglich: Conceptualization, Investigation, Visualization, Writing - original draft, Writing - review & editing, Supervision.

Acknowledgements

We thank K. Conrad and B. Crane for supplying the *Rs*LOV gene. We are grateful to B. Süß for discussion and supplying the TetR'(BD) construct. We are grateful to F. Lennartz (BESSY) for collecting diffraction data on *Rs*LOV D109G. This work was supported by the Alexander-von-Humboldt Foundation through a Sofja-Kovalevskaya Award (to A.M.) and by the Deutsche Forschungsgemeinschaft (grant MO2192/8-1 to A.M.).

Declaration of Competing Interest

The authors declare that they have no known competing financial interests or personal relationships that could have appeared to influence the work reported in this paper.

Appendix A. Supplementary material

Supplementary data to this article can be found online at https://doi.org/10.1016/j.jmb.2021. 167107.

Received 29 April 2021; Accepted 9 June 2021; Available online 17 June 2021

Keywords:

crystal structure; optogenetics; sensory photoreceptor; signal transduction; Tet repressor

References

- Hegemann, P., (2008). Algal sensory photoreceptors. *Annu. Rev. Plant Biol.*, **59**, 167–189. https://doi.org/ 10.1146/annurev.arplant.59.032607.092847.
- Möglich, A., Yang, X., Ayers, R.A., Moffat, K., (2010). Structure and function of plant photoreceptors. *Annu. Rev. Plant Biol.*, 61, 21–47. https://doi.org/10.1146/annurev-arplant-042809-112259.
- Ernst, O.P., Lodowski, D.T., Elstner, M., Hegemann, P., Brown, L.S., Kandori, H., (2014). Microbial and animal rhodopsins: structures, functions, and molecular mechanisms. *Chem. Rev.*, 114, 126–163. https://doi.org/ 10.1021/cr4003769.

- Fankhauser, C., Christie, J.M., (2015). Plant phototropic growth. Curr. Biol. CB., 25, R384–R389. https://doi.org/ 10.1016/j.cub.2015.03.020.
- Metz, S., Jäger, A., Klug, G., (2012). Role of a short light, oxygen, voltage (LOV) domain protein in blue light- and singlet oxygen-dependent gene regulation in Rhodobacter sphaeroides. *Microbiology*, 158, 368–379. https://doi.org/ 10.1099/mic.0.054700-0.
- Deisseroth, K., Feng, G., Majewska, A.K., Miesenböck, G., Ting, A., Schnitzer, M.J., (2006). Next-generation optical technologies for illuminating genetically targeted brain circuits. *J. Neurosci.*, 26, 10380–10386. https://doi.org/ 10.1523/JNEUROSCI.3863-06.2006.
- Ziegler, T., Möglich, A., (2015). Photoreceptor engineering. Front. Mol. Biosci., 2, 30. https://doi.org/10.3389/fmolb.2015.00030.
- Losi, A., Gardner, K.H., Möglich, A., (2018). Blue-light receptors for optogenetics. *Chem. Rev.*, 118, 10659– 10709. https://doi.org/10.1021/acs.chemrev.8b00163.
- Kennedy, M.J., Hughes, R.M., Peteya, L.A., Schwartz, J. W., Ehlers, M.D., Tucker, C.L., (2010). Rapid blue-light-mediated induction of protein interactions in living cells. Nat. Methods., 7, 973–975. https://doi.org/10.1038/nmeth.1524.
- Taslimi, A., Zoltowski, B., Miranda, J.G., Pathak, G.P., Hughes, R.M., Tucker, C.L., (2016). Optimized secondgeneration CRY2-CIB dimerizers and photoactivatable Cre recombinase. *Nat. Chem. Biol.*, 12, 425–430. https://doi. org/10.1038/nchembio.2063.
- G.P. Pathak, J.I. Spiltoir, C. Höglund, L.R. Polstein, S. Heine-Koskinen, C.A. Gersbach, J. Rossi, C.L. Tucker, Bidirectional approaches for optogenetic regulation of gene expression in mammalian cells using Arabidopsis cryptochrome 2, Nucleic Acids Res. 45 (2017) e167– e167. doi:10.1093/nar/gkx260.
- K. Meador, C.L. Wysoczynski, A.J. Norris, J. Aoto, M.R. Bruchas, C.L. Tucker, Achieving tight control of a photoactivatable Cre recombinase gene switch: new design strategies and functional characterization in mammalian cells and rodent, Nucleic Acids Res. 47 (2019) e97–e97. doi:10.1093/nar/gkz585.
- Wang, X., Chen, X., Yang, Y., (2012). Spatiotemporal control of gene expression by a light-switchable transgene system. *Nat. Methods.*, 9, 266–269. https://doi.org/ 10.1038/nmeth.1892.
- Chen, X., Liu, R., Ma, Z., Xu, X., Zhang, H., Xu, J., Ouyang, Q., Yang, Y., (2016). An extraordinary stringent and sensitive light-switchable gene expression system for bacterial cells. *Cell Res.*, 26, 854–857. https://doi.org/10.1038/cr.2016.74.
- Motta-Mena, L.B., Reade, A., Mallory, M.J., Glantz, S., Weiner, O.D., Lynch, K.W., Gardner, K.H., (2014). An optogenetic gene expression system with rapid activation and deactivation kinetics. *Nat. Chem. Biol.*, 10, 196–202. https://doi.org/10.1038/nchembio.1430.
- Wang, H., Vilela, M., Winkler, A., Tarnawski, M., Schlichting, I., Yumerefendi, H., Kuhlman, B., Liu, R., Danuser, G., Hahn, K.M., (2016). LOVTRAP: an optogenetic system for photoinduced protein dissociation. *Nat. Methods.*, 13, 755–758. https://doi.org/10.1038/ nmeth.3926.
- Reis, J.M., Xu, X., McDonald, S., Woloschuk, R.M., Jaikaran, A.S.I., Vizeacoumar, F.S., Woolley, G.A., Uppalapati, M., (2018). Discovering selective binders for

- photoswitchable proteins using phage display. *ACS Synth. Biol.*, **7**, 2355–2364. https://doi.org/10.1021/acssynbio.8b00123.
- Gil, A.A., Carrasco-López, C., Zhu, L., Zhao, E.M., Ravindran, P.T., Wilson, M.Z., Goglia, A.G., Avalos, J.L., Toettcher, J.E., (2020). Optogenetic control of protein binding using light-switchable nanobodies. *Nat. Commun.*, 11, 4044. https://doi.org/10.1038/s41467-020-17836-8.
- Carrasco-López, C., Zhao, E.M., Gil, A.A., Alam, N., Toettcher, J.E., Avalos, J.L., (2020). Development of light-responsive protein binding in the monobody nonimmunoglobulin scaffold. *Nat. Commun.*, 11, 4045. https:// doi.org/10.1038/s41467-020-17837-7.
- Kawano, F., Suzuki, H., Furuya, A., Sato, M., (2015). Engineered pairs of distinct photoswitches for optogenetic control of cellular proteins. *Nat. Commun.*, 6, 6256. https://doi.org/10.1038/ncomms7256.
- Strickland, D., Lin, Y., Wagner, E., Hope, C.M., Zayner, J., Antoniou, C., Sosnick, T.R., Weiss, E.L., Glotzer, M., (2012). TULIPs: tunable, light-controlled interacting protein tags for cell biology. *Nat. Methods.*, 9, 379–384. https://doi. org/10.1038/nmeth.1904.
- Lungu, O.I., Hallett, R.A., Choi, E.J., Aiken, M.J., Hahn, K. M., Kuhlman, B., (2012). Designing photoswitchable peptides using the AsLOV2 domain. *Chem. Biol.*, 19, 507–517. https://doi.org/10.1016/j.chembiol.2012.02.006.
- Guntas, G., Hallett, R.A., Zimmerman, S.P., Williams, T., Yumerefendi, H., Bear, J.E., Kuhlman, B., (2015). Engineering an improved light-induced dimer (iLID) for controlling the localization and activity of signaling proteins. *Proc. Natl. Acad. Sci. U. S. A.*, 112, 112–117. https://doi. org/10.1073/pnas.1417910112.
- Conrad, K.S., Bilwes, A.M., Crane, B.R., (2013). Light-induced subunit dissociation by a light-oxygen-voltage domain photoreceptor from Rhodobacter sphaeroides. *Biochemistry*, 52, 378–391. https://doi.org/10.1021/bi3015373.
- Christie, J.M., Reymond, P., Powell, G.K., Bernasconi, P., Raibekas, A.A., Liscum, E., Briggs, W.R., (1998).
 Arabidopsis NPH1: a flavoprotein with the properties of a photoreceptor for phototropism. *Science*, 282, 1698–1701.
- 26. Christie, J.M., (2007). Phototropin blue-light receptors. *Annu Rev Plant Biol.*, 58, 21–45.
- Conrad, K.S., Manahan, C.C., Crane, B.R., (2014).
 Photochemistry of flavoprotein light sensors. *Nat. Chem. Biol.*, 10, 801–809. https://doi.org/10.1038/nchembio.1633.
- Salomon, M., Christie, J.M., Knieb, E., Lempert, U., Briggs, W.R., (2000). Photochemical and mutational analysis of the FMN-binding domains of the plant blue light receptor, phototropin. *Biochemistry*, 39, 9401–9410.
- Yee, E.F., Diensthuber, R.P., Vaidya, A.T., Borbat, P.P., Engelhard, C., Freed, J.H., Bittl, R., Möglich, A., Crane, B. R., (2015). Signal transduction in light-oxygen-voltage receptors lacking the adduct-forming cysteine residue. *Nat. Commun.*, 6, 10079. https://doi.org/10.1038/ncomms10079.
- Möglich, A., (2019). Signal transduction in photoreceptor histidine kinases. *Protein Sci.*, 28, 1923–1946. https://doi. org/10.1002/pro.3705.
- Richter, F., Fonfara, I., Bouazza, B., Schumacher, C.H., Bratovič, M., Charpentier, E., Möglich, A., (2016). Engineering of temperature- and light-switchable Cas9

- variants. *Nucleic Acids Res.*, **44**, 10003–10014. https://doi.org/10.1093/nar/qkw930.
- Richter, F., Fonfara, I., Gelfert, R., Nack, J., Charpentier, E., Möglich, A., (2017). Switchable Cas9. Curr. Opin. Biotechnol., 48, 119–126. https://doi.org/10.1016/j.copbjo.2017.03.025.
- Grusch, M., Schelch, K., Riedler, R., Reichhart, E., Differ, C., Berger, W., Inglés-Prieto, Á., Janovjak, H., (2014). Spatio-temporally precise activation of engineered receptor tyrosine kinases by light. *EMBO J.*, 33, 1713–1726. https:// doi.org/10.15252/embj.201387695.
- Lu, H., Mazumder, M., Jaikaran, A.S.I., Kumar, A., Leis, E. K., Xu, X., Altmann, M., Cochrane, A., Woolley, G.A., (2019).
 A yeast system for discovering optogenetic inhibitors of eukaryotic translation initiation. ACS Synth. Biol., 8, 744–757. https://doi.org/10.1021/acssynbio.8b00386.
- X. Li, C. Zhang, X. Xu, J. Miao, J. Yao, R. Liu, Y. Zhao, X. Chen, Y. Yang, A single-component light sensor system allows highly tunable and direct activation of gene expression in bacterial cells, Nucleic Acids Res. 48 (2020) e33–e33. doi:10.1093/nar/gkaa044.
- Wu, D., Hu, Q., Yan, Z., Chen, W., Yan, C., Huang, X., Zhang, J., Yang, P., Deng, H., Wang, J., Deng, X., Shi, Y., (2012). Structural basis of ultraviolet-B perception by UVR8. *Nature*, 484, 214–219. https://doi.org/10.1038/nature10931.
- Hillen, W., Berens, C., (1994). Mechanisms underlying expression of tn10 encoded tetracycline resistance. *Annu. Rev. Microbiol.*, 48, 345–369. https://doi.org/10.1146/annurev.mi.48.100194.002021.
- Orth, P., Cordes, F., Schnappinger, D., Hillen, W., Saenger, W., Hinrichs, W., (1998). Conformational changes of the Tet repressor induced by tetracycline trapping. J. Mol. Biol., 279, 439–447. https://doi.org/ 10.1006/jmbi.1998.1775.
- Gossen, M., Freundlieb, S., Bender, G., Muller, G., Hillen, W., Bujard, H., (1995). Transcriptional activation by tetracyclines in mammalian cells. *Science*, 268, 1766– 1769. https://doi.org/10.1126/science.7792603.
- Orth, P., Schnappinger, D., Hillen, W., Saenger, W., Hinrichs, W., (2000). Structural basis of gene regulation by the tetracycline inducible Tet repressor-operator system. *Nat. Struct. Biol.*, 7, 215–219. https://doi.org/ 10.1038/73324.
- Lederer, T., Takahashi, M., Hillen, W., (1995). Thermodynamic analysis of tetracycline-mediated induction of tet repressor by a quantitative methylation protection assay. *Anal. Biochem.*, 232, 190–196. https://doi.org/10.1006/abio.1995.0006.
- Baumschlager, A., Rullan, M., Khammash, M., (2020). Exploiting natural chemical photosensitivity of anhydrotetracycline and tetracycline for dynamic and setpoint chemo-optogenetic control. *Nat. Commun.*, 11, 3834. https://doi.org/10.1038/s41467-020-17677-5.
- Tolia, N.H., Joshua-Tor, L., (2006). Strategies for protein coexpression in Escherichia coli. *Nat. Methods.*, 3, 55–64. https://doi.org/10.1038/nmeth0106-55.
- Zoltowski, B.D., Crane, B.R., (2008). Light activation of the LOV protein vivid generates a rapidly exchanging dimer. *Biochemistry*, 47, 7012–7019. https://doi.org/10.1021/bi8007017.
- 45. Herman, E., Sachse, M., Kroth, P.G., Kottke, T., (2013). Blue-light-induced unfolding of the $i\alpha$ helix allows for the

- dimerization of aureochrome-LOV from the diatom Phaeodactylum tricornutum. *Biochemistry*, **52**, 3094–3101. https://doi.org/10.1021/bi400197u.
- Harper, S.M., Neil, L.C., Gardner, K.H., (2003). Structural basis of a phototropin light switch. *Science*, 301, 1541– 1544. https://doi.org/10.1126/science.1086810.
- Goldenzweig, A., Goldsmith, M., Hill, S.E., Gertman, O., Laurino, P., Ashani, Y., Dym, O., Unger, T., Albeck, S., Prilusky, J., Lieberman, R.L., Aharoni, A., Silman, I., Sussman, J.L., Tawfik, D.S., Fleishman, S.J., (2016). Automated structure- and sequence-based design of proteins for high bacterial expression and stability. *Mol. Cell.*, 63, 337–346. https://doi.org/10.1016/j.molcel.2016.06.012.
- 48. Leman, J.K., Weitzner, B.D., Lewis, S.M., Adolf-Bryfogle, J., Alam, N., Alford, R.F., Aprahamian, M., Baker, D., Barlow, K.A., Barth, P., Basanta, B., Bender, B.J., Blacklock, K., Bonet, J., Boyken, S.E., Bradley, P., Bystroff, C., Conway, P., Cooper, S., Correia, B.E., Coventry, B., Das, R., De Jong, R.M., DiMaio, F., Dsilva, L., Dunbrack, R., Ford, A.S., Frenz, B., Fu, D.Y., Geniesse, C., Goldschmidt, L., Gowthaman, R., Gray, J.J., Gront, D., Guffy, S., Horowitz, S., Huang, P.-S., Huber, T., Jacobs, T. M., Jeliazkov, J.R., Johnson, D.K., Kappel, K., Karanicolas, J., Khakzad, H., Khar, K.R., Khare, S.D., Khatib, F., Khramushin, A., King, I.C., Kleffner, R., Koepnick, B., Kortemme, T., Kuenze, G., Kuhlman, B., Kuroda, D., Labonte, J.W., Lai, J.K., Lapidoth, G., Leaver-Fay, A., Lindert, S., Linsky, T., London, N., Lubin, J.H., Lyskov, S., Maguire, J., Malmström, L., Marcos, E., Marcu, O., Marze, N.A., Meiler, J., Moretti, R., Mulligan, V.K., Nerli, S., Norn, C., Ó'Conchúir, S., Ollikainen, N., Ovchinnikov, S., Pacella, M.S., Pan, X., Park, H., Pavlovicz, R.E., Pethe, M., Pierce, B.G., Pilla, K.B., Raveh, B., Renfrew, P.D., Burman, S.S. R., Rubenstein, A., Sauer, M.F., Scheck, A., Schief, W., Schueler-Furman, O., Sedan, Y., Sevv. A.M., Sgourakis. N.G., Shi, L., Siegel, J.B., Silva, D.-A., Smith, S., Song, Y., Stein, A., Szegedy, M., Teets, F.D., Thyme, S.B., Wang, R.-Y.-R., Watkins, A., Zimmerman, L., Bonneau, R., (2020). Macromolecular modeling and design in Rosetta: recent methods and frameworks. Nat. Methods., 17, 665-680. https://doi.org/10.1038/s41592-020-0848-2.
- Grau, F.C., Jaeger, J., Groher, F., Suess, B., Muller, Y.A., (2020). The complex formed between a synthetic RNA aptamer and the transcription repressor TetR is a structural and functional twin of the operator DNA-TetR regulator complex. *Nucleic Acids Res.*, 48, 3366–3378. https://doi. org/10.1093/nar/gkaa083.
- Schnappinger, D., Schubert, P., Pfleiderer, K., Hillen, W., (1998). Determinants of protein–protein recognition by four helix bundles: changing the dimerization specificity of Tet repressor. *EMBO J.*, 17, 535–543. https://doi.org/10.1093/ emboj/17.2.535.
- Heinig, M., Frishman, D., (2004). STRIDE: a web server for secondary structure assignment from known atomic coordinates of proteins. *Nucleic Acids Res.*, 32, W500– W502. https://doi.org/10.1093/nar/gkh429.
- Crosson, S., Rajagopal, S., Moffat, K., (2003). The LOV domain family: photoresponsive signaling modules coupled to diverse output domains. *Biochemistry*, 42, 2–10.
- Magerl, K., Dick, B., (2020). Dimerization of LOV domains of Rhodobacter sphaeroides (RsLOV) studied with FRET and stopped-flow experiments. *Photochem. Photobiol. Sci.*, 19, 159–170. https://doi.org/10.1039/C9PP00424F.

- Kainrath, S., Stadler, M., Reichhart, E., Distel, M., Janovjak, H., (2017). Green-light-induced inactivation of receptor signaling using cobalamin-binding domains. *Angew. Chem. Int. Ed.*, 56, 4608–4611. https://doi.org/ 10.1002/anie.201611998.
- Levskaya, A., Chevalier, A.A., Tabor, J.J., Simpson, Z.B., Lavery, L.A., Levy, M., Davidson, E.A., Scouras, A., Ellington, A.D., Marcotte, E.M., Voigt, C.A., (2005). Synthetic biology: Engineering Escherichia coli to see light. *Nature*, 438, 441–442. https://doi.org/ 10.1038/nature04405.
- Tabor, J.J., Levskaya, A., Voigt, C.A., (2011). Multichromatic control of gene expression in Escherichia coli. *J. Mol. Biol.*, 405, 315–324. https://doi.org/10.1016/j. jmb.2010.10.038.
- Ohlendorf, R., Vidavski, R.R., Eldar, A., Moffat, K., Möglich, A., (2012). From dusk till dawn: one-plasmid systems for light-regulated gene expression. *J. Mol. Biol.*, 416, 534–542. https://doi.org/10.1016/j.jmb.2012.01.001.
- Müller, K., Zurbriggen, M.D., Weber, W., (2015). An optogenetic upgrade for the Tet-OFF system. *Biotechnol. Bioeng.*, 112, 1483–1487. https://doi.org/10.1002/bit.25562.
- Elowitz, M.B., Leibler, S., (2000). A synthetic oscillatory network of transcriptional regulators. *Nature*, 403, 335– 338. https://doi.org/10.1038/35002125.
- Potvin-Trottier, L., Lord, N.D., Vinnicombe, G., Paulsson, J., (2016). Synchronous long-term oscillations in a synthetic gene circuit. *Nature*, 538, 514–517. https://doi. org/10.1038/nature19841.
- Hunsicker, A., Steber, M., Mayer, G., Meitert, J., Klotzsche, M., Blind, M., Hillen, W., Berens, C., Suess, B., (2009). An RNA aptamer that induces transcription. *Chem. Biol.*, 16, 173–180. https://doi.org/10.1016/j.chembiol.2008.12.008.
- Weber, A.M., Kaiser, J., Ziegler, T., Pilsl, S., Renzl, C., Sixt, L., Pietruschka, G., Moniot, S., Kakoti, A., Juraschitz, M., Schrottke, S., Steegborn, C., Bittl, R., Mayer, G., Möglich, A., (2019). A blue light receptor that mediates RNA binding and translational regulation. *Nat. Chem. Biol.*, 15, 1085–1092. https://doi.org/10.1038/s41589-019-0346-y.
- Pilsl, S., Morgan, C., Choukeife, M., Möglich, A., Mayer, G., (2020). Optoribogenetic control of regulatory RNA molecules. *Nat. Commun.*, 11, 4825. https://doi.org/ 10.1038/s41467-020-18673-5.
- Zimmerman, S.P., Hallett, R.A., Bourke, A.M., Bear, J.E., Kennedy, M.J., Kuhlman, B., (2016). Tuning the binding affinities and reversion kinetics of a light inducible dimer allows control of transmembrane protein localization. *Biochemistry*, 55, 5264–5271. https://doi.org/10.1021/acs. biochem.6b00529.
- Golonka, D., Fischbach, P., Jena, S.G., Kleeberg, J.R.W., Essen, L.-O., Toettcher, J.E., Zurbriggen, M.D., Möglich, A., (2019). Deconstructing and repurposing the lightregulated interplay between Arabidopsis phytochromes and interacting factors. *Commun. Biol.*, 2, 448. https://doi. org/10.1038/s42003-019-0687-9.
- Hallett, R.A., Zimmerman, S.P., Yumerefendi, H., Bear, J. E., Kuhlman, B., (2016). Correlating in vitro and in vivo activities of light-inducible dimers: a cellular optogenetics guide. ACS Synth. Biol., 5, 53–64. https://doi.org/10.1021/ acssynbio.5b00119.
- 67. Benedetti, L., Barentine, A.E.S., Messa, M., Wheeler, H., Bewersdorf, J., De Camilli, P., (2018). Light-activated

- protein interaction with high spatial subcellular confinement. *Proc. Natl. Acad. Sci. U. S. A.*, **115**, E2238–E2245. https://doi.org/10.1073/pnas.1713845115.
- Strickland, D., Yao, X., Gawlak, G., Rosen, M.K., Gardner, K.H., Sosnick, T.R., (2010). Rationally improving LOV domain-based photoswitches. *Nat. Methods.*, 7, 623–626. https://doi.org/10.1038/nmeth.1473.
- Shapiro, M.G., Homma, K., Villarreal, S., Richter, C.-P., Bezanilla, F., (2012). Infrared light excites cells by changing their electrical capacitance. *Nat. Commun.*, 3, 736. https://doi.org/10.1038/ncomms1742.
- Y. Zheng, F. Meng, Z. Zhu, W. Wei, Z. Sun, J. Chen, B. Yu, C. Lou, G.-Q. Chen, A tight cold-inducible switch built by coupling thermosensitive transcriptional and proteolytic regulatory parts, Nucleic Acids Res. 47 (2019) e137– e137. doi:10.1093/nar/gkz785.
- Fujii, Y., Tanaka, H., Konno, N., Ogasawara, Y., Hamashima, N., Tamura, S., Hasegawa, S., Hayasaki, Y., Okajima, K., Kodama, Y., (2017). Phototropin perceives temperature based on the lifetime of its photoactivated state. *Proc. Natl. Acad. Sci.*, 114, 9206–9211. https://doi. org/10.1073/pnas.1704462114.
- Legris, M., Klose, C., Burgie, E.S., Rojas, C.C.R., Neme, M., Hiltbrunner, A., Wigge, P.A., Schäfer, E., Vierstra, R.D., Casal, J.J., (2016). Phytochrome B integrates light and temperature signals in Arabidopsis. *Science*, 354, 897– 900. https://doi.org/10.1126/science.aaf5656.
- Gibson, D.G., Young, L., Chuang, R.-Y., Venter, J.C., Hutchison, C.A., Smith, H.O., (2009). Enzymatic assembly of DNA molecules up to several hundred kilobases. *Nat. Methods.*, 6, 343–345. https://doi.org/10.1038/nmeth.1318.
- Strack, R.L., Strongin, D.E., Bhattacharyya, D., Tao, W., Berman, A., Broxmeyer, H.E., Keenan, R.J., Glick, B.S., (2008). A noncytotoxic DsRed variant for whole-cell labeling. *Nat. Methods.*, 5, 955–957. https://doi.org/ 10.1038/nmeth.1264.
- 75. P.C. Cirino, K.M. Mayer, D. Umeno, Generating Mutant Libraries Using Error-Prone PCR, in: Dir. Evol. Libr. Creat., n.d.: pp. 3–9.
- Mathes, T., Vogl, C., Stolz, J., Hegemann, P., (2009). In vivo generation of flavoproteins with modified cofactors. *J. Mol. Biol.*, 385, 1511–1518. https://doi.org/10.1016/j.jmb.2008.11.001.

- Möglich, A., (2018). An open-source, cross-platform resource for nonlinear least-squares curve fitting. J. Chem. Educ., 95, 2273–2278. https://doi.org/10.1021/acs. ichemed.8b00649.
- W. Kabsch, XDS, Acta Crystallogr. D Biol. Crystallogr. 66 (2010) 125–132. doi:10.1107/S0907444909047337.
- Evans, P., (2006). Scaling and assessment of data quality.
 Acta Crystallogr. Sect. D., 62, 72–82. https://doi.org/ 10.1107/S0907444905036693.
- Krug, M., Weiss, M.S., Heinemann, U., Mueller, U., (2012).
 XDSAPP: a graphical user interface for the convenient processing of diffraction data using XDS. J. Appl. Crystallogr., 45, 568–572. https://doi.org/10.1107/S0021889812011715.
- Emsley, P., Cowtan, K., (2004). Coot: model-building tools for molecular graphics. Acta Crystallogr. D Biol. Crystallogr., 60, 2126–2132. https://doi.org/10.1107/ S0907444904019158.
- Murshudov, G.N., Vagin, A.A., Dodson, E.J., (1997). Refinement of macromolecular structures by the maximum-likelihood method. *Acta Crystallogr. Biol.* Crystallogr., 53, 240–255.
- Afonine, P.V., Grosse-Kunstleve, R.W., Echols, N., Headd, J.J., Moriarty, N.W., Mustyakimov, M., Terwilliger, T.C., Urzhumtsev, A., Zwart, P.H., Adams, P.D., (2012). Towards automated crystallographic structure refinement with phenix.refine. *Acta Crystallogr. D Biol. Crystallogr.*, 68, 352–367. https://doi.org/10.1107/S0907444912001308.
- Kabsch, W., (1976). A solution for the best rotation to relate two sets of vectors. *Acta Cryst. A.*, 32, 922–923. https://doi. org/10.1107/S0567739476001873.
- Iwahara, J., Tang, C., Marius Clore, G., (2007). Practical aspects of 1H transverse paramagnetic relaxation enhancement measurements on macromolecules. *J. Magn. Reson.*, 184, 185–195. https://doi.org/10.1016/j.jmr.2006.10.003.
- Baker, J.M., Boyce, F.M., (2014). High-throughput functional screening using a homemade dual-glow luciferase assay. *JoVE J. Vis. Exp.*,. https://doi.org/ 10.3791/50282 e50282.

Supporting Information

A light-oxygen-voltage receptor integrates light and temperature

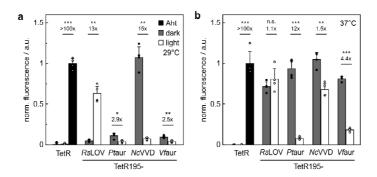
Julia Dietler, Roman Schubert, Tobias G. A. Krafft, Simone Meiler, Stephanie Kainrath, Florian Richter,
Kristian Schweimer, Michael Weyand, Harald Janovjak, Andreas Möglich

Supplementary Table S1. Data collection and refinement statistics for X-ray crystallography.

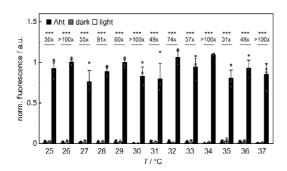
	RsLOV D109G ^a	RsLOV d2 ^a		
Data collection				
Space group	P 2 ₁ P 2 ₁ 2 ₁			
Cell dimensions				
a, b, c (Å)	90.96, 65.80, 122.72	58.06, 77.17, 155.00		
α, β, γ (°)	90, 94, 90	90, 90, 90		
Resolution (Å)	50.0 - 2.00 (2.12 - 2.00) ^b	50.0 - 1.90 (2.01 - 1.90) ^b		
R _{meas}	0.088 (3.441)	0.057 (0.254)		
Ι / σΙ	9.32 (0.40)	17.67 (5.53)		
Completeness (%)	99.6 (98.9)	99.6 (99.1)		
Redundancy	3.72 (3.50)	3.93 (3.88)		
CC _{1/2}	0.999 (0.189)	0.998 (0.961)		
Refinement				
Resolution (Å)	45.37 – 2.00 (2.03 – 2.00)	42.93 – 1.90 (1.94 – 1.90)		
No. reflections	97,821 (4,567)	55,587 (3,608)		
R _{work} / R _{free}	0.219 (0.503) / 0.263 (0.543)	0.176 (0.223) / 0.218 (0.286)		
No. atoms				
Protein	8,128	5,524		
Ligand/ion	234	140		
Water	172 544			
B-factors (Ų)				
Protein	75.08	27.73		
Ligand/ion	69.51 32.07			
Water	57.70 32.58			
R.m.s deviations				
Bond lengths (Å)	0.008	0.006		
Bond angles (°)	0.99	0.92		
PDB deposition	70BZ 70B0			

^a Data were collected from a single crystal each.

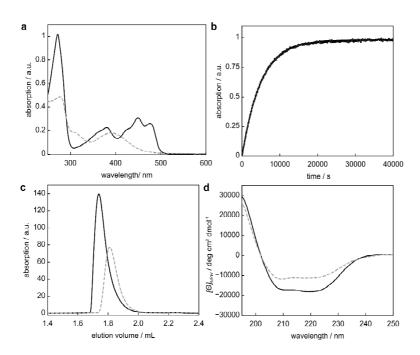
^b Values in parentheses are for highest-resolution shell.



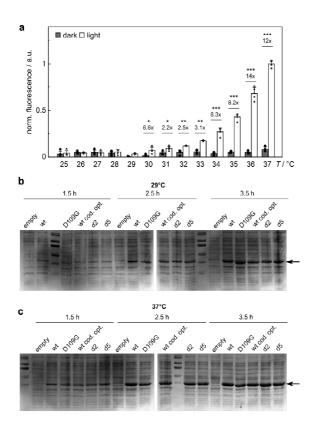
Supplementary Figure S1. *Ds*Red reporter fluorescence of *E. coli* CmpX13 cultures harboring TetR or TetR195-LOV constructs and incubated in darkness (grey bars), under blue light illumination (white bars), or in presence of Aht (black bars) at either **(a)** 29°C or **(b)** 37°C. All measurements represent mean \pm s.d. of four biologically independent samples and were normalized to the Aht-induced TetR system. Asterisks denote *p* values from a two-sided Welch's *t* test (* $p \le 0.05$, ** $p \le 0.01$, *** $p \le 0.001$, n.s. not significant).



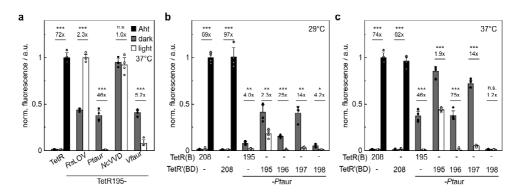
Supplementary Figure S2. DsRed reporter fluorescence of E. coli DH10b cultures harboring TetR and incubated in darkness (grey bars), under blue light illumination (white bars), or in presence of Aht (black bars) at varying temperatures. All measurements represent mean \pm s.d. of four biologically independent samples and were normalized to the Aht-induced TetR system at 29°C. Asterisks denote p values from a two-sided Welch's t test (*** $p \le 0.001$).



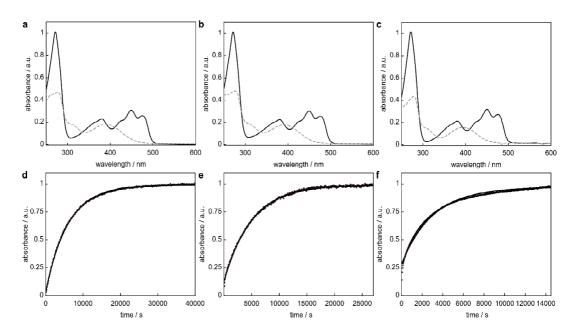
Supplementary Figure S3. Biochemical analyses of wild-type *Rs*LOV. **(a)** UV-vis absorbance spectra of the dark-adapted (black line) and light-adapted (grey dashed line) states. **(b)** Recovery reaction after saturating blue-light illumination followed by the absorbance at 450 nm. Data were normalized to the maximum absorbance and fitted to a single-exponential function. **(c)** Size-exclusion chromatography of *Rs*LOV in darkness (black line) and following blue-light exposure (grey dashed line). **(d)** Far-UV circular dichroism spectra of dark-adapted (black line) and light-adapted (grey dotted line) *Rs*LOV.



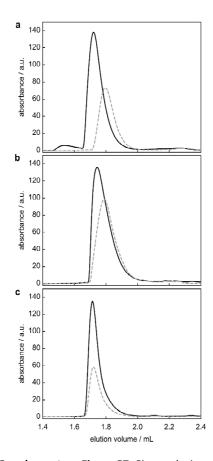
Supplementary Figure S4. (a) *Ds*Red reporter gene fluorescence of *E. coli* DH10b cells harboring TetR195-*Rs*LOV D109G and incubated in darkness (grey bars) or under blue light (white bars) at varying temperatures. All measurements represent mean \pm s.d. of four biologically independent samples and were normalized to the value at 37°C in the light. (b) Expression analysis of TetR195-*Rs*LOV variants in *E. coli* CmpX13 at 29°C analyzed by denaturing gel electrophoresis. The arrow indicates the band corresponding to the TetR195-*Rs*LOV variants. (c) As in panel b but the incubation temperature was 37°C. Asterisks denote *p* values from a two-sided Welch's *t* test (* $p \le 0.05$, ** $p \le 0.01$, *** $p \le 0.001$).



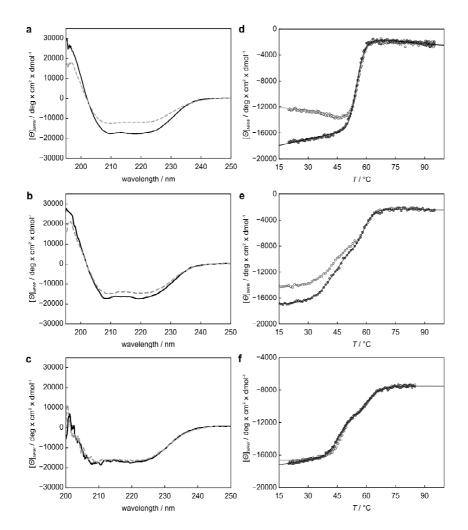
Supplementary Figure S5. (a) DsRed reporter fluorescence of E. coli DH10b cultures harboring TetR or TetR195-LOV variants and incubated at 37°C in darkness (grey bars), under blue light (white bars), or in presence of Aht (black bars). (b) DsRed reporter fluorescence of E. coli DH10b cultures harboring different TetR195 variants linked to the Ptaur LOV module and incubated at 29°C in darkness (grey bars), under blue light (white bars), or in presence of Aht (black bars). (c) As in panel b but cultures were incubated at 37°C. All measurements represent mean \pm s.d. of four biologically independent samples and were normalized to the Aht-induced TetR system. Asterisks denote p values from a two-sided Welch's t test (* $p \le 0.05$, ** $p \le 0.01$, *** $p \le 0.001$, n.s. not significant).



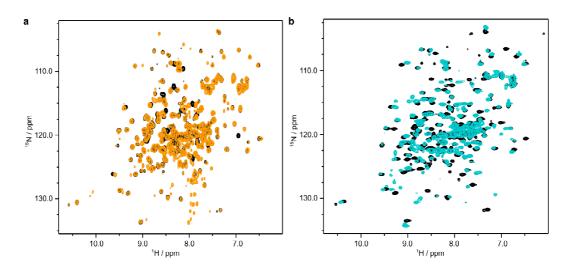
Supplementary Figure S6. Spectroscopic analyses of the *Rs*LOV D109G, d2 and d5 variants. **(a-c)** UV-vis absorbance spectra of dark-adapted (black line) and light-adapted (grey dotted line) *Rs*LOV D109G (a), d2 (b) and d5 (c). **(d-f)** Recovery reaction of *Rs*LOV D109G (d), d2 (e) and d5 (f) after saturating blue-light illumination followed by the absorbance at 450 nm. Data were normalized and fitted to a single-exponential function.



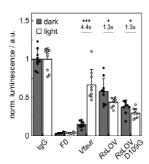
Supplementary Figure S7. Size-exclusion chromatography of 100 μ M *Rs*LOV D109G (panel a), d2 (panel b) and d5 (panel c) variant in darkness (black line) and following blue-light exposure (grey dashed line).



Supplementary Figure S8. (a-c) Far-UV circular dichroism spectra of the *Rs*LOV D109G (a), d2 (b) and d5 (c) variants in their dark-adapted (black line) and light-adapted (grey dashed line) states. (d-f) Thermal denaturation of *Rs*LOV D109G (d), d2 (e) and d5 (f) monitored by circular dichroism (CD) at 222 nm for the dark-adapted (filled circles) and light-adapted (open circles) states. The temperature was increased at a rate of 1°C min⁻¹, and data were fitted to two- or three-state unfolding transitions.



Supplementary Figure S9. **(a)** ¹H-¹⁵N HSQC spectra of dark-adapted *Rs*LOV wild type (black) and D109G (orange) at 29°C. **(b)** ¹H-¹⁵N HSQC spectra of *Rs*LOV D109G at 37°C in its dark-adapted (black) and light-adapted (cyan) states.



Supplementary Figure S10. HEK293T cells expressing mFGFR1 variants were incubated at 37°C in darkness (grey bars) or blue light (white), and luciferase activity was determined. Samples as in Fig. 6b. All measurements represent mean \pm s.d. of three biological replicates and were normalized to the IgG-coupled positive control. Asterisks denote p values from a two-sided Welch's t test (* $p \le 0.05$, *** $p \le 0.001$).

COMMUNICATION



www.advanced-bio.com

Photobiologically Directed Assembly of Gold Nanoparticles

Julia Dietler, Chen Liang, Saskia Frank, Ann-Kathrin Müller, Andreas Greiner,* and Andreas Möglich*

In nature, photoreceptor proteins undergo molecular responses to light, that exhibit supreme fidelity in time and space and generally occur under mild reaction conditions. To unlock these traits for material science, the light-induced homodimerization of light-oxygen-voltage (LOV) photoreceptors is leveraged to control the assembly of gold nanoparticles. Conjugated to genetically encodable LOV proteins, the nanoparticles are monodispersed in darkness but rapidly assemble into large aggregates upon blue-light exposure. The work establishes a new modality for reaction control in macromolecular chemistry and thus augurs enhanced precision in space and time in diverse applications of gold nanoparticles.

Adaptations to light abound in biology across wide time and length scales. At the molecular level, these adaptations rely on sensory photoreceptor proteins that absorb photons and initiate photochemical and biochemical reaction cascades with exquisite resolution in time and space. Often, these reactions entail the formation or dissolution of non-covalent interactions among proteins and other biomolecules. Notably, photoreceptors are genetically encoded and generally operate in aqueous milieu under mild reaction conditions. These core aspects are exemplified by the light-oxygen-voltage (LOV) photoreceptor class which respond to blue light via flavin nucleotide chromophores (Figure 1A). Certain LOV receptors undergo light-controlled homo- or heterodimerization reactions (Figure 1B), which have been harnessed to optogenetically control a cohort of cellular processes.

Here, we extend the concept of photobiological reaction control from biology to materials science. We develop the ondemand assembly of gold nanoparticles (AuNPs) as model nanoparticles via photobiological direction by associating LOV

J. Dietler, S. Frank, Prof. A. Möglich
Department of Biochemistry, Photobiochemistry
University of Bayreuth
Bayreuth D-95440, Germany
E-mail: andreas.moeglich@uni-bayreuth.de
C. Liang, A.-K. Müller, Prof. A. Greiner
Macromolecular Chemistry and Bavarian Polymer Institute
University of Bayreuth
Bayreuth D-95440, Germany

E-mail: andreas.greiner@uni-bayreuth.de

The ORCID identification number(s) for the author(s) of this article can be found under https://doi.org/10.1002/adbi.202000179.

© 2020 The Authors. Advanced Biology published by Wiley-VCH GmbH. This is an open access article under the terms of the Creative Commons Attribution License, which permits use, distribution and reproduction in any medium, provided the original work is properly cited.

DOI: 10.1002/adbi.202000179

receptors (Figure 1C). Nanoparticles in general are of fundamental interest for a variety of industrial processes.^[3,4] AuNPs in specific underpin diverse applications in, e.g., biological sensing and imaging,^[5–7] drug delivery,^[8] and intracellular gene regulation.^[9] Moreover, AuNPs of various shapes and sizes were ordered and arranged in defined architectures.^[5–12] Nanoparticle assembly was for instance controlled by various ligands,^[13–15] but also by external stimuli, such as magnetic fields or light.^[16–24] These advances notwithstanding, the controlled higherorder assembly in response to external

cues remains challenging, but worthwhile to explore because it could significantly extend the application scope of AuNPs. In particular, the interfacing of the inorganic nanoparticles with genetically encodable, adaptable, light-responsive proteins augurs innovative use cases. As a cue signal, light appears ideal as it can be applied non-invasively and supports high spatial and temporal precision, which is not least evidenced by ample applications in biology and biotechnology.^[2]

To achieve LOV-directed AuNP assembly, we envisioned a direct link between the organic photoreceptor proteins and the inorganic particles. Initial attempts to covalently couple the light-responsive proteins to citrate-capped AuNPs via gold sulfide bonds failed, because unspecific interactions (owing to cysteine residues within the protein and to the presence of salt ions, required for protein stability) invariably triggered nanoparticle aggregation and precipitation. [25,26] Therefore, we opted for the non-covalent attachment of the LOV receptors through nickel coordination chemistry. This strategy necessitates that the photoreceptors be equipped with hexa-histidine (His₆) tags and the AuNPs be functionalized with Ni2+-nitrilotriacetic acid (NTA) ligands (Figure 1C).[10,21,27] We selected two wellcharacterized LOV domains from Phaeodactylum tricornutum aureochrome 1a (Ptaur) and from Neurospora crassa Vivid (NcVVD), both previously shown to undergo light-induced homodimerization^[28,29] and used to bestow light sensitivity on cellular processes.^[2] Size-exclusion chromatography (SEC) confirmed that in their unmodified forms both LOV proteins adopt homogenous states in either darkness or blue light (Figure S1, Supporting Information); the apparent molecular size under blue light was higher, indicative of light-induced dimerization. Next, we introduced His6 tags at either the N or C termini of the LOV domains, separated by short glycine-serine linkers. N-terminal modification of Ptaur led to constitutive dimerization independent of light and accompanied by aggregation, whereas C-terminal modification incurred protein insolubility. The sensitivity of the Ptaur N- and C-terminal segments likely

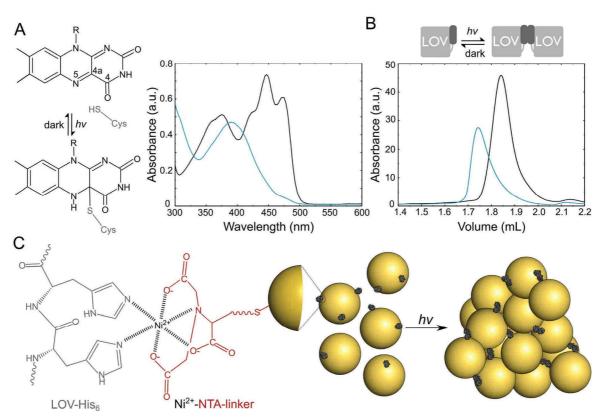


Figure 1. Photobiologically directed assembly of gold nanoparticles (AuNPs) by light-oxygen-voltage (LOV) photoreceptors. A) Simplified LOV photocycle, showing the oxidized quinone state of flavin nucleotide non-covalently bound within the LOV domain in the dark, and the light-induced formation of a covalent thioadduct between a conserved cysteine residue (Cys) and the C4a atom of the flavin molecule. The adduct form spontaneously recovers to restore the dark-adapted state. The photocycle can be observed spectroscopically by absorption of the dark-adapted (black) and light-adapted states (blue). B) Size-exclusion chromatography of NcVVD-His₆ in darkness (black traces) and following blue-light exposure (blue traces). C) To achieve light-induced AuNP assembly, associating LOV domains are immobilized on the particle surface by Ni²⁺-NTA coordination chemistry. Exposure to blue light triggers the dimerization of the LOV domain, which consequently drives the assembly of AuNPs.

owes to them contributing to the light-driven homodimerization. $^{[30,31]}$ Similarly, introduction of the His $_6$ tag at the N terminus of NcVVD caused protein insolubility, consistent with the crucial role of this protein segment in dimerization. $^{[32]}$ By contrast, appendage to the C terminus (NcVVD-His₆) was tolerated, and light-induced dimerization of NcVVD was preserved as assessed by SEC (Figure 1B).

To allow conjugation of the NcVVD-His6 protein to the particles, we synthesized citrate-capped AuNPs according to Frens^[33,34] and subsequently equipped their surface with Ni²⁺-NTA groups via ligand exchange and Ni²⁺ complexation (Figure S2, Supporting Information). Owing to the sensitivity of the surface plasmon resonance (SPR) signal to surface properties,[35] the functionalization with the Ni2+-NTA groups induced a shift of the SPR absorption band of the AuNPs, that could be followed spectroscopically (Figure S3, Supporting Information). Transmission electron microscopy (TEM) revealed that prior to and after Ni2+-NTA functionalization, the AuNPs did not associate and were essentially monodisperse with a mean diameter of (17.7 \pm 1.6) nm (Figure S4,

Supporting Information). Dynamic light scattering (DLS) showed similar average sizes of (21.8 \pm 3.6) and (30.6 \pm 3.4) nm for the citrate-capped and the Ni²⁺-NTA-ligated AuNPs, respectively (Figure S5, Supporting Information). Based on the functionalization of AuNPs with similar ligands, [36] we estimate that around 4000 NTA ligands are bound to the surface of each AuNP.

Next, we assessed the interaction of NcVVD-His6 and the Ni²⁺-NTA functionalized AuNPs. As light scattering scales with the sixth power of particle dimensions, the DLS signal is dominated by larger particles present in solution. To obtain a more accurate view of particle sizes and distributions, we hence switched to asymmetric flow field-flow fractionation (AF4) (Figures S6 and S7, Supporting Information). While the citratecapped and the Ni2+-NTA-functionalized AuNPs eluted with apparent radii of (11 \pm 2) nm and (12 \pm 2) nm, respectively, for the main particle fraction, addition of a fiftyfold molar excess of NcVVD-His₆ induced a shift to (18 \pm 2) nm. Given a protein diameter of ≈4 nm, these results indicate the association of LOV proteins to the AuNPs. When exposed to 450-nm light, the

2000179 (2 of 7)

www.advanced-bio.com

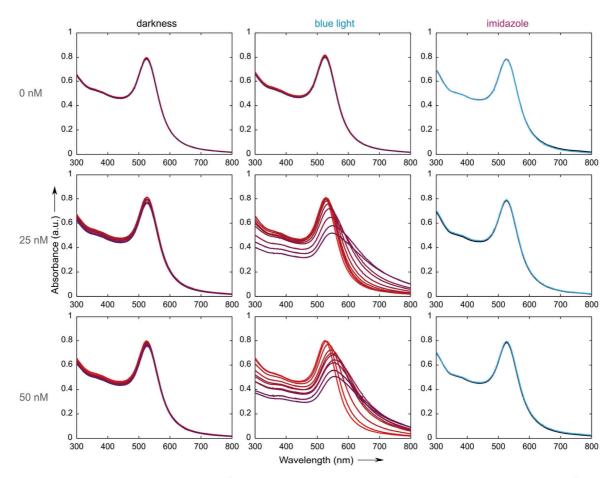


Figure 2. Blue-light exposure drives the assembly of Ni^{2+} -NTA functionalized AuNPs coupled to NcVVD-His $_6$. Time series of UV–vis spectra of Ni^{2+} -NTA functionalized AuNPs in the absence and presence of 25×10^{-9} or 50×10^{-9} m NcVVD-His $_6$. Spectra were acquired at 2, 5, 10, 15, 20, 30, 40, 60, and 90 min after protein addition (from top to bottom). Ni^{2+} -NTA functionalized AuNPs show a strong absorption with a maximum at 524 nm independent of illumination. In presence of NcVVD-His $_6$, blue light induces a broadening of the plasmon peak and a shift toward greater wavelengths, indicating the assembly of AuNPs. The velocity of light-directed assembly can be set by the LOV protein concentration. As control, Ni^{2+} -NTA functionalized AuNPs were incubated in the presence of imidazole without or with different concentrations of NcVVD-His $_6$ (right panels). After 90 min of incubation in either darkness (black traces) or under constant blue light (blue traces) no significant spectral changes could be detected. Imidazole competes with the His $_6$ tag for NTA binding and thus prevents light-induced particle assembly.

solution of *Nc*VVD-conjugated AuNPs rapidly changed color from light red to purple, indicative of altered plasmon resonance and nanoparticle assembly. The formation of such blue light-induced particle clusters was qualitatively confirmed by AF4 measurements during which a purple precipitate of high molecular weight formed on the analysis membrane (Figure S7, Supporting Information).

To better characterize the light-induced association reaction, we followed its kinetics by UV-vis absorption spectroscopy (**Figure 2**). In the absence of the LOV protein, the Ni²⁺-NTA-AuNPs at 0.9×10^{-9} M concentration exhibited broad absorption overlain by a narrower SPR band peaking at 524 nm, irrespective of whether the samples were kept in darkness or illuminated with blue light. Addition of 25×10^{-9} or 50×10^{-9} M NcVVD-His₆ did not induce significant spectral

changes provided the samples were kept in the dark. When exposed to 450-nm light, over the course of 90 min, the SPR band successively broadened, and its maximum shifted to longer wavelengths up to 630 nm. The substantial spectral shift of more than 100 nm reflects the formation of heterogeneous, large-scale nanoparticle assemblies. The kinetics of this process were faster for 50×10^{-9} m NcVVD-His $_6$ than for 25×10^{-9} m. By approximating the shape of the NcVVD-His $_6$ protein as a sphere of 4 nm diameter, we calculate that at maximum around 30 protein molecules can be accommodated on the surface of each particle. Notably, the NcVVD-His $_6$ concentrations of 25×10^{-9} and 50×10^{-9} m correspond to molar ratios of 28 and 56 proteins per nanoparticle, respectively. Reduction of the protein amount severely slowed down the assembly process to the extent that at 6.25×10^{-9} m NcVVD-His $_6$ almost no spectral

2000179 (3 of 7)

www.advanced-bio.com

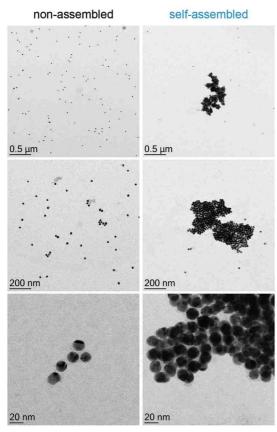


Figure 3. Light-induced assembly of nanoparticles. Transmission electron microscopy images of Ni^{2+} -NTA functionalized AuNPs in the presence of NcVVD-His $_6$ in darkness (left) or following blue-light exposure (right). In the absence of light, LOV-coupled AuNPs are evenly distributed and do not interact, whereas light-programmed association of the LOV receptors directs the assembly of the particles, culminating in the formation of extended networks with up to micrometer dimensions.

changes could be observed upon illumination (Figure S8, Supporting Information). Addition of imidazole, which competes for binding to the Ni²⁺-NTA group, abrogated any light-induced spectral changes (Figure 2).

We next analyzed by transmission electron microscopy (TEM) the size distribution of Ni²⁺-NTA-AuNPs conjugated with NcVVD-His₆ in darkness and under blue light (**Figure 3**). Prior to illumination, the AuNPs appeared monodisperse and evenly distributed on the TEM grid, with a minor population of particles in smaller groups but without forming immediate contact. By contrast, after exposure to blue light, most particles were in direct contact and formed stacked, amorphous assemblies of up to 1.5 μ m in size. Notably, the assemblies formed irreversibly as neither prolonged incubation in darkness nor the addition of imidazole could dissolve them. We ascribe this observation to fusion of the nanoparticles once they have been brought into spatial proximity. The AuNPs thus resisted attempts at dispersion.

Our results showcase AuNP assembly at will through photobiological direction by LOV receptors. By wedding inorganic and proteinaceous building blocks, we synthesize a composite system with emergent properties and thereby establish a new paradigm for reaction control in macromolecular chemistry. We thus lay the foundation for future applications at the interface of colloidal chemistry and biochemistry, as the principal strategy generally extends to diverse nanoparticles of various shape, composition and properties. The use of light triggers stands to permit the controlled nanoparticle assembly with superior spatial resolution, for example by lithography. Although not exploited here, we note that owing to genetic encoding and thereby identity, sensory photoreceptors can be readily attached to other proteins and biomolecules, or displayed on the surface of cells. [37] Doing so enables the defined incorporation of nanoparticles into complex biological circuits and reaction cascades. Of advantage, biological systems are generally malleable and can be adapted in their properties to meet specific application demands. As a case in point, the lifetime of the light-adapted state of LOV receptors, and therefore their effective light sensitivity at photostationary state, can be routinely varied across several orders of magnitude. [38,39] The combination of suitably modified, light-sensitive biological systems with nanoparticles thus augurs novel applications in biology and materials science alike. For instance, the light-triggered assembly of AuNPs, presently configured to be irreversible, may be harnessed for security purposes, such as monitoring the light exposure of sensitive materials.

Experimental Section

Expression and Purification of LOV Proteins: The genes of the N-terminally truncated short-LOV protein Neurospora crassa Vivid (NcVVD) (residues 37–186, including the mutations C71V and N56K)[29,32] and the A' α -LOV-J α module of Phaeodactylum tricornutum Aureo1a (Ptaur) (residues 235–378) were obtained by gene synthesis (GeneArt, Regensburg, Germany) and cloned by Gibson assembly^[40] into expression vectors. For the preparation of untagged protein and variants with N- or C-terminal His₆ tags, the vectors pET-19b-SUMO, pET-28c, and pET-41a were used, respectively. Where applicable, a (GS)₅-linker was inserted between the LOV core protein and the His₆ tags.

For expression, the plasmid constructs were transformed into Escherichia coli BL21(DE3) CmpX13 cells. [41] 800 mL of lysogeny broth (LB) medium, supplemented with 50 µg mL⁻¹ kanamycin, were inoculated with single clones and incubated at 37 °C and 200 rpm until an optical density at 600 nm of 0.6-0.8 was reached. At this point, expression was induced with 1×10^{-3} m isopropyl β -D-1-thiogalactopyranoside (IPTG), the temperature was lowered to 16 °C, and the incubation continued for ≈18 h under constant blue-light illumination (450 nm, 100 µW cm⁻²). The light intensity was determined with a power meter (model 842-PE, Newport) and a silicon photodetector (model 918D-UV-OD3, Newport). Cells were harvested by centrifugation and lysed by ultrasound. The cell lysate was cleared by centrifugation and purified by Ni:NTA affinity chromatography under exclusion of blue light. Fractions eluted by imidazole from the affinity column were analyzed by denaturing polyacrylamide gel electrophoresis (PAGE) and pooled. Proteins with terminal His6 tags expressed from the pET-28c and pET-41a vectors were directly dialyzed into storage buffer (50×10^{-3} M Tris, 300×10^{-3} M NaCl, 50% (w/v) glycerol, pH 8). In case of the SUMO-tagged LOV domains, the N-terminal His6-SUMO tags were removed by Senp2 cleavage, followed by a reverse Ni:NTA affinity chromatography. The resulting, untagged LOV protein was dialyzed into storage buffer as above. At all times during purification, proteins were handled under dim red light, and

2000179 (4 of 7)

www.advanced-bio.com

NcVVD constructs were kept in buffers containing 10% (w/v) glycerol to aid stability. Protein purity was assessed by denaturing PAGE analyses, and protein concentration was determined by UV–vis spectroscopy using an absorption coefficient of the flavin mononucleotide cofactor at 450 nm of 12 500 m $^{-1}$ cm $^{-1}$.

Synthesis of AuNPs: Gold chloride trihydrate (>99%), nickel (II) chloride (anhydrous, 98%), and N,N'-dicyclohexylcarbodiimide (DCC, 99%) were purchased from Alfa Aesar. Trisodium salt dihydrate (99%) and hydrazine acetate (97%) were bought from Acros Organics. 11-mercaptoundecanoic acid, $N_{\infty}N_{\alpha}$ -bis(carboxymethyl)-L-lysine, 1,2-dimethoxyethane (DME, 99%), N-hydroxysuccinimide (98%), and zinc (pure, powder) were purchased from Sigma-Aldrich. Acetyl chloride (≥98%) was purchased from Merck. Sodium hydrogen carbonate, chloroform, and dimethylformamide (DMF) were purchased from Fisher Chemical. Sodium sulphate, tris(hydroxymethyl)-aminomethan (Tris), sodium chloride, glycerol and imidazole were purchased from Carl Roth. Hydrochloric acid (37%) and acetic acid were purchased from VWR. Milli-Q water was used throughout the experiments. To avoid unwanted nucleation during the synthesis and aggregation of gold colloid solutions, all glassware and magnetic stir bars used in the syntheses were thoroughly cleaned in aqua regia (HCI/HNO₃ 3:1), rinsed in distilled water and then dried prior to use.

400 mL of an aqueous solution of HAuCl₄ (2.5×10^{-4} m) was heated to boiling, ensued by the addition of 10.4 mL trisodium citrate solution [1% (w/w)] under continuous stirring. Within 5 min of boiling, the solution gradually changed color from yellow to white, grey, faint blue, violet, and finally red, indicating the formation of AuNPs. The reaction mixture was boiled for another 30 min and then cooled down to ambient temperature during mild stirring. The solution of AuNPs was stable and stored at 4 °C.

Synthesis of Thiolated Nitrilotriacetic Acid (NTA) Ligand: The thiolated NTA group was synthesized by adapting a previously reported procedure (Figure S2, Supporting Information). [10,21,27]

Synthesis of Thiolated Nitrilotriacetic Acid (NTA) Ligand—Synthesis of 11-(acetylthio)undecanoic Acid: A solution of 11-mercaptoundecanoic acid (838 mg, 3.84 mmol) in 67 mL chloroform and 14 mL acetic acid was stirred for 15 min after zinc powder (2.2 g) was added. Then, the solution was cooled to 0 °C, subsequently treated with acetyl chloride (5.33 mL) and stirred overnight. Afterward, zinc was removed by filtration using a pad of Celite, and the filtrate was washed twice with 0.1 m HCI (30 mL) and water (30 mL). The organic deposit was dried above Na₂SO₄, filtered, and concentrated in vacuo. The residue was purified by column chromatography to give compound 1 650 mg (65%) as a white powder [¹H NMR (300 MHz, CDCl₃) & 2.85 (t, 2H), 2.37–2.31 (m, 5H), 1.67–1.48 (m, 4H), 1.37–1.20 (m, 12H)]

Synthesis of Thiolated Nitrilotriacetic Acid (NTA) Ligand—Synthesis of $N-[N_{\omega}, N_{\alpha}]$ bis(carboxymethyl)-L-lysine] 11-(acetylthio)dodecanamide: A solution of 11-(acetylthio)undecanoic acid (1, 164 mg, 0.63 mmol) and N-hydroxysuccinimide (NHS, 72.5 mg, 0.63 mmol) in 9 mL anhydrous 1,2-dimethoxyethane (DME) was cooled to 0 °C, and subsequently N,N'dicyclohexylcarbodiimide (157 mg, 0.76 mmol) was added. The solution was kept at 0 °C for 24 h, and afterward the white dicyclohexylurea precipitate was removed by filtration and rinsed with dry DME. The filtrate was concentrated in vacuo, and the resulting white powder NHS ester was used without further purification. The NHS ester was resuspended in acetone (0.63 mL) and ethanol (6.18 mL) and subsequently treated with a solution of $N_{co}N_{cc}$ bis (carboxymethyl)-L-lysine (164.92 mg, 0.63 mmol) and NaHCO₃ (211.68 mg, 2.52 mmol) in water (3.15 mL) at room temperature and stirred for 43 h under argon. Then, the ethanol was removed under reduced pressure and the residue was diluted with water (3.15 mL) and aqueous NaHCO $_3$ solution (0.25 M, 1.26 mL). The resulting white precipitate was filtered and discarded. After acidification of the filtrate with 1.0 M HCl to pH 3, the resulting colloidal suspension was centrifuged (4000 rpm, 25 °C, 20 min), leading to the production of crude product 3. The pellet was washed with water by repeating the resuspension/centrifugation twice. The resulting residue was lyophilized to give 156 mg (49%) of compound 3 as a pale white solid. [1H NMR (300 MHz, DMSO d_6) $\delta 3.45$ (d, 4H), 3.31 (t, J = 7.3 Hz, 2H), 2.98 (br, 2H), 2.81 (t, J = 7.2 Hz, 2H), 2.31 (s, 3H), 2.01 (t, *J* = 7.4 Hz, 2H), 1.64–1.11 (m, 22H).]

Synthesis of Thiolated Nitrilotriacetic Acid (NTA) Ligand—Synthesis of $N-[N_{\infty}N_{\alpha}-bis(Carboxymethyl)-L-lysine]$ 11-Mercaptododecanamide (NTA): Hydrazine acetate (147 mg, 1.59 mmol) was added to a solution of N-[$N_{\omega}N_{\alpha}$ -bis(carboxymethyl)-L-lysine] 11-(acetylthio)dodecanamide (compound 3, 53 mg, 0.105 mmol) in dimethylformaide (6.5 mL) and afterward bubbled with argon for 20 min at room temperature. The solution was then degassed and again stirred for 20 h under argon. The solvent was removed under reduced pressure, followed by the treatment with 0.05 N HCl (20 mL). The resulting colloidal suspension was centrifuged (4000 rpm, 25 °C, 20 min) to give crude product 4, denoted NTA hereafter. The supernatant was removed, and the residue was then washed with water by repeating resuspension / centrifugation twice. The product was lyophilized to give 36 mg (74%) of compound 4 as a pale white solid. [1 H NMR (300 MHz, DMSO- d_6) δ 3.47 (d, 4H), 3.31 (t, J=7.3 Hz, 1H), 2.98 (br, 2H), 2.44 (t, J=7.2 Hz, 2H), 2.01 (t, J=7.4 Hz, 2H), 1.66–1.10(m, 22H). $^{13}\mathrm{C}$ NMR (75 MHz, DMSO- d_6) δ 174.03, 173.30, 171.92, 64.34, 53.43, 38.26, 35.46, 33.46, 29.37, 28.94, 28.81, 28.54, 27.80, 25.36, 23.81, 23.15] Mass spectrometry: calculated $(M+1)^+ = 463.247$, observed $(M+1)^+ = 463.2469$

Synthesis of Thiolated Nitrilotriacetic Acid (NTA) Ligand—Preparation of Ni²⁺-NTA Functionalized AuNPs in Buffer via Ligand Exchange: 1 mg NTA (4) was dissolved in 3 mL of 50×10^{-3} m Tris, 300×10^{-3} m NaCl, 10% (w/v) glycerol, pH 8.0. Next, 5 mL of gold nanoparticle solution was added to the solution, and the mixture was stirred at room temperature overnight. The mixture was then centrifuged at 6000 rpm for 20 min, the supernatant was removed, and the precipitated AuNPs were re-dispersed in the same buffer. $3.5 \, \mu L$ NiCl₂ ($12.5 \, mg/20 \, mL$) was added to the AuNP solution, followed by incubation at ambient temperature for $20 \, min$. The solution of Ni²⁺-NTA-AuNPs was centrifuged at $6000 \, rpm$ for $20 \, min$ again. The final supernatant was removed, and the Ni²⁺-NTA-AuNPs were resuspended in 50×10^{-3} m Tris, 300×10^{-3} m NaCl, 10% (w/v) glycerol, pH 8.0. The particles were kept at $4 \, ^{\circ}C$ until further use.

The molar concentration of gold atoms, $c_{\rm Au}$, was determined by inductively coupled plasma optical emission spectrometry, see below. To calculate the concentration of AuNPs, a spherical shape and a uniform face-centered cubic lattice (fcc) structure of the synthesized AuNPs was assumed. The average number of gold atoms per nanoparticle (N) was calculated by Equation (1), where ρ denotes the density for fcc gold (19.3 g cm⁻³), M is the atomic weight of gold (197 g mol⁻¹), and d is the diameter of the AuNPs (17.7 nm, as measured by TEM)^[42]

$$N = \pi/6 \times (\rho d^3/M) \tag{1}$$

The molar concentration of the AuNPs, c_{NP} , was then calculated according to Equation (2)

$$c_{\mathsf{NP}} = c_{\mathsf{Au}}/\mathsf{N} \tag{2}$$

Analytical Methods—Size-Exclusion Chromatography: Size-exclusion chromatography was performed on an ÄKTA pure system and a Superdex 200 Increase 3.2/300 analytical column at 4 $^{\circ}$ C. The column was equilibrated with buffer containing 50 × 10 $^{-3}$ M Tris/HCl, 100 × 10 $^{-3}$ M NaCl and 5 × 10 $^{-3}$ M $^{\circ}$ Mercraptoethanol at pH 8.0, and operated at a flow rate of 0.05 mL min $^{-1}$. Samples were centrifuged at 13200 × g and injected in 30 μ L aliquots at a concentration of 50 × 10 $^{-6}$ M. Light-adapted samples were generated by irradiation with blue light (450 nm, 30 mW cm $^{-2}$, 2 min) immediately prior to injection. The run of the light-adapted sample was performed under constant blue light, while the run of the dark-state sample was conducted under exclusion of light. The elution of the samples was followed by absorption measurements at 280 nm.

Analytical Methods—Transmission Electron Microscopy (TEM): TEM micrographs were obtained on a ZEISS EM922 Omega microscope at an acceleration voltage of 200 keV. Functionalized AuNPs $(0.9 \times 10^{-9} \text{ M})$ were incubated with $50 \times 10^{-9} \text{ M}$ NcVVD-His either in the absence or presence of blue light irradiation (450 nm, 30 mW cm $^{-2}$) for 10 min at 4 °C. Then, individual samples were prepared by dripping the protein-AuNPs solution on a carbon-covered copper grid and drying at room temperature overnight. The

2000179 (5 of 7)

www.advanced-bio.com

images were evaluated with ImageJ. For each sample at least 100 AuNPs were counted.

Analytical Methods—Asymmetric Flow Field-Flow Fractionation (AF4): AF4 measurements were carried out using an AF2000 system with a Smart Stream Splitter from Postnova Analytics (Landsberg am Lech, Germany). The channel had a length and width of 295 and 30 mm, respectively, and was equipped with a spacer height of 350 µm. The separation was conducted on a NovaRC 10 kDa regenerated cellulose membrane. Detection was performed with a UV detector at a wavelength of 270 nm. In addition, the samples were analyzed inline by a multiple angle light scattering (MALS) detector (Postnova Analytics), with 21 observation angles and operated with linearly polarized laser light at 532 nm. Individual runs were conducted as stated in Table S1 in the Supporting Information using 50×10^{-3} M Tris/HCl, 300×10^{-3} M NaCl and 10% (w/v) glycerol at pH 8.0 as eluent. The temperature was kept at 8 °C during the measurement, and the samples were prepared as described in the TEM section. The run of the light-adapted samples was performed under constant illumination, whereas the run of the dark-adapted sample was conducted under exclusion of light. Data from the MALS detector were processed using the Postnova AF2000 control software. A spherical model was used for obtaining the radius of gyration based on the angular dependence of scattered light recorded by

Analytical Methods—Inductively Coupled Plasma Optical Emission Spectrometry: Measurements were performed on an Avio 200 instrument (Perkin Elmer) in radial viewed plasma with purged polychromator configurations. The measurement was calibrated with four standard solutions at concentrations of 0.1, 0.5, 1, and 10 mg L $^{-1}$.

Analytical Methods—Nuclear Magnetic Resonance (NMR) Spectroscopy:

1H NMR and
12C NMR spectroscopy was carried out on a Bruker Ultrashield 300 using deuterated chloroform and DMSO as solvents at 300 MHz. Spectra were calibrated by the signal of the residual protons of the deuterated solvents. Spectra were evaluated with the MestReNova software.

Analytical Methods—Mass Spectrometry (MS): Mass spectrometry was performed using direct infusion from an Ultimate 3000 UPLC system (Dionex, Sunnyvale, CA, USA) to a Hybrid Quadrupole Orbitrap system with electrospray ionization (ESI, Thermo Fisher Scientific, Waltham, MA, USA). For the MS analysis, ESI was operated in positive mode. Full scan was applied with a mass range of 80–1200 amu.

Analytical Methods—UV-vis (UV-vis) Absorption Spectroscopy: UV-vis absorption spectroscopy was carried out on an Agilent 8453 UV-vis apsorption spectroscopy system together with an Agilent 89090A temperature control accessory. Absorption spectra were recorded in 50 × 10 $^{-3}$ M Tris/HCl, 300 × 10 $^{-3}$ M NaCl, 10% (w/v) glycerol, pH 8.0 right after addition of 0 × 10 $^{-9}$, 6.25 × 10 $^{-9}$, 12.5 × 10 $^{-9}$, 25 × 10 $^{-9}$, or 50 × 10 $^{-9}$ M of NcVVD-His₆ to 0.9 × 10 $^{-9}$ M of Ni²+-NTA functionalized AuNPs. For kinetic measurements, light-adapted samples were constantly illuminated with 450-nm light (30 mW cm $^{-2}$), while dark-state samples were kept in darkness. Absorption spectra were recorded before addition of protein and after 2, 5, 10, 15, 20, 30, 40, 60, and 90 min of incubation at 4 °C in low-binding reaction tubes (Eppendorf, DNA LoBind). As a control, the AuNPs were incubated in the presence of 560 × 10 $^{-3}$ M imidazole and 0 × 10 $^{-9}$, 6.25 × 10 $^{-9}$, 12.5 × 10 $^{-9}$, 25 × 10 $^{-9}$, or 50 × 10 $^{-9}$ M NcVVD-His₆; the analysis was carried out as described above.

Supporting Information

Supporting Information is available from the Wiley Online Library or from the author.

Acknowledgements

Financial support was provided by University of Bayreuth and the Deutsche Forschungsgemeinschaft (grants MO2192/8-1 to A.M. and

SFB 840, project B8 to A.G.). We appreciate the support of the Keylab for optical and electron microscopy at the Bavarian Polymer Institute.

Open access funding enabled and organized by Projekt DEAL.

Conflict of Interest

The authors declare no conflict of interest.

Author Contributions

J.D. and C.L. contributed equally to this work. J. D. and C. L. contributed equally to the results of the manuscript. J.D. and S.F. cloned, expressed, purified, and analyzed LOV proteins; C.L. synthesized, derivatized, and analyzed AuNP. J.D., C.L., and S.F. assessed the light-dependent interplay of protein and nanoparticles and evaluated data. A-K.M., J.D., and C.L. performed and analyzed the AF4 measurements. J.D. and C.L. prepared figures. A.M. and A.G. conceived and supervised the project. J.D., C.L., A.M., and A.G. wrote the manuscript with input from all authors.

Data Availability Statement

All data underlying the main text and the supplementary materials are available as a supplementary zip archive.

Keywords

assembly, gold nanoparticles, photoresponsive materials, sensory photoreceptors, smart materials

Received: July 7, 2020 Revised: October 22, 2020 Published online:

- J. M. Christie, P. Reymond, G. K. Powell, P. Bernasconi, A. A. Raibekas, E. Liscum, W. R. Briggs, Science 1998, 282, 1698.
- [2] A. Losi, K. H. Gardner, A. Möglich, Chem. Rev. 2018, 118, 10659.
- [3] G. Chen, I. Roy, C. Yang, P. N. Prasad, Chem. Rev. 2016, 116, 2826.
- [4] W. J. Stark, P. R. Stoessel, W. Wohlleben, A. Hafner, Chem. Soc. Rev. 2015, 44, 5793.
- [5] N. L. Rosi, C. A. Mirkin, Chem. Rev. 2005, 105, 1547.
- [6] C. J. Murphy, A. M. Gole, J. W. Stone, P. N. Sisco, A. M. Alkilany, E. C. Goldsmith, S. C. Baxter, Acc. Chem. Res. 2008, 41, 1721.
- [7] C.-A. J. Lin, T.-Y. Yang, C.-H. Lee, S. H. Huang, R. A. Sperling, M. Zanella, J. K. Li, J.-L. Shen, H.-H. Wang, H.-I. Yeh, W. J. Parak, W. H. Chang, ACS Nano 2009, 3, 395.
- [8] G. Han, P. Ghosh, V. M. Rotello, Future Med. 2007, 2, 113.
- [9] N. L. Rosi, D. A. Giljohann, C. S. Thaxton, A. K. R. Lytton-Jean, M. S. Han, C. A. Mirkin, *Science* 2006, 312, 1027.
- [10] C. Xu, K. Xu, H. Gu, X. Zhong, Z. Guo, R. Zheng, X. Zhang, B. Xu, J. Am. Chem. Soc. 2004, 126, 3392.
- [11] Z. Fan, X. Chen, M. Köhn Serrano, H. Schmalz, S. Rosenfeldt, S. Förster, S. Agarwal, A. Greiner, Angew. Chem., Int. Ed. 2015, 54, 14539.
- [12] Z. Fan, M. K. Serrano, A. Schaper, S. Agarwal, A. Greiner, Adv. Mater. 2015, 27, 3888.
- [13] Y. Ofir, B. Samanta, V. M. Rotello, Chem. Soc. Rev. 2008, 37, 1814.
- [14] Q.-Y. Lin, J. A. Mason, Z. Li, W. Zhou, M. N. O'Brien, K. A. Brown, M. R. Jones, S. Butun, B. Lee, V. P. Dravid, K. Aydin, C. A. Mirkin, *Science* 2018, 359, 669.

2000179 (6 of 7)



ADVANCED BIOLOGY

www.advancedsciencenews.com www.advanced-bio.com

- [15] M. S. Köhn Serrano, T. A. F. König, J. S. Haataja, T. I. Löbling, H. Schmalz, S. Agarwal, A. Fery, A. Greiner, Macromol. Rapid Commun. 2016, 37, 215.
- [16] L. Zhang, L. Dai, Y. Rong, Z. Liu, D. Tong, Y. Huang, T. Chen, Langmuir 2015, 31, 1164.
- [17] P. K. Kundu, D. Samanta, R. Leizrowice, B. Margulis, H. Zhao, M. Börner, T. Udayabhaskararao, D. Manna, R. Klajn, *Nat. Chem.* 2015, 7, 646.
- [18] Y. Chen, Z. Wang, Y. He, Y. J. Yoon, J. Jung, G. Zhang, Z. Lin, Proc. Natl. Acad. Sci. 2018, 115, 1391.
- [19] J.-Y. Kim, J. Yeom, G. Zhao, H. Calcaterra, J. Munn, P. Zhang, N. Kotov, J. Am. Chem. Soc. 2019, 141, 11739.
- [20] Q. Wang, D. Li, J. Xiao, F. Guo, L. Qi, Nano Res. 2019, 12, 1563.
- [21] J. M. Abad, S. F. L. Mertens, M. Pita, V. M. Fernández, D. J. Schiffrin, J. Am. Chem. Soc. 2005, 127, 5689.
- [22] D. Huebner, C. Rossner, P. Vana, Polymer 2016, 107, 503.
- [23] J. Lai, Y. Xu, X. Mu, X. Wu, C. Li, J. Zheng, C. Wu, J. Chen, Y. Zhao, Chem. Commun. 2011, 47, 3822.
- [24] E. Jaquay, L. J. Martínez, N. Huang, C. A. Mejia, D. Sarkar, M. L. Povinelli, Nano Lett. 2014, 14, 5184.
- [25] S. Christau, T. Moeller, J. Genzer, R. Koehler, R. vonKlitzing, Macromolecules 2017, 50, 7333.
- [26] R. Pamies, J. G. H. Cifre, V. F. Espín, M. Collado-González, F. G. D. Baños, J. G. de laTorre, J. Nanoparticle Res. 2014, 16, 2376.

- [27] H.-Y. Park, K. Kim, S. Hong, H. Kim, Y. Choi, J. Ryu, D. Kwon, R. Grailhe, R. Song, *Langmuir* 2010, 26, 7327.
- [28] E. Herman, M. Sachse, P. G. Kroth, T. Kottke, Biochemistry 2013, 52, 3094.
- [29] B. D. Zoltowski, B. R. Crane, Biochemistry 2008, 47, 7012.
- [30] A. Banerjee, E. Herman, T. Kottke, L.-O. Essen, Structure 2016, 24, 171.
- [31] U. Heintz, I. Schlichting, eLife 2016, 5, 11860.
- [32] X. Wang, X. Chen, Y. Yang, Nat. Methods 2012, 9, 266.
- [33] G. Frens, Nat. Phys. Sci. 1973, 241, 20.
- [34] S. Panigrahi, S. Basu, S. Praharaj, S. Pande, S. Jana, A. Pal, S. K. Ghosh, T. Pal, J. Phys. Chem. C 2007, 111, 4596.
- [35] P. Kalimuthu, S. A. John, Mater. Chem. Phys. 2010, 122, 380.
- [36] A. M. Smith, L. E. Marbella, K. A. Johnston, M. J. Hartmann, S. E. Crawford, L. M. Kozycz, D. S. Seferos, J. E. Millstone, Anal. Chem. 2015, 87, 2771.
- [37] F. Chen, S. V. Wegner, ACS Synth. Biol. 2020, 9, 1169.
- [38] T. Ziegler, A. Möglich, Front. Mol. Biosci. 2015, 2, 30.
- [39] A. Pudasaini, K. K. El-Arab, B. D. Zoltowski, Front. Mol. Biosci. 2015, 2, 18.
- [40] D. G. Gibson, L. Young, R.-Y. Chuang, J. C. Venter, C. A. Hutchison, H. O. Smith, Nat. Methods 2009, 6, 343.
- [41] T. Mathes, C. Vogl, J. Stolz, P. Hegemann, J. Mol. Biol. 2009, 385, 1511.
- [42] X. Liu, M. Atwater, J. Wang, Q. Huo, Colloids Surf., B 2007, 58, 3.



Supporting Information

for Adv. Biosys., DOI: 10.1002/adbi.202000179

Photobiologically Directed Assembly of Gold Nanoparticles

Julia Dietler, Chen Liang, Saskia Frank, Ann-Kathrin Müller, Andreas Greiner,* and Andreas Möglich*

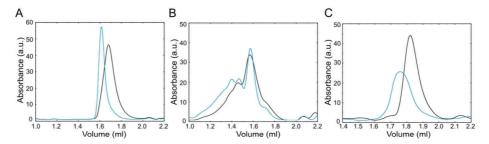
Copyright WILEY-VCH Verlag GmbH & Co. KGaA, 69469 Weinheim, Germany, 2020.

Supporting Information

Photobiologically Directed Assembly of Gold Nanoparticles

Julia Dietler[‡], Chen Liang[‡], Saskia Frank, Ann-Kathrin Müller, Andreas Greiner^{*}, Andreas Möglich^{*}

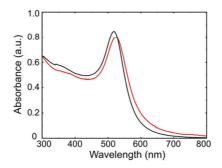
Figure S1. Light-induced changes in quaternary structure of LOV proteins.



Size-exclusion chromatography of (A) the unmodified *Pt*aur core domain, (B) His₆-*Pt*aur and (C) the unmodified *Nc*VVD domain in darkness (black traces) and upon blue-light exposure (blue traces). Both the untagged *Pt*aur and *Nc*VVD eluted as a single, homogenous peak in either darkness or under blue light. Under blue light, the apparent molecular weight is higher, indicating light-induced dimerization. However, the N-terminal modification of *Pt*aur (panel B) led to constitutive dimerization and formation of larger assemblies.

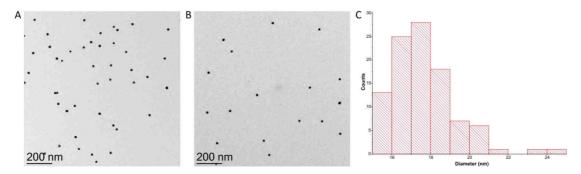
Figure S2. Synthesis of the NTA ligand and surface modification of gold nanoparticles via ligand exchange with subsequent Ni^{2+} coordination.

Figure S3. Modification of citrate-capped AuNPs with Ni²⁺-NTA.



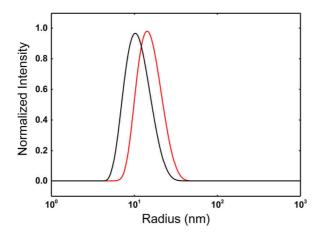
UV-vis spectra of citrate-capped AuNPs (black) and Ni^{2+} -NTA functionalized AuNPs (red) indicate a shift in maximum absorption from 518 nm towards 524 nm.

Figure S4. Analysis of gold nanoparticles by transmission electron microscopy (TEM).



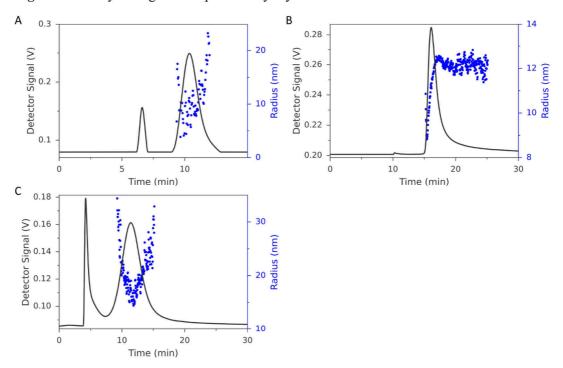
(A-B) TEM images of citrate-capped (A) and Ni^{2+} -NTA-functionalized AuNPs (B). (C) Size distribution of the Ni^{2+} -NTA-AuNPs.

Figure S5. Analysis of gold nanoparticles by dynamic light scattering.



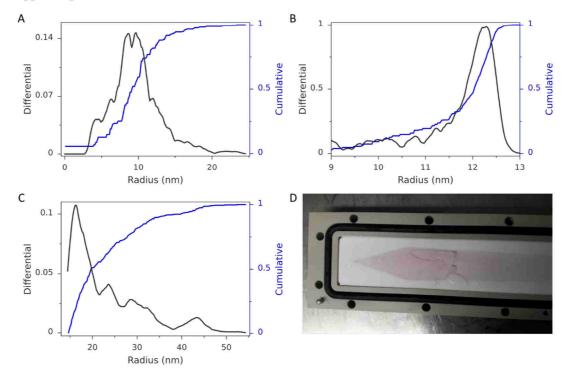
Distributions of the hydrodynamic radius of citrate-capped (black) and Ni^{2+} -NTA-functionalized AuNPs (red).

Figure S6. Analysis of gold nanoparticles by asymmetric flow field-flow fractionation.



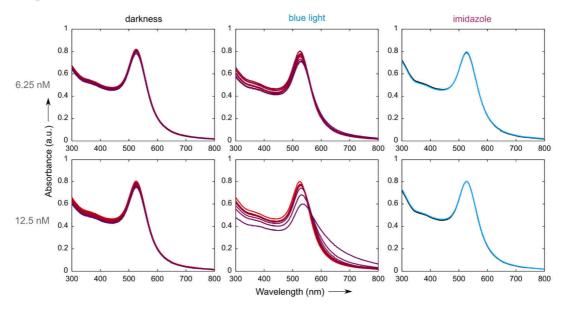
Elution profiles of citrate-capped AuNPs (A), Ni²⁺-NTA-functionalized AuNPs (B) and *Nc*VVD-His₆ coupled to Ni²⁺-NTA-AuNPs (C).

Figure S7. Coupling of NcVVD-His₆ to Ni²⁺-NTA-functionalized AuNPs increases the apparent particle size.



(A, B) Apparent particle sizes measured by AF4 of citrate-capped AuNPs (A) and Ni²⁺-NTA-functionalized AuNPs (B). The main particle fractions of citrate-capped and Ni²⁺-NTA-functionalized AuNPs eluted with apparent radii of (11 ± 2) nm and (12 ± 2) nm, respectively. (C) In the presence of NcVVD-His₆ but in absence of blue light the principal fraction of Ni²⁺-NTA-functionalized AuNPs eluted with an apparent radius of (18 ± 2) nm. (D) Illumination of the mixture of NcVVD-His₆ and Ni²⁺-NTA functionalized AuNPs promoted the formation of large particle clusters, which gave rise to a purple precipitate on the analysis membrane.

Figure S8. Blue-light exposure drives the assembly of Ni^{2+} -NTA-functionalized AuNPs coupled to NcVVD-His₆.



Time series of UV-vis spectra of Ni^{2+} -NTA-functionalized AuNPs in absence and presence of 6.25 nM or 12.5 nM NcVVD-His₆. Spectra were acquired at 2, 5, 10, 15, 20, 30, 40, 60 and 90 minutes (from top to bottom) after protein addition and incubation in darkness (left panels) or blue light (middle panels). The right panels show data obtained when 0.56 M imidazole was added to the particles. See figure 2 for details.

Table S1. Flow and time parameters of AF4 measurements.

Step	Parameter		Citrate- capped AuNPs	Ni ²⁺ -NTA- AuNPs	NcVVD-His6 coupled to Ni ²⁺ - NTA-AuNPs
	Injection volume (µL)		20	20	20
	Detector flow (mL min ⁻¹)		0.5	0.5	0.5
Focusing	Injection flow (mL min ⁻¹)		0.2	0.2	0.2
	Injection time (min)		5	9	3
	Crossflow (mL min ⁻¹)		0.7	0.7	0.5
	Transition time (min)		0.5	0.5	0.3
Elution	Step 1	Elution time (min)	3	3	0.5
	Step 2 Step 3	From (mL min ⁻¹)	0.7	0.7	0.5
		To (mL min ⁻¹)	0.7	0.7	0.5
		Type	const.	const.	const.
		Elution time (min)	20	20	25
		From (mL min ⁻¹)	0.7	0.7	0.5
		To (mL min ⁻¹)	0	0	0.05
		Type (Power)	0.15	0.15	0.3
		Elution time (min)	0	0	10
		From (mL min ⁻¹)	0	0	0.05
		To (mL min ⁻¹)	0	0	0
		Type	0	0	const.
Rinsing	Time (min)		5	5	5

5 Publikationsliste

Hennemann, J., Iwasaki, R.S., Grund, T.N., Diensthuber, R.P., Richter, F., Möglich, A., 2018. Optogenetic Control by Pulsed Illumination. Chembiochem 19, 1296–1304. https://doi.org/10.1002/cbic.201800030

Dietler, J., Stabel, R., Möglich, A., 2019. Pulsatile illumination for photobiology and optogenetics. Methods Enzymol. 624, 227–248.

https://doi.org/10.1016/bs.mie.2019.04.005

Dietler, J., Schubert, R., Krafft, T. G. A., Meiler, S., Kainrath, S., Richter, F., Schweimer, K., Weyand, M., Janovjak, H., Möglich, A., 2021. A Light-Oxygen-Voltage Sensor Integrates Light and Temperature. Journal of Molecular Biology, 433, 167107. https://doi.org/10.1016/j.jmb.2021.167107

Dietler, J., Liang, C., Frank, S., Müller, A., Greiner, A., Möglich, A., 2020. Photobiologically Directed Assembly of Gold Nanoparticles. Adv. Biol. 2000179.

https://doi.org/10.1002/adbi.202000179

6 Danksagung

Zuerst möchte ich Prof. Dr. Andreas Möglich für die lehrreichen Jahre (angefangen bei meiner Masterarbeit bis hin zur Promotion), den wissenschaftlichen Input mit den verbundenen Diskussionen und die jederzeit offene Tür bedanken. Nicht zuletzt haben sein immerwährender Optimismus und die motivierenden Gespräche zum Gelingen dieser Arbeit beigetragen.

Zudem geht ein großer Dank an die gesamte AG Möglich für eine großartige Zeit und sehr angenehme Arbeitsatmosphäre. Danke, für manch erfolgsbringende Tipps und Ratschläge, ausgelassene Unterhaltungen und dass man sich immer auf euch verlassen konnte.

Auch bei den Beschäftigten der Arbeitsgruppen von Prof. Dr. Birte Höcker und Prof. Dr. Clemens Steegborn möchte ich mich für die wissenschaftliche Hilfe und gute Zusammenarbeit bedanken.

Ein weiterer Dank gilt den Sekretärinnen für die tatkräftige Unterstützung in allen Belangen.

Ich möchte außerdem auch Cathrin, Josef und Andi danken, die mich während der Studienzeit und auch darüber hinaus begleitet haben. Danke für die unvergesslichen Praktika, ausgelassenen Abende und tiefsinnigen Gespräche. Insbesondere gilt auch mein Dank an Micha für die langjährige Freundschaft, die schönen gemeinsamen Erlebnisse und die Unterstützung in allen Lebenslagen.

An letzter und wichtigster Stelle möchte ich mich bei meiner gesamten Familie bedanken, die immer ein offenes Ohr für mich hat, mich in meinem Tun bestärkt, dieses aber auch kritisch hinterfragt. Danke, dass ihr mir Rückhalt gebt und mir immer neue Blickwinkel aufzeigt.

7 (Eidesstattliche) Versicherungen und Erklärungen

(§ 8 Satz 2 Nr. 3 PromO Fakultät)

Hiermit versichere ich eidesstattlich, dass ich die Arbeit selbstständig verfasst und keine anderen als die von mir angegebenen Quellen und Hilfsmittel benutzt habe (vgl. Art. 64 Abs. 1 Satz 6 BayHSchG).

(§ 8 Satz 2 Nr. 3 PromO Fakultät)

Hiermit erkläre ich, dass ich die Dissertation nicht bereits zur Erlangung eines akademischen Grades eingereicht habe und dass ich nicht bereits diese oder eine gleichartige Doktorprüfung endgültig nicht bestanden habe.

(§ 8 Satz 2 Nr. 4 PromO Fakultät)

Hiermit erkläre ich, dass ich Hilfe von gewerblichen Promotionsberatern bzw. –vermittlern oder ähnlichen Dienstleistern weder bisher in Anspruch genommen habe noch künftig in Anspruch nehmen werde.

(§ 8 Satz 2 Nr. 7 PromO Fakultät)

Hiermit erkläre ich mein Einverständnis, dass die elektronische Fassung der Dissertation unter Wahrung meiner Urheberrechte und des Datenschutzes einer gesonderten Überprüfung unterzogen werden kann.

(§ 8 Satz 2 Nr. 8 PromO Fakultät)

Hiermit erkläre ich mein Einverständnis, dass bei Verdacht wissenschaftlichen Fehlverhaltens Ermittlungen durch universitätsinterne Organe der wissenschaftlichen Selbstkontrolle stattfinden können.

Ort, Datum, Unterschrift